# ROLES OF CHONDROITIN SULFATE AND DERMATAN SULFATE AS REGULATORS FOR CELL AND TISSUE DEVELOPMENT

EDITED BY: Shuji Mizumoto, Jessica C. F. Kwok, Fuchuan Li, Roberto Perris and John Whitelock

PUBLISHED IN: Frontiers in Cell and Developmental Biology

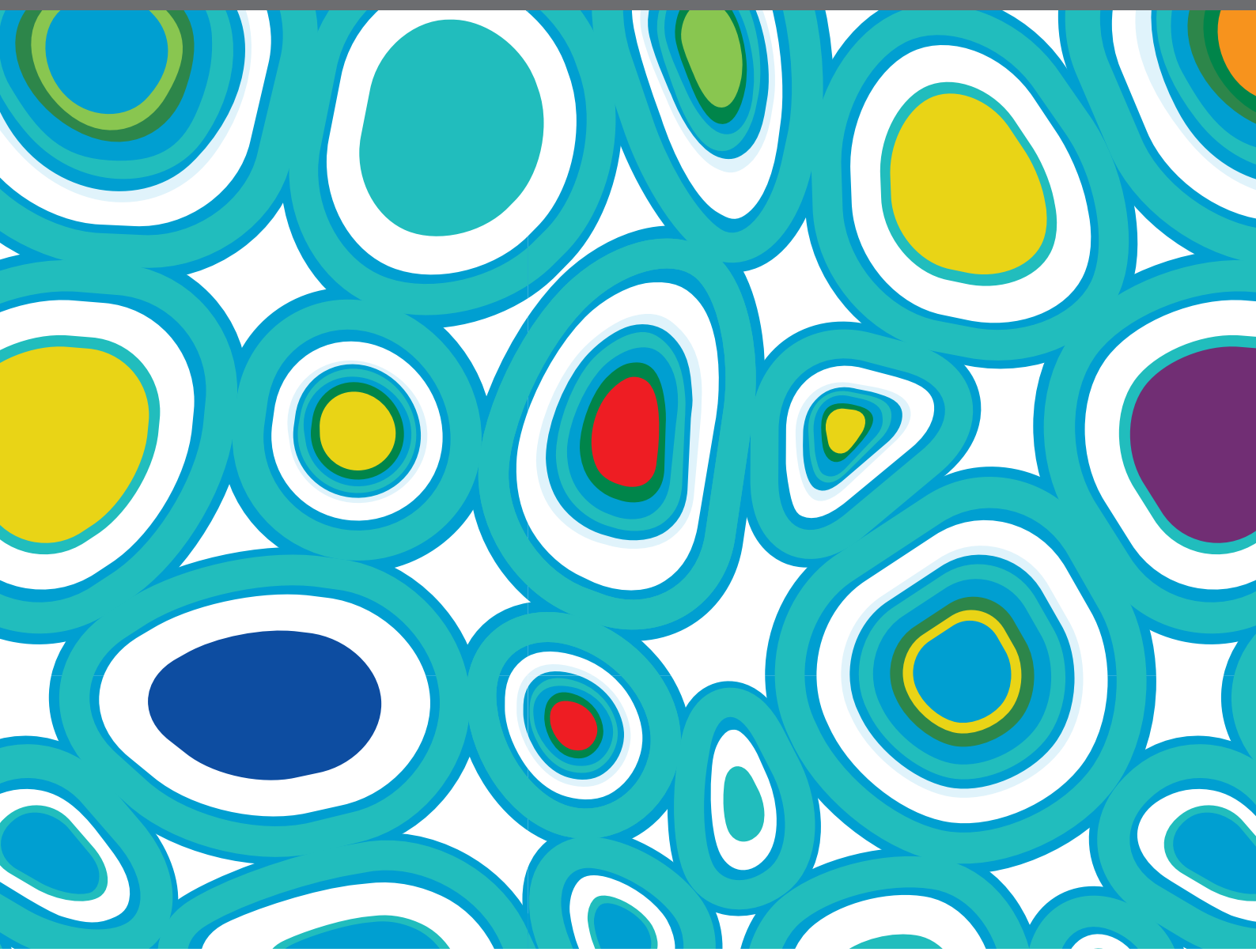

frontiers Research Topics

ISSN 1664-8714
ISBN 978-2-88976-478-5
DOI 10.3389/978-2-88976-478-5

## About Frontiers

Frontiers is more than just an open-access publisher of scholarly articles: it is a pioneering approach to the world of academia, radically improving the way scholarly research is managed. The grand vision of Frontiers is a world where all people have an equal opportunity to seek, share and generate knowledge. Frontiers provides immediate and permanent online open access to all its publications, but this alone is not enough to realize our grand goals.

## Frontiers Journal Series

The Frontiers Journal Series is a multi-tier and interdisciplinary set of open-access, online journals, promising a paradigm shift from the current review, selection and dissemination processes in academic publishing. All Frontiers journals are driven by researchers for researchers; therefore, they constitute a service to the scholarly community. At the same time, the Frontiers Journal Series operates on a revolutionary invention, the tiered publishing system, initially addressing specific communities of scholars, and gradually climbing up to broader public understanding, thus serving the interests of the lay society, too.

## Dedication to Quality

Each Frontiers article is a landmark of the highest quality, thanks to genuinely collaborative interactions between authors and review editors, who include some of the world's best academicians. Research must be certified by peers before entering a stream of knowledge that may eventually reach the public - and shape society; therefore, Frontiers only applies the most rigorous and unbiased reviews.
Frontiers revolutionizes research publishing by freely delivering the most outstanding research, evaluated with no bias from both the academic and social point of view. By applying the most advanced information technologies, Frontiers is catapulting scholarly publishing into a new generation.

## What are Frontiers Research Topics?

Frontiers Research Topics are very popular trademarks of the Frontiers Journals Series: they are collections of at least ten articles, all centered on a particular subject. With their unique mix of varied contributions from Original Research to Review Articles, Frontiers Research Topics unify the most influential researchers, the latest key findings and historical advances in a hot research area! Find out more on how to host your own Frontiers Research Topic or contribute to one as an author by contacting the Frontiers Editorial Office: frontiersin.org/about/contact

# ROLES OF CHONDROITIN SULFATE AND DERMATAN SULFATE AS REGULATORS FOR CELL AND TISSUE DEVELOPMENT

Topic Editors:
**Shuji Mizumoto,** Meijo University, Japan
**Jessica C. F. Kwok,** University of Leeds, United Kingdom
**Fuchuan Li,** Shandong University, China
**Roberto Perris,** University of Parma, Italy
**John Whitelock,** University of New South Wales, Australia

**Citation:** Mizumoto, S., Kwok, J. C. F., Li, F., Perris, R., Whitelock, J., eds. (2022). Roles of Chondroitin Sulfate and Dermatan Sulfate as Regulators for Cell and Tissue Development. Lausanne: Frontiers Media SA.
doi: 10.3389/978-2-88976-478-5

# Table of Contents

frontiers | Frontiers in Cell and Developmental Biology

EDITORIAL
published: 08 June 2022
doi: 10.3389/fcell.2022.941178

# Editorial: Roles of Chondroitin Sulfate and Dermatan Sulfate as Regulators for Cell and Tissue Development

*Shuji Mizumoto*[1]*, *Jessica C. F. Kwok*[2,3], *John M. Whitelock*[4], *Fuchuan Li*[5] and *Roberto Perris*[6]

[1]Department of Pathobiochemistry, Faculty of Pharmacy, Graduate School of Pharmacy, Meijo University, Nagoya, Japan, [2]Faculty of Biological Sciences, School of Biomedical Sciences, University of Leeds, Leeds, United Kingdom, [3]Centre for Reconstructive Neuroscience, Institute of Experimental Medicine, Czech Academy of Sciences, Prague, Czech Republic, [4]Graduate School of Biomedical Engineering, University of New South Wales, Adelaide, NSW, Australia, [5]National Glycoengineering Research Center, Shandong Key Laboratory of Carbohydrate Chemistry and Glycobiology, NMPA Key Laboratory for Quality Research and Evaluation of Carbohydrate-Based Medicine, Shandong University, Jinan, China, [6]Department of Chemical and Life Sciences and Environmental Sustainability, University of Parma, Parma, Italy

**Keywords: chondroitin sulfate, dermatan sulfate, proteoglycan, cell signal, stem cell, tissue morphogenesis**

## Editorial on the Research Topic

## Roles of Chondroitin Sulfate and Dermatan Sulfate as Regulators for Cell and Tissue Development

OPEN ACCESS

***Edited and reviewed by:***
*Ana Cuenda,*
*Spanish National Research Council (CSIC), Spain*

***Correspondence:**
*Shuji Mizumoto*
*mizumoto@meijo-u.ac.jp*

***Specialty section:***
*This article was submitted to Signaling, a section of the journal Frontiers in Cell and Developmental Biology*

***Received:*** *11 May 2022*
***Accepted:*** *23 May 2022*
***Published:*** *08 June 2022*

***Citation:***
*Mizumoto S, Kwok JCF, Whitelock JM, Li F and Perris R (2022) Editorial: Roles of Chondroitin Sulfate and Dermatan Sulfate as Regulators for Cell and Tissue Development. Front. Cell Dev. Biol. 10:941178. doi: 10.3389/fcell.2022.941178*

Chondroitin sulfate (CS) and dermatan sulfate (DS) are highly conserved glycosaminoglycans (GAGs) known to mediate many of the functions that proteoglycans (PGs) exert in a myriad of biological events taking place during embryogenesis, in the adult organism and in pathological conditions. CS was originally isolated from cartilage as early as at the end of the 19$^{th}$ century (Fischer and Boedeker, 1861), albeit its structural properties were resolved decades later (Levene and La Forge, 1913) and its complex sulfation patterns and domain arrangement remain a great challenges in this field. DS was first isolated from porcine skin by Karl Meyer in 1940s (Meyer and Chaffee, 1941) and was much later on found to share some of the characteristics of CS. As all sulfated GAGs, CS/DS chains are covalently attached to serine residue(s) of the core proteins of PGs through a specific and highly conserved GAG-protein tetrasaccharide linkage region encompassing glucuronic acid–galactose–galactose–xylose-(serine) (Lindahl and Rodén, 1966). In 1950s, the first CS-bearing PGs were isolated from bovine nasal septum (more specifically, aggrecan; Mathews and Lozaityte, 1958), while their counterpart first degrading enzyme, "chondroitinase ABC", was isolated from Proteus vulgaris (Dodgson and Lloyd, 1958).

The cloning of mammalian chondroitin synthases, DS-epimerases and chondroitin sulfotransferases significantly contributed to the gaining of a better understanding of the biosynthesis and homeostatic roles of CS/DS, with particular reference to the action of cytokinesis, the control of bone development, the assembly of collagen fibrils, and the regulation of cytokines as well as chemokines. These discoveries were followed by correlations between CS/DS synthesis and human genetic disorders, including spondyloepiphyseal dysplasia with congenital joint dislocations, Temtamy preaxial brachydactyly syndrome, and Ehlers-Danlos syndrome.

By combining the knowledge on the biosynthetic and catalytic activity of CS/DS enzymes and the use of transgenic technologies it has been possible to correlate the phenotypic traits of the brachymorphic mouse to a disturbed sulfation of CS of cartilage matrix PGs, as well as reconcile these synthetic GAG deficits to genetic abnormalities in humans. This transgenic mouse provided the first model for addressing the *in vivo* function of CS in that specific tissue and paved the way for

generating numerous other mouse mutants with altered expression of key CS/DS regulating molecules. It was, however, through the production of the first immunological tools that analyses of the distributional, structural and functional traits of CS/DS and their isoforms became more readily accomplishable. The pioneering, milestone work of Bruce Caterson and John Couchman (Couchman et al., 1984) opened this field and their work was soon followed by the impactful, but unfairly overlooked, studies of Michael Sorrell who was able to generate an array of monoclonal antibodies recognizing subdomains of the intact CS and DS chains (Sorrell et al., 1990).

Through the advent of more powerful technologies, including oligosaccharide libraries, microarrays, and sophisticated proteomic approaches, it has been possible delineate the complexity of the domain organization of CS, DS, and CS/DS hybrid chains and consequently gain a better understanding of the dynamics and structural-functional details of the molecular interactions that these GAGs, "wobble motifs", engage with a spectrum of proteins (Purushothaman et al., 2012).

Collectively, decades of studies on the structural properties and cellular and molecular functions of CS and DS have highlighted their importance in an ample spectrum of biological phenomena and have incited further investigations to be pursued to fully unveil their biological significance. This special issue was therefore proposed to expand our vision on what is currently known about the role of CSs and DSs in biological processes, spanning from those regulating embryonic development to those maintaining a proper tissue homeostasis, and on the methods and technologies currently used to analyse their structural-functional properties.

A study reported in this issue by Schaberg et al., highlights that in addition to the well-established function of heparan sulfate (HS) in growth factor signaling, CS may similarly participate in the modulation of fibroblast growth factor 2 (FGF2)-dependent cell-cycle progression in spinal cord neural stem and progenitor cells. Alongside this contribution, the article by Ogura and Nishihara describes how dermatan 4-*O*-sulfotransferase-1 (D4ST1) may control the differentiation state of murine embryonic stem cells, emphasizing how DS-PGs and D4ST1, as a promoter of 4-*O*-sulfation in DS-like HS, may influence signaling pathway(s) associated with cell differentiation. Comprehensively, these studies emphasize a critical role of CS, DS, and the PGs bearing such GAGs in the control of stem/progenitor cell development.

A parallel study by Nitahara-Kasahara et al., further demonstrates that D4st1 knockout mice display a myopathy-related phenotype including variation in fiber size and altered distribution in the muscle interstitium, resulting in a decreased exercise capacity. This finding suggests that D4ST1, and/or the DS-PGs affected by its deletion, regulate skeletal muscle myogenesis and muscle physiology, and highlights potential therapeutic approaches to be undertaken in patients of musculo-contractural Ehlers-Danlos syndrome caused by mutations in D4ST1. In their review, Mizumoto and Yamada elegantly summarize what we have learned through the use of CS/DS-deficient mice and how such mutants may be further exploited to improve our understanding of the role of the GAGs during both embryonic development and adult life.

Schwartz and Domowicz have reviewed in this issue the roles of CS-bearing PGs as regulators of skeletal development and as primary PGs affected by GAG-related disorders such as mucopolysaccharidoses and osteoarthritis. These authors specifically discuss the Indian hedgehog, BMPs, FGFs, and TGFs signaling pathways responsible for growth plate development, which are underlined to be elicited through the interaction of the growth factors with the CS chains of aggrecan, the prototype CS-bearing PG that may carry up to 100 such chains. Their essay provides a comprehensive view on the importance of aggrecan and other early expressed CS-bearing PGs during tissue development and the morphogenetic events leading to the formation of the specialized connective tissue structures building our skeleton.

Nadanaka et al., have contributed with an appealing article demonstrating that knockout of chondroitin 4-*O*-sulfotransferase-1 (C4ST1) in breast cancer cell lines results in the lack of CS side chains on syndecan-1, which thereby inhibits the cell surface shedding of sundecan-1 and causes a reduced rate of cell proliferation via the action of a small ubiquitin-like modifier of Akt. The observations would therefore imply that therapeutic targeting of C4ST1, as well as inhibited cleavage of syndecan-1, may be exploited for halting progression of breast cancer. In addition, the study proposed by Maciej-Hulme provides evidence for a specific effect hyaluronidase-4 (HYAL4), which specifically degrades CS but not hyaluronan, in cancer progression. Thus, the findings documented in these two articles strongly support the role attributed to CS in cancer development and suggest that alterations in CS distribution may be a key element to consider when addressing the biology of cancer and the search for novel diagnostic and therapeutic targets.

A perineuronal net is a layer of a lattice-like matrix enwrapping the surface of the soma and dendrites of neurons of the CNS. The perineuronal nets are mainly composed of CS-bearing PGs, which uniquely comprehend an array of aggrecan isoforms, hyaluronan, link proteins (HAPLNs), and tenascin-R. The contribution by Nojima et al., provides evidence that, at the calyx of Held synapses, HAPLN4 favors the perineuronal localization of brevican, but not that of aggrecan. Hence, the findings suggest that distinct HALPNs may regulate the localization of specific CS-bearing PGs, such as to finetune the formation and ultimate composition of neuronal class-specific perineuronal nets.

The work of Sakamoto et al. provides challenging inputs into the molecular mechanism by which CS influences the formation of dystrophic endbulbs, which are swollen axonal tips with multiple vacuoles. Upon injury in the CNS, CS-bearing PGs upregulated by the reactive astrocytes bind to receptor protein tyrosine phosphatase sigma (RTPTσ) to dephosphorylate cortactin, which then stabilizes actin microfilaments to facilitate lysosome autophagy. This finding may provide a novel view on therapeutic strategies to adopt for inducing axonal regeneration. As a corollary, Hayes and Melrose comprehensively review the function of a variety of neuronal CS/DS-PGs in the formation and morphogenesis of the CNS, by

also discussing the cell-surface ligands and putative receptors for CS-PGs, such as RTPTσ, contactin-1, semaphorins, and Nogo.

The study provided by Noborn et al., describes the recent advances in defining the CS glycoproteome using reversed phase nano-liquid chromatography-tandem mass spectrometry (nLC-MS/MS) to enabled the discovery of novel CS-PGs. This contribution provides further evidence of the complexity of CS/DSs and further emphasizes the powerfulness of mass spectrometric approaches to harness the dissection of this complexity.

Quantitative determination of the expression levels glycosyltransferases, sulfotransferases, and epimerases responsible for the biosynthesis of GAGs bound to PGs may provide valuable information on the resulting overall abundance of GAGs that may be bound to their partner PGs, as well as on the degree and variability of the sulfation patterns of these moieties. Huang et al., report the application potential of a recently developed, comprehensive glycosylation mapping tool based on gene expression profiles from RNA-seq data, GlycoMaple, designed to enable the visualization and assessment of glycan structures (Huang et al., 2021). The authors also demonstrate that the expression levels of genes encoding constituents of the CS/DS biosynthetic pathways that were established though the tool for normal brain, pancreatic tumors and breast cancer were consistent with those previously published through biochemical means. These findings suggest that new insight into GAG profiles may be gathered for various human diseases through the use of the GlycoMaple software tool, provided that the supportive RNAseq data is available.

Finally, Zhang and Chi provided a very informative review the known CS/DS-protein interaction that may take place in different disease conditions, including tumor growth and metastasis formation, nerve tissue repair, virus infection, and atherosclerosis. They also describe the analytical tools that may be employed for the characterization of these interactions.

Conclusively, we hope that the collection of articles embodied in this special issue will be useful for researchers of the field and scientists of other fields who may appreciate acquiring information about the biological and pathological importance of CS and DS, as well as the PGs carrying such GAGs. We are particularly thankful to all authors of these interesting and stimulating articles and would also like to acknowledge the splendid work of the Editorial and Editorial Staff in compiling the Topic Issue.

## AUTHOR CONTRIBUTIONS

SM prepared the draft of the manuscript, while JK, JW, FL, and RP provided the revision.

## REFERENCES


Couchman, J. R., Caterson, B., Christner, J. E., and Baker, J. R. (1984). Mapping by Monoclonal Antibody Detection of Glycosaminoglycans in Connective Tissues. *Nature* 307, 650–652. doi:10.1038/307650a0

Dodgson, K. S., and Lloyd, A. G. (1958). The Degradation of Cartilage Chrondroitin Sulphate by the Chondroitinase of Proteus Vulgaris. *Biochem. J.* 68, 88–94. doi:10.1042/bj0680088

Fischer, G., and Boedeker, C. (1861). Künstliche Bildung von Zucker aus Knorpel (Chondrogen), und über die Umsetzung des genossenen Knorpels im menschlichen Körper. *Ann. Chem. Pharm.* 117, 111–118. doi:10.1002/jlac.18611170109

Huang, Y.-F., Aoki, K., Akase, S., Ishihara, M., Liu, Y.-S., Yang, G., et al. (2021). Global Mapping of Glycosylation Pathways in Human-Derived Cells. *Dev. Cell* 56, 1195–1209. doi:10.1016/j.devcel.2021.02.023

Levene, P. A., and La Forge, F. B. (1913). On Chondroitin Sulphuric Acid. *J. Biol. Chem.* 15, 69–79. doi:10.1016/s0021-9258(18)88542-8

Lindahl, U., and Rodén, L. (1966). The Chondroitin 4-Sulfate-Protein Linkage. *J. Biol. Chem.* 241, 2113–2119. doi:10.1016/s0021-9258(18)96674-3

Mathews, M. B., and Lozaityte, I. (1958). Sodium Chondroitin Sulfate-Protein Complexes of Cartilage. I. Molecular Weight and Shape. *Archives Biochem. Biophysics* 74, 158–174. doi:10.1016/0003-9861(58)90210-8

Meyer, K., and Chaffee, E. (1941). The Mucopolysaccharides of Skin. *J. Biol. Chem.* 138, 491–499. doi:10.1016/s0021-9258(18)51374-0

Purushothaman, A., Sugahara, K., and Faissner, A. (2012). Chondroitin Sulfate "wobble Motifs" Modulate Maintenance and Differentiation of Neural Stem Cells and Their Progeny. *J. Biol. Chem.* 287, 2935–2942. doi:10.1074/jbc.R111.298430

Sorrell, J. M., Mahmoodian, F., Schafer, I. A., Davis, B., and Caterson, B. (1990). Identification of Monoclonal Antibodies that Recognize Novel Epitopes in Native Chondroitin/dermatan Sulfate Glycosaminoglycan Chains: Their Use in Mapping Functionally Distinct Domains of Human Skin. *J. Histochem Cytochem.* 38, 393–402. doi:10.1177/38.3.1689338


**Conflict of Interest:** The authors declare that the research was conducted in the absence of any commercial or financial relationships that could be construed as a potential conflict of interest.

frontiers in Cell and Developmental Biology

ORIGINAL RESEARCH
published: 25 May 2021
doi: 10.3389/fcell.2021.659428

# Cleavage of Syndecan-1 Promotes the Proliferation of the Basal-Like Breast Cancer Cell Line BT-549 Via Akt SUMOylation

*Satomi Nadanaka, Yaqiang Bai and Hiroshi Kitagawa**

*Laboratory of Biochemistry, Kobe Pharmaceutical University, Kobe, Japan*

OPEN ACCESS

**Edited by:**
*Shuji Mizumoto,*
*Meijo University, Japan*

**Reviewed by:**
*Pyong Woo Park,*
*Boston Children's Hospital and Harvard Medical School, United States*
*Mette Ørskov Agerbaek,*
*University of Copenhagen, Denmark*

***Correspondence:**
*Hiroshi Kitagawa*
*kitagawa@kobepharma-u.ac.jp*

**Specialty section:**
*This article was submitted to Signaling, a section of the journal Frontiers in Cell and Developmental Biology*

**Received:** *27 January 2021*
**Accepted:** *20 April 2021*
**Published:** *25 May 2021*

**Citation:**
*Nadanaka S, Bai Y and Kitagawa H (2021) Cleavage of Syndecan-1 Promotes the Proliferation of the Basal-Like Breast Cancer Cell Line BT-549 Via Akt SUMOylation. Front. Cell Dev. Biol. 9:659428. doi: 10.3389/fcell.2021.659428*

Basal-like breast cancer is characterized by an aggressive clinical outcome and presence of metastasis, for which effective therapies are unavailable. We have previously shown that chondroitin 4-*O*-sulfotransferase-1 (C4ST-1) controls the invasive properties of the basal-like breast cancer cell line BT-549 by inducing matrix metalloproteinase (MMP) expression through the N-cadherin/β-catenin pathway. Here we report that C4ST-1 controls the proliferation of BT-549 cells via the MMP-dependent cleavage of syndecan-1. Syndecan-1 is a membrane-bound proteoglycan associated with an aggressive phenotype and poor prognosis in breast cancer. In addition, the cleavage of syndecan-1 at a specific juxtamembrane cleavage site is implicated in the pathophysiological response in breast cancer. Knockout of C4ST-1 remarkably suppressed both the cleavage of syndecan-1 and proliferation of BT-549 cells. Kinases (AKT1, ERK1/2, PI3K, and STAT3) comprising cancer proliferative pathways are phosphorylated in C4ST-1 knockout cells at a level similar to that in parental BT-549 cells, whereas levels of phosphorylated S6 kinase and SUMOylated AKT (hyperactivated AKT observed in breast cancer) decreased in C4ST-1 knockout cells. An MMP inhibitor, GM6001, suppressed the small ubiquitin-like modifier (SUMO) modification of AKT, suggesting that cleavage of syndecan-1 by MMPs is involved in the SUMO modification of AKT. Forced expression of the cytoplasmic domain of syndecan-1, which is generated by MMP-dependent cleavage, increased the SUMO modification of AKT and global protein SUMOylation. Furthermore, syndecan-1 C-terminal domain-expressing BT-549 cells were more proliferative and sensitive to a potent SUMOylation inhibitor, tannic acid, compared with BT-549 cells transfected with an empty expression vector. These findings assign new functions to the C-terminal fragment of syndecan-1 generated by MMP-dependent proteolysis, thereby broadening our understanding of their physiological importance and implying that the therapeutic inhibition of syndecan-1 cleavage could affect the progression of basal-like breast cancer.

**Keywords: proteoglycan, chondroitin sulfate, breast cancer, syndecan-1, SUMOylation**

## INTRODUCTION

Chondroitin sulfate (CS), a glycosaminoglycan (GAG), is present on the cell surface and in the extracellular matrix (Sugahara et al., 2003). There is ample evidence for the pro-tumorigenic role of CS in the enhancement of cell proliferation, cell motility, and metastasis. CS is a linear sulfated polymer consisting of repeating disaccharide units of glucuronic acid (GlcUA) and *N*-acetylgalactosamine (GalNAc) [-GlcUA-GalNAc-]$_n$. During the synthesis of the CS backbone, various sulfotransferases catalyze sulfation. Chondroitin-4-*O*-sulfotransferase (C4ST-1) is involved in the biosynthesis of A-units [GlcUA-GalNAc(4-*O*-sulfate)] and E-disaccharide units [GlcUA-GalNAc(4,6-*O*-disulfates)] (Nadanaka et al., 2008; Mikami and Kitagawa, 2013; Nadanaka et al., 2020). Specific sulfation patterns are believed to underlie the distinct functional roles of CS not only under physiological conditions but also in tumor development and progression (Nadanaka et al., 2018).

Previously, C4ST-1 (Gene symbol: CHST11) was shown to be upregulated in breast cancer cells (Iida et al., 2015). In addition, the gene expression of *C4ST-1* has been correlated with the progression of breast cancer (Hazan et al., 2000). Most recently, Behrens et al. (2020) reported a new role of C4ST-1 in the induction of epithelial–mesenchymal transition and stem cell-like properties in breast cancer. These aggressive tumor phenotypes are thought to be exerted via protein–sugar interactions that are defined by specific sulfation patterns generated by C4ST-1. A few binding partners of CS produced by C4ST-1 have been identified. CS produced by C4ST-1 functions as a P-selectin ligand in aggressive breast cancer cells (Cooney et al., 2011). In addition, we have previously reported that the binding of CS produced by C4ST-1 to N-cadherin triggers endocytosis-dependent activation of the N-cadherin/β-catenin pathway to enhance the metastatic properties of the basal-like breast cancer cell line BT-549 (Nadanaka et al., 2018). However, the molecular mechanism underlying the tumor-promoting functions induced by C4ST-1 is not completely understood.

We have shown that CS produced by C4ST-1 induces the expression of matrix metalloproteinase 9 (MMP9) through the activation of the N-cadherin/β-catenin pathway (Nadanaka et al., 2018). Binding of C4ST-1-synthesized CS to N-cadherin triggers endocytosis and proteolysis of N-cadherin. Further, the C-terminal domain of N-cadherin forms a complex with β-catenin is released and translocates into the nucleus, where the target genes such as MMP9 are transcriptionally induced by β-catenin. Increased expression of MMP9 enhances invasion activity of BT-549 cells. In contrast, C4ST-1 knockout decreases the β-catenin-dependent transcriptional induction of MMP9 and subsequently suppresses the enhanced invasion activity of BT-549 cells. Recently, we found that the proliferation of C4ST-1-knockout BT-549 cells was decreased compared with that of parental BT-549 cells. These results have raised the possibility that breast cancer cells acquire not only invasive properties but also proliferative capacity by taking advantage of MMP9. However, it remains unclear what substrate proteins are cleaved by MMP9 in BT-549 cells. Syndecan-1 (SDC1), a cell surface proteoglycan, is thought to serve as a promising substrate for MMPs (Manon-Jensen et al., 2013). SDC1 has been implicated in promoting breast cancer progression and is highly expressed in basal-like breast cancers (Rousseau et al., 2011; Nguyen et al., 2013; Sayyad et al., 2019). In addition, the cleavage of SDC1 by MMPs is involved in tumor invasion and proliferation (Su et al., 2008; Wang et al., 2014; Szatmari et al., 2015; Jang et al., 2020). These findings prompted us to examine whether the proliferation of BT-549 cells is controlled by the cleavage of SDC1 by MMPs. Here we examined how MMPs promote the proliferation of BT-549 cells through the proteolysis of SDC1.

## MATERIALS AND METHODS

### Cell Culture and Stable Transfection

The human breast cancer cell line BT-549 (ATCC® HTB-122™), ER-, and ERBB2-negative (triple-negative and basal B subtype) breast cancer cell lines were obtained from American Type Culture Collection (ATCC) (Lacroix and Leclercq, 2004; Kao et al., 2009). The origin of BT-549 cells is "papillary, invasive ductal carcinoma," a non-frequent type (Bambang et al., 2013). C4ST-1-knockout BT-549 cells were generated using Crispr-Cas9 genome editing system as described previously (Nadanaka et al., 2018). Both cells were cultured in RPMI 1640 supplemented with 10% heat-inactivated fetal bovine serum (FBS), 100 units/mL penicillin, 100 μg/mL streptomycin, and 1% L-glutamine. The expression plasmids [p3xFLAG-CMV-14, p3xFLAG-CMV-14-hSDC1 (full-length), and p3xFLAG-CMV-14-hSDC1 (Δ 29–245)] were transfected into BT-549 cells using Lipofectamine 3000 (Invitrogen) according to the manufacturer's instructions. Transfectants were cultured in the presence of 25 μg/mL G418. Colonies surviving in the presence of 25 μg/mL G418 were collected and propagated for further experiments.

### Plasmid Construction

The human syndecan-1 (SDC1) gene (NM_001006946) was obtained from a HeLa cDNA library by polymerase chain reaction (PCR) using the following primers.

Forward primer for the amplification of full-length SDC1:

5′-CCATCGATGCCACC**ATG**AGGC-3′ (underline, *Cla*I site; bold, start codon).

Reverse primer for the amplification of full-length SDC1:

5′-GCTCTAGAGGCATAGAATTCCTCCTGTTTG-3′ (underline, *Xba*I site).

p3xFLAG-CMV-14-hSDC1 was constructed by inserting the *Cla*I-*Xba*I fragments of a PCR product into the *Cla*I and *Xba*I sites of p3xFLAG-CMV-14 (#E4901, Sigma-Aldrich, St. Louis, MO). An expression vector of the C-terminal fragment of SDC1, p3xFLAG-CMV-14-hSDC1 (CTF), was constructed by site-directed deletion mutagenesis by inverse PCR using the following primers and KOD One DNA polymerase (TOYOBO, Osaka, Japan). The human SDC1 core protein contains MMPs cleavage sites (Gly$^{82}$ – Leu$^{83}$, Glu$^{236}$ – Gln$^{237}$, and Gly$^{245}$ – Leu$^{246}$) (Manon-Jensen et al., 2013) and a transmembrane region

($Val^{252}$ – $Tyr^{276}$). Thus, the C-terminal fragment of SDC1 generated by MMPs ($Leu^{246}$ – $Tyr^{309}$) was expressed by fusing to the N-terminal region, including a signal peptide ($Met^{1}$ – $Leu^{28}$).

Forward primer for mutagenesis:

5′-CTCACAGGGCCTCCTGGACAGGAAAG-3′

Reverse primer for mutagenesis:

5′-ATTAGTAGCCACAATTTGCGGCAGGGC-3′

An expression vector of the N-terminal fragment of SDC1, p3xFLAG-CMV-14-hSDC1 (NTF), was constructed by site-directed deletion mutagenesis by inverse PCR using the following primers and KOD One DNA polymerase (TOYOBO, Osaka, Japan).

Forward primer for mutagenesis:

5′-ACTAGAGGATCCCGGGCTGAC-3′

Reverse primer for mutagenesis:

5′-GCCGGTGGGTTCTGGAGACG-3′

Integrity of the resulting plasmids was confirmed by sequencing the entire coding region and the ligation joints.

## Proliferation Assay

Cells were plated on 24-well plates at 5,000 cells/well and cultured for 3 days in the presence or absence of 5 munits/well of chondroitinase ABC (Chase ABC) (Seikagaku Biobusinesses, Tokyo, Japan) or 20 μM GM6001 (MMP inhibitor, #BML-EI300-0001, Enzo, Famingdale, NY, United States). To achieve exhaustive digestion of cellular CS chains, cells were digested in the serum-free media ASF Medium 104 (Ajinomoto Co., Inc., Tokyo, Japan) for 4 days, and 5 munits/well of chondroitinase ABC was added twice at 0 and 2 days. Anti-chondroitin sulfate antibody (clone 2B6) (#PRPG-BC-M02, Cosmo Bio Co., Ltd., Tokyo, Japan) was used to confirm chondroitinase ABC activity. After the cells were washed with phosphate-buffered saline (PBS), cellular lactate dehydrogenase was released from cells by adding 200 μL of lysis buffer containing 0.18% (w/v) Triton X-100. The enzyme activity of cellular lactate dehydrogenase was measured as an indicator of cell viability using the CytoTox-ONE$^{TM}$ Homogeneous Membrane Integrity Assay (Promega, Madison, WI, United States). To examine the proliferative pathways of BT-549 cells, GSK690693 (AKT inhibitor, #S1113, Selleck Chemicals, Houston, TX, United States) and tannic acid (SUMOylation inhibitor, #403040, Sigma-Aldrich, St. Louis, MO, United States) were used at indicated concentrations.

For determining the growth curve, cells were seeded on a 6-cm dish at a concentration of $2 \times 10^4$ cells/dish and cultured for 0, 1, 2, 4, 6, 8, 10, 13, and 15 days. The cells were harvested, stained with crystal violet-citric acid staining solution, and counted using a hemocytometer.

## Clonogenic Assay

Clonogenic assay was performed according to a method described previously (Kawamura et al., 2013). In brief, BT-549 cells were trypsinized to obtain single cell suspensions and seeded at a density of 50 cells/well in 6-well plates. The cells were then cultured for 9 days, fixed, and stained with crystal violet. Colonies consisting of more than 50 cells were counted.

## Flow Cytometry

Cells ($1 \times 10^5$ cells) treated with or without 25 μM GM6001 for 4 days were fixed with PBS containing 4% paraformaldehyde on ice for 30 min. After washing with PBS, the cells were incubated with PBS containing 2% BSA on ice for 30 min, and then stained with the anti-SDC1 antibody (dilution ratio 1:200) (HPA006185, Sigma-Aldrich) on ice. After 2 h, the cells were washed and incubated with rabbit IgG antibody conjugated with Alexa 488 (dilution ratio 1:200) on ice for 1 h. The cells were analyzed using a BD Accuri$^{TM}$ C6 flow cytometer (BD Biosciences, San Jose, CA, United States).

## Immunoblotting

For detecting the MMP-dependent cleavage of SDC1, the cells were cultured in the presence or absence of 25μM GM6001 for 4 days. The medium conditioned for 4 days by the cells was collected and centrifuged at 13,000 rpm for 10 min. Supernatants were incubated with 10 μL of protein G-Sepharose beads for 2 h at 4°C to remove serum immunoglobulin. After centrifugation at 4,000 rpm for 2 min, the resulting supernatants were subject to immunoblotting. The cells were washed with PBS and solubilized with M-PER (Thermo Fisher Scientific, Waltham, MA, United States) containing a protease inhibitor cocktail (Nacalai Tesque, Kyoto, Japan) for 30 min on ice. Cell lysates were centrifuged at 13,500 rpm for 10 min, and the resulting supernatants were analyzed by immunoblotting. For detecting SDC1, the supernatants were digested with or without 0.5 munits of heparitinase (HSase), 0.5 munits of heparinase (Hepase), and 1 munits of Chase ABC for 30 min at 37°C. All these glycosaminoglycan lyases (GAGase) were purchased from Seikagaku Biobusinesses (Tokyo, Japan).

For analysis of signaling pathways, the cells were solubilized with lysis buffer [1% Triton X-100, 20 mM Tris-HCl (pH 7.5), 0.15 M NaCl, 1 mM EDTA, 10% glycerol, 10 μM MG132, protease and phosphatase inhibitor cocktail (Nacalai Tesque, Kyoto, Japan)] for 30 min on ice. The protein concentration of each sample was determined by Pierce$^{TM}$ BCA Protein Assay Kit (Thermo Fisher Scientific).

To detect the SUMOylated AKT, the cells were solubilized with M-PER (10 μM MG132, protease and a phosphatase inhibitor cocktail, and 4 mM *N*-ethylmaleimide) for 30 min on ice, and cell lysates were centrifuged at 13,000 rpm for 10 min. Supernatants were incubated with anti-phospho-AKT (Ser473) antibody (dilution ratio 1:500) (#9271, Cell Signaling Technology, Danvers, MA) or anti-AKT antibody (dilution ratio 1:500) (#9272, Cell Signaling Technology, Danvers, MA) at 4°C overnight. After adding 10 μL of Protein G-Sepharose, each sample was incubated for 2 h at 4°C. The Protein G-Sepharose beads recovered by centrifugation were washed with lysis buffer.

To analyze the SUMOylated proteins, SUMO-QAPTURE-T® kit (#BML-UW1000A, Enzo Famingdale, NY, United States) was used. Each sample was resolved on Bullet PAGE One precast gels (5–15%), transferred to polyvinylidene fluoride membranes,

and incubated overnight with the antibodies mentioned in **Supplementary Table 1**.

## Knockdown of MMP2, 7, 9, and 14 by siRNA

Cells were transfected with the following siRNAs corresponding to MMP2, MMP7, MMP9, and MMP14. Silencer® Select siMMP2 (Cat. #4427038, Assay ID: s8852), siMMP7 (Cat. #4427037, Assay ID: s8858), siMMP14 (Cat. #4427038, Assay ID: s8878), and MMP9 siRNA (Cat. # sc-29400) were purchased from Thermo Fisher Scientific and Santa Cruz Biotechnology, Inc., respectively. Cells were transfected with 5 nM siRNA(MMP2, MMP7, and MMP14) or 25 nM (MMP9) using Lipofectamine 2000 (Thermo Fisher Scientific) according to the manufacturer's protocol and cultured for 2 days. Each siRNA-induced gene knockdown was assessed by real-time PCR.

Total RNA was isolated from the cells using the Maxwell® 16 LEV simplyRNA purification kit (Promega). For reverse transcription, 1 μg of total RNA was treated with Moloney murine leukemia virus reverse transcriptase (Invitrogen) using random primers [non-adeoxyribonucleotide mixture; $pd(N)_9$] (Takara Bio Inc., Shiga, Japan). Quantitative real-time PCR was performed using FastStart DNA Master Plus SYBR Green I in LightCycler® 96 (Roche Applied Science) according to the manufacturer's protocols. The housekeeping gene *G3PDH* was used as an internal control for quantification. The primers used for real-time PCR are mentioned in **Supplementary Table 2**.

## Statistics and Reproducibility

Data are expressed as the mean ± standard deviation of the mean. Statistical significance was determined using the Tukey–Kramer multiple comparison method and Student's *t*-test. Statistical analyses were performed using KaleidaGraph version 4.5.1. For all analyses, $n$ = number of experiments and differences were considered statistically significant at a $p$-value of $<0.05$. All experiments were reproduced with similar results a minimum of three times, and the exact number of repetitions is provided in the figure legends.

# RESULTS

## Deficiency for C4ST-1 Suppresses the Proliferation of BT-549 Cells

The cell growth curve was plotted to compare the time-dependent increase in cell number between *C4ST-1* knockout cells (C4ST-1 KO cells) and parental BT-549 cells (**Figure 1A**). In addition, cell growth of these two cell lines was measured using the CytoTox-ONE™ cell growth assay kit (**Figure 1B**). Furthermore, the ability of cells in culture to grow and divide into groups was assessed by the colony formation assay (**Figure 1C**). These results indicate that cell growth was remarkably suppressed by the loss of *C4ST-1* expression. We next examined the expression of *cyclin D1*, which has been reported as the target of β-catenin because a previous study showed that C4ST-1 upregulates β-catenin-dependent transcriptional activities (Nadanaka et al., 2018). Deficiency of C4ST-1 significantly decreased the expression of *cyclin D1* in C4ST-1 KO cells than in parental BT-549 cells (**Figure 1D**). We examined the effect of CS removal by digestion with Chase ABC on the proliferation of these two cell lines (**Figure 1E**). The proliferation of BT-549 cells was significantly attenuated by digestion with Chase ABC. The effect of Chase ABC on cellular CS chains was confirmed using anti-CS antibody (clone 2B6), which recognizes unsaturated disaccharide neoepitopes generated after the digestion of CS chains by Chase ABC (**Figure 1F**). We next investigated whether MMPs are involved in the proliferation of BT-549 cells (**Figure 1G**) because the loss of *C4ST-1* expression decreases the expression of *MMP9*, which is a target gene of β-catenin (Nadanaka et al., 2018). The proliferation of BT-549 cells was significantly inhibited by treatment with GM6001 (an MMP inhibitor), whereas C4ST-1 KO cells were not affected. These results suggest that MMPs play an important role in C4ST-1-dependent proliferation of BT-549 cells.

## Loss of *C4ST-1* Expression Suppresses the MMP-Mediated Cleavage of SDC1

As shown in **Figure 2A**, SDC1 is a hybrid-type transmembrane proteoglycan that consists of both CS and heparan sulfate chains. MMP cleavage sites and the HS ($Ser^{37}$, $Ser^{45}$, and $Ser^{47}$) and CS attachment sites ($Ser^{206}$ and $Ser^{216}$) on SDC1 have been reported in a previous study (Manon-Jensen et al., 2013). These MMP cleavage sites and HS/CS attachment sites are shown in **Figure 2A**. Full-length SDC1 core proteins were detected in the cell lysates after digestion in combination with Chase ABC, HSase, and Hepase (**Figure 2B**, arrow). It is estimated that the SDC1 fragments generated by MMPs provide a band of approximately 32.5 kDa because the anti-SDC1 antibody developed against amino acids 139–237 was used in this study (**Figure 2A**). The approximately 32.5 kDa band was detected in the BT-549 cell-conditioned medium digested with and without Chase ABC (**Figure 2B**, open triangle), suggesting that $Ser^{206}$ and $Ser^{216}$ are not modified with CS chains in BT-549 cells. Our previous study showed that CS chains are attached to a SDC1 core protein (Nadanaka et al., 2018), suggesting that $Ser^{37}$, $Ser^{45}$, or $Ser^{47}$ can be modified with CS chains. This 32.5 kDa band disappeared after treating BT-549 cells with GM6001. These results suggest that the MMP-mediated proteolysis of SDC1 occurs in BT-549 cells. On the other hand, the cleavage of SDC1 by MMPs was strongly inhibited in C4ST-1 KO cells, suggesting that C4ST-1 controls MMP-mediated cleavage of SDC1.

We next compared the surface expression of SDC1 among BT-549 cells, GM6001-treated BT-549 cells, and C4ST-1 KO cells (**Figure 2C**). Consistent with the results shown in **Figure 2B**, the surface expression of SDC1 in C4ST-1 KO cells was higher than that in BT-549 cells. In addition, treatment of BT-549 cells with GM6001 increased the surface expression of SDC1.

A previous study reported that MMP2, MMP7, MMP9, and MMP14 are involved in the proteolysis of SDC1 (Manon-Jensen et al., 2013). In addition, all these MMPs are transcriptionally regulated by β-catenin. Thus, we confirmed that these MMPs are implicated in the cleavage of SDC1. We first compared the

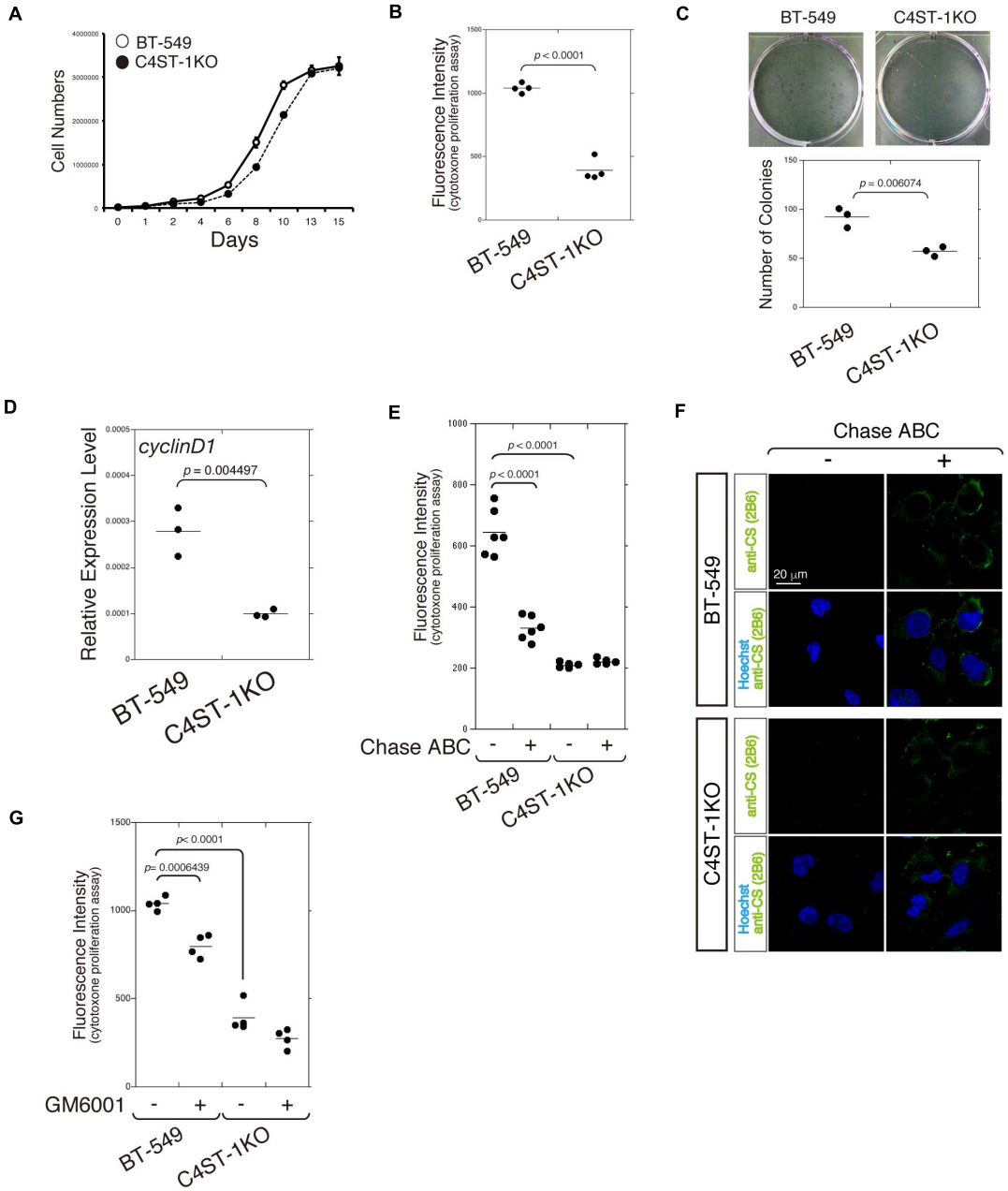


**FIGURE 1 |** C4ST-1 deficiency suppresses the proliferation of BT-549 cells. **(A)** Growth curves of parental BT-549 and C4ST-1 KO cells. **(B)** Proliferation of BT-549 ($n$ = 4) and C4ST-1 KO cells ($n$ = 4) was measured by CytoTox-ONE$^{TM}$ Assay. **(C)** Proliferation of BT-549 and C4ST-1 KO cells was examined by colony formation assay. Both the cell types were seeded at a concentration of 50 cells/well in 6-well plate and cultured for 9 days. The colonies were stained with crystal violet, and observed under a light microscope (Left). The number of colonies of BT-549 ($n$ = 3) and C4ST-1 KO cells ($n$ = 3) was compared (Right). **(D)** The level of cyclin D1 in BT-549 and C4ST-1 KO cells was measured by real-time PCR ($n$ = 3 each). **(E)** Proliferation of BT-549 ($n$ = 4) and C4ST-1 KO cells ($n$ = 4) treated with or without Chase ABC was examined by CytoTox-ONE$^{TM}$ Assay. Cells were digested in the serum-free medium ASF Medium 104 for 4 days by adding 5 munits/well of Chase ABC twice at 0 and 2 days. **(F)** Cells digested with or without Chase ABC were stained by anti-CS antibody (clone 2B6), which detects the terminal unsaturated disaccharide of CS chains generated by Chase ABC. **(G)** Proliferation of BT-549 ($n$ = 4) and C4ST-1 KO cells ($n$ = 4) treated with or without GM6001 was measured. Statistical significance was determined using Student's $t$-test. Statistical analyses were performed using KaleidaGraph version 4.5.1.

expression level of MMP2, MMP9, and MMP14 between BT-549 and C4ST-1KO cells (**Figure 2D**). The expression levels of three MMPs were significantly lower in C4ST-1KO cells than in BT-549 cells. Knockdown of each MMP suppressed the cleavage of SDC1 (**Figures 2E,F**) and attenuated the proliferation of BT-549 cells (**Figure 2G**). These results suggest that MMP-dependent proteolysis of SDC1 is associated with the proliferation of BT-549 cells. Furthermore, knockdown of β-catenin had a

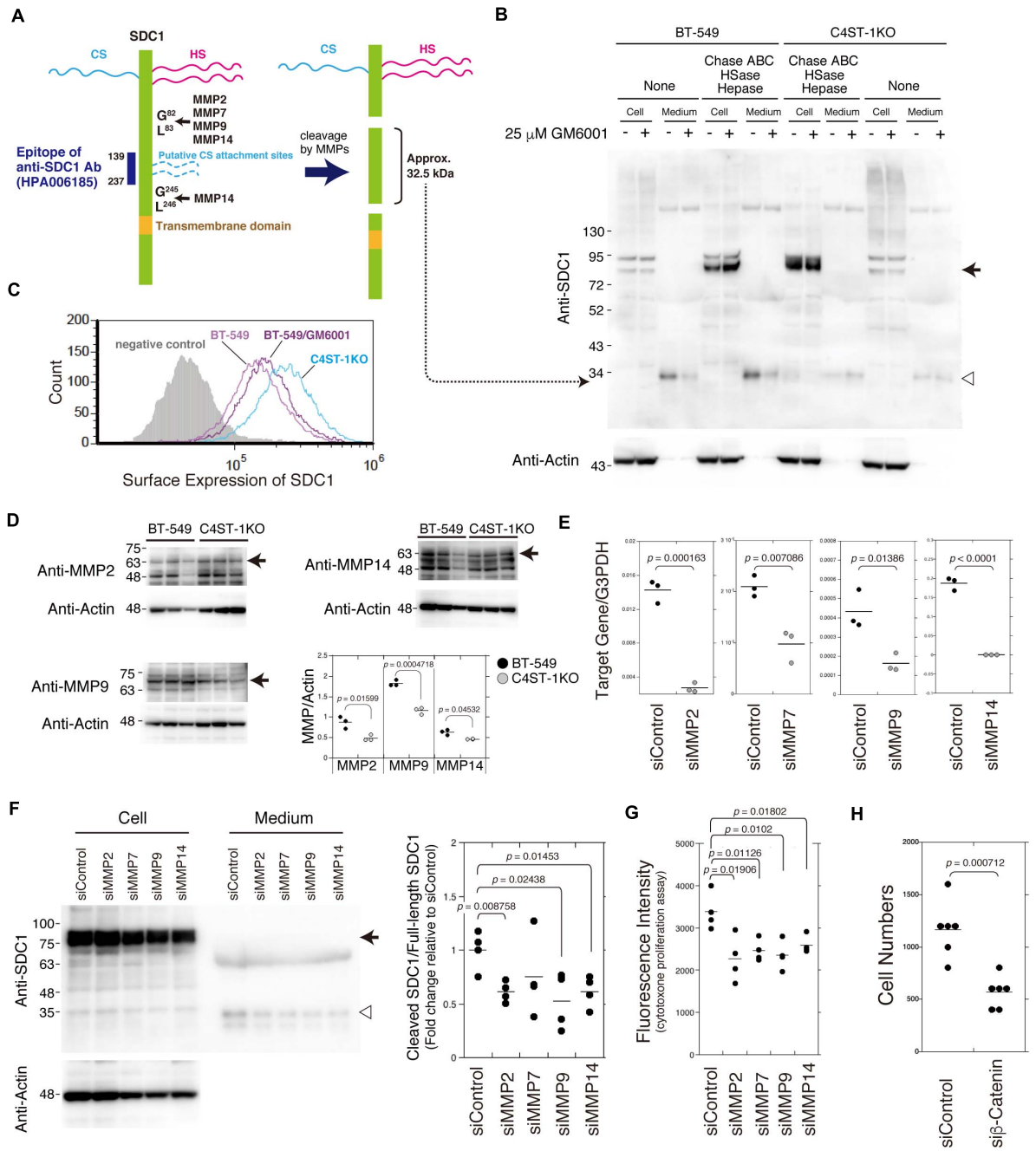


**FIGURE 2 |** Inhibition of the cleavage of SDC1 by loss of *C4ST-1* expression. **(A)** Schematic representation of the cleavage sites of MMPs, HS/CS attachment sites on SDC1, and the epitope of the anti-SDC1 antibody used in this study. CS chains are indicated by dashed lines because $Ser^{206}$ and $Ser^{216}$ are not modified with CS chains in BT-549 cells. In addition, CS chains are attached to $Ser^{37}$, $Ser^{45}$, or $Ser^{47}$, because a SDC1 core protein is modified with CS chains according to our previous study (Nadanaka et al., 2018). Anti-SDC1 antibody used in this study recognizes the SDC1 fragment (approx. 32.5 kDa) after cleavage by MMPs. **(B)** BT-549 and C4ST-1 KO cells were incubated in the presence (+) or absence (–) of GM6001. Cell lysates and conditioned medium prepared from each cell were treated with (+) or without (–) Chase ABC, HSase, and Hepase, and then subject to immunoblotting using the anti-SDC1 antibody. Arrow and open triangle indicate the core protein of full-length SDC1 and the SDC1 fragment after cleavage by MMPs, respectively. **(C)** The surface expression of SDC1 in BT-549 and BT-549 treated with GM6001, and C4ST-1KO cells were examined by flow cytometry. **(D)** The expression level of MMP2, MMP9, and MMP14 in BT-549 and C4ST-1KO cells was examined by immunoblotting. **(E)** The levels of MMP2, MMP7, MMP9, and MMP14 in BT-549 cells transfected either with si-Control or si-MMP2, 7, 9, or 14 were measured by real-time PCR. **(F)** The effect of knockdown of MMP2, 7, 9, or 14 on the cleavage of SDC1 was examined. Arrow and open triangle indicate the core protein of full-length SDC1 and the SDC1 fragment after cleavage by MMPs, respectively. At the right side, the ratio of cleaved SDC1 to full-length SDC1 is shown as fold change relative to that of siControl. **(G)** The effect of knockdown of MMP2, MMP7, MMP9, and MMP14 on the proliferation of BT-549 cells ($n$ = 4, each) was examined by CytoTox-ONE$^{TM}$ Assay. **(H)** The effect of knockdown of β-catenin on the proliferation of BT-549 cells ($n$ = 6) was investigated. Statistical significance was determined using Student's $t$-test.

stronger effect on the proliferation of BT-549 cells (**Figure 2H**), implying that these four MMPs act on the cleavage of SDC1 in various combinations.

## Knockout of *C4ST-1* Downregulates the Proliferation of BT-549 Cells Via SUMOylation of AKT

Several signaling pathways involved in the proliferation and survival of breast cancer cells are illustrated in **Figure 3A**. We examined the activation of the key oncogenic protein kinases (PI3K, AKT1, ERK1/2, and STAT3) of each signaling pathway in BT-549 and C4ST-1 KO cells (**Figures 3B,C**). The phosphorylation levels of PI3K, AKT, ERK, and STAT3 were not affected by the loss of *C4ST-1* expression. The activation of the AKT downstream kinase, S6 kinase (S6K), was inhibited in C4ST-1 KO cells (**Figures 3B,C**). AKT is post-translationally modified by phosphorylation as well as the small ubiquitin-like modifier (SUMO) protein. SUMO modification regulates AKT activity and cell proliferation, and cancer progression is enhanced via the SUMOylation-mediated signaling pathway. Therefore, we examined whether AKT1 SUMOylation is affected by the loss of C4ST-1. Blockage of SUMOylation by tannic acid, an inhibitor of SUMOylation, strongly inhibited the proliferation of BT-549 and C4ST-1 KO cells at concentrations above 7.5 μM (**Figure 3D**). Of note, compared with BT-549 cells, C4ST-1 KO cells showed slight but significant resistance to 5 and 7.5 μM tannic acid. In addition, the proliferation of BT-549 cells was inhibited by the AKT inhibitor GSK690693; moreover, BT-549 cells were more resistant to GSK690693 than C4ST-1KO cells (**Figure 3D**). We next investigated the SUMO modification of AKT1 in BT-549 and C4ST-1 KO cells (**Figure 3E**). SUMO modification of phosphorylated AKT1 (pAKT1) was decreased in C4ST-1 KO cells than in BT-549 cells. In addition, treatment with GM6001 inhibited the SUMOylation of pAKT1. These results suggest that C4ST-1 regulates the SUMO modification of AKT1 mediated by MMPs. SUMOylation of AKT1 by C4ST-1 is, however, only one of many mechanisms of controlling cell proliferation in BT-549 cells because cell proliferation of C4ST-1KO cells was inhibited by tannic acid.

## C-Terminal Fragment of SDC1 Generated by MMPs Induces SUMO Modification of AKT1

We tested the possibility that the N- and C-terminal fragment of SDC1 generated by MMPs controls the proliferation of BT-549 cells through the SUMO modification of AKT1. SDC1 is degraded into the N-terminal extracellular fragment (ectodomain) and C-terminal cytoplasmic fragment by MMPs (**Figure 4A**). We established BT-549 cells stably expressing either the full-length [SDC1(FL)], the N-terminal fragment [SDC1(NTF)], or the C-terminal fragment of SDC1 tagged with FLAG [SDC1(CTF)]. Cell lysates or conditioned medium prepared from the SDC1(FL)-, SDC1(NTF)-, or SDC1(CTF)-expressing cells was analyzed by immunoblotting using the anti-FLAG antibody. SDC1(NTF) was expressed and secreted into the medium (**Figure 4B**). SDC1(NTF) and SDC1(FL) were expressed as proteoglycans bearing GAG chains. In addition, SDC1(CTF) was detected because of the proteolytic processing of SDC1(FL) (**Figure 4C**). In the SDC1(CTF)-expressing cells, the C-terminal fragment of SDC1 was detected (**Figure 4C**).

A previous study suggests that tagging the C-terminus leads to the mislocalization of SDC1 to the apical surface in polarized epithelial cells (Maday et al., 2008). Thus, we next examined the cellular localization of SDC1(FL) and SDC1(CTF) (**Figure 4D**). Two types of antibodies against SDC1 were used, and their specificities are shown in **Figure 4A**. Anti-SDC1 antibody (HPA00618) recognizes the N-terminal side of a MMP14 cleavage site ($Gly^{245}$-$Leu^{246}$), while anti-SDC1 antibody (D4YH) binds to the C-terminal side of the transmembrane region. Endogenous SDC1 was localized on the cell surface and in the perinuclear region in BT-549 cells. Localization of SDC1 in the perinuclear region was visualized clearly by anti-SDC1 antibody (D4YH) (**Figure 4D**), suggesting that the processed C-terminal fragments of SDC1 is localized in the perinuclear region. Cellular localization of exogenously expressed SDC1(FL) and SDC1(CTF) was examined using anti-FLAG antibody. SDC1(FL) was localized at the cell surface and the perinuclear region in a similar pattern to endogenous SDC1, while SDC1(CTF) was localized in the perinuclear region. Double staining with anti-SDC1 antibody and anti-FLAG antibody indicated that the localization of SDC1(FL) was barely affected by the C-terminal FLAG tag. In addition, the localization pattern of SDC1(CTF) visualized by anti-FLAG antibody was merged with the staining pattern obtained using anti-SDC1 antibody (D4Y7H).

Proliferation of BT-549 cells was significantly increased by the expression of either SDC1(FL), SDC1(NTF), or SDC1(CTF) (**Figure 4E**). Cell proliferation is more affected by the expression of SDC1(CTF) than SDC1(NTF). Thus, we examined the effect of SDC1(CTF) on cell proliferation in this study. The inhibitory effect of GM6001 treatment on proliferation was weakened by the expression of either SDC1(FL) or SDC1(CTF) (**Figure 5A**). Furthermore, cell proliferation was relatively sensitive to tannic acid due to the expression of SDC1(CTF) (**Figure 5B**). These results suggest that SUMOylation has a greater effect on growth signaling of SDC1(CTF)-expressing BT-549 cells compared with empty vector-expressing BT-549 cells. We next determined the levels of SUMOylated proteins using a commercial SUMO-QAPTURE-T kit (**Figure 5C**). The SUMOylated protein-enriched bound fraction isolated from cells expressing SDC1(CTF) contained much more AKT1 and SUMOylated proteins than the empty vector-expressing BT-549 cells. These results indicate that the C-terminal fragment of SDC1 regulates the proliferation of BT-549 cells mediated by SUMO modification of AKT1.

# DISCUSSION

## Role of MMPs in Breast Cancer

MMPs are members of the metzincin group of zinc-dependent endopeptidases that are responsible for degrading and remodeling the extracellular matrix during cancer progression. We previously showed that CS produced by C4ST-1 induces the

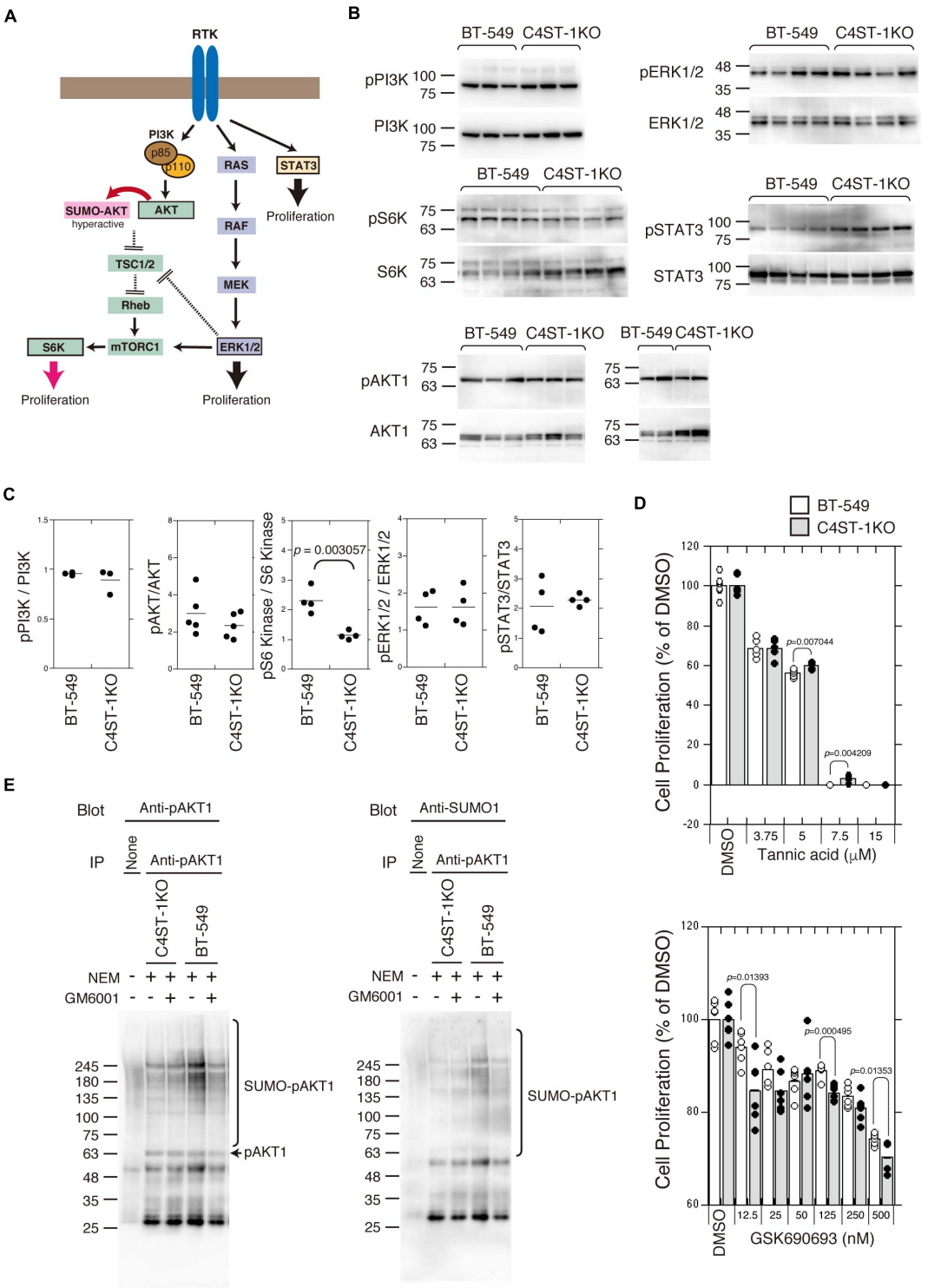


**FIGURE 3 |** Suppression of SUMOylation of AKT1 by the loss of *C4ST-1* expression. **(A)** Some of the signaling pathways involved in cancer proliferation examined in this study are shown. **(B)** Phosphorylation of PI3K, AKT1, S6K, ERK1/2, and STAT3 in BT-549 and C4ST-1 KO cells was examined by immunoblotting using phospho-specific antibodies and total antibodies. **(C)** Phosphorylation of PI3K ($n$ = 3), AKT1 ($n$ = 5), S6K ($n$ = 4), ERK1/2 ($n$ = 4), and STAT3 ($n$ = 4) in BT-549 and C4ST-1 KO cells was quantified by calculating the ratios of phosphorylated to total protein. **(D)** The effect of tannic acid and AKT inhibitor (GSK690693) on the proliferation of BT-549 and C4ST-1KO cells. **(E)** SUMOylation of AKT1 in BT-549 and C4ST-1 KO cells were examined. Both the cells were treated with (+) or without (–) GM6001, and lysed in the absence (–) or presence (+) of *N*-ethylmaleimide (NEM), which inhibits SUMO proteases. Immunoprecipitated phospho-AKT1 proteins were subject to immunoblotting using anti-pAkt1 and anti-SUMO1 antibodies.

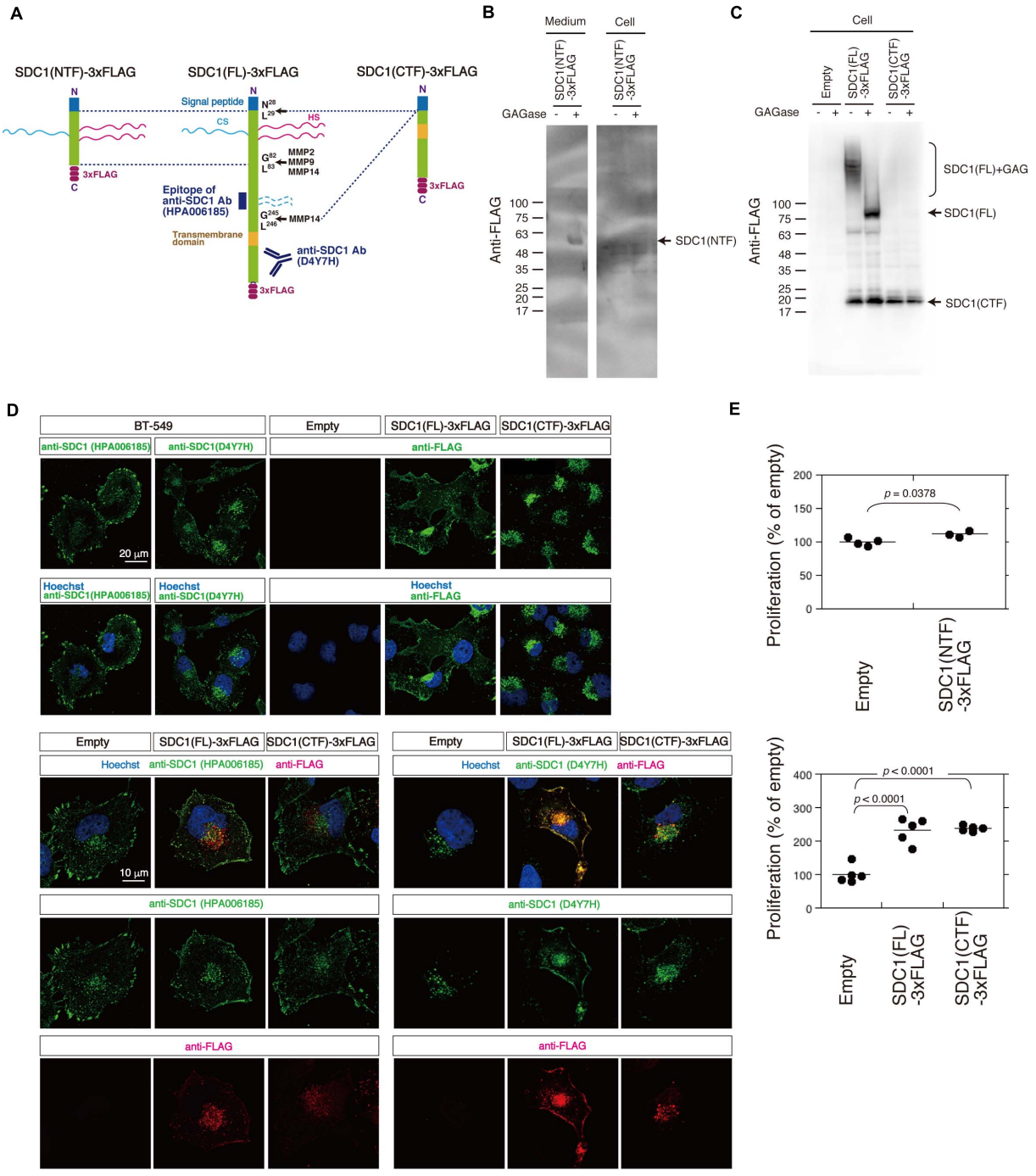


**FIGURE 4 |** Cellular localization of SDC1(FL)-3xFLAG and SDC1(CTF)-3xFLAG and the effect of SDC1 fragments on cell proliferation after cleavage of MMPs. **(A)** SDC1(FL)-3xFLAG, SDC1(NTF)-3xFLAG, and SDC1(CTF)-3xFLAG were schematically illustrated. Recognition sites of anti-SDC1 antibodies used in this study are shown. **(B)** The Expression of SDC1(NTF)-3xFLAG was confirmed by immunoblotting. Conditioned medium and cell lysate was digested with (+) or without (–) GAGase (the mixture of Chase ABC, HSase, and Hepase). SDC1(NTF)-3xFLAG was detected in medium digested with GAGase. **(C)** The expression of SDC1(FL)-3xFLAG or SDC1(CTF)-3xFLAG in stable clones of BT-549 cells overexpressing SDC1(FL)-3xFLAG and SDC1(CTF)-3xFLAG was confirmed by immunoblotting. Each cell lysate was digested with (+) or without (–) GAGase (the mixture of chondroitinase ABC, heparitinase, and heparinase). SDC1(FL)-3xFLAG modified with GAG chains is represented by "SDC1(FL) + GAG." BT-549 cells stably expressing the empty vector p3xFLAG-CMV14 is represented as "empty." **(D)** Expression pattern of exogenously expressed SDC1(FL)-3xFLAG and SDC1(CTF)-3xFLAG was compared with that of endogenous SDC1 by immunofluorescence method using anti-SDC1 antibodies (HPA00618 and D4Y7H) and anti-FLAG antibody. **(E)** Proliferation of BT-549 cells overexpressing the empty vector ($n$ = 4) and SDC1(NTF)-3xFLAG ($n$ = 3), or proliferation of BT-549 cells overexpressing the empty vector ($n$ = 5), SDC1(FL)-3xFLAG ($n$ = 5), and SDC1(CTF)-3xFLAG ($n$ = 5) was measured.

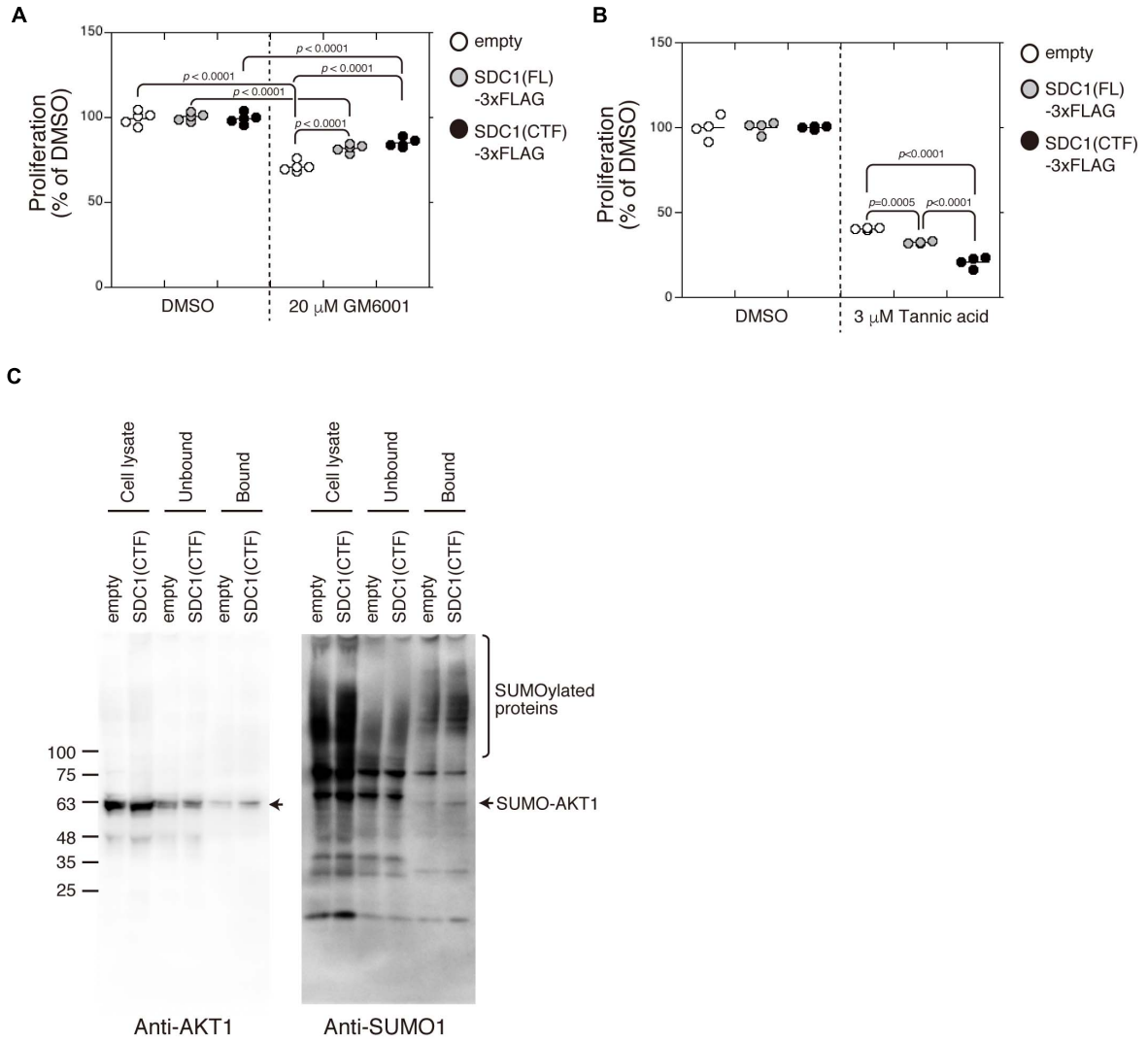


**FIGURE 5 |** Enhancement of cell proliferation through the SUMOylation of AKT1 upregulated by the expression of the C-terminal fragment of SDC1. **(A)** The effect of GM6001 on the proliferation of BT-549 cells overexpressing the empty vector ($n$ = 5), SDC1(FL)-3xFLAG ($n$ = 5), and SDC1(CTF)-3xFLAG ($n$ = 5) was examined. **(B)** The effect of tannic acid on the proliferation of BT-549 cells overexpressing the empty vector ($n$ = 4), SDC1(FL)-3xFLAG ($n$ = 4), and SDC1(CTF)-3xFLAG ($n$ = 4) was examined. **(C)** SUMOylated proteins in BT-549 cells overexpressing the empty vector and SDC1(CTF)-3xFLAG were captured using the SUMO-QAPTURE-T kit, and subject to immunoblotting using the anti-Akt1 and anti-SUMO1 antibodies.

expression of MMP9 mediated via the N-cadherin/β-catenin pathway and upregulates the invasive activity of BT-549 cells. MMP-2, MMP-9, and MMP-14, which are involved in the cleavage of SDC1, facilitate cell invasion and metastasis. In addition, these MMPs may regulate tumor proliferation by degradation of the extracellular matrix and basement membrane. MMPs can free growth factors from attachment to matrix components or the cell surface from where they can act on receptors. For example, MMP9 degrades insulin-like growth factor binding protein, which prevents insulin-like growth factor (IGF) from acting on its receptors. Thus, MMP9 can liberate active IGF and induce the activation of the IGF receptor pathway to promote tumor growth (Park et al., 2015). Graphical abstract of this study is shown in **Figure 6**. We showed that C4ST-1 deficiency could suppress cell proliferation and cleavage of SDC1 by MMPs through controlling the expression of MMPs. Although we previously showed that loss of C4ST-1 remarkably suppresses the modification of SDC1 with CS chains (Nadanaka et al., 2018), it remains unclear whether this alteration of glycosylation makes hard to cleave SDC1 using MMPs. In addition, we examined the mechanism underlying SDC1 cleavage-dependent cell proliferation. We found that the C-terminal fragment of SDC1 generated by MMPs enhanced cell proliferation through SUMOylation of AKT1. However, some issues need to be addressed. We demonstrated cell proliferation-controlling system taking advantage of SDC1 cleavage by MMPs only in a BT-549 cell line. Further studies are needed to examine whether proliferation of basal-like breast cancer cells is ubiquitously

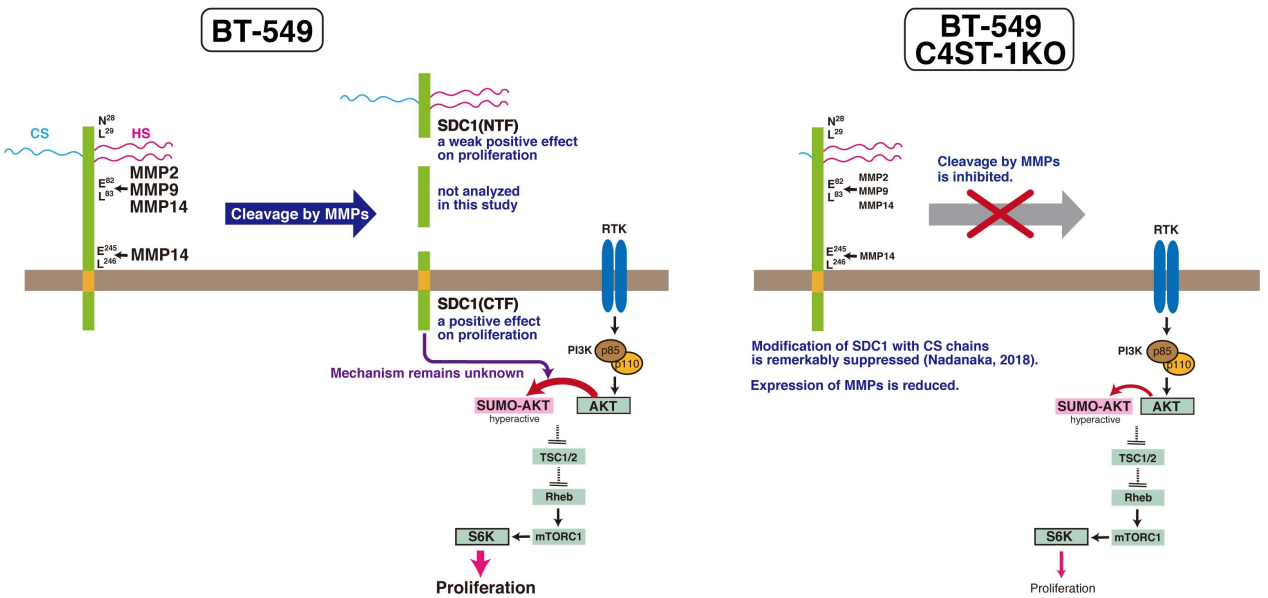


**FIGURE 6 |** C4ST-1 controls BT-549 cell proliferation by regulating the cleavage of SDC1 by MMPs. SDC1 expressed at the cell surface is cleaved by MMPs, and the N-terminal and the C-terminal fragments of SDC1 are generated. Both fragments, SDC1(NTF) and SDC1(CTF), have a positive effect on cell proliferation, and cell proliferation is more affected by SDC1(CTF) than by SDC1(NTF). SDC1(CTF) is involved in SUMOylation of AKT1, although the mechanism underlying SUMOylation by SDC1(CTF) remains unclear. SUMOylation of AKT1 enhances proliferation through S6 kinase signaling pathway. In C4ST-1KO cells, the cleavage of SDC1 by MMPs is suppressed because of reduced expression of MMPs. SUMOylation of AKT1 is inhibited because of decreased SDC1(CTF), and proliferation is slowed down.

regulated by this system. In addition, it remains unclear how the C-terminal fragment of SDC1 controls SUMOylation of AKT1.

In this study, we focused on the cleavage of SDC1 to examine the mechanism underlying C4ST-1-regulated cell proliferation. However, CS chains produced by C4ST-1 may play important roles in controlling proliferation signaling. The biological importance of specific sulfation of CS chains has been reported. A gene trap mutation of *C4ST-1* in mice causes severe chondrodysplasia associated with alterations of growth factor signaling including TGF-β signaling and BMP signaling (Klüppel et al., 2005). In addition, we have previously analyzed CS chains produced in C4ST-1KO cells (Nadanaka et al., 2018). The amount of CS chains decreased by almost half in C4ST-1KO cells compared to that in BT-549 cells. The 4-*O*-sulfated structures were decreased while the 6-*O*-sulfated structures were increased in C4ST-1KO cells, compared with BT-549 cells. Thus, we cannot exclude the possibility that decreased growth factor signaling in C4ST-1 KO cells retards cell proliferation.

The 4-*O*-sulfation of CS is catalyzed by C4ST-1, C4ST-2 (Gene symbol: CHST12), and C4ST-3 (Gene symbol: CHST13) (Mikami and Kitagawa, 2013). However, C4ST-2 and C4ST-3 cannot compensate for the loss of C4ST-1 because a deficiency or experimental knockdown of C4ST-1 results in a drastic decrease in cellular and whole-body level of CS (Klüppel et al., 2005; Uyama et al., 2006). C4ST-1 plays a distinct regulatory role not only in CS 4-*O*-sulfation but also in the amount of CS synthesis (Klüppel et al., 2005; Uyama et al., 2006). Consistent with this finding, we indicated that none of the CS chains are attached to a SDC1 core protein in C4ST-1KO cells (Nadanaka et al., 2018). Thus, it is suggested that C4ST-1 contributes greatly to the biosynthesis of CS chains involved in cell proliferation.

## Role of SDC1 Proteolysis in Tumor Progression

SDC1 is predominantly known as a cell surface proteoglycan that acts as a co-receptor for a variety of growth factor receptors. However, SDC1 is not always localized on the cell surface. It undergoes proteolytic cleavage in a process known as shedding, and releases its extracellular domain (ectodomain) and cytoplasmic domain. Ectodomain shedding reduces the number of membrane-bound type SDC1, serving as a surface receptor, thus downregulating signal transduction. The shed ectodomain contains intact HS chains, allowing the ectodomain to retain its ability to bind growth factors and other extracellular matrix components. Thus, a soluble ectodomain can compete with membrane-bound SDC1 for extracellular ligands (Steinfeld et al., 1996). Nikolova et al. (2009) showed that the overexpression of full-length SDC1 increases cell proliferation of the human breast cancer cell line MCF-7, whereas the shed ectodomain of SDC1 decreases proliferation. In addition, they indicated that the invasion of MCF-7 cells is promoted by the expression of the soluble ectodomain of SDC1. Moreover, shed SDC1 from stromal fibroblasts has been reported to be essential for breast carcinoma angiogenesis (Maeda et al., 2006) and growth of breast cancer cells was stimulated by shed SDC1 from stromal fibroblasts via the activation of FGF-2 (Su et al., 2007, 2008). Chemotherapy-induced SDC1 shedding is

mediated by disintegrin and metalloproteinases (ADAMs), and shed SDC1 promotes growth factor signaling (Ramani and Sanderson, 2014). Furthermore, SDC1 shedding correlates with the enhancement of both vascular endothelial growth factor and hepatocyte growth factor signaling and affects angiogenesis (Purushothaman et al., 2010; Ramani et al., 2011). Taken together, the shed ectodomain of SDC1 acts on cancer cells and has powerful effects on their behavior in a context-dependent manner.

Once SDC1 is shed from the cell surface by ADAM17, the remaining transmembrane C-terminal fragment undergoes intramembrane proteolysis by γ-secretase and is degraded by the proteasome in A549 lung cancer cells (Pasqualon et al., 2015a). The C-terminal transmembrane fragment mediates SDC1-dependent functions in cell proliferation, migration, invasion, and metastasis formation (Pasqualon et al., 2015b), whereas the cytoplasmic C-terminal fragment of SDC1 generated by γ-secretase inhibits SDC1-dependent tumor cell migration and invasion by increasing the phosphorylation of Src and focal adhesion kinase (Pasqualon et al., 2015a). In addition, the transmembrane C-terminal fragment does not affect the proliferation of A549 lung cancer cells in the presence of endogenous SDC1 (Pasqualon et al., 2015b). In this study, we examined the effect of the transmembrane C-terminal fragment cleaved at $Gly^{245}$-$Leu^{246}$ by MMP14 on cell proliferation. The expression of this fragment enhances the cell proliferation of BT-549 human breast cancer cells even in the presence of endogenous SDC1. This discrepancy may be explained as follows: ADAM17 cleaves at $Val^{252}$-$Leu^{253}$ of SDC1, releasing the transmembrane C-terminal fragment of SDC1 (amino acid position 253–310), whereas MMP14 produces the transmembrane C-terminal fragment of SDC1 (amino acid position 246–310). Thus, the transmembrane C-terminal fragment of SDC1 (amino acid position 246–310) may be processed in a distinct mechanism from the transmembrane C-terminal fragment of SDC1 (amino acid position 253–310). The two types of cytoplasmic C-terminal fragments of SDC1 generated in a distinct manner may have different effects on cell proliferation. Further studies are needed to explain the distinct functions of these transmembrane C-terminal fragments of SDC1.

## Significance of SUMOylation Required to Maintain the Basal-Like Cancer Subtype

SUMOylation involves the post-translational modification of proteins through the covalent attachment of SUMO proteins to lysine in target proteins, and affects several aspects of oncogenesis and cancer progression (Bettermann et al., 2012). There is a growing body of evidence that the SUMOylation of transcription factors affects transcriptional regulation (Gill, 2003). In addition, the SUMOylation of the serine threonine kinase AKT1 regulates cell proliferation by controlling AKT1 phosphorylation and activity (De La Cruz-Herrera et al., 2015; Lin et al., 2016). Lin et al. (2016) suggested that global SUMOylation occurs through the phosphorylation of Ubc9 and SUMO1 directly mediated by AKT1. Thus, AKT1 is suggested to play an important role in the SUMOylation of a large number of substrate proteins in the cells. Furthermore, the SUMOylation of TFAP2A transcription factor is involved in the transition from the luminal subtype to the basal-like subtype of breast cancer (Bogachek et al., 2014). Because the SUMOylation of TFAP2A blocks its ability to induce the expression of luminal genes, inhibition of the SUMO pathway induces a mesenchymal-to-epithelial transition, characterized by the repression of basal-associated gene expression and induction of luminal-associated genes. These findings indicate that the cleavage of SDC1 controls the SUMOylation of transcription factors associated with the maintenance of the basal-like cancer phenotypes through the SUMOylation of AKT1.

In this study, we found that the C-terminal fragment of SDC1 generated by MMPs could be involved in the SUMOylation of AKT1 in BT-549 cells and that the SDC1-dependent SUMO pathway enhances cell proliferation. Braun et al. (2012) reported that the SDC1 cytoplasmic domain interacts with the ubiquitin and SUMO-1 E3 ligase Topors. They discussed the role of the binding of SDC1 to Topors. Topors is a growth promoter for arterial smooth muscle cells, and SDC1 prevents its growth-promoting activities by inhibiting the ligase activity of Topors by directly binding to Topors. Although the findings reported by Braun et al. are inconsistent with our results, they have not examined whether the binding of SDC1 to Topors affects the SUMOylation pathway in the cells. Recently, Topors has been reported to function as a regulator of chromatin structure (Ji et al., 2020). In addition, the full-length form of SDC1 can translocate to the nucleus, although the complete route of full-length SDC1 internalization has not been elucidated (Brockstedt et al., 2002). Thus, the C-terminal fragment of SDC1 is suggested to induce SUMOylation by a Topors-independent mechanism.

The C-terminal domain of syndecan may serve as a platform to conjugate SUMO to proteins. A membrane-associated guanylate kinase protein, CASK, which is SUMOylated in neurons, has been reported to be a binding partner of syndecan 2 (Chao et al., 2008). Although it has not been investigated whether syndecan 2 is needed for SUMOylation of CASK, both SUMOylated CASK and syndecan 2 contribute to spine maturation. Thus, it is implicated that SUMOylation of substrate proteins such as CASK can be facilitated by forming a complex with syndecan. Moreover, a SUMO-specific isopeptidase, SENP2, has been reported to bind to intracellular membranes where it interacts with membrane-associated proteins (Odeh et al., 2018). As shown in **Figure 4D**, the C-terminal fragment of SDC1 is localized in the perinuclear region, probably in the Golgi. Membrane-associated proteins such as the C-terminal fragment of SDC1 may have the potential to regulate SUMOylation through binding to SUMO enzymes, although the mechanism by which SUMOylation is regulated at the membrane is largely unexplored.

## DATA AVAILABILITY STATEMENT

The raw data supporting the conclusions of this article will be made available by the authors, without undue reservation.

## AUTHOR CONTRIBUTIONS

SN and YB performed the research and analyzed the data. SN and HK wrote the manuscript, conceived, and designed the study. HK coordinated the study. All authors reviewed the results and approved the final version of the manuscript.

## FUNDING

This work was supported in part by Grants-in-Aid for Scientific Research on Innovative Areas 23110003 (to HK) and Scientific Research (B) 25293014 and 20H03386 (to HK) and (C) 25460080 (to SN), and by the Support Program for Strategic Research Foundation at Private Universities 2012–2016 (to HK) from the Ministry of Education, Culture, Sports, Science, and Technology, Japan.

## ACKNOWLEDGMENTS

We thank Yurika Yoshida, Kouki Hamabe, and Itaru Nagashima for technical support.

## SUPPLEMENTARY MATERIAL

The Supplementary Material for this article can be found online at: https://www.frontiersin.org/articles/10.3389/fcell.2021.659428/full#supplementary-material

## REFERENCES

Bambang, I. F., Lee, Y. K., Richardson, D. R., and Zhang, D. (2013). Endoplasmic reticulum protein 29 regulates epithelial cell integrity during the mesenchymal-epithelial transition in breast cancer cells. *Oncogene* 32, 1240–1251. doi: 10.1038/onc.2012.149

Behrens, A., Jousheghany, F., Yao-Borengasser, A., Siegel, E. R., Kieber-Emmons, T., and Monzavi-Karbassi, B. (2020). Carbohydrate (Chondroitin 4) Sulfotransferase-11-Mediated Induction of Epithelial-Mesenchymal Transition and Generation of Cancer Stem Cells. *Pharmacology* 105, 246–259. doi: 10.1159/000506710

Bettermann, K., Benesch, M., Weis, S., and Haybaeck, J. (2012). SUMOylation in carcinogenesis. *Cancer Lett.* 316, 113–125. doi: 10.1016/j.canlet.2011.10.036

Bogachek, M. V., Chen, Y., Kulak, M. V., Woodfield, G. W., Cyr, A. R., Park, J. M., et al. (2014). Sumoylation pathway is required to maintain the basal breast cancer subtype. *Cancer Cell* 25, 748–761. doi: 10.1016/j.ccr.2014.04.008

Braun, K. R., Dewispelaere, A. M., Bressler, S. L., Fukai, N., Kenagy, R. D., Chen, L., et al. (2012). Inhibition of PDGF-B induction and cell growth by syndecan-1 involves the ubiquitin and SUMO-1 ligase, Topors. *PLoS One* 7:e43701. doi: 10.1371/journal.pone.0043701

Brockstedt, U., Dobra, K., Nurminen, M., and Hjerpe, A. (2002). Immunoreactivity to cell surface syndecans in cytoplasm and nucleus: tubulin-dependent rearrangements. *Exp. Cell Res.* 274, 235–245. doi: 10.1006/excr.2002.5477

Chao, H. W., Hong, C. J., Huang, T. N., Lin, Y. L., and Hsueh, Y. P. (2008). SUMOylation of the MAGUK protein CASK regulates dendritic spinogenesis. *J. Cell Biol.* 182, 141–155. doi: 10.1083/jcb.200712094

Cooney, C. A., Jousheghany, F., Yao-Borengasser, A., Phanavanh, B., Gomes, T., Kieber-Emmons, A. M., et al. (2011). Chondroitin sulfates play a major role in breast cancer metastasis: a role for CSPG4 and CHST11 gene expression in forming surface P-selectin ligands in aggressive breast cancer cells. *Breast Cancer Res.* 13:R58.

De La Cruz-Herrera, C. F., Campagna, M., Lang, V., Del Carmen, Gonzalez-Santamaria, J., Marcos-Villar, L., et al. (2015). SUMOylation regulates AKT1 activity. *Oncogene* 34, 1442–1450. doi: 10.1038/onc.2014.48

Gill, G. (2003). Post-translational modification by the small ubiquitin-related modifier SUMO has big effects on transcription factor activity. *Curr. Opin. Genet. Dev.* 13, 108–113. doi: 10.1016/s0959-437x(03)00021-2

Hazan, R. B., Phillips, G. R., Qiao, R. F., Norton, L., and Aaronson, S. A. (2000). Exogenous expression of N-cadherin in breast cancer cells induces cell migration, invasion, and metastasis. *J. Cell Biol.* 148, 779–790. doi: 10.1083/jcb.148.4.779

Iida, J., Dorchak, J., Clancy, R., Slavik, J., Ellsworth, R., Katagiri, Y., et al. (2015). Role for chondroitin sulfate glycosaminoglycan in NEDD9-mediated breast cancer cell growth. *Exp. Cell Res.* 330, 358–370. doi: 10.1016/j.yexcr.2014.11.002

Jang, B., Kim, A., Hwang, J., Song, H. K., Kim, Y., and Oh, E. S. (2020). Emerging Role of Syndecans in Extracellular Matrix Remodeling in Cancer. *J. Histochem. Cytochem.* 68, 863–870. doi: 10.1369/0022155420930112

Ji, L., Huo, X., Zhang, Y., Yan, Z., Wang, Q., and Wen, B. (2020). TOPORS, a tumor suppressor protein, contributes to the maintenance of higher-order chromatin architecture. *Biochim. Biophys. Acta Gene Regul. Mech.* 1863:194518. doi: 10.1016/j.bbagrm.2020.194518

Kao, J., Salari, K., Bocanegra, M., Choi, Y. L., Girard, L., Gandhi, J., et al. (2009). Molecular profiling of breast cancer cell lines defines relevant tumor models and provides a resource for cancer gene discovery. *PLoS One* 4:e6146. doi: 10.1371/journal.pone.0006146

Kawamura, E., Fielding, A. B., Kannan, N., Balgi, A., Eaves, C. J., Roberge, M., et al. (2013). Identification of novel small molecule inhibitors of centrosome clustering in cancer cells. *Oncotarget* 4, 1763–1776. doi: 10.18632/oncotarget.1198

Klüppel, M., Wight, T. N., Chan, C., Hinek, A., and Wrana, J. L. (2005). Maintenance of chondroitin sulfation balance by chondroitin-4-sulfotransferase 1 is required for chondrocyte development and growth factor signaling during cartilage morphogenesis. *Development* 132, 3989–4003. doi: 10.1242/dev.01948

Lacroix, M., and Leclercq, G. (2004). Relevance of breast cancer cell lines as models for breast tumours: an update. *Breast Cancer Res. Treat* 83, 249–289. doi: 10.1023/b:brea.0000014042.54925.cc

Lin, C. H., Liu, S. Y., and Lee, E. H. (2016). SUMO modification of Akt regulates global SUMOylation and substrate SUMOylation specificity through Akt phosphorylation of Ubc9 and SUMO1. *Oncogene* 35, 595–607. doi: 10.1038/onc.2015.115

Maday, S., Anderson, E., Chang, H. C., Shorter, J., Satoh, A., Sfakianos, J., et al. (2008). A PDZ-binding motif controls basolateral targeting of syndecan-1 along the biosynthetic pathway in polarized epithelial cells. *Traffic* 9, 1915–1924. doi: 10.1111/j.1600-0854.2008.00805.x

Maeda, T., Desouky, J., and Friedl, A. (2006). Syndecan-1 expression by stromal fibroblasts promotes breast carcinoma growth in vivo and stimulates tumor angiogenesis. *Oncogene* 25, 1408–1412. doi: 10.1038/sj.onc.1209168

Manon-Jensen, T., Multhaupt, H. A., and Couchman, J. R. (2013). Mapping of matrix metalloproteinase cleavage sites on syndecan-1 and syndecan-4 ectodomains. *FEBS J.* 280, 2320–2331. doi: 10.1111/febs.12174

Mikami, T., and Kitagawa, H. (2013). Biosynthesis and function of chondroitin sulfate. *Biochim. Biophys. Acta* 1830, 4719–4733. doi: 10.1016/j.bbagen.2013.06.006

Nadanaka, S., Ishida, M., Ikegami, M., and Kitagawa, H. (2008). Chondroitin 4-O-sulfotransferase-1 modulates Wnt-3a signaling through control of E disaccharide expression of chondroitin sulfate. *J. Biol. Chem.* 283, 27333–27343. doi: 10.1074/jbc.m802997200

Nadanaka, S., Kinouchi, H., and Kitagawa, H. (2018). Chondroitin sulfate-mediated N-cadherin/beta-catenin signaling is associated with basal-like breast cancer cell invasion. *J. Biol. Chem.* 293, 444–465. doi: 10.1074/jbc.m117.814509

Nadanaka, S., Miyata, S., Yaqiang, B., Tamura, J. I., Habuchi, O., and Kitagawa, H. (2020). Reconsideration of the Semaphorin-3A Binding Motif Found in Chondroitin Sulfate Using Galnac4s-6st-Knockout Mice. *Biomolecules* 10:1499. doi: 10.3390/biom10111499

Nguyen, T. L., Grizzle, W. E., Zhang, K., Hameed, O., Siegal, G. P., and Wei, S. (2013). Syndecan-1 overexpression is associated with nonluminal subtypes and poor prognosis in advanced breast cancer. *Am. J. Clin. Pathol.* 140, 468–474. doi: 10.1309/ajcpz1d8calhdxcj

Nikolova, V., Koo, C. Y., Ibrahim, S. A., Wang, Z., Spillmann, D., Dreier, R., et al. (2009). Differential roles for membrane-bound and soluble syndecan-1 (CD138) in breast cancer progression. *Carcinogenesis* 30, 397–407. doi: 10.1093/carcin/bgp001

Odeh, H. M., Coyaud, E., Raught, B., and Matunis, M. J. (2018). The SUMO-specific isopeptidase SENP2 is targeted to intracellular membranes via a predicted N-terminal amphipathic alpha-helix. *Mol. Biol. Cell* 29, 1878–1890. doi: 10.1091/mbc.e17-07-0445

Park, J. H., Rasch, M. G., Qiu, J., Lund, I. K., and Egeblad, M. (2015). Presence of insulin-like growth factor binding proteins correlates with tumor-promoting effects of matrix metalloproteinase 9 in breast cancer. *Neoplasia* 17, 421–433. doi: 10.1016/j.neo.2015.04.003

Pasqualon, T., Pruessmeyer, J., Jankowski, V., Babendreyer, A., Groth, E., Schumacher, J., et al. (2015a). A cytoplasmic C-terminal fragment of syndecan-1 is generated by sequential proteolysis and antagonizes syndecan-1 dependent lung tumor cell migration. *Oncotarget* 6, 31295–31312. doi: 10.18632/oncotarget.5174

Pasqualon, T., Pruessmeyer, J., Weidenfeld, S., Babendreyer, A., Groth, E., Schumacher, J., et al. (2015b). A transmembrane C-terminal fragment of syndecan-1 is generated by the metalloproteinase ADAM17 and promotes lung epithelial tumor cell migration and lung metastasis formation. *Cell Mol. Life Sci.* 72, 3783–3801. doi: 10.1007/s00018-015-1912-4

Purushothaman, A., Uyama, T., Kobayashi, F., Yamada, S., Sugahara, K., Rapraeger, A. C., et al. (2010). Heparanase-enhanced shedding of syndecan-1 by myeloma cells promotes endothelial invasion and angiogenesis. *Blood* 115, 2449–2457. doi: 10.1182/blood-2009-07-234757

Ramani, V. C., and Sanderson, R. D. (2014). Chemotherapy stimulates syndecan-1 shedding: A potentially negative effect of treatment that may promote tumor relapse. *Matrix Biol.* 35, 215–222. doi: 10.1016/j.matbio.2013.10.005

Ramani, V. C., Yang, Y., Ren, Y., Nan, L., and Sanderson, R. D. (2011). Heparanase plays a dual role in driving hepatocyte growth factor (HGF) signaling by enhancing HGF expression and activity. *J. Biol. Chem.* 286, 6490–6499. doi: 10.1074/jbc.m110.183277

Rousseau, C., Ruellan, A. L., Bernardeau, K., Kraeber-Bodere, F., Gouard, S., Loussouarn, D., et al. (2011). Syndecan-1 antigen, a promising new target for triple-negative breast cancer immuno-PET and radioimmunotherapy. A preclinical study on MDA-MB-468 xenograft tumors. *EJNMMI Res.* 1:20. doi: 10.1186/2191-219x-1-20

Sayyad, M. R., Puchalapalli, M., Vergara, N. G., Wangensteen, S. M., Moore, M., Mu, L., et al. (2019). Syndecan-1 facilitates breast cancer metastasis to the brain. *Breast Cancer Res. Treat* 178, 35–49. doi: 10.1007/s10549-019-05347-0

Steinfeld, R., Van Den Berghe, H., and David, G. (1996). Stimulation of fibroblast growth factor receptor-1 occupancy and signaling by cell surface-associated syndecans and glypican. *J. Cell Biol.* 133, 405–416. doi: 10.1083/jcb.133.2.405

Su, G., Blaine, S. A., Qiao, D., and Friedl, A. (2007). Shedding of syndecan-1 by stromal fibroblasts stimulates human breast cancer cell proliferation via FGF2 activation. *J. Biol. Chem.* 282, 14906–14915. doi: 10.1074/jbc.m611739200

Su, G., Blaine, S. A., Qiao, D., and Friedl, A. (2008). Membrane type 1 matrix metalloproteinase-mediated stromal syndecan-1 shedding stimulates breast carcinoma cell proliferation. *Cancer Res.* 68, 9558–9565. doi: 10.1158/0008-5472.can-08-1645

Sugahara, K., Mikami, T., Uyama, T., Mizuguchi, S., Nomura, K., and Kitagawa, H. (2003). Recent advances in the structural biology of chondroitin sulfate and dermatan sulfate. *Curr. Opin. Struct. Biol.* 13, 612–620. doi: 10.1016/j.sbi.2003.09.011

Szatmari, T., Otvos, R., Hjerpe, A., and Dobra, K. (2015). Syndecan-1 in Cancer: Implications for Cell Signaling. Differentiation, and Prognostication. *Dis. Markers* 2015:796052.

Uyama, T., Ishida, M., Izumikawa, T., Trybala, E., Tufaro, F., Bergstrom, T., et al. (2006). Chondroitin 4-O-sulfotransferase-1 regulates E disaccharide expression of chondroitin sulfate required for herpes simplex virus infectivity. *J. Biol. Chem.* 281, 38668–38674. doi: 10.1074/jbc.m609320200

Wang, X., Zuo, D., Chen, Y., Li, W., Liu, R., He, Y., et al. (2014). Shed Syndecan-1 is involved in chemotherapy resistance via the EGFR pathway in colorectal cancer. *Br. J. Cancer* 111, 1965–1976. doi: 10.1038/bjc.2014.493

**Conflict of Interest:** The authors declare that the research was conducted in the absence of any commercial or financial relationships that could be construed as a potential conflict of interest.

frontiers in Cell and Developmental Biology

ORIGINAL RESEARCH
published: 08 June 2021
doi: 10.3389/fcell.2021.643060

# Sulfation of Glycosaminoglycans Modulates the Cell Cycle of Embryonic Mouse Spinal Cord Neural Stem Cells

*Elena Schaberg[1], Ursula Theocharidis[1], Marcus May[1], Katrin Lessmann[1], Timm Schroeder[2] and Andreas Faissner[1]**

[1] Department for Cell Morphology and Molecular Neurobiology, Ruhr University Bochum, Bochum, Germany, [2] Department of Biosystems Science and Engineering, ETH Zürich, Zurich, Switzerland

OPEN ACCESS

**Edited by:**
*Shuji Mizumoto, Meijo University, Japan*

**Reviewed by:**
*Dalit Sela-Donenfeld, The Hebrew University of Jerusalem, Israel*
*Shinji Miyata, Tokyo University of Agriculture and Technology, Japan*
*Lohitash Karumbaiah, University of Georgia, United States*
*Hiroshi Kitagawa, Kobe Pharmaceutical University, Japan*

***Correspondence:**
*Andreas Faissner*
*andreas.faissner@rub.de*

**Specialty section:**
*This article was submitted to Signaling, a section of the journal Frontiers in Cell and Developmental Biology*

**Received:** *17 December 2020*
**Accepted:** *18 May 2021*
**Published:** *08 June 2021*

**Citation:**
*Schaberg E, Theocharidis U, May M, Lessmann K, Schroeder T and Faissner A (2021) Sulfation of Glycosaminoglycans Modulates the Cell Cycle of Embryonic Mouse Spinal Cord Neural Stem Cells. Front. Cell Dev. Biol. 9:643060. doi: 10.3389/fcell.2021.643060*

In the developing spinal cord neural stem and progenitor cells (NSPCs) secrete and are surrounded by extracellular matrix (ECM) molecules that influence their lineage decisions. The chondroitin sulfate proteoglycan (CSPG) DSD-1-PG is an isoform of receptor protein tyrosine phosphatase-beta/zeta (RPTPβ/ζ), a *trans*-membrane receptor expressed by NSPCs. The chondroitin sulfate glycosaminoglycan chains are sulfated at distinct positions by sulfotransferases, thereby generating the distinct DSD-1-epitope that is recognized by the monoclonal antibody (mAb) 473HD. We detected the epitope, the critical enzymes and RPTPβ/ζ in the developing spinal cord. To obtain insight into potential biological functions, we exposed spinal cord NSPCs to sodium chlorate. The reagent suppresses the sulfation of glycosaminoglycans, thereby erasing any sulfation code expressed by the glycosaminoglycan polymers. When NSPCs were treated with chlorate and cultivated in the presence of FGF2, their proliferation rate was clearly reduced, while NSPCs exposed to EGF were less affected. Time-lapse video microscopy and subsequent single-cell tracking revealed that pedigrees of NSPCs cultivated with FGF2 were strongly disrupted when sulfation was suppressed. Furthermore, the NSPCs displayed a protracted cell cycle length. We conclude that the inhibition of sulfation with sodium chlorate interferes with the FGF2-dependent cell cycle progression in spinal cord NSPCs.

**Keywords: chondroitin sulfate proteoglycan, extracellular matrix, single-cell tracking, spinal cord, sodium chlorate, sulfation, stem cell niche**

## INTRODUCTION

The extracellular matrix (ECM) is a crucial determining structure in the developing central nervous system (CNS) that influences cell proliferation, lineage decisions and differentiation processes of neural stem and progenitor cells (NSPCs) (Barros et al., 2011; Theocharidis et al., 2014; Faissner and Reinhard, 2015). The ECM consists of glycoproteins, proteoglycans and complex glycans that either

loosely pervade the pericellular space as interstitial ECM or assemble to complex interactomes, e.g., collagen fibrils or basal membranes. The ECM regulates a large range of cellular behaviors by activating distinct receptor systems, for example cell based heterodimeric integrin receptors (Barros et al., 2011). Based on bioinformatic analyses of the ECM constituents around 300 genes have been attributed to the core matrisome, about 35 of which encode proteoglycans (Hynes and Naba, 2012; Naba et al., 2012). The latter consist of a protein core and at least one covalently bound glycosaminoglycan (GAG) carbohydrate chain. Based on the type of glycan proteoglycans can be classified, e.g., in chondroitin sulfates (CSPG) and heparan sulfate proteoglycans (HSPGs) (Iozzo and Schaefer, 2015). The GAGs consist of long chains of carbohydrate dimers that are sulfated at distinct positions and thereby endowed with specific docking sites for proteins such as morphogens, cytokines or other ECM compounds (Purushothaman et al., 2012; Mikami and Kitagawa, 2017). Sulfated proteoglycans are expressed during CNS development, provide signaling cues and are involved in a variety of processes such as cell proliferation, differentiation, migration of neural progenitors or synaptogenesis (Iozzo and Schaefer, 2015; Maeda, 2015; Smith et al., 2015; Mikami and Kitagawa, 2017; Song and Dityatev, 2018).

Chondroitin sulfate GAGs (CS-GAGs) and heparan sulfate GAGs (HS-GAGs) are the two most commonly expressed GAGs in the developing CNS (Smith et al., 2015). Distinct sulfotransferases modify the GAGs in a spatially and temporally regulated manner and are expressed in neurogenic regions of the developing and adult brain and in neural stem cells in culture (Akita et al., 2008). Enzymatic digestion of CS-GAGs by chondroitinase ABC (ChABC) reduced proliferation and differentiation of cortical progenitors (von Holst et al., 2006; Sirko et al., 2007). The sulfation of GAG chains occurs by the transfer of sulfate groups from the donor 3′-phosphoadenosine 5′-phosphosulfate (PAPS). This enzymatic reaction can be competitively inhibited by sodium chlorate ($NaClO_3$) (Sirko et al., 2010a). Sodium chlorate is a strong oxidant that has been used as herbicide until it was banned in the European Union in 2009 and is still applied as food supplement in live animal stocks in agriculture (Smith et al., 2012). We have shown previously that chlorate suppresses the sulfation of CS-GAGs in general, ablates the DSD-1-CS-epitope that is expressed by phosphacan and RPTP-β/ζ and thereby attenuates the proliferation of telencephalic NSPCs and spinal cord-derived neurospheres (Clement et al., 1998; Akita et al., 2008; Karus et al., 2012). In order to assess the potential functions of proteoglycans from the phosphacan/RPTP-β/ζ family we examined their expression and the presence of distinct CS-sulfotransferases during spinal cord development. To gain insight into the influence of sulfated GAGs on the cell cycle, we performed time-lapse video microscopy and single cell tracking of spinal cord progenitors treated with sodium chlorate, as a potent pharmacological sulfation inhibitor (Eilken et al., 2009; Rieger et al., 2009; Sirko et al., 2010a; Costa et al., 2011; Hoppe et al., 2016; May et al., 2018). Here, we show that the proliferation and lineage relationship of spinal cord-derived NSPCs cultivated in the presence of FGF2 are strongly altered by suppressing sulfation. This observation can be explained by an elongated cell cycle *in vitro*.

# MATERIALS AND METHODS

All experiments conform to the relevant regulatory standards.

## Animals

Wild-type SV129 mice (*Mus musculus*) were used in accordance with the European Council Directive of September 22, 2010 (2010/63/EU) for care of laboratory animals and approved by the animal care committee of North Rhine-Westphalia, Germany, based at the LANUV (Landesamt für Umweltschutz, Naturschutz und Verbraucherschutz, Nordrhein-Westphalen, Recklinghausen, Germany). The study was supervised by the animal welfare commissioner of Ruhr-University. Male and female SV129 mice were housed individually with a constant 12-h light-dark cycle and access to food and water *ad libitum*. All efforts were made to reduce the number of animals in the experiments. For the experiments we used embryos of both sexes from time mated pregnant SV129 mice. The day of the vaginal plug was defined as embryonic day (E) 0.5 and the age of the embryos was verified by the determination of the Theiler stage. The experiments were performed with embryos at the age of embryonic day 15.5 (E15.5).

## Tissue Preparation for Spinal Cord Sections

E15.5 mouse embryos were decapitated and the tail was removed prior to an overnight incubation of the trunks in 4% (w/v) paraformaldehyde (PFA, Carl ROTH, Karlsruhe, Germany), dissolved in phosphate-buffered saline (PBS, 137 mM NaCl, 3 mM KCl, 6.5 mM $Na_2HOP_4$+$2H_2O$, 1.5 mM $KH_2PO_4$, pH 7.3) at 4°C. The tissue was dehydrated in 20% (w/v) sucrose in DEPC-PBS (PBS treated with 0.1% (v/v) diethyl pyrocarbonate (DEPC, AppliChem, Darmstadt, Germany) over night before autoclaving) for 2 days before the embedding in Leica (Leica Biosystems, Richmond, IL, United States) tissue freezing medium. Horizontal cryosections with 14 μm thickness were cut in the lumbo-sacral region of the embryos at the Leica CM3050S cryostat and thaw-mounted on SuperFrost Plus glass slides (Menzel GmbH, Braunschweig, Germany). Animals from at least three different litters were used for the experiments and processed simultaneously. Figures show representative results from the independent experiments.

## Immunohistochemistry

A detailed list of primary antibodies can be found in **Supplementary Table 2**. Cryosections were rehydrated and blocked in PBS (including 1.7% (w/v) NaCl) + 10% (v/v) goat serum for 1 h before the antibodies βIII-tubulin (Sigma, 1:300), polyclonal anti-phosphacan (batch: KAF13[2], 1:300) and 473HD against the DSD-1-epitope (1:300; both (Faissner et al., 1994)) were applied in PBT1 [PBS with 1% (w/v) BSA (bovine serum albumin, ROTH) and 0.1% (v/v) triton-X100 (AppliChem)] with

5% (v/v) goat serum (Jackson ImmunoResearch). For the better accessibility of nuclear antigens the sections for the Islet-1/2 staining were boiled in 0.01 M citrate buffer for 10 min and then cooled down in the buffer for 5 min at room temperature and 10 min on ice. They were washed in 1× PBS before the application of the primary antibodies 473HD and Isl-1/2 (clone 39.4D5, DSHB; 1:200 hybridoma supernatant) in PBT-1. All primary antibodies were incubated for 2 h at room temperature and subsequently over night at 4°C and then washed twice with PBS. The secondary antibodies (α-rat-IgM Cy3, 1:600 and α-rabbit-AF488, 1:400, both from Jackson ImmunoResearch) were added in PBS/A (PBS with 0.1% (w/v) BSA) for 2 h at room temperature. To detect cell nuclei bisbenzimide (DAPI, Sigma) was included in the secondary antibody solution at a final concentration of 1:100,000. After washing twice with PBS, the sections were mounted with immumount (Shandon/Thermo Fisher Scientific) and analyzed by fluorescent microscopy at the AxioZoom V16 using ZEN 2009 pro Software (Carl Zeiss AG).

## Reverse Transcription Polymerase Chain Reaction (RT-PCR)

Spinal cord tissue from the lumbo-sacral part was isolated from E15.5 embryos and instantly frozen on dry ice. Total RNA was isolated from the tissue using the Sigma Mammalian GenElute-Total RNA miniprep Kit with an interposed DNase digestion step (On-Column DNaseI Digestion Set, Sigma). 1 μg of RNA was reverse-transcribed to cDNA using the first strand cDNA synthesis kit from Thermo Fisher Scientific adapted to a published protocol (von Holst et al., 2007; Sirko et al., 2010a). PCRs for the detection of RPTP-β/ζ /DSD-1-PG, the sulfotransferases and β-actin were performed using the primers and cycling conditions that can be found in **Supplementary Table 3**. All PCRs contained 1 μl cDNA, 5 pmol of each primer (synthesized by Sigma), 5 nmol dNTPs (Thermo Fisher Scientific), 10× reaction buffer and 1.25 U Taq-polymerase (both from Sigma) and were incubated in a Master Cycler Gradient (Eppendorf).

## *In situ* Hybridizations

Primers for the cloning of all used probes can be found in **Supplementary Table 3**. The probe detecting DSD-1-PG/ RPTP-β/ζ was generated based on the cDNA sequence of the mouse *ptprz1* gene within the common part of the isoforms in the carbonic anhydrase domain and spacer region (Garwood et al., 1999). The sequence was amplified from embryonic mouse brain cDNA and cloned into the pCRII-TOPO vector (Thermo Fisher Scientific) according to manufacturer's instructions. Vectors were isolated with the QIAprep Spin miniprep kit (QIAGEN) and cut with the restriction enzymes XhoI and HindIII (Thermo Fisher Scientific) for linearization. T7 and Sp6 RNA polymerases (Thermo Fisher Scientific) were used in combination with the DIG RNA labeling kit (Roche) to synthesize the sense and anti-sense riboprobes, respectively.

The sections for the *in situ* hybridizations were treated according to the protocol from Akita et al. (2008) with the aforementioned *ptprz1* riboprobes and the sulfotransferase probes listed in **Supplementary Table 3**. The cryosections were dried at room temperature, primed in 0.1 M TAE (triethanolamine, pH 8.0) and then acetylated with 0.25% (v/v) acetic anhydride in 0.1 M TAE for 10 min before two washing steps with 50 mM PB (phosphate buffer, $NaH_2PO_4/Na_2HPO_4$, pH 7.3). We performed a pre-incubation step in hybridization buffer (50% (v/v) formamide, 10% (w/v) dextran sulfate, 1× Denhardt's reagent (Sigma), 100 μg $ml^{-1}$ yeast RNA, 250 μg $ml^{-1}$ salmon sperm DNA (Roche), 2× SSC (standard saline citrate, prepared as 20× SSC: 3 M NaCl, 0.3 M sodium citrate, pH 7.0), 50 mM sodium phosphate, pH 7.0, 0.2% (w/v) SDS) for 2 h at 60°C. In the meantime, the probes were denatured in 20 μl hybridization buffer (without SDS) for 5 min at 80°C before they were cooled on ice and supplemented with the respective amount of hybridization buffer to achieve the correct concentration and SDS. The hybridization was carried out over night at 60°C with probes against *ptprz1*, *Chst11*, *Ust*, *Chst3,* and *Chst7* and their respective sense control probes in a concentration of 1:100. On the next day the sections were stringently washed at 60°C in the following buffers: 4× SSC for 10 min, 2 × SSC containing 50% (v/v) formamide for 20 min twice, 2× SSC for 10 min, 0.2× SSC for 20 min twice, Tris–NaCl buffer (0.15 M NaCl, 0.1 M Tris–HCl, pH 7.5) for 10 min twice. Before the antibody was applied the sections were blocked in Tris–NaCl buffer containing 1% (w/v) skimmed milk powder. The anti-digoxigenin-AP coupled Fab fragments (Roche) were incubated at a concentration of 1:2000 in blocking buffer over night at 4°C on the sections. The sections were washed three times in Tris–NaCl buffer before the application of the alkaline phosphatase substrates nitroblue tetrazolium (NBT, 0.34 mg $ml^{-1}$, Roche) and 5-bromo-4-chloro-3-indolyl phosphate (BCIP, 0.18 mg, Roche) in detection buffer containing 5% (w/v) polyvinyl alcohol, 0.1 M NaCl, 50 mM $MgCl_2$, 0.1 M Tris–HCl, pH 9.5. The development of the color reaction was carried out at 37°C and stopped with 1 mM EDTA, 10 mM Tris–HCl, pH 7.5 when positive signals were visible as strong purple color under microscopic control. Sense controls were stopped simultaneously. The micrographs were taken with the AxioZoom V16 (Carl Zeiss AG) using ZEN 2009 pro software.

## Neurosphere Culture

The neurosphere culture system of spinal cord progenitors has been described (Karus et al., 2011). Dissection of the embryos for cell culture experiments was carried out in MEM (minimal essential medium, Sigma). The spinal cords of E15.5 old embryos were isolated and enzymatically digested with 30 U $ml^{-1}$ Papain, 40 μg $ml^{-1}$ DNaseI (both from Worthington) in the presence of 0.24 mg $ml^{-1}$ L-Cysteine in MEM (Sigma). After centrifugation of the single cell suspension for 5 min at 1000 rpm the cell sediment was re-suspended in neurosphere medium consisting of DMEM/F-12 (1:1), 0.2 mg $ml^{-1}$ L-glutamine (all from Sigma), 2% (v/v) B27, 100 U $ml^{-1}$ penicillin, 100 μg $ml^{-1}$ streptomycin (all from Invitrogen/Thermo Fisher Scientific), 20 ng $ml^{-1}$ FGF2, 20 ng $ml^{-1}$ EGF (both PeproTech) and 0.25 U $ml^{-1}$ heparin (Sigma) for 6–7 days at 37°C and 6% (v/v) $CO_2$ to get neurospheres (von Holst et al., 2006; Sirko et al., 2010a). For chlorate treatment we added 30 mM sodium

chlorate (Sigma) pre-diluted in medium to the cultures as described previously (Akita et al., 2008; Sirko et al., 2010a; Karus et al., 2012).

## Single Cell Culture for Time-Lapse Video Microscopy

To prepare a single cell suspension the neurospheres were centrifuged for 5 min at 80 *g* and the resulting cell pellets were enzymatically digested with 0.05% (w/v) trypsin-EDTA in HBSS (Invitrogen/Thermo Fisher Scientific) for 5 min at 37°C. By adding 1 ml ovomucoid [1 mg $ml^{-1}$ trypsin inhibitor (Sigma), 50 μg $ml^{-1}$ BSA, 40 μg $ml^{-1}$ DNaseI (Worthington) in L-15 medium (Sigma)] the digestion was stopped and after the mechanical dissociation the single cell suspension was centrifuged for 5 min at 80 *g*. Neurosphere medium was added and the cells were re-suspended. For time-lapse video microscopy 24 well plates (Thermo Fisher Scientific) were sequentially coated with 0.001% (v/v) poly-d-lysin (Sigma) in $H_2O$, followed by 10 μg $ml^{-1}$ laminin-1 (Invitrogen/Thermo Fisher Scientific) in PBS for 1 h at 37°C each. 30,000 cells/well were plated in neurosphere medium containing either 20 ng $ml^{-1}$ EGF or 20 ng $ml^{-1}$ FGF2 with 0.25 U $ml^{-1}$ heparin (Sigma) and incubated at 37°C and 6% (v/v) $CO_2$ for 4 days during the acquisition in order to perform time-lapse video microscopy. For chlorate treatment 30 mM sodium chlorate (Sigma) were added to the cultures. Each condition was performed in duplicates. The chlorate treated cells were cultivated and filmed simultaneously to the untreated cells on the same plate. At the same time, NSPCs isolated from the spinal cord of tenascin-C-deficient mice were analyzed in an analogous manner for an independent experimental approach. The dataset regarding the untreated control cells served as reference both for the chlorate-treated and the tenascin-C depleted NSPCs and has been published in the latter context (May et al., 2018). Here, as the experiments have been conducted in parallel, this data set of the control cells was used as reference to evaluate the influence of inhibited sulfation on spinal cord-derived NSPCs.

## Time Lapse Video Microscopy

The time lapse microscopy of spinal cord progenitors was performed at the Axiovert 200 M with the AxioCam HRm camera and a self-written VBA module remote (Eilken et al., 2009) controlling the Zeiss Axiovision program 4.8.2 (all Zeiss). Additionally, the devices Tempcontrol 37-2 digital and CTI-Controller 3700 digital (both PeCon) were used to create defined culture conditions with 37°C and 6% (v/v) $CO_2$. Phase contrast images were taken every 5 min for at least 90 h. Five fields of view were defined for each well. Single cell tracking was performed using tTt, a computer program developed for the cell tracking and the generation of lineage trees on single cell level (Rieger et al., 2009; Hilsenbeck et al., 2016). Individual mother cells and their generated progeny were tracked over the cultivation period of 4 days. The duration between two cell divisions could be determined with high precision due to short intervals between the phase contrast images. Finally, full lineage trees originating from an individual stem cell could be constructed in that manner. A previous study of the laboratory illustrates this procedure, documenting the simultaneous construction of lineage trees in parallel with the time-lapse video (May et al., 2018). Movies were created using ImageJ 1.45r (National Institutes of Health) software and are played at a speed of five frames per second (see **Supplementary Material**). As cell culture dynamics could be monitored with high temporal resolution, quantification of proliferation and cell death events could be performed with ongoing cultivation. A detailed visualization of both processes has been published before (May et al., 2018).

## Data Analysis

To analyze the time-lapse video microscopy data the Kruskal–Wallis-Test with Dunn's multiple comparisons test or the Mann–Whitney *U*-Test was used. A minimum of three independent experiments for each condition was performed. The data are illustrated as Box Whisker Plots with percentiles from 5 to 95%. All statistics and graphs were performed using GraphPad Prism® software (Version 7, GraphPad Inc). *P*-values are given as $^{*}P \leq 0.05$, $^{**}P \leq 0.1$ and $^{***}P \leq 0.001$.

# RESULTS

## Proteoglycans of the CS Type Are Present in the Developing Spinal Cord

In the neurogenic regions in the developing and adult brain CSPGs from the RPTP-β/ζ type can be found (Akita et al., 2008). The members of this family consist of a short and a long transmembrane receptor variant and the soluble CSPG phosphacan (Maurel et al., 1994), also described as the homolog DSD-1-PG in the mouse CNS (Faissner et al., 1994; Garwood et al., 1999). In order to obtain an overview about the expression of these CSPGs in the embryonic day 15.5 (E15.5) spinal cord immunohistochemistry was performed. We have previously shown that at this stage, subsequent to a period of intensive proliferation a phase of gliogenesis can be observed that is strongly modulated by the glycoprotein tenascin-C of the stem cell niche, indicating a significant role of the extracellular matrix (Karus et al., 2011; Faissner et al., 2017). The expression of RPTP-β/ζ was restricted to the CNS (**Figure 1A**) and could not be detected in any other non-neural tissues in horizontal sections of mouse embryos (data not shown). There was a clear expression in the spinal cord that was stronger in its ventral than in its dorsal half (**Figure 1A**). The proteins could be found in the intermediate as well as in the mantle regions.

The monoclonal antibody 473HD recognizes a specific subtype of GAG side chains and this motif is exposed by phosphacan/DSD-1-PG and the long isoform of the RPTP-β/ζ receptor (Faissner et al., 1994; Ito et al., 2005). Both contain a peptide sequence where GAG chains can be attached (Garwood et al., 1999). Its expression resembled the pattern seen for the RPTP-β/ζ staining, with a prominent overlay in the ventral part of the spinal cord (**Figures 1A′,A″**). The 473HD epitope was, however, not confined to the CNS but also clearly present in cartilage (see **Figures 1A′–C′**) and gut (data not shown). Thus, outside of the CNS the 473HD epitope seems to appear also on

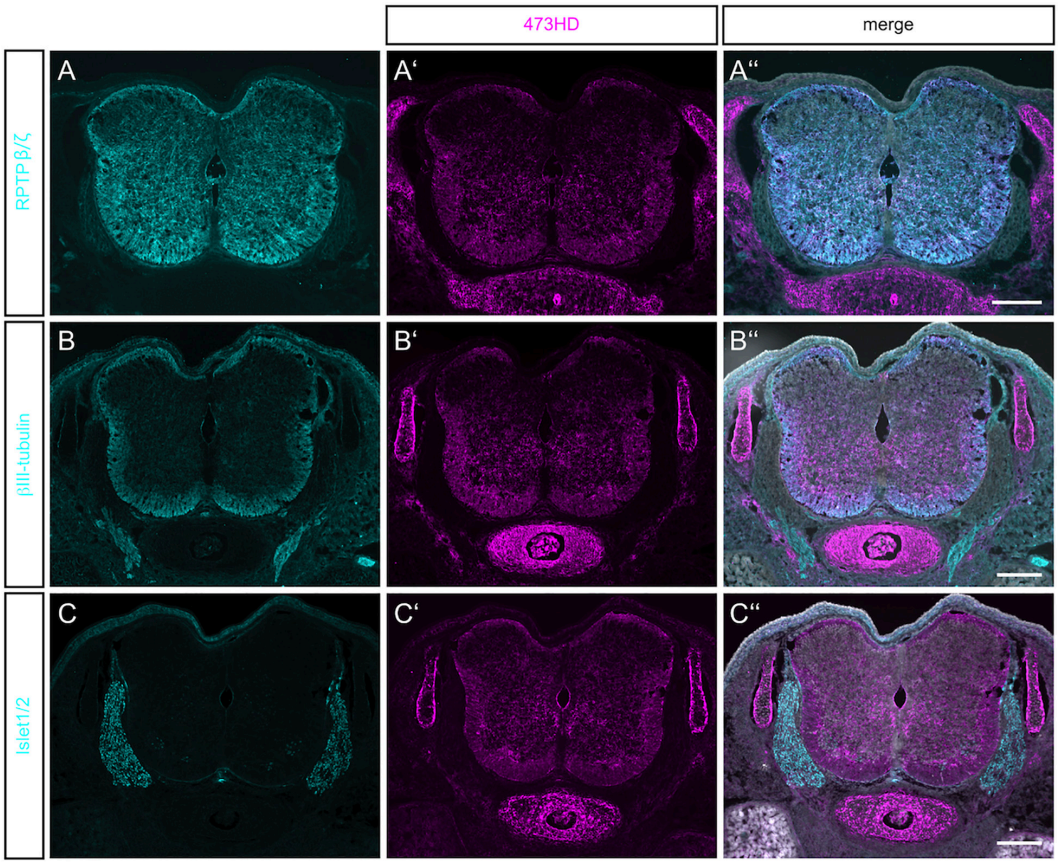


**FIGURE 1 |** Detection of RPTPβ/ζ/DSD-1-PG in the embryonic spinal cord. **(A)** Immunohistochemistry with the polyclonal antibody anti-phosphacan revealed the expression of the CSPGs RPTP-β/ζ and DSD-1-PG/phosphacan in E15.5 mouse spinal cord. No labeling could be observed outside the CNS. **(A′)** The monoclonal antibody 473HD recognizes a specific carbohydrate motif on CSPGs that is present on RPTP-β/ζ /DSD-1-PG. Immuno-positive structures could also be found outside the CNS, especially in the underlying cartilage. **(A″)** The overlay of both labels and the nuclear DAPI staining (in white) showed a co-localization in the spinal cord, but solely 473HD-positive structures outside the CNS. **(B)** Young neurons in the developing spinal cord could be labeled with βIII-tubulin which is present especially in the ventral marginal zone. There, the expression partially overlapped with 473HD staining **(B′,B″) (C,C′,C″)**. The immune-positive signals for 473HD surrounded scattered Isl-1/2-positive nuclei in the ventral spinal cord but showed no reactivity in the dorsal root ganglia (DRG) where Isl-1/2-positive motoneuron nuclei were arranged. Scale bars: 200 μm.

other proteoglycans beyond those recognized by the polyclonal RPTP-β/ζ antibodies (Ito et al., 2005). This is in accordance with an earlier study that reported expression of the DSD-1-epitope by Schwann cells in the sciatic nerve, in association with the CSPGs decorin and versican (Braunewell et al., 1995). 473HD expression overlapped with the signals obtained for βIII-tubulin immunostaining in the ventral mantle zone of the spinal cord, indicating a close association with motoneuron processes (**Figures 1B′,B″**). To have a closer look on this cell type we stained for the LIM homeobox transcription factors Islet-1 and -2 (Isl-1/2) (**Figure 1C**). The 473HD signal surrounded the large motoneuron cell bodies in the ventral basal plate (**Figure 1C′**) where single post-mitotic motoneuron nuclei were positive for Isl-1/2 (**Figure 1C″**). There was no overlap between 473HD and Isl-1/2 staining in the dorsal root ganglia (DRGs). 473HD was completely absent from the DRGs whereas the latter displayed clear expression of Isl-1/2. The association with motoneurons in the ventral spinal cord seemed to be concentrated to the stem and precursor cell stages in the ventral spinal cord as progenitors for post-mitotic motoneurons.

On the mRNA level all major isoforms of RPTP-β/ζ could be amplified by RT-PCR (**Figure 2A** upper panel), as well as the soluble DSD-1-PG (**Figure 2A** lower panel) indicating that both the long receptor and the secreted form were present and could represent core proteins of glycosylated proteoglycans. This approach did not, however, reveal the cellular source of the RPTP-β/ζ variants. Therefore, *in situ* hybridizations using a probe raised against the common constant part of DSD-1-PG/phosphacan and RPTP-β/ζ (**Figure 2B**) were performed. The proteoglycans were expressed in the spinal cord and produced by radial glia cells that surrounded the central canal. The signal was more intense in the ventral portion of the ventricular zone. This was consistent with previous findings that the 473HD epitope localizes with the nestin-positive neural stem/progenitor cells in the brain (von Holst et al., 2006) and spinal cord (Karus et al., 2012) and was more prominent in association with ventrally localized

motoneurons than sensory neurons in the dorsal part. It has to be pointed out that DSD-1-PG/phosphacan is a secreted CSPG and thus can diffuse through the interstitial space of the developing spinal cord where it may be immobilized by selective receptor systems. For example, the transmembrane receptor RPTP-σ has been identified a CSPG receptor that is expressed by neurons and may convey inhibitory properties of CSPGs for axon outgrowth (Shen et al., 2009; Lang et al., 2015). Therefore, the distribution territory of the DSD-1-epitope on the one hand and the location of cells producing the core proteins do not necessarily overlap, which may explain different expression patterns.

## Sulfotransferases for CSPGs Are Expressed in the Spinal Cord

Previous investigations strongly suggested that DSD-1-PG/phosphacan and RPTP-β/ζ are the major, if not the sole core carrier proteins of the DSD-1-epitope in the CNS (Faissner et al., 1994; Schnadelbach et al., 1998; Garwood et al., 1999). The epitope contains the CSD unit that is sulfated at two positions (Clement et al., 1998; Sugahara et al., 2003). In a quest for enzymes that are required for the synthesis of this unit we next examined which CS-sulfotransferases are expressed in the developing spinal cord. We have previously detected several of these enzymes in the stem cell compartment of the developing and adult telencephalic neural stem cell niche (Akita et al., 2008). We focused on spinal cord tissue for the analysis of the expression of sulfotransferases that modulate the sulfation status of CSPGs. The reaction pathways catalyzed by these enzymes have been reviewed elsewhere (Sugahara and Mikami, 2007; Akita et al., 2008; Mikami and Kitagawa, 2017). We found different isoforms of the modifying enzymes at chondroitin 4-sulfate (Chst11, Chst12, and Chst13), chondroitin 6-sulfate (Chst3 and Chst7) as well as Chst15 and Ust via RT-PCR analysis in spinal cord tissue samples (**Figure 2C**). Interestingly, in the spinal cord we could detect the enzyme Chst13 that is not present in E13 brain tissue (Akita et al., 2008) or forebrain neurospheres that were used as positive control. Having established the expression of the mRNAs, it was of interest to specify the cellular sources of the sulfotransferase enzymes. Therefore, *in situ* hybridization was performed. Examining the mRNA distribution in the tissue by *in situ* hybridization the expression of the sulfotransferases *Chst11*, *Ust*, *Chst3,* and *Chst7* could be localized to the gray matter of the ventricular zone and the intermediate layer, but not in the white matter of the marginal layer (**Figure 2D**). Sulfotransferases could also clearly be detected in dorsal root ganglia, as visible on the sections hybridized with *Chst11*, *Chst3,* and *Chst7* probes (**Figure 2D**). These structures were neither positive for polyclonal phosphacan antibodies, nor the mAb 473HD (compare to **Figure 1**), which suggested that other proteoglycans are potential targets for sulfation by these enzymes.

## Proliferation and Cell Death Are Strongly Affected After Sodium Chlorate Treatment *in vitro*

Sulfated GAGs are essential for normal proliferation and cell cycle progression of spinal cord progenitors *in vitro* (Karus et al., 2012). The significance of those sulfation patterns can be tested by addition of sodium chlorate to cell cultures that competitively inhibits the synthesis of phosphoadenosine phosphosulfate (PAPS), the universal donor for sulfotransferases. Thereby, sodium chlorate blocks the sulfation of GAGs. This treatment efficiently reduces the expression level of the sulfation-dependent DSD-1-epitope (Clement et al., 1998; Karus et al., 2012). In order to gain deeper insight in the role of sulfation for the biology of NSPCs, we analyzed the total number of cell divisions and dying cells of control cultures without further addition of sodium chlorate and chlorate-treated (chlorate, $NaClO_3$) progenitors over 2.5 days in phase contrast images obtained by time-lapse video microscopy (**Figure 3**). We noted a 2–3 fold reduction in cell divisions of chlorate-treated progenitors compared to control cultivated in the presence of either EGF or FGF2 (EGF, con: 382 ± 54, EGF+chlorate: 242 ± 36; $p < 0.009$; con $N = 4$, EGF+chlorate $N = 3$; FGF2, con: 477 ± 57, FGF2+chlorate: 182 ± 36; $p < 0.001$; con $N = 4$, FGF2+chlorate $N = 3$) (**Figure 3A**). Interestingly, the rate of cell death of spinal cord progenitors maintained in EGF was increased upon sodium chlorate treatment in comparison to the control, whereas progenitors kept in FGF2 and chlorate were barely affected in their survival (EGF, con: 35 ± 2, EGF+chlorate: 59 ± 6; $p < 0.001$ con $N = 4$, EGF+chlorate $N = 3$; FGF2, con: 33 ± 6, FGF2+chlorate: 32 ± 7; con $N = 4$, FGF2+chlorate $N = 3$) (**Figure 3B**). These results reveal the importance of sulfated GAGs for cell division and cell survival of spinal cord progenitors.

## Time-Lapse Video Microscopy Gives Insight Into Cell Cycle Behavior of Spinal Cord Progenitors

Sulfation of spinal cord progenitors is important for normal cell cycle progression, because inhibition of sulfation maintained more cells in the G2-phase and less on the M-phase of the cell cycle at embryonic stage E12.5, a phase of intense proliferation (Karus et al., 2012). With the aim to clarify the role of sulfated GAGs for the cell cycle in more detail, time-lapse video microscopy and single cell tracking of E15.5 spinal cord progenitors was performed. In this setting, cell divisions can be conveniently spotted and counted on the culture substrate, as reported previously (May et al., 2018). Thereby, the proliferative activity in the culture could be estimated. Dying cells could be identified as the cell bodies shrunk and eventually disappeared from the culture substrate. We compared untreated with chlorate treated progenitors exposed to EGF and FGF2. After 90 h, control progenitors proliferated and showed a higher cell density under both EGF (**Supplementary Movie 1**) and FGF2 (**Supplementary Movie 3**) conditions (**Figure 4A**). In contrast, the cell density visible after chlorate treatment was lower (**Figure 4A**). The focus of the current investigation was on the proliferation behavior of progenitors. Therefore, individual dividing cells were traced through several generations and their pedigrees constructed. Representative lineage trees of control progenitors showed synchronous cell cycles with a symmetric division mode of sibling cells exposed to EGF and FGF2 (**Figures 4B,D**, respectively). This phenomenon could also be observed for progenitors cultivated

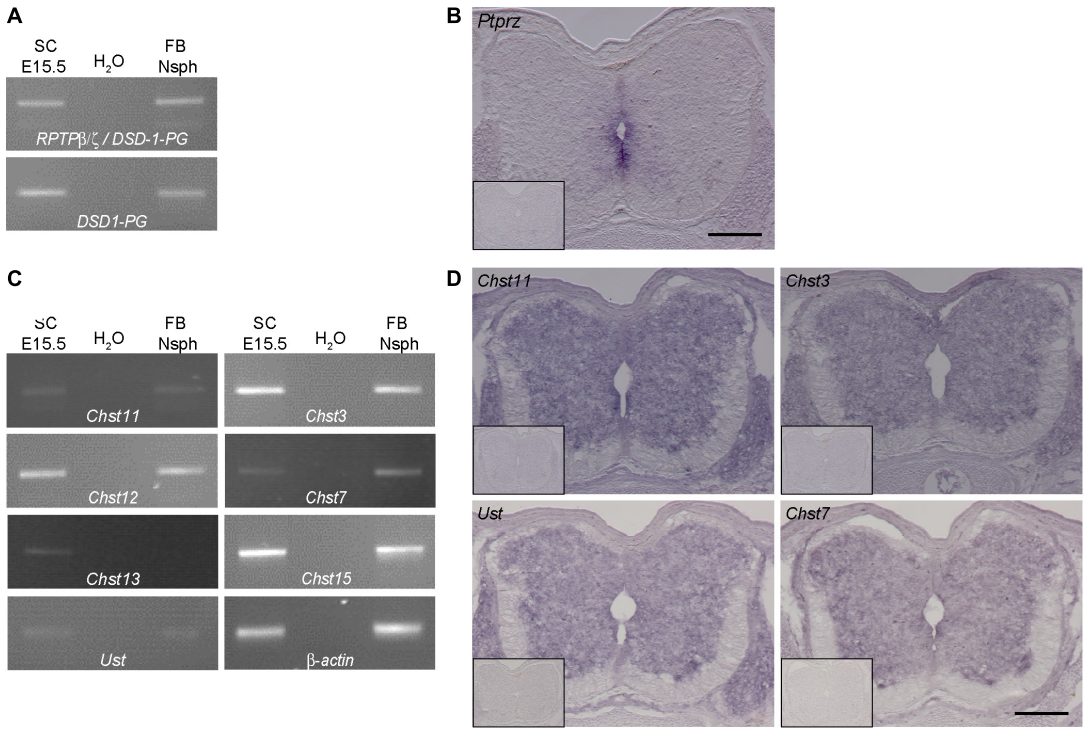


**FIGURE 2 |** Expression analysis of RPTP-β/ζ /DSD-1-PG and CS-/DS-sulfotransferases in the developing spinal cord. **(A)** RT-PCR analysis revealed the presence of *DSD-1-PG/phosphacan* and RPTP-β/ζ mRNAs in tissue isolated from E15.5 spinal cords (E15.5 SC). The isoforms could be detected individually using primers located in the specific sequences of the mRNA (Garwood et al., 1999). **(B)** The mRNA of the *ptprz1* gene coding for a constant part of the RPTP-β/ζ and DSD-1 proteoglycan sequences was produced by cells surrounding the central canal, as could be seen by *in situ* hybridizations. Sections that were incubated with the sense riboprobe did not show any positive signals (insert). **(C)** *Chst11, Chst12, Chst13, Chst3,* and *Chst7* as well as *Chst15* and *Ust* genes could be detected in E15.5 spinal cord mRNA via RT-PCR. A representative spinal cord sample is shown together with the no-template control ($H_2O$) and a positive control consisting of cDNA from neurospheres derived from embryonic brain tissue (Akita et al., 2008). Interestingly, although not present in telencephalic mRNA *Chst13* could be detected in E15.5 spinal cord tissue. β-*Actin* served as the reference gene. **(D)** Representative *in situ* hybridizations on E15.5 spinal cord sections showed positive signals for *Chst3, Chst7, Chst11, and Ust* in the central and intermediate zones of the spinal cord, but not in the marginal layer. Sulfotransferase message could be detected in the ventral as well as the dorsal spinal cord and the DRG. Sense controls (inserts) did not show detectable signals. Scale bars: 200 μm.

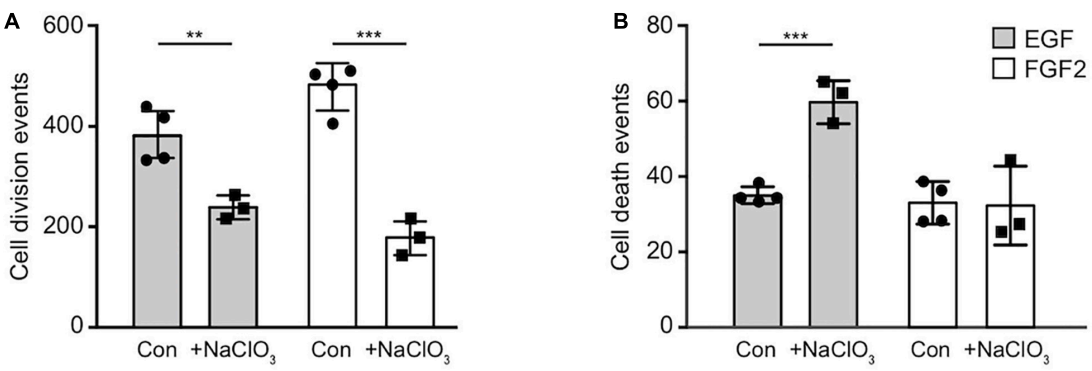


**FIGURE 3 |** Inhibition of sulfation reduced the cell division both in response to EGF and FGF2 and increased cell death in an EGF-dependent manner. The total number of cell divisions and events of cell death was analyzed over a period of 2.5 days recorded by time-lapse video microscopy. **(A)** There was a strong reduction in the number of cell divisions of spinal cord progenitors exposed to either EGF or FGF2 caused by exposure to chlorate. **(B)** Cell death rates of progenitors appeared enhanced when treated with chlorate in the presence of EGF. Error bars indicate SD, $^{**}p \leq 0.01$, $^{***}p \leq 0.001$ (*t*-test); $N = 3$.

with chlorate and EGF (**Figure 4C** and **Supplementary Movie 2**). In contrast, chlorate-treated progenitors in the presence of FGF2 displayed a markedly different behavior (**Supplementary Movie 4**). The division mode appeared asymmetric and the sibling cells divided less synchronously (**Figure 4E**). Quantification of the cell cycle length illustrated that the mitogen FGF2 accelerated the cell cycle of normally sulfated spinal cord progenitors in the 2nd, 3rd, and 4th generation in comparison with EGF [compare to May et al. (2018)].

## Sodium Chlorate Interfered With the Cell Cycle of Progenitors Exposed to FGF2

Comparing the different generations of every single condition helped to derive an estimate for the cell cycle length (**Supplementary Table 1**). It should be kept in mind that the data of the first generation were not precisely circumscribed, because the cell cycle state of the initially tracked mother cell was unknown when the tracking began. Therefore, the depicted time frames appear shorter than in the subsequent generations. In the second generation, the cell cycle length was the longest of all conditions, decreased with ongoing generation, and finally reached equivalence between control and treatment condition (**Figure 5** and **Supplementary Table 1**). However, the inhibition of sulfation in the presence of FGF2 notably changed the behavior of the progenitors and led to an elongated cell cycle length in all generations (**Figure 5** and **Supplementary Table 1**). Untreated control cells were compared with chlorate-treated cells in every single generation. We could observe a particularly strong difference concerning the cell cycle length after inhibition of sulfation in the 3rd, 4th, and 5th generation (**Supplementary Table 1**, **Figures 5C–E**; 3rd generation, con: 15.4 h vs. chlorate: 21.8 h; 4th generation, con: 13.9 h vs. chlorate: 20.8 h; 5th generation, con: 14.8 h vs. chlorate 22.2 h; control $N = 4$, chlorate $N = 3$). We conclude that sulfated GAGs are essential for normal cell cycle progression driven by FGF2.

## Inhibition of Sulfation Does Not Interfere With EGF Signaling

The analysis of the impact of sodium chlorate treatment of progenitors cultivated in the presence of EGF yielded a different result. Apart from generation 3 (**Supplementary Table 1**, **Figure 6C**; con: 18.2 h vs. chlorate: 20.6 h), where chlorate-treated cells divided more slowly than in the control condition, all other generations did not display any significant differences regarding cell cycle length (**Supplementary Table 1** and **Figures 6A–F**). In the light of this result, we conclude that the inhibition of sulfation led to a significant reduction in cell division events and a significant increase of cell death in the presence of EGF (**Figures 3A,B**), but did not affect the lineage progression in spinal cord progenitors.

# DISCUSSION

It is known HS-GAGs are necessary for normal FGF2 signaling and therefore HS-GAGs have an indirect influence on proliferation and differentiation (Eswarakumar et al., 2005; Matsuo and Kimura-Yoshida, 2013; Woodbury and Ikezu, 2014). Sulfated GAGs of proteoglycans play an important role in numerous processes during development and in adulthood (Iozzo and Schaefer, 2015; Wiese and Faissner, 2015; Mikami and Kitagawa, 2017). CS-GAGs are strongly expressed in stem cell niches of the CNS and regulate proliferation and differentiation of progenitors both in the cortex and spinal cord (Engel et al., 1996; Karus et al., 2012; Song and Dityatev, 2018). It has been shown that the DSD-1-epitope, a unique CS-motif, is expressed in the developing spinal cord and on radial glia cells of the cortex. The specific monoclonal antibody 473HD that recognizes the DSD-1-epitope reduces neurosphere formation when added to NSPC cultures, which reflects a functional role of the epitope in the stem cell niche (von Holst et al., 2006; Karus et al., 2012). The enzymatic digestion of specific CS-motifs by ChABC *in vivo* and *in vitro* decreases proliferation and self-renewal of telencephalic progenitors. Furthermore, this treatment leads to an increased number of differentiated astrocytes at the expense of neurons in a neurosphere differentiation assay (Sirko et al., 2007, 2010b). In contrast, spinal cord progenitors generate more immature neurons after inhibition of sulfation *in vitro* (Karus et al., 2012).

The proteoglycans of the RPTP-β/ζ family with its soluble member DSD-1-PG, the mouse homolog of phosphacan (Garwood et al., 1999; Faissner et al., 2006) were detected in the E15.5 spinal cord. Its presence in the close vicinity to neural stem and progenitor cells has been observed before in other CNS regions and developmental stages (von Holst et al., 2006; Sirko et al., 2007, 2010b; Akita et al., 2008; Klausmeyer et al., 2011; Karus et al., 2012), but whether these cells are indeed the source for these proteoglycans was unknown. We confirmed this by *in situ* hybridizations for the determining gene construct of *ptprz1* detecting the mRNAs of the RPTP-β/ζ transmembrane receptors and DSD-1-PG/phosphacan, the proteoglycan isoform derived therefrom. The signals surrounded the central canal of the spinal cord where the cell bodies of the progenitors are located. Immunohistochemistry with antibodies revealed the distribution of the molecules along the radial glia cell fibers stretching from the central canal to the surface of the spinal cord. The distribution of RPTP-β/ζ isoforms follows a gradient, with a more pronounced expression toward the ventral half of the spinal cord, where the motoneurons are located (Wiese and Faissner, 2015). Interestingly, motoneuron axons are guided by RPTP-β/ζ variants *in vitro* (Klausmeyer et al., 2011). The differential distribution may reflect diffusion of the proteoglycan and immobilization by specific receptor systems or an intrinsic difference of dorsal versus ventrally located NSPCs. We have reported that astrocyte progenitors assemble in the ventral half of the spinal cord at E15.5 (Karus et al., 2011). Significant heterogeneity of astrocytes has been concluded from transcriptome studies and bioinformatic analysis (John Lin et al., 2017; Fu et al., 2021). However, tools to enrich and separately study these asserted subpopulations in the spinal cord still remain to be developed.

Although the proteoglycans of the RPTP-β/ζ family are restricted to the CNS, the CS-GAG chains associated with these proteoglycans are widely distributed. Thus, the particular DSD-1 carbohydrate structure that is recognized by the mAb 473HD

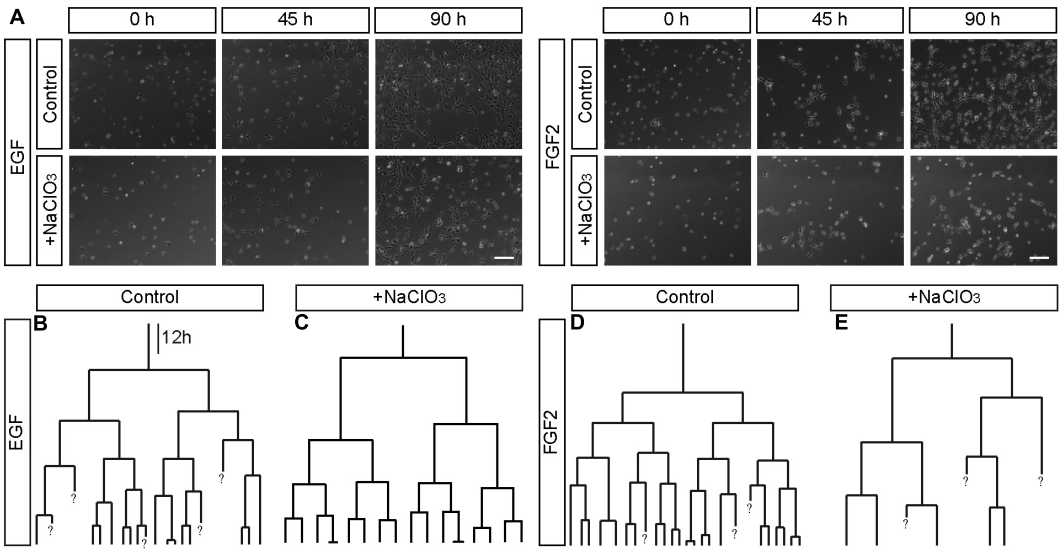


**FIGURE 4 |** Representative phase contrast images and lineage trees of spinal cord progenitors *in vitro*. **(A)** Phase contrast images obtained by time-lapse video microscopy at 0, 45, and 90 h of untreated (control, con) and chlorate-treated ($NaClO_3$) spinal cord progenitors exposed to EGF or FGF2. Untreated progenitors displayed higher cell densities after 90 h of cultivation than chlorate-treated cells. Additionally to the phase contrast images, exemplary movie sequences of all four conditions are included (**Supplementary Movies 1–4**). **(B–E)** Representative lineage trees of control and chlorate treated progenitors tracked in the presence of EGF **(B,C)** or FGF2 **(D,E)** are shown. There were some apparent differences between untreated control cells **(B,D)** and those exposed to inhibition of sulfation [$NaClO_3$, **(C,E)**]. The cell divisions of most sibling-cells occurred in a highly synchronous way. Chlorate-treated cells in the presence of FGF2 divided asynchronously in comparison to control cells and produced strongly distorted lineage trees. A question mark "?" indicates cells which were not traceable any further. Scale bar: 100 μm. The dataset of the control has been used in a previous study conducted in parallel (May et al., 2018).

is attached to the long receptor form of RPTP-β/ζ and to DSD-1-PG, which appear to be the major, if not exclusive core carrier proteins in the central nervous system (Faissner et al., 1994; Garwood et al., 1999). However, immunohistochemistry detected the epitope also in cartilage where CSPGs such as aggrecan, decorin and biglycan are prominent, as well as the HSPGs perlecan, the syndecans and glypicans (Knudson and Knudson, 2001). The strong interaction of the 473HD antibody with the CS-domain D from shark cartilage has been shown in a detailed epitope characterization (Ito et al., 2005). An association with versican and decorin in the human sciatic nerve has been previously inferred (Braunewell et al., 1995). Thus, the DSD-1-epitope is presumably exposed by other core proteins in embryonic mesenchyme derived tissues.

The CS/DS-proteoglycan side chains are modified by sulfotransferases that add sulfate groups to the GAGs at 2-S, 4-S, or 6-S positions, which generates docking sites for a variety of proteins (Sugahara and Mikami, 2007; Purushothaman et al., 2012). A family of specialized enzymes creates a production line that modifies the glycan chains and restructures the CS-GAG structure and charge. We could detect the mRNA expression of diverse sulfotransferases that modify CSPGs (Akita et al., 2008; Mikami and Kitagawa, 2017) and found that the enzyme Chst13 is exclusively present in the spinal cord, but not in the forebrain neurosphere mRNA that we used as control. This is consistent with previous results where Chst13 could not be detected in forebrain tissue (Akita et al., 2008). The analysis of the four sulfotransferases that we analyzed by *in situ* hybridizations revealed expression in the cellular compartment of the developing spinal cord and in the adjacent tissues of the dorsal root ganglia. The enzymes modify GAG chains of the CSPG and DSPG types of which different members control cellular events in diverse tissues and are not clearly restricted to the central nervous system. Keratinocytes for example show hyperproliferation in a knockout model of Chst3 (Kitazawa et al., 2021). In contrast, the overexpression of another sulfotransferase, Chst15, is associated with tumor growth in pancreatic cancer (Matsuda et al., 2019). Interestingly, several reports have highlighted a significant role of sulfotransferases in the context of human pathophysiology, e.g., in the connective tissue (Mizumoto et al., 2013). As the DSD-1-epitope comprises the CS-D-A-D motif, at least the three distinct sulfotransferases are required for the biosynthesis of the A-, C-, and D-unit (Ito et al., 2005; Miyata and Kitagawa, 2017). The analysis of their respective roles for NSPC proliferation represents a challenging task for future studies.

Although proteoglycans are involved in cell proliferation little is known about the influence of the sulfated GAGs on the cell cycle itself. That is why we focused on the analysis of the cell cycle length of spinal cord progenitors by the use of time-lapse video microscopy and single cell tracking. The cell division events of progenitors treated with sodium chlorate were dramatically reduced compared to untreated progenitors. Inhibition of sulfation intensively interfered with FGF2-dependent cell cycle progression and altered the division mode. Generally, progenitors exposed to FGF2 divided faster

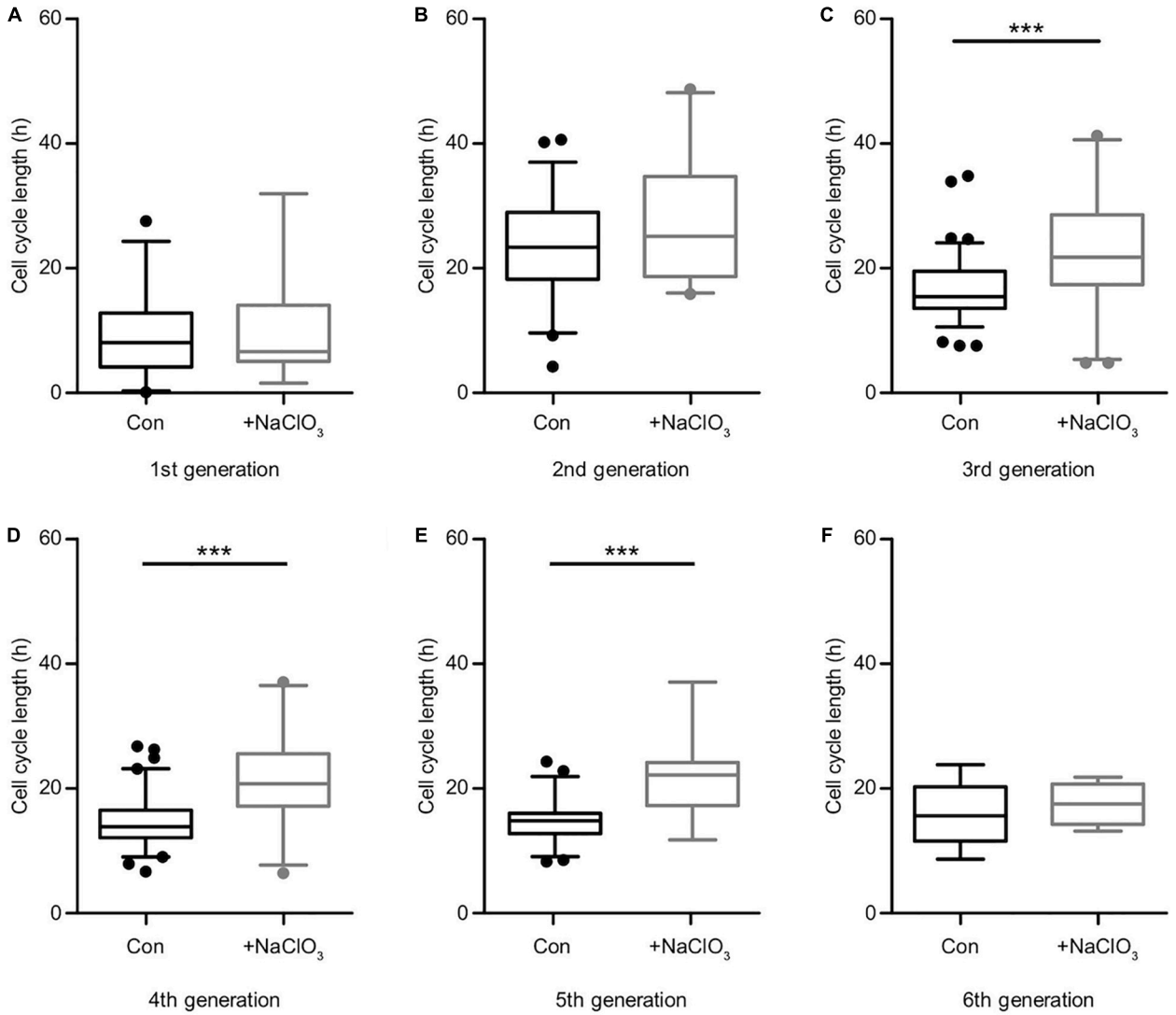


**FIGURE 5 |** Suppression of sulfation lengthened the cell cycle in the presence of FGF2. Cell cycle lengths of control (black boxes) versus chlorate-treated (gray boxes) spinal cord progenitors maintained in the presence of FGF2 were compared. The cells from the first generation **(A)** were captured at different starting points of their division cycle and could only be tracked for an undefined portion of the running cell cycle. From the second generation **(B)** on the cell cycle lengths could be compared statistically. The inhibition of sulfation led to a slower cell division of progenitors treated with chlorate. The prolongation of the cell cycle was particularly striking between the 3rd up to the 5th round of division **(C–E)**. The sixth generation **(F)** was only traceable for a few cells (compare to the lineage tree in **Figure 4E**) ***$p \leq 0.001$ (Mann–Whitney *U*-test); con: $N = 4$; chlorate: $N = 3$.

compared with EGF treated progenitors, but after inhibition of the sulfation we observed the opposite effect. NSPCs from the embryonic spinal cord only sparsely display mitotic events without growth factor treatment (data not shown). It is assumed that the addition of growth factors to the medium overall reduces the cell cycle length. This has in fact been confirmed for adult neural stem cells of the subventricular zone, which are able to proliferate *in vitro* also in the absence of any exogenously supplied factors (Costa et al., 2011).

Sodium chlorate inhibits the synthesis of the universal sulfate donor PAPS and thereby also interferes with the sulfation of proteins (Baeuerle and Huttner, 1986). Sulfation of proteins is operated by tyrosylprotein sulfotransferases (TPST1 and TPST2 enzymes) and occurs at free tyrosine residues (Beisswanger et al., 1998). It has been reported for a number of proteins, where it may contribute to sorting and protein interactions. The biological functions of protein tyrosine sulfation are presently not well understood and under ongoing investigation (Yang et al., 2015). However, there is general agreement that sodium chlorate treatment is not toxic for animal cells in culture (Baeuerle and Huttner, 1986; Clement et al., 1998). Along these lines, as the treatment of neural cells with sodium chlorate also does not reduce the expression levels of the carrier core proteins DSD-1PG/phosphacan and RPTP-β/ζ (Akita et al., 2008), we are

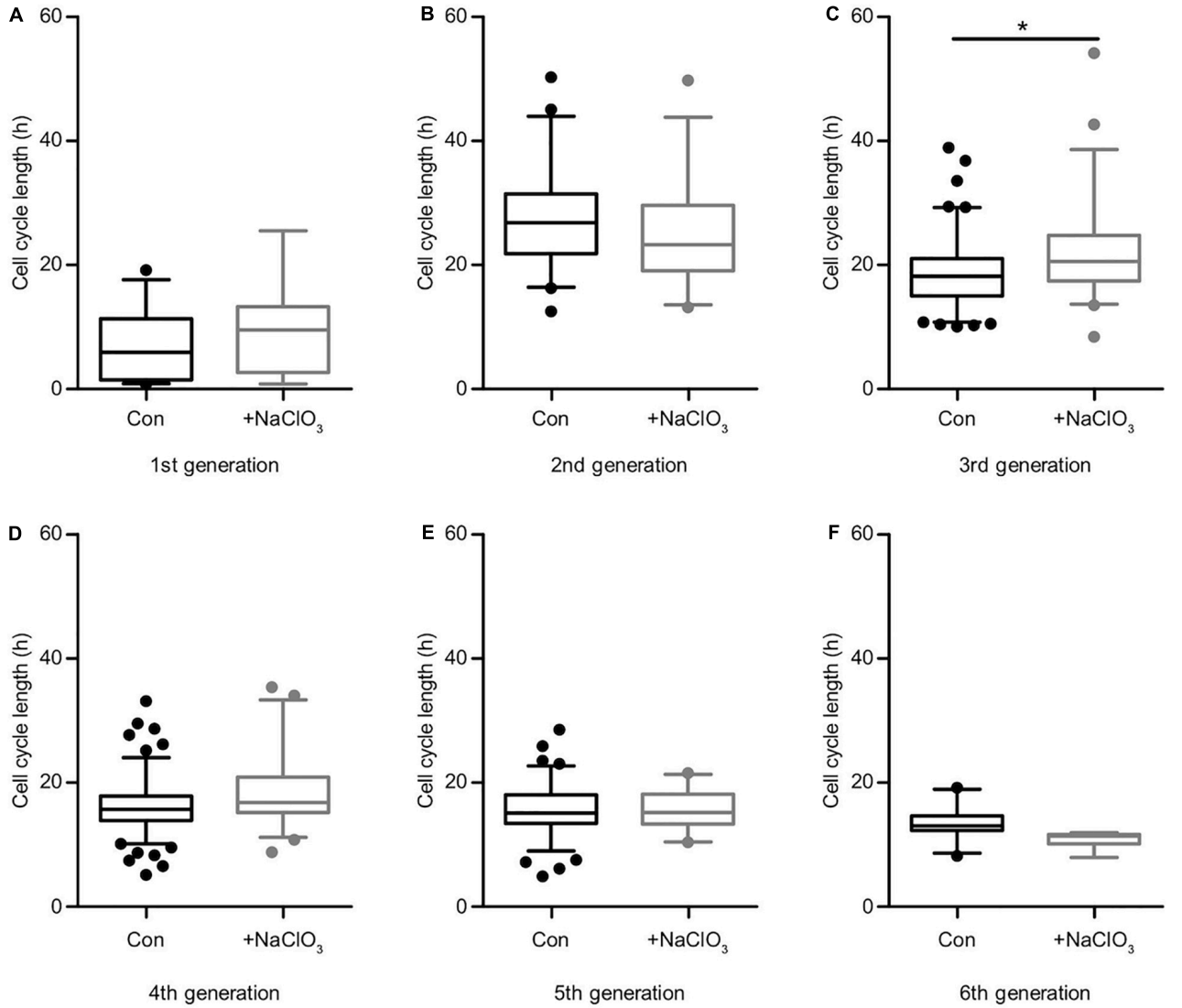


**FIGURE 6 |** Sulfation of spinal cord progenitors had a minor influence on the cell cycle in the presence of EGF. The cell cycle lengths of control (black boxes) and chlorate-treated (gray boxes) spinal cord progenitors cultivated in the presence of EGF are shown for the first **(A)**, second **(B)**, third **(C)**, fourth **(D)**, fifth **(E)** and the sixth generation **(F)**. In the third generation **(C)** the inhibition of sulfation led to a slightly slower cell division compared to untreated cells. In all other generations, the suppression of sulfation had no significant influence on the cell cycle length. $^{*}p \leq 0.05$ (Mann-Whitney *U*-test); control: $N = 4$; chlorate: $N = 3$.

convinced that the major impact of sodium chlorate in our studies targeted the GAG-compartment.

Heparan sulfate GAGs are expressed in the subventricular zone of the CNS and are involved in the FGF2 signaling pathway (Lamanna et al., 2008; Yamaguchi et al., 2010; Matsuo and Kimura-Yoshida, 2013; Ravikumar et al., 2020). Interference with FGF2 signaling by the use of sodium chlorate led to a longer cell cycle length of spinal cord progenitors. This is in line with previous findings where less neurospheres were generated after inhibition of sulfation and exposure to FGF2 (Karus et al., 2012). The FGF2 signaling pathway is disrupted, because FGF2 needs a specific HS-GAG-motif to bind the FGF-receptor (Bowman and Bertozzi, 1999). In contrast, EGF does not bind to HSPGs (Higashiyama et al., 1993) and accordingly, EGF-dependent cell cycling is not critically affected by chlorate treatment in our experiments. CS-GAGs also play a role, because treatment of telencephalic NSPCs with ChABC reduced proliferation in response to FGF2, but not to EGF (Sirko et al., 2010b). Although we could measure only a minor influence of EGF on the cell cycle length of progenitors after sodium chlorate treatment, the total number of cell divisions was reduced. This effect was even more severe when the cells where exposed to FGF2. However, the rate of cell death in response to chlorate exposure was only increased in NSPCs cultivated in the presence of EGF. This was surprising, because it has been reported that sodium chlorate is not toxic for cells (Baeuerle and Huttner, 1986; Karus et al., 2012). On the other hand, chlorate treatment results in a relative accumulation of cells in the G2-phase of the cell cycle, which

predisposes for cell death (Rieder, 2011; Karus et al., 2012). In agreement with this finding, NSPCs with suppressed sulfation displayed a longer cell cycle. Interestingly, HS-GAGs that are also targeted by chlorate are required to leave the self-renewal mode and switch to differentiation (Kraushaar et al., 2010).

In summary, we provide evidence that sulfated proteoglycans have an impact on the cell cycle of spinal cord progenitors. Different from approaches that were based on the degradation of CS-GAGs by chondroitinases we focused on the sulfation of the GAG-chains and demonstrate that these exert intrinsic effects on their own, independently of the core protein. Thereby, the results of the present study extend previous findings and illustrate the heterogeneity of the functions of GAGs and the importance of specific sulfation patterns for EGF and notably FGF2 related signaling and cell cycle progression.

## DATA AVAILABILITY STATEMENT

The raw data supporting the conclusions of this article will be made available by the authors, without undue reservation.

## ETHICS STATEMENT

Wild-type SV129 mice (*Mus musculus*) were used in accordance with the European Council Directive of September 22, 2010 (2010/63/EU) for care of laboratory animals and approved by the animal care committee of North Rhine-Westphalia, Germany, based at the LANUV (Landesamt für Umweltschutz, Naturschutz und Verbraucherschutz, Nordrhein-Westphalen, Recklinghausen, Germany). The study was supervised by the animal welfare commissioner of Ruhr-University.

## AUTHOR CONTRIBUTIONS

ES performed the experiments, analyzed the data, wrote the manuscript, and prepared the figures. UT developed the experimental design, performed the experiments, analyzed the data, and wrote the manuscript. MM performed the video microscopy experiments, analyzed the data, and wrote the manuscript. KL performed the video microscopy experiments. TS developed the video microscopy analysis and provided the software. AF developed the experimental design, supervised the work, revised the manuscript, and funded the study. All authors have read and approved the manuscript.

## FUNDING

We are grateful for grant support by the German Research Foundation (DFG, SPP 1757/1,2 and FA 159/20-1,2) to AF. We acknowledge support by the DFG Open Access Publication Funds of the Ruhr-Universität Bochum.

## ACKNOWLEDGMENTS

We thank Prof. Magdalena Götz for critical comments on the manuscript and for hosting ES during a training stage in her laboratory and the introduction to the method of video microscopy, Anke Mommsen for excellent technical assistance, and Lars Roll for supervising the animal colony. The phosphacan/ RPTPβ/ζ riboprobe was generated by Aliana Neubaur in the course of her project. We also thank Prof. Stefan Wiese for the Isl-1/2 antibody and helpful discussions.

## SUPPLEMENTARY MATERIAL

The Supplementary Material for this article can be found online at: https://www.frontiersin.org/articles/10.3389/fcell.2021.643060/full#supplementary-material

## REFERENCES

Akita, K., von Holst, A., Furukawa, Y., Mikami, T., Sugahara, K., and Faissner, A. (2008). Expression of multiple chondroitin/dermatan sulfotransferases in the neurogenic regions of the embryonic and adult central nervous system implies that complex chondroitin sulfates have a role in neural stem cell maintenance. *Stem Cells* 26, 798–809. doi: 10.1634/stemcells.2007-0448

Baeuerle, P. A., and Huttner, W. B. (1986). Chlorate–a potent inhibitor of protein sulfation in intact cells. *Biochem. Biophys. Res. Commun.* 141, 870–877. doi: 10.1016/s0006-291x(86)80253-4

Barros, C. S., Franco, S. J., and Muller, U. (2011). Extracellular matrix: functions in the nervous system. *Cold Spring Harb. Perspect. Biol.* 3:a005108. doi: 10.1101/cshperspect.a005108

Beisswanger, R., Corbeil, D., Vannier, C., Thiele, C., Dohrmann, U., Kellner, R., et al. (1998). Existence of distinct tyrosylprotein sulfotransferase genes: molecular characterization of tyrosylprotein sulfotransferase-2. *Proc. Natl. Acad. Sci. U.S.A.* 95, 11134–11139. doi: 10.1073/pnas.95.19.11134

Bowman, K. G., and Bertozzi, C. R. (1999). Carbohydrate sulfotransferases: mediators of extracellular communication. *Chem. Biol.* 6, R9–R22. doi: 10.1016/S1074-5521(99)80014-3

Braunewell, K. H., Martini, R., LeBaron, R., Kresse, H., Faissner, A., Schmitz, B., et al. (1995). Up-regulation of a chondroitin sulphate epitope during regeneration of mouse sciatic nerve: evidence that the immunoreactive molecules are related to the chondroitin sulphate proteoglycans decorin and versican. *Eur. J. Neurosci.* 7, 792–804. doi: 10.1111/j.1460-9568.1995.tb00682.x

Clement, A. M., Nadanaka, S., Masayama, K., Mandl, C., Sugahara, K., and Faissner, A. (1998). The DSD-1 carbohydrate epitope depends on sulfation, correlates with chondroitin sulfate D motifs, and is sufficient to promote neurite outgrowth. *J. Biol. Chem.* 273, 28444–28453. doi: 10.1074/jbc.273.43.28444

Costa, M. R., Ortega, F., Brill, M. S., Beckervordersandforth, R., Petrone, C., Schroeder, T., et al. (2011). Continuous live imaging of adult neural stem cell division and lineage progression in vitro. *Development* 138, 1057–1068. doi: 10.1242/dev.061663

Eilken, H. M., Nishikawa, S., and Schroeder, T. (2009). Continuous single-cell imaging of blood generation from haemogenic endothelium. *Nature* 457, 896–900. doi: 10.1038/nature07760

Engel, M., Maurel, P., Margolis, R. U., and Margolis, R. K. (1996). Chondroitin sulfate proteoglycans in the developing central nervous system. I. cellular sites of synthesis of neurocan and phosphacan. *J. Comp. Neurol.* 366, 34–43. doi: 10.1002/(sici)1096-9861(19960226)366:1<34::aid-cne3>3.0.co;2-l

Eswarakumar, V. P., Lax, I., and Schlessinger, J. (2005). Cellular signaling by fibroblast growth factor receptors. *Cytokine Growth Factor Rev.* 16, 139–149. doi: 10.1016/j.cytogfr.2005.01.001

Faissner, A., Clement, A., Lochter, A., Streit, A., Mandl, C., and Schachner, M. (1994). Isolation of a neural chondroitin sulfate proteoglycan with neurite outgrowth promoting properties. *J. Cell Biol.* 126, 783–799. doi: 10.1083/jcb.126.3.783

Faissner, A., Heck, N., Dobbertin, A., and Garwood, J. (2006). DSD-1-Proteoglycan/Phosphacan and receptor protein tyrosine phosphatase-beta isoforms during development and regeneration of neural tissues. *Adv. Exp. Med. Biol.* 557, 25–53. doi: 10.1007/0-387-30128-3_3

Faissner, A., and Reinhard, J. (2015). The extracellular matrix compartment of neural stem and glial progenitor cells. *Glia* 63, 1330–1349. doi: 10.1002/glia.22839

Faissner, A., Roll, L., and Theocharidis, U. (2017). Tenascin-C in the matrisome of neural stem and progenitor cells. *Mol. Cell Neurosci.* 81, 22–31. doi: 10.1016/j.mcn.2016.11.003

Fu, Y., Yang, M., Yu, H., Wang, Y., Wu, X., Yong, J., et al. (2021). Heterogeneity of glial progenitor cells during the neurogenesis-to-gliogenesis switch in the developing human cerebral cortex. *Cell Rep.* 34:108788. doi: 10.1016/j.celrep.2021.108788

Garwood, J., Schnadelbach, O., Clement, A., Schutte, K., Bach, A., and Faissner, A. (1999). DSD-1-proteoglycan is the mouse homolog of phosphacan and displays opposing effects on neurite outgrowth dependent on neuronal lineage. *J. Neurosci.* 19, 3888–3899. doi: 10.1523/jneurosci.19-10-03888.1999

Higashiyama, S., Abraham, J. A., and Klagsbrun, M. (1993). Heparin-binding EGF-like growth factor stimulation of smooth muscle cell migration: dependence on interactions with cell surface heparan sulfate. *J. Cell Biol.* 122, 933–940. doi: 10.1083/jcb.122.4.933

Hilsenbeck, O., Schwarzfischer, M., Skylaki, S., Schauberger, B., Hoppe, P. S., Loeffler, D., et al. (2016). Software tools for single-cell tracking and quantification of cellular and molecular properties. *Nat. Biotechnol.* 34, 703–706. doi: 10.1038/nbt.3626

Hoppe, P. S., Schwarzfischer, M., Loeffler, D., Kokkaliaris, K. D., Hilsenbeck, O., Moritz, N., et al. (2016). Early myeloid lineage choice is not initiated by random PU.1 to GATA1 protein ratios. *Nature* 535, 299–302. doi: 10.1038/nature18320

Hynes, R. O., and Naba, A. (2012). Overview of the matrisome–an inventory of extracellular matrix constituents and functions. *Cold Spring Harb. Perspect. Biol.* 4:a004903. doi: 10.1101/cshperspect.a004903

Iozzo, R. V., and Schaefer, L. (2015). Proteoglycan form and function: a comprehensive nomenclature of proteoglycans. *Matrix Biol.* 42, 11–55. doi: 10.1016/j.matbio.2015.02.003

Ito, Y., Hikino, M., Yajima, Y., Mikami, T., Sirko, S., von Holst, A., et al. (2005). Structural characterization of the epitopes of the monoclonal antibodies 473HD, CS-56, and MO-225 specific for chondroitin sulfate D-type using the oligosaccharide library. *Glycobiology* 15, 593–603. doi: 10.1093/glycob/cwi036

John Lin, C. C., Yu, K., Hatcher, A., Huang, T. W., Lee, H. K., Carlson, J., et al. (2017). Identification of diverse astrocyte populations and their malignant analogs. *Nat. Neurosci.* 20, 396–405. doi: 10.1038/nn.4493

Karus, M., Denecke, B., ffrench-Constant, C., Wiese, S., and Faissner, A. (2011). The extracellular matrix molecule tenascin C modulates expression levels and territories of key patterning genes during spinal cord astrocyte specification. *Development* 138, 5321–5331. doi: 10.1242/dev.067413

Karus, M., Samtleben, S., Busse, C., Tsai, T., Dietzel, I. D., Faissner, A., et al. (2012). Normal sulfation levels regulate spinal cord neural precursor cell proliferation and differentiation. *Neural Dev.* 7:20. doi: 10.1186/1749-8104-7-20

Kitazawa, K., Nadanaka, S., Kadomatsu, K., and Kitagawa, H. (2021). Chondroitin 6-sulfate represses keratinocyte proliferation in mouse skin, which is associated with psoriasis. *Commun. Biol.* 4:114. doi: 10.1038/s42003-020-01618-5

Klausmeyer, A., Conrad, R., Faissner, A., and Wiese, S. (2011). Influence of glial-derived matrix molecules, especially chondroitin sulfates, on neurite growth and survival of cultured mouse embryonic motoneurons. *J. Neurosci. Res.* 89, 127–141. doi: 10.1002/jnr.22531

Knudson, C. B., and Knudson, W. (2001). Cartilage proteoglycans. *Semin. Cell Dev. Biol.* 12, 69–78. doi: 10.1006/scdb.2000.0243

Kraushaar, D. C., Yamaguchi, Y., and Wang, L. (2010). Heparan sulfate is required for embryonic stem cells to exit from self-renewal. *J. Biol. Chem.* 285, 5907–5916. doi: 10.1074/jbc.M109.066837

Lamanna, W. C., Frese, M. A., Balleininger, M., and Dierks, T. (2008). Sulf loss influences N-, 2- O-, and 6-O-sulfation of multiple heparan sulfate proteoglycans and modulates fibroblast growth factor signaling. *J. Biol. Chem.* 283, 27724–27735. doi: 10.1074/jbc.M802130200

Lang, B. T., Cregg, J. M., DePaul, M. A., Tran, A. P., Xu, K., Dyck, S. M., et al. (2015). Modulation of the proteoglycan receptor PTPsigma promotes recovery after spinal cord injury. *Nature* 518, 404–408. doi: 10.1038/nature13974

Maeda, N. (2015). Proteoglycans and neuronal migration in the cerebral cortex during development and disease. *Front. Neurosci.* 9:98. doi: 10.3389/fnins.2015.00098

Matsuda, Y., Fujii, Y., Matsukawa, M., Ishiwata, T., Nishimura, M., and Arai, T. (2019). Overexpression of carbohydrate sulfotransferase 15 in pancreatic cancer stroma is associated with worse prognosis. *Oncol. Lett.* 18, 4100–4105. doi: 10.3892/ol.2019.10764

Matsuo, I., and Kimura-Yoshida, C. (2013). Extracellular modulation of Fibroblast Growth Factor signaling through heparan sulfate proteoglycans in mammalian development. *Curr. Opin. Genet. Dev.* 23, 399–407. doi: 10.1016/j.gde.2013.02.004

Maurel, P., Rauch, U., Flad, M., Margolis, R. K., and Margolis, R. U. (1994). Phosphacan, a chondroitin sulfate proteoglycan of brain that interacts with neurons and neural cell-adhesion molecules, is an extracellular variant of a receptor-type protein tyrosine phosphatase. *Proc. Natl. Acad. Sci. U.S.A.* 91, 2512–2516. doi: 10.1073/pnas.91.7.2512

May, M., Denecke, B., Schroeder, T., Gotz, M., and Faissner, A. (2018). Cell tracking in vitro reveals that the extracellular matrix glycoprotein Tenascin-C modulates cell cycle length and differentiation in neural stem/progenitor cells of the developing mouse spinal cord. *Biol. Open* 7:bio027730. doi: 10.1242/bio.027730

Mikami, T., and Kitagawa, H. (2017). Sulfated glycosaminoglycans: their distinct roles in stem cell biology. *Glycoconj J.* 34, 725–735. doi: 10.1007/s10719-016-9732-9

Miyata, S., and Kitagawa, H. (2017). Formation and remodeling of the brain extracellular matrix in neural plasticity: roles of chondroitin sulfate and hyaluronan. *Biochim. Biophys. Acta Gen. Subj.* 1861, 2420–2434. doi: 10.1016/j.bbagen.2017.06.010

Mizumoto, S., Ikegawa, S., and Sugahara, K. (2013). Human genetic disorders caused by mutations in genes encoding biosynthetic enzymes for sulfated glycosaminoglycans. *J. Biol. Chem.* 288, 10953–10961. doi: 10.1074/jbc.R112.437038

Naba, A., Clauser, K. R., Hoersch, S., Liu, H., Carr, S. A., and Hynes, R. O. (2012). The matrisome: in silico definition and in vivo characterization by proteomics of normal and tumor extracellular matrices. *Mol. Cell Proteomics* 11:M111014647. doi: 10.1074/mcp.M111.014647

Purushothaman, A., Sugahara, K., and Faissner, A. (2012). Chondroitin sulfate "wobble motifs" modulate maintenance and differentiation of neural stem cells and their progeny. *J. Biol. Chem.* 287, 2935–2942. doi: 10.1074/jbc.R111.298430

Ravikumar, M., Smith, R. A. A., Nurcombe, V., and Cool, S. M. (2020). Heparan sulfate proteoglycans: key mediators of stem cell function. *Front. Cell Dev. Biol.* 8:581213. doi: 10.3389/fcell.2020.581213

Rieder, C. L. (2011). Mitosis in vertebrates: the G2/M and M/A transitions and their associated checkpoints. *Chromosome Res.* 19, 291–306. doi: 10.1007/s10577-010-9178-z

Rieger, M. A., Hoppe, P. S., Smejkal, B. M., Eitelhuber, A. C., and Schroeder, T. (2009). Hematopoietic cytokines can instruct lineage choice. *Science* 325, 217–218. doi: 10.1126/science.1171461

Schnadelbach, O., Mandl, C., and Faissner, A. (1998). Expression of DSD-1-PG in primary neural and glial-derived cell line cultures, upregulation by TGF-beta, and implications for cell-substrate interactions of the glial cell line Oli-neu. *Glia* 23, 99–119. doi: 10.1002/(sici)1098-1136(199806)23:2<99::aid-glia2>3.0.co;2-z

Shen, Y., Tenney, A. P., Busch, S. A., Horn, K. P., Cuascut, F. X., Liu, K., et al. (2009). PTPsigma is a receptor for chondroitin sulfate proteoglycan, an inhibitor of neural regeneration. *Science* 326, 592–596. doi: 10.1126/science.1178310

Sirko, S., Akita, K., Von Holst, A., and Faissner, A. (2010a). Structural and functional analysis of chondroitin sulfate proteoglycans in the neural stem cell niche. *Methods Enzymol.* 479, 37–71. doi: 10.1016/S0076-6879(10)79003-0

Sirko, S., von Holst, A., Weber, A., Wizenmann, A., Theocharidis, U., Gotz, M., et al. (2010b). Chondroitin sulfates are required for fibroblast growth factor-2-dependent proliferation and maintenance in neural stem cells and for epidermal growth factor-dependent migration of their progeny. *Stem Cells* 28, 775–787. doi: 10.1002/stem.309

Sirko, S., von Holst, A., Wizenmann, A., Gotz, M., and Faissner, A. (2007). Chondroitin sulfate glycosaminoglycans control proliferation, radial glia cell differentiation and neurogenesis in neural stem/progenitor cells. *Development* 134, 2727–2738. doi: 10.1242/dev.02871

Smith, D. J., Oliver, C. E., Taylor, J. B., and Anderson, R. C. (2012). Invited review: Efficacy, metabolism, and toxic responses to chlorate salts in food and laboratory animals. *J. Anim. Sci.* 90, 4098–4117. doi: 10.2527/jas.2011-4997

Smith, P. D., Coulson-Thomas, V. J., Foscarin, S., Kwok, J. C., and Fawcett, J. W. (2015). GAG-ing with the neuron": the role of glycosaminoglycan patterning in the central nervous system. *Exp. Neurol.* 274(Pt B), 100–114. doi: 10.1016/j.expneurol.2015.08.004

Song, I., and Dityatev, A. (2018). Crosstalk between glia, extracellular matrix and neurons. *Brain Res. Bull.* 136, 101–108. doi: 10.1016/j.brainresbull.2017.03.003

Sugahara, K., and Mikami, T. (2007). Chondroitin/dermatan sulfate in the central nervous system. *Curr. Opin. Struct. Biol.* 17, 536–545. doi: 10.1016/j.sbi.2007.08.015

Sugahara, K., Mikami, T., Uyama, T., Mizuguchi, S., Nomura, K., and Kitagawa, H. (2003). Recent advances in the structural biology of chondroitin sulfate and dermatan sulfate. *Curr. Opin. Struct. Biol.* 13, 612–620. doi: 10.1016/j.sbi.2003.09.011

Theocharidis, U., Long, K., Ffrench-Constant, C., and Faissner, A. (2014). Regulation of the neural stem cell compartment by extracellular matrix constituents. *Prog. Brain Res.* 214, 3–28. doi: 10.1016/B978-0-444-63486-3.00001-3

von Holst, A., Egbers, U., Prochiantz, A., and Faissner, A. (2007). Neural stem/progenitor cells express 20 tenascin C isoforms that are differentially regulated by Pax6. *J. Biol. Chem.* 282, 9172–9181. doi: 10.1074/jbc.m608067200

von Holst, A., Sirko, S., and Faissner, A. (2006). The unique 473HD-Chondroitinsulfate epitope is expressed by radial glia and involved in neural precursor cell proliferation. *J. Neurosci.* 26, 4082–4094. doi: 10.1523/jneurosci.0422-06.2006

Wiese, S., and Faissner, A. (2015). The role of extracellular matrix in spinal cord development. *Exp. Neurol.* 274(Pt B), 90–99. doi: 10.1016/j.expneurol.2015.05.018

Woodbury, M. E., and Ikezu, T. (2014). Fibroblast growth factor-2 signaling in neurogenesis and neurodegeneration. *J. Neuroimmune. Pharmacol.* 9, 92–101. doi: 10.1007/s11481-013-9501-5

Yamaguchi, Y., Inatani, M., Matsumoto, Y., Ogawa, J., and Irie, F. (2010). Roles of heparan sulfate in mammalian brain development current views based on the findings from Ext1 conditional knockout studies. *Prog. Mol. Biol. Transl. Sci.* 93, 133–152. doi: 10.1016/S1877-1173(10)93007-X

Yang, Y. S., Wang, C. C., Chen, B. H., Hou, Y. H., Hung, K. S., and Mao, Y. C. (2015). Tyrosine sulfation as a protein post-translational modification. *Molecules* 20, 2138–2164. doi: 10.3390/molecules20022138

**Conflict of Interest:** The authors declare that the research was conducted in the absence of any commercial or financial relationships that could be construed as a potential conflict of interest.

frontiers in Cell and Developmental Biology

MINI REVIEW
published: 16 June 2021
doi: 10.3389/fcell.2021.702179

# Axonal Regeneration by Glycosaminoglycan

*Kazuma Sakamoto[1,2]*, Tomoya Ozaki[1] and Kenji Kadomatsu[1,2]*

*[1] Department of Biochemistry, Nagoya University Graduate School of Medicine, Nagoya, Japan, [2] Institute for Glyco-Core Research (iGCORE), Nagoya University, Nagoya, Japan*

Like other biomolecules including nucleic acid and protein, glycan plays pivotal roles in various cellular processes. For instance, it modulates protein folding and stability, organizes extracellular matrix and tissue elasticity, and regulates membrane trafficking. In addition, cell-surface glycans are often utilized as entry receptors for viruses,including SARS-CoV-2. Nevertheless, its roles as ligands to specific surface receptors have not been well understood with a few exceptions such as selectins and siglecs. Recent reports have demonstrated that chondroitin sulfate and heparan sulfate, both of which are glycosaminoglycans, work as physiological ligands on their shared receptor, protein tyrosine phosphatase sigma (PTPσ). These two glycans differentially determine the fates of neuronal axons after injury in our central nervous system. That is, heparan sulfate promotes axonal regeneration while chondroitin sulfate inhibits it, inducing dystrophic endbulbs at the axon tips. In our recent study, we demonstrated that the chondroitin sulfate (CS)-PTPσ axis disrupted autophagy flux at the axon tips by dephosphorylating cortactin. In this minireview, we introduce how glycans work as physiological ligands and regulate their intracellular signaling, especially focusing on chondroitin sulfate.

**Keywords: chondroitin sulfate, heparan sulfate, axonal regeneration, PTPσ, autophagy, dystrophic endbulb**

OPEN ACCESS

***Edited by:***
*Shuji Mizumoto,*
*Meijo University, Japan*

***Reviewed by:***
*Shinji Miyata,*
*Tokyo University of Agriculture and Technology, Japan*
*Jerry Silver,*
*Case Western Reserve University, United States*

****Correspondence:***
*Kazuma Sakamoto*
*sakamoto@med.nagoya-u.ac.jp*

***Specialty section:***
*This article was submitted to Signaling, a section of the journal Frontiers in Cell and Developmental Biology*

***Received:*** *29 April 2021*
***Accepted:*** *25 May 2021*
***Published:*** *16 June 2021*

***Citation:***
*Sakamoto K, Ozaki T and Kadomatsu K (2021) Axonal Regeneration by Glycosaminoglycan. Front. Cell Dev. Biol. 9:702179. doi: 10.3389/fcell.2021.702179*

## INTRODUCTION

The human neural circuit, composed of the central nervous system (CNS) and the peripheral nervous system (PNS), reaches approximately 1 million km and is formed mainly by neural axons. An axon is a structure that is elongated from the cell body and relays information to its target cells, including neurons, glands, and muscles, by conducting electrical pulses and releasing neurotransmitters.

Axonal injury to our mature CNS, including spinal cord injury and traumatic brain injury, is still an untreatable condition, even with current medical knowledge. It was already recognized and described as "incurable" in the Edwin Smith Surgical Papyrus published between 2,500 and 1,900 BC in Egypt (Hughes, 1988). Emerging evidence has revealed that the lack of trophic factors and the existence of inhibitory environmental cues in the adult CNS made it difficult for nerve axons to spontaneously regenerate. Once damaged, axons enter a dormant state. Regeneration is possible only under certain circumstances.

Upon injury, the distal parts of axons that are separated from the cell body, undergo Wallerian degeneration. The fragmented and degenerated axonal shafts are phagocytosed and removed by microglia or macrophages. The process seems to be important for the regeneration of axons by the surviving neurons. In PNS, Wallerian degeneration is mediated mainly by peripheral macrophages and is accomplished quickly and completely, which is thought to be a factor in the high regeneration capacity of PNS axons. In the CNS, on the other hand, Wallerian degeneration is largely delayed

and finished incompletely, probably because of the poor phagocytic capacity of microglia, major phagocytic cells in the CNS. In the 1980s, Aguayo and his colleagues clearly demonstrated that CNS axons regenerated through the implanted sciatic nerve "bridge," confirming that the difference in environmental cues between the CNS and the PNS defined each axon's regeneration capability (David and Aguayo, 1981; Benfey and Aguayo, 1982).

In addition to Wallerian degeneration, matrix remodeling after injury largely differs between the CNS and the PNS. In the CNS, the lesion site is surrounded by activated astrocytes (reactive astrocytes), forming a so-called glial scar (Silver and Miller, 2004). This scar is important for fixing the damaged blood-brain barrier (BBB), covering the lesion, protecting tissues from infections, and secreting various regeneration factors (Anderson et al., 2016). However, the glial scar also produces chondroitin sulfate (CS) proteoglycans, which are molecules that inhibit axonal regeneration (Snow et al., 1990, 1991; Rauch et al., 1991; Asher et al., 2000). When the regenerating axon tip makes contact with the CS proteoglycan (CSPG), it stops further extension and enters a dormant state called the dystrophic endbulb.

In this review, we briefly summarize how glycans work as physiological ligands and regulate axonal regeneration by mediating intracellular signaling.

## DYSTROPHIC ENDBULB

In 1928, Santiago Ramon Cajal found swollen axonal tips with multiple vacuoles in a lesion of a canine spinal cord. He reported that the structure was closely associated with poor axonal regeneration ability in the CNS. That structure is now recognized as the dystrophic endbulb or the dystrophic endball. The dystrophic endbulb contains a disorganized cytoskeleton and accumulations of membrane. It is formed acutely after injury can persist for several decades at lesions in human patients (Ruschel et al., 2015). Therefore, the structure was regarded as a therapeutic target for traumatic CNS injury, as Cajal suggested. However, the cellular and molecular mechanisms underlying the formation of dystrophic endbulb were unclear. Silver and his colleagues demonstrated that the increasing concentration gradient of CS that mimicked the *in vitro* glial scar was sufficient to induce dystrophic endbulbs on cultured adult dorsal root ganglion neurons (Tom et al., 2004). Defects in lysosomal secretion, including that of Cathepsin B, which might be important for matrix degradation and axonal elongation, were also suggested to be a characteristic of dystrophic endbulb (Tran et al., 2018; Tran and Silver, 2021).

## ROLES OF GLYCOSAMINOGLYCANS IN CNS

CS is a glycosaminoglycan (GAG) and an unbranched polymer chain, which consists of the repeating disaccharide unit, glucuronic acid–*N*-acetylgalactosamine (GlcA-GalNAc) (**Figure 1**; Margolis and Margolis, 1993; Kadomatsu and Sakamoto, 2014; Sakamoto and Kadomatsu, 2017). In addition to CS, GAG contains heparan sulfate (HS), keratan sulfate, and hyaluronan. Except for HA, GAG is modified with sulfate groups and covalently attached to specific core proteins, forming proteoglycan (PG). HS is a linear polysaccharide and consists of repeating disaccharide unit, uronic acid and *N*-acetylglucosamine. The sequential modifications, *N*-deacetylation of *N*-acetylglucosamines, *N*-sulfation of glucosamines, and *O*-sulfations at the C2-position of uronic acids as well as C3- and/or C6-position of glucosamines can be occurred. Regarding its roles in axonal elongation and its inhibition, HS, which is a linear polysaccharide of repeated disaccharide of uronic acid and was revealed to be a positive regulator (Wang and Denburg, 1992; Aricescu et al., 2002). For example, mice lacking *EXT1*, one of the essential enzymes for the synthesis of HS, showed abnormal commissure formation of the corpus callosum (Inatani et al., 2003). On the other hand, CS and keratan sulfate were revealed to be negative regulators in axonal elongation. In addition to dystrophic endbulb-forming activity *in vitro* as described above, several works based on chondroitinase ABC, a CS-degrading enzyme with bacterial origin, clearly demonstrated that CS was involved in the inhibition of axonal regeneration after injury *in vivo*. Enzymatic digestion of CS side chains on PG by the enzyme dramatically enhanced both anatomical and functional plasticity after various SCI models (Moon et al., 2001; Bradbury et al., 2002). Importantly, combined with intermittent hypoxia, chondroitinase ABC promoted robust restoration of ventilation after SCI, the impairment of which is a major cause of mortality in human patients (Warren et al., 2018). A recent work also showed that C-ABC improved both anatomical and functional outcomes after spinal cord hemisection in monkey (Rosenzweig et al., 2019). Keratan sulfate was also demonstrated to inhibit axonal regeneration both *in vitro* and *in vivo* (Snow et al., 1990; Smith-Thomas et al., 1994; Ito et al., 2010; Imagama et al., 2011). It is noteworthy that CS and keratan sulfate often share proteoglycans, such as aggrecan and phosphacan (Rauch et al., 1991; Margolis and Margolis, 1993).

CS is a long glycan chain with approximately 50–100 saccharides on average. The C2-position of GlcA and the C4- and/or C6-positions of GalNAc can be sulfated, resulting in different disaccharide compositions including A-unit (GlcA-GalNAc4S), C-unit (GlcA-GalNAc6S), D-unit (GlcA2S-GalNAc6S), and E-unit (GlcA-GalNAc4S,6S), where 2S, 4S, and 6S stand for 2- O-, 4- O-, and 6-O-sulfate, respectively. Thus, a single chain of CS is heterogeneous in both length and structure and has been proposed to contain a "functional domain" to interact with other specific molecules (Mikami et al., 2009; Dickendesher et al., 2012). In mammalian CNS, CSPGs, neurocan, versican, brevican, aggrecan, NG2, and phosphacan, contribute to assemble into an extracellular matrix. Along with the development of the CNS, CS is enriched especially around inhibitory neurons and synapses in a well-organized manner, in what is known as a "perineurnal net," where it regulates synaptic plasticity (Pizzorusso et al., 2002, 2006; Frischknecht et al., 2009; Gogolla et al., 2009; Miyata et al., 2012). Upon injury,

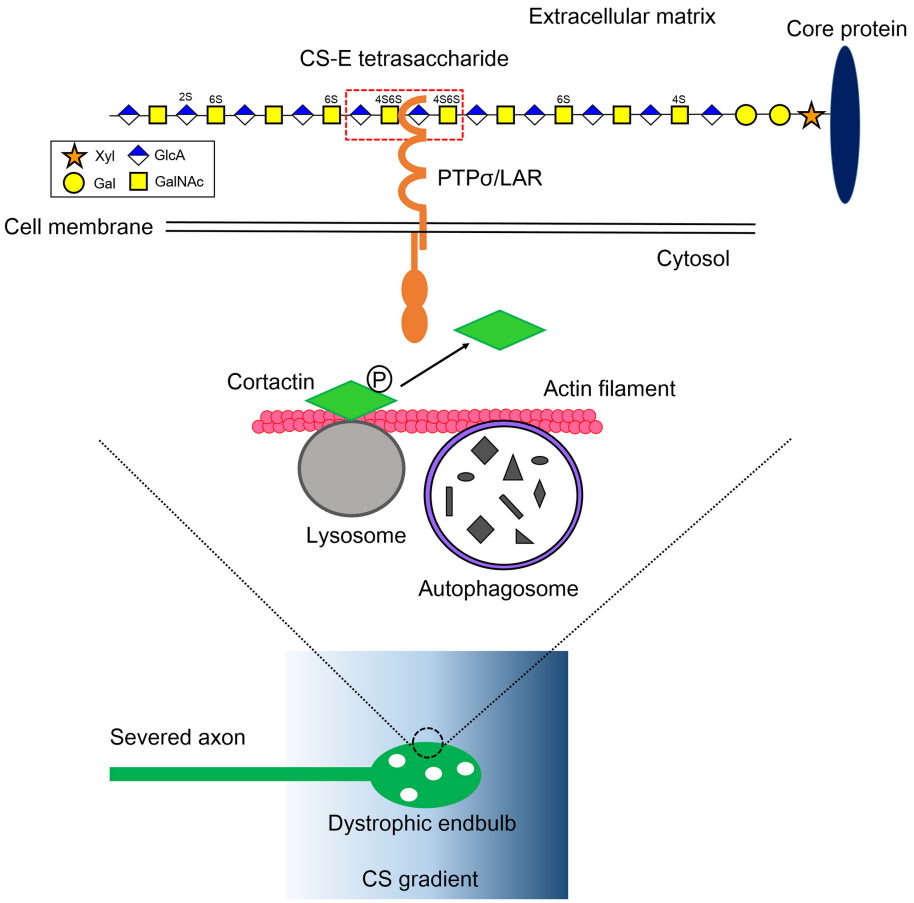


**FIGURE 1 |** Mechanistic insight into the formation of dystrophic endbulb by CS. The severed axons run into the gradient of CS originated from the perineuronal net and the reactive astrocyte in the lesion. The CS-E tetrasaccharide segment, which rarely appears on a CS chain, preferentially monomerizes and activates its axonal receptor PTPσ/LAR. Contrary, HS protects the formation of dystrophic endball by inducing clustering of the receptors. RPTP dephosphorylates cortactin, which is localized onto the lysosome surface and stabilizes actin fibers to facilitate autolysosome formation. As a consequence, the CS-RPTP axis disrupts autophagy flux, inducing the failure of fusion between autophagosomes and lysosomes, and thus abnormal accumulation of autophagosomes. That leadsto transforms of axon tips to dystrophic endbulb. Xyl, xylose; Gal, galactose; GlcA, glucuronic acid; GalNAc, *N*-acetylgalactosamine; P, tyrosine phosphorylation.

this organized CS matrix might be disrupted and diffused in a disorganized manner and, together with CS newly synthesized by the glial scar, inhibits regeneration of the dissected axons, transforming the dystrophic endbulb at its tip (Silver and Miller, 2004). However, the action mechanisms of CS on axons remained unclear for about two decades after CS was recognized as a major inhibitory cue for axonal regeneration in our CNS. This was largely because specific neuronal receptors for CS had not been identified.

## PROTEIN TYROSINE PHOSPHATASE SIGMA FUNCTIONS AS A CS RECEPTOR

It was a big surprise that protein tyrosine phosphatase sigma (PTPσ) and leukocyte common antigen-related (LAR) were identified as neuronal receptors for CS (Shen et al., 2009; Fisher et al., 2011), because these two molecules had already been reported as receptors for HS and found to be positively involved in axon guidance (Aricescu et al., 2002; Johnson et al., 2006). Both PTPσ and LAR, together with PTPδ, belong to the type IIa RPTP (receptor-type protein tyrosine phosphatase) family (Tonks, 2006). They are type I transmembrane proteins that each possess three immunoglobulin-like domains and typically four or eight fibronectin repeats. Two tandem repeats of the PTP domain composed of catalytically active D1 and inactive D2 form the intracellular domain (Tonks, 2006). The catalytic activity is regulated by receptor monomerization and multimerization. As a monomer, the D1 domain is free and active, while the D1 domain is *cis*-inhibited by the D2 domain as a multimer. Both CS and HS share the same binding domain on the first immunoglobulin-like domain of PTPσ and LAR, in which the basic amino acids form clusters at the surface, implying its ionic interaction with the sulfate groups of CS and HS (Aricescu et al., 2002; Shen et al., 2009). The additional binding site at the juxtamembrane domain on PTPσ for HS was also reported (Katagiri et al., 2018). On the basis of biochemical and structural analyses, the "switch model" of PTPσ by HS and CS was proposed, in which HS

induced receptor clustering, on the other hand, CS promoted receptor monomerization (Coles et al., 2011). However, how these two sulfated glycans act in such an opposing manner remained unclear, as did the specific substrates for PTPσ that are responsible for forming the dystrophic endbulb.

## DISRUPTION OF AUTOPHAGY IN DYSTROPHIC ENDBULB BY CS

In our recent work, we tried to explore deeply how CS and HS differentially regulate PTPσ, which ultimately determines axonal fate after injury (Sakamoto et al., 2019). The heterogeneity of glycan sulfation patterns in a single chain of GAG makes it harder to determine which segment binds to PTPσ. To overcome this, we synthesized and prepared a pure CS and HS oligosaccharides library with defined lengths and sulfation patterns. The surface plasmon resonance method was initially used to determine the interactions between CS variants and PTPσ. We found that CS-E, which has a highly proportion of E-unit (GlcA-GalNAc4S,6S), showed the best affinity to PTPσ among the CS variants, CS-A, CS-C, CS-D, and CS-E (Sakamoto et al., 2019). We found that CS-E, which has C4- and C6-sulfation on GalNAc residues, showed the best affinity to PTPσ. We then tested PTPσ with different lengths of CS-E and determined that the minimal binding segment of CS-E was a tetrasaccharide (**Figure 1**; Sakamoto et al., 2019). It is noteworthy that CS-E is a rare sulfation pattern and accounts for only a small percentage of the total CS in the injuredCNS in mice (Properzi et al., 2005). This means the frequency of CS-E tetrasaccharide can be estimated to be one at most in a single CS chain, and the CS chain is a preferable structure that can induce monomerization and activation of PTPσ (**Figure 1**). In contrast, with similar methods, we found that HS with one or more sulfate groups was sufficient to interact with PTPσ (Sakamoto et al., 2019). These structures account for nearly half of the total HS in the injured CNS (Properzi et al., 2008). Again, the results imply that the HS chain is preferable for inducing multimerization and inactivation of the receptor. This idea was confirmed by a cell culture experiment and synthetic CS/HS oligosaccharides. Although how these two distinct GAG chains with different levels of sulfation interact with PTPσ is still unclear, these data demonstrated that the frequency of the binding domain, defined by both the sulfation pattern and length in CS and HS, determined the action mode of each glycan on PTPσ .

To understand what a dystrophic endbulb is, and the consequence of PTPσ activation by CS, we deeply observed adystrophic endbulb formed on a CS gradient *in vitro* by electron microscopy. We found that autophagosomes abnormally accumulated in the dystrophic endbulb. Immunostaining with LC3, a specific marker for autophagosome, supported the results. More importantly, autophagosomes also accumulated at the tips of the dissected corticospinal tract in a mouse model of SCI (Sakamoto et al., 2019).

Autophagy is an intracellular degradation system for organelles and cytoplasmic components (Mizushima and Komatsu, 2011). Phagophore,a bowl-like membrane structure which is often formed at the contact site between endoplasmic reticulum and mitochondria,engulfs and encloses these components, producing autophagosome. The autophagosome then fuses with lysosome and is converted to autolysosome. As a consequence, components of autophagosome are delivered into lysosome and degraded by lysosomal enzymes. In axons, autophagy occurs preferentially at the axon tips and autophagosomes are retrogradely transported on microtubules to the cell body, fusing with lysosome during transport (Maday et al., 2012; Maday and Holzbaur, 2014). Because elongating axons have a high turnover of molecules and organelles including cytoskeleton, mitochondria, and membrane, the process seems to be essential to homeostasis for the elongation of axon tips. There are two mechanisms for the accumulation of autophagosomes (1) activation of autophagy and (2) disruption of autophagy flux, especially at the fusion step between autophagosomes and lysosomes. Immunocytochemical analysis using tandem-fluorescent LC3 (Kimura et al., 2007), which can distinguish between autophagosome and autolysosome, revealed that autophagy flux was severely disrupted in the dystrophic endbulb. Importantly, the knockdown of Syntaxin 17, Vamp 8, or Snap 29 by RNA interference, each of which is an essential soluble *N*-ethylmaleimide-sensitive factor attachment protein receptor (SNARE) for autophagosome-lysosome fusion (Itakura et al., 2012), successfully transformed healthy growth cones into dystrophic endbulb-like structures and significantly suppressed axonal elongation in cultured mouse dorsal root ganglion neuron. Consistent with this, treatments of the growth cones with chloroquine or bafilomycin A1, either of which inhibited the fusion between autophagosomes and lysosomes, gave similar results. Taken together, these results clearly demonstrated that disruption of autophagy flux was essential and sufficient for the formation of dystrophic endbulbs (**Figure 1**).

To link the PTPσ-autophagy axis, we focused on finding the specific substrate for PTPσ that is involved at the fusion step between autophagosomes and lysosomes (Sakamoto et al., 2019). Cortactin is an actin-binding protein thatis required for the process (Lee et al., 2010; Hasegawa et al., 2016). It has several tyrosine phosphorylation sites, among which the tyrosine 421 and 466 phosphorylation sites are essential for its actin-stabilizing activity (Hasegawa et al., 2016). Some of these tyrosine-phosphorylated cortactins are specifically localized to the lysosome surface by the protein-lipid interaction (Hasegawa et al., 2016), where they provide stabilized actin fibers to lysosomes to fuse with autophagosomes. In the primary cultured dorsal root ganglion neurons on a CSPG gradient, reduced phosphorylation at tyrosine 421 of cortactin was observed in the dystrophic endbulb compared to healthy growth cones. Furthermore, silencing cortactin resulted in dystrophic endbulb formation, similar to the case with CS treatment. Thus, we conclude that CS binds to PTPσ and the activated PTPσ dephosphorylates cortactin. This results in the disruption of the completion of the autophagy flux, causing the transformation of the growth cone into a dormant dystrophic endbulb (**Figure 1**).

## CONCLUDING REMARKS

CS and HS, each with different backbones and sulfation patterns, can bind to PTPσ. Currently, it is well known that CS inhibits axonal regeneration while HS promotes it. In a recent study we prepared a library of HS octasaccharides and found that, through these octasaccharides together with CS octasaccharides, PTPσ preferentially interacts with CS-E, a rare sulfation pattern in the natural CS chain, as well as with most HS oligomers bearing sulfate and sulfamate groups. Consequently, short and long stretches of natural CS and HS, respectively, bind to PTPσ. CS activates PTPσ, which dephosphorylates cortactin, a newly identified substrate for PTPσ, and disrupts autophagy flux at the autophagosome-lysosome fusion step. The failure of autophagy flux causes an accumulation of autophagosomes at the growth cone and is sufficient to turn the growth cone into a dystrophic endbulb. As a result, we conclude that the sulfation patterns determine the length of the GAG segment that binds to PTPσ and defines the fate of axonal regeneration through the PTPσ-cortactin-autophagy axis. Our results shed light on the mechanisms by which GAGs function as ligands to cell surface receptors. In addition, the present findings provide a new therapeutic strategy, including glycomimetics. Indeed, we recently showed that enoxaparin, a heparin oligosaccharide medicine clinically used as an anticoagulant, promoted functional recovery in a rat model of SCI, probably through the inactivation of PTPσ (Ito et al., 2021).

We cannot exclude the possibility that other intracellular mediators and mechanisms are involved in the formation of dystrophic endbulbs and in the inhibition of axonal regeneration. For instance, we recently identified a lot of interactors, including cortactin, for PTPσ by the proximity-dependent ligation assay (Gong et al., 2021). Further understanding toward dystrophic endbulbs is still needed to achieve complete regeneration of axons.

## AUTHOR CONTRIBUTIONS

KS wrote the manuscript. KS, TO, and KK discussed the manuscript. All authors contributed to the article and approved the submitted version.

## FUNDING

This work was supported by the Japan Society for the Promotion of Science (JSPS) KAKENHI Grant Nos. 19K07348 to KS and 19H03415 to KK, Grant from the Terumo Life Science Foundation to KS, and Grant from the Hori Science and Arts Foundation to KS.

## REFERENCES

Anderson, M. A., Burda, J. E., Ren, Y., Ao, Y., O'Shea, T. M., Kawaguchi, R., et al. (2016). Astrocyte scar formation aids central nervous system axon regeneration. *Nature* 532, 195–200. doi: 10.1038/nature17623

Aricescu, A. R., McKinnell, I. W., Halfter, W., and Stoker, A. W. (2002). Heparan sulfate proteoglycans are ligands for receptor protein tyrosine phosphatase sigma. *Mol. Cell Biol.* 22, 1881–1892. doi: 10.1128/mcb.22.6.1881-1892.2002

Asher, R. A., Morgenstern, D. A., and Fidler, P. S. (2000). Neurocan is upregulated in injured brain and in cytokine-treated astrocytes. *J. Neurosci.* 20, 2427–2438. doi: 10.1523/jneurosci.20-07-02427.2000

Benfey, M., and Aguayo, A. J. (1982). Extensive elongation of axons from rat brain into peripheral nerve grafts. *Nature* 296, 150–152. doi: 10.1038/296150a0

Bradbury, E. J., Moon, L. D., Popat, R. J., King, V. R., Bennett, G. S., Patel, P. N., et al. (2002). Chondroitinase ABC promotes functional recovery after spinal cord injury. *Nature* 416, 636–640. doi: 10.1038/416636a

Coles, C. H., Shen, Y., Tenney, A. P., Siebold, C., Sutton, G. C., Lu, W., et al. (2011). Proteoglycan-specific molecular switch for RPTPσ clustering and neuronal extension. *Science* 332, 484–488. doi: 10.1126/science.1200840

David, S., and Aguayo, A. J. (1981). Axonal elongation into peripheral nervous system "bridges" after central nervous system injury in adult rats. *Science* 214, 931–933. doi: 10.1126/science.6171034

Dickendesher, T. L., Baldwin, K. T., Mironova, Y. A., Koriyama, Y., Raiker, S. J., Askew, K. L., et al. (2012). NgR1 and NgR3 are receptors for chondroitin sulfate proteoglycans. *Nat. Neurosci.* 15, 703–712. doi: 10.1038/nn.3070

Fisher, D., Xing, B., Dill, J., Li, H., Hoang, H. H., Zhao, Z., et al. (2011). Leukocyte common antigen-related phosphatase is a functional receptor for chondroitin sulfate proteoglycan axon growth inhibitors. *J. Neurosci.* 31, 14051–14066. doi: 10.1523/JNEUROSCI.1737-11.2011

Frischknecht, R., Heine, M., Perrais, D., Seidenbecher, C. I., Choquet, D., and Gundelfinger, E. D. (2009). Brain extracellular matrix affects AMPA receptor lateral mobility and short-term synaptic plasticity. *Nat. Neurosci.* 12, 897–904. doi: 10.1038/nn.2338

Gogolla, N., Caroni, P., Lüthi, A., and Herry, C. (2009). Perineuronal nets protect fear memories from erasure. *Science* 325, 1258–1261. doi: 10.1126/science.1174146

Gong, Y., Abudureyimu, S., Kadomatsu, K., and Sakamoto, K. (2021). Identification of PTPRσ-interacting proteins by proximity-labelling assay. *J. Biochem.* 169, 187–194. doi: 10.1093/jb/mvaa141

Hasegawa, J., Iwamoto, R., Otomo, T., Nezu, A., Hamasaki, M., and Yoshimori, T. (2016). Autophagosome-lysosome fusion in neurons requires INPP5E, a protein associated with Joubert syndrome. *EMBO J.* 35, 1853–1867. doi: 10.15252/embj.201593148

Hughes, J. T. (1988). The Edwin Smith Surgical Papyrus: an analysis of the first case reports of spinal cord injuries. *Paraplegia* 26, 71–82. doi: 10.1038/sc.1988.15

Imagama, S., Sakamoto, K., Tauchi, R., Shinjo, R., Ohgomori, T., Ito, Z., et al. (2011). Keratan sulfate restricts neural plasticity after spinal cord injury. *J. Neurosci.* 31, 17091–17102. doi: 10.1523/jneurosci.5120-10.2011

Inatani, M., Irie, F., Plump, A. S., Tessier-Lavigne, M., and Yamaguchi, Y. (2003). Mammalian brain morphogenesis and midline axon guidance require heparan sulfate. *Science* 302, 1044–1046. doi: 10.1126/science.1090497

Itakura, E., Kishi-Itakura, C., and Mizushima, N. (2012). The hairpin-type tail-anchored SNARE syntaxin 17 targets to autophagosomes for fusion with endosomes/lysosomes. *Cell* 151, 1256–1269. doi: 10.1016/j.cell.2012.11.001

Ito, S., Ozaki, T., Morozumi, M., Imagama, S., Kadomatsu, K., and Sakamoto, K. (2021). Enoxaparin promotes functional recovery after spinal cord injury by antagonizing PTPRσ. *Exp. Neurol.* 340, 113679. doi: 10.1016/j.expneurol.2021.113679

Ito, Z., Sakamoto, K., Imagama, S., Matsuyama, Y., Zhang, H., Hirano, K., et al. (2010). N-acetylglucosamine 6-O-sulfotransferase-1-deficient mice show better functional recovery after spinal cord injury. *J. Neurosci.* 30, 5937–5947. doi: 10.1523/JNEUROSCI.2570-09.2010

Johnson, K. G., Tenney, A. P., Ghose, A., Duckworth, A. M., Higashi, M. E., Parfitt, K., et al. (2006). The HSPGs Syndecan and Dallylike bind the receptor phosphatase LAR and exert distinct effects on synaptic development. *Neuron* 49, 517–531. doi: 10.1016/j.neuron.2006.01.026

Kadomatsu, K., and Sakamoto, K. (2014). Sulfated glycans in network rewiring and plasticity after neuronal injuries. *Neurosci. Res.* 78, 50–54. doi: 10.1016/j.neures.2013.10.005

Katagiri, Y., Morgan, A. A., Yu, P., Bangayan, N. J., Junka, R., and Geller, H. M. (2018). Identification of novel binding sites for heparin in receptor protein-tyrosine phosphatase (RPTPσ): Implications for proteoglycan signaling. *J. Biol. Chem.* 293, 11639–11647. doi: 10.1074/jbc.RA118.003081

Kimura, S., Noda, T., and Yoshimori, T. (2007). Dissection of the autophagosome maturation process by a novel reporter protein, tandem fluorescent-tagged LC3. *Autophagy* 3, 452–460. doi: 10.4161/auto.4451

Lee, J. Y., Koga, H., Kawaguchi, Y., Tang, W., Wong, E., Gao, Y. S., et al. (2010). HDAC6 controls autophagosome maturation essential for ubiquitin-selective quality-control autophagy. *EMBO J.* 29, 969–980. doi: 10.1038/emboj.2009.405

Maday, S., and Holzbaur, E. L. (2014). Autophagosome biogenesis in primary neurons follows an ordered and spatially regulated pathway. *Dev. Cell* 30, 71–85. doi: 10.1016/j.devcel.2014.06.001

Maday, S., Wallace, K. E., and Holzbaur, E. L. (2012). Autophagosomes initiate distally and mature during transport toward the cell soma in primary neurons. *J. Cell Biol.* 196, 407–417. doi: 10.1083/jcb.201106120

Margolis, R. K., and Margolis, R. U. (1993). Nervous tissue proteoglycans. *Experientia* 49, 429–446. doi: 10.1007/bf01923587

Mikami, T., Yasunaga, D., and Kitagawa, H. (2009). Contactin-1 is a functional receptor for neuroregulatory chondroitin sulfate-E. *J. Biol. Chem.* 284, 4494–4499. doi: 10.1074/jbc.M809227200

Miyata, S., Komatsu, Y., Yoshimura, Y., Taya, C., and Kitagawa, H. (2012). Persistent cortical plasticity by upregulation of chondroitin 6-sulfation. *Nat. Neurosci.* 15, 414–422. doi: 10.1038/nn.3023

Mizushima, N., and Komatsu, M. (2011). Autophagy: renovation of cells and tissues. *Cell* 147, 728–741. doi: 10.1016/j.cell.2011.10.026

Moon, L. D., Asher, R. A., Rhodes, K. E., and Fawcett, J. W. (2001). Regeneration of CNS axons back to their target following treatment of adult rat brain with chondroitinase ABC. *Nat. Neurosci.* 4, 465–466. doi: 10.1038/87415

Pizzorusso, T., Medini, P., Berardi, N., Chierzi, S., Fawcett, J. W., and Maffei, L. (2002). Reactivation of ocular dominance plasticity in the adult visual cortex. *Science* 298, 1248–1251. doi: 10.1126/science.1072699

Pizzorusso, T., Medini, P., Landi, S., Baldini, S., Berardi, N., and Maffei, L. (2006). Structural and functional recovery from early monocular deprivation in adult rats. *Proc. Natl. Acad. Sci. U S A* 103, 8517–8522. doi: 10.1073/pnas.0602657103

Properzi, F., Carulli, D., Asher, R. A., Muir, E., Camargo, L. M., and van Kuppevelt, T. H. (2005). Chondroitin 6-sulphate synthesis is up-regulated in injured CNS, induced by injury-related cytokines and enhanced in axon-growth inhibitory glia. *Eur. J. Neurosci.* 21, 378–390. doi: 10.1111/j.1460-9568.2005.03876.x

Properzi, F., Lin, R., Kwok, J., Naidu, M., van Kuppevelt, T. H., and Ten Dam, G. B. (2008). Heparan sulphate proteoglycans in glia and in the normal and injured CNS: expression of sulphotransferases and changes in sulphation. *Eur. J. Neurosci.* 27, 593–604. doi: 10.1111/j.1460-9568.2008.06042.x

Rauch, U., Gao, P., Janetzko, A., Flaccus, A., Hilgenberg, L., Tekotte, H., et al. (1991). Isolation and characterization of developmentally regulated chondroitin sulfate and chondroitin/keratan sulfate proteoglycans of brain identified with monoclonal antibodies. *J. Biol. Chem.* 266, 14785–14801. doi: 10.1016/s0021-9258(18)98755-7

Rosenzweig, E. S., Salegio, E. A., Liang, J. J., Weber, J. L., Weinholtz, C. A., Brock, J. H., et al. (2019). Chondroitinase improves anatomical and functional outcomes after primate spinal cord injury. *Nat. Neurosci.* 22, 1269–1275. doi: 10.1038/s41593-019-0424-1

Ruschel, J., Hellal, F., Flynn, K. C., Dupraz, S., Elliott, D. A., Tedeschi, A., et al. (2015). Axonal regeneration. Systemic administration of epothilone B promotes axon regeneration after spinal cord injury. *Science* 348, 347–352. doi: 10.1126/science.aaa2958

Sakamoto, K., and Kadomatsu, K. (2017). Mechanisms of axon regeneration: The significance of proteoglycans. *Biochim. Biophys. Acta Gen. Subj.* 1861, 2435–2441. doi: 10.1016/j.bbagen.2017.06.005

Sakamoto, K., Ozaki, T., Ko, Y. C., Tsai, C. F., Gong, Y., Morozumi, M., et al. (2019). Glycan sulfation patterns define autophagy flux at axon tip via PTPRsigma-cortactin axis. *Nat. Chem. Biol.* 15, 699–709. doi: 10.1038/s41589-019-0274-x

Shen, Y., Tenney, A. P., Busch, S. A., Horn, K. P., Cuascut, F. X., Liu, K., et al. (2009). PTPsigma is a receptor for chondroitin sulfate proteoglycan, an inhibitor of neural regeneration. *Science* 326, 592–596. doi: 10.1126/science.1178310

Silver, J., and Miller, J. H. (2004). Regeneration beyond the glial scar. *Nat. Rev. Neurosci.* 5, 146–156. doi: 10.1038/nrn1326

Smith-Thomas, L. C., Fok-Seang, J., Stevens, J., Du, J. S., Muir, E., Faissner, A., et al. (1994). An inhibitor of neurite outgrowth produced by astrocytes. *J. Cell Sci.* 107(Pt 6), 1687–1695. doi: 10.1242/jcs.107.6.1687

Snow, D. M., Lemmon, V., Carrino, D. A., Caplan, A. I., and Silver, J. (1990). Sulfated proteoglycans in astroglial barriers inhibit neurite outgrowth in vitro. *Exp. Neurol.* 109, 111–130. doi: 10.1016/s0014-4886(05)80013-5

Snow, D. M., Watanabe, M., Letourneau, P. C., and Silver, J. (1991). A chondroitin sulfate proteoglycan may influence the direction of retinal ganglion cell outgrowth. *Development* 113, 1473–1485. doi: 10.1242/dev.113.4.1473

Tom, V. J., Steinmetz, M. P., Miller, J. H., Doller, C. M., and Silver, J. (2004). Studies on the development and behavior of the dystrophic growth cone, the hallmark of regeneration failure, in an in vitro model of the glial scar and after spinal cord injury. *J. Neurosci.* 24, 6531–6539. doi: 10.1523/JNEUROSCI.0994-04.2004

Tonks, N. K. (2006). Protein tyrosine phosphatases: from genes, to function, to disease. *Nat. Rev. Mol. Cell Biol.* 7, 833–846. doi: 10.1038/nrm2039

Tran, A. P., and Silver, J. (2021). Cathepsins in neuronal plasticity. *Neural. Regen Res.* 16, 26–35. doi: 10.4103/1673-5374.286948

Tran, A. P., Sundar, S., Yu, M., Lang, B. T., and Silver, J. (2018). Modulation of Receptor Protein Tyrosine Phosphatase Sigma Increases Chondroitin Sulfate Proteoglycan Degradation through Cathepsin B Secretion to Enhance Axon Outgrowth. *J. Neurosci.* 38, 5399–5414. doi: 10.1523/JNEUROSCI.3214-17.2018

Wang, L., and Denburg, J. L. (1992). A role for proteoglycans in the guidance of a subset of pioneer axons in cultured embryos of the cockroach. *Neuron* 8, 701–714. doi: 10.1016/0896-6273(92)90091-q

Warren, P. M., Steiger, S. C., Dick, T. E., MacFarlane, P. M., Alilain, W. J., and Silver, J. (2018). Rapid and robust restoration of breathing long after spinal cord injury. *Nat. Commun.* 9:4843. doi: 10.1038/s41467-018-06937-0

**Conflict of Interest:** The authors declare that the research was conducted in the absence of any commercial or financial relationships that could be construed as a potential conflict of interest.

frontiers in Cell and Developmental Biology

REVIEW
published: 02 August 2021
doi: 10.3389/fcell.2021.696640

# Neural Tissue Homeostasis and Repair Is Regulated via CS and DS Proteoglycan Motifs

*Anthony J. Hayes*[1] *and James Melrose*[2,3]*

[1] *Bioimaging Research Hub, Cardiff School of Biosciences, Cardiff University, Wales, United Kingdom,* [2] *Graduate School of Biomedical Engineering, University of New South Wales, Sydney, NSW, Australia,* [3] *Raymond Purves Bone and Joint Research Laboratories, Kolling Institute of Medical Research, Royal North Shore Hospital and The Faculty of Medicine and Health, The University of Sydney, St. Leonard's, NSW, Australia*

Chondroitin sulfate (CS) is the most abundant and widely distributed glycosaminoglycan (GAG) in the human body. As a component of proteoglycans (PGs) it has numerous roles in matrix stabilization and cellular regulation. This chapter highlights the roles of CS and CS-PGs in the central and peripheral nervous systems (CNS/PNS). CS has specific cell regulatory roles that control tissue function and homeostasis. The CNS/PNS contains a diverse range of CS-PGs which direct the development of embryonic neural axonal networks, and the responses of neural cell populations in mature tissues to traumatic injury. Following brain trauma and spinal cord injury, a stabilizing CS-PG-rich scar tissue is laid down at the defect site to protect neural tissues, which are amongst the softest tissues of the human body. Unfortunately, the CS concentrated in gliotic scars also inhibits neural outgrowth and functional recovery. CS has well known inhibitory properties over neural behavior, and animal models of CNS/PNS injury have demonstrated that selective degradation of CS using chondroitinase improves neuronal functional recovery. CS-PGs are present diffusely in the CNS but also form denser regions of extracellular matrix termed perineuronal nets which surround neurons. Hyaluronan is immobilized in hyalectan CS-PG aggregates in these perineural structures, which provide neural protection, synapse, and neural plasticity, and have roles in memory and cognitive learning. Despite the generally inhibitory cues delivered by CS-A and CS-C, some CS-PGs containing highly charged CS disaccharides (CS-D, CS-E) or dermatan sulfate (DS) disaccharides that promote neural outgrowth and functional recovery. CS/DS thus has varied cell regulatory properties and structural ECM supportive roles in the CNS/PNS depending on the glycoform present and its location in tissue niches and specific cellular contexts. Studies on the fruit fly, *Drosophila melanogaster* and the nematode *Caenorhabditis elegans* have provided insightful information on neural interconnectivity and the role of the ECM and its PGs in neural development and in tissue morphogenesis in a whole organism environment.

**Keywords: chondroitin sulfate, dermatan sulfate, proteoglycans, lecticans, neuroregulation, neural repair**

OPEN ACCESS

***Edited by:***
*Jessica C. F. Kwok,*
*University of Leeds, United Kingdom*

***Reviewed by:***
*Jun Zhou,*
*German Cancer Research Center (DKFZ), Germany*
*Reyna Hernandez-Benitez,*
*Salk Institute for Biological Studies, United States*

***Correspondence:**
*James Melrose*
*james.melrose@sydney.edu.au*
*orcid.org/0000-0001-9237-0524*

***Specialty section:***
*This article was submitted to Signaling, a section of the journal Frontiers in Cell and Developmental Biology*

***Received:*** *19 April 2021*
***Accepted:*** *13 July 2021*
***Published:*** *02 August 2021*

***Citation:***
*Hayes AJ and Melrose J (2021) Neural Tissue Homeostasis and Repair Is Regulated via CS and DS Proteoglycan Motifs. Front. Cell Dev. Biol. 9:696640. doi: 10.3389/fcell.2021.696640*

## INTRODUCTION

This chapter highlights the roles of chondroitin sulfate (CS) and dermatan sulfate (DS)-proteoglycans (PGs) in neural biology, heparan sulfate (HS)-PGs were outside the scope of this review and thus are only briefly touched on. However many excellent reviews exist on HS-PGs and their interactions with extracellular matrix (ECM) components in neural development, neural function and potential in neural repair biology (Condomitti and de Wit, 2018; Zhang P. et al., 2018; Roppongi et al., 2020; Xiong et al., 2020; Kamimura and Maeda, 2021; Sakamoto et al., 2021). Roles for HS-PGs in model developmental organisms such as *Drosophila melanogaster* and *Caenorhabditis elegans* have also been reviewed (Díaz-Balzac et al., 2014; Blanchette et al., 2017; Kamimura and Maeda, 2017; Saied-Santiago et al., 2017) and the interested reader is referred to these excellent publications for further information.

With the identification of the multiple molecular determinants that provide neuronal connectivity, and with new insights into the modulatory extracellular information regulating axon guidance, neural network and synapse formation, a better understanding of the complexity that neurons face in a living organism is beginning to emerge. Attention is now returning to an ancient regulator of cell-cell interaction: the ECM (Dityatev and Schachner, 2006; Dityatev et al., 2010; Miyata and Kitagawa, 2017; Nicholson and Hrabětová, 2017; Ferrer-Ferrer and Dityatev, 2018; Quraishe et al., 2018; Cope and Gould, 2019; Long and Huttner, 2019; Chelyshev et al., 2020; Jain et al., 2020; Wilson et al., 2020; Carulli and Verhaagen, 2021; Kamimura and Maeda, 2021; Shabani et al., 2021; Su et al., 2021). Among the many matrix components that influence neuronal connectivity, recent studies on the CS-PGs and HS-PGs indicate these ancient molecules form dynamic scaffolds that not only provide a protective environment around cells but are also a source of directive cues that modulate neuronal behavior and synaptic plasticity in tissue development (Haylock-Jacobs et al., 2011; Hayes and Melrose, 2018; Hayes et al., 2018; Karamanos et al., 2018; Hayes and Melrose, 2020a; Shabani et al., 2021).

### Roles of GAGs in the Evolution of Life and Electrochemical Properties of Tissues

Glycosaminoglycans (GAGs) and PGs are ancient molecules that evolved over a 500 million year period of invertebrate and vertebrate evolution (Yamada et al., 2011). Natural selection processes 'chose' GAGs with molecular recognition, information storage and transfer properties. The PGs that populated the glycocalyx surrounding cells thus had cell instructive properties through their GAG side chains that interacted with morphogens, growth factors, cytokines, cell receptors, cell adhesion molecules and neurotrophic peptides facilitating regulatory roles in embryonic neural development. GAGs also have electro-chemical properties through their sulfate and carboxyl groups that are ionized at physiological pH. GAG-electroconductive gels in the sensory pores of the skin of elasmobranch fish species (i.e., sharks, rays, and skates) have the capacity to detect protons produced by the muscular activity of prey fish species and this equips them with the ability to undergo electro-location to detect prey species, even under highly turbid water conditions where these are not visible (Bellono et al., 2017). Such gels have ultrasensitive proton detection capability, this information is transferred to a sensory nerve interface in the skin pores and then to the brain stem for signal interpretation.

All GAGs have proton detection capability (Josberger et al., 2016; Selberg et al., 2019) and are ancient molecules that were present during the early stages of the evolution of life (Yamada et al., 2011). It has been proposed that proton electrochemical ion gradients across membranes drove cellular metabolism and energy production during early evolution (Lane, 2017). In prokaryotic evolution, GAGs were mainly unsulfated or poorly sulfated; however, when eukaryotic cells evolved, sulfated GAGs predominated. Evolution of membrane polarization became possible in eukaryotic cells and membrane energetics emerged (Wilson and Lin, 1980; Niven and Laughlin, 2008; Dibrova et al., 2012; Lynch and Marinov, 2017). Membrane polarization involves the controlled movement of ions across cell membranes, GAGs had fundamental roles to play in these processes through their proton binding properties. All cells in multicellular organisms utilize membrane polarization when undergoing cell signaling, adhesion, proliferation, migration, and cytokinesis. Some cells such as neurons have developed electrical processes to a high level of precision, and this is the basis of the generation of electrical impulses in neural networks that remotely control cells and tissues in higher animals. Further eukaryotic evolution resulted in the development of a glycocalyx around cells. This contained PGs containing GAG side chains with the ability to instruct cellular behavior. The development of pericellular and extracellular matrices populated by PGs facilitated the development of tissues with variable biophysical properties due to these PGs and their co-operative interactions with structural proteins thus driving specialization with the ECM. Neural networks subsequently evolved to control these tissues of increasing complexity. Neurons are highly energetic cell types that utilize Na(+)/K(+)-ATPase pumps to generate energy. This process also generates chemical and electrical gradients across cell membranes. This membrane polarization process is essential for cell signaling and is aberrantly controlled in neurological diseases. Examination of the ECM PGs that control these neural processes has uncovered valuable therapeutic targets (Soleman et al., 2013; Maćkowiak et al., 2014; De Luca and Papa, 2016; Miyata and Kitagawa, 2016; Yang, 2020; Dityatev et al., 2021).

Glycosaminoglycan were fundamental entities in the formation and regulation of neural networks and tissues and the control of cell behavior during morphogenesis, tissue development and in ECM remodeling in tissue repair (Melrose, 2019b). The sulfation patterns of GAGs have roles in cellular molecular recognition and the regulation of physiological processes (Melrose, 2019b). GAG sulfotransferases and glycosyl transferases in progenitor/stem cell niches support the assembly of GAGs of diverse structure and sulfation patterns and are important in the development of pluripotent stem cell lineages with migratory properties (Stanley, 2016). This allows these cells to participate in tissue development and tissue repair.

Sulfate groups are important functional determinants on GAGs. Knock-out sulfotransferase and glycosyl transferase mice have demonstrated the important functional roles of GAGs in tissues (Stanley, 2016). Variable sulfation positions and densities on GAGs convey a range of functional attributes to tissues including an ability to act as electrical conduits to the cell. Sulfate groups are relatively bulky space-filling entities on GAGs, it was pertinent that all spatial orientations and permutations were explored during natural evolutionary selection processes to select GAGs with optimal interactivity. Natural selection forces thus explored many permutations of GAG structural form to optimize cell regulatory capability. Sulfate groups convey interactive molecular recognition and information transfer capability to GAGs and their interactions with growth factors, receptors, morphogens, ECM components, proteases, and protease inhibitory proteins regulate cell signaling processes in tissue morphogenesis and skeletogenesis. Knockout of glycosyl transferases, that are required for GAG assembly, has produced GAG-deficient mice (Stanley, 2016) that have allowed examination of the roles GAGs play in tissue form and function and how these regulate physiological processes in health and disease. The inherent charge transfer and storage properties of GAGs is a "glycocode" that provides sophisticated cell instructive information (Gabius, 2018; Hayes and Melrose, 2018; Hayes et al., 2018; Kaltner et al., 2019).

### CNS/PNS ECM PGs/GAGs, Cellular Regulation, and Neural Tissue Development

As already discussed, GAGs have electrochemical properties equipping them with cell regulatory abilities (Lane, 2017; Selberg et al., 2019). At the individual cell level, voltage gradients occur across cell membranes as so-called, action potentials (Strbak et al., 2016) which form part of the cell signaling and communication machinery of cells, i.e., membrane polarization-depolarization underlying the generation of electrical signaling in neural networks. Proton conductivity is important in many natural cellular processes including oxidative phosphorylation in mitochondria and energy production, uncoupling of membrane potentials during membrane polarization-de-polarization and neural potentiation, as well as in the priming of cells for proliferative events, apoptosis or cell migration (Wilson and Lin, 1980; Vellai et al., 1998; Niven and Laughlin, 2008; Dibrova et al., 2012; Lynch and Marinov, 2017). Electrochemical reactions control cell and tissue polarity and regulate cell behavior, ECM PGs facilitate electrocommunication between cells and their extracellular microenvironments. Cells sense changes in their microenvironments through micromechanical and electrochemical cues from the ECM allowing the cell to maintain a homeostatic tissue compositional balance thus providing optimal tissue functional properties (Guilak et al., 2021; Melrose et al., 2021). GAGs can detect proton gradients and are electroconductive entities that participate in microelectronic events during membrane polarization forming the basis of cell signaling (Wilson and Lin, 1980; Vellai et al., 1998; Niven and Laughlin, 2008; Dibrova et al., 2012; Lynch and Marinov, 2017). Neurons are particularly sensitive to electrostimulation in microelectronic events leading to polarization of the activated neuron cell membrane, however, membrane polarization occurs in all cells to some extent and is the basis of cell signaling during cellular attachment, migration and transmission of signals from cell to cell not only during development but also in neural repair and functional nerve recovery from trauma (Hortobágyi and Maffiuletti, 2011; Hayes and Melrose, 2020b). The GAG components of PGs participate in neurotrophic regulation of cellular movement in the development of neural networks and also in neural repair processes. A diverse collection of neuroregulatory molecules participate in these processes guided by cues from ECM PGs, which are discussed later in this chapter.

## THE CHONDROITIN SULFATE AND DERMATAN SULFATE COMPONENTS OF NEURAL PROTEOGLYCANS

Chondroitin sulfate is the most abundant GAG of the human body and CS side chains are found on a diverse range of PGs. CS is a linear GAG consisting of D-glucuronic acid glycosidically linked to *N*-acetyl galactosamine to form repeat disaccharides assembled into CS side chains (Zhang, 2010) on PGs up to ∼20 kDa in size (**Figure 1**). D-glucuronic acid also undergoes epimerization and inversion in structure to form L-iduronic acid in the related GAG, DS also known as CS-B (**Figure 2**).

Chondroitin sulfate is *O*-sulfated at C-4 or C-6 of the GalNAc, whereas in DS GalNAc is almost exclusively 4-*O*-sulfated and minor proportions of L-idoA may be *O*-sulfated at C-2 (Malmström et al., 2012). The conversion of GlcA into IdoA is variable ranging from one to almost 99% conversion of GlcA to IdoA (Malmström et al., 2012). IdoA residues are not regularly distributed along the CS/DS chain and occur in blocks of ≥6 IdoA residues, alternating IdoA/GlcA units, or as isolated IdoA units interspersed within stretches of unmodified GlcA (Tykesson et al., 2018). DS epimerase-1 and dermatan 4-*O*-sulfotransferase-1 form complexes that generate long epimerized 4-*O*-sulfated blocks. The presence of idoA in CS/DS alters its properties since a more flexible chain is generated that is more able to explore spatial orientations that maximize binding opportunities with prospective ligands (Ferro et al., 1990). IdoA substituted CS/DS influences cellular properties, such as migration, proliferation, differentiation, angiogenesis and regulates cytokine/growth factor activities (Thelin et al., 2013). CS and DS occur in significant amounts in the brain and have important roles to play in CNS development. DS sulfate epimerase 2 (DS-epi2) is ubiquitously expressed in the infant brain whereas DS epimerase 1 (DS-epi1) expression is faint at all developmental stages (Akatsu et al., 2011). DS-epi2 but not DS-epi1 plays dominant roles in the epimerization of CS/DS and has crucial roles to play in postnatal brain development. CS/DS hybrid chains have roles in the development of the cerebellum with the expression of crucial disulfated CS/DS disaccharides spatiotemporally regulated by specific sulfotransferase enzymes (Mitsunaga et al., 2006). Ubiquitous expression of chondroitin 4-*O*-sulfotransferase-1 (C4ST-1) and C4ST-2 in the postnatal mouse brain contrasts with dermatan 4-*O*-sulfotransferase-1 (D4ST-1) and uronyl 2-sulfotransferase

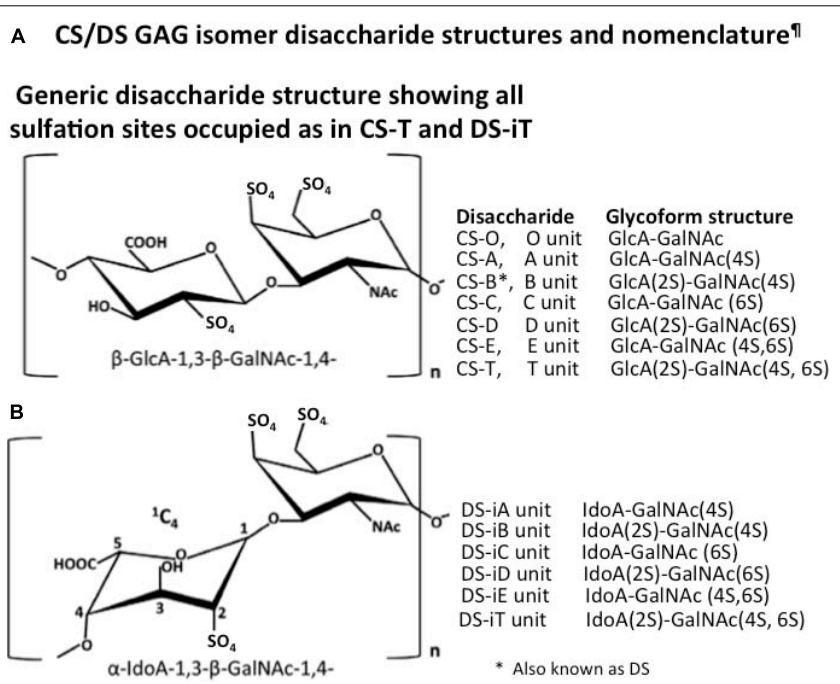


**FIGURE 1 |** Structure of the CS/DS disaccharides **(A)** and nomenclature of the CS and DS disaccharide glycoforms **(B)** as proposed by Malavaki et al. (2008).

(UST) expression which are restricted to the developing cerebellum. The proportions of DS-specific, 4-sulfated IdoA-GalNAc (iA) and 2-sulfated IdoA-GalNAc (iB) produced by sequential D4ST-1 and UST activity has been shown to be highest in CS/DS chains isolated from the developing cerebellum with a 10-fold increase in iB evident. GlcA/IdoA(2-*O*-sulfate)-GalNAc(6-*O*-sulfate) (D/iD) and GlcA/IdoA-GalNAc (4,6-*O*-disulfate) (E/iE) levels, however, decrease to 50 and 30%, respectively, in the developing cerebellum. Thus IdoA-containing iA and iB and D/iD and E/iE units in CS/DS hybrid chains both have important roles to play in the development of the cerebellum and postnatal brain development. The diverse structures that are possible with CS provide multifunctional properties to CS-PGs (Abbott and Nigussie, 2020), with dynamic changes in CS structure providing adaptable regulatory properties to PGs in tissue development and in pathological conditions (Galtrey and Fawcett, 2007). CS-PGs as components of perineuronal nets (PNNs) have neuroprotective properties and regulate neural plasticity and cognitive learning through specific CS mediated interactions (Dyck and Karimi-Abdolrezaee, 2015). PGs are ubiquitous secreted ECM components (**Figure 3**) that also occur attached to cell surfaces either as transmembrane or glycophosphatidylinositol (GPI)-anchored structures, and intracellularly as granular deposits in some cells (**Figures 4**, **5**). Perlecan is referred to as a HS-PG, however, in many tissues it is a hybrid CS/HS PG and is thus included in this review, particularly in view of its many interesting properties in neural tissues. The chain length of CS, 3D spatial presentation and density of its sulfate groups control its physicochemical and cell interactive and biological properties in tissues through interactions with a diverse range of ligands that regulate many physiological processes (Galtrey and Fawcett, 2007; Dyck and Karimi-Abdolrezaee, 2015). GAGs represent major ECM components of the brain, constituting up to 60% of its mass during early embryonic development and 20% in the adult central nervous system/peripheral nervous system (CNS/PNS). CS substituted PGs are one of the most abundant components of the CNS/PNS. HA is also a major component. HA has a simple structure and is the only non-sulfated GAG, but nevertheless has important biophysical properties which are important in the hydration and compartmentalization of the CNS/PNS. High molecular weight HA is anti-inflammatory, minimizes neuroinflammation and exhibits cell interactive properties that regulate cellular migration, proliferation and differentiation (Sherman et al., 2015). HA is also a component of the sub-ventricular and sub-granular dentate gyrus of the hippocampus which are two regions of the brain containing neuroprogenitor stem cell populations in niches known as fractones (Mercier et al., 2012; Mercier, 2016; Sato et al., 2019).

## DEVELOPMENTAL ANIMAL MODELS USED TO EXAMINE NEURAL DEVELOPMENT AND REGULATION IN A WHOLE ORGANISM ENVIRONMENT

Studies on the fruit fly, *D. melanogaster* (FitzGerald et al., 2006; Nishihara, 2010; Losada-Perez et al., 2016; Davis et al., 2019) and the nematode *C. elegans* (White et al., 1976; Mulcahy et al., 2018; Schafer, 2018; Kovács et al., 2020; White, 2020) have provided insightful information on the role of the ECM and some

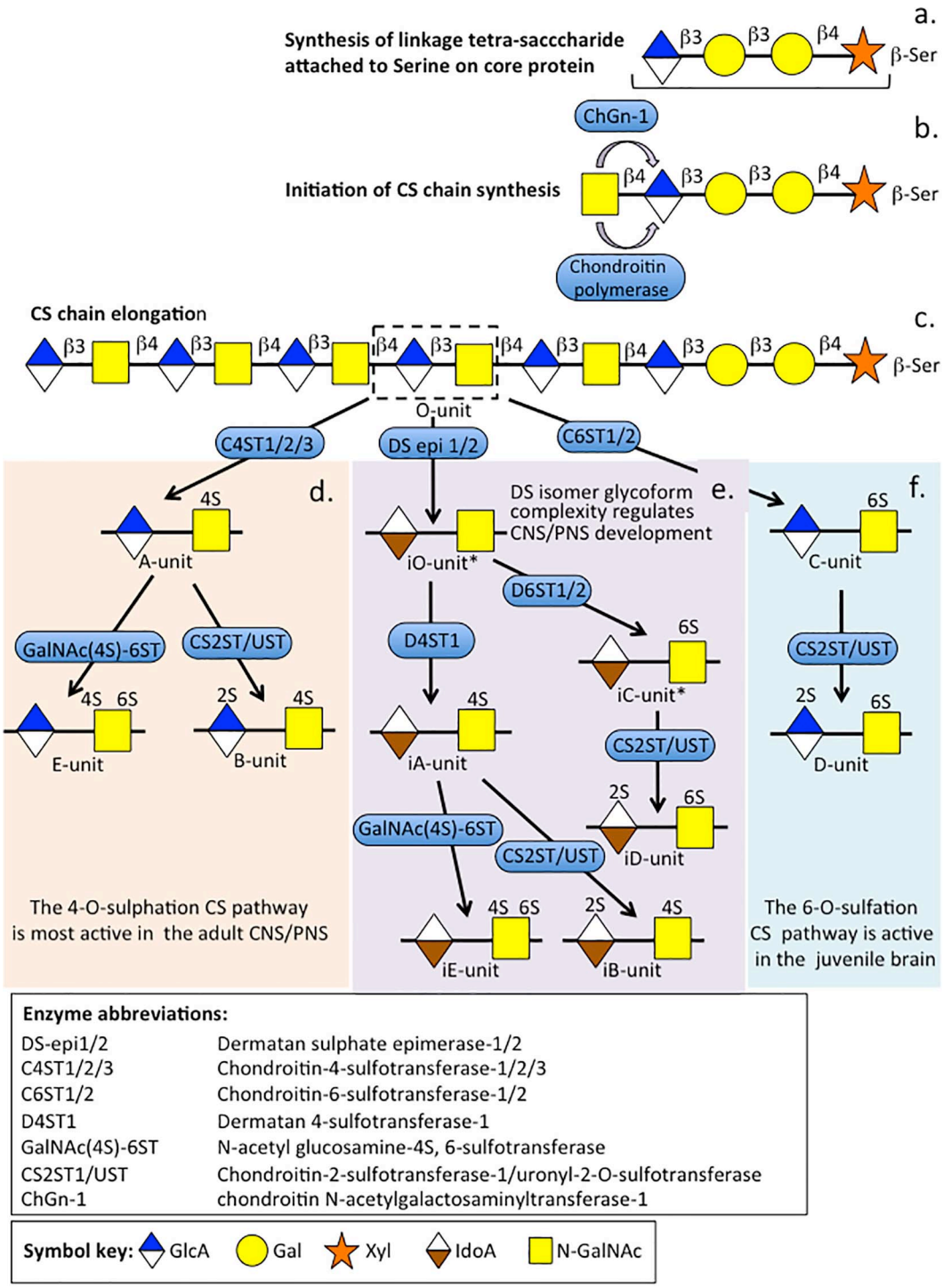


**FIGURE 2 |** The biosynthesis of CS and DS chains showing their diverse disaccharide glycoforms that are functional in the juvenile and adult CNS/PNS and during the development and repair of the CNS/PNS. Biosynthesis of the tetrasaccharide linker sequence by addition of a xylose residue to a serine residue in the proteoglycan core protein followed by addition of two Galactose and a GlcA residue **(a)**. Initiation of CS chain elongation occurs by addition of a GalNAc residue by chondroitin *N*-acetylgalactosaminyltransferase-1 or chondroitinpolymerase **(b)**. Elongation of the CS chain occurs by sequential additions of GlcA and GalNAc to the nascent non-reducing terminus by chondroitin polymerases **(c)**. The CS chain is sulfated by chondroitin-4 and 6-sulphotransferases, or the GlcA residue of the *O*-disaccharide unit is epimerized to IdoA with inversion in structure from a β-D conformation to an α-L conformation followed by a series of sulphotransferases and uronyl-2-sulphotransferase to form the CS-A, CS-B, CS-C, CS-D, CS-E and DS-iA, DS iB, CS-iC, DS-iD, and DS-iE isoforms as shown **(d–f)**. The 4-*O*-sulfation pathway is most active in the adult brain **(d)** while various DS isoforms regulate brain development and repair processes **(e)**. The 6-sulfation pathway **(f)** is most active in the juvenile brain. The DS-iO and DS-iC units have yet to be confirmed. Figure modified from Malmström et al. (2012) and Miyata and Kitagawa (2017).

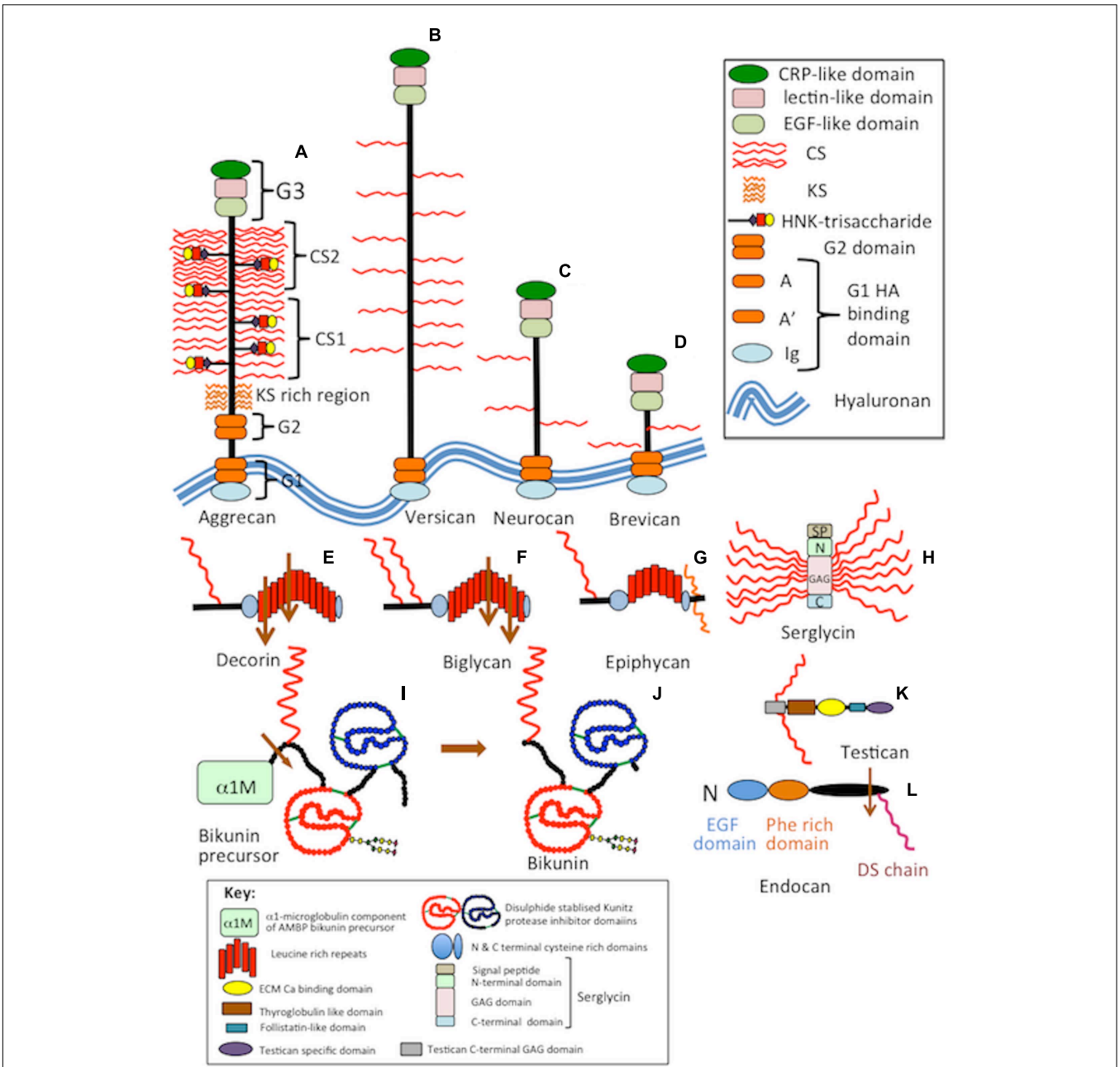


**FIGURE 3 |** Composite schematic depicting the structural organization of secreted CS-proteoglycans in the CNS/PNS. The lectican proteoglycans aggrecan, versican, neurocan, brevican **(A–D)**, selected members of the small leucine repeat proteoglycans, decorin, biglycan and epiphycan **(E–G)**, serglycin **(H)**, bikunin precursor protein and bikunin **(I,J)**, testican **(K)** and endocan **(L)**.

of its specific components in neural development and tissue morphogenesis in a whole organism environment. White et al. (1986) undertook the first complete mapping study of the nematode's nervous system using manual reconstruction of serial electron micrographs, to characterize the morphology of each of the 302 neurons in the adult nematode and their interconnected chemical and electrical synapses. This study is an invaluable guide on the *C. elegans* neural network and has significantly influenced studies on behavioral neurobiology and network science. The nervous system of *C. elegans* has a total of 302 invariantly organized neurons, that have been grouped into 118 categories. Neurons in *C. elegans* have simple morphologies displaying few, if any, branches and are generally highly connected through local synaptic connections with neighboring neurons, ∼ 5000 chemical synapses, 2000 neuromuscular junctions and 600 gap junctions have been identified in *C. elegans*. The specific patterns and functional properties of electrical synapses of the *C. elegans* nervous system

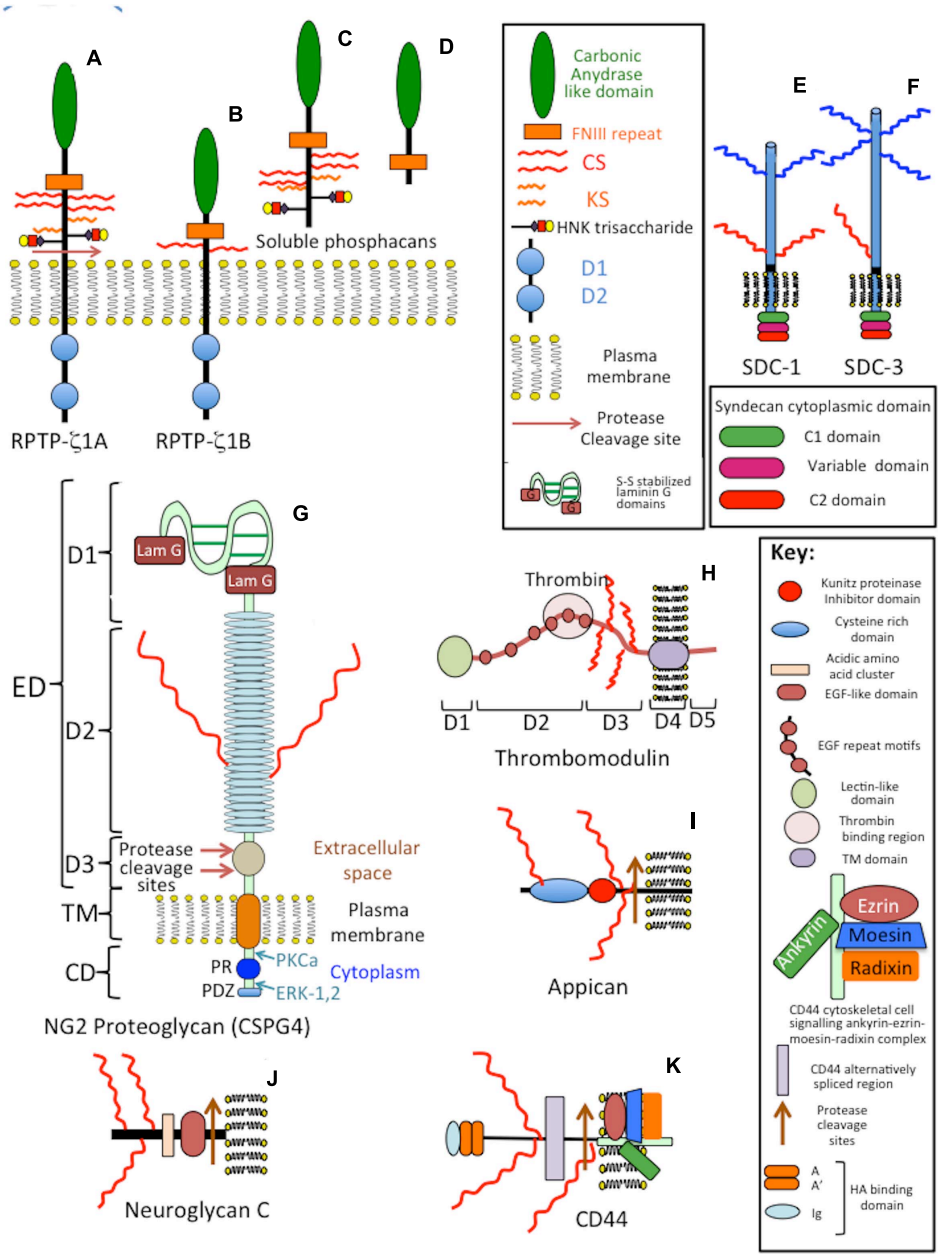


**FIGURE 4 |** Composite schematic depicting the structural organization of cell membrane attached CS-proteoglycans in the CNS/PNS. Phosphacan precursor, receptor protein tyrosine phosphatase (RPTP)-1A and 1B forms **(A,B)** and soluble phosphacan released by proteolysis of **(A)** as shown **(C)**. A non-glycanated truncated phosphacan variant has also been described **(D)**. Syndecan-1 (SDC-1) **(E)** and syndecan-3 (SDC-3) **(F)**. The transmembrane form of NG2 proteoglycan (CSPG4) **(G)** and its soluble form released from cells by protease cleavage close to the cell membrane **(H)**. The soluble form of CSPG4 becomes lodged in the ECM through interactions mediated by its LamG N-terminal motifs and by interactions of its central cysteine-rich domain with type IV and VI collagen. Thrombomodulin showing its terminal lectin-like domain, six EGF repeat modules, thrombin binding region which allows it to act as an anti-coagulant in the brain microvasculature and transmembrane cell attachment domain **(I)**. Appican **(J)**, neuroglycan-C **(K)**, and the HA-receptor CD-44 **(L)** with protease cleavage sites that results in the generation of soluble forms of these proteoglycans. The CS-E chains of appican bind strongly to the growth factors midkine and pleiotrophin, neuroglycan-C binds to ephrin cell surface receptors resulting in induction of cell signaling mediated by the ephrin cytoplasmic regions while sCD44 binds to HA in the ECM through its disulphide stabilized A, A′ and Ig folds. Several CAMs also act as CS-PG receptors through interaction with the CS side chains of these PGs (see **Figure 7**).

have been systematically examined through a genome- and nervous-system-wide analysis of the expression patterns of the invertebrate electrical synapse constituents, the innexins (Hu, 2007; Güiza et al., 2018; Bhattacharya et al., 2019). Innexins are transmembrane proteins that form gap junctions in invertebrates. Highly complex expression patterns are evident throughout the nervous system, and when animals enter an insulin-dependent arrest stage due to exposure to harsh environmental

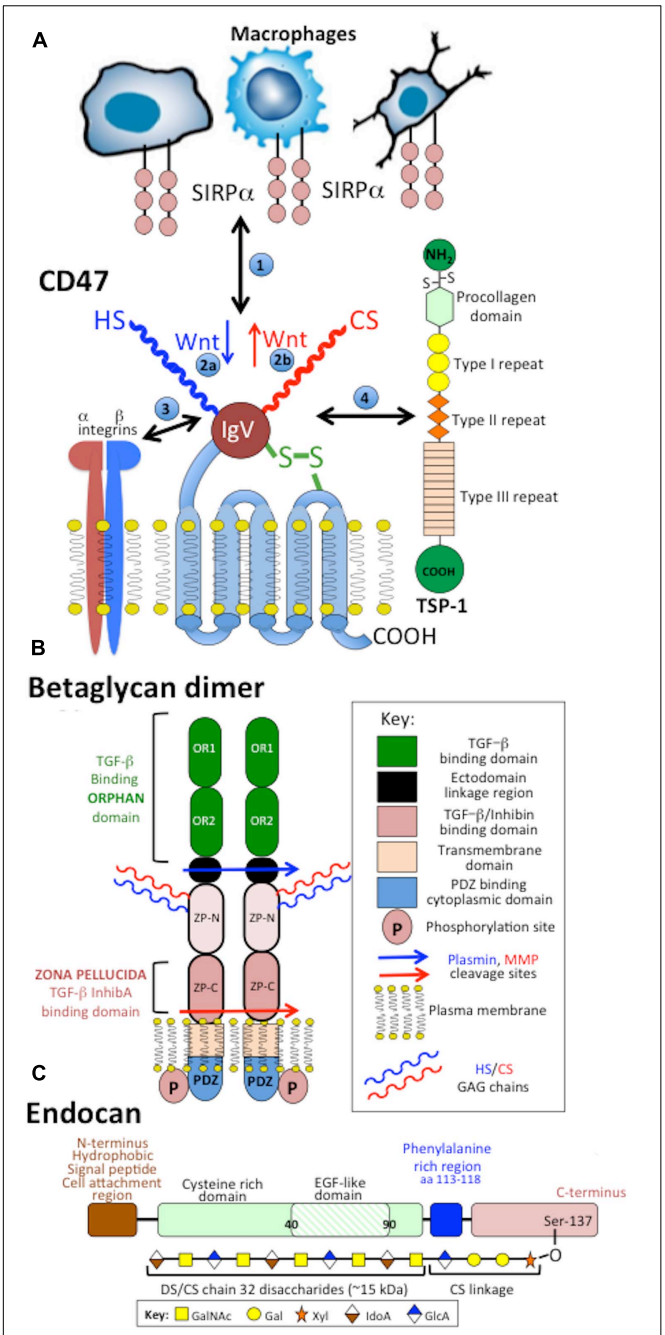


**FIGURE 5 |** Schematic depictions of the structural organization of the transmembrane CS-PG receptors CD47 showing its interactions with macrophages, integrins and thrombospondin-1 (TSP-1) **(A)**, betaglycan dimer **(B)** and endocan **(C)**. Betaglycan forms an active dimer on the cell surface. Protease cleavage sites are indicated which release fragments of the betaglycan ecto-domain. Endocan has an EGF-like and a phenylalanine rich domain and a single CS/DS GAG chain attached to its C-terminus.

conditions, termed the dauer stage, *C. elegans* larvae undergo Dauer arrest at the second molt (Cassada and Russell, 1975). Many insights into the signaling pathways and the molecular mechanisms that govern this developmental transition have been uncovered in the last decade. Dauer pheromone the major physiologic signal that promotes Dauer arrest, has been purified, identified, and synthesized and the vast majority of Dauer regulatory genes are now known (Jeong et al., 2005). Dauer pheromone (daumone, ascr#1) is the first *C. elegans* pheromone identified. Electrical synapse remodeling is responsible for the altered locomotory and chemosensory behavior of Dauer affected neurons (Starich et al., 2009). These neurons are regulated by a mechanism that involves FoxO transcription factors that mediate dynamic innexin expression plasticity in a neuron-type- and environment-specific manner (Hobert, 2010; Amran et al., 2021). *C. elegans* is a useful model for the examination of developmental processes regulated by ECM components (Hobert, 2010; Amran et al., 2021). HSPGs and chondroitin proteoglycans (CPGs) both have prominent roles to play in developmental processes in *C. elegans* (Saied-Santiago et al., 2017). Most ECM molecules in *C. elegans* are conserved and are homologues to mammalian proteins, however, fewer ECM protein isoforms are present and these exhibit less redundancy compared to in mammalian tissues. Furthermore, mutations in *C. elegans* produce comparable developmental defects to those evident in mammals. The small size, short lifespan of 3–4 days and defined neural interconnectivity of the *C. elegans* nervous system facilitate its use in systematic functional studies that have yielded valuable insights into neuronal differentiation (Chisholm and Jin, 2005). This information is also relevant to more complex neural systems since the basic cellular machinery of synaptic transmission is highly conserved across species. In *C. elegans,* 719 out of ∼20,000 genes (∼4%) of its genome encode matrisome proteins, including 181 collagens, 35 glycoproteins, 10 proteoglycans, and 493 matrisome-associated proteins, 173 out of the 181 collagen genes are unique to nematodes and are predicted to encode cuticular collagens (Teuscher et al., 2019).

Comparative genomic studies on human and *C. elegans* has identified orthologous genes in *C. elegans* that have comparable regulatory properties to human genes and demonstrated mechanisms relevant to human biology. *C. elegans* represents an experimental system that can be used in genetic approaches to address biological questions relevant to human development, physiology, and disease. Genetic based phenotype screens have identified *C. elegans* genes homologous to human disease-associated genes, and fundamental properties about their roles and mechanisms of action in pathological human tissues. Reverse genetic methods developed in *C. elegans* have expanded the repertoire of genetic approaches to examine the roles of specific genes in human disease processes. These methods have the ability to phenocopy loss-of-function mutations by feeding worms bacteria expressing double-stranded RNA, RNAi. Studies in *C. elegans* have also facilitated genome-wide screens or screens specifically targeting human disease genes and the large-scale generation of deletion or point mutations for functional genetic studies (Kim et al., 2018).

The *Drosophila* matrisome consists of 641 genes, 27 are homologs/orthologs to human core matrisome genes, 219 are homologs/orthologs to mammalian matrisome genes and the remaining 395 are genes are specific to *Drosophila* (Davis et al., 2019). Comparative genomic analyses have been

undertaken between human and *Drosophila* genomes and core promoter regions. Although fruit flies have a genome that is 25 times smaller than the human genome, many fruit fly genes have comparable genes in humans that control the same biological functions. Twelve fruit fly genome sequences are available in the FlyBase database[1], a collaboration of Harvard, Cambridge, Mass.; Indiana, Bloomington; and the University of Cambridge, United Kingdom. The fruit fly genome sequences are also available from NIH's National Center for Biotechnology Information[2], European Molecular Biology laboratory's Nucleotide Sequence Database, EMBL-Bank[3], and DNA Data Bank of Japan, DDBJ[4] (FitzGerald et al., 2006).

As found in higher organisms, PGs have important roles in cellular regulation critical to the development of metazoan organisms. *C. elegans,* however, produces a large amount of non-sulfated chondroitin (Chn) in addition to a small amount of low sulfation CS. Until recently, *C. elegans* was known to express nine Chn/CS-PGs dissimilar to vertebrate CS-PGs. A recent glycoproteomic study identified 15 additional CPGs in *C. elegans* and three of these were homologous to human proteins, thus selected CS-PG core proteins appear conserved throughout evolution (Noborn and Larson, 2021). Bioinformatic analysis of primary amino acid sequence data identified a broad range of functional domains in these *C. elegans* PGs, thus specific PG core protein mediated functional properties appeared to have evolved early in metazoan evolution.

*Drosophila melanogaster* has also proved to be a useful model for the investigation of developmental GAG functions *in vivo* confirming *in vitro* findings. HS and CS GAG side chains of PGs are structurally conserved between *Drosophila* and mammals, including humans. Mutant and RNAi fruit flies show that HS-PGs and CS-PGs play key roles in the regulation of developmental signaling pathways involving FGF, Wingless (Wg)/Wnt, Hedgehog, and Decapentaplegic (Dpp, a ligand of the TGFβ superfamily). Glycosyl transferases, sulfotransferases, sugar-nucleotide transporters including 3′-phosphoadenosine 5′-phosphosulfate (PAPS) transporters, all have important roles to play in GAG biosynthesis and the functional status of PGs in neuronal development and maintenance (Nishihara, 2010). It should be noted, however, that the major non-sulfated Chn in *C. elegans* has crucial roles in embryonic cell and tissue development and tissue morphogenesis. Since Chn is present on mammalian PG core proteins along with CS no studies have been possible to specifically target the functional roles of Chn in these PGs, however, insights into the biological properties of Chn in mammals can be gleaned from the use of Chn as a drug in the treatment of osteoarthritis (OA) (Singh et al., 2015). A meta-analysis of 43 reviews which analyzed the use of Chn for the treatment of OA and alleviation of joint pain yielded moderate to inconclusive results. However, Chn elicited a significant improvement in the anti-inflammatory profile of synoviocytes and chondrocytes in an OA model analyzed by multiplex and Western blot analysis. Chn significantly decreased the levels of several pro-inflammatory cytokines (IL-1β, IL-5, 6, 7, 9, 15, 17), anti-inflammatory cytokines (IL-4, IL-10), chemokines (IL-8, MCAF, MIP-1a, MIP-1b, RANTES) in synovial fluid samples and decreased expression of the OA biomarkers MyD88 and MMP-13 (Vassallo et al., 2021). Evidence therefore exists that Chn displays anti-inflammatory properties in mammalian tissues. However in *C. elegans* where Chn predominates over CS the biological properties of Chn have more profound effects on neural biology. A number of studies have demonstrated the fundamental biological roles played by Chn, CS, and DS, attached to the core proteins of cell surface and ECM PGs (Sugahara et al., 2003). PGs decorated with CS, DS, or HS have diverse roles in growth factor, morphogen and cytokine-mediated cell signaling through cellular receptors that play critical roles in the development of the CNS (Melrose et al., 2021). As discussed later in this chapter, these functions of PGs are closely associated with GAG sulfation patterns. Surprisingly, non-sulfated Chn is indispensable in the morphogenesis and cell division of *C. elegans*, as revealed by RNA interference experiments of the recently cloned *chondroitin synthase* gene and by the analysis of *squashed vulva* (sqv) gene mutants. It should be noted that while orthologous forms of human perlecan/HS-PG2 exist in *C. elegans (*UNC-52*)* and *D. melanogaster* (Trol) these have a different modular structure to human perlecan and are devoid of domain-I and thus they lack HS substitution (Celestrin et al., 2018). Thus the interactive properties provided by the HS chains of human perlecan do not occur in these orthologs and the interactive properties conveyed by these form of perlecan is due to modular components in their core proteins (Condomitti and de Wit, 2018; Martinez et al., 2018).

## The Instructional Properties of CS- and HS-PGs in Neural Development and Tissue Morphogenesis in *Caenorhabditis elegans*

Blocking of chondroitin synthesis results in cell proliferative defects in early embryogenesis in *C. elegans* and leads to early embryonic death (Mizuguchi et al., 2003). Mutations in eight sqv genes in *C. elegans* causes defects in embryonic cytokinesis and in vulval morphogenesis during postembryonic development. Sqv-1, 2, 3, 4, 6, 7, 8 control CS and HS biosynthesis, while sqv-5 encodes a bifunctional glycosyltransferase responsible for the biosynthesis of Chn, but not HS (Hwang et al., 2003a,b). Sqv mutations in *C. elegans* have lethal consequences due to disruption in cell proliferation and the lack of the formation of an extracellular space between the egg and the eggshell, apparently due to disruption in the normal GAG containing ECM structures. Cloning and characterization of the sqv-2 and -6 genes showed that sqv-6 encoded a protein similar to human xylosyltransferase, while sqv-2 encoded a protein similar to human galactosyltransferase II. SQV-6 and SQV-2 proteins act in concert with other SQV proteins to catalyze the stepwise formation of the PG core protein linkage tetrasaccharide GlcAβ1,3Galβ1, 3Galβ1,4Xylβ-*O*-(Ser), common to CS and HS (Hwang et al., 2003a,b). This linkage tetrasaccharide acts as an

[1]http://flybase.bio.indiana.edu

[2]www.ncbi.nlm.nih.gov

[3]www.ebi.ac.uk/embl/index.html

[4]www.ddbj.nig.ac.jp

acceptor molecule for the assembly of the CS and HS chains. Chain elongation is initiated by the addition of GlcNAc or GalNAc, with the former addition resulting in the biosynthesis of HS chains by sequential additions of GlcA and GlcNAc, while if GalNAc is the initial sugar added to the acceptor group this results in the synthesis of CS chains. These GAG chains are sulphated in a later biosynthetic stage at various positions on GlcNAc or GalNAc by specific sulfotransferases. GlcA can also be epimerised to IdoA and sulphated at O-2 in HS chains. HS chains can be sulphated at multiple positions. CS sulfation is an important functional determinant in the regulation mammalian neural tissue development and repair, however, in *C. elegans* and *D. melanogaster* the Chn chains are not sulphated but nevertheless have essential roles to play in early embryonic development and tissue morphogenesis in later developmental stages.

Vertebrates produce multiple CS-PGs with important roles in development and the mechanical performance of tissues. The Chn chains in *C. elegans* are not sulfated, but nevertheless they still play essential roles in embryonic development and vulval morphogenesis (Olson et al., 2006). *C. elegans* Chn PG core proteins, do not share sequence similarities with PGs from *D. melanogaster* or *Hydra vulgaris*. The *C. elegans* CPG-1 and CPG-2 PGs are expressed during embryonic development and bind chitin, which may have a structural role to play in the egg (Olson et al., 2006). Chitin is a widespread polymer in nature and is a polymer composed of *N*-Acetyl glucosamine. Chitin is a primary component of fungal cell walls, the exoskeletons of arthropods such as crustaceans and insects and the scales of fish. Depletion of CPG-1/CPG-2 results in multinucleated single-cell embryos in *C. elegans*, this is also observed with depletion of the SQV-5 chondroitin synthase protein, Chn chains of CPG1/CPG2 play essential roles in cytokinesis. This is achieved through regulation of GAG biosynthetic enzymes. *C. elegans* microRNA mir-79, an ortholog of mammalian miR-9, controls sugar-chain homeostasis by targeting two proteins in the PG GAG biosynthetic pathway: a chondroitin synthase (SQV-5; squashed vulva-5) and a uridine 5′-diphosphate-sugar transporter (SQV-7). Loss of mir-79 causes neurodevelopmental defects through dysregulation of SQV-5 and SQV-7. This results in a partial shutdown of HS biosynthesis that effects the LON-2/glypican pathway and disrupts neuronal migration. MicroRNA thus represents a regulatory axis that maintains PG homeostasis. Sqv genes 1–8 control the invagination of vulval epithelial cells, normal oocyte formation and embryogenesis. Sequencing of sqv-3, sqv-7, and sqv-8 genes indicated potential roles for the proteins they encode in glycolipid or glycoprotein biosynthesis. sqv-3, -7, and -8 affect the biosynthesis of GAGs and the bioactivity of PGs establishing their essential roles in tissue morphogenesis and pattern development in *C. elegans* (Bulik et al., 2000).

Sulfation of PG GAG side chains has critical roles to play in the cell regulatory properties of PGs and their roles in many essential physiological processes. Sulfation reactions involves activated sulfate, and the universal sulfate donor 3′-phosphoadenosine 5′-phosphosulfate (PAPS). In animals, PAPS is synthesized from ATP and inorganic sulfate by PAPS synthase, genetic defects in PAPS synthase 2, one of two PAPS synthase isozymes, causes dwarfism. In order to better understand the developmental role of sulfation in tissue PGs, a *C. elegans* PAPS synthase-homologous gene, pps-1 has been cloned and the depleted expression of its product, PPS-1 examined (Dejima et al., 2006). PPS-1 protein exhibits specific roles in the formation of PAPS *in vitro*. Disruption of the pps-1 gene by RNAi methods causes widespread developmental tissue defects, a decrease in GAG sulfation in the pps-1 null mutant exhibits larval lethality. Sulfation is essential for normal growth and the integrity of the epidermis in *C. elegans* and has been used as a model to demonstrate the role of HS modifications in a defined biological process. Genetic analyses suggest that syndecan/sdn-1 and HS 6-*O*-sulfotransferase, hst-6, function in a signaling pathway and glypican/lon-2 and HS 2-*O*-sulfotransferase, hst-2, function in a parallel pathway. HS modifications may be part regulated at the level of tissue expression of genes encoding for HS-PGs and HS modifying enzymes. There is a delicate balance in such HS modifications that may deleteriously effect cell migration, HS is a critical regulator of cell signaling in normal development and disease. HS-PGs have roles in the structural organization of neurochemical synapses, involving interactions with the core protein as well as the HS side chains (Cizeron et al., 2021). Specific modifications to HS contribute to a sugar code which provides specificity to synaptic interactions. SDN-1 is a unique *C. elegans* syndecan ortholog found in synaptic junctions. 3-*O* sulfation of SDN-1 maintains the ECM protein punctin/MADD-4/ (MAP kinase-activating death domain protein) that defines the synaptic domains, however, in mammals 3-*O* sulfation is a rare modification in HS despite the seven HS modifying enzymes that can produce 3-*O* sulfation.

Punctin/MADD-4, a member of the ADAMTSL ECM protein family, is a synaptic organizer in *C. elegans.* MADD is an enzyme encoded by the MADD gene. The Ig-like domain of MADD is the primary determinant for N-MADD-4B interactions with NLG-1 *in vitro* (Platsaki et al., 2020). At GABAergic neuromuscular junctions, the short isoform MADD-4B binds the ectodomain of neuroligin (NLG-1), which is also a postsynaptic organizer of inhibitory synapses (Tu et al., 2015). Proteolysis of MADD-4B generates *N*-MADD-4B, which contains four thrombospondin domains and one Ig-like domain that bind NLG-1 (Maro et al., 2015). A second processing event eliminates the C-terminal Ig-like domain of N-MADD-4B and its ability to bind NLG-1. The death domain of the type 1 tumor necrosis factor receptor (TNFR1) mediates the downstream effects of TNF. MADD interacts with TNFR1 residues and is a component of the TNFR1 signaling complex. The MADD death domain stimulates ERK and c-JUN N-terminal kinase MAP kinases inducing phosphorylation of cytosolic phospholipase A2. Thus, MADD links TNFR1, MAP kinase activation and arachidonic acid release, which may explain the pleiotropic effects of TNF.

Growth cones facilitate the repair of damaged neural tissue by promoting axon regeneration, syndecan, is required for growth cone function during axon regeneration in *C. elegans* (Edwards and Hammarlund, 2014; Gopal et al., 2016, 2021). In the absence of syndecan, regenerating growth cones are unstable and they collapse, impeding regrowth to target cells. Syndecan has two distinct functions during axon regeneration: (i) axon guidance

requiring its HS-dependent expression outside the nervous system (ii) intrinsic growth cone stabilization mediated by the SDC core protein independently of HS.

## The Instructional Properties of CS- and HS-Proteoglycans in Neural Development and Tissue Morphogenesis in *D. melanogaster*

Blocking Chn synthesis results in defects in cytokinesis and embryogenic development in *D. melanogaster* leading to early embryonic death. This demonstrates the essential developmental roles Chn plays in *Drosophila* embryonic cytokinesis and cell division. *Drosophila* has proved to be a useful model for the investigation of developmental GAG functions *in vivo* confirming *in vitro* findings with GAGs (FitzGerald et al., 2006; Nishihara, 2010). HS and CS GAG side chains of PGs are structurally conserved between *Drosophila* and mammals, including humans. CS sulfation is an important functional determinant in the regulation of mammalian neural tissue development and repair; however, in *C. elegans* and *D. melanogaster* the Chn chains are not sulfated but, nevertheless, have essential roles to play in early embryonic development and tissue morphogenesis in later developmental stages.

Windpipe (Wdp) is a novel CS-PG recently identified in *Drosophila*. Wdp is a single-pass transmembrane protein with leucine-rich repeat (LRR) motifs and has three extracellular CS chain attachment sites (Takemura et al., 2020). Wdp modulates the Hedgehog (Hh) cell signaling pathway. In the wing disk, overexpression of Wdp inhibits Hh signaling an effect that is dependent on its CS chains and protein interactive LRR motifs. The JAK/STAT (Janus Kinase/Signal Transducer and Activator of Transcription) signaling pathway regulates adult stem cell activities and is essential for the maintenance of intestinal homeostasis in *Drosophila*. Wdp interaction with the receptor Domeless (Dome) promotes its internalization and lysosomal degradation. Wdp thus acts as a negative feedback regulator of JAK/STAT cell signaling and is a novel regulatory component of JAK/STAT signaling in *Drosophila* adult intestines (Ren et al., 2015).

Glycosaminoglycans such as HS and CS have roles in intercellular signaling thus disruptions of genes encoding enzymes that mediate GAG biosynthesis have severe consequences in *Drosophila* and mice. Mutations in the *Drosophila* gene *sugarless*, encoding a uridine diphosphate (UDP)-glucose dehydrogenase, impairs developmental signaling through the Wnt family member Wingless, and FGF and Hedgehog signaling pathways. Undersulfated and oversulfated CS chains are implicated in neural development, cloning of a chondroitin synthase homolog in *Caenorhabditis elegans* and depletion in Chn expression results in defects in cytokinesis in early embryogenesis and early embryonic death demonstrating the essential role Chn plays in early developmental processes (Mizuguchi et al., 2003).

*Drosophila* has an NG2 homologue called kon-tiki (kon), that promotes CNS repair (Losada-Perez et al., 2016). Crush injury upregulates kon expression and induces glial cell proliferation and differentiation by activating glial genes and prospero (pros). Negative feedback loops with Notch and Pros allow Kon to drive the homeostatic regulation of neuronal repair with modulation of Kon levels in glia, potentially preventing or promoting CNS repair (Losada-Perez et al., 2016). The interplay between Kon, Notch, and Pros is therefore essential in neural repair in *Drosophila*. Prospero homeobox protein-1 is encoded by the *PROX1* gene in humans. This pan-neural protein has essential roles to play in the proper differentiation of neuronal lineages and in the expression of genes in the *Drosophila* CNS. Prospero is a sequence-specific DNA-binding protein that can act as a transcription factor through interaction with homeodomain proteins to differentially modulate their DNA-binding properties (Hassan et al., 1997; Yousef and Matthews, 2005). Functional interactions between Prospero and homeodomain proteins is supported by observations showing that Prospero, together with the homeodomain protein, Deformed, are required for proper regulation of a Deformed-dependent neural-specific transcriptional enhancer (Hassan et al., 1997). The DNA-binding and homeodomain protein-interactive properties of Prospero are localized in its highly conserved C-terminal region.

Syndecan (Sdc) is a conserved transmembrane HS-PG bearing CS chains on its ectodomain. In vertebrates, this extracellular domain of Sdc is shed and acts as a soluble effector of cellular communication events, and the Sdc cytoplasmic domain participates in intracellular signaling needed to maintain epithelial integrity. In *Drosophila*, Sdc has been shown to be necessary for Slit signaling-dependent axonal guidance during CNS development (Chanana et al., 2009). Sdc acts in a cell-autonomous manner in Slit-receiving cells and that its membrane-anchored extracellular domain is sufficient to mediate Slit signaling. The HS-PG Dally-like protein (Dlp), which lacks CS on its extracellular domain, can only partially substitute for Sdc function but its activity is not restricted to the Slit target cells. Sdc and Dlp act in a cooperative but non-redundant manner in neural tissues with Dlp transferring Slit from its site of expression to the target cells, where it interacts with CS-modified Sdc.

## *Caenorhabditis elegans* Netrins and Neural Development

UNCoordinated-6 (UNC-6) was the first *C. elegans* member of the netrin family that was discovered (Krahn et al., 2019). UNC-6 shares homology to human netrin-1, and is a key signaling molecule in the regulation of directional axonal migration in nematodes (Krahn et al., 2019). Similar to netrin-1, UNC-6 interacts with multiple receptors to guide axonal migration (Moore et al., 2007; Rajasekharan and Kennedy, 2009; Ogura et al., 2012). Netrin is a key guidance protein regulating the orientation of axonal growth during neural network formation in *C. elegans*. LON-2/glypican, modulates UNC-6/netrin signaling through interactions with the UNC-40/DCC (deleted in colorectal carcinoma) receptor (Yang et al., 2014). LON-2 expressed on the cell surface in the intestine and hypodermis in *C. elegans* and in *D. melanogaster* promotes growth factor binding in several developmental processes, negatively regulating the TGF-β receptor signaling pathway and

BMP-like signaling that regulates tissue growth and body length. N-terminal sequencing of the signal peptide of LON-2, identified a 14 cysteine domain of functional importance, SGXG GAG attachment site and C-terminal GPI anchor site showing that LON-2 is a member of the glypican family (Eisenhaber et al., 2000; Gumienny et al., 2007). The other *C. elegans* glypican, *gpn-1*, has no significant effect on the body size (Blanchette et al., 2015). Null mutations in *C. elegans* genes encoding HS biosynthetic enzymes that process the HS side chains of LON-2, significantly reduce body size. *hse-5*, *hst-2*, and *hst-6* encode *C. elegans* counterparts to mammalian glucuronyl C5-epimerase, 2 *O*-sulfotransferase, and 6 *O*-sulfotransferase, respectively. This demonstrates the important functional role HS plays in neural development in *C. elegans* and the importance of the HS sulfation patterns for this activity (Bülow and Hobert, 2004; Gysi et al., 2013; Díaz-Balzac et al., 2014; Saied-Santiago et al., 2017). HS chains of HS-PGs carry multiple structural modifications due to sulfation and epimerization of GlcA that influence their ligand binding properties. This is why HS-PGs have such diverse effects in tissue and axonal development. The core proteins of *C. elegans* SDN-1 and glypican/LON-2 and HS modifying enzymes thus both have roles in axonal guidance through interactions with UNC-6/Netrin (Rhiner et al., 2005). *C. elegans* SDN-1/syndecan control of neural migration and axonal guidance also occurs through regulation of Slit/Robo signaling in parallel with C5-epimerase HSE-5, and/or the 2O-sulfotransferase HST-2 activity, which provide distinct regulatory HS modification patterns on SDN-1.

## MAMMALIAN NEURONAL PROTEOGLYCANS

Neural PGs occur as large and small extracellular, cell surface and intracellular components. The salient features of neural PGs are summarized in **Table 1** and their structural organizations are shown schematically in **Figures 3–5**.

### Roles for the CS-Rich Lectican PG Family in Perineuronal Net Structures

The lectican family of neural PGs have similar structures to aggrecan but do not contain keratan sulfate (KS) or a G2 globular domain. Furthermore, their molecular dimensions are smaller due to shorter core proteins and less extensive distributions of CS side-chains (Yamaguchi, 2000). Lectican PGs occur as diffuse ECM components and as dense PNN structures attached to HA through interactions with lectican N-terminal HA-binding regions. This aggregate is stabilized by tenascin-R and Bral-1 (Hyaluronan and Proteoglycan Link Protein 2; HAPLN2). The form of aggrecan found in brain differs from that of cartilage aggrecan in that it contains less KS chains, and its CS chains are less densely distributed along the CS1 and CS2 core protein regions (Hayes and Melrose, 2020a). Some CS chains in neural aggrecan are replaced by HNK-1 trisaccharide which also attaches to the same core protein linkage tetrasaccharide as CS. Once the HNK-1 trisaccharide is assembled chain elongation ceases resulting in a reduction in CS chain density but introduces cell interactive properties. Neural aggrecan guides neural crest progenitor cell migration during embryonic neurogenesis and formation of the neural tube and notochord (Hayes and Melrose, 2020a). Preclinical spinal cord injury (SCI) and traumatic brain injury (TBI) animal model studies demonstrate that the enzymatic degradation of CS-PGs from gliotic scars using chondroitinase ABC improves neuronal functional recovery (Bradbury and Carter, 2011; Cheng et al., 2015; Muir et al., 2019). Endogenous degradation of the core protein of CS-PGs by ADAMTS-4 also improves neuronal functional recovery (Tauchi et al., 2012). While the CS-A and CS-C side chains of the lecticans inhibit neural repair, not all CS-PGs inhibit axonal re-growth (Mencio et al., 2021). PGs containing over-sulfated CS-B, and CS-E promote neurite outgrowth and functional recovery (Bovolenta and Fernaud-Espinosa, 2000). The EGF-like motif in the G3 domain of the lecticans has also been shown to regulate cell migration and tissue repair (Aguirre et al., 2007; Du et al., 2010). Overexpression of human EGFR in CNP (hEGFR) mice accelerates remyelination and functional recovery following focal demyelination. Progenitor cells over-expressing NG2 PG also improve re-myelination through EGFR mediated cell signaling (Keirstead and Blakemore, 1999; Aguirre et al., 2007). PNNs surrounding the soma and dendrites of a number of neuronal cell types are prevalent during neural development and maturation (Carulli and Verhaagen, 2021). A similar structure, the perinodal ECM surrounds the axonal nodes of Ranvier and appear after re-myelination, acting as a protective ion-diffusion barrier (Bekku and Oohashi, 2019; Fawcett et al., 2019). Perinodal structures in the Nodes of Ranvier also contain PNN components such as brevican and versican V2 (Bekku et al., 2009; Dours-Zimmermann et al., 2009).

Perineuronal net are variably distributed in the brain, the somatosensory frontal lobes of the cerebral cortex have a particularly high density of PNNs, however, they are sparsely distributed in the sub-ventricular and sub-granular dentate gyrus of the hippocampus. These regions contain neuro-progenitor stem cell niches termed fractones (Mercier and Arikawa-Hirasawa, 2012; Sato et al., 2019). Abnormal PNN formation impacts on neural development and may result in degenerative synaptic pathology in schizophrenia (Pantazopoulos et al., 2021), bipolar disorder, major depression, and autism spectrum disorders (Sorg et al., 2016). CS-PGs in PNNs control synaptic plasticity, and have roles in memory in the aging brain, deterioration of PNNs contribute to the age-dependent decline in brain function. Recent work has revealed the importance of PNNs in the control of CNS plasticity. Digestion, blocking or removal of PNNs impedes functional recovery after a variety of CNS lesions. Deficient PNN numbers are implicated in a number of psychiatric disorders and suggested as therapeutic targets in their treatment (Dityatev et al., 2021). Incorrect assembly of PNNs or degradation of PNN components by excessive MMP activity can lead to the development of epilepsy (Rankin-Gee et al., 2015; Dubey et al., 2017; Mencio et al., 2021). Deficient levels of HA in PNN structures promote epilepsy and spontaneous convulsions in animal models (Perkins et al., 2017). The CS-PGs of PNNs have important functional roles to play in perisynaptic structures that prevent the development

**TABLE 1 |** Extracellular, cell associated and intracellular CS-proteoglycans of the CNS/PNS.

| Protein | Distribution | Roles | References |
|---|---|---|---|
| **Large lectican neural proteoglycans** | | | |
| Aggrecan (ACAN) (CSPG1) | Present as diffuse ECM component between the dense ECM of PNNs which contain HA and the lecticans | Roles in tissue hydration, space-filling in CNS/PNS, neuroprotective in PNNs, synapse formation, roles in synaptic plasticity memory, cognitive learning | Kiani et al., 2002; Hayes and Melrose, 2020a |
| Versican (VCAN) (CSPG2) | Widespread in CNS/PNS occurs as V0, V1, V2, V3 isoforms | Promotes proliferation, differentiation, cell migration, tissue development, repair, tissue morphogenesis. G1 and G3 stimulate cell migration. Versikine G1 fragment of Versican V2 is an Alarmin in innate immunity with TLR4. | Schmalfeldt et al., 1998; Wu et al., 2004; Xiang et al., 2006; Schmitt, 2016; Islam and Watanabe, 2020 |
| Neurocan (NCAM) (CSPG3) | 150 kDa lectican CS-PG<br>Widespread CNS/PNS PG | Interacts with HA, NCAM, modulates cell binding, regulates neurite outgrowth through interactions with Sdc-1, Gpc-3, and PTN. | Margolis and Margolis, 1994; Margolis et al., 1996; Rauch et al., 2001; Sullivan et al., 2018; Schmidt et al., 2020 |
| Brevican (CSPG7) | Widespread CNS/PNS PG, present in the post synaptic gap where it may relay neurotransmitters to adjacent communicating neurons | Binds to astrocytes and neurons regulates axon and dendritic maturation, upregulated in glial scars. GPI anchored brevican described. BEHAB is a bioactive fragment that promotes glioblastoma development. | Yamaguchi, 1996; Gary and Hockfield, 2000; Matthews et al., 2000; Giamanco and Matthews, 2020 |
| **Large non-lectican neural proteoglycans** | | | |
| RPTPR-ζ Phosphacan | Populations of phosphacan contain variable levels of CS, KS, or HNK-1 trisaccharide substitution<br>Cell surface (RPTPR-ζ) and soluble PG (phosphacan) forms | RPTPR-ζ, single pass type 1 TM PG-phosphatase receptor, regulates SC repair and neurogenesis, soluble phosphacan ectodomain, has truncated forms with neurite outgrowth activity. | Garwood et al., 2003; Faissner et al., 2006; Eill et al., 2020 |
| NG2 (CSPG4) | Widely distributed TM Oligodendrocyte PG, a soluble form is released from cell by proteases | Stimulates endothelial cell proliferation, sequesters FGF-2 and PDGF. Collagen VI receptor activates FAK/ERK1/ERK2 signaling. Up-regulated in SCI and tumors. | Jones et al., 2002; Wigley et al., 2007; Tamburini et al., 2019 |
| Betaglycan | 250–280 kDa CS/HS TM homodimeric PG | Binds inhibin, FGF-2, Wnt TGF-β HS inhibits and CS promotes Wnt signaling. Fragments of betaglycan are released by plasmin and MMPs. binding to inhibin antagonises activin signaling | Lewis et al., 2000; Gray et al., 2001; Bilandzic and Stenvers, 2011; Miller et al., 2012; Kim et al., 2019 |
| Perlecan (HSPG2) | HS/CS hybrid PG of BBB, NMJ, BM, and of fractone stem cell niche | Stabilizes BBB and motor neuron endplate BM. Regulates neuroprogenitor proliferation by FGF-2 in SVZ and dentate gyrus fractones. Domain V promotes neurogenesis, BBB repair | Cho et al., 2012; Kerever et al., 2014; Celestrin et al., 2018 |
| **Small neural proteoglycans** | | | |
| Neuroglycan-C (CSPG5, CALEB) Acidic, Leu-rich EGF Brain PG | Part-time TM PG, growth and differentiation factor involved in neuritogenesis | Core protein EGF domain, CS-E side chains, ligand for ErbB3. Binds PTN to promote neurite outgrowth. | Watanabe et al., 1995; Kinugasa et al., 2004; Shuo et al., 2007; Nakanishi et al., 2010 |
| Syndecan-1. Syndecan-3 (Sdc1, Sdc3) | TM CS/HS CNS/PNS PGs | Sdc-1 and 3 interact with midkine, and PTN, roles in neural development, neurite outgrowth, neural proliferation | Couchman et al., 2015; Gopal et al., 2016 |
| Decorin (DCN) | ∼92.5 kDa class I SLRP containing one N-terminal CS or DS chain, 42 kDa core protein, and 12 LRRs. Widely distributed in CNS/PNS and around gliotic scars | Pluripotent, regulates IL-1, VEGF2, CTGF, TGF-β EGF, IGF-1, participates in ECM assembly, cell growth, differentiation, proliferation, adhesion, and migration. Regulates inflammation, fibrosis, fibrillogenesis, TGF-β bioavailability. "Mayday" and "Decorunt" DCN fragments. Mayday attracts MSCs into tissue defects | Lee et al., 2014; Zhang W. et al., 2018 |
| Biglycan (BGN) | ∼200 kDa class I SLRP containing two N-terminal CS or DS chains and a 42 kDa core protein and 12 LRRs | Structural ECM component, TLR-2, 4 interactive DAMP Alarmin protein in innate immunity, modulates growth factor (TGF-β, TNFα, BMP-2, 4, 6; WISP-1) and cytokine functions and is a stabilizing component of synapses. also interacts with complement system. An *en silico* generated BGN fragment (P2K) is a TGF-β inhibitor. | Amenta et al., 2012; Nastase et al., 2012; Chen et al., 2018, 2020; Xie et al., 2020 |

*(Continued)*

**TABLE 1 |** Continued

| Protein | Distribution | Roles | References |
|---|---|---|---|
| Epiphycan (EPN) DSPG3,PG-Lb | Epiphycan (EPN) also known as DSPG3 or PG-Lb is a CS/DS substituted 133 kDa SLRP with a 46 kDa core protein and contains 7 LRR repeats. EPN is a Cochlear SLRP | Epiphycan (EPN) is a CS/DS 133 kDa SLRP with a 46 kDa core protein and c7 LRR repeats. EPN has roles in auditory cochlear neuronal interactions, EPN deficiency leads to deafness. | Johnson et al., 1997; Hanada et al., 2017 |
| Appican (APP) | APP is a 100–110 kDa type I TM PG alternatively spliced APLP2 is also found in neural tissues | APP has neuroregulatory properties through PTN: CS-E interactions | Pangalos et al., 1996 |
| Bikunin/ITI | Bikunin is the light chain of ITI and has a mass of 25–26 kDa, contains a single CS chain. | Multifunctional Kunitz protease inhibitor PG, anti-metastatic, immune-modulator, growth promoter. Stabilizes HA by crosslinking ITI HCs to HA | Hamasuna et al., 2001; Lord et al., 2013, 2020 |
| Serglycin (SGN) | Mast cells, platelets, macrophages, T-cell, NK cells | Mast cell SGN is substituted with heparin, macrophage, NK killer, T-cell SGN has CS (CS-A, CS-E) side chains | Kolset and Pejler, 2011; Roy et al., 2017 |
| Endocan | 50 kDa Endothelial cell DS cell surface PG also found circulating in bloodstream | DS chain binds L-, *P*-Selectin FN, chemokines, cytokines. RANTES, SDF-1β, IL-8, MCP-1, IFN-γ, PF-4, MK, PTN, FGF-2, FGF -7 | Maurage et al., 2009; Kali and Shetty, 2014; Gaudet et al., 2020 |
| Testican-1, 2, 3 | Testican-1 and -2 are CS/HS PGs, of the BM-40/SPARC/osteonectin family. Testican 3 is a brain specific HS PG | Testican-1 is upregulated in neurons and astrocytes following brain injury. Testican 1-3 regulate MT_MMP and cathepsin L activity in neural tissues. | Marr et al., 2000; Iseki et al., 2011; Hartmann et al., 2013 |
| CD 141 | Thrombomodulin is a component of the endothelium, thrombin inhibitor | Inhibits thrombin in the endothelium protein C-anticoagulant system. Has anti-inflammatory barrier-stabilizing properties in ischemic stroke, enhancing vessel recovery and BBB repair. | |
| CD44 | V3 splice variants bear CS chains | Binds Ezrin, fibrin/fibrinogen, FN, HA, OPN, Selectins-P,-E,-L. | Dzwonek and Wilczynski, 2015; Mooney et al., 2016 |
| CD47 | Neuron 50 KDa, 4 span TM CS-PG receptor | Neuroimmune regulatory protein, TSP-1 receptor, binds SIRPα. Regulates neuronal migration, proliferation and vascular cell survival, in innate and adaptive immunity, increases tissue resilience | Zhang H. et al., 2015; Matlung et al., 2017; Bedoui et al., 2018; Hutter et al., 2019; Li et al., 2021 |
| Astrochondrin | Astrocyte cell surface PG | Binds laminin and type IV collagen in microvasculature and meninges. | Streit et al., 1993 |
| Photomedin | Brain-specific glycoprotein of the eye neuroepithelium. member of the olfactomedin protein family | Photomedin interacts with CS-E to regulate axonal growth and differentiation of neural sensory epithelium | Furutani et al., 2005 |
| FORSE-1 PG (forebrain-surface-embryonic) | LeX-substituted 286 kDa neuro-progenitor cell glycoprotein/PG | Lewis-X, SSEA-1 or CD15, Galβ(1-4)Fucα(1-3)GlcNAc-R oligosaccharide epitopes in FORSE-1 have roles in embryonic neural development | Gooi et al., 1981; Hakomori et al., 1981; Allendoerfer et al., 1995, 1999; Kelly et al., 2019 |

*ADAM-TS, a disintegrin and metalloproteinase with thrombospondin motifs; BBB, blood brain barrier; BM, basement membrane; BMP, bone morphogenic protein; CNS, central nervous system; CS, chondroitin sulfate; DS, dermatan sulfate; ECM, extracellular matrix; ERK, extracellular regulated kinase; FAK, focal adhesion kinase; FGF-2, fibroblast growth factor-2; HA, hyaluronic acid; HS, heparan sulfate; IL1, interleukin-1; LRR, leucine rich repeat; MMP, matrix metalloproteinase; MS, mass spectrometry; NCAM, neural cell adhesion molecule; PCM, pericellular matrix; PNS, peripheral nervous system; SLRP, small leucine repeat proteoglycan; SV, sub-ventricular; TLR4, Toll-like receptor-4; TM, transmembrane; TNF-α, tumor necrosis factor-α; MK, midkine; PTN, pleiotrophin; FN, fibronectin; TSP, thrombospondin; SGN, serglycin; ITI, inter-α-trypsin inhibitor; SVZ, sub-ventricular zone; WISP-1, Wnt1-inducible-signaling pathway protein 1, CCN4; SDF-1, stromal cell derived factor-1, CXCL12; MCP-1, monocyte chemoattractant protein-1, CCL2; RANTES, Regulated upon Activation, Normal T Cell Expressed and Presumably Secreted, chemokine ligand 5 (CCL5); PF-4, platelet factor-4; SSEA-1, stage specific embryonic antigen-1; DAMP, danger associated molecular pattern; SPARC, secreted protein acidic and rich in cysteine.*

of Alzheimer's disease (AD) (Morawski et al., 2012), cortical regions with abundant levels of ECM CS-PGs are less affected by degenerative features associated with the development of AD (Bruckner et al., 1999). PNNs also have important roles to play in Schizophrenia and Bipolar disorder (Berretta, 2012; Mauney et al., 2013). In unaffected individuals, the density of PNNs in the prefrontal cortex increases during pre-puberty and early adolescence. However, in patients with schizophrenia, a 70% reduction in PNN numbers in the prefrontal cortex has been observed (Mauney et al., 2013). The organization and function of PNNs is also disturbed in bipolar disorder (Gandal et al., 2018). Stem cells have been administered to promote recovery of normal PNN structure in an attempt to reverse these debilitating conditions (Forostyak et al., 2014). With an appreciation of PNNs and their important contributions to synaptic stability (Miyata et al., 2018), plasticity, memory and cognitive learning in normal brain tissues this has led to the identification of abnormalities in PNN assembly or expression of PNN components associated with particular neurodegerative conditions (Yamaguchi, 2000; Wen et al., 2018). Thus PNNs have

become a therapeutic focus in the treatment of these conditions (Dityatev et al., 2006, 2010, 2021).

## NEURAL PROTEOGLYCANS

### Aggrecan

In the CNS/PNS, aggrecan core protein contains KS, HNK-1 trisaccharide and CS side chains (Hayes and Melrose, 2020a) that convey unique tissue-specific functional properties (**Figure 3A**). Aggrecan's ability to form macro-aggregates with HA provides water imbibing, space-filling and matrix stabilizing properties to the PNS/CNS ECM and in brain establishes ionic gradients and microcompartments important for the optimal activity of neural cell populations.

The ability of the aggrecan core protein to assemble CS and KS chains at high density provides its well-known water-imbibing properties. Specific arrangements of GAG chains on aggrecan are functional determinant providing unique tissue context-dependent regulatory properties over neural cell populations. The aggrecan core protein KS and CS side chains and N-linked oligosaccharides all display neurite outgrowth-inhibitory activity (Hering et al., 2020). The cell mediatory properties of aggrecan's GAGs thus convey diverse regulatory roles in tissue development and in neuroprotective matrix stabilization of PNNs. Variation in the sulfation position and density on the CS side chains can influence morphogen and growth factor binding relevant to tissue development (Reichsman et al., 1996; Nandini and Sugahara, 2006; Nadanaka et al., 2008; Whalen et al., 2013; Mizumoto et al., 2015).

### Versican

Versican is a large member of the lectican family (Yamaguchi, 2000) with a 400 kDa core protein modestly substituted with CS side chains (**Figure 3B**). Versican occurs as four alternatively spliced isoforms, VO, V1, V2, V3 (Yamaguchi, 2000). Versican was named after its versatile roles as a cell instructional and ECM organizational functional PG in tissue development, cell migration, adhesion, proliferation, and differentiation. Versican V1 promotes neuritogenesis (Wu et al., 2004). Versican interacts with HA through its G1 globular domain, C-type lectin G3 motifs interact with tenascin-R to stabilize HA-versican macro-aggregates (Bignami et al., 1993) and with HNK-1-substituted cell adhesion proteins (Bignami et al., 1993), HNK-1 glycolipids (Miura et al., 2001), and sulfated GAGs (Miura et al., 1999). Free G1, G3 versican domains released by proteases have regulatory properties in cell adhesion, proliferation, apoptosis, migration, angiogenesis, invasion, and metastasis. Versican G3 domain regulates neurite growth and synaptic transmission of hippocampal neurons by activating EGFR (Xiang et al., 2006). NgR2 interacts with versican G3 suppressing axonal plasticity (Bäumer et al., 2014) and has a dominant-negative effect on astrocytoma cell proliferation (Wu et al., 2001). An 80 kDa N-terminal matricryptic fragment of versican (versikine) generated by ADAMTS-4 (a disintegrin and metalloproteinase with thrombospondin motifs) cleavage acts as an alarmin in the innate immune response (Yamada et al., 2011). Interactions between myeloma stromal and myeloid cells generates versikine, a DAMP (damage-associated molecular pattern) that may facilitate immune sensing of myeloma tumors (Hope et al., 2016). Versikine also occurs during connective tissue remodeling during embryonic development (Nandadasa et al., 2014). Versican V2 is highly expressed in the adult brain (Schmalfeldt et al., 1998), promotes angiogenesis (Yang and Yee, 2013), and interactions with neurons (Horii-Hayashi et al., 2008). Versican V1 induces neural differentiation and neuritogenesis (Wu et al., 2004). Versican isoforms are differentially distributed in gliomas, medulloblastomas, schwannomas, neurofibromas, and meningiomas. Versican V2 is the major isoform found in gliomas. Versican V0 and V1 are found in all tissues, Versican V3 is found in all tissues except medulloblastomas.

### Neurocan

Neurocan has a widespread distribution in the CNS/PNS and is a component of PNNs (Schmidt et al., 2020) and regulates synaptic signaling (Sullivan et al., 2018). Neurocan (**Figure 3C**) has roles in neurodegenerative disorders (Lin et al., 2021). β-amyloid increases neurocan expression in astrocytes through Sox9 influencing the development of AD. Mutations in the neurocan gene predispose to bipolar disorder and schizophrenia (Mühleisen et al., 2012; Raum et al., 2015). Neurocan regulates neural migration and axonal development in the cerebral cortex influencing the folding of the occipital and pre-frontal lobes and an increased probability of developing schizophrenia (Schultz et al., 2014).

### Brevican

Brevican is the smallest lectican CS-PG family member (**Figure 3D**) present in PNNs in some cases, but aggrecan and versican are the principal lecticans in PNNs (Yamaguchi, 1996). Brain-enriched hyaluronan-binding protein (BEHAB) is an N-terminally cleaved (Matthews et al., 2000) bioactive fragment of brevican that is dramatically increased in human gliomas (Nutt et al., 2001; Viapiano et al., 2008) where it promotes glial cell motility and the aggressiveness of gliomas (Yamaguchi, 1996; Gary and Hockfield, 2000; Nutt et al., 2001; Viapiano et al., 2008; Giamanco and Matthews, 2020).

## OTHER NON-LECTICAN LARGE NEURAL PROTEOGLYCANS

### Phosphacan/Receptor Protein Tyrosine Phosphatase-Zeta (RPTP-ζ)

A cell membrane bound precursor form of phosphacan (RPTP-ζ) (**Figures 4A,B**) is processed by proteases to release a soluble PG ectodomain (**Figure 4C**) called phosphacan (Chow et al., 2008), truncated and non-GAG substituted forms of phosphacan have also been described (**Figure 4D**) with neurite outgrowth promoting activity (Fujikawa et al., 2017). This property is thus due to the core protein in some phosphacan species

while neurite outgrowth activity may also be conveyed by GAG components, such as oversulfated CS-B and CS-E, in other phosphacan glycoforms (Dobbertin et al., 2003; Hikino et al., 2003). Phosphacan populations bearing KS and HNK-1 have also been described as well as the more common CS-glycanated form (Melrose, 2019b). Phosphacan promotes PNN formation (Eill et al., 2020). RPTP-ζphosphacan contain extracellular carbonic anhydrase (CAH) and fibronectin type III repeat domains, which foster protein–protein interactions (Milev et al., 1994; Lamprianou et al., 2011). A truncated 90 kDa phosphacan form is not a PG, but is substituted with the HNK-1 trisaccharide which facilitates interactive properties with a number of cell adhesion and ECM molecules (Garwood et al., 2003). Phosphacan promotes neuron–glial interactions, neuronal differentiation, myelination, and axonal repair. The CAH carbonic anhydrase domain of phosphacan promotes protein–protein recognition, induces cell adhesion, neurite outgrowth of primary neurons, and differentiation of neuroblastoma cells (Adamsky et al., 2001); contactin is a phosphacan neuronal receptor that regulates neural development and axonal repair.

## NG2 Proteoglycan/CSPG4

CSPG4 modular transmembrane CS-PG also occurs as a soluble protease generated form (Schäfer and Tegeder, 2018; **Figure 4G**). CSPG4 is expressed by oligodendrocyte precursor cells (OPCs), NG2 glia (Butt et al., 2019), pericytes (Girolamo et al., 2013), activated astrocytes in damaged neural tissues (Anderson et al., 2016) and fibroblasts and macrophages associated with the meninges (Tamburini et al., 2019). NG2/CSPG4 is the largest complex macromolecule of the neuron surfaceome (Tamburini et al., 2019). OPCs are sensitive to electrophysiological stimulation through synaptic interactions that induce cellular proliferation and tissue repair.

The 290 kDa ectodomain of CSPG4 is released from OPCs by ADAM10 (α-secretase) (Moransard et al., 2011; Clarke et al., 2012; Huang et al., 2014) and are a major source of neural CSPG4 (Jones et al., 2002). Neurons, astrocytes, and microglial cells do not express CSPG4. Glioblastoma cells (Moransard et al., 2011; Huang et al., 2014), endothelial cells and pericytes in gliotic scars express CSPG4 (Jones et al., 2002; McTigue et al., 2006). NG2 PG binds type V and VI collagen through its central non-globular domain (Clarke et al., 2012; Huang et al., 2014) and with integrins (Sakry and Trotter, 2016). C-terminal LamG domains of NG2 interact with BM components and are crucial for formation of synaptic neuroligin-neurexin complexes and glial cell signaling (Jeong et al., 2017) and also interact with matriglycan-dystroglycan, perlecan, agrin and type XVIII collagen to localize NG2PG in motor neuron endplates in the neuromuscular junction (NMJ) (Walimbe et al., 2020).

## Betaglycan

Betaglycan homo-dimeric transmembrane (TM) CS/HS PG (Mythreye and Blobe, 2009; Bilandzic and Stenvers, 2011) contains inhibin, FGF-2, Wnt, and TGF-β binding sites (Boyd et al., 1990; Segarini, 1991; Massagué et al., 1992; Sandbrink et al., 1996; Miyazono, 1997; Lewis et al., 2000; Gray et al., 2001; Kim et al., 2019; Bernard et al., 2020; **Figure 5B**). The HS chains of betaglycan bind FGF-2. Wnt signaling is regulated independently of TGF-β (Jenkins et al., 2018). HS inhibits Wnt signaling, while CS promotes Wnt signaling (Jenkins et al., 2016, 2018). Betaglycan *N*-and *O*- linked oligosaccharides and GAG chains, modulate betaglycan's growth factor-mediated, vascular and cancer cell migratory properties (Pantazaka and Papadimitriou, 2014) and Inhibin A and B binding (Makanji et al., 2007). Fragments of betaglycan released by plasmin and MMPs act as circulating antagonists to normal betaglycan interactions. Inhibin/activin subunits and betaglycan are co-localized in the human brain (MacConell et al., 2002; Miller et al., 2012). Betaglycan-FGF-2 mediate neural proliferation and differentiation in neuroblastoma (Knelson et al., 2013). TGF-β also enhances glioma migration and invasion. TGF-β TbetaR I-III signaling phosphorylates Sma and MAD-related protein (SMAD), soluble TbetaR-I-III antagonize this process (Naumann et al., 2008). TGF-β enhances adult neurogenesis in the sub-ventricular zone (SVZ) and supports pro-neurogenic roles for TGF-β (Battista et al., 2006; Mathieu et al., 2010). Activins and inhibins, stimulate or inhibit secretion of FSH and the differentiation, proliferation and function of many cell types (Vale et al., 2004). Activin receptors highly expressed in neuronal cells, and activin mRNA are upregulated by neuronal activity. Models of TBI display enhanced activin A expression exacerbated by hypoxic/ischemic injury, mechanical irritation, and chemical damage (Florio et al., 2007). FGF-2 is neuroprotective and prevents apoptosis by strengthening anti-apoptotic pathways promoting neurogenesis in the adult hippocampus by upregulation of activin A activity (Woodruff, 1998; Alzheimer and Werner, 2002; Florio et al., 2007).

# THE SMALL NEURAL PROTEOGLYCANS

## Neuroglycan C

Neuroglycan C is a part time (Oohira et al., 2004) brain specific TM (Watanabe et al., 1995; Yasuda et al., 1998; Shuo et al., 2004) 150 kDa CS-PG (**Figure 4J**) with a 120 kDa core protein that can also be shed by MMPs (Shuo et al., 2007), GAG-free forms of CSPG5 have also been described. Neuroglycan C, is a novel member of the neuregulin family (Kinugasa et al., 2004), interacting with pleiotropin (Nakanishi et al., 2010) producing neurite outgrowth-promoting activity mediated by phosphatidylinositol 3-kinase and protein kinase C (Nakanishi et al., 2006). CSPG5 forms peri-synaptic structures in the postnatal adult rat cortex (Jüttner et al., 2013). Impaired CSPG5 properties are evident in schizophrenia (So et al., 2010). Alternatively spliced forms have been identified in the human brain, recombinant CSPG5 induces phosphorylation of Erb2 and Erb3 and induces proliferation of neocorticol neurons (Kinugasa et al., 2004; Nakanishi et al., 2006). The neurite outgrowth promoting activity of neuroglycan C resides in its EGF and acidic amino acid domains (Nakanishi et al., 2006).

## Syndecans

Syndecan transmembrane HS/CS-PGs (**Figures 4E,F**) modulate cell adhesion, cell–cell interactions and ligand-receptor interactions that regulate neural plasticity, promote neural growth and development (Couchman et al., 2015; Gopal et al., 2021). Sdc-3 and Sdc-4 are found throughout the nervous system and have roles in motor neuron development (Liu et al., 2020), Slit/Robo signaling and guidance of axonal development (Steigemann et al., 2004). Sdc3 is a co-receptor for Heparin-Binding Growth-Associated Molecule (HB-GAM)/midkine-induced neurite outgrowth in perinatal rat brain neurons. HB-GAM acts as a local, synaptic factor that promotes presynaptic and postsynaptic differentiation during neural development. Sdc3 also has roles in adult neuronal synaptic plasticity in the hippocampus in rat models following injury and regulates the neuronal internodal axonal ECM during re-myelination in growth, remodeling and repair (Steigemann et al., 2004). Sdc3 and Sdc4 promote functional recovery of neural tissues re-organizing sodium and potassium channels (Steigemann et al., 2004). Oligodendrocytes are sensitive to electro-stimulation, and this maintains their membrane polarization required for the promotion of axonal repair processes. Sdc1 is upregulated by neurons following TBI and SCI (Murakami et al., 2015). Sdc1 and Sdc3 knockdown in dorsal root ganglia (DRG) neurons induces short neurite extensions suggesting roles in nerve regeneration, synaptic formation and plasticity (Akita et al., 2004; Steigemann et al., 2004). Syndecans shed from the cell surface by MMPs, act as soluble growth factor co-receptors that regulate cell migration acting antagonistically with cell surface syndecans competing for FGF and VEGF binding (Gopal et al., 2021) and interact with integrins potentially influencing cellular behavior, adhesion, spreading, migration, proliferation, tissue morphogenesis and pathogenetic tissue changes (Couchman et al., 2015).

## Decorin

Decorin (**Figure 3E**) regulates cellular survival, migratory, proliferative and angiogenic signaling and collagen fibril formation, sequesters TGF-β and antagonizes receptor tyrosine kinase family members, including EGFR and IGF-IR (Schönherr et al., 2005; Iozzo et al., 2011; Neill et al., 2012). MayDay, a ∼12 kDa N-terminal chemotactic factor, generated by macrophage-induced MMP-12 cleavage of decorin, recruits mesenchymal stem cells (MSCs) to damaged tissue regions *in vitro* and *in vivo,* promoting tissue repair (Dempsey et al., 2020). *In situ* hybridization (ISH) has localized decorin in areas of microvascular proliferation within gliomas and may be a therapeutic target in anti-angiogenic therapy (Patel et al., 2020) or approaches targeting TGF-β activity in tumors (Birch et al., 2020). Decorin protects neuronal tissue from the damaging effects of anti-oxidants and neuroinflammation following TBI by inactivation and has anti-tumor activity by inhibiting glioma cell migration (Yao et al., 2016). Decorin inhibits TGF-β activity, fibrous scar formation in neural tissues following trauma.

## Biglycan

Biglycan (**Figure 3F**) is synthesized by astrocytes (Koops et al., 1996) and immune cells (Mohan et al., 2010) and has neurotrophic activity, stimulates glial cell proliferation (Kikuchi et al., 2000) and neuronal cell survival (Koops et al., 1996). It is part of the proteome of the normal human retrobulbar optic nerve (Zhang et al., 2016) and is massively upregulated around gliotic scars following trauma (Stichel et al., 1995). NF-κB upregulates biglycan, protecting human neuroblastoma cells from nitric oxide (NO)-induced cell death by inhibiting AMPK-mTOR mediated autophagy and intracellular reactive oxygen species (ROS) production from mitochondrial oxidative bursts (Wang et al., 2015), targeting Erk1/2 and p38 signaling pathways to prevent NO-induced neuronal cell apoptosis (Chen et al., 2020). Biglycan regulates neuroinflammation (Xie et al., 2020) through M1 microglial cell activation in the early stages of subarachnoid hemorrhage, targeting Erk1/2 and p38 signaling pathways (Chen et al., 2018). Biglycan binds to Notch-3 and accumulates in cerebral autosomal dominant arteriopathy with subcortical infarcts and leukoencephalopathy (CADASIL) (Zhang X. et al., 2015). Transcriptomic profiling of the hypothalamus and hippocampus, supports a central regulatory role for biglycan (bgn) in molecular pathways linking metabolic events with the immune response, and neuronal plasticity (Ying et al., 2018). Transcriptomic profiling of hypothalamus, hippocampus, and liver supports regulatory roles for Bgn in molecular pathways involved in metabolism, the immune response, and neuronal plasticity (Ying et al., 2018).

## Epiphycan

The synaptic poles of inner hair cells of the cochlea have audio-sensory properties and are surrounded by basket-like ECM structures with similar roles to the PNNs of neurons in the CNS (Sonntag et al., 2015). Epiphycan (**Figure 3G**) and aggrecan are cochlear components and of the gel-filled tectorial membrane which detects auditory signals and transmits these to sensory hair cells (Melrose, 2019a). Epiphycan is expressed by cochlear supporting cells and is necessary for normal hearing. Epiphycan mRNA is abundantly expressed in the cochlea in the organ of Corti of neonatal and adult mice. The cochlea of epiphycan knockout (KO) mice display a normal morphology, however, the auditory brain-stem response is altered since epiphycan is necessary for normal auditory function (Hanada et al., 2017). These PNN like structures surround high function neuron types which respond to signals received from inner sensory hair cells, transducing audio signals into mechanical stimuli and receptor-mediated action potentials which are sent to spiral ganglion neurons (Sonntag et al., 2015). These neuron types operate at very high discharge rates and efficiently convey signals to the auditory brainstem for further processing. The hearing loss evident in cartilage matrix deficiency (CMD) mice is related to aggrecan deficiency in the cochlea (Melrose, 2019a).

## Appican

Two variants of the related amyloid precursor-like protein 2 (APLP2) carry single CS-E side chains, which bind midkine

and pleiotrophin (Thinakaran and Sisodia, 1994; Shioi et al., 1995; Thinakaran et al., 1995). Multiple splice variants of amyloid-beta precursor protein (APP) (**Figure 4I**) and APLP2 arise from alternative splicing of three exons in APP and two exons in APLP2 (Kitaguchi et al., 1988; Ponte et al., 1988). The CS attachment site on APP/APLP2 is located adjacent to the membrane-spanning domain through deletion of 18 (APP) or 12 (APLP2) amino acids (Thinakaran et al., 1995). Splice variants also occur lacking CS side chains. APP and APLP are widely distributed in the CNS/PNS, APP is expressed by glial cells in the CNS/PNS.

## Bikunin/ITI

Bikunin (inter-α-trypsin inhibitor light chain) is synthesized by neurons (Chen et al., 2016), occurring as a tissue form and small circulating PG containing a single CS chain (**Figure 3J**). Bikunin displays anti-inflammatory, anti-protease, anti-microbial, anti-viral properties and also functions as a growth factor (Fries and Blom, 2000; Lord et al., 2020). Bikunin is expressed in brain tissue (Takano et al., 1999; Kim et al., 2020) and accumulates in brain tumors. Bikunin CS chains contain embedded disulfated CS-D motifs (Lord et al., 2013, 2020). A related Kunitz protease inhibitor, placental bikunin (hepatocyte growth factor activator inhibitor type-2) has been reported to inhibit glioblastoma tumor invasion (Hamasuna et al., 2001), however, this is a dissimilar protein to serum bikunin. Traumatic impact to the brain and spinal cord can release nuclear components such as histone H1 into the circulation or cerebrospinal fluid (CSF). Histone H1 has neuro-stimulatory effects and activates the innate immune response in the CNS mediated by microglial cells (Gilthorpe et al., 2013). This promotes neural cell survival, up-regulates major histocompatibility complex (MHC) class II antigen expression and is a powerful microglial chemoattractant. Release of histone H1 from the degenerative CNS drives a positive immune response (Gilthorpe et al., 2013) but can also be cytotoxic. Plasma immune tolerance induction (ITI) neutralizes the cytotoxic effects of histone H1, decreasing histone-induced platelet aggregation (Chaaban et al., 2015) through complexation of the histone with the negatively charged CS GAG chains of ITI (Chaaban et al., 2015). Hypoxic-ischemic encephalopathy predisposes infants to long-term cognitive decline impacting on life quality and healthcare resources (Chen et al., 2019). ITI regulates neonatal inflammation, decreases damage to brain tissues (Chen et al., 2019) and neuronal cell death, attenuates glial responses and leucocyte invasion with long-term beneficial effects in neonatal models of brain injury (Koehn et al., 2020).

## Serglycin

Serglycin (**Figure 3H**) is a small intracellular PG present in secretory granules of hemopoietic and endothelial cells (Kolset and Tveit, 2008) with regulatory properties over immune cells (Kolset and Pejler, 2011). It also promotes the development and aggressiveness of many tumor types including glioblastoma and is a glioblastoma biomarker (Roy et al., 2017; Manou et al., 2020). Suppression of serglycin in LN-18 shSRGN mutant cells results in retarded glioma proliferation, migration and invasive potential (Manou et al., 2020). Serglycin expression is elevated in astrocyte-glioma co-cultures. Astrocytes promote glioblastoma growth and is a potential glioma therapeutic target (Mega et al., 2020).

## Endocan

Endocan (**Figures 3L**, **5C**) is a small endothelial cell surface DS-PG found in cerebral blood vessels and is a small circulating PG in the blood stream (Frahm et al., 2013). Human umbilical vein endothelial cells (HUVECs) produce a truncated, alternatively spliced form of endocan which is neither glycosylated or secreted (Tsai et al., 2002). Circulating PGs are relatively rare; examples include endocan, bikunin, and macrophage colony stimulating factor-1 (Aitkenhead et al., 2002; Zhao et al., 2004). Endocan shares no homologies with other ECM PGs (De Freitas and Lassalle, 2015), does not contain LRRs or C-type lectin domains. Endocan, endothelial cell specific molecule-1 (ESM-1) encoded by the ESM-1 gene is an atypical DS-PG, with a single DS chain and distinctive structural and functional properties (Xing et al., 2016; Sun et al., 2019). Endocan is expressed by endothelial cells, regulated by proinflammatory pro-angiogenic molecules, has matrix-binding properties and is a marker of endothelial cell activation. TNF-α, IL-1, TGF-β1, FGF-2, and VEGF-2 induce endocan expression *in vitro*, IFN-γ inhibits TNF-α induced upregulation of endocan (Scherpereel et al., 2003). Endocan is associated with neuroinflamation in highly vascularized tumors in meningiomas, gliomas and lung cancer (Maurage et al., 2009) and with new blood vessel development in glioma (Maurage et al., 2009), pituitary adenoma, renal cell carcinoma, pediatric brain injury (Lele et al., 2019) and is a biomarker of cerebral damage (Morleo et al., 2019). Endocan expression is upregulated in human cytomegaloviral infection which increases glioma development in brain tissues (Scherpereel et al., 2003; Xing et al., 2016) leading to its suggestion as a therapeutic target in glioma (Atukeren et al., 2016). Endocan binds to lymphocytes and monocytes through high affinity interactions with integrin CD11a/CD18 lymphocyte function associated antigen-1 (LFA-1). A protease cleaved form of endocan (p14) antagonizes these interactions (Gaudet et al., 2020). Endocan promotes adhesion of monocytes and endothelial cells (Sun et al., 2019). The DS chains of endocan bind and activate hepatocyte growth factor (HGF) *in vitro* (Lyon et al., 1998; Mythreye and Blobe, 2009), L- and *P*-Selectins, fibronectin, chemokines, cytokines, RANTES, Stromal Cell-Derived Factor-1β (SDF-1β), IL-8, monocyte chemoattractant protein-1 (MCP-1), IFN-γ, and platelet factor-4 (PF-4), midkine, pleiotrophin, FGF-2, and FGF-7 (Sarrazin et al., 2006).

## Testican

Testican-1 and -2 are CS/HS PGs (**Figure 3K**), of the BM-40/SPARC/osteonectin family of extracellular calcium-binding proteins consisting of a signal peptide, a follistatin-like domain, a central Ca2+-binding domain, a thyroglobulin-like domain, and a C-terminal GAG attachment region. Testican-1 and 2 are expressed by multiple neuronal cell types in olfactory bulb, cerebral cortex, thalamus, hippocampus, cerebellum, and medulla (Marr et al., 2000). Neuronal testican-1 is upregulated following brain trauma (Iseki et al., 2011) and is also expressed by

activated astrocytes. Testican-1 modulates neuronal attachment and MMP activation (Bocock et al., 2003; Edgell et al., 2004), inhibits membrane type MMPs and cathepsin-L but not cathepsin-B. Testican-1 contains a single thyropin domain highly homologous to domains in cysteine proteinase inhibitors, the CS chains of testican-1 are essential for inhibition of cathepsin-L. Testican-2 is a HS/CS PG, has GAG-substituted and GAG-free forms that inhibit neurite extension, regulating neuronal growth and development (Schnepp et al., 2005). Testican-2 abrogates the inhibition of metallothionein-1(MT1)-MMP- or MT3-MMP-mediated pro-MMP-2 activation by testican-1 (Nakada et al., 2003). Testican-3, a HS-PG exclusive to brain tissues suppresses MT1-MMP mediated activation of MMP-2 and tumor invasion (Hartmann et al., 2013).

## Thrombomodulin (CD141)

Thrombomodulin (**Figure 4H**) inhibits thrombin as part of the anticoagulant protein C-system in the endothelium, is anti-inflammatory and promotes barrier-stabilization. Thrombomodulin is a protective factor in the brain during ischemic stroke, enhancing vessel post-ischemic recovery in the blood brain barrier. Thrombin's physiological roles in the brain stabilize normal brain function in synaptic transmission and plasticity through direct or indirect activation of Protease-Activated Receptor-1 (PAR1) and has neuroprotective roles in neurological diseases (Krenzlin et al., 2016).

## Cluster of Differentiation 44

Cluster of differentiation 44 (CD44), a major transmembrane glycoprotein HA receptor (**Figure 4K**) in the CNS/PNS, has roles in cell division, migration, adhesion, and cell–cell and cell–ECM signaling (Dzwonek and Wilczynski, 2015). Alternatively spliced CD44v3 is a CS-PG, 20 isoforms of CD44 have been reported associated with several kinds of tumors. CD44 expression is highly dynamic and transitions between different isoforms during tumor development (Lah et al., 2020). In glioma, CD44 and integrins attach the cell to ECM forming focal adhesion complexes and generate traction forces that facilitate cell spreading, essential in the cell migratory machinery in glioma cell invasion (Mooney et al., 2016). In the normal brain, CD44 is a major HA receptor that interacts with osteopontin, collagens, and MMPs stabilisating and remodeling the CNS/PNS ECM (Dzwonek and Wilczynski, 2015). HA is highly interactive through CD44, conveying cell instructional cues, and ECM stabilization, hydration and space-filling properties thus maintaining tissue compartmentalisation, ionic gradients and niches important in the metabolism of neural cell populations (Sherman et al., 2015; Peters and Sherman, 2020), including neural progenitor stem cell niches (Preston and Sherman, 2011).

## Cluster of Differentiation 47

Cluster of differentiation 47 (CD47) (**Figure 5A**), originally named integrin-associated protein (IAP) is a receptor for thrombospondin-1 (TSP-1) regulates cellular migration, proliferation, and the survival of vascular cells, in innate and adaptive immune regulation (Barclay and Van den Berg, 2014; Murata et al., 2014). TSP-1 acts via CD47 to inhibit NO signaling in the vascular system supporting blood pressure by regulation limiting endothelial nitric oxide synthase (eNOS) activation and endothelial-dependent vasorelaxation. CD47 is a ligand for signal regulatory protein α (SIRPα), also known as SHPS-1/BIT/CD172a). The CD47-SIRPα signaling system is a cell-cell communication system (Zhang H. et al., 2015; Matlung et al., 2017; Weiskopf, 2017). CD47-SIRPα interactions have been termed an innate immune checkpoint in macrophages (Li et al., 2021). Blockade of anti-phagocytic CD47-SIRPα interactions using humanized antibodies to CD47 (Hu5F9-G4) has yielded promising results in preclinical studies of a number of human malignancies including pediatric brain tumors: medulloblastoma, atypical teratoid rhabdoid tumors, primitive neuroectodermal tumor, pediatric glioblastoma, and diffuse intrinsic pontine glioma (Gholamin et al., 2017) and accelerates the clearance of hematomas in experimental intraventricular hemorrhage (Ye et al., 2021). Thus by targeting the immunological checkpoint complex CD47-SIRPα, the development of glioblastoma can be inhibited, the function of phagocytic, dendritic and T-lymphocytes enhanced and the efficiency of tumor cell removal improved by innate and adaptive immune responses (Hutter et al., 2019; Hu et al., 2020; Kuo et al., 2020; Zhang et al., 2020).

## Astrochondrin

Some specialized CNS proteins such as astrochondrin, a cell surface CS-PG of astrocytes carry L2/HNK-1 and L5 carbohydrate structures interactive with ECM components such as laminin and type IV collagen this may facilitate interaction of astrocyte foot processes with the brain microvasculature and meningeal membranes (Streit et al., 1993).

## Photomedin

Photomedin is another brain-specific glycoprotein of the eye neuroepithelium that interacts with CS-E (Furutani et al., 2005). Photomedin is a member of the olfactomedin protein family and has regulatory roles in axonal growth and differentiation of sensory cilia in the neural epithelium.

## FORSE-1 (Forebrain-Surface-Embryonic) Proteoglycan

FORSE-1 contains LeX-carbohydrate, stage specific embryonic antigen-1 (SSEA-1) or CD15, terminal Galβ(1-4)Fucα(1-3)GlcNAc-R oligosaccharide epitopes with roles in embryonic neural development (Allendoerfer et al., 1995, 1999; Kelly et al., 2019).

# CS-PGs REGULATION OF NEURONAL CELL SIGNALING

Neural cell populations including astrocytes, oligodendrocytes, neurons, endothelial cells and pericytes of the brain microvasculature and microglial cells synthesize a range of CS-PGs that interact with a variety of cell surface molecules

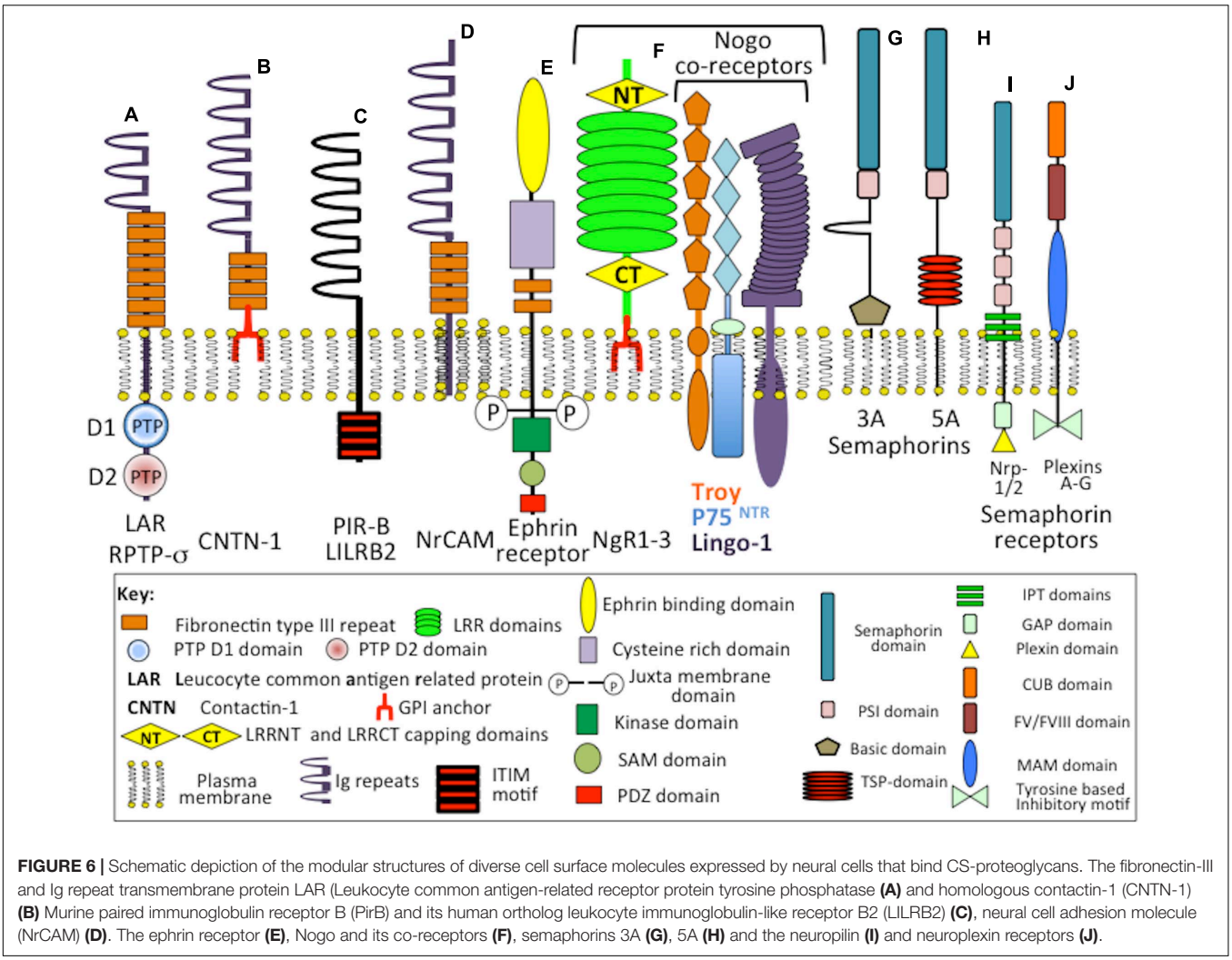


**FIGURE 6 |** Schematic depiction of the modular structures of diverse cell surface molecules expressed by neural cells that bind CS-proteoglycans. The fibronectin-III and Ig repeat transmembrane protein LAR (Leukocyte common antigen-related receptor protein tyrosine phosphatase **(A)** and homologous contactin-1 (CNTN-1) **(B)** Murine paired immunoglobulin receptor B (PirB) and its human ortholog leukocyte immunoglobulin-like receptor B2 (LILRB2) **(C)**, neural cell adhesion molecule (NrCAM) **(D)**. The ephrin receptor **(E)**, Nogo and its co-receptors **(F)**, semaphorins 3A **(G)**, 5A **(H)** and the neuropilin **(I)** and neuroplexin receptors **(J)**.

and receptors (**Figure 6**). These modulate cellular processes that control CNS/PNS function and repair (Djerbal et al., 2017; **Figure 7**). CS-PGs contribute to the structural integrity and compartmentalisation of the brain ECM and have important organizational functional roles in brain regions (Dityatev et al., 2010). CS-PGs operate at multiple functional levels involving interactions with growth factors, receptors, adhesion molecules, neural guidance proteins and ECM proteins (Djerbal et al., 2017). Transmembrane CS-PGs are active during cell-cell crosstalk, they may also be secreted or released from the cell surface by proteases to act remotely from their cells of origin and may antagonize normal transmembrane PG interactions (**Figure 7F**). CS-PGs are not uniformly distributed in the CNS/PNS but occur concentrated in neural growth cones and PNNs strategically positioned to control processes occurring at the cell-tissue interface (Shimbo et al., 2013; Sugitani et al., 2020). Growth cone receptor protein tyrosine phosphatases (RPTPs) bind with high affinity to CS-PGs, this controls axonal growth and provides guidance cues during regeneration, plasticity and neuronal development and in repair responses (Djerbal et al., 2017). CS-PGs attached to RPTP members can also exert repulsive guidance cues and inhibit neuritogenesis (**Figure 6A**). Lectican PG family members (neurocan, brevican, versican, aggrecan) are diffusely distributed in the CNS ECM and are also components of the denser PNNs. The CS component of CS-PGs vary in composition with tissue development. During embryonic development CS-C is a predominant isoform while CS-A is more abundant in adult neural tissues (**Figure 2**). The sulphation patterns and charge density are important functional determinants of CS glycoforms. The more highly charged CS-E, B and D are components of PNN PGs, CS-A and CS-C are diffusely distributed in the ECM distant from PNN structures (Djerbal et al., 2017). The chemo-repellent semaphorin 3A (SEMA3A), a component of PNNs (Battistini and Tamagnone, 2016; Fard and Tamagnone, 2020), interacts with CS-E and B but not CS-D, thus such interactions are not purely mediated by charge; saccharide sequences in CS chains also determine the interactive properties of CS-PGs and their core proteins also contain ECM interactive modules. Selective binding of midkine (MK) and brain-derived neurotrophic factor (BDNF) to CS-E of some CS-PGs leads to neurite outgrowth. The Nogo receptors NgR1 and NgR3 bind to Nogo and inhibit neurite outgrowth. NgR1 and NgR3 also

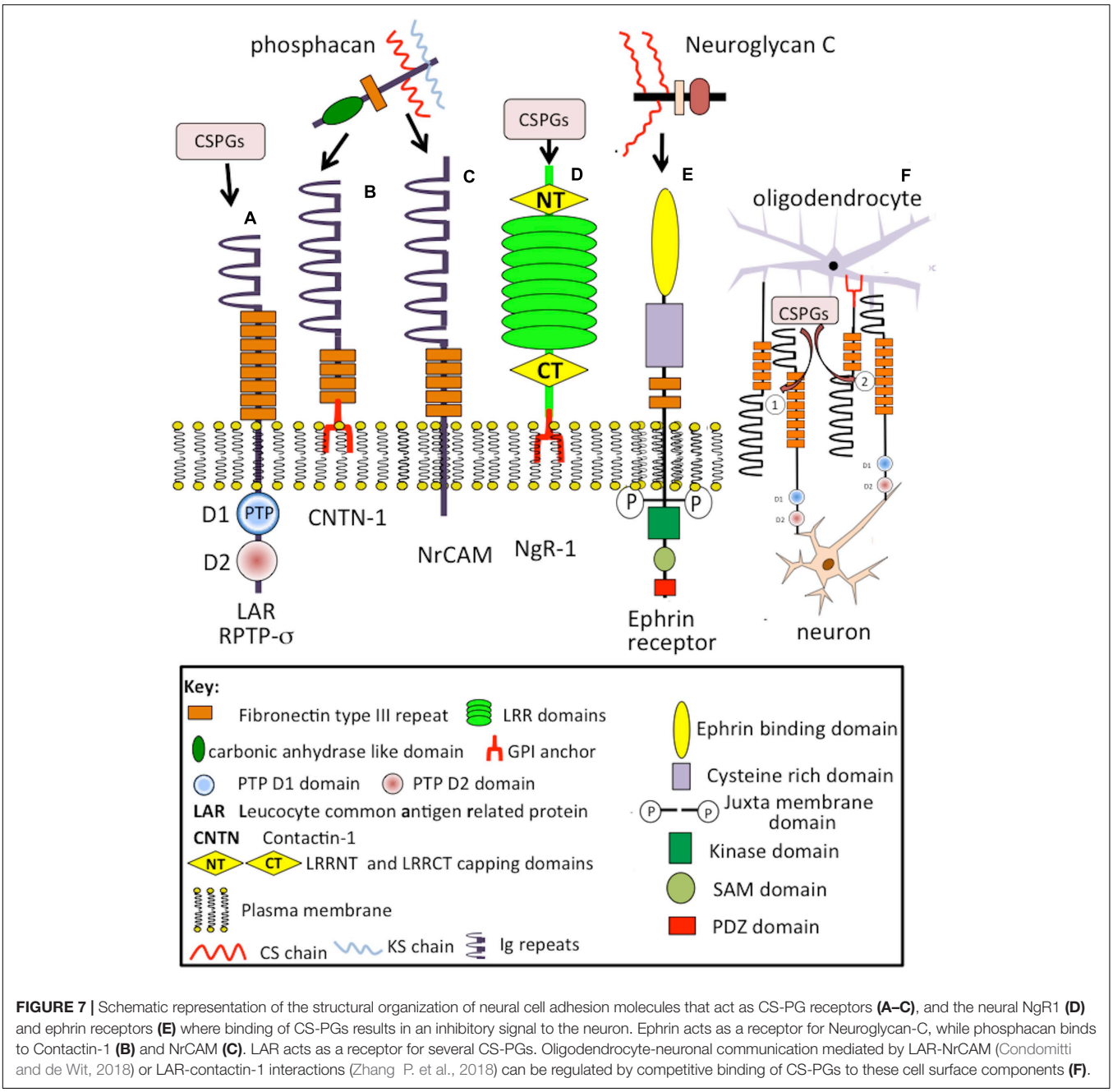


**FIGURE 7 |** Schematic representation of the structural organization of neural cell adhesion molecules that act as CS-PG receptors **(A–C)**, and the neural NgR1 **(D)** and ephrin receptors **(E)** where binding of CS-PGs results in an inhibitory signal to the neuron. Ephrin acts as a receptor for Neuroglycan-C, while phosphacan binds to Contactin-1 **(B)** and NrCAM **(C)**. LAR acts as a receptor for several CS-PGs. Oligodendrocyte-neuronal communication mediated by LAR-NrCAM (Condomitti and de Wit, 2018) or LAR-contactin-1 interactions (Zhang P. et al., 2018) can be regulated by competitive binding of CS-PGs to these cell surface components **(F)**.

bind specifically to CS-B, CS-D, and CS-E with high affinity, and this inhibits neurite outgrowth. Cell adhesion molecules are operative in cell–cell and cell–ECM interactions that regulate tissue integrity, cellular communication and cellular migration during CNS development and repair following trauma and are evident as pathological functional changes in neurological disorders. Neural cell adhesion molecule (NCAM) in particular, has specific roles in the promotion of neurite outgrowth of motor neurons that improves locomotor functional recovery following SCI. NCAM and neuroglia cell adhesion molecule (NgCAM) bind with high affinity to the CS-PG phosphacan, reducing neurite outgrowth and adhesion. Chondroitinase ABC moderately reduces phosphacan-NCAM binding showing this interaction is mainly mediated through phosphacan core protein interactions (**Figure 7**). Neurocan binding to NCAM and NgCAM also inhibits neurite outgrowth but unlike phosphacan, chondroitinase ABC abrogates this, showing that neurocan-NCAM interactions are mediated through CS. NCAM and NgCAM act as receptors for phosphacan and neurocan. Contactin-1 is a further GPI anchored cell adhesion molecule (CAM) that facilitates axonal growth and dendritic interactions that promote neurogenesis, CS-E binds contactin-1 with significant affinity and promotes neural growth. Thus, CS-PG binding to contactin-1 can modulate contactin-1 interactions

that normally mediate cell-cell interaction (**Figure 7F**). CS-PG5 (neuroglycan C) forms peri-synaptic matrix assemblies that regulate neuronal synaptic activity in the cerebral cortex of rats (Pintér et al., 2020).

The semaphorins are a family of guidance proteins of embryonic peripheral nerve projections and have roles in synaptogenesis and the maintenance of neural interconnections in adulthood thus maintaining cerebral homeostasis. SEMA3A is upregulated following CNS injury, causes growth cone collapse by signaling through synaptic neuropilin-1 (Nrp-1) and plexin receptors and is also known as collapsin-1. SEMA3A in PNNs can modulate synaptic morphology and function (Goshima et al., 2002; Mecollari et al., 2014; Battistini and Tamagnone, 2016; Alto and Terman, 2017; Fard and Tamagnone, 2020). SEMA3A interacts with CS-E with high affinity and neuropilin-1 (Nrp-1) in SEMA3A-Nrp-plexin signaling complexes to potently inhibit neural sprouting following SCI, and also inhibits neural growth factor (NGF) (Mecollari et al., 2014; Fard and Tamagnone, 2020) (**Figure 6**). Compared to SEMA3A, SEMA5A is less well studied, but also has important functional roles in CNS development and response to injury (Conrad et al., 2010). SEMA5A contains a cluster of thrombospondin (TSP) repeats which promote neural outgrowth. CS-PGs interact with this TSP repeat region producing a neuro-repulsive response whereas HS-PGs produce a neuro-attractive response. Thus, CS has important SEMA5A regulatory properties. A proteomic surface plasmon resonance and microarray study by Conrad et al. (2010), showed that interactions with neurotrophic factors was not confined to the highly charged CS-E glycoforms and that significant interactions also occurred between CS-A and Sema 3E, Sema 6B and ephrin A3 (Conrad et al., 2010).

## CONCLUSION

This chapter has shown the impressive diversity in CS-PG form and function in the CNS/PNS. CS-PGs undertake many essential roles in neural tissues through the provision of a functional ECM for the many different cell populations resident in the CNS/PNS. The intricacies of some of the cell regulatory properties conveyed by CS-PGs have been illustrated, as has the complex interplay between distinct neural cell populations in the maintenance of CNS/PNS tissue function and homeostasis. Aberrations in the assembly of the ECM through processing defects in component CS-PGs can have serious functional consequences in brain tissues and can lead to neurodegenerative diseases. Such defects underline the fundamental importance of the ECM in normal tissue function and the potential of CS-PGs as promising therapeutic targets for future treatment of many of these neurodegenerative conditions.

## AUTHOR CONTRIBUTIONS

JM obtained the funding, conceptualized the study, and wrote the initial draft of the manuscript. AH assisted in manuscript writing and editing and had intellectual input into data interpretation. Both authors approved the final version of the manuscript.

## FUNDING

This study was supported by the NHMRC Project Grant 512167.

## REFERENCES

Abbott, L., and Nigussie, F. (2020). Adult neurogenesis in the mammalian dentate gyrus. *Anat. Histol. Embryol.* 49, 3–16. doi: 10.1111/ahe.12496

Adamsky, K., Schilling, J., Garwood, J., Faissner, A., and Peles, E. (2001). Glial tumor cell adhesion is mediated by binding of the FNIII domain of receptor protein tyrosine phosphatase beta (RPTPbeta) to tenascin C. *Oncogene* 20, 609–618. doi: 10.1038/sj.onc.1204119

Aguirre, A., Dupree, J. L., Mangin, J. M., and Gallo, V. (2007). A functional role for EGFR signaling in myelination and remyelination. *Nat. Neurosci.* 10, 990–1002. doi: 10.1038/nn1938

Aitkenhead, M., Wang, S. J., Nakatsu, M. N., Mestas, J., Heard, C., and Hughes, C. C. (2002). Identification of endothelial cell genes expressed in an in vitro model of angiogenesis: induction of ESM-1, (beta)ig-h3, and NrCAM. *Microvasc. Res.* 63, 159–171. doi: 10.1006/mvre.2001.2380

Akatsu, C., Mizumoto, S., Kaneiwa, T., Maccarana, M., Malmström, A., Yamada, S., et al. (2011). Dermatan sulfate epimerase 2 is the predominant isozyme in the formation of the chondroitin sulfate/dermatan sulfate hybrid structure in postnatal developing mouse brain. *Glycobiology* 21, 565–574. doi: 10.1093/glycob/cwq208

Akita, K., Toda, M., Hosoki, Y., Inoue, M., Fushiki, S., Oohira, A., et al. (2004). Heparan sulphate proteoglycans interact with neurocan and promote neurite outgrowth from cerebellar granule cells. *Biochem. J.* 383, 129–138. doi: 10.1042/bj20040585

Allendoerfer, K., Durairaj, A., Matthews, G. A., and Patterson, P. H. (1999). Morphological domains of Lewis-X/FORSE-1 immunolabeling in the embryonic neural tube are due to developmental regulation of cell surface carbohydrate expression. *Dev. Biol.* 211, 208–219. doi: 10.1006/dbio.1999.9308

Allendoerfer, K., Magnani, J. L., and Patterson, P. H. (1995). FORSE-1, an antibody that labels regionally restricted subpopulations of progenitor cells in the embryonic central nervous system, recognizes the Le(x) carbohydrate on a proteoglycan and two glycolipid antigens. *Mol. Cell. Neurosci.* 6, 361–395.

Alto, L., and Terman, J. R. (2017). Semaphorins and their signaling mechanisms. *Methods Mol. Biol.* 1493, 1–25. doi: 10.1007/978-0-387-70956-7_1

Alzheimer, C., and Werner, S. (2002). Fibroblast growth factors and neuroprotection. *Adv. Exp. Med. Biol.* 513, 335–351. doi: 10.1007/978-1-4615-0123-7_12

Amenta, A., Creely, H. E., Mercado, M. L., Hagiwara, H., McKechnie, B. A., Lechner, B. E., et al. (2012). Biglycan is an extracellular MuSK binding protein important for synapse stability. *J. Neurosci.* 32, 2324–2334. doi: 10.1523/jneurosci.4610-11.2012

Amran, A., Pigatto, L., Pocock, R., and Gopal, S. (2021). Functions of the extracellular matrix in development: lessons from *Caenorhabditis elegans*. *Cell. Signal.* 84:110006. doi: 10.1016/j.cellsig.2021.110006

Anderson, M., Burda, J. E., Ren, Y., Ao, Y., O'Shea, T. M., Kawaguchi, R., et al. (2016). Astrocyte scar formation aids central nervous system axon regeneration. *Nature* 532, 195–200. doi: 10.1038/nature17623

Atukeren, P., Kunbaz, A., Turk, O., Kemerdere, R., Ulu, M. O., Turkmen Inanir, N., et al. (2016). Expressions of endocan in patients with meningiomas and gliomas. *Dis. Markers* 2016:7157039.

Barclay, A., and Van den Berg, T. K. (2014). The interaction between signal regulatory protein alpha (SIRPα) and CD47: structure, function, and therapeutic target. *Annu. Rev. Immunol.* 32, 25–50. doi: 10.1146/annurev-immunol-032713-120142

Battista, D., Ferrari, C. C., Gage, F. H., and Pitossi, F. J. (2006). Neurogenic niche modulation by activated microglia: transforming growth factor beta increases

neurogenesis in the adult dentate gyrus. *Eur. J. Neurosci.* 23, 83–93. doi: 10.1111/j.1460-9568.2005.04539.x

Battistini, C., and Tamagnone, I. (2016). Transmembrane semaphorins, forward and reverse signaling: have a look both ways. *Cell. Mol. Life Sci.* 73, 1609–1622. doi: 10.1007/s00018-016-2137-x

Bäumer, B., Kurz, A., Borrie, S. C., Sickinger, S., Dours-Zimmermann, M. T., Zimmermann, D. R., et al. (2014). Nogo receptor homolog NgR2 expressed in sensory DRG neurons controls epidermal innervation by interaction with Versican. *J. Neurosci.* 34, 1633–1646. doi: 10.1523/jneurosci.3094-13.2014

Bedoui, Y., Neal, J. W., and Gasque, P. (2018). The neuro-immune-regulators (NIREGs) promote tissue resilience; a vital component of the host's defense strategy against neuroinflammation. *J. Neuroimmune Pharmacol.* 13, 309–329. doi: 10.1007/s11481-018-9793-6

Bekku, Y., and Oohashi, T. (2019). Under the ECM dome: the physiological role of the perinodal extracellular matrix as an ion diffusion barrier. *Adv. Exp. Med. Biol.* 1190, 107–122. doi: 10.1007/978-981-32-9636-7_8

Bekku, Y., Rauch, U., Ninomiya, Y., and Oohashi, T. (2009). Brevican distinctively assembles extracellular components at the large diameter nodes of Ranvier in the CNS. *J. Neurochem.* 108, 1266–1276. doi: 10.1111/j.1471-4159.2009.05873.x

Bellono, N. W., Leitch, D. B., and Julius, D. (2017). Molecular basis of ancestral vertebrate electroreception. *Nature* 543, 391–396. doi: 10.1038/nature21401

Bernard, D., Smith, C. L., and Brûlé, E. (2020). A tale of two proteins: betaglycan, IGSF1, and the continuing search for the inhibin B receptor. *Trends Endocrinol. Metab.* 31, 37–45. doi: 10.1016/j.tem.2019.08.014

Berretta, S. (2012). Extracellular matrix abnormalities in schizophrenia. *Neuropharmacology* 62, 1584–1597. doi: 10.1016/j.neuropharm.2011.08.010

Bhattacharya, A., Aghayeva, U., Berghoff, E. G., and Hobert, O. (2019). Plasticity of the electrical connectome of *C. elegans*. *Cell* 176, 1174–1189.e16.

Bignami, A., Hosley, M., and Dahl, D. (1993). Hyaluronic acid and hyaluronic acid-binding proteins in brain extracellular matrix. *Anat. Embryol. (Berl.)* 188, 419–433.

Bilandzic, M., and Stenvers, K. L. (2011). Betaglycan: a multifunctional accessory. *Mol. Cell. Endocrinol.* 339, 180–189. doi: 10.1016/j.mce.2011.04.014

Birch, J., Coull, B. J., Spender, L. C., Watt, C., Willison, A., Syed, N., et al. (2020). Multifaceted transforming growth factor-beta (TGFβ) signalling in glioblastoma. *Cell. Signal.* 72:109638. doi: 10.1016/j.cellsig.2020.109638

Blanchette, C., Perrat, P. N., Thackeray, A., and Bénard, C. Y. (2015). Glypican is a modulator of netrin-mediated axon guidance. *PLoS Biol.* 13:e1002183. doi: 10.1371/journal.pbio.1002183

Blanchette, C., Thackeray, A., Perrat, P. N., Hekimi, S., and Bénard, C. Y. (2017). Functional requirements for heparan sulfate biosynthesis in morphogenesis and nervous system development in *C. elegans*. *PLoS Genet.* 13:e1006525. doi: 10.1371/journal.pgen.1006525

Bocock, J., Edgell, C. J., Marr, H. S., and Erickson, A. H. (2003). Human proteoglycan testican-1 inhibits the lysosomal cysteine protease cathepsin L. *Eur. J. Biochem.* 270, 4008–4015. doi: 10.1046/j.1432-1033.2003.03789.x

Bovolenta, P., and Fernaud-Espinosa, I. (2000). Nervous system proteoglycans as modulators of neurite outgrowth. *Prog. Neurobiol.* 61, 113–132. doi: 10.1016/s0301-0082(99)00044-1

Boyd, F., Cheifetz, S., Andres, J., Laiho, M., and Massagué, J. (1990). Transforming growth factor-beta receptors and binding proteoglycans. *J. Cell Sci.* 13, 131–138. doi: 10.1242/jcs.1990.supplement_13.12

Bradbury, E. J., and Carter, L. M. (2011). Manipulating the glial scar: chondroitinase ABC as a therapy for spinal cord injury. *Brain Res. Bull.* 84, 306–316. doi: 10.1016/j.brainresbull.2010.06.015

Bruckner, G. H. D., Härtig, W., Drlicek, M., Arendt, T., and Brauer, K. (1999). Cortical areas abundant in extracellular matrix chondroitin sulphate proteoglycans are less affected by cytoskeletal changes in Alzheimer's disease. *Neuroscience* 92, 791–805. doi: 10.1016/s0306-4522(99)00071-8

Bulik, D., Wei, G., Toyoda, H., Kinoshita-Toyoda, A., Waldrip, W. R., Esko, J. D., et al. (2000). sqv-3, -7, and -8, a set of genes affecting morphogenesis in *Caenorhabditis elegans*, encode enzymes required for glycosaminoglycan biosynthesis. *Proc. Natl. Acad. Sci. U.S.A.* 97, 10838–10843. doi: 10.1073/pnas.97.20.10838

Bülow, H., and Hobert, O. (2004). Differential sulfations and epimerization define heparan sulfate specificity in nervous system development. *Neuron* 41, 723–736. doi: 10.1016/s0896-6273(04)00084-4

Butt, A., Papanikolaou, M., and Rivera, A. (2019). Physiology of oligodendroglia. *Adv. Exp. Med. Biol.* 1175, 117–128. doi: 10.1007/978-981-13-9913-8_5

Carulli, D., and Verhaagen, J. (2021). An extracellular perspective on CNS maturation: perineuronal nets and the control of plasticity. *Int. J. Mol. Sci.* 22:2434. doi: 10.3390/ijms22052434

Cassada, R., and Russell, R. L. (1975). The dauerlarva, a post-embryonic developmental variant of the nematode *Caenorhabditis elegans*. *Dev. Biol.* 46, 326–342. doi: 10.1016/0012-1606(75)90109-8

Celestrin, K., Díaz-Balzac, C. A., Tang, L. T. H., Ackley, B. D., and Bülow, H. E. (2018). Four specific immunoglobulin domains in UNC-52/Perlecan function with NID-1/Nidogen during dendrite morphogenesis in *Caenorhabditis elegans*. *Development* 145:dev158881.

Chaaban, H., Keshari, R. S., Silasi-Mansat, R., Popescu, N. I., Mehta-D'Souza, P., Lim, Y. P., et al. (2015). Inter-α inhibitor protein and its associated glycosaminoglycans protect against histone-induced injury. *Blood* 125, 2286–2296. doi: 10.1182/blood-2014-06-582759

Chanana, B., Steigemann, P., Jäckle, H., and Vorbrüggen, G. (2009). Reception of Slit requires only the chondroitin-sulphate-modified extracellular domain of Syndecan at the target cell surface. *Proc. Natl. Acad. Sci. U.S.A.* 106, 11984–11988. doi: 10.1073/pnas.0901148106

Chelyshev, Y. A., Kabdesh, I. M., and Mukhamedshina, Y. O. (2020). Extracellular matrix in neural plasticity and regeneration. *Cell. Mol. Neurobiol.* doi: 10.1007/s10571-020-00986-0

Chen, S., Guo, D., Lei, B., Bi, J., and Yang, H. (2020). Biglycan protects human neuroblastoma cells from nitric oxide-induced death by inhibiting AMPK-mTOR mediated autophagy and intracellular ROS level. *Biotechnol. Lett.* 42, 657–668. doi: 10.1007/s10529-020-02818-z

Chen, S., Guo, D., Zhang, W., Xie, Y., Yang, H., Cheng, B., et al. (2018). Biglycan, a nitric oxide-downregulated proteoglycan, prevents nitric oxide-induced neuronal cell apoptosis via targeting Erk1/2 and p38 signaling pathways. *J. Mol. Neurosci.* 66, 68–76. doi: 10.1007/s12031-018-1151-x

Chen, X., Nakada, S., Donahue, J. E., Chen, R. H., Tucker, R., Qiu, J., et al. (2019). Neuroprotective effects of inter-alpha inhibitor proteins after hypoxic-ischemic brain injury in neonatal rats. *Exp. Neurol.* 317, 244–259. doi: 10.1016/j.expneurol.2019.03.013

Chen, X., Rivard, L., Naqvi, S., Nakada, S., Padbury, J. F., Sanchez-Esteban, J., et al. (2016). Expression and localization of Inter-alpha Inhibitors in rodent brain. *Neuroscience* 324, 69–81. doi: 10.1016/j.neuroscience.2016.03.009

Cheng, C., Lin, C. T., Lee, M. J., Tsai, M. J., Huang, W. H., Huang, M. C., et al. (2015). Local delivery of high-dose chondroitinase ABC in the sub-acute stage promotes axonal outgrowth and functional recovery after complete spinal cord transection. *PLoS One* 10:e0138705. doi: 10.1371/journal.pone.0138705

Chisholm, A., and Jin, Y. (2005). Neuronal differentiation in *C. elegans*. *Curr. Opin. Cell Biol.* 17, 682–689. doi: 10.1016/j.ceb.2005.10.004

Cho, J., Chak, K., Andreone, B. J., Wooley, J. R., and Kolodkin, A. L. (2012). The extracellular matrix proteoglycan perlecan facilitates transmembrane semaphorin-mediated repulsive guidance. *Genes Dev.* 26, 2222–2235. doi: 10.1101/gad.193136.112

Chow, J., Fujikawa, A., Shimizu, H., Suzuki, R., and Noda, M. (2008). Metalloproteinase- and gamma-secretase-mediated cleavage of protein-tyrosine phosphatase receptor type Z. *J. Biol. Chem.* 283, 30879–30889. doi: 10.1074/jbc.m802976200

Cizeron, M., Granger, L., Bülow, H. E., and Bessereau, J. L. (2021). Specific heparan sulfate modifications stabilize the synaptic organizer MADD-4/Punctin at *C. elegans* neuromuscular junctions. *Genetics* iyab073. doi: 10.1093/genetics/iyab073

Clarke, L., Young, K. M., Hamilton, N. B., Li, H., Richardson, W. D., and Attwell, D. (2012). Properties and fate of oligodendrocyte progenitor cells in the corpus callosum, motor cortex, and piriform cortex of the mouse. *J. Neurosci.* 32, 8173–8185. doi: 10.1523/jneurosci.0928-12.2012

Condomitti, G., and de Wit, J. (2018). Heparan sulfate proteoglycans as emerging players in synaptic specificity. *Front. Mol. Neurosci.* 11:14. doi: 10.3389/fnmol.2018.00014

Conrad, A. H., Zhang, Y., Tasheva, E. S., and Conrad, G. W. (2010). Proteomic analysis of potential keratan sulfate, chondroitin sulfate a, and hyaluronic acid molecular interactions. *Invest. Ophthalmol. Vis. Sci.* 51, 4500–4515. doi: 10.1167/iovs.09-4914

Cope, E., and Gould, E. (2019). Adult neurogenesis, glia, and the extracellular matrix. *Cell Stem Cell* 24, 690–705. doi: 10.1016/j.stem.2019.03.023

Couchman, J., Gopal, S., Lim, H. C., Nørgaard, S., and Multhaupt, H. A. (2015). Fell-muir lecture: syndecans: from peripheral coreceptors to mainstream regulators of cell behaviour. *Int. J. Exp. Pathol.* 96, 1–10. doi: 10.1111/iep.12112

Davis, M., Horne-Badovinac, S., and Naba, A. (2019). In-silico definition of the *Drosophila melanogaster* matrisome. *Matrix Biol. Plus* 4:100015. doi: 10.1016/j.mbplus.2019.100015

De Freitas, C. N., and Lassalle, P. (2015). Highlight on mouse endocan. *Circ. Res.* 116, e69–e70.

De Luca, C., and Papa, M. (2016). Looking inside the matrix: perineuronal nets in plasticity, maladaptive plasticity and neurological disorders. *Neurochem. Res.* 41, 1507–1515. doi: 10.1007/s11064-016-1876-2

Dejima, K., Seko, A., Yamashita, K., Gengyo-Ando, K., Mitani, S., Izumikawa, T., et al. (2006). Essential roles of 3′-phosphoadenosine 5′-phosphosulfate synthase in embryonic and larval development of the nematode *Caenorhabditis elegans*. *J. Biol. Chem.* 281, 11431–11440. doi: 10.1074/jbc.m601509200

Dempsey, S., Miller, C. H., Schueler, J., Veale, R. W. F., Day, D. J., and May, B. C. H. (2020). A novel chemotactic factor derived from the extracellular matrix protein decorin recruits mesenchymal stromal cells in vitro and in vivo. *PLoS One* 15:e0235784. doi: 10.1371/journal.pone.0235784

Díaz-Balzac, C., Lázaro-Peña, M. I., Tecle, E., Gomez, N., and Bülow, H. E. (2014). Complex cooperative functions of heparan sulfate proteoglycans shape nervous system development in *Caenorhabditis elegans*. *G3 (Bethesda)* 4, 1859–1870. doi: 10.1534/g3.114.012591

Dibrova, D., Chudetsky, M. Y., Galperin, M. Y., Koonin, E. V., and Mulkidjanian, A. Y. (2012). The role of energy in the emergence of biology from chemistry. *Orig. Life Evol. Biosph.* 42:5.

Dityatev, A., and Schachner, M. (2006). The extracellular matrix and synapses. *Cell Tissue Res.* 326, 647–654. doi: 10.1007/s00441-006-0217-1

Dityatev, A., Frischknecht, R., and Seidenbecher, C. I. (2006). Extracellular matrix and synaptic functions. *Results Probl. Cell Differ.* 43, 69–97. doi: 10.1007/400_025

Dityatev, A., Seidenbecher, C. I., and Schachner, M. (2010). Compartmentalization from the outside: the extracellular matrix and functional microdomains in the brain. *Trends Neurosci.* 33, 503–512. doi: 10.1016/j.tins.2010.08.003

Dityatev, A., Seidenbecher, C., and Morawski, M. (2021). Brain extracellular matrix: an upcoming target in neurological and psychiatric disorders. *Eur J Neurosci.* 12, 3807–3810. doi: 10.1111/ejn.15336

Djerbal, L., Lortat-Jacob, H., and Kwok, J. (2017). Chondroitin sulfates and their binding molecules in the central nervous system. *Glycoconj. J.* 34, 363–376. doi: 10.1007/s10719-017-9761-z

Dobbertin, A., Rhodes, K. E., Garwood, J., Properzi, F., Heck, N., Rogers, J. H., et al. (2003). Regulation of RPTPbeta/phosphacan expression and glycosaminoglycan epitopes in injured brain and cytokine-treated glia. *Mol. Cell. Neurosci.* 24, 951–971. doi: 10.1016/s1044-7431(03)00257-4

Dours-Zimmermann, M., Maurer, K., Rauch, U., Stoffel, W., Fässler, R., and Zimmermann, D. R. (2009). Versican V2 assembles the extracellular matrix surrounding the nodes of ranvier in the CNS. *J. Neurosci.* 29, 7731–7742. doi: 10.1523/jneurosci.4158-08.2009

Du, W., Yang, B. B., Shatseva, T. A., Yang, B. L., Deng, Z., Shan, S. W., et al. (2010). Versican G3 promotes mouse mammary tumor cell growth, migration, and metastasis by influencing EGF receptor signaling. *PLoS One* 5:e13828. doi: 10.1371/journal.pone.0013828

Dubey, D., McRae, P. A., Rankin-Gee, E. K., Baranov, E., Wandrey, L., Rogers, S., et al. (2017). Increased metalloproteinase activity in the hippocampus following status epilepticus. *Epilepsy Res.* 132, 50–58. doi: 10.1016/j.eplepsyres.2017.02.021

Dyck, S., and Karimi-Abdolrezaee, S. (2015). Chondroitin sulfate proteoglycans: key modulators in the developing and pathologic central nervous system. *Exp. Neurol.* 269, 169–187. doi: 10.1016/j.expneurol.2015.04.006

Dzwonek, J., and Wilczynski, G. M. (2015). CD44: molecular interactions, signaling and functions in the nervous system. *Front. Cell. Neurosci.* 9:175. doi: 10.3389/fncel.2015.00175

Edgell, C., BaSalamah, M. A., and Marr, H. S. (2004). Testican-1: a differentially expressed proteoglycan with protease inhibiting activities. *Int. Rev. Cytol.* 236, 101–122. doi: 10.1016/s0074-7696(04)36003-1

Edwards, T., and Hammarlund, M. (2014). Syndecan promotes axon regeneration by stabilizing growth cone migration. *Cell Rep.* 8, 272–283. doi: 10.1016/j.celrep.2014.06.008

Eill, G. J., Sinha, A., Morawski, M., Viapiano, M. S., and Matthews, R. T. (2020). The protein tyrosine phosphatase RPTPzeta/phosphacan is critical for perineuronal net structure. *J. Biol. Chem.* 295, 955–968. doi: 10.1074/jbc.ra119.010830

Eisenhaber, B., Bork, P., Yuan, Y., Löffler, G., and Eisenhaber, F. (2000). Automated annotation of GPI anchor sites: case study *C. elegans*. *Trends Biochem. Sci.* 25, 340–341. doi: 10.1016/s0968-0004(00)01601-7

Faissner, A., Heck, N., Dobbertin, A., and Garwood, J. (2006). DSD-1-proteoglycan/phosphacan and receptor protein tyrosine phosphatase-beta isoforms during development and regeneration of neural tissues. *Adv. Exp. Med. Biol.* 557, 25–53. doi: 10.1007/0-387-30128-3_3

Fard, D., and Tamagnone, L. (2020). Semaphorins in health and disease. *Cytokine Growth Factor Rev.* 57, 55–63. doi: 10.1016/j.cytogfr.2020.05.006

Fawcett, J., Oohashi, T., and Pizzorusso, T. (2019). The roles of perineuronal nets and the perinodal extracellular matrix in neuronal function. *Nat. Rev. Neurosci.* 20, 451–465. doi: 10.1038/s41583-019-0196-3

Ferrer-Ferrer, M., and Dityatev, A. (2018). Shaping synapses by the neural extracellular matrix. *Front. Neuroanat.* 12:40. doi: 10.3389/fnana.2018.00040

Ferro, D., Provasoli, A., Ragazzi, M., Casu, B., Torri, G., Bossennec, V., et al. (1990). Conformer populations of L-iduronic acid residues in glycosaminoglycan sequences. *Carbohydr. Res.* 195, 157–167. doi: 10.1016/0008-6215(90)84164-p

FitzGerald, P., Sturgill, D., Shyakhtenko, A., Oliver, B., and Vinson, C. (2006). Comparative genomics of *Drosophila* and human core promoters. *Genome Biol.* 7:R53.

Florio, P., Gazzolo, D., Luisi, S., and Petraglia, F. (2007). Activin A in brain injury. *Adv. Clin. Chem.* 43, 117–130. doi: 10.1016/s0065-2423(06)43004-3

Forostyak, S. H. A., Turnovcova, K., Svitil, P., Jendelova, P., and Sykova, E. (2014). Intrathecal delivery of mesenchymal stromal cells protects the structure of altered perineuronal nets in SOD1 rats and amends the course of ALS. *Stem Cells* 32, 3163–3172. doi: 10.1002/stem.1812

Frahm, K., Nash, C. P., and Tobet, S. A. (2013). Endocan immunoreactivity in the mouse brain: method for identifying nonfunctional blood vessels. *J. Immunol. Methods* 398-399, 27–32. doi: 10.1016/j.jim.2013.09.005

Fries, E., and Blom, A. M. (2000). Bikunin not just a plasma proteinase inhibitor. *Int. J. Biochem. Cell Biol.* 32, 125–137. doi: 10.1016/s1357-2725(99)00125-9

Fujikawa, A., Chow, J. P. H., Matsumoto, M., Suzuki, R., Kuboyama, K., Yamamoto, N., et al. (2017). Identification of novel splicing variants of protein tyrosine phosphatase receptor type Z. *J. Biochem.* 162, 381–390. doi: 10.1093/jb/mvx042

Furutani, Y., Manabe, R., Tsutsui, K., Yamada, T., Sugimoto, N., Fukuda, S., et al. (2005). Identification and characterization of photomedins: novel olfactomedin-domain-containing proteins with chondroitin sulphate-E-binding activity. *Biochem. J.* 389, 675–684. doi: 10.1042/bj20050120

Gabius, H. (2018). The sugar code: why glycans are so important. *Biosystems* 164, 102–111. doi: 10.1016/j.biosystems.2017.07.003

Galtrey, C., and Fawcett, J. W. (2007). The role of chondroitin sulfate proteoglycans in regeneration and plasticity in the central nervous system. *Brain Res. Rev.* 54, 1–18. doi: 10.1016/j.brainresrev.2006.09.006

Gandal, M., Zhang, P., Hadjimichael, E., Walker, R. L., Chen, C., Liu, S., et al. (2018). Transcriptome-wide isoform-level dysregulation in ASD, schizophrenia, and bipolar disorder. *Science* 362:eaat8127. doi: 10.1126/science.aat8127

Garwood, J., Heck, N., Reichardt, F., and Faissner, A. (2003). Phosphacan short isoform, a novel non-proteoglycan variant of phosphacan/receptor protein tyrosine phosphatase-beta, interacts with neuronal receptors and promotes neurite outgrowth. *J. Biol. Chem.* 278, 24164–24173. doi: 10.1074/jbc.m211721200

Gary, S., and Hockfield, S. (2000). BEHAB/brevican: an extracellular matrix component associated with invasive glioma. *Clin. Neurosurg.* 47, 72–82.

Gaudet, A., Portier, L., Mathieu, D., Hureau, M., Tsicopoulos, A., Lassalle, P., et al. (2020). Cleaved endocan acts as a biologic competitor of endocan in the control of ICAM-1-dependent leukocyte diapedesis. *J. Leukoc. Biol.* 107, 833–841. doi: 10.1002/jlb.3ab0320-612rr

Gholamin, S., Mitra, S. S., Feroze, A. H., Liu, J., Kahn, S. A., Zhang, M., et al. (2017). Disrupting the CD47-SIRPα anti-phagocytic axis by a humanized anti-CD47 antibody is an efficacious treatment for malignant pediatric brain tumors. *Sci. Transl. Med.* 9:eaaf2968. doi: 10.1126/scitranslmed.aaf2968

Giamanco, K., and Matthews, R. T. (2020). The role of BEHAB/Brevican in the tumor microenvironment: mediating glioma cell invasion and motility. *Adv. Exp. Med. Biol.* 1272, 117–132. doi: 10.1007/978-3-030-48457-6_7

Gilthorpe, J., Oozeer, F., Nash, J., Calvo, M., Bennett, D. L., Lumsden, A., et al. (2013). Extracellular histone H1 is neurotoxic and drives a pro-inflammatory response in microglia. *F1000 Res.* 2:148. doi: 10.12688/f1000research.2-148.v1

Girolamo, F., Dallatomasina, A., Rizzi, M., Errede, M., Walchli, T., Mucignat, M. T., et al. (2013). Diversified expression of NG2/CSPG4 isoforms in glioblastoma and human foetal brain identifies pericyte subsets. *PLoS One* 8:e84883. doi: 10.1371/journal.pone.0084883

Gooi, H., Feizi, T., Kapadia, A., Knowles, B. B., Solter, D., and Evans, M. J. (1981). Stage-specific embryonic antigen involves alpha 1 goes to 3 fucosylated type 2 blood group chains. *Nature* 292, 156–158. doi: 10.1038/292156a0

Gopal, S., Arokiasamy, S., Pataki, C., Whiteford, J. R., and Couchman, J. R. (2021). Syndecan receptors: pericellular regulators in development and inflammatory disease. *Open Biol.* 11:200377.

Gopal, S., Couchman, J., and Pocock, R. (2016). Redefining the role of syndecans in *C. elegans* biology. *Worm* 5:e1142042. doi: 10.1080/21624054.2016.1142042

Goshima, Y., Ito, T., Sasaki, Y., and Nakamura, F. (2002). Semaphorins as signals for cell repulsion and invasion. *J. Clin. Invest.* 109, 993–998. doi: 10.1172/jci0215467

Gray, P., Bilezikjian, L. M., and Vale, W. (2001). Antagonism of activin by inhibin and inhibin receptors: a functional role for betaglycan-glycan. *Mol. Cell. Endocrinol.* 180, 47–53. doi: 10.1016/s0303-7207(01)00515-9

Guilak, F., Hayes, A. J., and Melrose, J. (2021). Perlecan in pericellular mechanosensory cell-matrix communication, extracellular matrix stabilisation and mechanoregulation of load-bearing connective tissues. *Int. J. Mol. Sci.* 22:2716. doi: 10.3390/ijms22052716

Güiza, J., Barría, I., Sáez, J. C., and Vega, J. L. (2018). Innexins: expression, regulation, and functions. *Front. Physiol.* 9:1414. doi: 10.3389/fphys.2018.01414

Gumienny, T., MacNeil, L. T., Wang, H., de Bono, M., Wrana, J. L., and Padgett, R. W. (2007). Glypican LON-2 is a conserved negative regulator of BMP-like signaling in *Caenorhabditis elegans*. *Curr. Biol.* 17, 159–164. doi: 10.1016/j.cub.2006.11.065

Gysi, S., Rhiner, C., Flibotte, S., Moerman, D. G., and Hengartner, M. O. (2013). A network of HSPG core proteins and HS modifying enzymes regulates netrin-dependent guidance of D-type motor neurons in *Caenorhabditis elegans*. *PLoS One* 8:e74908. doi: 10.1371/journal.pone.0074908

Hakomori, S., Nudelman, E., Levery, S., Solter, D., and Knowles, B. B. (1981). The hapten structure of a developmentally regulated glycolipid antigen (SSEA-1) isolated from human erythrocytes and adenocarcinoma: a preliminary note. *Biochem. Biophys. Res. Commun.* 100, 1578–1586. doi: 10.1016/0006-291x(81)90699-9

Hamasuna, R., Kataoka, H., Meng, J. Y., Itoh, H., Moriyama, T., Wakisaka, S., et al. (2001). Reduced expression of hepatocyte growth factor activator inhibitor type-2/placental bikunin (HAI-2/PB) in human glioblastomas: implication for anti-invasive role of HAI-2/PB in glioblastoma cells. *Int. J. Cancer* 93, 339–345. doi: 10.1002/ijc.1349

Hanada, Y., Nakamura, Y., Ishida, Y., Takimoto, Y., Taniguchi, M., Ozono, Y., et al. (2017). Epiphycan is specifically expressed in cochlear supporting cells and is necessary for normal hearing. *Biochem. Biophys. Res. Commun.* 492, 379–385. doi: 10.1016/j.bbrc.2017.08.092

Hartmann, U., Hülsmann, H., Seul, J., Röll, S., Midani, H., Breloy, I., et al. (2013). Testican-3: a brain-specific proteoglycan member of the BM-40/SPARC/osteonectin family. *J. Neurochem.* 125, 399–409. doi: 10.1111/jnc.12212

Hassan, B., Li, L., Bremer, K. A., Chang, W., Pinsonneault, J., and Vaessin, H. (1997). Prospero is a panneural transcription factor that modulates homeodomain protein activity. *Proc. Natl. Acad. Sci. U.S.A.* 94, 10991–10996. doi: 10.1073/pnas.94.20.10991

Hayes, A., and Melrose, J. (2018). Glycans and glycosaminoglycans in neurobiology: key regulators of neuronal cell function and fate. *Biochem. J.* 475, 2511–2545. doi: 10.1042/bcj20180283

Hayes, A., and Melrose, J. (2020a). Aggrecan, the primary weight-bearing cartilage proteoglycan, has context-dependent, cell-directive properties in embryonic development and neurogenesis: aggrecan glycan side chain modifications convey interactive biodiversity. *Biomolecules* 10:E1244.

Hayes, A., and Melrose, J. (2020b). Electro-stimulation, a promising therapeutic treatment modality for tissue repair: emerging roles of sulfated glycosaminoglycans as electro-regulatory mediators of intrinsic repair processes. *Adv. Ther.* 3:2000151. doi: 10.1002/adtp.202000151

Hayes, A., Sugahara, K., Farrugia, B., Whitelock, J. M., Caterson, B., and Melrose, J. (2018). Biodiversity of CS-proteoglycan sulphation motifs: chemical messenger recognition modules with roles in information transfer, control of cellular behaviour and tissue morphogenesis. *Biochem. J.* 475, 587–620. doi: 10.1042/bcj20170820

Haylock-Jacobs, S., Keough, M. B., Lau, L., and Yong, V. W. (2011). Chondroitin sulphate proteoglycans: extracellular matrix proteins that regulate immunity of the central nervous system. *Autoimmun. Rev.* 10, 766–772. doi: 10.1016/j.autrev.2011.05.019

Hering, T., Beller, J. A., Calulot, C. M., and Snow, D. M. (2020). Contributions of chondroitin sulfate, keratan sulfate and N-linked oligosaccharides to inhibition of neurite outgrowth by aggrecan. *Biology (Basel)* 9:E29.

Hikino, M., Mikami, T., Faissner, A., Vilela-Silva, A. C., Pavão, M. S., and Sugahara, K. (2003). Oversulfated dermatan sulfate exhibits neurite outgrowth-promoting activity toward embryonic mouse hippocampal neurons: implications of dermatan sulfate in neuritogenesis in the brain. *J. Biol. Chem.* 278, 43744–43754. doi: 10.1074/jbc.m308169200

Hobert, O. (2010). "Neurogenesis in the nematode *Caenorhabditis elegans*," in *WormBook*, ed. The *C. elegans* Research Community (New York, NY :WormBook). doi: 10.1895/wormbook.1.12.2

Hope, C., Foulcer, S., Jagodinsky, J., Chen, S. X., Jensen, J. L., Patel, S., et al. (2016). Immunoregulatory roles of versican proteolysis in the myeloma microenvironment. *Blood* 128, 680–685. doi: 10.1182/blood-2016-03-705780

Horii-Hayashi, N., Okuda, H., Tatsumi, K., Ishizaka, S., Yoshikawa, M., and Wanaka, A. (2008). Localization of chondroitin sulfate proteoglycan versican in adult brain with special reference to large projection neurons. *Cell Tissue Res.* 334, 163–177. doi: 10.1007/s00441-008-0698-1

Hortobágyi, T., and Maffiuletti, N. A. (2011). Neural adaptations to electrical stimulation strength training. *Eur. J. Appl. Physiol.* 111, 2439–2449. doi: 10.1007/s00421-011-2012-2

Hu, J., Xiao, Q., Dong, M., Guo, D., Wu, X., and Wang, B. (2020). Glioblastoma immunotherapy targeting the innate immune checkpoint CD47-SIRPα Axis. *Front. Immunol.* 11:593219. doi: 10.3389/fimmu.2020.593219

Hu, P. J. (2007). "Dauer," in *WormBook*, ed. The *C. elegans* Research Community (New York, NY: WormBook). doi: 10.1895/wormbook.1.144.1

Huang, W., Zhao, N., Bai, X., Karram, K., Trotter, J., Goebbels, S., et al. (2014). Novel NG2-CreERT2 knock-in mice demonstrate heterogeneous differentiation potential of NG2 glia during development. *Glia* 62, 896–913. doi: 10.1002/glia.22648

Hutter, G., Theruvath, J., Graef, C. M., Zhang, M., Schoen, M. K., Manz, E. M., et al. (2019). Microglia are effector cells of CD47-SIRPα antiphagocytic axis disruption against glioblastoma. *Proc. Natl. Acad. Sci. U.S.A.* 116, 997–1006. doi: 10.1073/pnas.1721434116

Hwang, H., Olson, S. K., Brown, J. R., Esko, J. D., and Horvitz, H. R. (2003a). The *Caenorhabditis elegans* genes sqv-2 and sqv-6, which are required for vulval morphogenesis, encode glycosaminoglycan galactosyltransferase II and xylosyltransferase. *J. Biol. Chem.* 278, 11735–11738. doi: 10.1074/jbc.c200518200

Hwang, H., Olson, S. K., Esko, J. D., and Horvitz, H. R. (2003b). *Caenorhabditis elegans* early embryogenesis and vulval morphogenesis require chondroitin biosynthesis. *Nature* 423, 439–443. doi: 10.1038/nature01634

Iozzo, R., Buraschi, S., Genua, M., Xu, S. Q., Solomides, C. C., Peiper, S. C., et al. (2011). Decorin antagonizes IGF receptor I (IGF-IR) function by interfering with IGF-IR activity and attenuating downstream signaling. *J. Biol. Chem.* 286, 34712–34721. doi: 10.1074/jbc.m111.262766

Iseki, K., Hagino, S., Zhang, Y., Mori, T., Sato, N., Yokoya, S., et al. (2011). Altered expression pattern of testican-1 mRNA after brain injury. *Biomed. Res.* 32, 373–378. doi: 10.2220/biomedres.32.373

Islam, S., and Watanabe, H. (2020). Versican: a dynamic regulator of the extracellular matrix. *J. Histochem. Cytochem.* 68, 763–775. doi: 10.1369/0022155420953922

Jain, D., Mattiassi, S., Goh, E. L., and Yim, E. K. F. (2020). Extracellular matrix and biomimetic engineering microenvironment for neuronal differentiation. *Neural Regen. Res.* 15, 573–585. doi: 10.4103/1673-5374.266907

Jenkins, L., Horst, B., Lancaster, C. L., and Mythreye, K. (2018). Dually modified transmembrane proteoglycans in development and disease. *Cytokine Growth Factor Rev.* 39, 124–136. doi: 10.1016/j.cytogfr.2017.12.003

Jenkins, L., Singh, P., Varadaraj, A., Lee, N. Y., Shah, S., Flores, H. V., et al. (2016). Altering the proteoglycan state of transforming growth factor β Type III receptor (TβRIII)/betaglycan modulates canonical Wnt/β-catenin signaling. *J. Biol. Chem.* 291, 25716–25728. doi: 10.1074/jbc.m116.748624

Jeong, J., Paskus, J. D., and Roche, K. W. (2017). Posttranslational modifications of neuroligins regulate neuronal and glial signaling. *Curr. Opin. Neurobiol.* 45, 130–138. doi: 10.1016/j.conb.2017.05.017

Jeong, P.-Y., Jung, M., Yim, Y.-H., Kim, H., Park, M., Hong, E., et al. (2005). Chemical structure and biological activity of the *Caenorhabditis elegans* dauer-inducing pheromone. *Nature* 433, 541–545. doi: 10.1038/nature03201

Johnson, H., Rosenberg, L., Choi, H. U., Garza, S., Höök, M., and Neame, P. J. (1997). Characterization of epiphycan, a small proteoglycan with a leucine-rich repeat core protein. *J. Biol. Chem.* 272, 18709–18717. doi: 10.1074/jbc.272.30.18709

Jones, L., Yamaguchi, Y., Stallcup, W. B., and Tuszynski, M. H. (2002). NG2 is a major chondroitin sulfate proteoglycan produced after spinal cord injury and is expressed by macrophages and oligodendrocyte progenitors. *J. Neurosci.* 22, 2792–2803. doi: 10.1523/jneurosci.22-07-02792.2002

Josberger, E., Hassanzadeh, P., Deng, Y., Sohn, J., Rego, M. J., Amemiya, C. T., et al. (2016). Proton conductivity in ampullae of Lorenzini jelly. *Sci. Adv.* 2:e1600112. doi: 10.1126/sciadv.1600112

Jüttner, R., Montag, D., Craveiro, R. B., Babich, A., Vetter, P., and Rathjen, F. G. (2013). Impaired presynaptic function and elimination of synapses at premature stages during postnatal development of the cerebellum in the absence of CALEB (CSPG5/neuroglycan C). *Eur. J. Neurosci.* 38, 3270–3280. doi: 10.1111/ejn.12313

Kali, A., and Shetty, K. S. (2014). Endocan: a novel circulating proteoglycan. *Indian J. Pharmacol.* 46, 579–583. doi: 10.4103/0253-7613.144891

Kaltner, H., Abad-Rodríguez, J., Corfield, A. P., Kopitz, J., and Gabius, H. J. (2019). The sugar code: letters and vocabulary, writers, editors and readers and biosignificance of functional glycan-lectin pairing. *Biochem. J.* 476, 2623–2655. doi: 10.1042/bcj20170853

Kamimura, K., and Maeda, N. (2017). Heparan sulfate proteoglycans in *Drosophila* neuromuscular development. *Biochim. Biophys. Acta Gen. Subj.* 1861, 2442–2446. doi: 10.1016/j.bbagen.2017.06.015

Kamimura, K., and Maeda, N. (2021). Glypicans and heparan sulfate in synaptic development, neural plasticity, and neurological disorders. *Front. Neural Circuits* 15:595596. doi: 10.3389/fncir.2021.595596

Karamanos, N., Piperigkou, Z., Theocharis, A. D., Watanabe, H., Franchi, M., Baud, S., et al. (2018). Proteoglycan chemical diversity drives multifunctional cell regulation and therapeutics. *Chem. Rev.* 118, 9152–9232. doi: 10.1021/acs.chemrev.8b00354

Keirstead, H., and Blakemore, W. F. (1999). The role of oligodendrocytes and oligodendrocyte progenitors in CNS remyelination. *Adv. Exp. Med. Biol.* 468, 183–197. doi: 10.1007/978-1-4615-4685-6_15

Kelly, A., O'Malley, A., Redha, M., O'Keeffe, G. W., and Barry, D. S. (2019). The distribution of the proteoglycan FORSE-1 in the developing mouse central nervous system. *J. Anat.* 234, 216–226. doi: 10.1111/joa.12907

Kerever, A., Mercier, F., Nonaka, R., de Vega, S., Oda, Y., Zalc, B., et al. (2014). Perlecan is required for FGF-2 signaling in the neural stem cell niche. *Stem Cell Res.* 12, 492–505. doi: 10.1016/j.scr.2013.12.009

Kiani, C., Chen, L., Wu, Y. J., Yee, A. J., and Yang, B. B. (2002). Structure and function of aggrecan. *Cell Res.* 12, 19–32. doi: 10.1038/sj.cr.7290106

Kikuchi, A., Tomoyasu, H., Kido, I., Takahashi, K., Tanaka, A., Nonaka, I., et al. (2000). Haemopoietic biglycan produced by brain cells stimulates growth of microglial cells. *J. Neuroimmunol.* 106, 78–86. doi: 10.1016/s0165-5728(99)00258-1

Kim, B., De La Monte, S., Hovanesian, V., Patra, A., Chen, X., Chen, R. H., et al. (2020). Ontogeny of inter-alpha inhibitor protein (IAIP) expression in human brain. *J. Neurosci. Res.* 98, 869–887. doi: 10.1002/jnr.24565

Kim, S., Henen, M. A., and Hinck, A. P. (2019). Structural biology of betaglycan and endoglin, membrane-bound co-receptors of the TGF-beta family. *Exp. Biol. Med. (Maywood)* 244, 1547–1558. doi: 10.1177/1535370219881160

Kim, W., Underwood, R. S., Greenwald, I., and Shaye, D. D. (2018). OrthoList 2: a new comparative genomic analysis of human and *Caenorhabditis elegans* genes. *Genetics* 210, 445–461. doi: 10.1534/genetics.118.301307

Kinugasa, Y., Ishiguro, H., Tokita, Y., Oohira, A., Ohmoto, H., and Higashiyama, S. (2004). Neuroglycan C, a novel member of the neuregulin family. *Biochem. Biophys. Res. Commun.* 321, 1045–1049. doi: 10.1016/j.bbrc.2004.07.066

Kitaguchi, N., Takahashi, Y., Tokushima, Y., Shiojiri, S., and Ito, H. (1988). Novel precursor of Alzheimer's disease amyloid protein shows protease inhibitory activity. *Nature* 331, 530–532. doi: 10.1038/331530a0

Knelson, E., Gaviglio, A. L., Tewari, A. K., Armstrong, M. B., Mythreye, K., and Blobe, G. C. (2013). Type III TGF-β receptor promotes FGF2-mediated neuronal differentiation in neuroblastoma. *J. Clin. Invest.* 123, 4786–4798. doi: 10.1172/jci69657

Koehn, L., Chen, X., Logsdon, A. F., Lim, Y. P., and Stonestreet, B. S. (2020). novel neuroprotective agents to treat neonatal hypoxic-ischemic encephalopathy: inter-alpha inhibitor proteins. *Int. J. Mol. Sci.* 21:9193. doi: 10.3390/ijms21239193

Kolset, S. O., and Pejler, G. (2011). Serglycin: a structural and functional chameleon with wide impact on immune cells. *J. Immunol.* 187, 4927–4933. doi: 10.4049/jimmunol.1100806

Kolset, S., and Tveit, H. (2008). Serglycin–structure and biology. *Cell. Mol. Life Sci.* 65, 1073–1085. doi: 10.1007/s00018-007-7455-6

Koops, A., Kappler, J., Junghans, U., Kuhn, G., Kresse, H., and Müller, H. W. (1996). Cultured astrocytes express biglycan, a chondroitin/dermatan sulfate proteoglycan supporting the survival of neocortical neurons. *Brain Res. Mol. Brain Res.* 41, 65–73. doi: 10.1016/0169-328x(96)00067-8

Kovács, I., Barabási, D. L., and Barabási, A. L. (2020). Uncovering the genetic blueprint of the *C. elegans* nervous system. *Proc. Natl. Acad. Sci. U.S.A.* 117, 33570–33577. doi: 10.1073/pnas.2009093117

Krahn, N., Meier, M., Reuten, R., Koch, M., Stetefeld, J., and Patel, T. R. (2019). Solution structure of *C. elegans* UNC-6: a nematode paralogue of the axon guidance protein Netrin-1. *Biophys. J.* 116, 2121–2130. doi: 10.1016/j.bpj.2019.04.033

Krenzlin, H., Lorenz, V., Danckwardt, S., Kempski, O., and Alessandri, B. (2016). The importance of thrombin in cerebral injury and disease. *Int. J. Mol. Sci.* 17:84. doi: 10.3390/ijms17010084

Kuo, T., Chen, A., Harrabi, O., Sockolosky, J. T., Zhang, A., Sangalang, E., et al. (2020). Targeting the myeloid checkpoint receptor SIRPα potentiates innate and adaptive immune responses to promote anti-tumor activity. *J. Hematol. Oncol.* 13:160.

Lah, T., Novak, M., and Breznik, B. (2020). Brain malignancies: glioblastoma and brain metastases. *Semin. Cancer Biol.* 60, 262–273. doi: 10.1016/j.semcancer.2019.10.010

Lamprianou, S., Chatzopoulou, E., Thomas, J. L., Bouyain, S., and Harroch, S. (2011). A complex between contactin-1 and the protein tyrosine phosphatase PTPRZ controls the development of oligodendrocyte precursor cells. *Proc. Natl. Acad. Sci. U.S.A.* 108, 17498–17503. doi: 10.1073/pnas.1108774108

Lane, N. (2017). Proton gradients at the origin of life. *Bioessays* 39:1600217. doi: 10.1002/bies.201600217

Lee, S., Zhang, X., and Wang, M. M. (2014). Vascular accumulation of the small leucine-rich proteoglycan decorin in CADASIL. *Neuroreport* 25, 1059–1063. doi: 10.1097/wnr.0000000000000230

Lele, A., Alunpipatthanachai, B., Qiu, Q., Clark-Bell, C., Watanitanon, A., Moore, A., et al. (2019). Plasma levels, temporal trends and clinical associations between biomarkers of inflammation and vascular homeostasis after pediatric traumatic brain injury. *Dev. Neurosci.* 41, 177–192. doi: 10.1159/000502276

Lewis, K., Gray, P. C., Blount, A. L., MacConell, L. A., Wiater, E., Bilezikjian, L. M., et al. (2000). Betaglycan binds inhibin and can mediate functional antagonism of activin signalling. *Nature* 404, 411–414. doi: 10.1038/35006129

Li, Z., Li, Y., Gao, J., Fu, Y., Hua, P., Jing, Y., et al. (2021). The role of CD47-SIRPα immune checkpoint in tumor immune evasion and innate immunotherapy. *Life Sci.* 273, 779150.

Lin, J. Z., Duan, M. R., Lin, N., and Zhao, W. J. (2021). The emerging role of the chondroitin sulfate proteoglycan family in neurodegenerative diseases. *Rev. Neurosci.* doi: 10.1515/revneuro-2020-0146

Liu, C., Kuo, Y. C., Wang, C. Y., Hsu, C. C., Ho, Y. J., Chiang, Y. C., et al. (2020). Syndecan-3 contributes to the regulation of the microenvironment

at the node of Ranvier following end-to side neurorrhaphy: sodium image analysis. *Histochem. Cell Biol.* 155, 355–367. doi: 10.1007/s00418-020-01936-z

Long, K., and Huttner, W. B. (2019). How the extracellular matrix shapes neural development. *Open Biol.* 9:180216. doi: 10.1098/rsob.180216

Lord, M., Day, A. J., Youssef, P., Zhuo, L., Watanabe, H., Caterson, B., et al. (2013). Sulfation of the bikunin chondroitin sulfate chain determines heavy chain. hyaluronan complex formation. *J. Biol. Chem.* 288, 22930–22941. doi: 10.1074/jbc.m112.404186

Lord, M., Melrose, J., Day, A. J., and Whitelock, J. M. (2020). The inter-α-trypsin inhibitor family: versatile molecules in biology and pathology. *J. Histochem. Cytochem.* 68, 907–927. doi: 10.1369/0022155420940067

Losada-Perez, M., Harrison, N., and Hidalgo, A. (2016). Molecular mechanism of central nervous system repair by the *Drosophila* NG2 homologue kon-tiki. *J. Cell Biol.* 214, 587–601. doi: 10.1083/jcb.201603054

Lynch, M., and Marinov, G. K. (2017). Membranes, energetics, and evolution across the prokaryote-eukaryote divide. *Elife* 6:e20437.

Lyon, M., Deakin, J. A., Rahmoune, H., Fernig, D. G., Nakamura, T., and Gallagher, J. T. (1998). Hepatocyte growth factor/scatter factor binds with high affinity to dermatan sulfate. *J. Biol. Chem.* 273, 271–278. doi: 10.1074/jbc.273.1.271

MacConell, L., Leal, A. M., and Vale, W. W. (2002). The distribution of betaglycan protein and mRNA in rat brain, pituitary, and gonads: implications for a role for betaglycan in inhibin-mediated reproductive functions. *Endocrinology* 143, 1066–1075. doi: 10.1210/endo.143.3.8707

Maćkowiak, M., Mordalska, P., and Wędzony, K. (2014). Neuroligins, synapse balance and neuropsychiatric disorders. *Pharmacol. Rep.* 66, 830–835. doi: 10.1016/j.pharep.2014.04.011

Makanji, Y., Harrison, C. A., Stanton, P. G., Krishna, R., and Robertson, D. M. (2007). Inhibin A and B in vitro bioactivities are modified by their degree of glycosylation and their affinities to betaglycan. *Endocrinology* 148, 2309–2316. doi: 10.1210/en.2006-1612

Malavaki, C., Mizumoto, S., Karamanos, N., and Sugahara, K. (2008). Recent advances in the structural study of functional chondroitin sulfate and dermatan sulfate in health and disease. *Connect. Tissue Res.* 49, 133–139. doi: 10.1080/03008200802148546

Malmström, A., Bartolini, B., Thelin, M. A., Pacheco, B., and Maccarana, M. (2012). Iduronic acid in chondroitin/dermatan sulfate: biosynthesis and biological function. *J. Histochem. Cytochem.* 60, 916–925. doi: 10.1369/0022155412459857

Manou, D., Bouris, P., Kletsas, D., Götte, M., Greve, B., Moustakas, A., et al. (2020). Serglycin activates pro-tumorigenic signaling and controls glioblastoma cell stemness, differentiation and invasive potential. *Matrix Biol. Plus* 6–7:100033. doi: 10.1016/j.mbplus.2020.100033

Margolis, R., and Margolis, R. K. (1994). Aggrecan-versican-neurocan family proteoglycans. *Methods Enzymol.* 245, 105–126. doi: 10.1016/0076-6879(94)45008-0

Margolis, R., Rauch, U., Maurel, P., and Margolis, R. U. (1996). Neurocan and phosphacan: two major nervous tissue-specific chondroitin sulfate proteoglycans. *Perspect. Dev. Neurobiol.* 3, 273–290.

Maro, G., Gao, S., Olechwier, A. M., Hung, W. L., Liu, M., Özkan, E., et al. (2015). MADD-4/punctin and neurexin organize *C. elegans* GABAergic postsynapses through neuroligin. *Neuron* 86, 1420–1432. doi: 10.1016/j.neuron.2015.05.015

Marr, H., Basalamah, M. A., Bouldin, T. W., Duncan, A. W., and Edgell, C. J. (2000). Distribution of testican expression in human brain. *Cell Tissue Res.* 302, 139–144. doi: 10.1007/s004410000277

Martinez, J., Dhawan, A., and Farach-Carson, M. C. (2018). Modular proteoglycan perlecan/HSPG2: mutations, phenotypes, and functions. *Genes (Basel)* 9:556. doi: 10.3390/genes9110556

Massagué, J., Andres, J., Attisano, L., Cheifetz, S., López-Casillas, F., Ohtsuki, M., et al. (1992). TGF-beta receptors. *Mol. Reprod. Dev.* 32, 99–104.

Mathieu, P., Piantanida, A. P., and Pitossi, F. (2010). Chronic expression of transforming growth factor-beta enhances adult neurogenesis. *Neuroimmunomodulation* 17, 200–201. doi: 10.1159/000258723

Matlung, H., Szilagyi, K., Barclay, N. A., and van den Berg, T. K. (2017). The CD47-SIRPα signaling axis as an innate immune checkpoint in cancer. *Immunol. Rev.* 276, 145–164. doi: 10.1111/imr.12527

Matthews, R., Gary, S. C., Zerillo, C., Pratta, M., Solomon, K., Arner, E. C., et al. (2000). Brain-enriched hyaluronan binding (BEHAB)/brevican cleavage in a glioma cell line is mediated by a disintegrin and metalloproteinase with thrombospondin motifs (ADAMTS) family member. *J. Biol. Chem.* 275, 22695–22703. doi: 10.1074/jbc.m909764199

Mauney, S., Athanas, K. M., Pantazopoulos, H., Shaskan, N., Passeri, E., Berretta, S., et al. (2013). Developmental pattern of perineuronal nets in the human prefrontal cortex and their deficit in schizophrenia. *Biol. Psychiatry* 74, 427–435. doi: 10.1016/j.biopsych.2013.05.007

Maurage, C., Adam, E., Minéo, J. F., Sarrazin, S., Debunne, M., Siminski, R. M., et al. (2009). Endocan expression and localization in human glioblastomas. *J. Neuropathol. Exp. Neurol.* 68, 633–641. doi: 10.1097/nen.0b013e3181a52a7f

McTigue, D., Tripathi, R., and Wei, P. (2006). NG2 colocalizes with axons and is expressed by a mixed cell population in spinal cord lesions. *J. Neuropathol. Exp. Neurol.* 65, 406–420. doi: 10.1097/01.jnen.0000218447.32320.52

Mecollari, V., Nieuwenhuis, B., and Verhaagen, J. (2014). A perspective on the role of class III semaphorin signaling in central nervous system trauma. *Front. Cell. Neurosci.* 8:328. doi: 10.3389/fncel.2014.00328

Mega, A., Hartmark Nilsen, M., Leiss, L. W., Tobin, N. P., Miletic, H., Sleire, L., et al. (2020). Astrocytes enhance glioblastoma growth. *Glia* 68, 316–327. doi: 10.1002/glia.23718

Melrose, J. (2019a). Functional consequences of keratan sulfate sulfation in electrosensory tissues and in neuronal regulation. *Adv. Biosyst.* 3:e1800327.

Melrose, J. (2019b). Keratan sulfate (KS)-proteoglycans and neuronal regulation in health and disease: the importance of KS-glycodynamics and interactive capability with neuroregulatory ligands. *J. Neurochem.* 149, 170–194. doi: 10.1111/jnc.14652

Melrose, J., Hayes, A. J., and Bix, G. (2021). The CNS/PNS extracellular matrix provides instructive guidance cues to neural cells and neuroregulatory proteins in neural development and repair. *Int. J. Mol. Sci.* 22:5583. doi: 10.3390/ijms22115583

Mencio, C., Hussein, R. K., Yu, P., and Geller, H. M. (2021). The role of chondroitin sulfate proteoglycans in nervous system development. *J. Histochem. Cytochem.* 69, 61–80. doi: 10.1369/0022155420959147

Mercier, F. (2016). Fractones: extracellular matrix niche controlling stem cell fate and growth factor activity in the brain in health and disease. *Cell. Mol. Life Sci.* 73, 4661–4674. doi: 10.1007/s00018-016-2314-y

Mercier, F., and Arikawa-Hirasawa, E. (2012). Heparan sulfate niche for cell proliferation in the adult brain. *Neurosci. Lett.* 510, 67–72. doi: 10.1016/j.neulet.2011.12.046

Mercier, F., Kwon, Y. C., and Douet, V. (2012). Hippocampus/amygdala alterations, loss of heparan sulfates, fractones and ventricle wall reduction in adult BTBR T+ tf/J mice, animal model for autism. *Neurosci. Lett.* 506, 208–213. doi: 10.1016/j.neulet.2011.11.007

Milev, P., Friedlander, D. R., Sakurai, T., Karthikeyan, L., Flad, M., Margolis, R. K., et al. (1994). Interactions of the chondroitin sulfate proteoglycan phosphacan, the extracellular domain of a receptor-type protein tyrosine phosphatase, with neurons, glia, and neural cell adhesion molecules. *J. Cell Biol.* 127, 1703–1715. doi: 10.1083/jcb.127.6.1703

Miller, M., Lambert-Messerlian, G. M., Eklund, E. E., Heath, N. L., Donahue, J. E., and Stopa, E. G. (2012). Expression of inhibin/activin proteins and receptors in the human hypothalamus and basal forebrain. *J. Neuroendocrinol.* 24, 962–972. doi: 10.1111/j.1365-2826.2012.02289.x

Mitsunaga, C., Mikami, T., Mizumoto, S., Fukuda, J., and Sugahara, K. (2006). Chondroitin sulfate/dermatan sulfate hybrid chains in the development of cerebellum. Spatiotemporal regulation of the expression of critical disulfated disaccharides by specific sulfotransferases. *J. Biol. Chem.* 281, 18942–18952. doi: 10.1074/jbc.m510870200

Miura, R., Aspberg, A., Ethell, I. M., Hagihara, K., Schnaar, R. L., Ruoslahti, E., et al. (1999). The proteoglycan lectin domain binds sulfated cell surface glycolipids and promotes cell adhesion. *J. Biol. Chem.* 274, 11431–11438. doi: 10.1074/jbc.274.16.11431

Miura, R., Ethell, I. M., and Yamaguchi, Y. (2001). Carbohydrate-protein interactions between HNK-1-reactive sulfoglucuronyl glycolipids and the proteoglycan lectin domain mediate neuronal cell adhesion and neurite outgrowth. *J. Neurochem.* 76, 413–424. doi: 10.1046/j.1471-4159.2001.00042.x

Miyata, S., and Kitagawa, H. (2016). Chondroitin sulfate and neuronal disorders. *Front. Biosci. (Landmark Ed.)* 21:1330–1340. doi: 10.2741/4460

Miyata, S., and Kitagawa, H. (2017). Formation and remodeling of the brain extracellular matrix in neural plasticity: roles of chondroitin sulfate and

hyaluronan. *Biochim. Biophys. Acta Gen. Subj.* 1861, 2420–2434. doi: 10.1016/j.bbagen.2017.06.010

Miyata, S., Nadanaka, S., Igarashi, M., and Kitagawa, H. (2018). Structural variation of chondroitin sulfate chains contributes to the molecular heterogeneity of perineuronal nets. *Front. Integr. Neurosci.* 12:3. doi: 10.3389/fnint.2018.00003

Miyazono, K. (1997). TGF-beta receptors and signal transduction. *Int. J. Hematol.* 65, 97–104.

Mizuguchi, S., Uyama, T., Kitagawa, H., Nomura, K. H., Dejima, K., Gengyo-Ando, K., et al. (2003). Chondroitin proteoglycans are involved in cell division of *Caenorhabditis elegans*. *Nature* 423, 443–448. doi: 10.1038/nature01635

Mizumoto, S., Yamada, S., and Sugahara, K. (2015). Molecular interactions between chondroitin-dermatan sulfate and growth factors/receptors/matrix proteins. *Curr. Opin. Struct. Biol.* 34, 35–42. doi: 10.1016/j.sbi.2015.06.004

Mohan, H., Krumbholz, M., Sharma, R., Eisele, S., Junker, A., Sixt, M., et al. (2010). Extracellular matrix in multiple sclerosis lesions: fibrillar collagens, biglycan and decorin are upregulated and associated with infiltrating immune cells. *Brain Pathol.* 20, 966–975.

Mooney, K., Choy, W., Sidhu, S., Pelargos, P., Bui, T. T., Voth, B., et al. (2016). The role of CD44 in glioblastoma multiforme. *J. Clin. Neurosci.* 34, 1–5. doi: 10.1016/j.jocn.2016.05.012

Moore, S., Tessier-Lavigne, M., and Kennedy, T. E. (2007). Netrins and their receptors. *Adv. Exp. Med. Biol.* 621, 17–31. doi: 10.1007/978-0-387-76715-4_2

Moransard, M., Dann, A., Staszewski, O., Fontana, A., Prinz, M., and Suter, T. (2011). NG2 expressed by macrophages and oligodendrocyte precursor cells is dispensable in experimental autoimmune encephalomyelitis. *Brain* 134, 1315–1330. doi: 10.1093/brain/awr070

Morawski, M. B. G., Jäger, C., Seeger, G., Matthews, R. T., and Arendt, T. (2012). Involvement of perineuronal and perisynaptic extracellular matrix in Alzheimer's disease neuropathology. *Brain Pathol.* 22, 547–561. doi: 10.1111/j.1750-3639.2011.00557.x

Morleo, B., Teresinski, G., Rousseau, G., Tse, R., Tettamanti, C., Augsburger, M., et al. (2019). Biomarkers of cerebral damage in fatal hypothermia: preliminary results. *Am. J. Forensic. Med. Pathol.* 40, 242–245. doi: 10.1097/paf.0000000000000484

Mühleisen, T., Mattheisen, M., Strohmaier, J., Degenhardt, F., Priebe, L., Schultz, C. C., et al. (2012). Association between schizophrenia and common variation in neurocan (NCAN), a genetic risk factor for bipolar disorder. *Schizophr. Res.* 138, 69–73. doi: 10.1016/j.schres.2012.03.007

Muir, E., De Winter, F., Verhaagen, J., and Fawcett, J. (2019). Recent advances in the therapeutic uses of chondroitinase ABC. *Exp. Neurol.* 321:113032. doi: 10.1016/j.expneurol.2019.113032

Mulcahy, B., Witvliet, D., Holmyard, D., Mitchell, J., Chisholm, A. D., Meirovitch, Y., et al. (2018). A pipeline for volume electron microscopy of the *Caenorhabditis elegans* nervous system. *Front Neural Circuits* 12:94. doi: 10.3389/fncir.2018.00094

Murakami, K., Tanaka, T., Bando, Y., and Yoshida, S. (2015). Nerve injury induces the expression of syndecan-1 heparan sulfate proteoglycan in primary sensory neurons. *Neuroscience* 300, 338–350. doi: 10.1016/j.neuroscience.2015.05.033

Murata, Y., Kotani, T., Ohnishi, H., and Matozaki, T. (2014). The CD47-SIRPα signalling system: its physiological roles and therapeutic application. *J. Biochem.* 155, 335–344. doi: 10.1093/jb/mvu017

Mythreye, K., and Blobe, G. C. (2009). Proteoglycan signaling co-receptors: roles in cell adhesion, migration and invasion. *Cell. Signal.* 21, 1548–1558. doi: 10.1016/j.cellsig.2009.05.001

Nadanaka, S., Ishida, M., Ikegami, M., and Kitagawa, H. (2008). Chondroitin 4-O-sulfotransferase-1 modulates Wnt-3a signaling through control of E disaccharide expression of chondroitin sulfate. *J. Biol. Chem.* 283, 27333–27343. doi: 10.1074/jbc.m802997200

Nakada, M., Miyamori, H., Yamashita, J., and Sato, H. (2003). Testican 2 abrogates inhibition of membrane-type matrix metalloproteinases by other testican family proteins. *Cancer Res.* 63, 3364–3369.

Nakanishi, K., Aono, S., Hirano, K., Kuroda, Y., Ida, M., Tokita, Y., et al. (2006). Identification of neurite outgrowth-promoting domains of neuroglycan C, a brain-specific chondroitin sulfate proteoglycan, and involvement of phosphatidylinositol 3-kinase and protein kinase C signaling pathways in neuritogenesis. *J. Biol. Chem.* 281, 24970–24978. doi: 10.1074/jbc.m601498200

Nakanishi, K., Tokita, Y., Aono, S., Ida, M., Matsui, F., Higashi, Y., et al. (2010). Neuroglycan C, a brain-specific chondroitin sulfate proteoglycan, interacts with pleiotrophin, a heparin-binding growth factor. *Neurochem. Res.* 35, 1131–1137. doi: 10.1007/s11064-010-0164-9

Nandadasa, S., Foulcer, S., and Apte, S. S. (2014). The multiple, complex roles of versican and its proteolytic turnover by ADAMTS proteases during embryogenesis. *Matrix Biol.* 35, 34–41. doi: 10.1016/j.matbio.2014.01.005

Nandini, C., and Sugahara, K. (2006). Role of the sulfation pattern of chondroitin sulfate in its biological activities and in the binding of growth factors. *Adv. Pharmacol.* 53, 253–279. doi: 10.1016/s1054-3589(05)53012-6

Nastase, M., Young, M. F., and Schaefer, L. (2012). Biglycan: a multivalent proteoglycan providing structure and signals. *J. Histochem. Cytochem.* 60, 963–975. doi: 10.1369/0022155412456380

Naumann, U., Maass, P., Gleske, A. K., Aulwurm, S., Weller, M., and Eisele, G. (2008). Glioma gene therapy with soluble transforming growth factor-beta receptors II and III. *Int. J. Oncol.* 33, 759–765.

Neill, T., Schaefer, L., and Iozzo, R. V. (2012). Decorin: a guardian from the matrix. *Am. J. Pathol.* 181, 380–387.

Nicholson, C., and Hrabětová, S. (2017). Brain extracellular space: the final frontier of neuroscience. *Biophys. J.* 113, 2133–2142. doi: 10.1016/j.bpj.2017.06.052

Nishihara, S. (2010). Glycosyltransferases and transporters that contribute to proteoglycan synthesis in *Drosophila*: identification and functional analyses using the heritable and inducible RNAi system. *Methods Enzymol.* 480, 323–351. doi: 10.1016/s0076-6879(10)80015-1

Niven, J., and Laughlin, S. B. (2008). Energy limitation as a selective pressure on the evolution of sensory systems. *J. Exp. Biol.* 211, 1792–1804. doi: 10.1242/jeb.017574

Noborn, F., and Larson, G. (2021). Characterization of *C. elegans* chondroitin proteoglycans and their large functional and structural heterogeneity; evolutionary aspects on structural differences between humans and the nematode. *Adv. Exp. Med. Biol.* 21, 155–170. doi: 10.1007/5584_2020_485

Nutt, C., Zerillo, C. A., Kelly, G. M., and Hockfield, S. (2001). Brain enriched hyaluronan binding (BEHAB)/brevican increases aggressiveness of CNS-1 gliomas in Lewis rats. *Cancer Res.* 61, 7056–7059.

Ogura, K., Asakura, T., and Goshima, Y. (2012). Localization mechanisms of the axon guidance molecule UNC-6/Netrin and its receptors, UNC-5 and UNC-40, in *Caenorhabditis elegans*. *Dev. Growth Differ.* 54, 390–397. doi: 10.1111/j.1440-169x.2012.01349.x

Olson, S., Bishop, J. R., Yates, J. R., Oegema, K., and Esko, J. D. (2006). Identification of novel chondroitin proteoglycans in *Caenorhabditis elegans*: embryonic cell division depends on CPG-1 and CPG-2. *J. Cell Biol.* 173, 985–994. doi: 10.1083/jcb.200603003

Oohira, A., Shuo, T., Tokita, Y., Nakanishi, K., and Aono, S. (2004). Neuroglycan C, a brain-specific part-time proteoglycan, with a particular multidomain structure. *Glycoconj. J.* 21, 53–57. doi: 10.1023/b:glyc.0000043748.90896.83

Pangalos, M. N., Shioi, J., Efthimiopoulos, S., Wu, A., and Robakis, N. K. (1996). Characterization of appican, the chondroitin sulfate proteoglycan form of the Alzheimer amyloid precursor protein. *Neurodegeneration* 5, 445–451. doi: 10.1006/neur.1996.0061

Pantazaka, E., and Papadimitriou, E. (2014). Chondroitin sulfate-cell membrane effectors as regulators of growth factor-mediated vascular and cancer cell migration. *Biochim. Biophys. Acta* 1840, 2643–2650. doi: 10.1016/j.bbagen.2014.01.009

Pantazopoulos, H., Katsel, P., Haroutunian, V., Chelini, G., Klengel, T., and Berretta, S. (2021). Molecular signature of extracellular matrix pathology in schizophrenia. *Eur. J. Neurosci.* 12, 3960–3987. doi: 10.1111/ejn.15009

Patel, K., Yao, J., Raymond, C., Yong, W., Everson, R., Liau, L. M., et al. (2020). Decorin expression is associated with predictive diffusion MR phenotypes of anti-VEGF efficacy in glioblastoma. *Sci. Rep.* 10:14819.

Perkins, K., Arranz, A. M., Yamaguchi, Y., and Hrabetova, S. (2017). Brain extracellular space, hyaluronan, and the prevention of epileptic seizures. *Rev. Neurosci.* 28, 869–892.

Peters, A., and Sherman, L. S. (2020). Diverse roles for hyaluronan and hyaluronan receptors in the developing and adult nervous system. *Int. J. Mol. Sci.* 21:5988. doi: 10.3390/ijms21175988

Pintér, A., Hevesi, Z., Zahola, P., Alpár, A., and Hanics, J. (2020). Chondroitin sulfate proteoglycan-5 forms perisynaptic matrix assemblies in the adult rat cortex. *Cell. Signal.* 74:109710. doi: 10.1016/j.cellsig.2020.109710

Platsaki, S., Zhou, X., Pinan-Lucarré, B., Delauzun, V., Tu, H., Mansuelle, P., et al. (2020). The Ig-like domain of Punctin/MADD-4 is the primary determinant for interaction with the ectodomain of neuroligin NLG-1. *J. Biol. Chem.* 295, 16267–16279. doi: 10.1074/jbc.ra120.014591

Ponte, P., Gonzalez-DeWhitt, P., Schilling, J., Miller, J., Hsu, D., Greenberg, B., et al. (1988). A new A4 amyloid mRNA contains a domain homologous to serine proteinase inhibitors. *Nature* 331, 525–527. doi: 10.1038/331525a0

Preston, M., and Sherman, L. S. (2011). Neural stem cell niches: roles for the hyaluronan-based extracellular matrix. *Front. Biosci. (Schol. Ed.)* 3:1165–1179. doi: 10.2741/218

Quraishe, S., Forbes, L. H., and Andrews, M. R. (2018). The extracellular environment of the CNS: influence on plasticity, sprouting, and axonal regeneration after spinal cord injury. *Neural Plast.* 2018:2952386.

Rajasekharan, S., and Kennedy, T. E. (2009). The netrin protein family. *Genome Biol.* 10:239. doi: 10.1186/gb-2009-10-9-239

Rankin-Gee, E., McRae, P. A., Baranov, E., Rogers, S., Wandrey, L., and Porter, B. E. (2015). Perineuronal net degradation in epilepsy. *Epilepsia* 56, 1124–4433. doi: 10.1111/epi.13026

Rauch, U., Feng, K., and Zhou, X. H. (2001). Neurocan: a brain chondroitin sulfate proteoglycan. *Cell. Mol. Life Sci.* 58, 1842–1856. doi: 10.1007/pl00000822

Raum, H., Dietsche, B., Nagels, A., Witt, S. H., Rietschel, M., Kircher, T., et al. (2015). A genome-wide supported psychiatric risk variant in NCAN influences brain function and cognitive performance in healthy subjects. *Hum. Brain Mapp.* 36, 378–390. doi: 10.1002/hbm.22635

Reichsman, F., Smith, L., and Cumberledge, S. (1996). Glycosaminoglycans can modulate extracellular localization of the wingless protein and promote signal transduction. *J. Cell Biol.* 135, 809–827.

Ren, W., Zhang, Y., Li, M., Wu, L., Wang, G., Baeg, G. H., et al. (2015). Windpipe controls *Drosophila* intestinal homeostasis by regulating JAK/STAT pathway via promoting receptor endocytosis and lysosomal degradation. *PLoS Genet.* 11:e1005180. doi: 10.1371/journal.pgen.1005180

Rhiner, C., Gysi, S., Fröhli, E., Hengartner, M. O., and Hajnal, A. (2005). Syndecan regulates cell migration and axon guidance in *C. elegans*. *Development* 132, 4621–4633. doi: 10.1242/dev.02042

Roppongi, R., Dhume, S. H., Padmanabhan, N., Silwal, P., Zahra, N., Karimi, B., et al. (2020). LRRTMs organize synapses through differential engagement of neurexin and PTPσ. *Neuron* 106, 108–125.e112.

Roy, A., Attarha, S., Weishaupt, H., Edqvist, P. H., Swartling, F. J., Bergqvist, M., et al. (2017). Serglycin as a potential biomarker for glioma: association of serglycin expression, extent of mast cell recruitment and glioblastoma progression. *Oncotarget* 8, 24815–24827. doi: 10.18632/oncotarget.15820

Saied-Santiago, K., Townley, R. A., Attonito, J. D., da Cunha, D. S., Díaz-Balzac, C. A., Tecle, E., et al. (2017). Coordination of heparan sulfate proteoglycans with Wnt signaling to control cellular migrations and positioning in *Caenorhabditis elegans*. *Genetics* 206, 1951–1967. doi: 10.1534/genetics.116.198739

Sakamoto, K., Ozaki, T., Suzuki, Y., and Kadomatsu, K. (2021). Type IIa RPTPs and glycans: roles in axon regeneration and synaptogenesis. *Int. J. Mol. Sci.* 22:5524. doi: 10.3390/ijms22115524

Sakry, D., and Trotter, J. (2016). The role of the NG2 proteoglycan in OPC and CNS network function. *Brain Res.* 1638, 161–166. doi: 10.1016/j.brainres.2015.06.003

Sandbrink, R., Masters, C. L., and Beyreuther, K. (1996). APP gene family. Alternative splicing generates functionally related isoforms. *Ann. N. Y. Acad. Sci.* 777, 281–287. doi: 10.1111/j.1749-6632.1996.tb34433.x

Sarrazin, S., Adam, E., Lyon, M., Depontieu, F., Motte, V., Landolfi, C., et al. (2006). Endocan or endothelial cell specific molecule-1 (ESM-1): a potential novel endothelial cell marker and a new target for cancer therapy. *Biochim. Biophys. Acta* 1765, 25–37. doi: 10.1016/j.bbcan.2005.08.004

Sato, Y., Kiyozumi, D., Futaki, S., Nakano, I., Shimono, C., Kaneko, N., et al. (2019). Ventricular-subventricular zone fractones are speckled basement membranes that function as a neural stem cell niche. *Mol. Biol. Cell* 30, 56–68. doi: 10.1091/mbc.e18-05-0286

Schäfer, M., and Tegeder, I. (2018). NG2/CSPG4 and progranulin in the posttraumatic glial scar. *Matrix Biol.* 6, 571–588. doi: 10.1016/j.matbio.2017.10.002

Schafer, W. (2018). The worm connectome: back to the future. *Trends Neurosci.* 41, 763–765. doi: 10.1016/j.tins.2018.09.002

Scherpereel, A., Gentina, T., Grigoriu, B., Sénéchal, S., Janin, A., Tsicopoulos, A., et al. (2003). Overexpression of endocan induces tumor formation. *Cancer Res.* 63, 6084–6089.

Schmalfeldt, M., Dours-Zimmermann, M. T., Winterhalter, K. H., and Zimmermann, D. R. (1998). Versican V2 is a major extracellular matrix component of the mature bovine brain. *J. Biol. Chem.* 273, 15758–15764. doi: 10.1074/jbc.273.25.15758

Schmidt, S., Arendt, T., Morawski, M., and Sonntag, M. (2020). Neurocan contributes to perineuronal net development. *Neuroscience* 442, 69–86. doi: 10.1016/j.neuroscience.2020.06.040

Schmitt, M. (2016). Versican vs versikine: tolerance vs attack. *Blood* 128, 612–613. doi: 10.1182/blood-2016-06-721092

Schnepp, A., Komp Lindgren, P., Hülsmann, H., Kröger, S., Paulsson, M., and Hartmann, U. (2005). Mouse testican-2. Expression, glycosylation, and effects on neurite outgrowth. *J. Biol. Chem.* 280, 1274–1280.

Schönherr, E., Sunderkötter, C., Iozzo, R. V., and Schaefer, L. (2005). Decorin, a novel player in the insulin-like growth factor system. *J. Biol. Chem.* 280, 15767–15772. doi: 10.1074/jbc.m500451200

Schultz, C., Mühleisen, T. W., Nenadic, I., Koch, K., Wagner, G., Schachtzabel, C., et al. (2014). Common variation in NCAN, a risk factor for bipolar disorder and schizophrenia, influences local cortical folding in schizophrenia. *Psychol. Med.* 44, 811–820. doi: 10.1017/s0033291713001414

Segarini, P. (1991). TGF-beta receptors. *Ciba Found. Symp.* 157, 29–50.

Selberg, J., Jia, M., and Rolandi, M. (2019). Proton conductivity of glycosaminoglycans. *PLoS One.* 14:e0202713. doi: 10.1371/journal.pone.0202713

Shabani, Z., Ghadiri, T., Karimipour, M., Sadigh-Eteghad, S., Mahmoudi, J., Mehrad, H., et al. (2021). Modulatory properties of extracellular matrix glycosaminoglycans and proteoglycans on neural stem cells behavior: highlights on regenerative potential and bioactivity. *Int. J. Biol. Macromol.* 171, 366–381. doi: 10.1016/j.ijbiomac.2021.01.006

Sherman, L., Matsumoto, S., Su, W., Srivastava, T., and Back, S. A. (2015). Hyaluronan synthesis, catabolism, and signaling in neurodegenerative diseases. *Int. J. Cell Biol.* 2015:368584.

Shimbo, M., Ando, S., Sugiura, N., Kimata, K., and Ichijo, H. (2013). Moderate repulsive effects of E-unit-containing chondroitin sulfate (CSE) on behavior of retinal growth cones. *Brain Res.* 1491, 34–43. doi: 10.1016/j.brainres.2012.11.011

Shioi, J., Pangalos, M. N., Ripellino, J. A., Vassilacopoulou, D., Mytilineou, C., Margolis, R. U., et al. (1995). The Alzheimer amyloid precursor proteoglycan (appican) is present in brain and is produced by astrocytes but not by neurons in primary neural cultures. *J. Biol. Chem.* 270, 11839–11844. doi: 10.1074/jbc.270.20.11839

Shuo, T., Aono, S., Matsui, F., Tokita, Y., Maeda, H., Shimada, K., et al. (2004). Developmental changes in the biochemical and immunological characters of the carbohydrate moiety of neuroglycan C, a brain-specific chondroitin sulfate proteoglycan. *Glycoconj. J.* 20, 267–278. doi: 10.1023/b:glyc.0000025821.22618.33

Shuo, T., Aono, S., Nakanishi, K., Tokita, Y., Kuroda, Y., Ida, M., et al. (2007). Ectodomain shedding of neuroglycan C, a brain-specific chondroitin sulfate proteoglycan, by TIMP-2- and TIMP-3-sensitive proteolysis. *J. Neurochem.* 102, 1561–1568. doi: 10.1111/j.1471-4159.2007.04658.x

Singh, J., Noorbaloochi, S., MacDonald, R., and Maxwell, L. J. (2015). Chondroitin for osteoarthritis. *Cochrane Database Syst. Rev.* 1:CD005614.

So, H., Fong, P. Y., Chen, R. Y., Hui, T. C., Ng, M. Y., Cherny, S. S., et al. (2010). Identification of neuroglycan C and interacting partners as potential susceptibility genes for schizophrenia in a Southern Chinese population. *Am. J. Med. Genet. B Neuropsychiatr. Genet.* 153B, 103–113.

Soleman, S., Filippov, M. A., Dityatev, A., and Fawcett, J. W. (2013). Targeting the neural extracellular matrix in neurological disorders. *Neuroscience* 253, 194–213. doi: 10.1016/j.neuroscience.2013.08.050

Sonntag, M., Blosa, M., Schmidt, S., Rübsamen, R., and Morawski, M. (2015). Perineuronal nets in the auditory system. *Hear Res.* 329, 21–32. doi: 10.1016/j.heares.2014.12.012

Sorg, B., Berretta, S., Blacktop, J. M., Fawcett, J. W., Kitagawa, H., Kwok, J. C., et al. (2016). Casting a wide net: role of perineuronal nets in neural plasticity. *J. Neurosci.* 36, 11459–11468. doi: 10.1523/jneurosci.2351-16.2016

Stanley, P. (2016). What have we learned from glycosyltransferase knockouts in mice? *J. Mol. Biol.* 428, 3166–3182. doi: 10.1016/j.jmb.2016.03.025

Starich, T., Xu, J., Skerrett, I. M., Nicholson, B. J., and Shaw, J. E. (2009). Interactions between innexins UNC-7 and UNC-9 mediate electrical synapse specificity in the *Caenorhabditis elegans* locomotory nervous system. *Neural Dev.* 11:16. doi: 10.1186/1749-8104-4-16

Steigemann, P., Molitor, A., Fellert, S., Jäckle, H., and Vorbrüggen, G. (2004). Heparan sulfate proteoglycan syndecan promotes axonal and myotube guidance by slit/robo signaling. *Curr. Biol.* 14, 225–230. doi: 10.1016/j.cub.2004.01.006

Stichel, C., Kappler, J., Junghans, U., Koops, A., Kresse, H., and Müller, H. W. (1995). Differential expression of the small chondroitin/dermatan sulfate proteoglycans decorin and biglycan after injury of the adult rat brain. *Brain Res.* 704, 263–274. doi: 10.1016/0006-8993(95)01131-5

Strbak, O., Kanuchova, Z., and Krafcik, A. (2016). Proton gradients as a key physical factor in the evolution of the forced transport mechanism across the lipid membrane. *Orig. Life Evol. Biosph.* 46, 523–531. doi: 10.1007/s11084-016-9496-z

Streit, A., Nolte, C., Rásony, T., and Schachner, M. (1993). Interaction of astrochondrin with extracellular matrix components and its involvement in astrocyte process formation and cerebellar granule cell migration. *J. Cell Biol.* 120, 799–814. doi: 10.1083/jcb.120.3.799

Su, M., Soomro, S. H., Jie, J., and Fu, H. (2021). Effects of the extracellular matrix on myelin development and regeneration in the central nervous system. *Tissue Cell* 69:101444. doi: 10.1016/j.tice.2020.101444

Sugahara, K., Mikami, T., Uyama, T., Mizuguchi, S., Nomura, K., and Kitagawa, H. (2003). Recent advances in the structural biology of chondroitin sulfate and dermatan sulfate. *Curr. Opin. Struct. Biol.* 13, 612–620. doi: 10.1016/j.sbi.2003.09.011

Sugitani, K., Egorova, D., Mizumoto, S., Nishio, S., Yamada, S., Kitagawa, H., et al. (2020). Hyaluronan degradation and release of a hyaluronan-aggrecan complex from perineuronal nets in the aged mouse brain. *Biochim. Biophys. Acta Gen. Subj.* 1865:129804. doi: 10.1016/j.bbagen.2020.129804

Sullivan, C., Gotthard, I., Wyatt, E. V., Bongu, S., Mohan, V., Weinberg, R. J., et al. (2018). Perineuronal net protein neurocan inhibits NCAM/EphA3 repellent signaling in GABAergic interneurons. *Sci. Rep.* 8:6143.

Sun, H., Zhang, H., Li, K., Wu, H., Zhan, X., Fang, F., et al. (2019). ESM-1 promotes adhesion between monocytes and endothelial cells under intermittent hypoxia. *J. Cell Physiol.* 234, 1512–1521. doi: 10.1002/jcp.27016

Takano, M., Mori, Y., Shiraki, H., Horie, M., Okamoto, H., Narahara, M., et al. (1999). Detection of bikunin mRNA in limited portions of rat brain. *Life Sci.* 65, 757–762. doi: 10.1016/s0024-3205(99)00302-1

Takemura, M., Noborn, F., Nilsson, J., Bowden, N., Nakato, E., Baker, S., et al. (2020). Chondroitin sulfate proteoglycan Windpipe modulates Hedgehog signaling in *Drosophila*. *Mol. Biol. Cell* 31, 813–824. doi: 10.1091/mbc.e19-06-0327

Tamburini, E., Dallatomasina, A., Quartararo, J., Cortelazzi, B., Mangieri, D., Lazzaretti, M., et al. (2019). Structural deciphering of the NG2/CSPG4 proteoglycan multifunctionality. *FASEB J.* 33, 3112–3128. doi: 10.1096/fj.201801670r

Tauchi, R., Imagama, S., Natori, T., Ohgomori, T., Muramoto, A., Shinjo, R., et al. (2012). The endogenous proteoglycan-degrading enzyme ADAMTS-4 promotes functional recovery after spinal cord injury. *J. Neuroinflammation* 9:53.

Teuscher, A., Jongsma, E., Davis, M. N., Statzer, C., Gebauer, J. M., Naba, A., et al. (2019). The in-silico characterization of the *Caenorhabditis elegans* matrisome and proposal of a novel collagen classification. *Matrix Biol. Plus* 1:100001. doi: 10.1016/j.mbplus.2018.11.001

Thelin, M., Bartolini, B., Axelsson, J., Gustafsson, R., Tykesson, E., Pera, E., et al. (2013). Biological functions of iduronic acid in chondroitin/dermatan sulfate. *FEBS J.* 280, 2431–2446. doi: 10.1111/febs.12214

Thinakaran, G., and Sisodia, S. S. (1994). Amyloid precursor-like protein 2 (APLP2) is modified by the addition of chondroitin sulfate glycosaminoglycan at a single site. *J. Biol. Chem.* 269, 22099–22104. doi: 10.1016/s0021-9258(17)31761-1

Thinakaran, G., Slunt, H. H., and Sisodia, S. S. (1995). Novel regulation of chondroitin sulfate glycosaminoglycan modification of amyloid precursor protein and its homologue, APLP2. *J. Biol. Chem.* 270, 16522–16525. doi: 10.1074/jbc.270.28.16522

Tsai, J., Zhang, J., Minami, T., Voland, C., Zhao, S., Yi, X., et al. (2002). Cloning and characterization of the human lung endothelial-cell-specific molecule-1 promoter. *J. Vasc. Res.* 39, 148–159. doi: 10.1159/000057763

Tu, H., Pinan-Lucarré, B., Ji, T., Jospin, M., and Bessereau, J. L. (2015). *C. elegans* punctin clusters GABA(A) receptors via neuroligin binding and UNC-40/DCC recruitment. *Neuron* 86, 1407–1419. doi: 10.1016/j.neuron.2015.05.013

Tykesson, E., Hassinen, A., Zielinska, K., Thelin, M. A., Frati, G., Ellervik, U., et al. (2018). Dermatan sulfate epimerase 1 and dermatan 4-O-sulfotransferase 1 form complexes that generate long epimerized 4-O-sulfated blocks. *J. Biol. Chem.* 293, 13725–13735. doi: 10.1074/jbc.ra118.003875

Vale, W., Wiater, E., Gray, P., Harrison, C., Bilezikjian, L., and Choe, S. (2004). Activins and inhibins and their signaling. *Ann. N. Y. Acad. Sci.* 1038, 142–147.

Vassallo, V., Stellavato, A., Cimini, D., Pirozzi, A. V. A., Alfano, A., Cammarota, M., et al. (2021). Unsulfated biotechnological chondroitin by itself as well as in combination with high molecular weight hyaluronan improves the inflammation profile in osteoarthritis in vitro model. *J. Cell Biochem.* doi: 10.1002/jcb.29907

Vellai, T., Takács, K., and Vida, G. (1998). A new aspect to the origin and evolution of eukaryotes. *J. Mol. Evol.* 46, 499–507. doi: 10.1007/pl00006331

Viapiano, M., Hockfield, S., and Matthews, R. T. (2008). BEHAB/brevican requires ADAMTS-mediated proteolytic cleavage to promote glioma invasion. *J. Neurooncol.* 88, 261–272. doi: 10.1007/s11060-008-9575-8

Walimbe, A., Okuma, H., Joseph, S., Yang, T., Yonekawa, T., Hord, J. M., et al. (2020). POMK regulates dystroglycan function via LARGE1-mediated elongation of matriglycan. *Elife* 9:e61388.

Wang, L., Cheng, B. F., Yang, H. J., Wang, M., and Feng, Z. W. (2015). NF-κB protects human neuroblastoma cells from nitric oxide-induced apoptosis through upregulating biglycan. *Am. J. Transl. Res.* 7, 1541–1552.

Watanabe, E., Maeda, N., Matsui, F., Kushima, Y., Noda, M., and Oohira, A. (1995). Neuroglycan C, a novel membrane-spanning chondroitin sulfate proteoglycan that is restricted to the brain. *J. Biol. Chem.* 270, 26876–26882. doi: 10.1074/jbc.270.45.26876

Weiskopf, K. (2017). Cancer immunotherapy targeting the CD47/SIRPα axis. *Eur. J. Cancer* 76, 100–109. doi: 10.1016/j.ejca.2017.02.013

Wen, T., Binder, D. K., Ethell, I. M., and Razak, K. A. (2018). The perineuronal 'safety' net? Perineuronal net abnormalities in neurological disorders. *Front. Mol. Neurosci.* 11:270. doi: 10.3389/fnmol.2018.00270

Whalen, D., Malinauskas, T., Gilbert, R. J., and Siebold, C. (2013). Structural insights into proteoglycan-shaped Hedgehog signaling. *Proc. Natl. Acad. Sci. U.S.A.* 110, 16420–16425. doi: 10.1073/pnas.1310097110

White, J. (2020). Of worms and men. *J. Neurogenet.* 34, 255–258. doi: 10.1080/01677063.2020.1834543

White, J., Southgate, E., Thomson, J. N., and Brenner, S. (1976). Factors which determine connectivity in the nervous system of *C. elegans*. *Cold Spring Harb. Symp. Quant. Biol.* 48:633640.

White, J., Southgate, E., Thomson, J. N., and Brenner, S. (1986). The structure of the nervous system of the nematode *Caenorhabditis elegans*. *Philos. Trans. R. Soc. Lond. B Biol. Sci.* 314, 1–340. doi: 10.1098/rstb.1986.0056

Wigley, R., Hamilton, N., Nishiyama, A., Kirchhoff, F., and Butt, A. M. (2007). Morphological and physiological interactions of NG2-glia with astrocytes and neurons. *J. Anat.* 10, 661–670. doi: 10.1111/j.1469-7580.2007.00729.x

Wilson, E., Knudson, W., and Newell-Litwa, K. (2020). Hyaluronan regulates synapse formation and function in developing neural networks. *Sci. Rep.* 10:16459.

Wilson, T., and Lin, E. C. (1980). Evolution of membrane bioenergetics. *J. Supramol. Struct.* 13, 421–446. doi: 10.1002/jss.400130403

Woodruff, T. (1998). Regulation of cellular and system function by activin. *Biochem. Pharmacol.* 55, 953–963. doi: 10.1016/s0006-2952(97)00477-2

Wu, Y., Sheng, W., Chen, L., Dong, H., Lee, V., Lu, F., et al. (2004). Versican V1 isoform induces neuronal differentiation and promotes neurite outgrowth. *Mol. Biol. Cell* 15, 2093–2104. doi: 10.1091/mbc.e03-09-0667

Wu, Y., Zhang, Y., Cao, L., Chen, L., Lee, V., Zheng, P. S., et al. (2001). Identification of the motif in versican G3 domain that plays a dominant-negative effect on astrocytoma cell proliferation through inhibiting versican secretion and binding. *J. Biol. Chem.* 276, 14178–14186. doi: 10.1074/jbc.m100618200

Xiang, Y., Dong, H., Wan, Y., Li, J., Yee, A., Yang, B. B., et al. (2006). Versican G3 domain regulates neurite growth and synaptic transmission of hippocampal neurons by activation of epidermal growth factor receptor. *J. Biol. Chem.* 281, 19358–19368. doi: 10.1074/jbc.m512980200

Xie, Y., Peng, J., Pang, J., Guo, K., Zhang, L., Yin, S., et al. (2020). Biglycan regulates neuroinflammation by promoting M1 microglial activation in early brain injury after experimental subarachnoid hemorrhage. *J. Neurochem.* 152, 368–380. doi: 10.1111/jnc.14926

Xing, Y., Wang, Y., Wang, S., Wang, X., Fan, D., Zhou, D., et al. (2016). Human cytomegalovirus infection contributes to glioma disease progression via upregulating endocan expression. *Transl. Res.* 177, 103–126.

Xiong, A., Spyrou, A., and Forsberg-Nilsson, K. (2020). Involvement of heparan sulfate and heparanase in neural development and pathogenesis of brain tumors. *Adv. Exp. Med. Biol.* 1221, 365–403. doi: 10.1007/978-3-030-34521-1_14

Yamada, S., Sugahara, K., and Ozbek, S. (2011). Evolution of glycosaminoglycans: comparative biochemical study. *Commun. Integr. Biol.* 4, 150–158. doi: 10.4161/cib.4.2.14547

Yamaguchi, Y. (1996). Brevican: a major proteoglycan in adult brain. *Perspect. Dev. Neurobiol.* 3, 307–317.

Yamaguchi, Y. (2000). Lecticans: organizers of the brain extracellular matrix. *Cell. Mol. Life Sci.* 57, 276–289. doi: 10.1007/pl00000690

Yang, W., and Yee, A. J. (2013). Versican V2 isoform enhances angiogenesis by regulating endothelial cell activities and fibronectin expression. *FEBS Lett.* 587, 185–192. doi: 10.1016/j.febslet.2012.11.023

Yang, X. (2020). Chondroitin sulfate proteoglycans: key modulators of neuronal plasticity, long-term memory, neurodegenerative, and psychiatric disorders. *Rev. Neurosci.* 31, 555–568. doi: 10.1515/revneuro-2019-0117

Yang, Y., Lee, W. S., Tang, X., and Wadsworth, W. G. (2014). Extracellular matrix regulates UNC-6 (netrin) axon guidance by controlling the direction of intracellular UNC-40 (DCC) outgrowth activity. *PLoS One* 9:e97258. doi: 10.1371/journal.pone.0097258

Yao, T., Zhang, C. G., Gong, M. T., Zhang, M., Wang, L., and Ding, W. (2016). Decorin-mediated inhibition of the migration of U87MG glioma cells involves activation of autophagy and suppression of TGF-β signaling. *FEBS Open Bio* 31, 707–719. doi: 10.1002/2211-5463.12076

Yasuda, Y., Tokita, Y., Aono, S., Matsui, F., Ono, T., Sonta, S., et al. (1998). Cloning and chromosomal mapping of the human gene of neuroglycan C (NGC), a neural transmembrane chondroitin sulfate proteoglycan with an EGF module. *Neurosci. Res.* 32, 313–322. doi: 10.1016/s0168-0102(98)00098-4

Ye, F., Hua, Y., Keep, R. F., Xi, G., and Garton, H. J. L. (2021). CD47 blocking antibody accelerates hematoma clearance and alleviates hydrocephalus after experimental intraventricular hemorrhage. *Neurobiol. Dis.* 155:105384. doi: 10.1016/j.nbd.2021.105384

Ying, Z., Byun, H. R., Meng, Q., Noble, E., Zhang, G., Yang, X., et al. (2018). Biglycan gene connects metabolic dysfunction with brain disorder. *Biochim. Biophys. Acta Mol. Basis Dis.* 1864, 3679–3687. doi: 10.1016/j.bbadis.2018.10.002

Yousef, M., and Matthews, B. W. (2005). Structural basis of Prospero-DNA interaction: implications for transcription regulation in developing cells. *Structure* 13, 601–607. doi: 10.1016/j.str.2005.01.023

Zhang, H., Li, F., Yang, Y., Chen, J., and Hu, X. (2015). SIRP/CD47 signaling in neurological disorders. *Brain Res.* 1623, 74–80. doi: 10.1016/j.brainres.2015.03.012

Zhang, L. (2010). Glycosaminoglycan (GAG) biosynthesis and GAG-binding proteins. *Prog. Mol. Biol. Transl. Sci.* 93, 1–17. doi: 10.1016/s1877-1173(10)93001-9

Zhang, P., Karani, R., Turner, R. L., Dufresne, C., Ferri, S., Van Eyk, J. E., et al. (2016). The proteome of normal human retrobulbar optic nerve and sclera. *Proteomics* 16, 2592–2596. doi: 10.1002/pmic.201600229

Zhang, P., Lu, H., Peixoto, R. T., Pines, M. K., Ge, Y., Oku, S., et al. (2018). Heparan sulfate organizes neuronal synapses through neurexin partnerships. *Cell* 174, 1450–1464.e23.

Zhang, W., Ge, Y., Cheng, Q., Zhang, Q., Fang, L., and Zheng, J. (2018). Decorin is a pivotal effector in the extracellular matrix and tumour microenvironment. *Oncotarget* 9, 5480–5491. doi: 10.18632/oncotarget.23869

Zhang, W., Huang, Q., Xiao, W., Zhao, Y., Pi, J., Xu, H., et al. (2020). Advances in anti-tumor treatments targeting the CD47/SIRPα axis. *Front. Immunol.* 11:18. doi: 10.3389/fimmu.2020.00018

Zhang, X., Lee, S. J., Young, M. F., and Wang, M. M. (2015). The small leucine-rich proteoglycan BGN accumulates in CADASIL and binds to NOTCH3. *Transl. Stroke Res.* 6, 148–155. doi: 10.1007/s12975-014-0379-1

Zhao, X., Ramsey, K. E., Stephan, D. A., and Russell, P. (2004). Gene and protein expression changes in human trabecular meshwork cells treated with transforming growth factor-beta. *Invest. Ophthalmol. Vis. Sci.* 45, 4023–4034. doi: 10.1167/iovs.04-0535

**Conflict of Interest:** The authors declare that the research was conducted in the absence of any commercial or financial relationships that could be construed as a potential conflict of interest.

**Publisher's Note:** All claims expressed in this article are solely those of the authors and do not necessarily represent those of their affiliated organizations, or those of the publisher, the editors and the reviewers. Any product that may be evaluated in this article, or claim that may be made by its manufacturer, is not guaranteed or endorsed by the publisher.

## GLOSSARY

AD, Alzheimer's disease; ADAM, A disintegrin and metalloproteinase domain-containing protein; ADAMTSL, A disintegrin and metalloproteinase with thrombospondin motifs; AMPK, 5′ adenosine monophosphate-activated protein kinase; APLP2, amyloid precursor-like protein 2; APP, amyloid-beta precursor protein; BBB, blood brain barrier; BDNF, brain-derived neurotrophic factor; BEHAB, brain-enriched hyaluronan-binding protein; Bgn, biglycan; BMP, bone morphogenic protein; C4ST-1, chondroitin 4-*O*-sulfotransferase-1; C4ST-2, Chondroitin 4-*O*-sulfotransferase-2; CADASIL, cerebral autosomal dominant arteriopathy with subcortical infarcts and leukoencephalopathy; CAM, cell adhesion molecule; CD44, cluster of differentiation 44; CD47, cluster of differentiation 47; Chn, chondroitin; CMD, cartilage matrix deficiency; CNP, 2′,3′-cyclic nucleotide 3′-phosphodiesterase; CNS, central nervous system; CPG, chondroitin proteoglycans; CS, chondroitin sulfate; CSF, cerebrospinal fluid; CS-PG, chondroitin sulfate proteoglycan; D/iD, GlcA/IdoA(2-*O*-sulfate)-GalNAc(6-*O*-sulfate); D4ST-1, dermatan 4-*O*-sulfotransferase-1; DAMP, damage-associated molecular pattern; DCC, deleted in colorectal carcinoma; DDBJ, DNA Data Bank of Japan; Dlp, Dally-like protein; Dome, domeless; Dpp, decapentaplegic, a ligand of the TGFβ superfamily; DRG, dorsal root ganglion/ganglia; DS, dermatan sulfate; DS-PG, dermatan sulfate proteoglycan; E/iE, GlcA/IdoA-GalNAc (4,6-*O*-disulfate); ECM, extracellular matrix; EGF(R), epidermal growth factor (Receptor); eNOS, endothelial nitric oxide synthase; ESM-1, endothelial cell specific molecule-1; FGF, fibroblast growth factor; FORSE-1, forebrain surface embryonic-1; FSH, follicle-stimulating hormone; GPI, glycophosphatidylinositol; HA, hyaluronic acid; HAPLN2, hyaluronan and proteoglycan link protein 2; HB-GAM, heparin-binding growth-associated molecule; hEGFR, human epidermal growth factor receptor; HGF, hepatocyte growth factor; Hh, Hedgehog; HNK-1, human natural killer-1; HS, heparan sulfate; HS-PG, heparan sulfate proteoglycan; HSPG2, heparan sulfate proteoglycan 2 (perlecan); Hst, heparan sulfate sulfotransferase; HUVECs, human umbilical vein endothelial cells; iA, 4-sulfated IdoA-GalNAc; IAP, integrin-associated protein; iB, 2-sulfated IdoA-GalNAc; IFN-γ, interferon-γ; IGF-IR, insulin-like growth factor-1 receptor; IL, interleukin; ISH, *in situ* hybridization; ITI, immune tolerance induction; JAK/STAT, Janus kinase/signal transducer and activator of transcription; KO, knockout; Kon, Kon-tiki (NG2 homolog); KS, keratan sulfate; LFA-1, lymphocyte function associated antigen-1; LRR, leucine-rich repeat; MADD, muscle arm development defective; MAP, mitogen-activated protein; MCAF, monocyte chemotactic and activating factor; MCP-1, monocyte chemoattractant protein-1; MHC, major histocompatibility complex; MIP, macrophage inflammatory protein; MK, midkine; MMP, matrix metalloproteinase; MSC, mesenchymal stem cell; MT-1, metallothionein-1; mTOR, mechanistic target of rapamycin; NCAM, neural cell adhesion molecule; NF-κB, nuclear factor Kappa-light-chain-enhancer of activated B cells; NG2, neuron-glial antigen 2; NgCAM, neuroglia cell adhesion molecule; NGF, neural growth factor; NgR2, Nogo-66 Receptor Homolog2; NLG, neuroligin; NMJ, neuromuscular junction; NO, nitric oxide; Nrp-1, neuropilin 1; OA, osteoarthritis; OPC, oligodendrocyte precursor cells; PAP, 3′-phosphoadenosine 5′-phosphosulfate; PAPS, 3′-phosphoadenosine 5′-phosphosulfate; PAR1, protease-activated receptor-1, PG, proteoglycan; PNN, perineuronal net; PNS, peripheral nervous system; Pros, prospero; RANTES, regulated upon activation, normal T cell expressed and secreted; RNAi, ribonucleic acid interference; ROS, reactive oxygen species; RPTPs, receptor protein tyrosine phosphatases; RPTP-ζ, receptor protein tyrosine phosphatase-ζ; SCI, spinal cord injury; Sdc, syndecan; SDF-1β, stromal cell-derived factor-1β; SDN-1, syndecan homolog found in *Caenorhabditis elegans;* SEMA3A, semaphorin 3A; SEMA5A, semaphorin 5A; SIRPα, signal regulatory protein α; SMAD, Sma and MAD-related protein; SOX9, SRY-box transcription factor 9; Sqv, squashed vulva gene; SSEA-1, stage specific embryonic antigen-1; SVZ, subventricular zone; TBI, traumatic brain injury; TGF-β, transforming growth factor-β; TM, transmembrane; TNFR, tumor necrosis factor receptor; TNF-α, tumor necrosis factor-α; TSP-1, thrombospondin-1; UDP, uridine diphosphate; UNC, uncoordinated; UST, uronyl 2-sulfotransferase; VEGF, vascular endothelial growth factor; Wdp, windpipe; Wg, wingless.

frontiers in Cell and Developmental Biology

REVIEW
published: 06 August 2021
doi: 10.3389/fcell.2021.693563

# Chondroitin Sulfate/Dermatan Sulfate-Protein Interactions and Their Biological Functions in Human Diseases: Implications and Analytical Tools

*Bin Zhang and Lianli Chi**

*National Glycoengineering Research Center, Shandong University, Qingdao, China*

Chondroitin sulfate (CS) and dermatan sulfate (DS) are linear anionic polysaccharides that are widely present on the cell surface and in the cell matrix and connective tissue. CS and DS chains are usually attached to core proteins and are present in the form of proteoglycans (PGs). They not only are important structural substances but also bind to a variety of cytokines, growth factors, cell surface receptors, adhesion molecules, enzymes and fibrillary glycoproteins to execute series of important biological functions. CS and DS exhibit variable sulfation patterns and different sequence arrangements, and their molecular weights also vary within a large range, increasing the structural complexity and diversity of CS/DS. The structure-function relationship of CS/DS PGs directly and indirectly involves them in a variety of physiological and pathological processes. Accumulating evidence suggests that CS/DS serves as an important cofactor for many cell behaviors. Understanding the molecular basis of these interactions helps to elucidate the occurrence and development of various diseases and the development of new therapeutic approaches. The present article reviews the physiological and pathological processes in which CS and DS participate through their interactions with different proteins. Moreover, classic and emerging glycosaminoglycan (GAG)-protein interaction analysis tools and their applications in CS/DS-protein characterization are also discussed.

**Keywords: chondroitin sulfate, dermatan sulfate, protein, interaction, human disease, analytical methods**

OPEN ACCESS

***Edited by:***
*Jessica C. F. Kwok,*
*University of Leeds, United Kingdom*

***Reviewed by:***
*Dalit Sela-Donenfeld,*
*The Hebrew University of Jerusalem, Israel*
*Chao Cai,*
*Ocean University of China, China*
*Zhongfu Wang,*
*Northwest University, China*

***Correspondence:**
*Lianli Chi*
*lianlichi@sdu.edu.cn*

***Specialty section:***
*This article was submitted to Signaling, a section of the journal Frontiers in Cell and Developmental Biology*

***Received:*** *11 April 2021*
***Accepted:*** *20 July 2021*
***Published:*** *06 August 2021*

***Citation:***
*Zhang B and Chi L (2021) Chondroitin Sulfate/Dermatan Sulfate-Protein Interactions and Their Biological Functions in Human Diseases: Implications and Analytical Tools. Front. Cell Dev. Biol. 9:693563. doi: 10.3389/fcell.2021.693563*

## INTRODUCTION

Chondroitin sulfate (CS) and dermatan sulfate (DS) are acidic linear anionic polysaccharides in the glycosaminoglycan (GAG) family. CS is composed of repeated disaccharide units [→4GlcAβ1→3 GalNAcβ1→], where GlcA and GalNAc refer to D-glucuronic acid and N-acetylgalactosamine (Mikami and Kitagawa, 2013). The difference between the DS chain and CS chain is that the GlcA is epimerized to iduronic acid (IdoA) in the DS, and the CS and DS structures are usually found in a single CS-DS hybrid polysaccharide chain (Sugahara et al., 2003). The structure of CS/DS seems simple, but the hydroxyl groups at the C4 and C6 positions of GalNAc and the C2 position of GlcA/IdoA residues may undergo sulfation modification, thus yielding huge structural variations

(Mizumoto et al., 2015). According to the number and positions of sulfate groups, the disaccharide units can be divided into different types, as shown in **Figure 1**. A single polysaccharide chain generally contains different disaccharide units, and CS and DS are usually classified by their most abundant disaccharide units. For example, the CS-A chain contains not only the dominant A unit but also relatively small amounts of C units and O units (Wang W. et al., 2020). The diversity of CS/DS structures leads to different biological functions, but it also brings great challenges to the study of corresponding structure-function relationships.

Like most GAGs, CS and DS are located in the animal extracellular matrix (ECM), on the cell surface or associated with the plasma membrane (Li et al., 2019). Therefore, they seem to be strategically in a superior position to control various important processes that occur at the cell-tissue interface. CS/DS chains are covalently bound to the core protein to form CS/DS proteoglycans (CS/DSPG), which participate in the regulation of the extracellular environment and many biological and pathophysiological activities (Malavaki et al., 2008). In recent decades, increasing evidence has shown that CS/DS is involved in tumor occurrence and metastasis (Knutson et al., 1996; Tang et al., 2018), nervous system development (Avram et al., 2014; Shida et al., 2019), virus adsorption and infection (Aquino and Park, 2016; Yang et al., 2016), atherosclerosis and other diseases (Pomin, 2015; Stabler et al., 2017; Scuruchi et al., 2020). The CS/DS chain performs these functions by interacting with various target proteins, such as various growth factors, fibroblast growth factor (FGF), hepatocyte growth factor (HGF), pluripotent protein (PTN), cell surface receptor and intercellular adhesion factor (Pudelko et al., 2019).

The charge density and the position of sulfation on the CS/DS chains are the main factors that affect their ability to interact with target proteins, while a minimal chain length is usually required for binding (Bao et al., 2005; Yamaguchi et al., 2006). It was initially believed that the GAG-protein interaction was solely due to charge-charge interaction. On this basis, a number of consensus sequences on GAG binding proteins were found, including XBBXBX, XBBBXXBX, and XBBBXXBBBXXBBX, where B is a basic amino acid residue and X is a hydrophilic residue (Cardin and Weintraub, 1989; Sobel et al., 1992). In subsequent studies, it was found that non-ionic interactions (hydrogen bonds, hydrophobic interactions) and the secondary, tertiary structure or spatial distribution of basic amino acid residues may also have an important impact on the interaction between these two biomolecules (Margalit et al., 1993; Bae et al., 1994; Hileman et al., 1998). The CS-protein binding is much more complex than the simple charge to charge interaction has also been supported by that the CS chains bearing the same charge to mass ratio are frequently observed to exhibit difference in binding specificity and affinity. For examples, nephronectin bound strongly to CS-E, but failed to bind to CS-D, although both CS-D and CS-E are carrying two sulfate groups per disaccharide unit (Sato et al., 2013); The FGF family also showed distinct

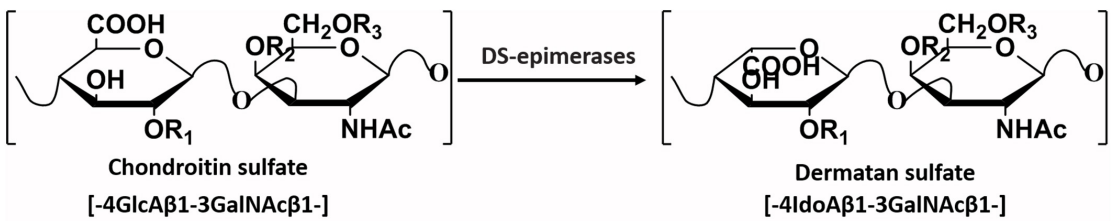


| Classification of CS/DS | Abundant disaccharide units | $R_1$ | $R_2$ | $R_3$ |
|---|---|---|---|---|
| CS-O/DS-O | O/iO unit | -H | -H | -H |
| CS-A/DS-A | A/iA unit | -H | $-SO_3H$ | -H |
| CS-C/DS-C | C/iC unit | -H | -H | $-SO_3H$ |
| CS-U/DS-U | U/iU unit | $-SO_3H$ | -H | -H |
| CS-B/DS-B | B/iB unit | $-SO_3H$ | $-SO_3H$ | -H |
| CS-D/DS-D | D/iD unit | $-SO_3H$ | -H | $-SO_3H$ |
| CS-E/DS-E | E/iE unit | -H | $-SO_3H$ | $-SO_3H$ |
| CS-T/DS-T | T/iT unit | $-SO_3H$ | $-SO_3H$ | $-SO_3H$ |

**FIGURE 1 |** The typical disaccharide units present in the backbone of the CS/DS chain. The major types of disaccharide units and sulfate group substitution positions that frequently exist in the CS/DS chains of different classifications are given.

affinities when binds to CS-D and CS-E, as the FGF3, 6, 8, and 22 bound strongly to CS-E, while the FGF5 bound moderately to CS-D (Asada et al., 2009). The binding between the CS and C-C motif chemokine ligand 5 (CCL5) was presented in **Figure 2** as an example. In addition to the basic BBXB binding motif, within the binding area of CS there are also hydrogen bonds, ionic bonds, and ring-stacking interaction that participate in the combination of the complex (Deshauer et al., 2015).

Characterization of the CS/DS-protein complex is of great significance for the design of more specifically targeted protein/GAG analogs and the subsequent development of more effective therapeutic drugs with fewer side effects. However, the structural motifs and interaction mechanisms between CS/DS and proteins are not fully understood due to the heterogeneity and complexity of CS/DS structures. The rapid development of analytical methods, including affinity approaches, mass spectrometry (MS), nuclear magnetic resonance (NMR), and computational approaches, makes it possible to study the GAG-protein complex with higher resolution, which will help in understanding the interaction mechanisms between CS/DS and various protein ligands and in the development of new treatment methods.

This review focuses on the interactions between CS/DS and proteins and their roles in human diseases. In addition, some classic and emerging GAG-protein interaction analysis tools and their applications in CS/DS-protein characterization are also discussed.

## HUMAN DISEASES RELATED TO CS/DS-PROTEIN INTERACTIONS

In the human body, CS/DS plays an important role in the physiological and pathological processes by interacting with a large number of proteins. The development of certain diseases is usually related to the imbalance of CS/DSPGs biosynthesis and changes in CS/DS chain structure. The major diseases that are related to the interaction between CS/DS and proteins are presented in **Figure 3**.

### Tumor Growth and Metastasis

Tumor-associated glycans and PGs play an important role in promoting the invasion and metastasis of malignant cells, participating in cell-cell and cell-ECM interactions, and promoting the adhesion and migration of tumor cells. In many tumor tissues, changes in the production level of PGs and the structure of GAG have been observed. Among PGs, the important role of HSPG in tumor adhesion, invasion, migration, proliferation and angiogenesis has been recognized for a long time (Afratis et al., 2012). In recent years, increasing evidence has shown that in addition to HSPGs, CS/DSPGs are also important regulatory molecules that affect tumor cell functions and phenotypes (Fuster and Esko, 2005). Versican and decorin are the main CSPGs that are overexpressed in the ECM of many malignant tumors, such as osteosarcoma, breast cancer, testicular

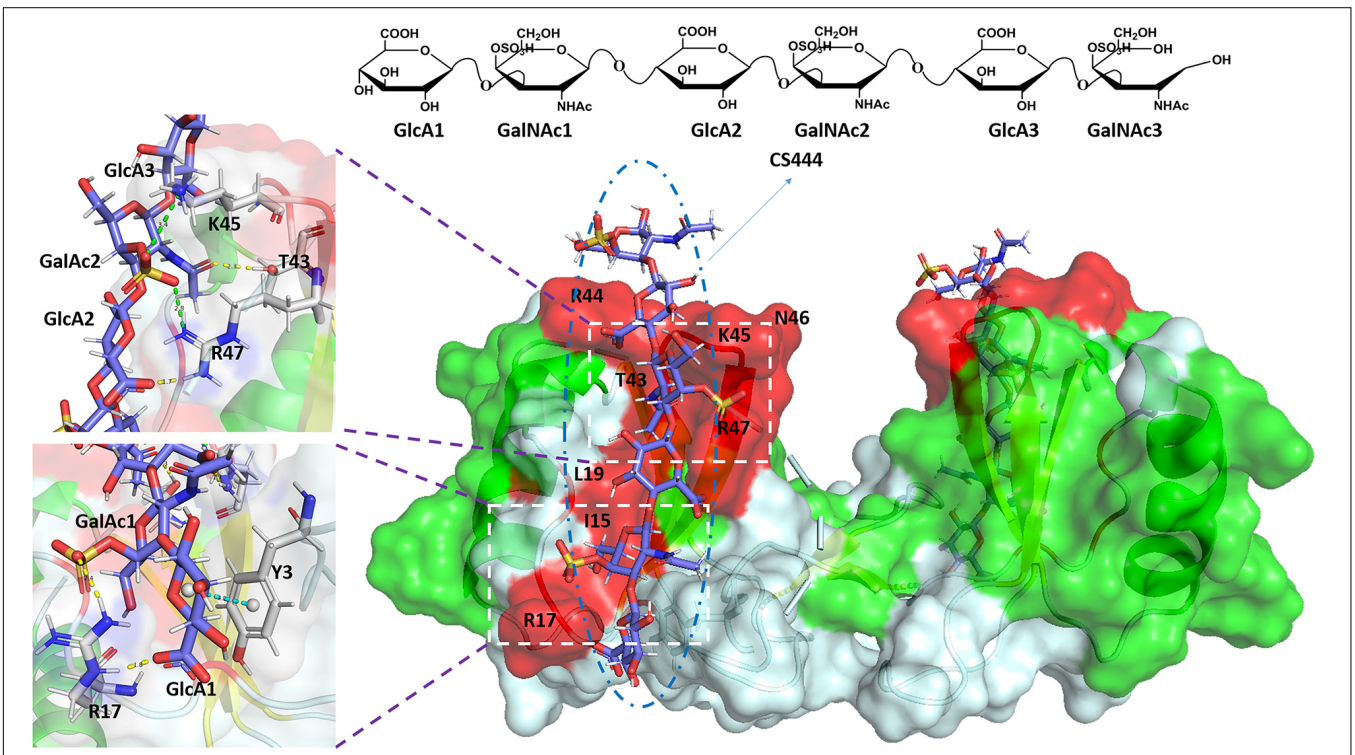


**FIGURE 2 |** Complex of CCL5 dimer and CS444. In the cartoon and surface hybrid model, the CS combined area is displayed in red. In the enlarged image, other non-covalent interactions are shown. The yellow dashed line represents hydrogen bonds, the green dashed line represents ionic bonds, and the blue dashed line represents ring-stacking interactions. The figure was prepared using the PDB file originally reported in the reference (Deshauer et al., 2015).

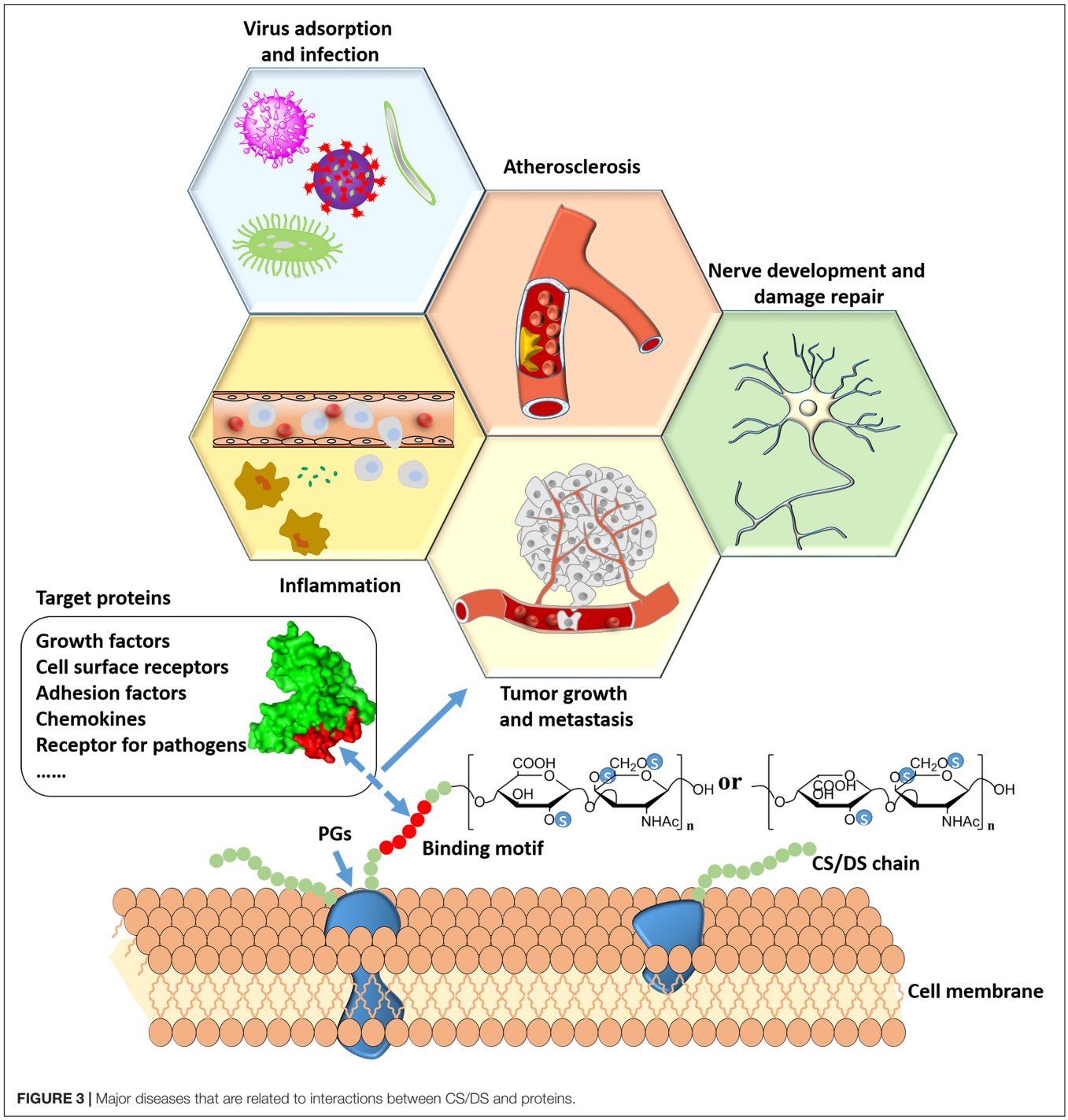


**FIGURE 3 |** Major diseases that are related to interactions between CS/DS and proteins.

cancer, colon cancer and pancreatic cancer (Labropoulou et al., 2006; Theocharis et al., 2006; Skandalis et al., 2011). Versican has been shown to induce the secretion of inflammatory factors by macrophages by activating the TLR2:TL6 complex, which can change the inflammatory microenvironment of tumors, thereby promoting tumor cell metastasis (Kim et al., 2009). Tumor cells spread to other organs through platelets. Studies have shown that CS/DS on the surface of breast cancer cells interacts with p-selectin ligands on endothelial cells and activated platelets, thereby promoting the spread of tumor cells (Cooney et al., 2011). The DS chain of endocan expressed in the capillaries of tumor tissues can bind to and activate HGF to promote tumor cell movement and proliferation (Delehedde et al., 2013).

The different sulfation patterns of the disaccharide repeating unit endow CS with different polyanionic properties, making CS have different biological activities. For example, the 6-*O*-sulfation of CS exhibited the dual role in the development, progression and metastasis of cancer. The monosulfated substitution provided

interaction surface for CS and influenced its binding to various cytokines and growth factors, cell surface receptors and other important proteins, which resulted in the complex role of CS/DS in tumor (Pudelko et al., 2019). In the case of disulfated CS, studies have shown that CS-E played a critical role in the tumorigenesis process. The ECM of ovarian cancer and adenocarcinoma cells can secrete excessive amounts of CS-E, which can combine with vascular endothelial growth factor (VEGF) to regulate VEGF signal transduction and CD44 molecular hydrolysis. Among them, VEGF can regulate the angiogenesis of tumor tissues, and the hydrolysis of CD44 molecules is beneficial to the metastasis of tumor cells, thereby enhancing the ability of tumor cells to metastasize (ten Dam et al., 2007; Sugahara et al., 2008). CS-E undergoes stronger binding to P-selectin on the surface of tumor cells and mediates signal transduction in the process of tumor metastasis. In addition, CS-E plays an important role in the migration of Lewis lung cancer cells by interacting with advanced glycation end products (RAGE) (Mizumoto et al., 2012). The specific changes in CS structures during tumorigenesis and development indicate their importance as potential biomarkers for cancer occurrence and for development and as therapeutic targets.

## Nerve Development and Damage Repair

CS is the GAG with the highest content in the matrix of the central nervous system (CNS), as CSPG accounts for about 20% of the total ECM of the CNS (Djerbal et al., 2017). Notably, many studies have shown that CSPG has a two-way function in the development of the nervous system. On the one hand, CSPG is involved in almost all processes of nervous system cell proliferation and differentiation, nerve migration, axon growth and synapse formation and stability, which is essential for the orderly development and maintenance of the nervous system (Mencio et al., 2021). The neural stem cell niche of embryonic and adult forebrain is rich in CS, which is essential for the development and maintenance of neural stem/progenitor cells mediated by FGF-2 (Sirko et al., 2010; Bian et al., 2011). Additionally, CSPGs can be combined with a variety of growth factors, such as midkine (MK), pleiotrophin (PTN), brain-derived neurotrophic factor (BDNF) and other neurotrophic factor family members, to regulate growth signal pathways and promote neuron growth (Rogers et al., 2011; Miller and Hsieh-Wilson, 2015). The CS on CSPGs can also be used as a guide for growth cones and promote the formation of neuron boundaries in the developing CNS (Dyck and Karimi-Abdolrezaee, 2015). On the other hand, CSPG is also involved in inhibiting the plasticity and regeneration of the adult CNS. CSPG is significantly upregulated in glial scar areas around CNS injuries such as those due to trauma and stroke, inhibits neuron growth and axon regeneration by binding to the receptor protein tyrosine phosphatases protein tyrosine phosphatase σ (RPTPσ) and LAR and to Nogo receptors (NgR1 and NgR3) (Brown et al., 2012; Griffith et al., 2017). In addition, neurocan (Ncan), as a CNS-specific CSPG, is involved in visual processing and top-down cognitive functions. Changes in Ncan are potential risk factors for bipolar disorder and schizophrenia (Schultz et al., 2014). Brevican (Bcan) is another specific CSPG of CNS. It not only participates in neuronal plasticity as a structural component, but is also considered to be related to CNS damage and Alzheimer's disease (Jang et al., 2020). The above studies show that the roles of CSPGs in the growth and development of the nervous system are extensive, complex, sometimes contradictory, and, of course, essential.

Currently, some *in vitro* studies have proven the specificity of the sulfation mode for some of the above processes. *In vitro* experiments have shown that CS-E and CS-D, which are rich in highly sulfated modifications, are very important for regulating the functions of CSPGs. They can interact with growth factors and inhibitory cell surface receptors (Miller and Hsieh-Wilson, 2015). For example, CS-D and CS-E can be combined with the growth factors MK and PTN to promote neuron growth, but CS-A and CS-C cannot (Deepa et al., 2002; Maeda et al., 2003). Moreover, CS-E can also participate in the inhibition of nerve damage repair by interacting with the cell surface receptors RPTPσ and NgRs (NgR1 and NgR3) (Dickendesher et al., 2012; Griffith et al., 2017). Therefore, further study of CS sulfation patterns in the nervous system and their interacting proteins will provide a molecular basis for the development of new therapies to promote neuronal growth and regeneration and CNS plasticity.

## Virus Adsorption and Infection

Most pathogens need to use GAG on the cell surface to promote their attachment and infect host cells, transfer from one cell to another, and evade host defense mechanisms. Many pathogenic microorganisms, such as viruses (e.g., dengue virus; Avirutnan et al., 2007), herpes simplex virus (HSV) (Uyama et al., 2006), vaccinia virus, and respiratory syncytial virus (RSV) (Klenk and Roberts, 2002), bacteria (e.g., *Borrelia burgdorferi*; Srinoulprasert et al., 2006) and fungi (e.g., Penicillium), can express proteins that bind to CS/DS on the cell surface, thereby promoting the infection of host cells.

The adsorption and invasion of many pathogens rely on CS/DS motifs with specific sulfation modification patterns on the host cell surface. The non-structural protein NS1 secreted by the dengue virus can bind to HS and CS-E on the surface of host cells and mediate the accumulation of NS1 on microvascular endothelial cells, leading to immune-mediated vascular damage and leakage (Avirutnan et al., 2007). Plasmodium invades erythrocytes and secretes the VAR2CSA protein. VAR2CSA can specifically bind to CS-A on the surface of vascular endothelial cells to make infected erythrocytes adhere to the blood vessel wall and cause falciparum malaria (Clausen et al., 2012; Rieger et al., 2015). HSV is a typical representative herpesvirus that can effectively bind to GAG and other receptors on the cell surface to infect host cells. Among HSV receptors, HS has been extensively studied, but there are also studies showing that CS-E is also important (Uyama et al., 2006). In addition, during the infection process of Penicillium, its conidia can adhere to CS-B and HS on the surface of epithelial cells to exert an infectious effect (Srinoulprasert et al., 2006). In short, these observations emphasize the biological significance of the interactions between CS/DS and pathogens in infectious diseases, which provides a theoretical basis for the development of antiviral drugs based on CS/DS.

## Atherosclerosis

Atherosclerosis (ATH) is a chronic, dynamic and evolving process that involves changes in the morphology and structure of arterial vessels, leading to the formation of atherosclerotic plaques, which ultimately leads to myocardial infarction or stroke (Scuruchi et al., 2020). PGs are considered essential molecules for maintaining vascular homeostasis, and changes in their regulation are key factors in the induction and development of ATH. The most representative vascular PGs are CSPGs and DS-containing DSPGs, such as versican, biglycan, and decorin. The deposition of low-density lipoprotein (LDL) in the arteries has been considered the initiating factor in the development of atherosclerosis. CSPGs significantly increase in early atherosclerotic lesions and play an important role in lipid retention, modification and final accumulation (Karangelis et al., 2010). Biglycan is considered the most likely to participate in the retention of lipids in the vascular intima because it can interact with apolipoprotein B (apoB) and high-density lipoprotein (HDL) (Scuruchi et al., 2020). In addition, decorin, which is a small CS/DSPG, interacts with type I collagen accumulated in atherosclerotic lesions and binds to LDL to enhance the retention of lipoproteins in the arterial wall (Pentikainen et al., 1997). There is also direct evidence that CS/DSPGs are involved in arteriosclerosis, the absence of chondroitin sulfate N-acetylgalactosaminyltransferase-2 can reduce lipoprotein retention in the early stage of atherosclerosis and reduce the migration of aortic smooth muscle cells (Adhikara et al., 2019). CSPG binds to lipoproteins mainly through its GAG chain. The accumulation of the LDL-GAG complex triggers a local inflammatory response to further promote the development of atherosclerosis (Nakashima et al., 2008).

The length of the CS chain and the sulfation modification mode are the main factors that affect the interaction between LDL and CSPG. The interaction between chondroitin-6-sulfate and LDL plays a vital role in atherosclerotic diseases. The increase in chondroitin-6-sulfate in early lesions of atherosclerosis leads to the accumulation, oxidation and hydrolysis of LDL and promotes the development of atherosclerosis (Karangelis et al., 2010; Cilpa et al., 2011).

## Other Diseases

In addition to the abovementioned physiological and pathological processes, CS/DS also plays a key regulatory role in inflammation, autoimmune diseases, genetic diseases, kidney diseases and other diseases. Studies have shown that CS/DSPGs promote the inflammatory response by binding immune receptors such as Toll-like receptors, selectin, CD44 and β1 integrin, which helps drive the development of traumatic brain/spinal cord injury and multiple sclerosis (Stephenson and Yong, 2018). The overexpression of chondroitin-6-sulfate in endothelial cells, which results in an imbalance of the chondroitin-6-sulfate and chondroitin-4-sulfate ratio, may be the main cause of chronic inflammatory diseases of the skin, such as skin lupus erythematosus and dermatomyositis (DM) (Kim and Werth, 2011). Defects in the core proteins of CS/DSPGs or mutations in CS/DS glycosyltransferases, epimerases, and sulfotransferases lead to a number of diseases, including congenital corneal stromal dystrophy, Meester-Loeys syndrome, and connective tissue diseases (Mizumoto et al., 2017; Kosho et al., 2019; Lautrup et al., 2020). The expression of CS/DS and DSPG is increased in a variety of fibrotic kidney diseases, including interstitial fibrosis, diabetic nephropathy, mesangial sclerosis and nephrosclerosis. Studies have shown that DSPGs regulate the formation of collagen fibrils in the body, so they play a role in kidney disease (Joladarashi et al., 2011; Lensen et al., 2015). In addition, CS/DS can also promote wound healing and improve osteoarthritis (Islam et al., 2020).

As mentioned above, CS/DS plays an important regulatory role in many physiological and pathological processes. An accurate understanding of the CS/DS mechanism in these processes will help in developing CS/DS-based polysaccharide drugs, along with new therapies and applications. The rapid progress of analytical methods will promote the decryption of the molecular basis of CS/DS-protein interactions. The following section will introduce the analytical methods used for characterizing GAG-protein interactions in recent years and their applications in CS/DS-proteins.

# ANALYTICAL TOOLS AND APPROACHES FOR CHARACTERIZATION OF GAG-PROTEIN INTERACTIONS

At present, many analytical methods for revealing the molecular mechanism and binding motifs of GAG-protein complexes have been developed, including affinity methods, MS, NMR, and computational approaches. The following reviews the progress and applications of various analytical methods in the analysis of CS/DS-protein complexes. Modern analytical tools that can be used to characterize the binding between CS/DS and proteins are categorized into different groups based on their purposes and summarized in **Figure 4**.

## Affinity Approaches

Many affinity-based analytical techniques and tools are used to explore the role of biomolecular interactions in physiological and pathological phenomena, including affinity chromatography, gel mobility shift assays (GMSA), isothermal titration calorimetry (ITC), biosensor-based surface plasmon resonance (SPR), biolayer interferometry (BLI), and quartz crystal microbalance (QCM) techniques. In research in recent decades, the above methods have not only been used to prove interactions between GAGs and proteins but have also been used to screen the interacting sequences of GAGs and proteins.

### Affinity Chromatography

Affinity chromatography is a method used to separate interesting GAGs or interesting proteins from a mixture based on the highly specific macromolecular binding between GAG and the target protein. This method generally involves coupling interesting proteins or interesting GAGs to agarose and coating them onto affinity columns (Maimone and Tollefsen, 1990; Tollefsen, 1992; Barkalow and Schwarzbauer, 1994). Binding is usually carried

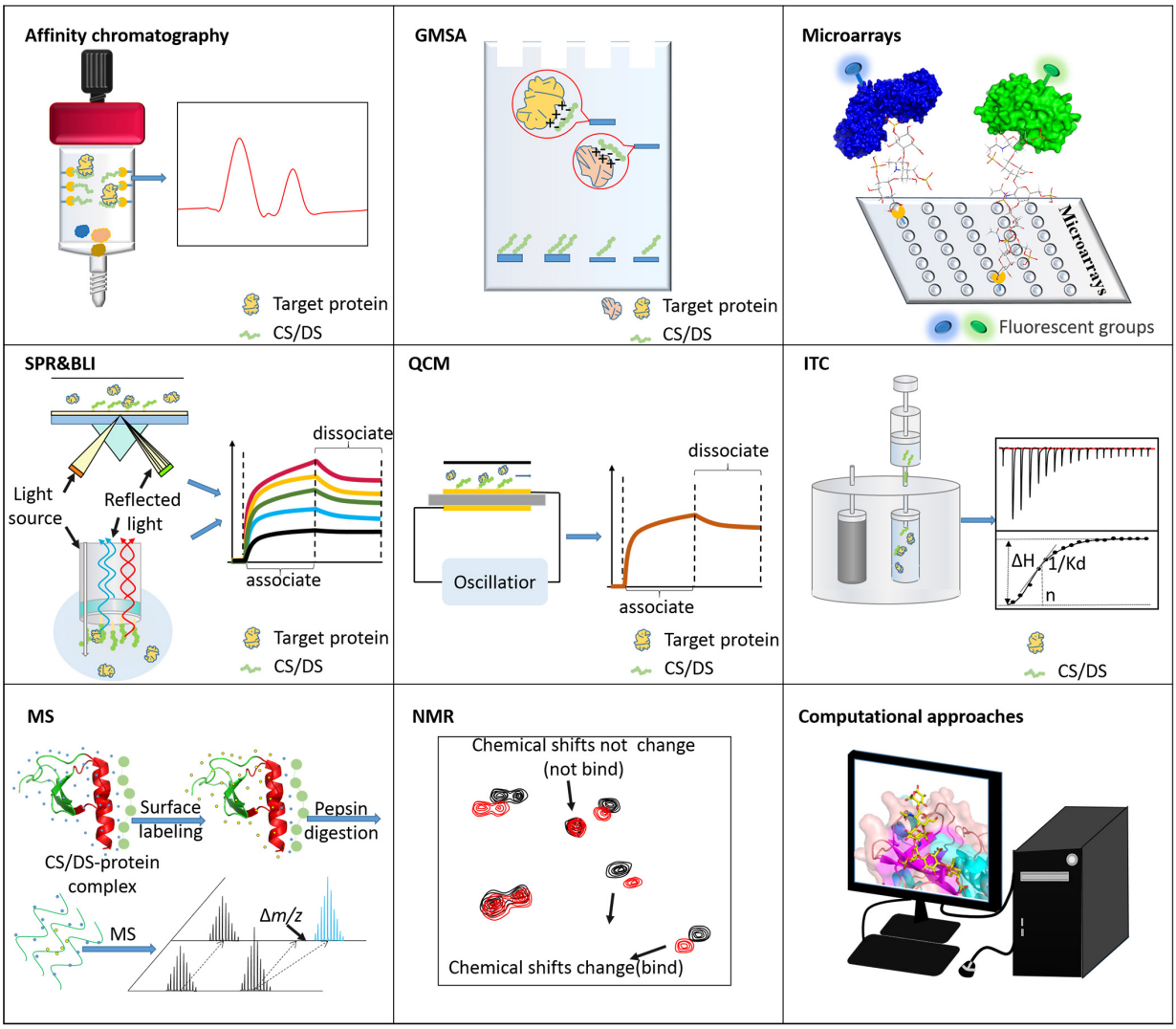


**FIGURE 4 |** Tools for analyzing CS/DS-protein interactions. Affinity chromatography is usually used to isolate binding molecules or fragments. GMSA and microarrays are used to screen the CS/DS or proteins that bind to each other. ITC, SPR, BLI, and QCM can measure the binding strength between CS/DS and proteins. MS and NMR are applied to characterize the structure/sequence of binding motifs. Computational approaches are powerful for simulating the binding postures of these two types of biomolecules.

out under physiological conditions, and then the target binding substance is eluted with increasing NaCl concentrations. GAGs are usually depolymerized into oligosaccharides to determine the binding domain of GAGs. For example, through affinity chromatography, Maimone and Tollefsen (1990) screened the DS hexasaccharide [IdoA(2S)-GalNAc(4S)-IdoA(2S)-GalNAc(4S)-IdoA(2S)-ATalR(4S)] with high affinity to heparin cofactor II (HCII). Bao et al. (2005) determined that under physiological salt concentrations, octasaccharide is the smallest CS/DS oligosaccharide that can interact with PTN. Similarly, site-directed amino acid mutations can identify key protein binding sites (Bao et al., 2005). In addition, based on the specific interactions of GAG-proteins, affinity chromatography also separates target proteins. Liangsupree et al. (2019) used immobilized chondroitin-6-sulfate to quickly separate plasma LDL. Toledo et al. (2020) used immobilized VAR2CSA to screen CSPGs that can interact with it. However, due to its inherent low resolution, elucidating of the GAG binding domain obtained by affinity chromatography often requires further separation and characterization.

## GMSA

GMSA can show different electrophoretic mobility rates according to the size of the analyte molecule and the nature and size of the charge. It has been successfully applied to the interaction between GAG and proteins. Generally, AMAC is used to label the reducing end of GAG, and the offset of the GAG-protein complex band and the free GAG band is displayed by fluorescence irradiation to determine the binding affinity (Lyon et al., 2004). GMSA can simultaneously

compare the relative protein affinities/selectivities of different oligosaccharides. Deakin et al. (2009) revealed that the binding of HGF/scatter factor (SF) to GAG depends on the degree of sulfation and not the position of sulfation. In addition, GMSA can also be used to measure protein binding sites. Boren et al. (1998) conducted a site-directed mutagenesis experiment and identified the basic amino acid whose interaction site between LDL and chondroitin-4-sulfate is located between residues 3,359 and 3,369.

## ITC

ITC can directly obtain the enthalpy, entropy, free energy (binding constant), and stoichiometry in a single analysis. The binding constant can reflect the binding ability of two molecules, so ITC is also used for GAG-protein interaction analysis. To verify the structure of the interaction between CS-A and the VAR2CSA protein, which is a member of the erythrocyte membrane protein-1 family of *Plasmodium falciparum*, Singh et al. (2008). mutated Lys1507 and Lys1510 in the domain DBL3X to Ala, and the results of ITC analysis showed that their binding to CSA was significantly weakened, thus proving the binding site of CS-A on VAR2CSA. This work provides a new target for the development of a malaria vaccine (Singh et al., 2008). ITC can also be used to characterize GAG binding motif characteristics. Nguyen et al. (2019) used ITC to characterize the interactions between heparin oligosaccharides of different lengths and interleukin (IL)-12 when studying the molecular mechanism by which heparin induces and regulates the biological activity of human interleukin-12. The results showed that only heparin molecules longer than octasaccharide could enhance the activity of IL-12, and the more sulfate groups there were, the stronger the interaction (Nguyen et al., 2019).

## SPR, BLI, and QCM

SPR can directly and quantitatively analyze unlabeled molecular interactions in real time and has been successfully used for the biophysical characterization of glycosaminoglycan (GAG) protein interactions. BLI is an SPR alternative technology developed later with a higher throughput and flexibility. As an example of a study detecting the binding motif of GAG, Zhang et al. (2015) used heparin biosensors to map the interactions between tissue inhibitor of metalloproteinases-3 (TIMP-3) and heparin and other GAGs via surface plasmonic resonance spectroscopy. The results show that TIMP-3 is a heparin-binding protein. The competition surface plasmon resonance results show that the interaction between TIMP-3 and heparin is chain length-dependent, in which *N*-sulfo and 6-*O*-sulfo groups play a key role in the interaction. Of the other GAGs, only CS-E and CS-B exhibit strong combination with TIMP-3 (Zhang et al., 2015). In the binding motif of the detection protein, to further understand the potential of *Borrelia burgdorferi* surface-localized membrane protein 1 (Lmp1)-interacting host molecule and the Lmp1 region that may participate in this interaction, Yang et al. (2016) placed a variety of host extracellular ligands on the chip and flowed the three discrete domains (Lmp1N, Lmp1 M, and Lmp1C) of recombinant Lmp 1 through the chip. The SPR results show that Lmp1 M interacts with chondroitin-6-sulfate and promotes the adhesion of Lmp 1 to host cells (Yang et al., 2016).

Different from SPR and BLI, QCM is an acoustic biosensor that uses the piezoelectric effect. The number of molecules bound on the surface determines the frequency of the QCM crystal, so the kinetic rate constant [association ($k_a$) and dissociation ($k_d$) rate constants] and affinity between the ligand and the analyte can be evaluated. Therefore, QCM has also been successfully used to characterize the interaction between GAGs and proteins. D'Ulivo et al. (2010) used QCM to study the interaction between LDL and chondroitin-6-sulfate. Three peptides involved in the interaction with glycosaminoglycans were selected from apo-B and fixed to polystyrene and carboxyl sensor chips. Chondroitin-6-sulfate was injected as an analyte on the peptide coating surface, and the estimated dissociation constant indicated that the interaction occurred through the positive residues lysine and arginine of ApoB-100 (D'Ulivo et al., 2010).

## Microarrays

The high sensitivity and high throughput has made glycan microarray a core technology for analyzing GAG-mediated biological events. It is suitable for comparing binding strengths between ligand oligosaccharides and searching for specific oligosaccharide ligands (Yamaguchi et al., 2006). The key step in the construction of glycan microarrays is to immobilize glycans on the solid phase by non-covalent or covalent methods. Of course, many immobilization methods have been discussed (Palma et al., 2014; Song et al., 2015; Gao et al., 2019). Some of the GAGs used for glycan microarrays are characteristic oligosaccharides prepared by enzymatic hydrolysis or chemical desulfurization of natural GAG. Yamaguchi et al. (2006) used chondroitinase ACI to degrade DS into a series of oligosaccharides to prepare neoglycolipid microarrays and studied the interactions with HGF/SF, RANTES, KGF/FGF-7 and HCII. The results show that HGF/SF, KGF/FGF-7 and HCII can preferentially bind to DS oligosaccharide fragments longer than 8-mers, while the binding of RANTES depends on the strength of the charge (Yamaguchi et al., 2006). Shipp and Hsieh-Wilson desulfurized natural sources of HP and CS at different positions to prepare oligosaccharide microarrays interacting with various growth factors, proving that members of the FGF family and various axon guide proteins have obvious vulcanization preferences (Shipp and Hsieh-Wilson, 2007). Other GAGs used to construct glycan microarrays come from chemical or enzymatic synthesis, which greatly increases the number of glycans available for analysis in glycan microarrays. Tully et al. (2006) reported the first example of synthesizing CS microarrays and identified the interaction between CS-E and tumor necrosis factor-α (TNF-α) for the first time. Chemical-enzymatic synthesis promotes the efficient preparation of glycans with specific lengths and sulfation patterns, for example, three homogeneous CS-E oligosaccharides, including CS-E heptasaccharide, CS-E tridecasaccharide and CS-E non-adecasaccharide, have been produced recently (Li et al., 2020). Adoption of these chemically-enzymatically synthesized CS structures into glycan microarray will help to expand its potential to reveal more GAG-mediated biological events.

## MS

MS techniques have been maturely applied to GAG sequence mapping, protein epitope mapping and GAG binding protein structural characterization due to their high sensitivity, tolerance to low-purity samples, and ability to characterize single amino acid/sugar residues and modifications. In recent years, the MS methods used to characterize GAG-protein complexes have mainly included surface-labeling MS, cross-linking MS, ion mobility (IM) MS, and the recently emerged native MS. Among them, surface-labeling MS, which is more mature, is used to characterize the CS/DS-protein case. The principle of surface labeling is that chemical probes preferentially modify the parts of biomolecules exposed to the solvent, and the amino acids buried in the folded protein core or interacting proteins are not labeled. Then, proteolysis and LC/MS/MS are used to monitor the labeling site and degree of the protein (Lossl et al., 2016). According to different labeling methods, surface labels can be divided into covalent labels and non-covalent labels. Hydroxyl radical footprinting (HRF) uses hydroxyl radicals to rapidly oxidize amino acid side chains (Maleknia and Downard, 2014), which is a covalent labeling method for characterizing GAG-protein complexes. Wang K. et al. (2020) used hydroxyl radical HRF to characterize the binding sites between CS and the protein VAR2CSA expressed by the parasite. Hydroxyl radicals were used to rapidly oxidize the recombinantly expressed DBL1-ID2 protein with and without CS. After treatment with chymotrypsin, LC-MS/MS was used to compare the oxidation differences of each peptide. Finally, it was found that the peptide with the largest redox is peptide 543-558, which proves that the surface of the DBL2 and Hb1 groove acts as a CS binding region (Wang K. et al., 2020). The irradiation conditions of HRF must be carefully controlled to avoid secondary modification of the protein. Hydrogen-deuterium exchange (HDX) on the peptide backbone is a method to characterize the non-covalent labeling of protein-ligand complexes (Gallagher and Hudgens, 2016). The protein-ligand interaction changes the HDX rate of protein in deuterium water, which can provide rich information about the dynamic structure of protein-ligand complexes, including GAG-protein complexes. Tommy Hofmann performed a HDX experiment with IL-8 with and without CS. Through MS detection, the H/D exchange information of the entire IL-8 sequence was obtained. In the presence of CS, a significant reduction in H/D exchange was observed in the C-terminal α-helix region (containing amino acids 70–77) and loop (containing amino acids 27–29), which is the binding site of CS (Hofmann et al., 2015). HDX-MS analyzes GAG-protein complexes at the physiological pH, temperature and salt concentration, so it is a very promising technique for characterizing GAG-protein interactions.

## NMR

NMR is one of the most commonly used and valuable analytical methods for studying GAG-protein interactions. Commonly used NMR methods include chemical shift perturbation (CSP), saturation transfer difference (STD), and the transferred nuclear Overhauser effect (trNOE) (Pomin and Wang, 2018). The essence of the CSP method is to identify GAG-binding residues by assuming that when GAG is in contact with a protein, the atoms belonging to GAG-binding residues will show greater changes in chemical shifts. The atomic chemical shift of proteins is usually obtained by $^{15}$N-edited heteronuclear single quantum coherence ($^{15}$N-HSQC) spectra of $^{15}$N-labeled proteins titrated with different GAG oligosaccharide concentrations (Pomin, 2014). Based on this method, Deshauer et al. (2015) studied the interaction of the chemokine CCL5 with medium-sized CS. The $^{15}$N-HSQC spectrum of CS titration showed that in addition to the BBXB motif in the 40 s loop, the CCL5 dimer also has a CS binding epitope located in the N loop, including the R17, L19 and I15 residues (Deshauer et al., 2015). By comparing the NMR spectra of the saturated state (on-resonance) and unsaturated state (off-resonance) of the interaction between the protein and the ligand in the solution (Vignovich and Pomin, 2020), the STD method can determine how GAG binds to protein during the formation of the GAG-protein complex. Yu et al. (2014) used saturated STD NMR to characterize the interaction of a synthesized heparin octasaccharide with FGF-2 and FGF-10. According to the STD value, the octasaccharide chain contained 2-*O*-sulfate and *N*- sulfate groups that participated in the binding of FGF-2, while 2-*O*-sulfate and 6-*O*-sulfate specifically participated in the binding of FGF-10 (Yu et al., 2014). The trNOE NMR method can provide information about the conformational changes of GAG oligosaccharides when interacting with proteins by identifying the changes in the NOE signal in the ligand molecule induced by the protein. Kunze et al. (2014) used the trNOE NMR method to study the binding of heparin tetrasaccharide (ΔUA2S-GlcNS6S-IdoA2S-GlcNS6S) and IL-10. The NOESY and ROESY profiles show that in the absence of IL-10, the NOE/ROE signal of the GAG ligand is close to zero. When IL-10 is present, in addition to a single positive NOE between H2 and H3 of the non-reduced terminal disaccharide GlCNS6s, several strongly negative NOEs were observed in heparin tetroglycosis, suggesting an appropriate molecular interaction between IL-10 and heparin (Kunze et al., 2014). Additional cases of using CSP, STD, and trNOE analysis to determine the protein binding motifs of GAG-protein complexes have been reported by other groups (Bechara et al., 2013; Mobius et al., 2013; Gao et al., 2018; Penk et al., 2019). NMR is an irreplaceable technique for the analysis of GAG-protein complexes. However, NMR requires highly skilled operators, and relatively low sensitivity is the main disadvantage of NMR.

## Computational Approaches

The complexity and heterogeneity of natural GAGs limit the in-depth study of the structure of GAG-protein interactions using various analytical tools. The latest developments in computational tools and technologies have made significant progress in the field of GAG modeling, and as an alternative strategy, they have promoted the study of GAG-protein interactions. Of course, various calculation methods and techniques have been discussed (Almond, 2018; Sankaranarayanan et al., 2018). Raghuraman et al. (2006) developed a CVLS method using the genetic algorithm-based automatic docking program GOLD and built up a heparin library consisting of a total of 6,859 unique heparin hexasaccharide

sequences. Based on this method, several high-affinity and high-specificity heparin sequences were identified by AT recognition, and the binding mode of heparin pentasaccharide was accurately predicted (Raghuraman et al., 2006). Later, they applied CVLS to the DS-HCII system and screened 16 highly specific hexasaccharides from among 192 possible DS hexasaccharide topologies. Among them, 13 topologies were predicted to bind to the heparin binding site of HCII in a new binding mode at a 60-degree angle relative to the D helix (Raghuraman et al., 2010). The above prediction results based on CVLS are consistent with existing experimental data. Rogers et al. (2011) combined the carbohydrate microarray method with computational modeling to clarify the CS-E-neurotrophin (NT)-tyrosine receptor kinase (Trk) interaction. A continuous CS-E binding site spans the NT-Trk complex, which provides a potential mechanism explaining how CS regulates the formation of the complex and the NT signaling pathway. Later, cell experiments proved that CS plays an active role in cell signal transduction by regulating the NT-Trk interaction (Rogers et al., 2011). The GAG-Dock method successfully predicted the binding modes and sites of CS-A, CS-D, CS-E and heparin hexasaccharide to the axon growth-related protein RPTPσ and Nogo receptor. Among these interactions, it is predicted that when heparin participates in the binding of RPTPσ, multiple sulfate groups are exposed to the solvent, which can bind to other RPTPσ, and all the sulfate groups of CS-E point to the GAG binding site of RPTPσ, which explains the opposite effect of CS-E and heparin on neurite growth when interacting with RPTPσ (Griffith et al., 2017). Of course, the use of computational tools to predict the GAG-protein binding mode and site has been adopted by an increasing number of research groups (Pichert et al., 2012; Namachivayam et al., 2015; Ryan et al., 2016). In fact, various computing tools and websites have been developed to make the operation simple, and non-computational researchers can also perform calculation predictions (Sankaranarayanan et al., 2018).

## CONCLUSION AND REMARKS

Similar to other GAGs, CS/DS is involved in a large number of biological processes. In the body, CS/DS directly or indirectly participates in a variety of physiological and pathological processes by interacting with a variety of protein ligands, such as growth factors, cell surface receptors, and adhesion molecules. The characterization of a wide range of CS/DS-protein interactions is essential for mapping the biological functions of CS/DS and finding new therapies that target specific CS/DS-protein interactions. Due to the complexity and heterogeneity of the CS/DS structure, the molecular basis of most CS/DS-protein interactions is still unclear. The rapid development of multiple analytical tools and analytical methods will facilitate uncovering more of the mystery behind CS/DS-protein interactions and provide a template for the development of novel therapeutics based on CS/DS-protein interactions.

## AUTHOR CONTRIBUTIONS

Both authors contributed to the article and approved the submitted version.

## FUNDING

This study was supported by the National Natural Science Foundation of China (21877072) and the Natural Science Foundation of Shandong Province (ZR2019MB014).

## REFERENCES

Adhikara, I. M., Yagi, K., Mayasari, D. S., Ikeda, K., Kitagawa, H., Miyata, O., et al. (2019). Chondroitin sulfate N-acetylgalactosaminyltransferase-2 deletion alleviates lipoprotein retention in early atherosclerosis and attenuates aortic smooth muscle cell migration. *Biochem. Biophys. Res. Commun.* 509, 89–95. doi: 10.1016/j.bbrc.2018.12.068

Afratis, N., Gialeli, C., Nikitovic, D., Tsegenidis, T., Karousou, E., Theocharis, A. D., et al. (2012). Glycosaminoglycans: key players in cancer cell biology and treatment. *FEBS J.* 279, 1177–1197. doi: 10.1111/j.1742-4658.2012.08529.x

Almond, A. (2018). Multiscale modeling of glycosaminoglycan structure and dynamics: current methods and challenges. *Curr. Opin. Struct. Biol.* 50, 58–64. doi: 10.1016/j.sbi.2017.11.008

Aquino, R. S., and Park, P. W. (2016). Glycosaminoglycans and infection. *Front. Biosci.* 21, 1260–1277. doi: 10.2741/4455

Asada, M., Shinomiya, M., Suzuki, M., Honda, E., Sugimoto, R., Ikekita, M., et al. (2009). Glycosaminoglycan affinity of the complete fibroblast growth factor family. *Biochim. Biophys. Acta* 1790, 40–48. doi: 10.1016/j.bbagen.2008.09.001

Avirutnan, P., Zhang, L., Punyadee, N., Manuyakorn, A., Puttikhunt, C., Kasinrerk, W., et al. (2007). Secreted NS1 of dengue virus attaches to the surface of cells via interactions with heparan sulfate and chondroitin sulfate E. *PLoS Pathog.* 3:e183. doi: 10.1371/journal.ppat.0030183

Avram, S., Shaposhnikov, S., Buiu, C., and Mernea, M. (2014). Chondroitin sulfate proteoglycans: structure-function relationship with implication in neural development and brain disorders. *Biomed. Res. Int.* 2014:642798. doi: 10.1155/2014/642798

Bae, J., Desai, U. R., Pervin, A., Caldwell, E. E., Weiler, J. M., and Linhardt, R. J. (1994). Interaction of heparin with synthetic antithrombin III peptide analogues. *Biochem. J.* 301(Pt 1), 121–129. doi: 10.1042/bj3010121

Bao, X., Muramatsu, T., and Sugahara, K. (2005). Demonstration of the pleiotrophin-binding oligosaccharide sequences isolated from chondroitin sulfate/dermatan sulfate hybrid chains of embryonic pig brains. *J. Biol. Chem.* 280, 35318–35328. doi: 10.1074/jbc.M507304200

Barkalow, F. J., and Schwarzbauer, J. E. (1994). Interactions between fibronectin and chondroitin sulfate are modulated by molecular context. *J. Biol. Chem.* 269, 3957–3962. doi: 10.1016/s0021-9258(17)41727-3

Bechara, C., Pallerla, M., Zaltsman, Y., Burlina, F., Alves, I. D., Lequin, O., et al. (2013). Tryptophan within basic peptide sequences triggers glycosaminoglycan-dependent endocytosis. *FASEB J.* 27, 738–749. doi: 10.1096/fj.12-216176

Bian, S., Akyuz, N., Bernreuther, C., Loers, G., Laczynska, E., Jakovcevski, I., et al. (2011). Dermatan sulfotransferase Chst14/D4st1, but not chondroitin sulfotransferase Chst11/C4st1, regulates proliferation and neurogenesis of neural progenitor cells. *J. Cell Sci.* 124(Pt 23), 4051–4063. doi: 10.1242/jcs.088120

Boren, J., Olin, K., Lee, I., Chait, A., Wight, T. N., and Innerarity, T. L. (1998). Identification of the principal proteoglycan-binding site in LDL. A single-point mutation in apo-B100 severely affects proteoglycan interaction without affecting LDL receptor binding. *J. Clin. Invest.* 101, 2658–2664. doi: 10.1172/JCI2265

Brown, J. M., Xia, J., Zhuang, B., Cho, K. S., Rogers, C. J., Gama, C. I., et al. (2012). A sulfated carbohydrate epitope inhibits axon regeneration after injury. *Proc. Natl. Acad. Sci. U.S.A.* 109, 4768–4773. doi: 10.1073/pnas.1121318109

Cardin, A. D., and Weintraub, H. J. (1989). Molecular modeling of protein-glycosaminoglycan interactions. *Arteriosclerosis* 9, 21–32. doi: 10.1161/01.atv.9.1.21

Cilpa, G., Koivuniemi, A., Hyvonen, M. T., and Riekkola, M. L. (2011). A molecular dynamics approach for the association of apolipoproteinB-100 and chondroitin-6-sulfate. *J. Phys. Chem. B* 115, 4818–4825. doi: 10.1021/jp110987r

Clausen, T. M., Christoffersen, S., Dahlback, M., Langkilde, A. E., Jensen, K. E., Resende, M., et al. (2012). Structural and functional insight into how the *Plasmodium falciparum* VAR2CSA protein mediates binding to chondroitin sulfate A in placental malaria. *J. Biol. Chem.* 287, 23332–23345. doi: 10.1074/jbc.M112.348839

Cooney, C. A., Jousheghany, F., Yao-Borengasser, A., Phanavanh, B., Gomes, T., Kieber-Emmons, A. M., et al. (2011). Chondroitin sulfates play a major role in breast cancer metastasis: a role for CSPG4 and CHST11 gene expression in forming surface P-selectin ligands in aggressive breast cancer cells. *Breast Cancer Res.* 13:R58. doi: 10.1186/bcr2895

Deakin, J. A., Blaum, B. S., Gallagher, J. T., Uhrin, D., and Lyon, M. (2009). The binding properties of minimal oligosaccharides reveal a common heparan sulfate/dermatan sulfate-binding site in hepatocyte growth factor/scatter factor that can accommodate a wide variety of sulfation patterns. *J. Biol. Chem.* 284, 6311–6321. doi: 10.1074/jbc.M807671200

Deepa, S. S., Umehara, Y., Higashiyama, S., Itoh, N., and Sugahara, K. (2002). Specific molecular interactions of oversulfated chondroitin sulfate E with various heparin-binding growth factors. Implications as a physiological binding partner in the brain and other tissues. *J. Biol. Chem.* 277, 43707–43716. doi: 10.1074/jbc.M207105200

Delehedde, M., Devenyns, L., Maurage, C. A., and Vives, R. R. (2013). Endocan in cancers: a lesson from a circulating dermatan sulfate proteoglycan. *Int. J. Cell Biol.* 2013:705027. doi: 10.1155/2013/705027

Deshauer, C., Morgan, A. M., Ryan, E. O., Handel, T. M., Prestegard, J. H., and Wang, X. (2015). Interactions of the chemokine CCL5/RANTES with medium-sized chondroitin sulfate ligands. *Structure* 23, 1066–1077. doi: 10.1016/j.str.2015.03.024

Dickendesher, T. L., Baldwin, K. T., Mironova, Y. A., Koriyama, Y., Raiker, S. J., Askew, K. L., et al. (2012). NgR1 and NgR3 are receptors for chondroitin sulfate proteoglycans. *Nat. Neurosci.* 15, 703–712. doi: 10.1038/nn.3070

Djerbal, L., Lortat-Jacob, H., and Kwok, J. (2017). Chondroitin sulfates and their binding molecules in the central nervous system. *Glycoconj. J.* 34, 363–376. doi: 10.1007/s10719-017-9761-z

D'Ulivo, L., Saint-Guirons, J., Ingemarsson, B., and Riekkola, M. L. (2010). Quartz crystal microbalance, a valuable tool for elucidation of interactions between apoB-100 peptides and extracellular matrix components. *Anal. Bioanal. Chem.* 396, 1373–1380. doi: 10.1007/s00216-009-3371-y

Dyck, S. M., and Karimi-Abdolrezaee, S. (2015). Chondroitin sulfate proteoglycans: key modulators in the developing and pathologic central nervous system. *Exp. Neurol.* 269, 169–187. doi: 10.1016/j.expneurol.2015.04.006

Fuster, M. M., and Esko, J. D. (2005). The sweet and sour of cancer: glycans as novel therapeutic targets. *Nat. Rev. Cancer* 5, 526–542. doi: 10.1038/nrc1649

Gallagher, E. S., and Hudgens, J. W. (2016). Mapping protein-ligand interactions with proteolytic fragmentation, hydrogen/deuterium exchange-mass spectrometry. *Methods Enzymol.* 566, 357–404. doi: 10.1016/bs.mie.2015.08.010

Gao, C., Wei, M., McKitrick, T. R., McQuillan, A. M., Heimburg-Molinaro, J., and Cummings, R. D. (2019). Glycan microarrays as chemical tools for identifying glycan recognition by immune proteins. *Front. Chem.* 7:833. doi: 10.3389/fchem.2019.00833

Gao, Q., Yang, J. Y., Moremen, K. W., Flanagan, J. G., and Prestegard, J. H. (2018). Structural characterization of a heparan sulfate pentamer interacting with LAR-Ig1-2. *Biochemistry* 57, 2189–2199. doi: 10.1021/acs.biochem.8b00241

Griffith, A. R., Rogers, C. J., Miller, G. M., Abrol, R., Hsieh-Wilson, L. C., and Goddard, W. A. III (2017). Predicting glycosaminoglycan surface protein interactions and implications for studying axonal growth. *Proc. Natl. Acad. Sci. U.S.A.* 114, 13697–13702. doi: 10.1073/pnas.1715093115

Hileman, R. E., Jennings, R. N., and Linhardt, R. J. (1998). Thermodynamic analysis of the heparin interaction with a basic cyclic peptide using isothermal titration calorimetry. *Biochemistry* 37, 15231–15237. doi: 10.1021/bi980212x

Hofmann, T., Samsonov, S. A., Pichert, A., Lemmnitzer, K., Schiller, J., Huster, D., et al. (2015). Structural analysis of the interleukin-8/glycosaminoglycan interactions by amide hydrogen/deuterium exchange mass spectrometry. *Methods* 89, 45–53. doi: 10.1016/j.ymeth.2015.02.011

Islam, S., Chuensirikulchai, K., Khummuang, S., Keratibumrungpong, T., Kongtawelert, P., Kasinrerk, W., et al. (2020). Accumulation of versican facilitates wound healing: implication of its initial ADAMTS-cleavage site. *Matrix Biol.* 87, 77–93. doi: 10.1016/j.matbio.2019.10.006

Jang, D. G., Sim, H. J., Song, E. K., Kwon, T., and Park, T. J. (2020). Extracellular matrixes and neuroinflammation. *BMB Rep.* 53, 491–499. doi: 10.5483/BMBRep.2020.53.10.156

Joladarashi, D., Salimath, P. V., and Chilkunda, N. D. (2011). Diabetes results in structural alteration of chondroitin sulfate/dermatan sulfate in the rat kidney: effects on the binding to extracellular matrix components. *Glycobiology* 21, 960–972. doi: 10.1093/glycob/cwr029

Karangelis, D. E., Kanakis, I., Asimakopoulou, A. P., Karousou, E., Passi, A., Theocharis, A. D., et al. (2010). Glycosaminoglycans as key molecules in atherosclerosis: the role of versican and hyaluronan. *Curr. Med. Chem.* 17, 4018–4026. doi: 10.2174/092986710793205354

Kim, J. S., and Werth, V. P. (2011). Identification of specific chondroitin sulfate species in cutaneous autoimmune disease. *J. Histochem. Cytochem.* 59, 780–790. doi: 10.1369/0022155411411304

Kim, S., Takahashi, H., Lin, W. W., Descargues, P., Grivennikov, S., Kim, Y., et al. (2009). Carcinoma-produced factors activate myeloid cells through TLR2 to stimulate metastasis. *Nature* 457, 102–106. doi: 10.1038/nature07623

Klenk, K., and Roberts, S. R. (2002). Use of a vesicular stomatitis virus complementation system to analyze respiratory syncytial virus binding. *Virus Res.* 90, 327–335. doi: 10.1016/S0168-1702(02)00250-2

Knutson, J. R., Iida, J., Fields, G. B., and McCarthy, J. B. (1996). CD44/chondroitin sulfate proteoglycan and alpha 2 beta 1 integrin mediate human melanoma cell migration on type IV collagen and invasion of basement membranes. *Mol. Biol. Cell* 7, 383–396. doi: 10.1091/mbc.7.3.383

Kosho, T., Mizumoto, S., Watanabe, T., Yoshizawa, T., Miyake, N., and Yamada, S. (2019). Recent advances in the pathophysiology of musculocontractural Ehlers-Danlos syndrome. *Genes* 11:43. doi: 10.3390/genes11010043

Kunze, G., Gehrcke, J. P., Pisabarro, M. T., and Huster, D. (2014). NMR characterization of the binding properties and conformation of glycosaminoglycans interacting with interleukin-10. *Glycobiology* 24, 1036–1049. doi: 10.1093/glycob/cwu069

Labropoulou, V. T., Theocharis, A. D., Ravazoula, P., Perimenis, P., Hjerpe, A., Karamanos, N. K., et al. (2006). Versican but not decorin accumulation is related to metastatic potential and neovascularization in testicular germ cell tumours. *Histopathology* 49, 582–593. doi: 10.1111/j.1365-2559.2006.02558.x

Lautrup, C. K., Teik, K. W., Unzaki, A., Mizumoto, S., Syx, D., Sin, H. H., et al. (2020). Delineation of musculocontractural Ehlers-Danlos syndrome caused by dermatan sulfate epimerase deficiency. *Mol. Genet. Genomic Med.* 8:e1197. doi: 10.1002/mgg3.1197

Lensen, J. F., van der Vlag, J., Versteeg, E. M., Wetzels, J. F., van den Heuvel, L. P., Berden, J. H., et al. (2015). Differential expression of specific dermatan sulfate domains in renal pathology. *PLoS One* 10:e0134946. doi: 10.1371/journal.pone.0134946

Li, J., Sparkenbaugh, E. M., Su, G., Zhang, F., Xu, Y., Xia, K., et al. (2020). Enzymatic synthesis of chondroitin sulfate e to attenuate bacteria lipopolysaccharide-induced organ damage. *ACS Cent. Sci.* 6, 1199–1207. doi: 10.1021/acscentsci.0c00712

Li, Q., Wu, X., Na, X., Ge, B., Wu, Q., Guo, X., et al. (2019). Impaired cognitive function and altered hippocampal synaptic plasticity in mice lacking dermatan sulfotransferase Chst14/D4st1. *Front. Mol. Neurosci.* 12:26. doi: 10.3389/fnmol.2019.00026

Liangsupree, T., Multia, E., Metso, J., Jauhiainen, M., Forssen, P., Fornstedt, T., et al. (2019). Rapid affinity chromatographic isolation method for LDL in human plasma by immobilized chondroitin-6-sulfate and anti-apoB-100 antibody monolithic disks in tandem. *Sci. Rep.* 9:11235. doi: 10.1038/s41598-019-47750-z

Lossl, P., van de Waterbeemd, M., and Heck, A. J. (2016). The diverse and expanding role of mass spectrometry in structural and molecular biology. *EMBO J.* 35, 2634–2657. doi: 10.15252/embj.201694818

Lyon, M., Deakin, J. A., Lietha, D., Gherardi, E., and Gallagher, J. T. (2004). The interactions of hepatocyte growth factor/scatter factor and its NK1 and NK2 variants with glycosaminoglycans using a modified gel mobility shift assay – elucidation of the minimal size of binding and activatory oligosaccharides. *J. Biol. Chem.* 279, 43560–43567. doi: 10.1074/jbc.M408510200

Maeda, N., He, J., Yajima, Y., Mikami, T., Sugahara, K., and Yabe, T. (2003). Heterogeneity of the chondroitin sulfate portion of phosphacan/6B4 proteoglycan regulates its binding affinity for pleiotrophin/heparin binding growth-associated molecule. *J. Biol. Chem.* 278, 35805–35811. doi: 10.1074/jbc.M305530200

Maimone, M. M., and Tollefsen, D. M. (1990). Structure of a dermatan sulfate hexasaccharide that binds to heparin cofactor-ii with high-affinity. *J. Biol. Chem.* 265, 18263–18271.

Malavaki, C., Mizumoto, S., Karamanos, N., and Sugahara, K. (2008). Recent advances in the structural study of functional chondroitin sulfate and dermatan sulfate in health and disease. *Connect Tissue Res.* 49, 133–139. doi: 10.1080/03008200802148546

Maleknia, S. D., and Downard, K. M. (2014). Advances in radical probe mass spectrometry for protein footprinting in chemical biology applications. *Chem. Soc. Rev.* 43, 3244–3258. doi: 10.1039/c3cs60432b

Margalit, H., Fischer, N., and Ben-Sasson, S. A. (1993). Comparative analysis of structurally defined heparin binding sequences reveals a distinct spatial distribution of basic residues. *J. Biol. Chem.* 268, 19228–19231.

Mencio, C. P., Hussein, R. K., Yu, P., and Geller, H. M. (2021). The role of chondroitin sulfate proteoglycans in nervous system development. *J. Histochem. Cytochem.* 69, 61–80. doi: 10.1369/0022155420959147

Mikami, T., and Kitagawa, H. (2013). Biosynthesis and function of chondroitin sulfate. *Biochim. Biophys. Acta* 1830, 4719–4733. doi: 10.1016/j.bbagen.2013.06.006

Miller, G. M., and Hsieh-Wilson, L. C. (2015). Sugar-dependent modulation of neuronal development, regeneration, and plasticity by chondroitin sulfate proteoglycans. *Exp. Neurol.* 274(Pt B), 115–125. doi: 10.1016/j.expneurol.2015.08.015

Mizumoto, S., Kosho, T., Yamada, S., and Sugahara, K. (2017). Pathophysiological significance of dermatan sulfate proteoglycans revealed by human genetic disorders. *Pharmaceuticals* 10:34. doi: 10.3390/ph10020034

Mizumoto, S., Takahashi, J., and Sugahara, K. (2012). Receptor for advanced glycation end products (RAGE) functions as receptor for specific sulfated glycosaminoglycans, and anti-RAGE antibody or sulfated glycosaminoglycans delivered in vivo inhibit pulmonary metastasis of tumor cells. *J. Biol. Chem.* 287, 18985–18994. doi: 10.1074/jbc.M111.313437

Mizumoto, S., Yamada, S., and Sugahara, K. (2015). Molecular interactions between chondroitin-dermatan sulfate and growth factors/receptors/matrix proteins. *Curr. Opin. Struct. Biol.* 34, 35–42. doi: 10.1016/j.sbi.2015.06.004

Mobius, K., Nordsieck, K., Pichert, A., Samsonov, S. A., Thomas, L., Schiller, J., et al. (2013). Investigation of lysine side chain interactions of interleukin-8 with heparin and other glycosaminoglycans studied by a methylation-NMR approach. *Glycobiology* 23, 1260–1269. doi: 10.1093/glycob/cwt062

Nakashima, Y., Wight, T. N., and Sueishi, K. (2008). Early atherosclerosis in humans: role of diffuse intimal thickening and extracellular matrix proteoglycans. *Cardiovasc. Res.* 79, 14–23. doi: 10.1093/cvr/cvn099

Namachivayam, K., Coffing, H. P., Sankaranarayanan, N. V., Jin, Y., MohanKumar, K., Frost, B. L., et al. (2015). Transforming growth factor-beta2 is sequestered in preterm human milk by chondroitin sulfate proteoglycans. *Am. J. Physiol. Gastrointest. Liver Physiol.* 309, G171–G180. doi: 10.1152/ajpgi.00126.2015

Nguyen, K. G., Gillam, F. B., Hopkins, J. J., Jayanthi, S., Gundampati, R. K., Su, G., et al. (2019). Molecular mechanisms of heparin-induced modulation of human interleukin 12 bioactivity. *J. Biol. Chem.* 294, 4412–4424. doi: 10.1074/jbc.RA118.006193

Palma, A. S., Feizi, T., Childs, R. A., Chai, W., and Liu, Y. (2014). The neoglycolipid (NGL)-based oligosaccharide microarray system poised to decipher the meta-glycome. *Curr. Opin. Chem. Biol.* 18, 87–94. doi: 10.1016/j.cbpa.2014.01.007

Penk, A., Baumann, L., Huster, D., and Samsonov, S. A. (2019). NMR and molecular modeling reveal specificity of the interactions between CXCL14 and glycosaminoglycans. *Glycobiology* 29, 715–725. doi: 10.1093/glycob/cwz047

Pentikainen, M. O., Oorni, K., Lassila, R., and Kovanen, P. T. (1997). The proteoglycan decorin links low density lipoproteins with collagen type I. *J. Biol. Chem.* 272, 7633–7638. doi: 10.1074/jbc.272.12.7633

Pichert, A., Samsonov, S. A., Theisgen, S., Thomas, L., Baumann, L., Schiller, J., et al. (2012). Characterization of the interaction of interleukin-8 with hyaluronan, chondroitin sulfate, dermatan sulfate and their sulfated derivatives by spectroscopy and molecular modeling. *Glycobiology* 22, 134–145. doi: 10.1093/glycob/cwr120

Pomin, V. H. (2014). Biological findings from the recent NMR-based studies of glycosaminoglycan-protein interactions. *Glycobiology* 24, 991–1003. doi: 10.1093/glycob/cwu065

Pomin, V. H. (2015). Sulfated glycans in inflammation. *Eur. J. Med. Chem.* 92, 353–369. doi: 10.1016/j.ejmech.2015.01.002

Pomin, V. H., and Wang, X. (2018). Glycosaminoglycan-protein interactions by nuclear magnetic resonance (NMR) spectroscopy. *Molecules* 23:2314. doi: 10.3390/molecules23092314

Pudelko, A., Wisowski, G., Olczyk, K., and Kozma, E. M. (2019). The dual role of the glycosaminoglycan chondroitin-6-sulfate in the development, progression and metastasis of cancer. *FEBS J.* 286, 1815–1837. doi: 10.1111/febs.14748

Raghuraman, A., Mosier, P. D., and Desai, U. R. (2006). Finding a needle in a haystack: development of a combinatorial virtual screening approach for identifying high specificity heparin/heparan sulfate sequence(s). *J. Med. Chem.* 49, 3553–3562. doi: 10.1021/jm060092o

Raghuraman, A., Mosier, P. D., and Desai, U. R. (2010). Understanding dermatan sulfate-heparin cofactor II interaction through virtual library screening. *ACS Med. Chem. Lett.* 1, 281–285. doi: 10.1021/ml100048y

Rieger, H., Yoshikawa, H. Y., Quadt, K., Nielsen, M. A., Sanchez, C. P., Salanti, A., et al. (2015). Cytoadhesion of *Plasmodium falciparum*-infected erythrocytes to chondroitin-4-sulfate is cooperative and shear enhanced. *Blood* 125, 383–391. doi: 10.1182/blood-2014-03-561019

Rogers, C. J., Clark, P. M., Tully, S. E., Abrol, R., Garcia, K. C., Goddard, W. A. III, et al. (2011). Elucidating glycosaminoglycan-protein-protein interactions using carbohydrate microarray and computational approaches. *Proc. Natl. Acad. Sci. U.S.A.* 108, 9747–9752. doi: 10.1073/pnas.1102962108

Ryan, E., Shen, D., and Wang, X. (2016). Structural studies reveal an important role for the pleiotrophin C-terminus in mediating interactions with chondroitin sulfate. *FEBS J.* 283, 1488–1503. doi: 10.1111/febs.13686

Sankaranarayanan, N. V., Nagarajan, B., and Desai, U. R. (2018). So you think computational approaches to understanding glycosaminoglycan-protein interactions are too dry and too rigid? Think again! *Curr. Opin. Struct. Biol.* 50, 91–100. doi: 10.1016/j.sbi.2017.12.004

Sato, Y., Shimono, C., Li, S., Nakano, I., Norioka, N., Sugiura, N., et al. (2013). Nephronectin binds to heparan sulfate proteoglycans via its MAM domain. *Matrix Biol.* 32, 188–195. doi: 10.1016/j.matbio.2013.01.005

Schultz, C. C., Muhleisen, T. W., Nenadic, I., Koch, K., Wagner, G., Schachtzabel, C., et al. (2014). Common variation in NCAN, a risk factor for bipolar disorder and schizophrenia, influences local cortical folding in schizophrenia. *Psychol. Med.* 44, 811–820. doi: 10.1017/S0033291713001414

Scuruchi, M., Poti, F., Rodriguez-Carrio, J., Campo, G. M., and Mandraffino, G. (2020). Biglycan and atherosclerosis: lessons from high cardiovascular risk conditions. *Biochim. Biophys. Acta Mol. Cell Biol. Lipids* 1865:158545. doi: 10.1016/j.bbalip.2019.158545

Shida, M., Mikami, T., Tamura, J. I., and Kitagawa, H. (2019). Chondroitin sulfate-D promotes neurite outgrowth by acting as an extracellular ligand for neuronal integrin alphaVbeta3. *Biochim. Biophys. Acta Gen. Subj.* 1863, 1319–1331. doi: 10.1016/j.bbagen.2019.06.004

Shipp, E. L., and Hsieh-Wilson, L. C. (2007). Profiling the sulfation specificities of glycosaminoglycan interactions with growth factors and chemotactic proteins using microarrays. *Chem. Biol.* 14, 195–208. doi: 10.1016/j.chembiol.2006.12.009

Singh, K., Gittis, A. G., Nguyen, P., Gowda, D. C., Miller, L. H., and Garboczi, D. N. (2008). Structure of the DBL3x domain of pregnancy-associated malaria protein VAR2CSA complexed with chondroitin sulfate A. *Nat. Struct. Mol. Biol.* 15, 932–938. doi: 10.1038/nsmb.1479

Sirko, S., von Holst, A., Weber, A., Wizenmann, A., Theocharidis, U., Gotz, M., et al. (2010). Chondroitin sulfates are required for fibroblast growth factor-2-dependent proliferation and maintenance in neural stem cells and for epidermal

growth factor-dependent migration of their progeny. *Stem Cells* 28, 775–787. doi: 10.1002/stem.309

Skandalis, S. S., Labropoulou, V. T., Ravazoula, P., Likaki-Karatza, E., Dobra, K., Kalofonos, H. P., et al. (2011). Versican but not decorin accumulation is related to malignancy in mammographically detected high density and malignant-appearing microcalcifications in non-palpable breast carcinomas. *BMC Cancer* 11:314. doi: 10.1186/1471-2407-11-314

Sobel, M., Soler, D. F., Kermode, J. C., and Harris, R. B. (1992). Localization and characterization of a heparin binding domain peptide of human von Willebrand factor. *J. Biol. Chem.* 267, 8857–8862.

Song, X., Heimburg-Molinaro, J., Smith, D. F., and Cummings, R. D. (2015). Glycan microarrays of fluorescently-tagged natural glycans. *Glycoconj. J.* 32, 465–473. doi: 10.1007/s10719-015-9584-8

Srinoulprasert, Y., Kongtawelert, P., and Chaiyaroj, S. C. (2006). Chondroitin sulfate B and heparin mediate adhesion of *Penicillium marneffei* conidia to host extracellular matrices. *Microb. Pathog.* 40, 126–132. doi: 10.1016/j.micpath.2005.12.001

Stabler, T. V., Montell, E., Verges, J., Huebner, J. L., and Kraus, V. B. (2017). Chondroitin sulfate inhibits monocyte chemoattractant protein-1 release from 3T3-L1 adipocytes: a new treatment opportunity for obesity-related inflammation? *Biomark. Insights* 12:1177271917726964. doi: 10.1177/1177271917726964

Stephenson, E. L., and Yong, V. W. (2018). Pro-inflammatory roles of chondroitin sulfate proteoglycans in disorders of the central nervous system. *Matrix Biol.* 71-72, 432–442. doi: 10.1016/j.matbio.2018.04.010

Sugahara, K. N., Hirata, T., Tanaka, T., Ogino, S., Takeda, M., Terasawa, H., et al. (2008). Chondroitin sulfate E fragments enhance CD44 cleavage and CD44-dependent motility in tumor cells. *Cancer Res.* 68, 7191–7199. doi: 10.1158/0008-5472.CAN-07-6198

Sugahara, K., Mikami, T., Uyama, T., Mizuguchi, S., Nomura, K., and Kitagawa, H. (2003). Recent advances in the structural biology of chondroitin sulfate and dermatan sulfate. *Curr. Opin. Struct. Biol.* 13, 612–620. doi: 10.1016/j.sbi.2003.09.011

Tang, F., Lord, M. S., Stallcup, W. B., and Whitelock, J. M. (2018). Cell surface chondroitin sulphate proteoglycan 4 (CSPG4) binds to the basement membrane heparan sulphate proteoglycan, perlecan, and is involved in cell adhesion. *J. Biochem.* 163, 399–412. doi: 10.1093/jb/mvy008

ten Dam, G. B., van de Westerlo, E. M., Purushothaman, A., Stan, R. V., Bulten, J., Sweep, F. C., et al. (2007). Antibody GD3G7 selected against embryonic glycosaminoglycans defines chondroitin sulfate-E domains highly up-regulated in ovarian cancer and involved in vascular endothelial growth factor binding. *Am. J. Pathol.* 171, 1324–1333. doi: 10.2353/ajpath.2007.070111

Theocharis, A. D., Tsolakis, I., Tzanakakis, G. N., and Karamanos, N. K. (2006). Chondroitin sulfate as a key molecule in the development of atherosclerosis and cancer progression. *Adv. Pharmacol.* 53, 281–295.

Toledo, A. G., Pihl, J., Spliid, C. B., Persson, A., Nilsson, J., Pereira, M. A., et al. (2020). An affinity chromatography and glycoproteomics workflow to profile the chondroitin sulfate proteoglycans that interact with malarial VAR2CSA in the placenta and in cancer. *Glycobiology* 30, 989–1002. doi: 10.1093/glycob/cwaa039

Tollefsen, D. M. (1992). The interaction of glycosaminoglycans with heparin cofactor II: structure and activity of a high-affinity dermatan sulfate hexasaccharide. *Adv. Exp. Med. Biol.* 313, 167–176. doi: 10.1007/978-1-4899-2444-5_17

Tully, S. E., Rawat, M., and Hsieh-Wilson, L. C. (2006). Discovery of a TNF-alpha antagonist using chondroitin sulfate microarrays. *J. Am. Chem. Soc.* 128, 7740–7741. doi: 10.1021/ja061906t

Uyama, T., Ishida, M., Izumikawa, T., Trybala, E., Tufaro, F., Bergstrom, T., et al. (2006). Chondroitin 4-O-sulfotransferase-1 regulates E disaccharide expression of chondroitin sulfate required for herpes simplex virus infectivity. *J. Biol. Chem.* 281, 38668–38674. doi: 10.1074/jbc.M609320200

Vignovich, W. P., and Pomin, V. H. (2020). Saturation transfer difference in characterization of glycosaminoglycan-protein interactions. *SLAS Technol.* 25, 307–319. doi: 10.1177/2472630320921130

Wang, K., Dagil, R., Lavstsen, T., Misra, S., Spliid, C., Wang, Y., et al. (2020). Cryo-EM reveals the architecture of placental malaria VAR2CSA and provides molecular insight into chondroitin sulfate binding. *Research Square* [Preprint] doi: 10.21203/rs.3.rs-121821/v1

Wang, W., Shi, L., Qin, Y., and Li, F. (2020). Research and application of chondroitin sulfate/dermatan sulfate-degrading enzymes. *Front. Cell Dev. Biol.* 8:560442. doi: 10.3389/fcell.2020.560442

Yamaguchi, K., Tamaki, H., and Fukui, S. (2006). Detection of oligosaccharide ligands for hepatocyte growth factor/scatter factor (HGF/SF), keratinocyte growth factor (KGF/FGF-7), RANTES and heparin cofactor II by neoglycolipid microarrays of glycosaminoglycan-derived oligosaccharide fragments. *Glycoconj. J.* 23, 513–523. doi: 10.1007/s10719-006-7151-z

Yang, X., Lin, Y. P., Heselpoth, R. D., Buyuktanir, O., Qin, J., Kung, F., et al. (2016). Middle region of the *Borrelia burgdorferi* surface-located protein 1 (Lmp1) interacts with host chondroitin-6-sulfate and independently facilitates infection. *Cell. Microbiol.* 18, 97–110. doi: 10.1111/cmi.12487

Yu, F., Roy, S., Arevalo, E., Schaeck, J., Wang, J., Holte, K., et al. (2014). Characterization of heparin-protein interaction by saturation transfer difference (STD) NMR. *Anal. Bioanal. Chem.* 406, 3079–3089. doi: 10.1007/s00216-014-7729-4

Zhang, F., Lee, K. B., and Linhardt, R. J. (2015). SPR biosensor probing the interactions between TIMP-3 and heparin/GAGs. *Biosensors* 5, 500–512. doi: 10.3390/bios5030500

**Conflict of Interest:** The authors declare that the research was conducted in the absence of any commercial or financial relationships that could be construed as a potential conflict of interest.

**Publisher's Note:** All claims expressed in this article are solely those of the authors and do not necessarily represent those of their affiliated organizations, or those of the publisher, the editors and the reviewers. Any product that may be evaluated in this article, or claim that may be made by its manufacturer, is not guaranteed or endorsed by the publisher.

frontiers in Cell and Developmental Biology

MINI REVIEW
published: 13 August 2021
doi: 10.3389/fcell.2021.695970

# Expanding the Chondroitin Sulfate Glycoproteome — But How Far?

*Fredrik Noborn[1]*, Mahnaz Nikpour[1], Andrea Persson[1], Jonas Nilsson[1,2] and Göran Larson[1]*

[1] Department of Laboratory Medicine, Institute of Biomedicine, Sahlgrenska Academy at the University of Gothenburg, Gothenburg, Sweden, [2] Proteomics Core Facility, Sahlgrenska Academy at the University of Gothenburg, Gothenburg, Sweden

Chondroitin sulfate proteoglycans (CSPGs) are found at cell surfaces and in connective tissues, where they interact with a multitude of proteins involved in various pathophysiological processes. From a methodological perspective, the identification of CSPGs is challenging, as the identification requires the combined sequencing of specific core proteins, together with the characterization of the CS polysaccharide modification(s). According to the current notion of CSPGs, they are often considered in relation to a functional role in which a given proteoglycan regulates a specific function in cellular physiology. Recent advances in glycoproteomic methods have, however, enabled the identification of numerous novel chondroitin sulfate core proteins, and their glycosaminoglycan attachment sites, in humans and in various animal models. In addition, these methods have revealed unexpected structural complexity even in the linkage regions. These findings indicate that the number and structural complexity of CSPGs are much greater than previously perceived. In light of these findings, the prospect of finding additional CSPGs, using improved methods for structural and functional characterizations, and studying novel sample matrices in humans and in animal models is discussed. Further, as many of the novel CSPGs are found in low abundance and with not yet assigned functions, these findings may challenge the traditional notion of defining proteoglycans. Therefore, the concept of proteoglycans is considered, discussing whether "a proteoglycan" should be defined mainly on the basis of an assigned function or on the structural evidence of its existence.

**Keywords: proteoglycans, glycosaminoglycans, chondroitin sulfate, core proteins, glycoproteomics, attachment site**

OPEN ACCESS

***Edited by:***
*John Whitelock, University of New South Wales, Australia*

***Reviewed by:***
*Jasmeen S. Merzaban, King Abdullah University of Science and Technology, Saudi Arabia*
*Nikos Karamanos, University of Patras, Greece*

****Correspondence:***
*Fredrik Noborn*
*Fredrik.Noborn@gu.se*

***Specialty section:***
*This article was submitted to Signaling, a section of the journal Frontiers in Cell and Developmental Biology*

***Received:*** *15 April 2021*
***Accepted:*** *27 July 2021*
***Published:*** *13 August 2021*

***Citation:***
*Noborn F, Nikpour M, Persson A, Nilsson J and Larson G (2021) Expanding the Chondroitin Sulfate Glycoproteome — But How Far? Front. Cell Dev. Biol. 9:695970. doi: 10.3389/fcell.2021.695970*

## INTRODUCTION

The concept of chondroitin sulfate proteoglycans (CSPGs) as discrete molecular entities first emerged during the late 1950s. At that time, chondroitin sulfate (CS) and protein complexes had been identified in hyaline cartilage, but the nature of the complexes remained elusive, and it was unclear whether the CS to protein association involved a covalent bond or not (Shatton and Schubert, 1954). In a pioneering study by Helen Muir, she showed that the CS chains were indeed covalently linked to the protein counterpart (Muir, 1958). A few years later, it was found that the CS polysaccharides are attached to serine residues of the core proteins via a tetrasaccharide linkage region, composed of Glucuronic acid (GlcA)—Galactose (Gal)—Galactose (Gal)—Xylose (Xyl) (Lindahl and Roden, 1966; Roden and Smith, 1966). Since then, an increasing number of different

CSPGs have been identified, each distinguished by the primary sequence of the core protein and with different numbers of CS chains attached (Olson et al., 2006; Iozzo and Schaefer, 2015; Pomin and Mulloy, 2018; Toledo et al., 2020).

CSPGs are important components in connective tissue and fine-tunes a wide range of cellular processes, including neural development, growth factor signaling and inflammation (Hatano and Watanabe, 2020; Hussein et al., 2020). However, the structural identification of CSPGs is often difficult, as the identification requires the combined sequencing of specific core proteins together with the structural verification of any potential CS polysaccharides. Consequently, studies on identifying novel CSPGs, using earlier established biochemical techniques, were mostly focused on the characterization of single core proteins in a defined cellular or physiological context (Krusius and Ruoslahti, 1986; Fisher et al., 1989). Such techniques are typically based on different read out assays following enzymatic depolymerization with bacterial lyases and/or site directed mutagenesis of cloned proteins.

The lack of suitable analytical methods for large-scale analyses of CSPGs in biological samples has for a long time limited the ability to identify both novel CSPGs and assess the degree of heterogeneity of the CS glycoproteome across various systems.

This mini review will specifically focus on the recent advances in glycoproteomics to identify and characterize CSPGs in complex sample mixtures in humans and animal model systems. These methods include trypsin digestion, enrichment of acidic glycopeptides by strong anion-exchange chromatography (SAX), and incubation with chondroitinase ABC to reduce the length and complexity of the CS chains. The samples are then analyzed with reversed phase nano-liquid chromatography-tandem mass spectrometry (nLC-MS/MS) and evaluated by glycopeptide search algorithms, resulting in the discovery and characterization of several novel CSPGs both in vertebrates and invertebrates. In light of these findings, the structural and conceptual insights that can be provided by such attachment site-specific analysis of the CS glycoproteome are discussed. Further, as many of the novel CSPGs are found in low abundance and with no yet assigned functions, these findings may challenge the traditional notion of proteoglycans, in which the described proteoglycans often have an assigned function. Finally, the concept of the CS glycoproteome is discussed in relation to whether the glycoproteomic space should be regarded as a static or a dynamic entity.

## A GLYCOPROTEOMIC APPROACH TO IDENTIFY NOVEL PROTEOGLYCANS

In glycobiology, mass spectrometry-based strategies for investigating protein glycosylation (glycoproteomics) have become an increasingly important tool (Nilsson et al., 2009; Thaysen-Andersen et al., 2016; Narimatsu et al., 2018). Such strategies, well-covered in excellent reviews, are typically based on enrichment of glycopeptides and subsequent analysis with nLC-MS/MS to provide site-specific information of *N*- and *O*-glycans (Nilsson, 2016; Darula and Medzihradszky, 2018; Madsen et al., 2020; Chernykh et al., 2021). To further develop this concept, we established a glycoproteomic protocol for global characterization of CS-glycopeptides in human urine and cerebrospinal fluid (CSF) (Noborn et al., 2015; Noborn et al., 2021). At first, bikunin (also known as protein AMBP) was used as a model CSPG since it was relatively well characterized, available in large quantities from human urine and also used in some countries as a pharmaceutical agent to treat acute pancreatitis (Ly et al., 2011; Lord et al., 2020). Human bikunin has a single CS chain of 27–39 monosaccharides attached to the N-terminal end (Ser-10) of the core protein (Lord et al., 2013). We incubated pharmaceutical grade bikunin with chondroitinase ABC that generated free disaccharides and a residual hexasaccharide structure still attached to the core protein. Digestion with trypsin generated a defined CS-glycopeptide suitable in size for nLC-MS/MS analysis. The analysis enabled the identification of several specific glycosidic and bikunin peptide fragments, serving as a proof-of-concept that site-specific analysis of CSPGs is indeed a feasible strategy. We then enriched trypsin-digested CSPGs from human urine and CSF and incubated the enriched samples with chondroitinase ABC, and thereafter analyzed the resulting CS-glycopeptides by nLC-MS/MS. Generated data were evaluated through proteomic software with adjustments to allow for glycopeptide identification, enabling the identification of 13 novel human CSPGs in addition to 13 already established CSPGs. In **Tables 1A,B**, the novel proteoglycans identified in humans and different model systems through glycoproteomics are shown. Interestingly, several of the novel human CSPGs were traditionally defined as prohormones, which was surprising, as prohormones are not typically regarded to belong to the proteoglycan superfamily (Noborn et al., 2015). This approach demonstrates the structural and conceptual insights that can be provided by global attachment site-specific analysis of the CS glycoproteome.

A similar strategy was developed for complex proteoglycans of the extracellular matrix (hyalectans) from human and bovine sources (Klein et al., 2018). In addition to CS chains, hyalectan proteoglycans are also rich *N*- and mucin-type *O*-glycosylations that decorate large parts of the proteins. The abundant glycosylation impairs effective peptide identification and reduces the overall sequence coverage achieved by mass-spectrometric based methods. By using a combination of efficient enrichment procedures for glycosylated peptides and advanced MS/MS-software analysis, the authors were able to improve the peptide sequence coverage of these complex proteoglycans and identify a number of new attachment sites, including both *N*-, mucin type *O*- and CS-glycosylations.

## GLYCOPROTEOMICS: NOVEL CSPGs LEADING TO NOVEL HYPOTHESES

Although glycoproteomic approaches assist in identifying novel CSPGs, the functional relevance of a CS modification on cellular physiology is often unclear and cannot be inferred from only the CS structure or from the core protein alone.

**TABLE 1 | A.** Novel human proteoglycans identified through glycoproteomics.

***Human***

| Protein name | Uniprot ID | Modification[a] | Site(s)[b] | References |
|---|---|---|---|---|
| Brain-specific angiogenesis inhibitor 2 | O60241 | CS | 266* | Noborn et al., 2015 |
| CD99L2 protein | H0Y4H3 | CS | 141* | Noborn et al., 2015 |
| Cholecystokinin | P06307 | CS | 31 | Noborn et al., 2015 |
| Collagen and calcium-binding EGF domain containing protein 1 | Q6UXH8 | CS | 385 | Noborn et al., 2015 |
| Dermcidin | P81605 | CS | 30* | Noborn et al., 2015 |
| Laminin subunit alpha-4 | Q16363 | CS | 40* | Noborn et al., 2015 |
| Laminin subunit gamma 2 | Q13753 | CS | 803* | Toledo et al., 2020 |
| Matrix-remodeling associated protein 5 | Q9NR99 | CS | 702* | Noborn et al., 2015 |
| Meprin A subunit alpha | Q16819 | CS | 631* | Nasir et al., 2016 |
| Natriuretic peptides B | P16860 | CS | 41* | Toledo et al., 2020 |
| Neurexin-1 | Q9ULB1 | HS | 1,355 | Zhang et al., 2018 |
| Neurexin-2 | Q9P2S2 | HS | 1,400 | Zhang et al., 2018 |
| Neurexin-3 | Q9Y4C0 | HS | 1,315 | Zhang et al., 2018 |
| Neuropeptide W | Q8N729 | CS | 133* | Noborn et al., 2015 |
| Neuroserpin | Q99574 | CS | 403 | Noborn et al., 2015 |
| Nidogen-2 | Q14112 | CS | 452*, 358* | Toledo et al., 2020 |
| Osteopontin | P10451 | CS | 234*, 308* | Noborn et al., 2015 |
| Plexin domain-containing protein 1 | Q8IUK5 | CS | 33 | Noborn et al., 2015 |
| Retinoic acid responder protein | P49788 | CS | 40 | Nasir et al., 2016 |
| Secretogranin-1 | P05060 | CS | 93*, 239* | Noborn et al., 2015 |
| Secretogranin-3 | Q8WXD2 | CS | 37 | Noborn et al., 2015 |
| Sushi repeat-containing protein SRPX | P78539 | CS | 34* | Toledo et al., 2020 |

**B.** Novel proteoglycans identified in different model systems through glycoproteomics.

| Protein name | Uniprot ID/Accession number | Modification[b] | Site(s)[b] | References |
|---|---|---|---|---|
| ***Caenorabditis elegans*** | | | | |
| CLE-1A protein/CPG-10 | Q9U9K7 | Chn | 581 | Noborn et al., 2018 |
| COLlagen/CPG-11 | Q22651 | Chn | 336* | Noborn et al., 2018 |
| C-type lectin domain containing protein 180/CPG-12 | Q19970 | Chn | 275, 290 | Noborn et al., 2018 |
| Dauer Up-Regulated, isoform b/CPG-13 | Q7JLY2 | Chn | 368 | Noborn et al., 2018 |
| High Incidence of Males, isoform b/CPG-14 | NCBINP_001024582.1 | Chn | 4,850* | Noborn et al., 2018 |
| LiPocalin-Related protein/CPG-15 | Q23163 | Chn | 172* | Noborn et al., 2018 |
| FiBrilliN homolog/CPG-16 | Q23587 | Chn | 1,079* | Noborn et al., 2018 |
| Papilin/CPG-17 | O76840 | Chn | 775* | Noborn et al., 2018 |
| Protein C45E5.4/CPG-18 | Q18642 | Chn | 38* | Noborn et al., 2018 |
| Protein C06G1.2/CPG-19 | Q17742 | Chn | 35* | Noborn et al., 2018 |
| Protein K08B4.2/CPG-20 | Q9TYY6 | Chn | 167* | Noborn et al., 2018 |
| Protein R17.3/CPG-21 | O18003 | Chn | 111* | Noborn et al., 2018 |
| Protein T10E9.3/CPG-22 | O01603 | Chn | 382, 399 | Noborn et al., 2018 |
| Protein Y39B6B.y/CPG-23 | NCBI PIR T45051 | Chn | 313* | Noborn et al., 2018 |
| Protein Y41D4B.26/CPG-24 | Q8WSN8 | Chn | 194 | Noborn et al., 2018 |
| ***Danio rerio*** | | | | |
| Uncharacterized protein si:ch73-306e8.2 isoform X1 | XP_00133717.3 | CS | 103* | Delbaere et al., 2020 |
| ***Drosophila melanogaster*** | | | | |
| Protein Windpipe | Q9W266 | CS | 282, 335, 337 | Takemura et al., 2020 |
| ***Rat INS-1 832/13, murine MIN-6 and NIT-1 cell lines*** | | | | |
| Chromogranin-A | P10354 | HS | 433 | Nikpour et al., 2021 |
| Immunoglobulin superfamily member 10 | Q3V1M1 | CS | 679 | Nikpour et al., 2021 |
| Islet Amyloid Polypeptide | P12969 | CS | 28 | Nikpour et al., 2021 |
| Secretogranin-1 | P35314 | HS | 236 | Nikpour et al., 2021 |

[a] *Glycosaminoglycan modifications: CS, chondroitin sulfate; HS, heparan sulfate; or Chn, chondroitin.*

[b] *Glycosaminoglycan attachment sites denote serine amino acid numbers, determined unambiguously by nLC-MS/MS or ambiguously for glycopeptides containing two or more serine residues (*). Numbers relate to the corresponding protein ID.*

However, the identification of novel CSPGs, as well as defining novel attachment site modifications of established CSPGs, generate novel hypotheses that can be experimentally tested. Here we exemplify with a few cases of how such global or targeted glycoproteomic approaches can be combined with hypothesis-driven research to investigate structure-function relationships of CSPGs.

We recently identified the Windpipe protein as a novel CSPGs in *Drosophila melanogaster* and found that the core protein carried three separate CS chains in its extracellular domain (Takemura et al., 2020). Genetic engineering combined with morphological analyses demonstrated that Windpipe inhibited Hedgehog (Hh) signaling in a CS dependent manner. Interestingly, Windpipe-overexpression resulted in reduced wing size compared with control flies. However, the wing size was restored in genetically modified flies in which all the three CS attachment serine residues were substituted with alanine residues (thereby precluding CS modification). This study thus demonstrates a novel role of a specific CSPG in regulating Hh signaling and illustrate the potential of combining glycoproteomics with molecular and cell biological studies in a well-defined model system.

Several protein hormones are stored as amyloid-like aggregates in the secretory granules of endocrine cells (Maji et al., 2009). Most of the protein hormones require mild acidic pH and the addition of low molecular weight heparin or CS for their aggregation *in vitro*. Our finding that several prohormones carry CS chains lead us to hypothesize that the CS side chains may facilitate self-assembly of the prohormones (Noborn et al., 2015). Indeed, binding studies showed that CS promoted the assembly of the chromogranin A core protein under acidic condition, giving a possible explanation to previous observations that chromogranin A has an inherent property to assemble in the acidic milieu of secretory granules. Whether the CS side chains of other prohormones (e.g., secretogranin-1 and 3) may also influence the assembly of their respective core protein remains to be determined.

Furthermore, an affinity-enriched glycoproteomic approach was recently employed to explore the involvement of CSPGs in the pathogenesis of pregnancy-associated malaria. The disease is caused by the parasite *Plasmodium falciparum* and has potentially very severe clinical outcome for both mother and child (Toledo et al., 2020; Tomlinson et al., 2020). The parasite induces expression of the malarial protein VAR2CSA on the surface of infected erythrocytes, which enables their binding to structural variants of CS in the placental intervillous space of pregnant women (Kane and Taylor-Robinson, 2011). This interaction is dependent on the size and sulfation-type of the polysaccharide, as longer chains with higher degree of C4-*O*- sulfation of GalNAc residues display stronger binding (Sugiura et al., 2016; Ma et al., 2021). A VAR2CSA-affinity column was recently used to enrich for CSPGs, capable of binding the VAR2CSA-protein, in human placenta. The enriched fraction was then analyzed through a CS glycoproteomic workflow, showing that a collection of different core proteins, rather than a single core protein, carried CS chains that were capable of binding the VAR2CSA-protein (Toledo et al., 2020). This indicates that several different CSPGs may serve as attachment factors for malaria-infected erythrocytes, which provides new insight into the disease etiology. Notably, CS and heparan sulfate (HS) also constitute attachment factors for many enveloped and non-enveloped viruses (Olofsson and Bergström, 2005). Interestingly, recent studies show that cell surface HS act as a co-receptor to ACE2 and is essential for SARS-CoV-2 infection (Clausen et al., 2020; Mycroft-West et al., 2020). To our knowledge, however, the information of a potential HS core protein (or group of core proteins) involved in such processes is scarce (Daly et al., 2020). A glycoproteomic enrichment strategy, similar to the VAR2CSA-CS enrichment approach, may provide information on this issue.

## PROTEOGLYCAN LINKAGE REGION COMPLEXITY

The CS linkage region has previously been perceived as a relatively uniform entity with limited structural variability. MS/MS-analysis of chondroitinase ABC-digested bikunin described a defined hexasaccharide structure with *O*-sulfations of the GalNAc residue and of the outer Gal residue (Ly et al., 2011). In addition to sulfation, other linkage region modifications have been reported, e.g., sialylation and phosphorylation (Sugahara et al., 1988; Kitagawa et al., 2008; Lu et al., 2010; Wen et al., 2014). However, the reports have been limited to only a few separate experimental systems and information on potential combinations of linkage region modifications is still scarce. To this aim, our glycoproteomic analysis of human bikunin and other proteoglycans from urine, CSF, and plasma have revealed an unexpected linkage region complexity, with different combinations of sulfation, phosphorylation and sialylation (Gomez Toledo et al., 2015; Noborn et al., 2015; Nasir et al., 2016; Nilsson et al., 2017). Furthermore, the structural variability of human bikunin was further increased by large variations in the mucin type *O*-linked glycosylation found nearby the CS site (Gomez Toledo et al., 2015). Moreover, an unexpected fucose (deoxy-hexose) modification was found on the xylose residue of the linkage region of human bikunin and decorin and on two novel human CSPGs; retinoic acid responder protein 1 and meprin A (Gomez Toledo et al., 2015; Nasir et al., 2016). This was surprising as fucosylated CS chains have previously only been described in sea cucumbers, a member of the phylum of Echinodermata (Myron et al., 2014; Dwivedi and Pomin, 2020). Notably, this fucose modification in human CS was located on xylose (and not on the CS chain), i.e., close to the protein component. This position is similar to the fucose modifications on *N*-glycans, which also may occur at the innermost GlcNAc residue linked to Asn in the consensus amino acid sequence (core fucosylation) (Plomp et al., 2017; Schneider et al., 2017; Wang and Ravetch, 2019). This kind of *N*-glycan fucosylation occurs both in invertebrate and vertebrate species and modifies the functional effects of the corresponding proteins, e.g., by regulating the inflammatory immune responses by modifying the *N*-glycans of the Fc chains of IgG1 molecules. This is of major importance when designing and introducing monoclonal antibodies for immune therapy, since the afucosylated variants show an increased antibody-dependent cellular cytotoxicity (ADCC) (Pereira et al., 2018). What functional effects the

core fucosylation of xylose of CSPG may have remains to be determined.

Furthermore, we have observed a non-canonical linkage region trisaccharide (GlcA-Gal-Xyl-*O*-) on glycopeptides of bikunin from urine of healthy donors. This trisaccharide thus lacks one Gal residue of the traditional linkage region, and results in a residual pentasaccharide structure upon chondroitinase ABC digestion (Persson et al., 2019). Interestingly, mutations in the *B3GALT6* gene, which codes for galactosyltransferase II (β3GalT6) is associated with Ehlers-Danlos–like syndromes, characterized by a spectrum of skeletal and connective tissue "linkeropathy" disorders (Malfait et al., 2013). The β3GalT6 enzyme is responsible for adding the second Gal residue in the GAG linkage region and mutations in the gene results in reduced GAG biosynthesis and appearance of the trisaccharide linkage region in a zebrafish *b3galt6* knock-out model (Delbaere et al., 2020). Whether patients with *B3GALT6* mutations also have increased levels of the non-canonical trisaccharide linkage region of bikunin in their urine remains to be determined. Taken together, at least 14 different variants of the bikunin linkage region (including canonical and non-canonical sequences) have now been described, thus demonstrating a much greater variability than previously appreciated (Gomez Toledo et al., 2015; Noborn et al., 2015; Nilsson et al., 2017; Persson et al., 2019). Xylose phosphorylation has been shown to function as a molecular switch to regulate the proteoglycan biosynthesis (Wen et al., 2014). The removal of xylose phosphorylation by 2-phosphoxylose phosphatase is considered a prerequisite for the polymerization of the linkage regions into longer chains (Koike et al., 2014). However, the influence of the other linkage modifications (or the combinations thereof) on the downstream GAG biosynthesis is yet unknown. Nevertheless, knowledge of linkage region complexity provides a theoretical framework for future functional-structural studies of CS biosynthesis. Moreover, analysis of extended site-specific CS chains, in theory achieved by using partial chondroitinase ABC digestion, may assist in further understanding of how these modifications affect the biosynthesis and thus the final structures of CS. In addition, this may provide information on how certain core protein determinants (e.g., amino acid sequences) may influence the CS structures. The concept of core protein specific structures have been difficult to address since most established proteoglycan workflows involve the separation of the CS polysaccharides and the core proteins. Ideally, site-specific analysis of full-length CS structures is desirable, as this type of information is likely required to fully explore the structural-functional basis of CSPGs.

Further development of the glycoproteomic concept has enabled site-specific characterization of both CS and HS sites (Noborn et al., 2016). To this aim, perlecan (also known as basement membrane specific proteoglycan) was chosen as a model proteoglycan since it is known to be substituted with both CS and HS chains (Iozzo, 2005; Noborn et al., 2015). A trypsin-digested perlecan sample, derived from Engelbreth-Holm-Swarm mouse sarcoma, was enriched on a SAX column and digested with heparinase or chondroitinase ABC, generating residual tetrasaccharide and hexasaccharide structures still attached to the peptide. This allowed for the identification of a glycopeptide derived from the N-terminal domain of perlecan, which encompassed the three previously known HS sites (Iozzo and Sanderson, 2011). In addition, the combination of chondroitinase and heparinase digestion revealed a "hybrid site" in the C-terminal domain, carrying either an HS or a CS chain (Noborn et al., 2016). This was surprising since it demonstrated that a single GAG attachment site is capable of carrying either HS or CS chains, thus, revealing a less appreciated level of proteoglycan heterogeneity. The identification of such "hybrid sites" is likely to be biologically important as HS and CS often display opposite effects on cellular physiology (Coles et al., 2011; Doody et al., 2015). Furthermore, similar glycoproteomic protocols have been used to identify novel HSPGs, and to investigate the functional role of HSPGs in neuronal synapse formation (Zhang et al., 2018; Montoliu-Gaya et al., 2021; Nikpour et al., 2021).

## EXPANDING THE PROTEOGLYCAN GLYCOPROTEOME — BUT HOW FAR?

Glycosylation is one of the most ubiquitous forms of post-translational modification and is expected to be present on more than half of all mammalian proteins (Apweiler et al., 1999; Schjoldager et al., 2020). However, despite its high abundance, GAG modifications are considered to occur only on a very minor proportion of the 20,000–25,000 proteins encoded by the human genome. Although glycoproteomic studies of various sample matrices have significantly increased our structural knowledge of proteoglycans, fewer than 80 core proteins carrying CS have so far been identified in humans (Noborn et al., 2015; Nasir et al., 2016; Toledo et al., 2020). A list of all CSPGs known to date in humans was recently published by Toledo et al. (2020). The number of human core proteins carrying HS are even less, and so far only a little more than 20 HSPGs have been established (Zhang et al., 2018; Nikpour et al., 2021). Moreover, while proteoglycans in vertebrates have been the focus of several structural studies, the information about proteoglycans in invertebrates is scarce and the reports are restricted to only a few species (Noborn and Larson, 2021). Thus, only a limited number of CSPGs have been identified in *Drosophila melanogaster*, which is surprising since it is one of the most studied invertebrates (Momota et al., 2011; Zhu et al., 2019; Takemura et al., 2020). Future studies employing glycoproteomic approaches will likely identify novel CSPGs of invertebrates and further expand our knowledge of the proteoglycan glycoproteome in different species.

The enzymatic transfer of a Xyl residue to certain Ser residues in the proteoglycan core protein initiates GAG biosynthesis (Briggs and Hohenester, 2018). The Xyl-modified Ser residue is typically followed by a Gly residue (-SG-) and is associated with a cluster of acidic residues in close proximity, indicating that certain motifs of the amino acid sequence influence the initiation process (Esko and Zhang, 1996). Such motifs may assist in the prediction of potential GAG sites of core proteins and provides insights into the potential space of the GAG glycoproteome. When we recently mapped the chondroitin (Chn) glycoproteome in *C. elegans*, this resulted in the identification of 15 novel core proteins in addition to the 9 previously established core

proteins (Olson et al., 2006; Noborn et al., 2018). Bioinformatic analysis of protein sequences in the regions of the glycosylated Ser residues showed a highly stringent attachment motif E/D-G/A-S-G. A search in the Swiss-Prot database using this motif retrieved 19 additional potential CPGs, indicating that possibly additional CPGs are yet to be found in the nematode (Noborn et al., 2018). However, it is unclear why these assumed CPGs escaped detection by the glycoproteomic analysis. This may simply relate to the sensitivity of the assay and that the glycopeptides corresponding to these potential CPGs were below the detection threshold. On the other hand, it may also suggest that some motifs are only occasionally occupied, or substituted with HS instead of Chn. Nevertheless, this demonstrates the ambiguity of using only attachment motifs as a strategy to identify proteoglycans, and that glycoproteomic analysis is needed to determine the GAG glycoproteome in any given sample system. The basic strategies for proteoglycan identification and the different levels of structural- and functional understanding of their roles in any biological system is schematically illustrated in **Figure 1**.

The prohormone chromogranin-A (CgA) is one of the main proteins in secretory granules of endocrine cells and the precursor for several bioactive peptides (Kim et al., 2001). CgA has previously been established as a CSPG and carries a CS chain in the C-terminal end (Ser-424) of the human core protein (Gowda et al., 1990; Noborn et al., 2015). Our recent glycoproteomic analysis of cultured insulin-secreting cells, demonstrate that CgA in rodents, but not in humans, also carries

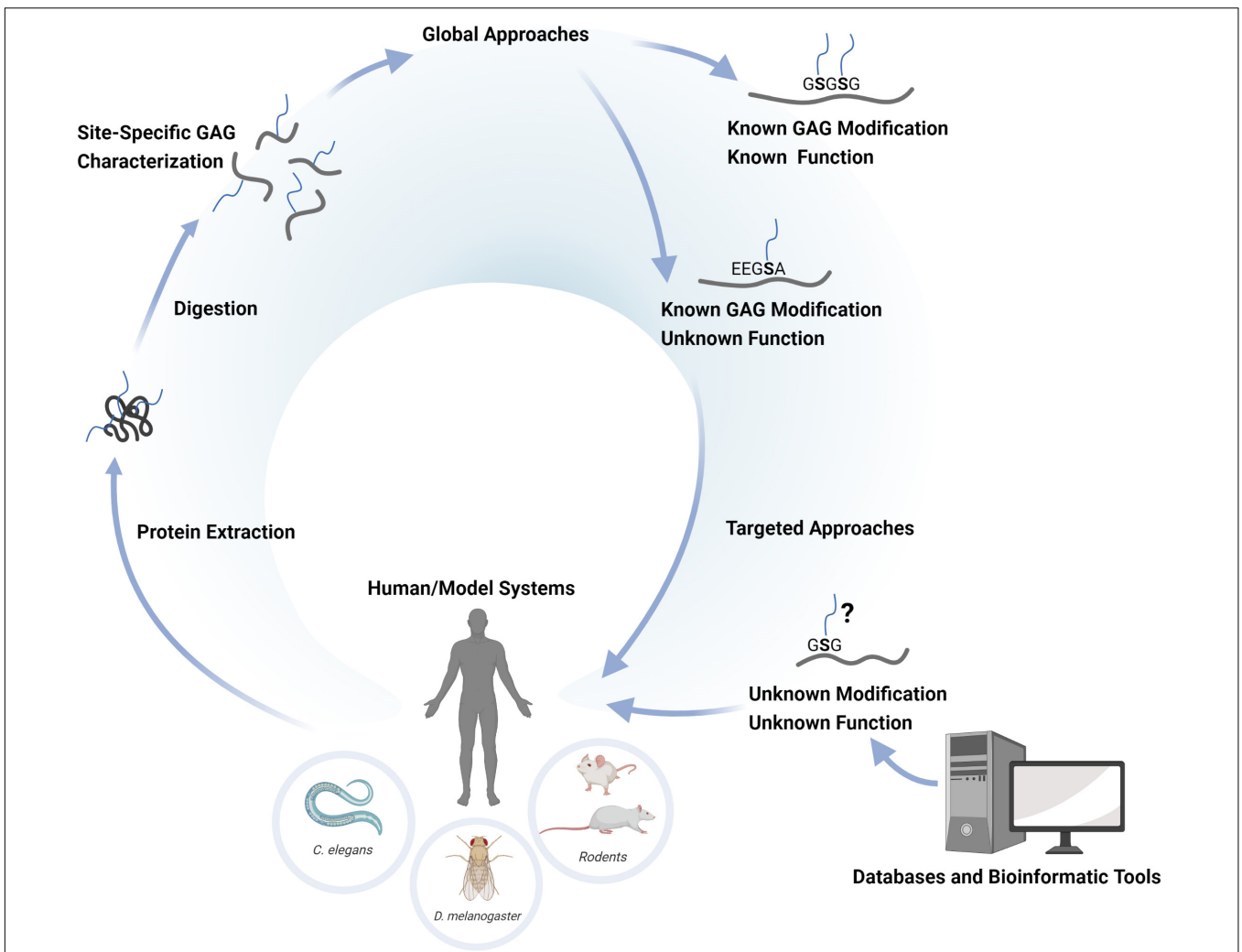


**FIGURE 1 |** Schematic illustration of the basic concepts concerning glycoproteomic identification of proteoglycans. The identification is achieved by the extraction of proteoglycans from human tissues or from various experimental systems (*C. elegans*, *D. melanogaster*, etc.), followed by the digestion with trypsin and chondroitinase ABC to enrich and generate defined CS-glycopeptides. The glycopeptides are then analyzed by nLC-MS/MS and the data is evaluated through glycopeptide search algorithms. This approach provides a global site-specific characterization of the CSPGs present in the sample system of interest. The identified CSPGs may be previously known CSPGs with known functions, or novel CSPGs for which the functions are yet unknown. The use of targeted approaches (e.g. molecular engineering) may assist in exploring the potential function of novel CSPGs in the sample system of interest. Bioinformatic analysis of the proteome sequences of a given model system may provide information of potential GAG-attachment sites. An assumed GAG-site may thus be verified in vivo using targeted glycoproteomic approaches and functional read-outs.

HS at the same C-terminal site, making this another "hybrid site" (Noborn et al., 2016; Nikpour et al., 2021). Although the glycosite is highly conserved between species (Noborn et al., 2015), this highlights the importance of cell-targeted mapping and that GAG modifications found in one cell type or tissue or species may not simply be inferred to another sample system. These findings also support the view that the GAG glycoproteome should not be regarded as a static entity, but rather a dynamic system that changes with the cellular physiology. A key issue for the future is to comprehend the biological factors that eventually will govern the expansion of the GAG glycoproteome.

## DISCUSSION

As with any research area, the characterization of any particular biomolecule is critical for the understanding of its role in biological and pathological processes. The identification and structural characterization of proteoglycans is no exception. According to our current understanding of CSPGs, these are often regarded in a functional context, in which any given proteoglycan regulate a specific function in cellular pathophysiology. For example, decorin, a small leucine-rich extracellular matrix proteoglycan, is well-studied for its role as a suppressor of tumor cell growth (Neill et al., 2016; Appunni et al., 2019). Decorin binds and antagonizes various receptor tyrosine kinases, thereby inhibiting downstream oncogenic signaling and reducing tumor growth (Reszegi et al., 2020; Hu X. et al., 2021). Apart from their involvement in cancer, CSPGs are also in focus of other research areas, including neurogenesis and spinal cord injury (Maeda, 2015). Following damage to the central nervous system, axons fail to regenerate due to the formation of a glial scar, which is composed of extracellular matrix components including CSPGs (Hussein et al., 2020). The production of several CSPG family members is differentially regulated in the glial scar as neurocan, brevican and versican are increased, while aggrecan is reduced (Mukhamedshina et al., 2019). How the individual CSPGs contribute to the pathogenesis is yet unclear, but their relevance is illustrated by the interest of using chondroitinase ABC as a therapeutic agent (Bradbury et al., 2002; Hu et al., 2018; Hu J. et al., 2021). Although detailed structural-functional understanding of PGs many times remains unknown, the examples given in this review point to essential roles of CSPGs in various pathophysiological conditions and demonstrate the significant progress that has been made in the field in recent years.

The recent advances in glycoproteomics have enabled the identification of several novel CS core proteins in humans and in various animal models. With such techniques, additional CS core proteins and novel GAG modifications will likely be discovered with no yet assigned function/s. Thus, one should consider whether "a proteoglycan" should be defined mainly on the basis of an assigned function or on structural evidence of its existence. Importantly, glycoproteomic strategies have the potential of finding many novel proteoglycans and provide global structural information that may contribute to our conceptual understanding of the complex family of proteoglycans. However, viewing proteoglycans from a "structure only" perspective will meet its limitations. The development of even more advanced glycoproteomics strategies will presumably identify proteoglycans at low abundances and/or at low levels of occupancy. This suggests that caution is needed in the interpretation of the data as minute amounts of any given proteoglycan may have little or no relevance for our understanding of any given biological system. Therefore, using glycoproteomics in a clearly defined biological or pathological context will likely be a necessary future strategy, since it will set constraints on the interpretation of the structural information derived. This will likely assist in determining which proteoglycans are relevant for understanding the underlying biological mechanisms in any given system. Nonetheless, glycoproteomic strategies will surely assist in further expanding the knowledge of proteoglycan core proteins and their functions. In the perspective of the present pandemic of COVID-19, the importance of proteoglycans as attachment factors/receptors or co-receptors of pathogenic viruses cannot be underestimated and detailed structural information of the host GAGs and their core protein structures will most likely be warranted to understand the molecular details of virus infections as well as to design novel anti-viral drugs.

## AUTHOR CONTRIBUTIONS

FN and GL did the writing and provided the main concepts discussed in this mini review. MN, AP, and JN assisted in the organization and editing of the publication and contributed to the table and the figure. All authors contributed to the article and approved the submitted version.

## FUNDING

This review covers the recent advancement of glycoproteomic analysis of proteoglycans, and discusses the basis of site-specific glycan characterization, which has been an important concept in glycobiology during the last decade. As a principal investigator, GL has been conducting basic and applied research in this area and has been funded by several agencies during this time, and most lately from Vetenskapsrådet (Swedish Research Council 2017-00955) and Swedish Governmental grants to the Sahlgrenska University Hospital, Västra Götalandsregionen under the ALF-agreement (ALFGBG-721971). As a research team, we sincerely thank all these agencies, which are each listed in the respective publications which they supported.

## ACKNOWLEDGMENTS

We thank Lena Kjellén and Paul O′Callaghan (Uppsala University) for valuable intellectual discussions. We also thank the proteomics Core Facility at the Sahlgrenska Academy, University of Gothenburg which performed most of the nLC-MS/MS-analyses referenced in this manuscript. The illustration was created with Biorender.com.

## REFERENCES


Appunni, S., Anand, V., Khandelwal, M., Gupta, N., Rubens, M., and Sharma, A. (2019). Small Leucine Rich Proteoglycans (decorin, biglycan and lumican) in cancer. *Clin. Chim. Acta* 491, 1–7. doi: 10.1016/j.cca.2019.01.003

Apweiler, R., Hermjakob, H., and Sharon, N. (1999). On the frequency of protein glycosylation, as deduced from analysis of the SWISS-PROT database. *Biochim. Biophys. Acta* 1473, 4–8. doi: 10.1016/s0304-4165(99)00165-8

Bradbury, E. J., Moon, L. D., Popat, R. J., King, V. R., Bennett, G. S., Patel, P. N., et al. (2002). Chondroitinase ABC promotes functional recovery after spinal cord injury. *Nature* 416, 636–640.

Briggs, D. C., and Hohenester, E. (2018). Structural Basis for the Initiation of Glycosaminoglycan Biosynthesis by Human Xylosyltransferase 1. *Structure* 26, 801–809.e3.

Chernykh, A., Kawahara, R., and Thaysen-Andersen, M. (2021). Towards structure-focused glycoproteomics. *Biochem. Soc. Trans.* 49, 161–186. doi: 10.1042/bst20200222

Clausen, T. M., Sandoval, D. R., Spliid, C. B., Pihl, J., Perrett, H. R., Painter, C. D., et al. (2020). SARS-CoV-2 Infection Depends on Cellular Heparan Sulfate and ACE2. *Cell* 183, 1043–1057.e15.

Coles, C. H., Shen, Y., Tenney, A. P., Siebold, C., Sutton, G. C., Lu, W., et al. (2011). Proteoglycan-specific molecular switch for RPTPsigma clustering and neuronal extension. *Science* 332, 484–488. doi: 10.1126/science.1200840

Daly, J. L., Simonetti, B., Klein, K., Chen, K. E., Williamson, M. K., Anton-Plagaro, C., et al. (2020). Neuropilin-1 is a host factor for SARS-CoV-2 infection. *Science* 370, 861–865.

Darula, Z., and Medzihradszky, K. F. (2018). Analysis of Mammalian O-Glycopeptides-We Have Made a Good Start, but There is a Long Way to Go. *Mol. Cell Proteomics* 17, 2–17. doi: 10.1074/mcp.mr117.000126

Delbaere, S., De Clercq, A., Mizumoto, S., Noborn, F., Bek, J. W., Alluyn, L., et al. (2020). b3galt6 Knock-Out Zebrafish Recapitulate β3GalT6-Deficiency Disorders in Human and Reveal a Trisaccharide Proteoglycan Linkage Region. *Front. Cell Dev. Biol.* 8:597857. doi: 10.3389/fcell.2020.597857

Doody, K. M., Stanford, S. M., Sacchetti, C., Svensson, M. N., Coles, C. H., Mitakidis, N., et al. (2015). Targeting phosphatase-dependent proteoglycan switch for rheumatoid arthritis therapy. *Sci. Transl. Med.* 7:288ra276.

Dwivedi, R., and Pomin, V. H. (2020). Marine Antithrombotics. *Mar. Drugs* 18:514. doi: 10.3390/md18100514

Esko, J. D., and Zhang, L. (1996). Influence of core protein sequence on glycosaminoglycan assembly. *Curr. Opin. Struct. Biol.* 6, 663–670. doi: 10.1016/s0959-440x(96)80034-0

Fisher, L. W., Termine, J. D., and Young, M. F. (1989). Deduced protein sequence of bone small proteoglycan I (biglycan) shows homology with proteoglycan II (decorin) and several nonconnective tissue proteins in a variety of species. *J. Biol. Chem.* 264, 4571–4576. doi: 10.1016/s0021-9258(18)83781-4

Gomez Toledo, A., Nilsson, J., Noborn, F., Sihlbom, C., and Larson, G. (2015). Positive Mode LC-MS/MS Analysis of Chondroitin Sulfate Modified Glycopeptides Derived from Light and Heavy Chains of The Human Inter-alpha-Trypsin Inhibitor Complex. *Mol. Cell Proteomics* 14, 3118–3131. doi: 10.1074/mcp.m115.051136

Gowda, D. C., Hogue-Angeletti, R., Margolis, R. K., and Margolis, R. U. (1990). Chromaffin granule and PC12 cell chondroitin sulfate proteoglycans and their relation to chromogranin A. *Arch. Biochem. Biophys.* 281, 219–224. doi: 10.1016/0003-9861(90)90435-2

Hatano, S., and Watanabe, H. (2020). Regulation of Macrophage and Dendritic Cell Function by Chondroitin Sulfate in Innate to Antigen-Specific Adaptive Immunity. *Front. Immunol.* 11:232. doi: 10.3389/fimmu.2020.00232

Hu, H. Z., Granger, N., Pai, S. B., Bellamkonda, R. V., and Jeffery, N. D. (2018). Therapeutic efficacy of microtube-embedded chondroitinase ABC in a canine clinical model of spinal cord injury. *Brain* 141, 1017–1027. doi: 10.1093/brain/awy007

Hu, J., Rodemer, W., Zhang, G., Jin, L. Q., Li, S., and Selzer, M. E. (2021). Chondroitinase ABC Promotes Axon Regeneration and Reduces Retrograde Apoptosis Signaling in Lamprey. *Front. Cell Dev. Biol.* 9:653638. doi: 10.3389/fcell.2021.653638

Hu, X., Villodre, E. S., Larson, R., Rahal, O. M., Wang, X., Gong, Y., et al. (2021). Decorin-mediated suppression of tumorigenesis, invasion, and metastasis in inflammatory breast cancer. *Commun. Biol.* 4:72. doi: 10.1201/b14586-5

Hussein, R. K., Mencio, C. P., Katagiri, Y., Brake, A. M., and Geller, H. M. (2020). Role of Chondroitin Sulfation Following Spinal Cord Injury. *Front. Cell Neurosci.* 14:208. doi: 10.3389/fncel.2020.00208

Iozzo, R. V. (2005). Basement membrane proteoglycans: from cellar to ceiling. *Nat. Rev. Mol. Cell. Biol.* 6, 646–656. doi: 10.1038/nrm1702

Iozzo, R. V., and Sanderson, R. D. (2011). Proteoglycans in cancer biology, tumour microenvironment and angiogenesis. *J. Cell Mol. Med.* 15, 1013–1031. doi: 10.1111/j.1582-4934.2010.01236.x

Iozzo, R. V., and Schaefer, L. (2015). Proteoglycan form and function: a comprehensive nomenclature of proteoglycans. *Matrix Biol.* 42, 11–55. doi: 10.1016/j.matbio.2015.02.003

Kane, E. G., and Taylor-Robinson, A. W. (2011). Prospects and Pitfalls of Pregnancy-Associated Malaria Vaccination Based on the Natural Immune Response to Plasmodium falciparum VAR2CSA-Expressing Parasites. *Malar. Res. Treat.* 2011:764845.

Kim, T., Tao-Cheng, J. H., Eiden, L. E., and Loh, Y. P. (2001). Chromogranin A, an "on/off" switch controlling dense-core secretory granule biogenesis. *Cell* 106, 499–509. doi: 10.1016/s0092-8674(01)00459-7

Kitagawa, H., Tsutsumi, K., Ikegami-Kuzuhara, A., Nadanaka, S., Goto, F., Ogawa, T., et al. (2008). Sulfation of the galactose residues in the glycosaminoglycan-protein linkage region by recombinant human chondroitin 6-O-sulfotransferase-1. *J. Biol. Chem.* 283, 27438–27443. doi: 10.1074/jbc.m803279200

Klein, J. A., Meng, L., and Zaia, J. (2018). Deep Sequencing of Complex Proteoglycans: a Novel Strategy for High Coverage and Site-specific Identification of Glycosaminoglycan-linked Peptides. *Mol. Cell Proteomics* 17, 1578–1590. doi: 10.1074/mcp.ra118.000766

Koike, T., Izumikawa, T., Sato, B., and Kitagawa, H. (2014). Identification of phosphatase that dephosphorylates xylose in the glycosaminoglycan-protein linkage region of proteoglycans. *J. Biol. Chem.* 289, 6695–6708. doi: 10.1074/jbc.m113.520536

Krusius, T., and Ruoslahti, E. (1986). Primary structure of an extracellular matrix proteoglycan core protein deduced from cloned cDNA. *Proc. Natl. Acad. Sci. U. S. A.* 83, 7683–7687. doi: 10.1073/pnas.83.20.7683

Lindahl, U., and Roden, L. (1966). The chondroitin 4-sulfate-protein linkage. *J. Biol. Chem.* 241, 2113–2119. doi: 10.1016/s0021-9258(18)96674-3

Lord, M. S., Day, A. J., Youssef, P., Zhuo, L., Watanabe, H., Caterson, B., et al. (2013). Sulfation of the bikunin chondroitin sulfate chain determines heavy chain.hyaluronan complex formation. *J. Biol. Chem.* 288, 22930–22941. doi: 10.1074/jbc.m112.404186

Lord, M. S., Melrose, J., Day, A. J., and Whitelock, J. M. (2020). The Inter-alpha-Trypsin Inhibitor Family: versatile Molecules in Biology and Pathology. *J. Histochem. Cytochem.* 68, 907–927. doi: 10.1369/0022155420940067

Lu, H., Mcdowell, L. M., Studelska, D. R., and Zhang, L. (2010). Glycosaminoglycans in Human and Bovine Serum: detection of Twenty-Four Heparan Sulfate and Chondroitin Sulfate Motifs Including a Novel Sialic Acid-modified Chondroitin Sulfate Linkage Hexasaccharide. *Glycobiol. Insights* 2010, 13–28. doi: 10.4137/gbi.s4273

Ly, M., Leach, F. E. III., Laremore, T. N., Toida, T., Amster, I. J., and Linhardt, R. J. (2011). The proteoglycan bikunin has a defined sequence. *Nat. Chem. Biol.* 7, 827–833. doi: 10.1038/nchembio.673

Ma, R., Lian, T., Huang, R., Renn, J. P., Petersen, J. D., Zimmerberg, J., et al. (2021). Structural basis for placental malaria mediated by Plasmodium falciparum VAR2CSA. *Nat. Microbiol.* 6, 380–391. doi: 10.1038/s41564-020-00858-9

Madsen, T. D., Hansen, L. H., Hintze, J., Ye, Z., Jebari, S., Andersen, D. B., et al. (2020). An atlas of O-linked glycosylation on peptide hormones reveals diverse biological roles. *Nat. Commun.* 11:4033.

Maeda, N. (2015). Proteoglycans and neuronal migration in the cerebral cortex during development and disease. *Front. Neurosci.* 9:98. doi: 10.3389/fnins.2015.00098

Maji, S. K., Perrin, M. H., Sawaya, M. R., Jessberger, S., Vadodaria, K., Rissman, R. A., et al. (2009). Functional amyloids as natural storage of peptide hormones in pituitary secretory granules. *Science* 325, 328–332. doi: 10.1126/science.1173155

Malfait, F., Kariminejad, A., Van Damme, T., Gauche, C., Syx, D., Merhi-Soussi, F., et al. (2013). Defective initiation of glycosaminoglycan synthesis due to B3GALT6 mutations causes a pleiotropic Ehlers-Danlos-syndrome-like connective tissue disorder. *Am. J. Hum. Genet.* 92, 935–945. doi: 10.1016/j.ajhg.2013.04.016

Momota, R., Naito, I., Ninomiya, Y., and Ohtsuka, A. (2011). Drosophila type XV/XVIII collagen, Mp, is involved in Wingless distribution. *Matrix Biol.* 30, 258–266. doi: 10.1016/j.matbio.2011.03.008

Montoliu-Gaya, L., Tietze, D., Kaminski, D., Mirgorodskaya, E., Tietze, A. A., and Sterky, F. H. (2021). CA10 regulates neurexin heparan sulfate addition via a direct binding in the secretory pathway. *EMBO Rep.* 22:e51349.

Muir, H. (1958). The nature of the link between protein and carbohydrate of a chondroitin sulphate complex from hyaline cartilage. *Biochem. J.* 69, 195–204. doi: 10.1042/bj0690195

Mukhamedshina, Y. O., Povysheva, T. V., Nikolenko, V. N., Kuznecov, M. S., Rizvanov, A. A., and Chelyshev, Y. A. (2019). Upregulation of proteoglycans in the perilesion perimeter in ventral horns after spinal cord injury. *Neurosci. Lett.* 704, 220–228. doi: 10.1016/j.neulet.2019.04.006

Mycroft-West, C. J., Su, D., Pagani, I., Rudd, T. R., Elli, S., Gandhi, N. S., et al. (2020). Heparin Inhibits Cellular Invasion by SARS-CoV-2: structural Dependence of the Interaction of the Spike S1 Receptor-Binding Domain with Heparin. *Thromb. Haemost.* 120, 1700–1715. doi: 10.1055/s-0040-1721319

Myron, P., Siddiquee, S., and Al Azad, S. (2014). Fucosylated chondroitin sulfate diversity in sea cucumbers: a review. *Carbohydr. Polym.* 112, 173–178. doi: 10.1016/j.carbpol.2014.05.091

Narimatsu, H., Kaji, H., Vakhrushev, S. Y., Clausen, H., Zhang, H., Noro, E., et al. (2018). Current Technologies for Complex Glycoproteomics and Their Applications to Biology/Disease-Driven Glycoproteomics. *J. Proteome Res.* 17, 4097–4112. doi: 10.1021/acs.jproteome.8b00515

Nasir, W., Toledo, A. G., Noborn, F., Nilsson, J., Wang, M., Bandeira, N., et al. (2016). SweetNET: a Bioinformatics Workflow for Glycopeptide MS/MS Spectral Analysis. *J. Proteome Res.* 15, 2826–2840. doi: 10.1021/acs.jproteome.6b00417

Neill, T., Schaefer, L., and Iozzo, R. V. (2016). Decorin as a multivalent therapeutic agent against cancer. *Adv. Drug Deliv. Rev.* 97, 174–185. doi: 10.1016/j.addr.2015.10.016

Nikpour, M., Nilsson, J., Persson, A., Noborn, F., Vorontsov, E., and Larson, G. (2021). Proteoglycan profiling of human, rat and mouse insulin-secreting cells. *Glycobiology* doi: 10.1093/glycob/cwab035 [Epub Online ahead of print].

Nilsson, J. (2016). Liquid chromatography-tandem mass spectrometry-based fragmentation analysis of glycopeptides. *Glycoconj. J.* 33, 261–272. doi: 10.1007/s10719-016-9649-3

Nilsson, J., Noborn, F., Gomez Toledo, A., Nasir, W., Sihlbom, C., and Larson, G. (2017). Characterization of Glycan Structures of Chondroitin Sulfate-Glycopeptides Facilitated by Sodium Ion-Pairing and Positive Mode LC-MS/MS. *J. Am. Soc. Mass Spectrom.* 28, 229–241. doi: 10.1007/s13361-016-1539-1

Nilsson, J., Ruetschi, U., Halim, A., Hesse, C., Carlsohn, E., Brinkmalm, G., et al. (2009). Enrichment of glycopeptides for glycan structure and attachment site identification. *Nat. Methods* 6, 809–811. doi: 10.1038/nmeth.1392

Noborn, F., Gomez Toledo, A., Green, A., Nasir, W., Sihlbom, C., Nilsson, J., et al. (2016). Site-specific identification of heparan and chondroitin sulfate glycosaminoglycans in hybrid proteoglycans. *Sci. Rep.* 6:34537.

Noborn, F., Gomez Toledo, A., Nasir, W., Nilsson, J., Dierker, T., Kjellen, L., et al. (2018). Expanding the chondroitin glycoproteome of Caenorhabditis elegans. *J. Biol. Chem.* 293, 379–389. doi: 10.1074/jbc.m117.807800

Noborn, F., Gomez Toledo, A., Sihlbom, C., Lengqvist, J., Fries, E., Kjellen, L., et al. (2015). Identification of chondroitin sulfate linkage region glycopeptides reveals prohormones as a novel class of proteoglycans. *Mol. Cell Proteomics* 14, 41–49. doi: 10.1074/mcp.m114.043703

Noborn, F., and Larson, G. (2021). Characterization of C. elegans Chondroitin Proteoglycans and Their Large Functional and Structural Heterogeneity; Evolutionary Aspects on Structural Differences Between Humans and the Nematode. *Adv. Exp. Med. Biol.* 21, 155–170. doi: 10.1007/5584_2020_485

Noborn, F. N., Persson, M., Sihlbom, A., Nilsson, C., and Larson, J. (2021). A Glycoproteomic Approach to Identify Novel Proteoglycans. *Methods Mol. Biol. Glycosaminoglycans, 978-1-0716-1397-9, 481765_2_En*, 2303, ed. K. Balagurunathan, et al.

Olofsson, S., and Bergström, T. (2005). Glycoconjugate glycans as viral receptors. *Ann. Med.* 37, 154–172. doi: 10.1080/07853890510007340

Olson, S. K., Bishop, J. R., Yates, J. R., Oegema, K., and Esko, J. D. (2006). Identification of novel chondroitin proteoglycans in Caenorhabditis elegans: embryonic cell division depends on CPG-1 and CPG-2. *J. Cell Biol.* 173, 985–994. doi: 10.1083/jcb.200603003

Pereira, N. A., Chan, K. F., Lin, P. C., and Song, Z. (2018). The "less-is-more" in therapeutic antibodies: Afucosylated anti-cancer antibodies with enhanced antibody-dependent cellular cytotoxicity. *MAbs* 10, 693–711. doi: 10.1080/19420862.2018.1466767

Persson, A., Nilsson, J., Vorontsov, E., Noborn, F., and Larson, G. (2019). Identification of a non-canonical chondroitin sulfate linkage region trisaccharide. *Glycobiology* 29, 366–371. doi: 10.1093/glycob/cwz014

Plomp, R., Ruhaak, L. R., Uh, H. W., Reiding, K. R., Selman, M., Houwing-Duistermaat, J. J., et al. (2017). Subclass-specific IgG glycosylation is associated with markers of inflammation and metabolic health. *Sci. Rep.* 7:12325.

Pomin, V. H., and Mulloy, B. (2018). Glycosaminoglycans and Proteoglycans. *Pharmaceuticals (Basel)* 11:27.

Reszegi, A., Horvath, Z., Feher, H., Wichmann, B., Tatrai, P., Kovalszky, I., et al. (2020). Protective Role of Decorin in Primary Hepatocellular Carcinoma. *Front. Oncol.* 10:645. doi: 10.3389/fonc.2020.00645

Roden, L., and Smith, R. (1966). Structure of the neutral trisaccharide of the chondroitin 4-sulfate-protein linkage region. *J. Biol. Chem.* 241, 5949–5954. doi: 10.1016/s0021-9258(18)96362-3

Schjoldager, K. T., Narimatsu, Y., Joshi, H. J., and Clausen, H. (2020). Global view of human protein glycosylation pathways and functions. *Nat. Rev. Mol. Cell Biol.* 21, 729–749. doi: 10.1038/s41580-020-00294-x

Schneider, M., Al-Shareffi, E., and Haltiwanger, R. S. (2017). Biological functions of fucose in mammals. *Glycobiology* 27, 601–618. doi: 10.1093/glycob/cwx034

Shatton, J., and Schubert, M. (1954). Isolation of a mucoprotein from cartilage. *J. Biol. Chem.* 211, 565–573. doi: 10.1016/s0021-9258(18)71147-2

Sugahara, K., Yamashina, I., De Waard, P., Van Halbeek, H., and Vliegenthart, J. F. (1988). Structural studies on sulfated glycopeptides from the carbohydrate-protein linkage region of chondroitin 4-sulfate proteoglycans of swarm rat chondrosarcoma. Demonstration of the structure Gal(4-O-sulfate)beta 1-3Gal beta 1-4XYL beta 1-O-Ser. *J. Biol. Chem.* 263, 10168–10174. doi: 10.1016/s0021-9258(19)81492-8

Sugiura, N., Clausen, T. M., Shioiri, T., Gustavsson, T., Watanabe, H., and Salanti, A. (2016). Molecular dissection of placental malaria protein VAR2CSA interaction with a chemo-enzymatically synthesized chondroitin sulfate library. *Glycoconj. J.* 33, 985–994. doi: 10.1007/s10719-016-9685-z

Takemura, M., Noborn, F., Nilsson, J., Bowden, N., Nakato, E., Baker, S., et al. (2020). Chondroitin sulfate proteoglycan Windpipe modulates Hedgehog signaling in Drosophila. *Mol. Biol. Cell* 31, 813–824. doi: 10.1091/mbc.e19-06-0327

Thaysen-Andersen, M., Packer, N. H., and Schulz, B. L. (2016). Maturing Glycoproteomics Technologies Provide Unique Structural Insights into the N-glycoproteome and Its Regulation in Health and Disease. *Mol. Cell Proteomics* 15, 1773–1790. doi: 10.1074/mcp.o115.057638

Toledo, A. G., Pihl, J., Spliid, C. B., Persson, A., Nilsson, J., Pereira, M. A., et al. (2020). An Affinity-Chromatography and Glycoproteomics Workflow to Profile the Chondroitin Sulfate Proteoglycans that interact with malarial

VAR2CSA in the Placenta and in Cancer. *Glycobiology* 30, 989–1002. doi: 10.1093/glycob/cwaa039

Tomlinson, A., Semblat, J. P., Gamain, B., and Chene, A. (2020). VAR2CSA-Mediated Host Defense Evasion of Plasmodium falciparum Infected Erythrocytes in Placental Malaria. *Front. Immunol.* 11:624126. doi: 10.3389/fimmu.2020.624126

Wang, T. T., and Ravetch, J. V. (2019). Functional diversification of IgGs through Fc glycosylation. *J. Clin. Invest.* 129, 3492–3498. doi: 10.1172/jci130029

Wen, J., Xiao, J., Rahdar, M., Choudhury, B. P., Cui, J., Taylor, G. S., et al. (2014). Xylose phosphorylation functions as a molecular switch to regulate proteoglycan biosynthesis. *Proc. Natl. Acad. Sci. U. S. A.* 111, 15723–15728.

Zhang, P., Lu, H., Peixoto, R. T., Pines, M. K., Ge, Y., Oku, S., et al. (2018). Heparan Sulfate Organizes Neuronal Synapses through Neurexin Partnerships. *Cell* 174, 1450–1464.e23.

Zhu, F., Li, D., and Chen, K. (2019). Structures and functions of invertebrate glycosylation. *Open Biol.* 9:180232.

**Conflict of Interest:** The authors declare that the research was conducted in the absence of any commercial or financial relationships that could be construed as a potential conflict of interest.

**Publisher's Note:** All claims expressed in this article are solely those of the authors and do not necessarily represent those of their affiliated organizations, or those of the publisher, the editors and the reviewers. Any product that may be evaluated in this article, or claim that may be made by its manufacturer, is not guaranteed or endorsed by the publisher.

frontiers in Cell and Developmental Biology

BRIEF RESEARCH REPORT
published: 06 September 2021
doi: 10.3389/fcell.2021.709018

# Novel Insight Into Glycosaminoglycan Biosynthesis Based on Gene Expression Profiles

*Yi-Fan Huang[1], Shuji Mizumoto[2] and Morihisa Fujita[1]**

[1] *Key Laboratory of Carbohydrate Chemistry and Biotechnology, Ministry of Education, School of Biotechnology, Jiangnan University, Wuxi, China,* [2] *Department of Pathobiochemistry, Faculty of Pharmacy, Meijo University, Nagoya, Japan*

Glycosaminoglycans (GAGs) including chondroitin sulfate, dermatan sulfate, heparan sulfate, and keratan sulfate, except for hyaluronan that is a free polysaccharide, are covalently attached to core proteins to form proteoglycans. More than 50 gene products are involved in the biosynthesis of GAGs. We recently developed a comprehensive glycosylation mapping tool, GlycoMaple, for visualization and estimation of glycan structures based on gene expression profiles. Using this tool, the expression levels of GAG biosynthetic genes were analyzed in various human tissues as well as tumor tissues. In brain and pancreatic tumors, the pathways for biosynthesis of chondroitin and dermatan sulfate were predicted to be upregulated. In breast cancerous tissues, the pathways for biosynthesis of chondroitin and dermatan sulfate were predicted to be up- and down-regulated, respectively, which are consistent with biochemical findings published in the literature. In addition, the expression levels of the chondroitin sulfate-proteoglycan versican and the dermatan sulfate-proteoglycan decorin were up- and down-regulated, respectively. These findings may provide new insight into GAG profiles in various human diseases including cancerous tumors as well as neurodegenerative disease using GlycoMaple analysis.

**Keywords: dermatan sulfate (DS), chondroitin sulfate (CS), glycosaminoglycan (GAG), GlycoMaple, heparan sulfate (HS), hyaluronan (HA), keratan sulfate (KS), proteoglycan (PG)**

OPEN ACCESS

***Edited by:***
*Ayano Satoh,*
*Okayama University, Japan*

***Reviewed by:***
*Kristian Prydz,*
*University of Oslo, Norway*
*Nikos Karamanos,*
*University of Patras, Greece*

****Correspondence:***
*Morihisa Fujita*
*fujita@jiangnan.edu.cn*

***Specialty section:***
*This article was submitted to Signaling, a section of the journal Frontiers in Cell and Developmental Biology*

***Received:*** *13 May 2021*
***Accepted:*** *18 August 2021*
***Published:*** *06 September 2021*

***Citation:***
*Huang Y-F, Mizumoto S and Fujita M (2021) Novel Insight Into Glycosaminoglycan Biosynthesis Based on Gene Expression Profiles. Front. Cell Dev. Biol. 9:709018. doi: 10.3389/fcell.2021.709018*

## INTRODUCTION

Glycosaminoglycans (GAGs) are linear polysaccharides consisting of repeating disaccharide units. Among these are heparin, heparan sulfate (HS), chondroitin sulfate (CS), dermatan sulfate (DS), and keratan sulfate (KS), which are covalently bound to core proteins, forming proteoglycans (PGs) (Kjellen and Lindahl, 1991; Iozzo, 1998; Lindahl et al., 2015). Hyaluronan (HA) is a free polysaccharide (Lindahl and Rodén, 1972; Hascall, 2019). PGs are distributed in the extracellular matrix and on cell surfaces, and are crucially involved in a wide range of biological processes such as cell adhesion, the regulation of cellular signaling, and assembly of the extracellular matrix (Esko and Selleck, 2002; Häcker et al., 2005; Bülow and Hobert, 2006; Bishop et al., 2007; Sarrazin et al., 2011; Thelin et al., 2013; Xu and Esko, 2014; Mizumoto et al., 2015; Neill et al., 2015).

CS, DS, and HS are covalently linked to specific serine residues usually flanked by a glycine residue on core proteins via a common linker tetrasaccharide region, GlcAβ1–3Gaβ1–3Galβ1–4Xylβ1–*O*–, where GlcA, Gal, and Xyl stand for glucuronic acid, galactose, and xylose, respectively (Lindahl and Rodén, 1972; Sugahara and Kitagawa, 2000). The biosynthesis of the linker tetrasaccharide is initiated by the transfer of β-Xyl from uridine diphosphate

(UDP)-Xyl to the specific serine residue(s) on the core proteins of PGs by β-xylosyltransferase (XYLT) encoded by *XYLT1* or *XYLT2* (Götting et al., 2000; Pönighaus et al., 2007) at the endoplasmic reticulum, endoplasmic reticulum-Golgi intermediate compartment, or *cis*-Golgi apparatus (Prydz, 2015). Then, a second Gal is transferred from UDP-Gal to Xylβ-*O*-serine by β4-galactosyltransferase-I encoded by *B4GALT7* (Almeida et al., 1999; Okajima et al., 1999). The C2-position of Xyl is phosphorylated by xylosylkinase encoded by *FAM20B* (Koike et al., 2009). A third Gal is added to the second Gal residue on the Galβ1–4Xylβ-*O*-serine from UDP-Gal by β3-galactosyltransferase-II encoded by *B3GALT6* (Bai et al., 2001). β3-Glucuronosyltransferase-I encoded by *B3GAT3* transfers GlcA to Galβ1–3Galβ1–4Xylβ-*O*-serine from UDP-GlcA (Kitagawa et al., 1998). Then, a phosphate group in GlcAβ1–3Galβ1–3Galβ1–4Xyl(2-*O*-phosphate) is removed by 2-*O*-phosphoxylose phosphatase encoded by *PXYLP1* (Koike et al., 2014). The types of GAGs including CS, DS, or HS extended from the linker tetrasaccharide are determined by the structure of the core protein, sulfation and phosphorylation status on the tetrasaccharide, and the biochemical environment of GAGosome, which is a complex of enzymes and regulatory factors in the Golgi apparatus (Sugahara and Kitagawa, 2000; Presto et al., 2008; Prydz, 2015; Izumikawa, 2019).

Heparan sulfate consists of repeating disaccharide units of *N*-acetylglucosamine (GlcNAc) (Rodén et al., 1992), and GlcA that are polymerized onto the linker tetrasaccharide region of specific core proteins (Lidholt et al., 1989; Lindahl, 1989; Esko and Selleck, 2002; Kim et al., 2003). The initial GlcNAc residue is transferred from UDP-GlcNAc to the tetrasaccharide by α4-*N*-acetylglucosaminyltransferase (GlcNAcT)-I encoded by *exostosin-like 2* (*EXTL2*) or *EXTL3* (Kitagawa et al., 1999; Kim et al., 2001). Thereafter, polymerization of the HS-repeating disaccharide region, $[-3GalNAc\alpha1-4GlcA\beta1-]_n$, occurs by enzymatic activities designated as HS-β4-glucuronosyltransferase-II (HS-GlcAT-II) and GlcNAcT-II, which are catalyzed by a HS polymerase enzyme hetero-complex composed of exostosin 1 (EXT1) and EXT2 (Lind et al., 1998; McCormick et al., 1998; Kim et al., 2003). EXTL1 and EXTL3 also show GlcNAcT-II activity (Kim et al., 2001). The GlcNAc residue on the repeating unit is partially converted to *N*-sulfated glucosamine by a dual enzyme, *N*-deacetylase/*N*-sulfotransferase encoded by *NDST1*, *NDST2*, *NDST3*, or *NDST4* (Hashimoto et al., 1992; Eriksson et al., 1994; Aikawa and Esko, 1999; Aikawa et al., 2001). HS C5-epimerase encoded by *GLCE* converts GlcA residues, which are located on the non-reducing side of *N*-sulfated glucosamine in the repeating disaccharide region of HS, iduronic acid (IdoA) (Li et al., 1997). The disaccharide region can be further *O*-sulfated at the C2 position of IdoA by HS 2-*O*-sulfotransferases, and *O*-sulfated at C3 and C6 positions of GlcNAc or *N*-sulfated glucosamine by HS 3-*O*-sulfotransferases and HS 6-*O*-sulfotransferases, respectively. 3′-phosphoadenosine 5′-phosphosulfate (PAPS) is utilized as the substrate for the sulfation reaction (Kusche-Gullberg and Kjellen, 2003). PAPS is synthesized from ATP and an inorganic sulfate in the cytosol by PAPS synthase encoded by *PAPSS1* or *PAPSS2* (Venkatachalam, 2003). PAPS is transported into the Golgi lumen from the cytosol by two PAPS transporters encoded by *SLC35B2* and *SLC35B3* (Kamiyama et al., 2003, 2006).

The repeating disaccharide region of CS and DS, $[-4GlcA\beta1-3N$-acetylgalactosamine $(GalNAc)\beta1-]_n$ and $[-4IdoA\beta1-3GalNAc\beta1-]_n$, respectively, is also attached to a linker tetrasaccharide, GlcA-Gal-Gal-Xyl, on a serine residue of specific core proteins (Lindahl and Rodén, 1972; Fransson et al., 1993; Lamari and Karamanos, 2006). The initial GalNAc residue is transferred from UDP-GalNAc to the tetrasaccharide by β4-*N*-acetylgalactosaminyltransferase (GalNAcT)-I encoded by *CSGALNACT1* or *CSGALNACT*2 (Uyama et al., 2002, 2003). The CS-repeating disaccharide region is formed by the alternative addition of GlcA and GalNAc residues from UDP-GlcA and UDP-GalNAc to the non-reducing end of the linker region tetrasaccharide, GlcA-Gal-Gal-Xyl, by CS-GlcAT-II and GalNAcT-II activities, respectively, of a chondroitin synthase (CHSY) family member including CHSY1, CHSY3, chondroitin polymerizing factor (CHPF), and CHPF2 (Kitagawa et al., 2001, 2003; Izumikawa et al., 2007, 2008). The combination of any two heterocomplexes of these five proteins exerts polymerization activity to build the repeating disaccharide region of CS (Kitagawa et al., 2001, 2003; Izumikawa et al., 2007, 2008). After or during biosynthesis of the disaccharide region, GlcA residues in the chondroitin precursor chain are epimerized to IdoA by DS-epimerase encoded by *DSE* or *DSEL* (Maccarana et al., 2006; Pacheco et al., 2009). The CS and DS repeating disaccharide regions, $[-4GlcA\beta1-3GalNAc\beta1-]_n$ and $[-4IdoA\beta1-3GalNAc\beta1-]_n$, respectively, can be modified by sulfation at C4 and C6 positions of GalNAc and C2 position of GlcA and IdoA by chondroitin 4-*O*-sulfotransferases, chondroitin 6-*O*-sulfotransferases, and uronyl 2-*O*-sulfotransferase, respectively (Kusche-Gullberg and Kjellen, 2003).

Keratan sulfate consists of sulfated poly-*N*-acetyllactosamine, $[-4GlcNAc\beta1-3Gal\beta1-]_n$, which is bound to serine, threonine, or asparagine on specific core proteins through the linkage region such as O-linked or N-linked oligosaccharides, respectively (Stuhlsatz et al., 1989; Caterson and Melrose, 2018). The biosynthesis of the repeating disaccharide region of KS is initiated by β3-*N*-acetylglucosaminyltransferase encoded by *B3GNT7* (Seko and Yamashita, 2004; Kitayama et al., 2007). Thereafter, GlcNAc 6-*O*-sulfotransferase encoded by *CHST5* or *CHST6* transfers a sulfate group from PAPS to the GlcNAc residue (Akama et al., 2001, 2002; Narentuya et al., 2019), following the addition of a Gal residue to the GlcNAc6-*O*-sulfate residue by β4-galactosyltransferase encoded by *B4GALT4* (Seko et al., 2003; Kitayama et al., 2007). After the construction of polysaccharide, $[-4GlcNAc(6S)\beta1-3Gal\beta1-]_n$, KS Gal 6-*O*-sulfotransferase is encoded by *CHST1* (Fukuta et al., 1997; Akama et al., 2002). KS-PGs are distributed widely in the cornea, cartilage, and brain, and play important roles in collagen fibrillogenesis, tissue hydration, neurotransmission, and nerve regeneration (Caterson and Melrose, 2018).

Hyaluronan is a high molecular weight, natural polymer composed of a repeating disaccharide, $[-4GlcA\beta1-3GlcNAc\beta1-]_n$ (Rodén, 1980; Hascall and Esko, 2015; Abbruzzese et al., 2017; Hascall, 2019). HA is synthesized from cytosolic UDP-GlcNAc

and UDP-GlcA by hyaluronan synthase 1 (HAS1), HAS2, or HAS3 at the plasma membrane (Itano and Kimata, 2002), whereas other GAGs are synthesized in the secretory pathway. HAS1 and HAS2 contribute to the synthesis of longer hyaluronan ($\sim 2 \times 10^6$ Da and $> 2 \times 10^6$ Da, respectively), whereas HAS3 synthesizes a markedly shorter hyaluronan ($\sim 1 \times 10^6$ Da) (Itano et al., 1999). HA is a major component of the extracellular matrix, and is not covalently attached to a core protein (Lindahl and Rodén, 1972; Hascall, 2019). During the tissue injury and repair process, HA is actively produced and plays important roles (Liang et al., 2016).

The abundance of GAGs and their pattern of sulfation are dynamically altered, affecting GAG–protein interactions (Kjellen and Lindahl, 2018) during a number of physiological and pathological processes, such as differentiation, tumorigenesis, inflammation, and bacterial and viral infections (Sasisekharan et al., 2002; Bishop et al., 2007; Iozzo and Sanderson, 2011; Jiang et al., 2011; Kam and Alexander, 2014; Baghy et al., 2016; Morla, 2019). Therefore, the analyses of changes in content as well as sulfation pattern of GAGs are required to elucidate the pathogenesis. However, these analyses are complicated and require special techniques. We previously established GlycoMaple, a comprehensive glycosylation mapping tool based on genetic expression profiles (Huang et al., 2021). With this tool, the expression profiles of glycan-related genes are mapped into glycan metabolic pathways to visualize and estimate glycan biosynthesis or degradation using transcriptional data. Transcripts per million transcripts (TPM) values of genes in RNA-Seq analyses are commonly utilized to evaluate and compare gene expression levels among samples from distinct cells or tissues. By uploading RNA-Seq data, glycan metabolic pathways in the tissue of interest can be automatically drawn to understand the glycosylation process. In this study, the expression levels of genes involved in GAG biosynthetic pathways in various tissues and tumor tissues have been addressed using gene expression profile data available in public databases, thereby allowing the estimation and comparison of amounts as well as sulfation pattern of GAGs between normal and disease states.

## METHODS

Expression data of GAG-related genes (**Supplementary Table 1**) in 37 human tissues were downloaded from the Human Protein Atlas database[1] (**Supplementary Table 2**). TPM values of GAG-related genes (**Supplementary Table 1**) and PG genes (**Supplementary Table 3**) from healthy tissue in GTEx and primary tumor tissues in TCGA were obtained from UCSC Xena[2] (Goldman et al., 2020). Raw data ($\log_2$[TPM + 0.001]) in Xena were converted to TPM values (**Supplementary Tables 4, 6**). TPM values of samples were input in GlycoMaple, and then pathways were visualized (Huang et al., 2021). When several genes overlapped in a reaction, the maximum TPM value among the values of overlapping genes was used to represent this reaction. When several gene products comprised a reaction complex, the minimum TPM value of the subunit genes was used to represent the reaction. To compare GAG biosynthetic pathways between tumor and normal tissues, fold changes in expression of genes, whose median TPM + 1 values increased by >1.5 and decreased by <0.667, are shown as pink and green arrows, respectively, in the pathways. The heatmaps and boxplots for gene expression profiles were drawn by R (ver. 3.6.2) (R Foundation for Statistical Computing, Vienna, Austria). The data used for boxplots were converted to $\log_2$ (TPM + 1). The Wilcoxon matched-pairs signed rank test was used to compare gene expression levels between primary tumor and normal tissues.

[1]https://www.proteinatlas.org/download/rna_tissue_hpa.tsv.zip

[2]https://xenabrowser.net/

## RESULTS AND DISCUSSION

### GAG Expression Profiles of Human Tissues

We previously listed 950 human glycan-related genes and established a tool named GlycoMaple, which can visualize 19 human glycan metabolic pathways and estimate the glycan structures synthesized in cells or tissues (Huang et al., 2021). In this study, we focused on GAG biosynthetic pathways. Among 950 glycan-related genes, those involved in: (1) biosynthesis of GAG backbones, (2) sulfation modification of HS, (3) sulfation modification of CS and DS, (4) biosynthesis of KS, and (5) biosynthesis and catabolism of HA in GlycoMaple pathways, were selected as GAG-related genes (**Supplementary Figure 1**). In addition, genes encoding PAPS transporters (*SLC35B2* and *SLC35B3*), a UDP-Xyl and UDP-GlcNAc transporter (*SLC35B4*), and a UDP-Gal transporter (*SLC35A2*) were included. *PAPSS1* and *PAPSS2*, *CANT1*, and *IMPAD1/BPNT2* encoding PAPS synthases 1 and 2, calcium-activated nucleotidase 1/UDP-diphosphatase, and 3′-phosphoadenosine 5′-phosphate 3′-phosphatase, respectively, were also listed. Furthermore, genes encoding regulators of GAG biosynthesis such as maintenance of Golgi-resident glycosyltransferases (*GOLPH3*) (Chang et al., 2013), a Golgi-localized protease (*SPPL3*) (Kuhn et al., 2015), a transcriptional regulator (*ZNF263*) (Weiss et al., 2020), and an epigenetic factor (*KDM2B*) (Weiss et al., 2021) were also added to the list. In total, 66 genes were listed in these categories (**Supplementary Table 1**).

To evaluate GAG biosynthesis capability in human tissue, we used RNA-Seq data from 37 human tissues, obtained from the Human Protein Atlas (Pontén et al., 2008). TPM is a value that indicates how many transcripts are present in each transcript when there are 1 million total transcripts in the sample (Wagner et al., 2012). The TPM is a method frequently utilized for comparing samples. First, gene expression profiles in each reaction were compared among tissues (**Figure 1**). The tissues were clustered into two groups by gene expression profiles of GAG biosynthetic reactions. One cluster included the cerebral cortex, thyroid gland, placenta, testis, ovary, endometrium, smooth muscle, cervix/uterine, prostate, fallopian tube, seminal vesicle, adrenal gland, parathyroid gland, spleen, lymph node, skin, lung, urinary bladder, appendix, and gallbladder. This

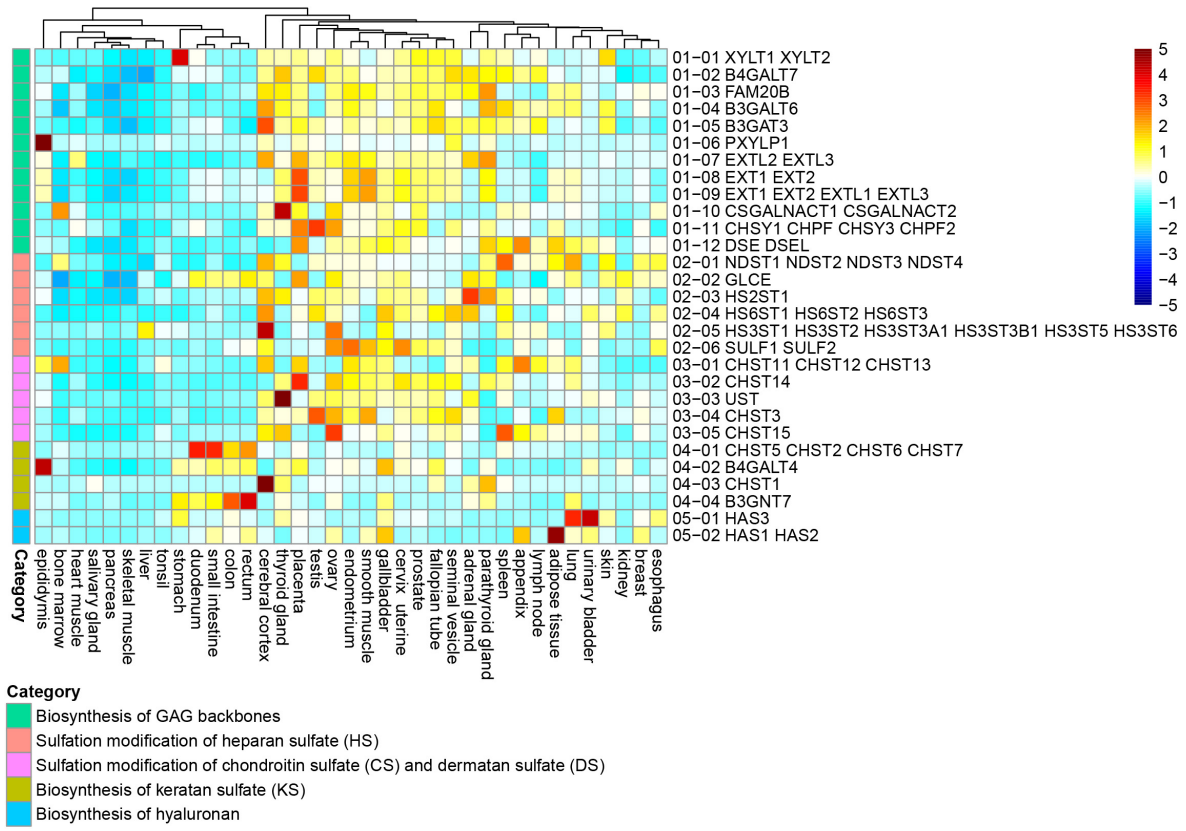


**FIGURE 1 |** Expression profiles of GAG-related genes in human tissues. Expression data of genes responsible for 29 reactions in five categories including biosynthesis of GAG backbones (green), sulfation of HS (red), sulfation of CS and DS (pink), biosynthesis of KS (ocher), and biosynthesis of HA (blue). Expression data were obtained from 37 human tissues of the Human Protein Atlas. The reaction numbers are correlated with **Supplementary Figure 1** and **Supplementary Table 1**. Transcripts per million transcripts (TPM) values in each of 29 reactions were normalized (*z*-score) and visualized as a heatmap.

cluster showed relatively higher expression of GAG-related genes, suggesting stronger productive ability of GAGs. In contrast, tissues such as the tonsil, liver, skeletal muscle, pancreas, salivary gland, and heart muscle were clustered together in the same tree because of lower expression of GAG-related genes. Certain digestive organs including the duodenum, small intestine, colon, and rectum were sub-clustered in this group because of the relatively low expression of genes involved in the biosynthesis of HS, CS, and DS. Instead, genes required for KS biosynthesis were expressed in the digestive tissues.

We next examined the Pearson correlation of 66 GAG-related gene expression in 37 human tissues to identify similarities in the expression patterns. In the Pearson correlation heatmap for GAG-related genes, many genes required for the biosynthesis of GAG backbones, including *XYLT1*, *XYLT2*, *FAM20B*, *B4GALT7*, *B3GALT6*, *B3GAT3*, *EXT1*, *EXT2*, *EXTL2*, *EXTL3*, *CHSY1*, *CHSY3*, *CHPF*, *CHPF2*, *CSGALNACT1*, *DSE*, and *DSEL*, clustered together (**Figure 2** and **Supplementary Table 2**). The expression patterns of regulator genes for GAG biosynthesis including *SPPL3*, *GOLPH3*, and *ZNF263*, and *SLC35B2*, *SLC35B4*, *PAPSS1*, and *IMPAD1*, which encode a PAPS transporter, UDP-Xyl/UDP-GlcNAc dual transporter, PAPS synthase 1, and 3′-phosphoadenosine 5′-phosphate 3′-phosphatase, respectively, were also correlated with genes required for biosynthesis of sulfated GAGs in human tissues (**Figure 2** and **Supplementary Table 2**). These findings suggest that expression levels of these genes are regulated by similar mechanisms such as regulation by corresponding signal transductions as well as transcriptional factors. On the other hand, some other genes encoding regulators and transporters were not clustered in the group (**Figure 2**). For example, the expression patterns of *SLC35A2*, whose gene product imports UDP-Gal into the lumen of the Golgi apparatus, were different from those of genes categorized as necessary for the biosynthesis of GAG backbones. This is reasonable because UDP-Gal is utilized not only for GAG biosynthesis, but also for biosynthesis of other glycans, such as *N*-glycans, mucin-type *O*-glycans, and glycolipid. *HAS1* and *HAS2*, which encode hyaluronan synthase to produce a higher molecular weight form of HA, shared close expression patterns (**Figure 2**), indicating linkage between gene function and transcriptional regulation. Genes required for sulfation of GAGs were distributed in different trees, although some of them, such as *NDST3*, *HS3ST2*, *HS3ST3*, and *HS3ST5*, showed correlated expression patterns in normal human tissues (**Figure 2** and **Supplementary Table 2**). It has been reported that several genes such as *B3GAT3*, *EXT2*, *GLCE*,

*NDST2*, *HS3ST1*, *HS3ST6*, *HS6ST1*, and *CSGALNACT2* are upregulated by treatment with 4-methylumbelliferyl-β-xyloside, which inhibits the biosynthesis of GAGs (Sasaki et al., 2019). Some of these genes possess enhancer elements named PG stress response elements, PGSE-A and PGSE-B, in their promoter region, which regulate the transcription activation upon Golgi stress caused by PG defects (Sasaki et al., 2019). Among these genes, *CSGALNACT2*, *NDST2*, and *HS3ST1* were clustered in the Pearson correlation heatmap (**Figure 2**), suggesting that their expression levels are regulated in a common manner.

## Prediction of Alterations in GAG Structure in Human Tumor Tissues

Because GAGs are involved in cell adhesion, migration, proliferation, and inflammation, changes in GAG levels can affect tumor development (Sasisekharan et al., 2002; Bishop et al., 2007; Iozzo and Sanderson, 2011; Mizumoto and Sugahara, 2013; Wei et al., 2020). The GlycoMaple tool can compare glycan metabolic pathways between two samples based on gene expression data. The comparison function enables us to reveal underlying changes of PGs or GAGs between normal and tumor tissues. We compared GAG biosynthetic pathways between several primary tumor and normal tissues using RNA-Seq data from two public databases: the Cancer Genome Atlas Program (TCGA) and Genotype-Tissue Expression Project (GTEx) (GTEx Consortium, 2017; Hoadley et al., 2018). TPM values of GAG-related genes were used as expression values, which were obtained from RNA-Seq data of primary tumor and normal tissue samples (brain, pancreas, breast, adrenal glands, and thyroid glands) processed in UCSC Xena (Goldman et al., 2020). Based on these expression values, GAG biosynthetic pathways were then analyzed using GlycoMaple.

Spatio/temporal expression of PGs and biosynthesis of GAGs are critical for establishment and maintenance of fundamental functions of the central nervous system (Karamanos et al., 2018). In brain cancers, various GAG and PG levels have been reported to change (Vitale et al., 2019). The medians of TPM from 662 primary brain tumors and 1,146 normal brain tissues were added into the glycosylation pathways. Pink and green arrows indicate whether expression of the genes (TPM + 1) coding the GAG biosynthetic enzymes were increased more than 1.5-fold and decreased to less than 0.667-fold, respectively, in primary tumors, when compared with the corresponding normal tissues (**Figure 3**). In primary brain tumor samples, many of the reaction steps in GAG biosynthesis were upregulated (**Figure 3**). In particular, almost all of the reactions involved in the biosynthesis of GAG backbones were markedly increased (**Figure 3A**). The expression levels of *XYLT1*, *XYLT2*, *B4GALT7*, *B3GALT6*, *PXYLP1*, *EXT1*, *EXT2*, *EXTL3*, *CHSY1*, *CHPF*, *CHPF2*, *CSGALNACT1*, *DSE*, and *DSEL* were increased (**Figure 3B**). In addition, sulfation of chondroitin and dermatan was predicted to increase in the brain during tumorigenesis, as contributed by *CHST3*, *CHST11*, *CHST12*, *CHST14*, *CHST15*, and *UST* (**Figures 3C,D**). Besides, the expression levels of several genes encoding core proteins of PG were increased to varying degrees (**Supplementary Figure 2A** and **Supplementary Table 4**). It has been reported that various PGs are upregulated in brain cancers. For example, high levels of HA receptors including *epican* (*CD44*) were correlated with poor prognosis in cancer patients (Yan and Wang, 2020). RNA levels for *fibronectin* (*FN1*), *brevican* (*BCAN*), *versican* (*VCAN*), *perlecan* (*HSPG2*), and several laminins were high in glioblastomas compared with in the normal brain (Dzikowski et al., 2021; von Spreckelsen et al., 2021). A high level of *CD74* was expressed in the monocytic subset of immune suppressive myeloid-derived suppressor cells and localized in the tumor microenvironment (Alban et al., 2020). *Glypican 2* (*GPC2*) was selectively expressed in neuroblastoma (Nagarajan et al., 2018). In our analysis, particularly, transcript levels of *CD44*, *BCAN*, *VCAN*, *CD74*, and *GPC2* increased more than five-fold and were the most upregulated PGs in brain tumor tissues, whereas only the expression of *GPC5* was downregulated among the PGs (**Supplementary Figure 2A** and **Supplementary Tables 4**, **5**). This prediction is consistent with previous reports that PGs help drive multiple oncogenic pathways in tumor cells and promote critical tumor–microenvironment interactions in cancer (Iozzo and Sanderson, 2011; Wade et al., 2013; Theocharis et al., 2015; Schaefer et al., 2017; Yan and Wang, 2020). Furthermore, the expression levels of genes involved in the regulation of GAG biosynthesis such as *SPPL3*, *GOLPH3*, *ZNF263*, and *KDM2B*; in the biosynthesis of a sulfate donor, PAPS synthase encoded by *PAPSS1* and *PAPSS2*; in the transport of PAPS encoded by *SLC35B2*; and in the catabolism of UDP and 3′-phosphoadenosine 5′-phosphate encoded by *CANT1* and *IMPAD1*, respectively, were also increased by more than 1.5 times in brain tumors compared with normal tissues (**Supplementary Figure 2B** and **Supplementary Table 4**). These results suggest that demand for the biosynthesis and sulfation of GAGs changes the expression of regulator genes, which might affect the amount as well as sulfation patterns of GAGs. In contrast, the expression levels of biosynthetic enzymes for HA and KS did not show a definite trend between normal and tumor tissues based upon GlycoMaple predictions (data not shown). This indicates that expression levels of biosynthetic enzymes for HA as well as KS and catabolic enzymes for HA might not significantly change, at least in the brain tumors examined.

We also analyzed GAG pathways in pancreatic carcinoma. GAGs are produced at low levels in healthy pancreatic tissue (Theocharis et al., 2000). In contrast, the amounts of GAGs in human pancreatic carcinoma are increased 4-fold, and in particular, show a 22-fold increase of CS and 12-fold increase of HA (Theocharis et al., 2000). The emerging expression of GAGs is considered to be a biological tumor marker for pancreatic tissues. The medians of TPM from 178 primary pancreatic tumors and 165 normal tissues were used to visualize the glycosylation pathways in GlycoMaple. Almost all steps involved in GAG biosynthesis including HS, CS, DS, KS, and HA were expressed in the pancreatic tumor tissues, and increased markedly compared with healthy tissues (**Supplementary Figure 3**), which was partially consistent with previous reports (Theocharis et al., 2000; Skandalis et al., 2006). It should be noted, however, that the reports showed no changes in the content or molecular size of HS, suggesting that *in silico* analysis is not always correct. In addition, it was reported that 6-*O*-sulfated CS on two PGs, versican

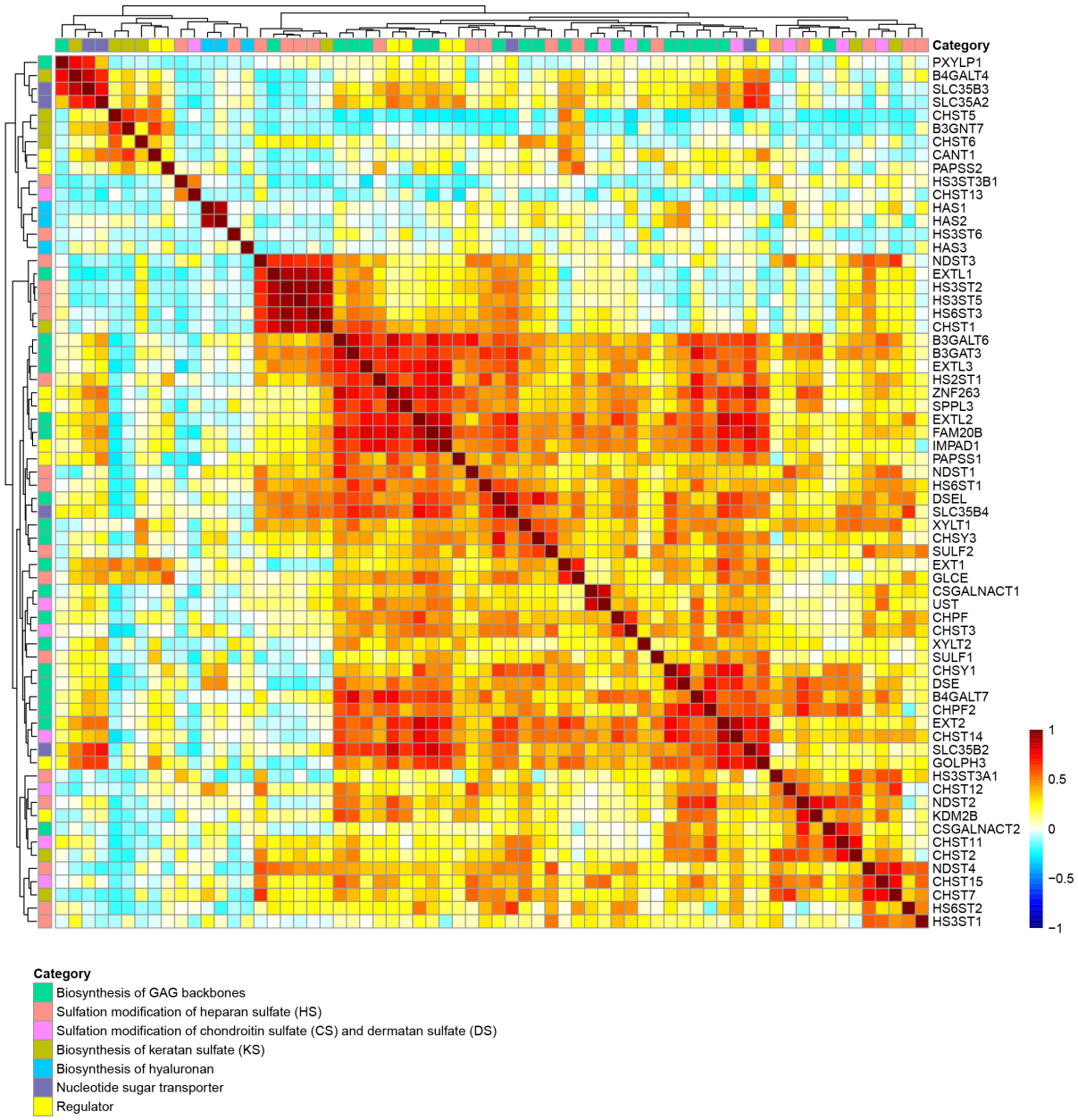


**FIGURE 2 |** Correlation of expression of GAG-related genes among human tissues. Similarity of expression patterns of 56 genes involved in GAG biosynthesis in 37 human tissues, including biosynthesis of GAG backbones (green), sulfation of HS (red), sulfation of CS and DS (pink), biosynthesis of KS (ocher), biosynthesis of HA (blue), nucleotide sugar transporters (purple), and regulators (yellow) were visualized as a Pearson correlation heatmap. The Pearson correlation values (–1 to 1) are presented as color changes (blue to red).

(*VCAN*) and decorin (*DCN*), was upregulated in pancreatic cancer (Skandalis et al., 2006). The *VCAN* expression level in pancreatic neuroendocrine tumor tissues was found to be higher than in normal pancreatic tissues (Gao et al., 2020). In this study, the RNA-seq data indicated that the expression levels of both *CHST3* and *CHST15* encoding chondroitin 6-*O*-sulfotransferase and GalNAc-4-*O*-sulfate 6-*O*-sulfotransferase in tumors were increased 4.0 and 3.5 times, respectively, in pancreatic tumors compared with that in normal tissues (**Supplementary Figure 3** and **Supplementary Table 4**). The expression levels of *VCAN* and *DCN* were increased 4.8 and 1.5 times, respectively (**Supplementary Table 4**). Besides, it has been reported that *endocan* (*ESM1*) expression in pancreatic neuroendocrine tumor correlates with poor clinical outcomes (Lin et al., 2017). The overexpression of *lumican* (*LUM*) and *biglycan* (*BGN*) has been reported in pancreatic cancers (Weber et al., 2001; Ishiwata et al., 2007). A high *syndecan 1* (*SDC1*) mRNA level tended to increase the mortality rate due to pancreatic cancer (Wu et al., 2020).

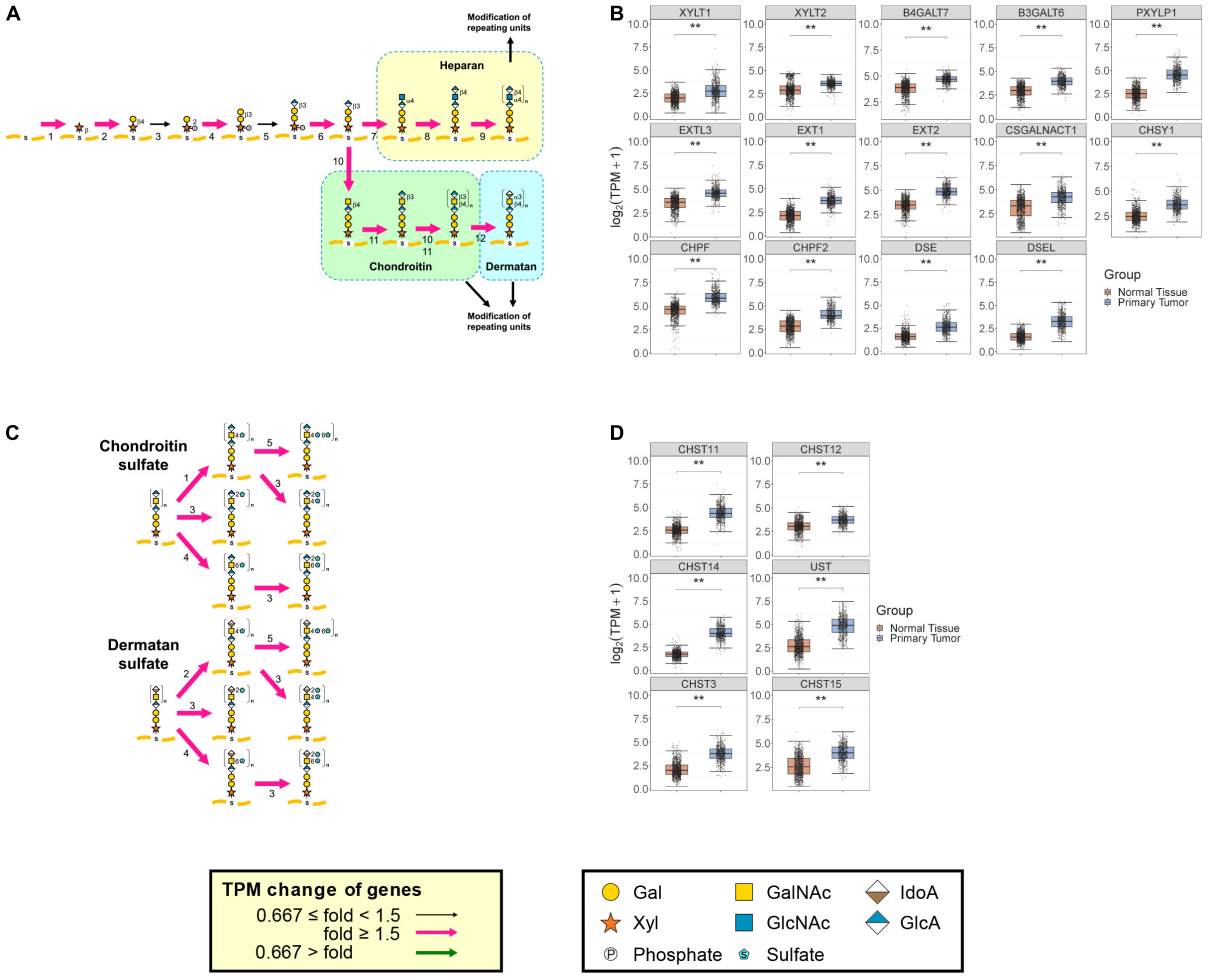


**FIGURE 3 |** Comparison of expression of GAG biosynthetic enzymes between primary brain tumors and normal tissues. Expression changes of genes responsible for reactions in pathways for biosynthesis of GAG backbones **(A)** and sulfation of CS and DS **(C)** between primary brain tumors (*N* = 662) and normal tissues (*N* = 1146) were visualized using GlycoMaple. Median TPM values of GAG-related genes in each sample were used for mapping. If several genes overlapped in a reaction, the maximum TPM value among the overlapping genes was used. When several gene products comprised a reaction complex, the minimum TPM value of the subunit genes was used. Fold changes of gene expression whose median TPM + 1 value was increased by >1.5 are shown as pink arrows. Genes that are significantly changed among tumor and normal tissues (Wilcoxon matched-pairs signed rank test; $^{**}P < 0.0001$) in GAG backbones **(B)** and sulfation of CS and DS **(D)** are shown as boxplots. The numbers of each step indicate the enzymes responsible for biosynthesis of GAG backbones **(A)** and sulfation of CS and DS **(B)**. **(A)** 1, *XYLT1* and *XYLT2*; 2, *B4GALT7*; 3, *FAM20B*; 4, *B3GALT6*; 5, *B3GAT3*; 6, *PXYLP1*; 7, *EXTL2* and *EXTL3*; 8 and 9, *EXT1* and *EXT2*; 10, *CSGALNACT1* and *CSGALNACT2*; 11, *CHSY1*, *CHSY3*, *CHPF*, and *CHPF2*; 12, *DSE* and *DSEL*. **(C)** 1, *CHST11*, *CHST12*, and *CHST13*; 2, *CHST14*; 3, *UST*; 4, *CHST3*; 5, *CHST15*.

In our analysis, expression of all PGs except for *neurocan* (*NCAN*), which showed almost no expression, were increased in pancreatic carcinoma (**Supplementary Figure 3F**). Particularly, *VCAN*, *ESM1*, *LUM*, *BGN*, and *SDC1* were the five most upregulated PGs. Similar to brain tumors, genes encoding transporters and regulators related to GAG biosynthesis were also upregulated in pancreatic tumors (**Supplementary Figure 3G** and **Supplementary Tables 4**, **5**).

In breast cancer, the DS content has been reported to decrease significantly, whereas the CS content increased in the central area of breast carcinoma tissues compared with fibroadenoma (Olsen et al., 1988). A similar change in GAG levels was observed in prostate cancer, where the DS level decreased and the CS level increased, when compared with normal tissue (De Klerk et al., 1984). GlycoMaple data including expression levels of biosynthetic enzymes for GAGs correlate well with these trends including the amounts of GAGs (**Figure 4**). In primary breast tumors, there is reduced expression of *DSE* and *DSEL*, which are the genes encoding DS epimerase converting GlcA to IdoA, to generate dermatan from the chondroitin precursor chain (**Figures 4A,B**). In addition, *CHPF* and *CHPF2*, whose products are required for the polymerization of chondroitin, were upregulated in breast cancer tissues (**Figures 4A,B**). Consistent with this result, down- and up-regulations of *DSE* and *CHPF*, respectively, were also observed in ductal carcinoma *in situ* compared with non-malignant breast tissue (Potapenko et al., 2015). It has also been demonstrated that among PG and GAG-related genes, *ACAN*, *VCAN*, *XYLT2*, *B3GALT6*, *CHSY1*, *CHPF*,

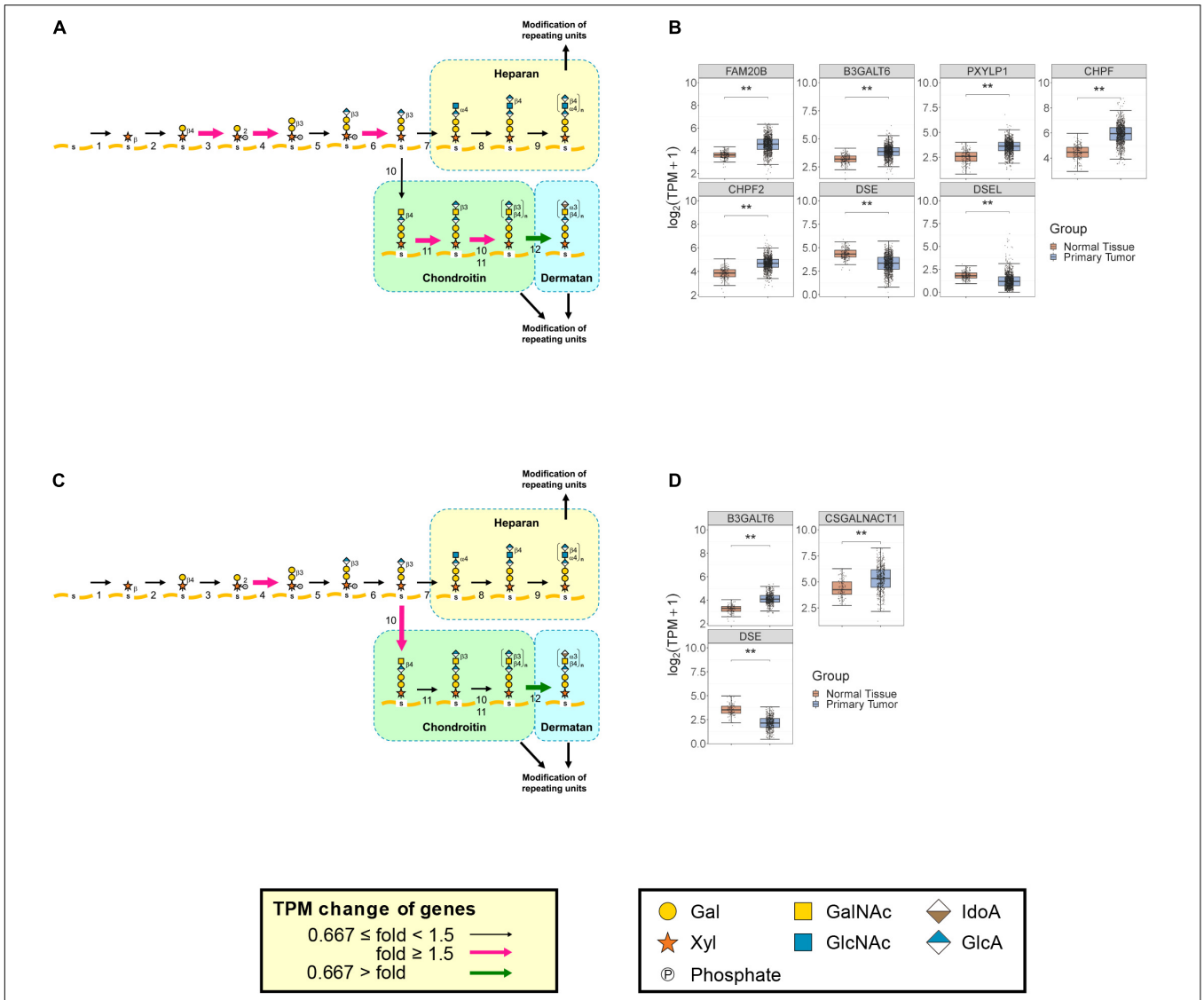


**FIGURE 4 |** Comparison of expression of GAG biosynthetic enzymes between breast and prostate primary tumors and normal tissues. Expression changes of genes responsible for biosynthetic pathways for GAG backbones between primary breast tumors ($N$ = 1092) and normal tissues ($N$ = 179) **(A)** or primary prostate tumors ($N$ = 495) and normal tissues ($N$ = 100) **(C)** were visualized using GlycoMaple, as described in **Figure 3**. Fold changes of gene expression whose median TPM + 1 value was increased by >1.5 and decreased by <0.667 are shown as pink and green arrows, respectively. GAG core biosynthesis genes that were significantly changed among tumor and normal tissues (Wilcoxon matched-pairs signed rank test; $^{**}P < 0.0001$) in breast **(B)** and prostate **(D)** are shown as boxplots. The numbers of each step are referred to in the legend of **Figure 3**.

*CHST11*, and *CHST15* were upregulated in malignant breast cancer tissue, while *CHST3* was downregulated (Potapenko et al., 2010). These findings were consistent with our data: expression levels of *ACAN*, *VCAN*, *B3GALT6*, *CHPF*, *CHST11*, and *CHST15* were increased more than 1.5 times in breast tumors, whereas expression of *CHST3* was 3.4-times decreased (**Figure 4B**, **Supplementary Figure 4A**, and **Supplementary Table 4**). In terms of PGs, it has been reported that *ESM1* was overexpressed in triple-negative breast cancer cell lines as well as in patient tissues, which is correlated with a poor prognosis (Fernandez-Vega et al., 2013). *SDC1* expression was activated, when compared with the very low level of expression in normal breast tissue, while expression of *DCN* decreased two—five-fold (Eshchenko et al., 2007). *BGN* was upregulated in human breast cancers, particularly in the tumor stroma compartment, compared with normal mammary glands (Cong et al., 2021). *VCAN* mRNA levels were upregulated in breast cancer tissues (Takahashi et al., 2012). In contrast, normal breast tissues exhibited high expression levels of *GPC3*, while the expression was reduced in tumors (Guereno et al., 2020). Despite the fact that *HSPG2* expression was correlated with poor patient survival and is considered as a therapeutic target in triple-negative breast cancer (Kalscheuer et al., 2019), the expression levels were two-fold higher in normal breast compared with breast cancer

tissues (Jansson et al., 2020). Our analysis also showed changes in expression of those genes: upregulation of *SDC1*, *ESM1*, *VCAN*, and *BGN*, and downregulation of *GPC3*, *HSPG2*, and *DCN* in breast cancer tissues (**Supplementary Figure 4A** and **Supplementary Tables 4**, **5**).

In primary prostate tumors, *DSE* expression was decreased to less than half (**Figures 4C,D**). In addition, a greater than two-fold increase was found in *CSGALNACT1*, whose product initiates the biosynthesis of the disaccharide region of the chondroitin chain (**Figures 4C,D**). These results are consistent with the findings of decreased DS and increased CS in pancreatic cancerous tissues (De Klerk et al., 1984), suggesting that GlycoMaple is a powerful tool for estimating changes of GAGs in diseased tissues. In terms of PGs, it has been reported that the expression of *fibromodulin* (*FMOD*) in malignant prostate tissues is significantly upregulated compared with that in benign tissues (Bettin et al., 2016). A significant decrease in tissue *DCN* expression is associated with tumor progression and metastasis in certain types of cancer including prostate cancer (Rezaie et al., 2020). The *GPC2* mRNA expression level was utilized to predict survival associated with prostate cancer (Xu et al., 2018). In our analysis, upregulations of *neuroglycan C* (*CSPG5*), *bamacan* (*SMC3*), and *collagen type IX alpha2* (*COL9A2*) and downregulations of *GPC1*, *GPC2*, *HSPG2*, *CSPG4*, and *DCN* were detected (**Supplementary Figure 4B** and **Supplementary Table 5**).

Finally, we estimated GAG changes in the adrenal and thyroid glands during tumorization. GlycoMaple analysis predicted decreased levels of CS and DS, because of the downregulation of *CSGALNACT1* and *DSE* in both the adrenal gland and thyroid gland tumors compared with that in normal tissues (**Supplementary Figure 5**). To date, there has been no report that GAG levels are changed in those tissues during tumorization. Therefore, it is worth examining the amounts of CS and DS in tumor tissues.

## CONCLUDING REMARKS

In this study, we analyzed the expression levels of GAG biosynthetic enzymes as well as PGs in various normal and tumor tissues. GAG biosynthetic levels differed, depending upon the tissue functions and requirements. Analyses of the amount and sulfation pattern of GAGs are not easy to perform and require relatively abundant starting materials. The estimation of glycan structures based on gene expression data could be performed easily from small amounts of samples, and is useful to discover properties of cells of interest and obtain clues to structural changes among cell types. We applied GlycoMaple analysis to visualize the expression of genes involved in GAG biosynthesis and PG levels and to estimate glycan changes based on gene expression. Comprehensive analysis using gene expression levels in human tissues revealed new findings showing that expression of some genes required for GAG biosynthesis are regulated in a similar manner. For example, expression of genes required for the biosynthesis of GAG backbones including CS, DS, HS, and HA may be similarly regulated. GlycoMaple estimation showed that GAG biosynthetic patterns and core proteins of PGs were markedly changed during tumor progression in some tissues, which correlated with previous research. The process of CS formation would be upregulated during the formation of many tumor types (Berto et al., 2001; Sakko et al., 2008; Svensson et al., 2011). However, there are several limitations in GlycoMaple analysis (Huang et al., 2021). First, estimations of GAG changes in tumors using GlycoMaple, are just predictions based on expression changes of genes related to GAG biosynthesis. Second, the estimation of glycans from GlycoMaple is not quantitative. Therefore, after identifying potential target pathways from these estimations, it is essential to validate GAG as well as PG levels using biochemical analyses. Nonetheless, GlycoMaple could provide a 'bird's eye view' of glycosylation pathways in cells/tissues of interest and clues for focusing on altered glycosylation pathways between diseased and normal tissues. Changes in glycosylation patterns during tumor progression were widely observed. In the future, GlycoMaple analysis could contribute to the development of biomarkers and clinical diagnostics using transcriptional data from clinical patient samples.

## DATA AVAILABILITY STATEMENT

The original contributions generated for this study are included in the article/**Supplementary Material**, further inquiries can be directed to the corresponding author.

## AUTHOR CONTRIBUTIONS

MF and Y-FH conceptualized and designed the study and wrote a draft of the manuscript. Y-FH conducted analyses and validated the results. SM strengthened the background of GAG. All authors checked and edited the manuscript.

## FUNDING

This work was supported by grants from the National Natural Science Foundation of China 32071278 and 31770853 (MF), the Program of Introducing Talents of Discipline to Universities 111-2-06, and the International Joint Research Laboratory for Investigation of Glycoprotein Biosynthesis at Jiangnan University. This work was also supported by a Grant-in-Aid for Scientific Research (C) from the Japan Society for the Promotion of Science (#19K07054) (SM).

## ACKNOWLEDGMENTS

We thank Rachel James, from Liwen Bianji, Edanz Group China, for editing the English text of a draft of this manuscript.

## SUPPLEMENTARY MATERIAL

The Supplementary Material for this article can be found online at: https://www.frontiersin.org/articles/10.3389/fcell.2021.709018/full#supplementary-material

## REFERENCES


Abbruzzese, F., Basoli, F., Costantini, M., Giannitelli, S. M., Gori, M., Mozetic, P., et al. (2017). Hyaluronan: an overview. *J. Biol. Regul. Homeost. Agents* 31(4 Suppl. 2), 9–22.

Aikawa, J., and Esko, J. D. (1999). Molecular cloning and expression of a third member of the heparan sulfate/heparin glcnac *N*-deacetylase/*N*-sulfotransferase family. *J. Biol. Chem.* 274, 2690–2695. doi: 10.1074/jbc.274.5.2690

Aikawa, J., Grobe, K., Tsujimoto, M., and Esko, J. D. (2001). Multiple isozymes of heparan sulfate/heparin glcnac *N*-deacetylase/GlcN *N*-sulfotransferase: structure and activity of the fourth member, NDST4. *J. Biol. Chem.* 276, 5876–5882. doi: 10.1074/jbc.M009606200

Akama, T. O., Misra, A. K., Hindsgaul, O., and Fukuda, M. N. (2002). Enzymatic synthesis in vitro of the disulfated disaccharide unit of corneal keratan sulfate. *J. Biol. Chem.* 277, 42505–42513. doi: 10.1074/jbc.M207412200

Akama, T. O., Nakayama, J., Nishida, K., Hiraoka, N., Suzuki, M., McAuliffe, J., et al. (2001). Human corneal GlcNac 6-*O*-sulfotransferase and mouse intestinal GlcNac 6-*O*-sulfotransferase both produce keratan sulfate. *J. Biol. Chem.* 276, 16271–16278. doi: 10.1074/jbc.M009995200

Alban, T. J., Bayik, D., Otvos, B., Rabljenovic, A., Leng, L., Jia-Shiun, L., et al. (2020). Glioblastoma myeloid-derived suppressor cell subsets express differential macrophage migration inhibitory factor receptor profiles that can be targeted to reduce immune suppression. *Front. Immunol.* 11:1191. doi: 10.3389/fimmu.2020.01191

Almeida, R., Levery, S. B., Mandel, U., Kresse, H., Schwientek, T., Bennett, E. P., et al. (1999). Cloning and expression of a proteoglycan UDP-galactose: beta-xylose β1,4-galactosyltransferase I. A seventh member of the human β4-galactosyltransferase gene family. *J. Biol. Chem.* 274, 26165–26171. doi: 10.1074/jbc.274.37.26165

Baghy, K., Tatrai, P., Regos, E., and Kovalszky, I. (2016). Proteoglycans in liver cancer. *World J. Gastroenterol.* 22, 379–393. doi: 10.3748/wjg.v22.i1.379

Bai, X., Zhou, D., Brown, J. R., Crawford, B. E., Hennet, T., and Esko, J. D. (2001). Biosynthesis of the linkage region of glycosaminoglycans: cloning and activity of galactosyltransferase II, the sixth member of the β1,3-galactosyltransferase family (β3GalT6). *J. Biol. Chem.* 276, 48189–48195. doi: 10.1074/jbc.M107339200

Berto, A. G., Oba, S. M., Michelacci, Y. M., and Sampaio, L. O. (2001). Galactosaminoglycans from normal myometrium and leiomyoma. *Braz. J. Med. Biol. Res.* 34, 633–637. doi: 10.1590/s0100-879x2001000500011

Bettin, A., Reyes, I., and Reyes, N. (2016). Gene expression profiling of prostate cancer-associated genes identifies fibromodulin as potential novel biomarker for prostate cancer. *Int. J. Biol. Markers* 31, e153–e162. doi: 10.5301/jbm.5000184

Bishop, J. R., Schuksz, M., and Esko, J. D. (2007). Heparan sulphate proteoglycans fine-tune mammalian physiology. *Nature* 446, 1030–1037. doi: 10.1038/nature05817

Bülow, H. E., and Hobert, O. (2006). The molecular diversity of glycosaminoglycans shapes animal development. *Annu. Rev. Cell Dev. Biol.* 22, 375–407. doi: 10.1146/annurev.cellbio.22.010605.093433

Caterson, B., and Melrose, J. (2018). Keratan sulfate, a complex glycosaminoglycan with unique functional capability. *Glycobiology* 28, 182–206. doi: 10.1093/glycob/cwy003

Chang, W. L., Chang, C. W., Chang, Y. Y., Sung, H. H., Lin, M. D., Chang, S. C., et al. (2013). The *Drosophila* GOLPH3 homolog regulates the biosynthesis of heparan sulfate proteoglycans by modulating the retrograde trafficking of exostosins. *Development* 140, 2798–2807. doi: 10.1242/dev.087171

Cong, L., Maishi, N., Annan, D. A., Young, M. F., Morimoto, H., Morimoto, M., et al. (2021). Inhibition of stromal biglycan promotes normalization of the tumor microenvironment and enhances chemotherapeutic efficacy. *Breast Cancer Res.* 23:51. doi: 10.1186/s13058-021-01423-w

De Klerk, D. P., Lee, D. V., and Human, H. J. (1984). Glycosaminoglycans of human prostatic cancer. *J. Urol.* 131, 1008–1012. doi: 10.1016/s0022-5347(17)50750-8

Dzikowski, L., Mirzaei, R., Sarkar, S., Kumar, M., Bose, P., Bellail, A., et al. (2021). Fibrinogen in the glioblastoma microenvironment contributes to the invasiveness of brain tumor-initiating cells. *Brain Pathol.* (in press). e12947. doi: 10.1111/bpa.12947

Eriksson, I., Sandbäck, D., Ek, B., Lindahl, U., and Kjellén, L. (1994). cDNA cloning and sequencing of mouse mastocytoma glucosaminyl *N*-deacetylase/*N*-sulfotransferase, an enzyme involved in the biosynthesis of heparin. *J. Biol. Chem.* 269, 10438–10443. doi: 10.1016/s0021-9258(17)34079-6

Eshchenko, T. Y., Rykova, V. I., Chernakov, A. E., Sidorov, S. V., and Grigorieva, E. V. (2007). Expression of different proteoglycans in human breast tumors. *Biochemistry* 72, 1016–1020. doi: 10.1134/s0006297907090143

Esko, J. D., and Selleck, S. B. (2002). Order out of chaos: assembly of ligand binding sites in heparan sulfate. *Annu. Rev. Biochem.* 71, 435–471. doi: 10.1146/annurev.biochem.71.110601.135458

Fernandez-Vega, I., Garcia, O., Crespo, A., Castanon, S., Menendez, P., Astudillo, A., et al. (2013). Specific genes involved in synthesis and editing of heparan sulfate proteoglycans show altered expression patterns in breast cancer. *BMC Cancer* 13:24. doi: 10.1186/1471-2407-13-24

Fransson, L.-A., Cheng, F., Yoshida, K., Heinegård, D., Malmström, A., and Schmidtchen, A. (1993). "Patterns of epimerization and sulphation in dermatan sulphate chains," in *Dermatan Sulphate Proteoglycans: Chemistry, Biology, Chemical Pathology*, ed. J. E. Scott (London: Portland Press), 11–25.

Fukuta, M., Inazawa, J., Torii, T., Tsuzuki, K., Shimada, E., and Habuchi, O. (1997). Molecular cloning and characterization of human keratan sulfate Gal-6-sulfotransferase. *J. Biol. Chem.* 272, 32321–32328. doi: 10.1074/jbc.272.51.32321

Gao, H., Cheng, Y., Chen, Y., Luo, F., Shao, Y., Sun, Z., et al. (2020). The expression of versican and its role in pancreatic neuroendocrine tumors. *Pancreatology* 20, 142–147. doi: 10.1016/j.pan.2019.11.009

Goldman, M. J., Craft, B., Hastie, M., Repecka, K., McDade, F., Kamath, A., et al. (2020). Visualizing and interpreting cancer genomics data via the Xena platform. *Nat. Biotechnol.* 38, 675–678. doi: 10.1038/s41587-020-0546-8

Götting, C., Kuhn, J., Zahn, R., Brinkmann, T., and Kleesiek, K. (2000). Molecular cloning and expression of human UDP-D-xylose: proteoglycan core protein β-D-xylosyltransferase and its first isoform XT-II. *J. Mol. Biol.* 304, 517–528. doi: 10.1006/jmbi.2000.4261

GTEx Consortium (2017). Genetic effects on gene expression across human tissues. *Nature* 550, 204–213. doi: 10.1038/nature24277

Guereno, M., Delgado Pastore, M., Lugones, A. C., Cercato, M., Todaro, L., Urtreger, A., et al. (2020). Glypican-3 (GPC3) inhibits metastasis development promoting dormancy in breast cancer cells by p38 MAPK pathway activation. *Eur. J. Cell Biol.* 99:151096. doi: 10.1016/j.ejcb.2020.151096

Häcker, U., Nybakken, K., and Perrimon, N. (2005). Heparan sulphate proteoglycans: the sweet side of development. *Nat. Rev. Mol. Cell Biol.* 6, 530–541. doi: 10.1038/nrm1681

Hascall, V. C. (2019). The journey of hyaluronan research in the journal of biological chemistry. *J. Biol. Chem.* 294, 1690–1696. doi: 10.1074/jbc.TM118.005836

Hascall, V., and Esko, J. D. (2015). "Hyaluronan," in *Essentials of Glycobiology*, eds A. Varki, R. D. Cummings, J. D. Esko, P. Stanley, G. W. Hart, M. Aebi, et al. (Cold Spring Harbor, NY: Cold Spring Harbor Laboratory Press), 197–206.

Hashimoto, Y., Orellana, A., Gil, G., and Hirschberg, C. B. (1992). Molecular cloning and expression of rat liver *N*-heparan sulfate sulfotransferase. *J. Biol. Chem.* 267, 15744–15750. doi: 10.1016/s0021-9258(19)49598-7

Hoadley, K. A., Yau, C., Hinoue, T., Wolf, D. M., Lazar, A. J., Drill, E., et al. (2018). Cell-of-origin patterns dominate the molecular classification of 10,000 tumors from 33 types of cancer. *Cell* 173, 291–304. doi: 10.1016/j.cell.2018.03.022

Huang, Y. F., Aoki, K., Akase, S., Ishihara, M., Liu, Y. S., Yang, G., et al. (2021). Global mapping of glycosylation pathways in human-derived cells. *Dev. Cell* 56, 1195–1209.e7. doi: 10.1016/j.devcel.2021.02.023

Iozzo, R. V. (1998). Matrix proteoglycans: from molecular design to cellular function. *Annu. Rev. Biochem.* 67, 609–652. doi: 10.1146/annurev.biochem.67.1.609

Iozzo, R. V., and Sanderson, R. D. (2011). Proteoglycans in cancer biology, tumor microenvironment and angiogenesis. *J. Cell. Mol. Med.* 15, 1013–1031. doi: 10.1111/j.1582-4934.2010.01236.x

Ishiwata, T., Cho, K., Kawahara, K., Yamamoto, T., Fujiwara, Y., Uchida, E., et al. (2007). Role of lumican in cancer cells and adjacent stromal tissues in human pancreatic cancer. *Oncol. Rep.* 18, 537–543.

Itano, N., and Kimata, K. (2002). Mammalian hyaluronan synthases. *IUBMB Life* 54, 195–199. doi: 10.1080/15216540214929

Itano, N., Sawai, T., Yoshida, M., Lenas, P., Yamada, Y., Imagawa, M., et al. (1999). Three isoforms of mammalian hyaluronan synthases have distinct enzymatic properties. *J. Biol. Chem.* 274, 25085–25092. doi: 10.1074/jbc.274.35.25085

Izumikawa, T. (2019). Regulatory mechanism of 2-*O*-phosphorylation of xylose in the glycosaminoglycan-linkage region of the tetrasaccharide. *Trend Glycosci. Glycotechnol.* 31, E57–E62. doi: 10.4052/tigg.1955.2E

Izumikawa, T., Koike, T., Shiozawa, S., Sugahara, K., Tamura, J., and Kitagawa, H. (2008). Identification of chondroitin sulfate glucuronyltransferase as chondroitin synthase-3 involved in chondroitin polymerization: chondroitin polymerization is achieved by multiple enzyme complexes consisting of chondroitin synthase family members. *J. Biol. Chem.* 283, 11396–11406. doi: 10.1074/jbc.M707549200

Izumikawa, T., Uyama, T., Okuura, Y., Sugahara, K., and Kitagawa, H. (2007). Involvement of chondroitin sulfate synthase-3 (chondroitin synthase-2) in chondroitin polymerization through its interaction with chondroitin synthase-1 or chondroitin-polymerizing factor. *Biochem. J.* 403, 545–552. doi: 10.1042/BJ20061876

Jansson, M., Billing, O., Herdenberg, C., Lundin, C., Tolockiene, E., Nazemroaya, A., et al. (2020). Expression and circulating levels of perlecan in breast cancer – implications for oestrogen dependent stromal remodeling. *J. Mammary Gland Biol. Neoplasia* 25, 69–77. doi: 10.1007/s10911-020-09447-2

Jiang, D., Liang, J., and Noble, P. W. (2011). Hyaluronan as an immune regulator in human diseases. *Physiol. Rev.* 91, 221–264. doi: 10.1152/physrev.00052.2009

Kalscheuer, S., Khanna, V., Kim, H., Li, S., Sachdev, D., DeCarlo, A., et al. (2019). Discovery of HSPG2 (Perlecan) as a therapeutic target in triple negative breast cancer. *Sci. Rep.* 9:12492. doi: 10.1038/s41598-019-48993-6

Kam, T., and Alexander, M. (2014). Drug-induced immune thrombocytopenia. *J. Pharm. Pract.* 27, 430–439. doi: 10.1177/0897190014546099

Kamiyama, S., Sasaki, N., Goda, E., Ui-Tei, K., Saigo, K., Narimatsu, H., et al. (2006). Molecular cloning and characterization of a novel 3′-phosphoadenosine 5′-phosphosulfate transporter, PAPST2. *J. Biol. Chem.* 281, 10945–10953. doi: 10.1074/jbc.M508991200

Kamiyama, S., Suda, T., Ueda, R., Suzuki, M., Okubo, R., Kikuchi, N., et al. (2003). Molecular cloning and identification of 3′-phosphoadenosine 5′-phosphosulfate transporter. *J. Biol. Chem.* 278, 25958–25963. doi: 10.1074/jbc.M302439200

Karamanos, N. K., Piperigkou, Z., Theocharis, A. D., Watanabe, H., Franchi, M., Baud, S., et al. (2018). Proteoglycan chemical diversity drives multifunctional cell regulation and therapeutics. *Chem. Rev.* 118, 9152–9232. doi: 10.1021/acs.chemrev.8b00354

Kim, B. T., Kitagawa, H., Tamura, J., Saito, T., Kusche-Gullberg, M., Lindahl, U., et al. (2001). Human tumor suppressor *EXT* gene family members *EXTL1* and *EXTL3* encode α1,4-*N*-acetylglucosaminyltransferases that likely are involved in heparan sulfate/heparin biosynthesis. *Proc. Natl. Acad. Sci. U.S.A.* 98, 7176–7181. doi: 10.1073/pnas.131188498

Kim, B. T., Kitagawa, H., Tanaka, J., Tamura, J., and Sugahara, K. (2003). *In vitro* heparan sulfate polymerization: crucial roles of core protein moieties of primer substrates in addition to the EXT1-EXT2 interaction. *J. Biol. Chem.* 278, 41618–41623. doi: 10.1074/jbc.M304831200

Kitagawa, H., Izumikawa, T., Uyama, T., and Sugahara, K. (2003). Molecular cloning of a chondroitin polymerizing factor that cooperates with chondroitin synthase for chondroitin polymerization. *J. Biol. Chem.* 278, 23666–23671. doi: 10.1074/jbc.m302493200

Kitagawa, H., Shimakawa, H., and Sugahara, K. (1999). The tumor suppressor EXT-like gene *EXTL2* encodes an α1, 4-*N*-acetylhexosaminyltransferase that transfers *N*-acetylgalactosamine and *N*-acetylglucosamine to the common glycosaminoglycan-protein linkage region. The key enzyme for the chain initiation of heparan sulfate. *J. Biol. Chem.* 274, 13933–13937. doi: 10.1074/jbc.274.20.13933

Kitagawa, H., Tone, Y., Tamura, J., Neumann, K. W., Ogawa, T., Oka, S., et al. (1998). Molecular cloning and expression of glucuronyltransferase I involved in the biosynthesis of the glycosaminoglycan-protein linkage region of proteoglycans. *J. Biol. Chem.* 273, 6615–6618. doi: 10.1074/jbc.273.12.6615

Kitagawa, H., Uyama, T., and Sugahara, K. (2001). Molecular cloning and expression of a human chondroitin synthase. *J. Biol. Chem.* 276, 38721–38726. doi: 10.1074/jbc.M106871200

Kitayama, K., Hayashida, Y., Nishida, K., and Akama, T. O. (2007). Enzymes responsible for synthesis of corneal keratan sulfate glycosaminoglycans. *J. Biol. Chem.* 282, 30085–30096. doi: 10.1074/jbc.M703695200

Kjellen, L., and Lindahl, U. (1991). Proteoglycans: structures and interactions. *Annu. Rev. Biochem.* 60, 443–475. doi: 10.1146/annurev.bi.60.070191.002303

Kjellen, L., and Lindahl, U. (2018). Specificity of glycosaminoglycan-protein interactions. *Curr. Opin. Struct. Biol.* 50, 101–108. doi: 10.1016/j.sbi.2017.12.011

Koike, T., Izumikawa, T., Sato, B., and Kitagawa, H. (2014). Identification of phosphatase that dephosphorylates xylose in the glycosaminoglycan-protein linkage region of proteoglycans. *J. Biol. Chem.* 289, 6695–6708. doi: 10.1074/jbc.m113.520536

Koike, T., Izumikawa, T., Tamura, J.-I., and Kitagawa, H. (2009). FAM20B is a kinase that phosphorylates xylose in the glycosaminoglycan–protein linkage region. *Biochem. J.* 421, 157–162. doi: 10.1042/bj20090474

Kuhn, P. H., Voss, M., Haug-Kroper, M., Schroder, B., Schepers, U., Brase, S., et al. (2015). Secretome analysis identifies novel signal Peptide peptidase-like 3 (Sppl3) substrates and reveals a role of Sppl3 in multiple Golgi glycosylation pathways. *Mol. Cell. Proteomics* 14, 1584–1598. doi: 10.1074/mcp.M115.048298

Kusche-Gullberg, M., and Kjellen, L. (2003). Sulfotransferases in glycosaminoglycan biosynthesis. *Curr. Opin. Struct. Biol.* 13, 605–611. doi: 10.1016/j.sbi.2003.08.002

Lamari, F. N., and Karamanos, N. K. (2006). Structure of chondroitin sulfate. *Adv. Pharmacol.* 53, 33–48. doi: 10.1016/S1054-3589(05)53003-5

Li, J.-P., Hagner-McWhirter, Å, Kjellén, L., Palgi, J., Jalkanen, M., and Lindahl, U. (1997). Biosynthesis of heparin/heparan sulfate: cdna cloning and expression of D-glucuronyl C5-epimerase from bovine lung. *J. Biol. Chem.* 272, 28158–28163. doi: 10.1074/jbc.272.44.28158

Liang, J., Jiang, D., and Noble, P. W. (2016). Hyaluronan as a therapeutic target in human diseases. *Adv. Drug Deliv. Rev.* 97, 186–203. doi: 10.1016/j.addr.2015.10.017

Lidholt, K., Kjellen, L., and Lindahl, U. (1989). Biosynthesis of heparin. Relationship between the polymerization and sulphation processes. *Biochem. J.* 261, 999–1007. doi: 10.1042/bj2610999

Lin, L. Y., Yeh, Y. C., Chu, C. H., Won, J. G. S., Shyr, Y. M., Chao, Y., et al. (2017). Endocan expression is correlated with poor progression-free survival in patients with pancreatic neuroendocrine tumors. *Medicine* 96:e8262. doi: 10.1097/MD.0000000000008262

Lind, T., Tufaro, F., McCormick, C., Lindahl, U., and Lidholt, K. (1998). The putative tumor suppressors EXT1 and EXT2 are glycosyltransferases required for the biosynthesis of heparan sulfate. *J. Biol. Chem.* 273, 26265–26268. doi: 10.1074/jbc.273.41.26265

Lindahl, U. (1989). "Biosynthesis of heparin and related polysaccharides," in *Heparin*, eds D. A. Lane and U. Lindahl (London: Edward Arnold), 159–189.

Lindahl, U., and Rodén, L. (1972). "Carbohydrate-protein linkages in proteoglycans of animal, plant and bacterial origin," in *Glycoproteins: Their Composition, Structure and Function*, ed. A. Gottschalk (Amsterdam: Elsevier), 491–517.

Lindahl, U., Couchman, J., Kimata, K., and Esko, J. D. (2015). "Proteoglycans and sulfated glycosaminoglycans," in *Essentials of Glycobiology*, eds A. Varki, R. D. Cummings, J. D. Esko, P. Stanley, G. W. Hart, M. Aebi, et al. (Cold Spring Harbor, NY: Cold Spring Harbor Laboratory Press), 207–221.

Maccarana, M., Olander, B., Malmström, J., Tiedemann, K., Aebersold, R., Lindahl, U., et al. (2006). Biosynthesis of dermatan sulfate: chondroitin-glucuronate C5-epimerase is identical to SART2. *J. Biol. Chem.* 281, 11560–11568. doi: 10.1074/jbc.M513373200

McCormick, C., Leduc, Y., Martindale, D., Mattison, K., Esford, L. E., Dyer, A. P., et al. (1998). The putative tumour suppressor EXT1 alters the expression of cell-surface heparan sulfate. *Nat. Genet.* 19, 158–161. doi: 10.1038/514

Mizumoto, S., and Sugahara, K. (2013). Glycosaminoglycans are functional ligands for receptor for advanced glycation end-products in tumors. *FEBS J.* 280, 2462–2470. doi: 10.1111/febs.12156

Mizumoto, S., Yamada, S., and Sugahara, K. (2015). Molecular interactions between chondroitin–dermatan sulfate and growth factors/receptors/matrix proteins. *Curr. Opin. Struct. Biol.* 34, 35–42. doi: 10.1016/j.sbi.2015.06.004

Morla, S. (2019). Glycosaminoglycans and glycosaminoglycan mimetics in cancer and inflammation. *Int. J. Mol. Sci.* 20:1963. doi: 10.3390/ijms20081963

Nagarajan, A., Malvi, P., and Wajapeyee, N. (2018). Heparan sulfate and heparan sulfate proteoglycans in cancer initiation and progression. *Front. Endocrinol.* 9:483. doi: 10.3389/fendo.2018.00483

Narentuya, Takeda-Uchimura, Y., Foyez, T., Zhang, Z., Akama, T. O., Yagi, H., et al. (2019). GlcNAc6ST3 is a keratan sulfate sulfotransferase for the protein-tyrosine phosphatase PTPRZ in the adult brain. *Sci. Rep.* 9:4387. doi: 10.1038/s41598-019-40901-2

Neill, T., Schaefer, L., and Iozzo, R. V. (2015). Oncosuppressive functions of decorin. *Mol. Cell. Oncol.* 2:e975645. doi: 10.4161/23723556.2014.975645

Okajima, T., Yoshida, K., Kondo, T., and Furukawa, K. (1999). Human homolog of *Caenorhabditis elegans sqv-3* gene is galactosyltransferase I involved in the biosynthesis of the glycosaminoglycan-protein linkage region of proteoglycans. *J. Biol. Chem.* 274, 22915–22918. doi: 10.1074/jbc.274.33.22915

Olsen, E. B., Trier, K., Eldov, K., and Ammitzboll, T. (1988). Glycosaminoglycans in human breast cancer. *Acta Obstet. Gynecol. Scand.* 67, 539–542. doi: 10.3109/00016348809029866

Pacheco, B., Malmström, A., and Maccarana, M. (2009). Two dermatan sulfate epimerases form iduronic acid domains in dermatan sulfate. *J. Biol. Chem.* 284, 9788–9795. doi: 10.1074/jbc.M809339200

Pönighaus, C., Ambrosius, M., Casanova, J., Prante, C., Kuhn, J., Esko, J., et al. (2007). Human xylosyltransferase II is involved in the biosynthesis of the uniform tetrasaccharide linkage region in chondroitin sulfate and heparan sulfate proteoglycans. *J. Biol. Chem.* 282, 5201–5206. doi: 10.1074/jbc.M611665200

Pontén, F., Jirström, K., and Uhlen, M. (2008). The human protein atlas—a tool for pathology. *J. Pathol.* 216, 387–393. doi: 10.1002/path.2440

Potapenko, I. O., Haakensen, V. D., Luders, T., Helland, A., Bukholm, I., Sorlie, T., et al. (2010). Glycan gene expression signatures in normal and malignant breast tissue; possible role in diagnosis and progression. *Mol. Oncol.* 4, 98–118. doi: 10.1016/j.molonc.2009.12.001

Potapenko, I. O., Luders, T., Russnes, H. G., Helland, A., Sorlie, T., Kristensen, V. N., et al. (2015). Glycan-related gene expression signatures in breast cancer subtypes; relation to survival. *Mol. Oncol.* 9, 861–876. doi: 10.1016/j.molonc.2014.12.013

Presto, J., Thuveson, M., Carlsson, P., Busse, M., Wile ìn, M., Eriksson, I., et al. (2008). Heparan sulfate biosynthesis enzymes EXT1 and EXT2 affect NDST1 expression and heparan sulfate sulfation. *Proc. Natl. Acad. Sci. U.S.A.* 105, 4751–4756. doi: 10.1073/pnas.0705807105

Prydz, K. (2015). Determinants of glycosaminoglycan (GAG) structure. *Biomolecules* 5, 2003–2022. doi: 10.3390/biom5032003

Rezaie, R., Falakian, Z., Mazloomzadeh, S., Ayati, M., Morakabati, A., Teimouri Dastjerdan, M. R., et al. (2020). While urine and plasma decorin remain unchanged in prostate cancer, prostatic tissue decorin has a prognostic value. *Iran. Biomed. J* 24, 229–235. doi: 10.29252/ibj.24.4.229

Rodén, L. (1980). "Structure and metabolism of connective tissue proteoglycans," in *The Biochemistry of Glycoproteins and Proteoglycans*, ed. W. J. Lennarz (New York: Plenum Press), 267–371. doi: 10.1007/978-1-4684-1006-8_7

Rodén, L., Ananth, S., Campbell, P., Curenton, T., Ekborg, G., Manzella, S., et al. (1992). "Heparin—an introduction," in *Heparin and Related Polysaccharides*, eds D. A. LaneIngemar, I. Björk, and U. Lindahl (New York: Plenum Press), 1–20. doi: 10.1007/978-1-4899-2444-5_1

Sakko, A. J., Butler, M. S., Byers, S., Reinboth, B. J., Stahl, J., Kench, J. G., et al. (2008). Immunohistochemical level of unsulfated chondroitin disaccharides in the cancer stroma is an independent predictor of prostate cancer relapse. *Cancer Epidemiol. Biomarkers Prev.* 17, 2488–2497. doi: 10.1158/1055-9965.EPI-08-0204

Sarrazin, S., Lamanna, W. C., and Esko, J. D. (2011). Heparan sulfate proteoglycans. *Cold Spring Harb. Perspect. Biol.* 3:a004952.

Sasaki, K., Komori, R., Taniguchi, M., Shimaoka, A., Midori, S., Yamamoto, M., et al. (2019). PGSE is a novel enhancer regulating the proteoglycan pathway of the mammalian Golgi stress response. *Cell Struct. Funct.* 44, 1–19. doi: 10.1247/csf.18031

Sasisekharan, R., Shriver, Z., Venkataraman, G., and Narayanasami, U. (2002). Roles of heparan-sulphate glycosaminoglycans in cancer. *Nat. Rev. Cancer* 2, 521–528. doi: 10.1038/nrc842

Schaefer, L., Tredup, C., Gubbiotti, M. A., and Iozzo, R. V. (2017). Proteoglycan neofunctions: regulation of inflammation and autophagy in cancer biology. *FEBS J.* 284, 10–26. doi: 10.1111/febs.13963

Seko, A., and Yamashita, K. (2004). β1, 3-N-acetylglucosaminyltransferase-7 (β3Gn-T7) acts efficiently on keratan sulfate-related glycans. *FEBS Lett.* 556, 216–220. doi: 10.1016/s0014-5793(03)01440-6

Seko, A., Dohmae, N., Takio, K., and Yamashita, K. (2003). β1,4-Galactosyltransferase (β4GalT)-IV is specific for GlcNAc 6-*O*-sulfate. β4GalT-IV acts on keratan sulfate-related glycans and a precursor glycan of 6-sulfosialyl-Lewis X. *J. Biol. Chem.* 278, 9150–9158. doi: 10.1074/jbc.m211480200

Skandalis, S. S., Kletsas, D., Kyriakopoulou, D., Stavropoulos, M., and Theocharis, D. A. (2006). The greatly increased amounts of accumulated versican and decorin with specific post-translational modifications may be closely associated with the malignant phenotype of pancreatic cancer. *Biochim. Biophys. Acta* 1760, 1217–1225. doi: 10.1016/j.bbagen.2006.03.021

Stuhlsatz, H. W., Keller, R., Becker, G., Oeben, M., Lennartz, L., Fischer, D. C., et al. (1989). "Structure of keratan sulphate proteoglycans: core proteins, linkage regions, carbohydrate chains," in *Keratan Sulphate Proteoglycans: Chemistry, Biology, Chemical Pathology*, eds H. Greiling and J. E. Scott (London: Portland Press), 1–11.

Sugahara, K., and Kitagawa, H. (2000). Recent advances in the study of the biosynthesis and functions of sulfated glycosaminoglycans. *Curr. Opin. Struct. Biol.* 10, 518–527. doi: 10.1016/s0959-440x(00)00125-1

Svensson, K. J., Christianson, H. C., Kucharzewska, P., Fagerstrom, V., Lundstedt, L., Borgquist, S., et al. (2011). Chondroitin sulfate expression predicts poor outcome in breast cancer. *Int. J. Oncol.* 39, 1421–1428. doi: 10.3892/ijo.2011.1164

Takahashi, Y., Kuwabara, H., Yoneda, M., Isogai, Z., Tanigawa, N., and Shibayama, Y. (2012). Versican G1 and G3 domains are upregulated and latent transforming growth factor-beta binding protein-4 is downregulated in breast cancer stroma. *Breast Cancer* 19, 46–53. doi: 10.1007/s12282-011-0264-7

Thelin, M. A., Bartolini, B., Axelsson, J., Gustafsson, R., Tykesson, E., Pera, E., et al. (2013). Biological functions of iduronic acid in chondroitin/dermatan sulfate. *FEBS J.* 280, 2431–2446. doi: 10.1111/febs.12214

Theocharis, A. D., Skandalis, S. S., Neill, T., Multhaupt, H. A., Hubo, M., Frey, H., et al. (2015). Insights into the key roles of proteoglycans in breast cancer biology and translational medicine. *Biochim. Biophys. Acta* 1855, 276–300. doi: 10.1016/j.bbcan.2015.03.006

Theocharis, A. D., Tsara, M. E., Papageorgacopoulou, N., Karavias, D. D., and Theocharis, D. A. (2000). Pancreatic carcinoma is characterized by elevated content of hyaluronan and chondroitin sulfate with altered disaccharide composition. *Biochim. Biophys. Acta* 1502, 201–206. doi: 10.1016/s0925-4439(00)00051-x

Uyama, T., Kitagawa, H., Tamura, J., and Sugahara, K. (2002). Molecular cloning and expression of human chondroitin *N*-acetylgalactosaminyltransferase: the key enzyme for chain initiation and elongation of chondroitin/dermatan sulfate on the protein linkage region tetrasaccharide shared by heparin/heparan sulfate. *J. Biol. Chem.* 277, 8841–8846. doi: 10.1074/jbc.M111434200

Uyama, T., Kitagawa, H., Tanaka, J., Tamura, J., Ogawa, T., and Sugahara, K. (2003). Molecular cloning and expression of a second chondroitin *N*-acetylgalactosaminyltransferase involved in the initiation and elongation of chondroitin/dermatan sulfate. *J. Biol. Chem.* 278, 3072–3078. doi: 10.1074/jbc.M209446200

Venkatachalam, K. (2003). Human 3′-phosphoadenosine 5′-phosphosulfate (PAPS) synthase: biochemistry, molecular biology and genetic deficiency. *IUBMB Life* 55, 1–11. doi: 10.1080/1521654031000072148

Vitale, D., Kumar Katakam, S., Greve, B., Jang, B., Oh, E. S., Alaniz, L., et al. (2019). Proteoglycans and glycosaminoglycans as regulators of cancer stem cell function and therapeutic resistance. *FEBS J.* 286, 2870–2882. doi: 10.1111/febs.14967

von Spreckelsen, N., Fadzen, C. M., Hartrampf, N., Ghotmi, Y., Wolfe, J. M., Dubey, S., et al. (2021). Targeting glioblastoma using a novel peptide specific to a deglycosylated isoform of brevican. *Adv. Ther.* 4:2000244. doi: 10.1002/adtp.202000244

Wade, A., Robinson, A. E., Engler, J. R., Petritsch, C., James, C. D., and Phillips, J. J. (2013). Proteoglycans and their roles in brain cancer. *FEBS J.* 280, 2399–2417. doi: 10.1111/febs.12109

Wagner, G. P., Kin, K., and Lynch, V. J. (2012). Measurement of mRNA abundance using RNA-seq data: RPKM measure is inconsistent among samples. *Theory Biosci.* 131, 281–285. doi: 10.1007/s12064-012-0162-3

Weber, C. K., Sommer, G., Michl, P., Fensterer, H., Weimer, M., Gansauge, F., et al. (2001). Biglycan is overexpressed in pancreatic cancer and induces G1-arrest in pancreatic cancer cell lines. *Gastroenterology* 121, 657–667. doi: 10.1053/gast.2001.27222

Wei, J., Hu, M., Huang, K., Lin, S., and Du, H. (2020). Roles of proteoglycans and glycosaminoglycans in cancer development and progression. *Int. J. Mol. Sci.* 21:5983. doi: 10.3390/ijms21175983

Weiss, R. J., Spahn, P. N., Chiang, A. W. T., Liu, Q., Li, J., Hamill, K. M., et al. (2021). Genome-wide screens uncover KDM2B as a modifier of protein binding to heparan sulfate. *Nat. Chem. Biol.* 17, 684–692. doi: 10.1038/s41589-021-00776-9

Weiss, R. J., Spahn, P. N., Toledo, A. G., Chiang, A. W. T., Kellman, B. P., Li, J., et al. (2020). ZNF263 is a transcriptional regulator of heparin and heparan sulfate biosynthesis. *Proc. Natl. Acad. Sci. U.S.A.* 117, 9311–9317. doi: 10.1073/pnas.1920880117

Wu, Y., Huang, H., Fervers, B., and Lu, L. (2020). Syndecan-1 and KRAS gene expression signature associates with patient survival in pancreatic cancer. *Pancreas* 49, 1187–1194. doi: 10.1097/MPA.0000000000001654

Xu, D., and Esko, J. D. (2014). Demystifying heparan sulfate–protein interactions. *Annu. Rev. Biochem.* 83, 129–157. doi: 10.1146/annurev-biochem-060713-035314

Xu, N., Wu, Y. P., Yin, H. B., Xue, X. Y., and Gou, X. (2018). Molecular network-based identification of competing endogenous RNAs and mRNA signatures that predict survival in prostate cancer. *J. Transl. Med.* 16:274. doi: 10.1186/s12967-018-1637-x

Yan, Z., and Wang, S. (2020). Proteoglycans as therapeutic targets in brain cancer. *Front. Oncol.* 10:1358. doi: 10.3389/fonc.2020.01358

**Conflict of Interest:** The authors declare that the research was conducted in the absence of any commercial or financial relationships that could be construed as a potential conflict of interest.

**Publisher's Note:** All claims expressed in this article are solely those of the authors and do not necessarily represent those of their affiliated organizations, or those of the publisher, the editors and the reviewers. Any product that may be evaluated in this article, or claim that may be made by its manufacturer, is not guaranteed or endorsed by the publisher.

frontiers in Cell and Developmental Biology

BRIEF RESEARCH REPORT
published: 17 September 2021
doi: 10.3389/fcell.2021.730550

# Assessment of Possible Contributions of Hyaluronan and Proteoglycan Binding Link Protein 4 to Differential Perineuronal Net Formation at the Calyx of Held

*Kojiro Nojima[1†], Haruko Miyazaki[1†], Tetsuya Hori[2], Lydia Vargova[3,4] and Toshitaka Oohashi[1*]*

[1] Department of Molecular Biology and Biochemistry, Okayama University Graduate School of Medicine, Dentistry and Pharmaceutical Sciences, Okayama, Japan, [2] Cellular and Molecular Synaptic Function Unit, Okinawa Institute of Science and Technology Graduate University, Okinawa, Japan, [3] Department of Neuroscience, Charles University, Second Faculty of Medicine, Prague, Czechia, [4] Department of Cellular Physiology, Institute of Experimental Medicine AS CR, Prague, Czechia

OPEN ACCESS

**Edited by:**
Shuji Mizumoto,
Meijo University, Japan

**Reviewed by:**
Shinji Miyata,
Tokyo University of Agriculture and Technology, Japan
Alexandra Yurievna Tsidulko,
Federal Research Center of Fundamental and Translational Medicine, Russia

***Correspondence:**
Toshitaka Oohashi
oohashi@cc.okayama-u.ac.jp

[†] These authors have contributed equally to this work and share first authorship

**Specialty section:**
This article was submitted to Signaling, a section of the journal Frontiers in Cell and Developmental Biology

**Received:** 25 June 2021
**Accepted:** 23 August 2021
**Published:** 17 September 2021

**Citation:**
Nojima K, Miyazaki H, Hori T, Vargova L and Oohashi T (2021) Assessment of Possible Contributions of Hyaluronan and Proteoglycan Binding Link Protein 4 to Differential Perineuronal Net Formation at the Calyx of Held. Front. Cell Dev. Biol. 9:730550. doi: 10.3389/fcell.2021.730550

The calyx of Held is a giant nerve terminal mediating high-frequency excitatory input to principal cells of the medial nucleus of the trapezoid body (MNTB). MNTB principal neurons are enwrapped by densely organized extracellular matrix structures, known as perineuronal nets (PNNs). Emerging evidence indicates the importance of PNNs in synaptic transmission at the calyx of Held. Previously, a unique differential expression of aggrecan and brevican has been reported at this calyceal synapse. However, the role of hyaluronan and proteoglycan binding link proteins (HAPLNs) in PNN formation and synaptic transmission at this synapse remains elusive. This study aimed to assess immunohistochemical evidence for the effect of HAPLN4 on differential PNN formation at the calyx of Held. Genetic deletion of *Hapln4* exhibited a clear ectopic shift of brevican localization from the perisynaptic space between the calyx of Held terminals and principal neurons to the neuropil surrounding the whole calyx of Held terminals. In contrast, aggrecan expression showed a consistent localization at the surrounding neuropil, together with HAPLN1 and tenascin-R, in both gene knockout (KO) and wild-type (WT) mice. An *in situ* proximity ligation assay demonstrated the molecular association of brevican with HAPLN4 in WT and HAPLN1 in gene KO mice. Further elucidation of the roles of HAPLN4 may highlight the developmental and physiological importance of PNN formation in the calyx of Held.

**Keywords: perineuronal net, chondroitin sulfate proteoglycan, calyx of Held, hyaluronan and proteoglycan binding link protein 4, synapse, *in situ* proximity ligation assay**

## INTRODUCTION

Perineuronal nets (PNNs) are pericellular coats of condensed matrix that enwrap the cell bodies and dendrites of certain neurons in the adult central nervous system. In the brain, PNNs are completed at the end of developmental critical periods for experience-dependent plasticity. They contribute to the stabilization of specific connection patterns, thus limiting plasticity. More recently, PNNs have

been revealed to have myriad actions in many central nervous system functions, including memory, psychiatric disease, and neurodegeneration (Fawcett et al., 2019; Carulli and Verhaagen, 2021). PNNs primarily consist of hyaluronan, chondroitin sulfate proteoglycans (CSPGs) of the lectican family, tenascin-R, and link proteins as a core extracellular matrix (ECM). Other ECM-affiliated molecules (such as semaphorin 3A) and ECM regulators (such as a disintegrin and metalloproteinase with thrombospondin motifs (ADAMTS) proteases) are also included. The heterogeneity of PNNs may arise from variations in molecular compositions as well as differences in the glycan structure of CSPGs.

Perineuronal nets are typically found around fast-spiking GABAergic interneurons expressing parvalbumin. However, of note is that they also exist surrounding other neurons, such as the medial nucleus of the trapezoid body (MNTB). Each principal cell within the MNTB is contacted by a single giant terminal called the calyx of Held, which is characterized by fast and highly reliable synaptic transmission (Borst and Soria van Hoeve, 2012; Joris and Trussell, 2018; Nakakubo et al., 2020). In addition, a unique and clearly distinct distribution pattern of the proteoglycans aggrecan and brevican on the surface of the MNTB principal neurons/calyx of Held has been reported (Blosa et al., 2013). Electrophysiological studies on genetic models deficient in PNN components or enzymatic chondroitin sulfate chain depletion models have highlighted the importance of PNN components and their physiological functions in the calyx of Held (Blosa et al., 2015; Balmer, 2016; Schmidt et al., 2020).

The hyaluronan and proteoglycan binding link proteins (HAPLNs) are key molecules in the formation and control of hyaluronan-based condensed perineuronal matrix in the adult brain (Carulli et al., 2010; Kwok et al., 2010; Bekku et al., 2012; Fawcett et al., 2019). *Hapln4*/*Bral2*-knockout (KO) mice have attenuated PNNs mainly expressed in the brainstem and cerebellum (Bekku et al., 2012). Moreover, the loss of HAPLN4 markedly affected the localization of brevican in all of the nuclei examined, whereas no effect was seen on aggrecan localization (Bekku et al., 2012). HAPLN4 is typically expressed in auditory brainstem neurons, including MNTB neurons (Bekku et al., 2003). Studies in *Hapln4*-KO mice detected higher hearing thresholds at high frequencies and weaker temporal resolution ability in KO mice than in wild-type (WT) mice (Popelář et al., 2017). We have also reported the effect of HAPLN4 deficiency on extracellular diffusion parameters in MNTB during aging (Sucha et al., 2020). These results suggest the importance of HAPLN4 in auditory function. Furthermore, *Hapln4*-KO mice have demonstrated that HAPLN4 is a selective regulator for the formation and transmission of GABAergic Purkinje synapses and deep cerebellar nuclei neurons (Edamatsu et al., 2018). These findings suggest that HAPLNs may regulate the micro-organization of PNN *via* specific interactions with lecticans (HAPLN4 with brevican and HAPLN1 with aggrecan) (Oohashi et al., 2015).

Previous electron microscopic investigations delineated the precise distribution pattern of aggrecan and brevican at the calyx of Held (Blosa et al., 2013), namely: brevican prominently localizes to the pericellular space between the calyx of Held terminals and principal neurons to seal the synaptic cleft. In contrast, aggrecan encloses the entire calyx of Held terminals and principal cells. The differential PNN formation of aggrecan and brevican might indicate their distinct functions on the cell/synapse surface.

These findings led us to conclude that different HAPLN–lectican molecular sets may orchestrate distinct PNNs with functional relevance. To verify this hypothesis, we evaluated the effect of the genetic deletion of *Hapln4* on the differential formation of PNNs using immunohistochemistry and *in situ* proximity ligation assay (PLA) in *Hapln4*-KO mice compared with WT mice.

# MATERIALS AND METHODS

## Animals

Homozygous *Hapln4*-KO mice aged 4 to 5 months and age-matched WT animals from a C57Bl/6 background were used in the experiments. The KO mice were generated by homologous recombination in embryonic stem cells, as described previously (Bekku et al., 2012). The animals were kept on a 12-h light/dark cycle, with a regular feeding and cage cleaning schedule. The mice were given free access to food and water. This study was conducted in strict accordance with the Policy on the Care and Use of Laboratory Animals, Okayama University. The protocol was approved by the Animal Care and Use Committee of the Okayama University (protocol number: OKU-2020743).

## Immunohistochemistry and *in situ* Proximity Ligation Assay

Immunohistochemistry was performed as previously described (Cicanic et al., 2018; Edamatsu et al., 2018). The animals were deeply anesthetized with isoflurane inhalation. To obtain specimens for cryosections, vascular perfusion *via* the left ventricle was performed with phosphate-buffered saline (PBS) and then with a fixative agent containing 4% paraformaldehyde in 0.1 M phosphate buffer (pH 7.4). The brains were removed and postfixed overnight at 4°C. The samples were immersed in 30% sucrose solution in PBS at 4°C, embedded in optimal cutting temperature compound (Sakura Finetek, Japan), and frozen. Then, 30 μm-thick coronal cryosections were cut on a cryostat (Leica CM 1,860) and further processed.

The sections were permeabilized with 0.2% Triton X-100 in PBS and then blocked in 10% donkey serum (Sigma, St. Louis, MO, United States; D9663) in PBS or a Duolink™ blocking solution. Regarding aggrecan immunolabeling, pretreatment with chondroitinase ABC (ChABC, 0.1 U/ml; Sigma, C2905) for 40 min at 37°C was required. The specimens were incubated overnight at 4°C with specific primary antibodies diluted in PBS with 0.2% Triton X-100 and 1.5% donkey serum. Then, the slices were incubated for 4 h at room temperature with secondary antibodies. The following primary

antibodies were used: goat anti-HAPLN4 polyclonal antibody (R&D Systems, Minneapolis, MN, United States; AF4085, RRID:AB_2116264; dilution 1:50), goat anti-HAPLN1 polyclonal antibody (R&D Systems; AF2608, RRID:AB_2116135; dilution 1:50), rabbit anti-aggrecan polyclonal antibody (Merk Millipore, Burlington, MA, United States; AB1031, RRID:AB_90460; dilution 1:150), rabbit anti-brevican polyclonal antibody ([+1058], Thon et al., 2000; dilution 1:2,000; kindly gifted by Dr. Takako Sasaki, Oita University), goat anti-tenascin-R polyclonal antibody (R&D Systems; AF3865, RRID:2207009; dilution 1:200), and guinea pig anti-vesicular glutamate transporter 1 (VGLUT1) polyclonal antibody (Synaptic systems, Göttingen, Germany, 135 304, RRID:AB_887878; dilution 1:100). Regarding immunohistochemistry, the following secondary antibodies were used: Alexa 488-conjugated donkey anti-goat IgG (Thermo Fisher Scientific, Tokyo, Japan; A11055, RRID:AB_2534102; dilution 1:400), Alexa 594-conjugated donkey anti-guinea pig IgG (Jackson ImmunoResearch, West Grove, PA, United States; 706-586-148, RRID:AB_2340475; dilution 1:400), and Alexa 647-conjugated donkey anti-rabbit IgG (Abcam, Cambridge, United Kingdom, ab150075, RRID:AB_2752244; dilution 1:400).

*In situ* PLA was conducted according to the instructions of the manufacturer (Sigma, Duolink®). After primary antibody incubation, the secondary antibodies conjugated with oligonucleotides (PLA probe MINUS and PLA probe PLUS) were added to the specimens and incubated for 2 h at room temperature. Further ligation and amplification reactions were performed. The ligation solution, consisting of two oligonucleotides and ligases, was added and incubated for 30 min at 37°C to cause the oligonucleotides to hybridize to the two PLA probes and join a closed circle when they are in close proximity (<40 nm apart). In the final rolling-circle amplification reaction, the amplification–polymerase solution was added and incubated for 100 min at 37°C. The control experiments were performed for each combination of PLA probes by omitting one of the primary antibodies.

A biotinylated HA-binding protein (b-HABP: Hokudo, Sapporo, Japan, BC41) derived from versican using recombinant human G1 domain was used for hyaluronan staining, as described previously (Bekku et al., 2010). Sections were incubated at 4°C overnight with b-HABP (dilution 1:100), followed by secondary labeling with Alexa 488-conjugated streptavidin (Thermo Fisher Scientific, S32354; dilution 1:400).

After tissue processing, the sections were mounted on microscope slides with a fluorescence mounting medium (Dako, S3023) or Duolink® *in situ* Mounting Medium with DAPI (Sigma). Fluorescent images were acquired using a confocal laser scanning microscope system (Carl Zeiss, LSM780). Confocal images were acquired at a resolution of 1,024 × 1,024 dpi. Laser intensity, gain, and offset were maintained at constant levels for each analysis. Staining intensities were analyzed using the plot profile tool in ImageJ FIJI software. Each experiment was repeated using three WT and three *Hapln4*-KO mice. All experiments were successively repeated at least two times in each mouse, and similar results were obtained. Hence, a representative result is shown in the figure.

# RESULTS

## Distribution of Hyaluronan and Proteoglycan Binding Link Protein 4 and Related Molecules in the Medial Nucleus of the Trapezoid Body

In a previous report, two distinct PNN-type proteoglycan expressions have been reported in the MNTB (Blosa et al., 2013), namely, brevican localization at the perisynaptic space between the calyx of Held terminals and principal neurons and aggrecan localization at the surrounding neuropil. To compare the precise distribution of HAPLN4 with other related molecules and confirm its localization in the context of these distinct PNNs, we performed immunohistochemistry.

In the MNTB of WT, linear immunolabeling of HAPLN4, which colocalized with that of brevican, was observed (**Figures 1C,D**; see arrowheads in the right panels), while a clear segregation of HAPLN4 and aggrecan immunoreactivity (**Figures 1A,B**; see arrows in the right panels) was noted. On the other hand, HAPLN1 immunostaining overlapped with that of aggrecan in the extracellular space of principal cells (**Figures 1E,F**; see arrowheads in the right panels). Notably, HAPLN1 immunoreactivity enwrapped the inner ring-like brevican immunostaining in stark contrast (**Figures 1G,H**; see arrowheads in the right panels). Furthermore, by fluorescence intensity profile analysis, we noticed that some weak staining of brevican localized to the surrounding extracellular space partially overlapped with that of HAPLN1, which indicates a potential interaction between brevican and HAPLN1 (**Figure 1H**; see arrowheads in the right panels).

## Ectopic Expression of Brevican in the Medial Nucleus of the Trapezoid Body of *Hyaluronan and Proteoglycan Binding Link Protein 4*-Knockout Mice

In our previous reports, the diffuse expression of brevican in the MNTB of the young adult *Hapln4*-KO (aged 2–4 months) has been reported (Bekku et al., 2012; Sucha et al., 2020). However, the detailed spatial relationship of PNN components around the MNTB principal cells is lacking. To clarify the special location of PNN components, giant glutamatergic synaptic terminals, and the calyces of Held, were visualized as histological markers by immunostaining for VGLUT1 (Blosa et al., 2013). Regarding MNTB in WT, linear immunostaining for HAPLN4 and brevican around each principal cell was surrounded by VGLUT1 staining (**Figures 2A,C**). In contrast, the immunoreaction of brevican in *Hapln4*-KO mice was prominently located around VGLUT1 staining (**Figure 2D**). This clearly demonstrates the ectopic shift of brevican localization at the surrounding extracellular space in the neuropil in the absence of HAPLN4 (**Figure 2B**). Moreover, we found another interesting aspect of HAPLN1-based PNN in MNTB. Immunostaining for HAPLN1 and aggrecan was consistently localized at the surrounding extracellular space in both genotypes (**Figures 2E–H**). To assess

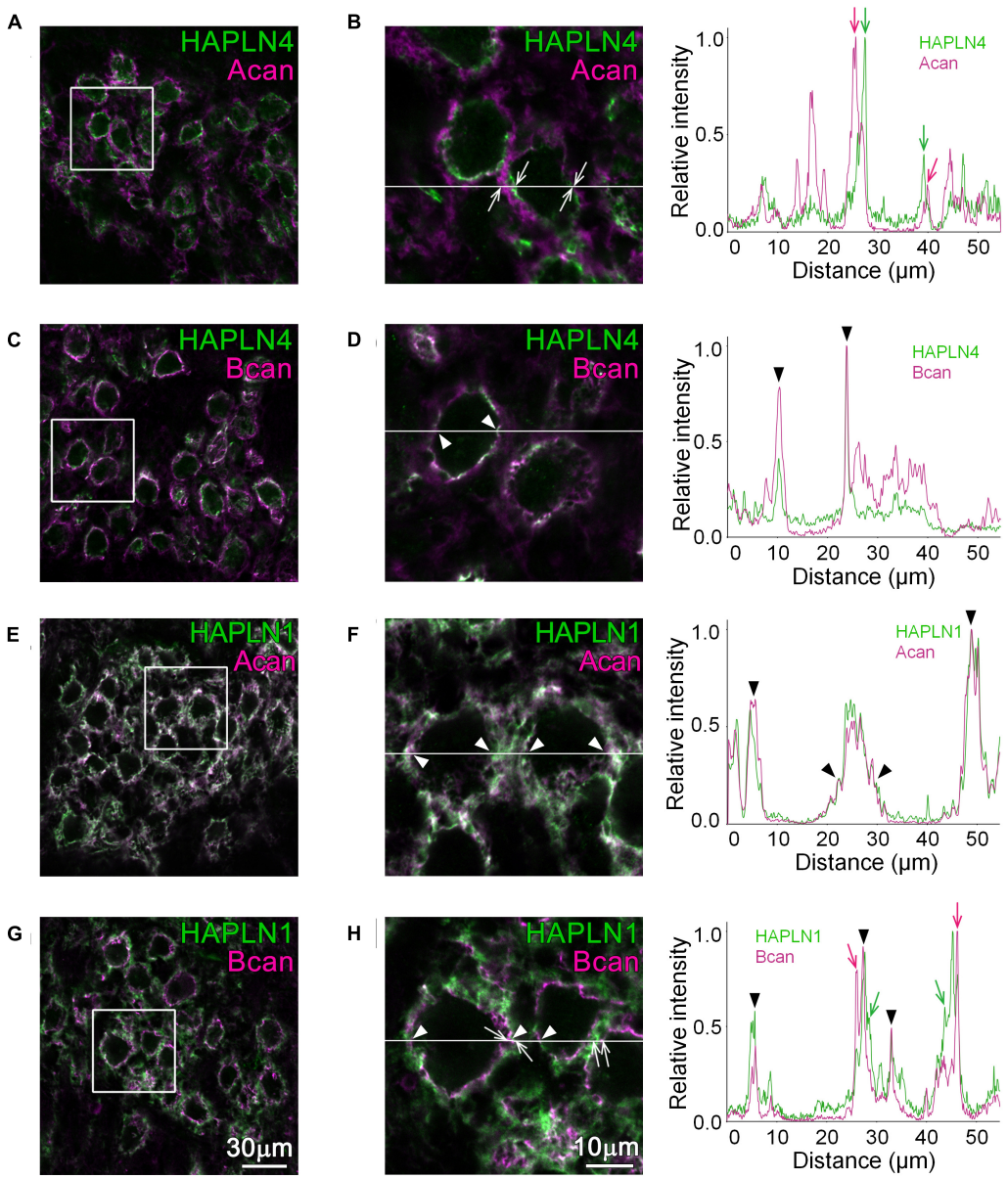


**FIGURE 1 |** Distribution of HAPLNs and lecticans in the medial nucleus of the trapezoid body (MNTB) of adult wild-type (WT) mice. Immunohistochemical detection of HAPLNs (green) and lecticans (magenta) in the MNTB of 4-month-old adult WT mice using HAPLN4 **(A–D)**, HAPLN1 **(E–H)**, aggrecan **(A,B,E,F)**, and brevican **(C,D,G,H)** immunostaining. The intensity profiles of the fluorescence signals along the white lines are shown in the rightmost panels. The fluorescence intensities are normalized by the highest intensities of individual proteins within the lines. Of note are the well-segregated signals between HAPLNs and CSPGs that are indicated by arrows (HAPLNs in green and CSPGs in magenta, respectively). The colocalized signals are indicated by arrowheads. Acan, aggrecan; Bcan, brevican. Scale bar = 30 μm in the left panels and 10 μm in the right panels.

the relative localization of HAPLN1 and brevican in *Hapln4*-KO, we compared the immunolocalization of these molecules and VGLUT1 by triple immunostaining in the same section (**Supplementary Figure 1**). The fluorescence intensity profile analysis showed the well-matched colocalization of HAPLN1 and brevican at the surrounding extracellular space in the neuropil in *Hapln4*-KO. In addition, we assessed the localization of tenascin-R, another important crosslinker of lecticans, in the PNN. The immunoreactivity of tenascin-R was prominent at the HAPLN1-positive surrounding extracellular space around VGLUT1 staining. However, it was barely detectable at the inner ring-like extracellular space between the calyx of Held terminals and the principal cells in both genotypes (**Figures 2I,J**). Hyaluronan labeling with b-HABP showed two distinct PNNs in both genotypes, namely, the inner ring-like PNNs in the perisynaptic space between the calyx of Held terminals and principal neurons and the PNNs at the surrounding extracellular space with neuropil-like morphology (**Supplementary Figure 2**).

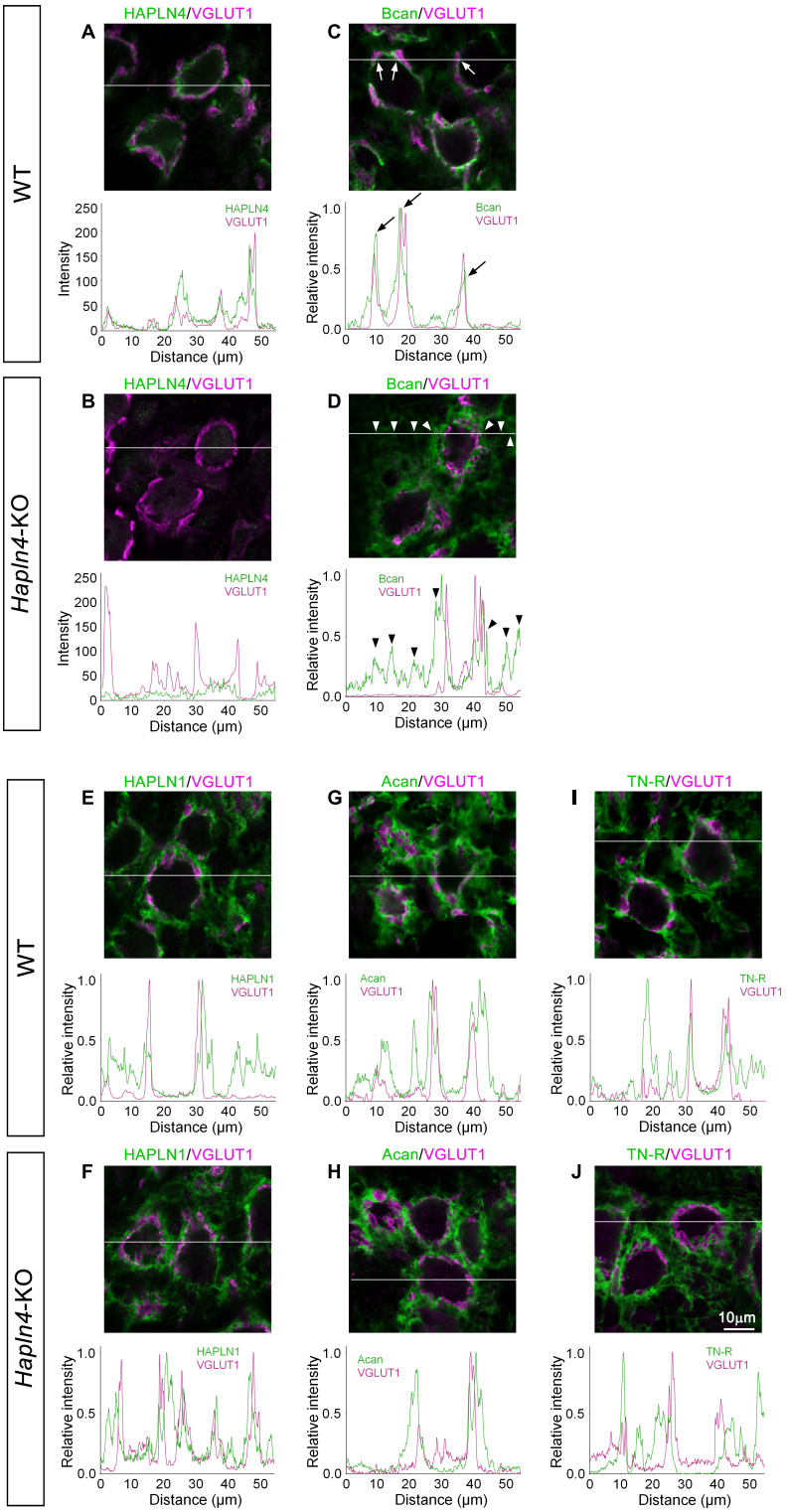


**FIGURE 2 |** Ectopic expression of brevican in the medial nucleus of the trapezoid body (MNTB) of *Hapln4*-KO mice. To clarify the spatial location of perineuronal net components, the immunoreactivity of HAPLNs **(A,B,E,F)**, brevican or aggrecan **(C,D,G,H)**, and tenascin-R **(I,J)** (green) is examined in the MNTB of 4-month-old adult mice using VGLUT1 as a marker of the calyces of Held (magenta). The intensity profiles of the fluorescence signals along the white lines are shown in the lower panels. The fluorescence intensities are normalized by the highest intensities of individual proteins within the lines except in **(A,B)**. Since these have a relatively low signal-to-noise ratio of the anti-HAPLN4 antibodies, the background is high when the intensities are normalized as previously described. Of note is the observed ectopic shift of brevican immunolocalization from the perisynaptic space in the wild type (arrows) to the surrounding extracellular space in the neuropil in *Hapln4*-KO (arrowheads). Acan, aggrecan; Bcan, brevican; TN-R, tenascin-R. The scale bar represents 10 μm.

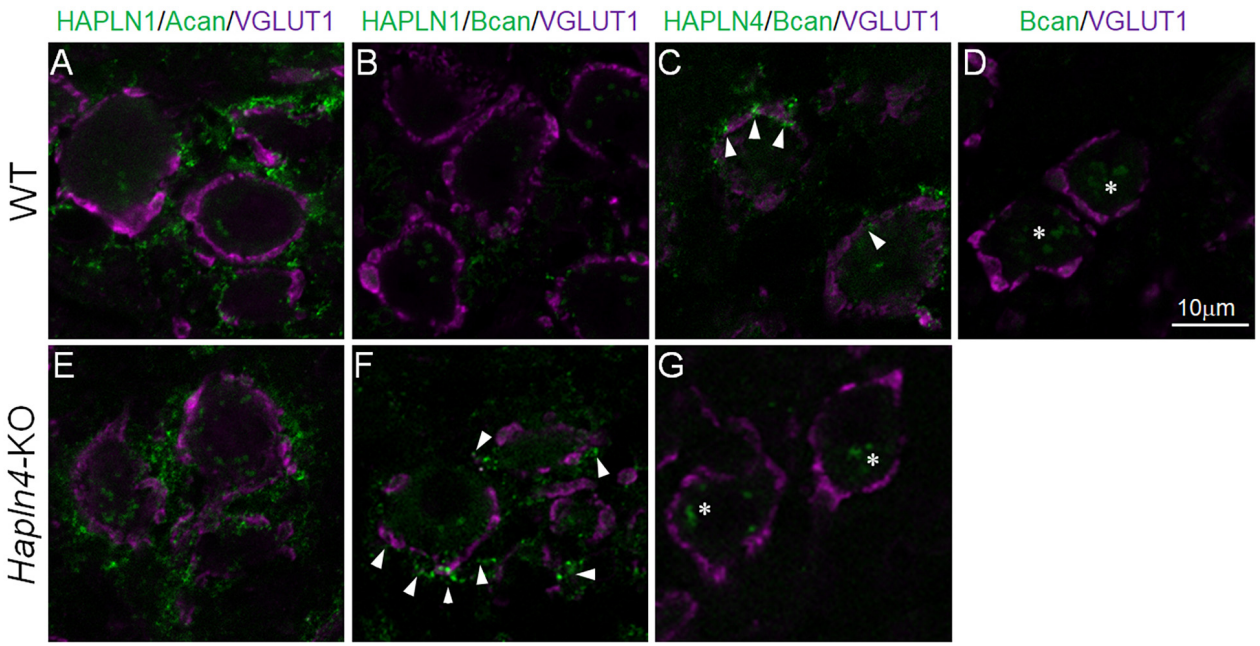


**FIGURE 3 |** Detection of specific HAPLN–lectican molecular interactions by an *in situ* proximity ligation assay (PLA). *In situ* PLA to visualize *in situ* endogenous HAPLN–lectican interactions (green) in the medial nucleus of the trapezoid body of 5-month-old adult WT **(A–D)** and KO **(E–G)** mice using VGLUT1 as a marker of the calyx of Held (magenta). A pair of primary antibodies of HAPLN4 and brevican shows dot signals at the edge or perisynaptic space of the calyx of Held terminals (**C**, arrowheads). Notably, in the absence of HAPLN4, brevican shows an ectopic shift of localization to the surrounding neuropil, where HAPLN1 might potentially stabilize brevican in the aberrant condition (**F**, arrowheads). The specificity of the PLA reaction is validated with two different negative controls: one is a reaction that omits the anti-HAPLN4 antibody on wild-type tissue **(D)**; the other is the PLA reaction of HAPLN4 and brevican using *Hapln4*-KO tissue **(G)**. The non-specific reactions in the negative controls are indicated by asterisks **(D,G)**. Acan, aggrecan; Bcan, brevican. The scale bar represents 10 μm.

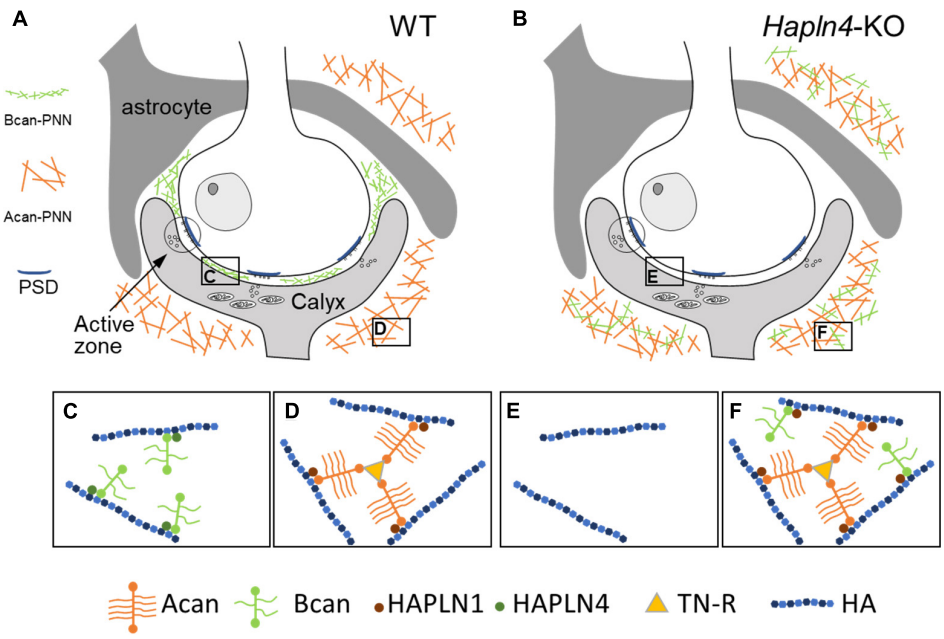


**FIGURE 4 |** Schematic representation of HAPLN-dependent perineuronal net (PNN) micro-organization at the calyx of Held synapses. **(A,C,D)** In wild-type mice, HAPLN4-brevican-type PNN is enriched in the perisynaptic space between the calyx of Held terminals and the principal neuron, and HAPLN1–aggrecan–tenascin-R-type PNN surrounds the whole calyx of Held terminals. **(B,E,F)** In *Hapln4*-KO, the ectopic expression of brevican is detectable with HAPLN1 association at the surrounding extracellular space in the neuropil in addition to the HAPLN1–aggrecan–tenascin-R complex. Acan, aggrecan; Bcan, brevican; TN-R, tenascin-R; HA, hyaluronan; PSD, postsynaptic density.

### Importance of Specific *Hyaluronan and Proteoglycan Binding Link Protein*–Lectican Molecular Interactions for Distinct Perineuronal Net Formation at the Calyx of Held

To better understand the molecular mechanism for the ectopic expression of brevican in the MNTB of *Hapln4*-KO, we introduced *in situ* PLA, a method that outperforms the *in situ* visualization of endogenous protein–protein interactions in tissue sections. By combining immunostaining for the caliceal marker VGLUT1, it becomes a powerful approach to identify differential interactions between HAPLNs and lecticans. The presence of PLA-positive green dots indicates the existence of HAPLN/lectican complexes (**Figure 3**).

A pair of primary antibodies of HAPLN1 and aggrecan generated abundant signals at the surrounding extracellular space with neuropil-like morphology around VGLUT1 staining in both WT and KO mice (**Figures 3A,E**). In contrast, another pair of primary antibodies of HAPLN4 and brevican could generate dot signals at the edge or perisynaptic space of the calyx of Held terminals (**Figure 3C**, arrowheads) in WT mice. An aberrant pair of primary antibodies of HAPLN1 and brevican showed prominent signals at the surrounding extracellular space in *Hapln4*-KO mice (**Figure 3F**, arrowheads), which were very similar to those between HAPLN1 and aggrecan interactions (**Figures 3A,E**), while this pair produced scarcely detectable signals in WT mice (**Figure 3B**).

This study provides direct evidence for differential interactions between HAPLNs and lecticans. In WT form, a specific combination of HAPLN and lectican is located at the specific extracellular milieu, in which HAPLN4 and brevican are located in the perisynaptic space near the synaptic cleft, HAPLN1, and aggrecan surrounding the whole calyx of Held terminals (**Figures 4A,C,D**). Notably, in the absence of HAPLN4, brevican showed an ectopic shift of localization to the surrounding neuropil, where HAPLN1 could potentially stabilize brevican in the aberrant condition (**Figures 4B,E,F**).

## DISCUSSION

In this study, we hypothesized that distinct HAPLNs would regulate the micro-organization of PNN *via* specific interactions with lecticans (Oohashi et al., 2015). Our results demonstrated that HAPLN4 is important for maintaining the specific localization of brevican in the perisynaptic space between the calyx of Held terminals and the principal neurons in the MNTB.

A query could be raised about how each HAPLN-dependent microorganization would be distinctively formed. The authors assumed that some of the following requirements were necessary to achieve this: (i) differences in binding affinity between HAPLNs and G1 domain of lecticans, (ii) tenascin-R crosslinking of aggrecan *via* the G3 domain, and (iii) HAPLN4 translocation through the axon and secretion from the calyx of Held terminal. Regarding the first requirement, we demonstrated a clear difference in HAPLN and lectican binding between WT and KO mice using *in situ* PLA (**Figure 3**). However, biochemical experiments are necessary to measure the binding affinity between HAPLNs and lecticans. Regarding the second requirement, tenascin-R has been shown to have a high affinity for the G3 domain of aggrecan and brevican (Aspberg, 2012). Moreover, it has been experimentally demonstrated that tenascin-R could promote the assembly of reticular PNNs *via* cross-linking of aggrecan (Morawski et al., 2014). In fact, tenascin-R was prominently expressed to surround the entire calyx of Held terminals (**Figure 2**). The cross-linking of aggrecan *via* tenascin-R in HAPLN1-based PNN may increase the structural integrity of the PNN. The third requirement has not been validated yet. However, there have been several supporting data from three previous reports that may explain the possibility of HAPLN4 axonal transport (Bekku et al., 2003; Carulli et al., 2007; Blosa et al., 2016). Further research is necessary to test this hypothesis.

Each principal neuron in the MNTB receives a single input from a giant axosomatic terminal: the calyx of Held. High transmission reliability and consistency in timing and amplitude have been confirmed in the mature calyx of Held synapses (Sonntag et al., 2011; Borst and Soria van Hoeve, 2012). Although the calyx of Held synapses are enwrapped by densely organized PNNs, the functional importance of PNN has not been elucidated until recently. However, based on the recent progress in understanding the formation of PNN (Sonntag et al., 2015), Morawski et al. (2014) have addressed the functional role of PNN components. They could take advantage of the accessibility of the calyx of Held synapses to patch-clamp recordings in brain slices from a genetic model deficient in PNN components (Blosa et al., 2015; Schmidt et al., 2020). In brevican-deficient mice, the speed of pre- to post-synaptic action potential transmission was reduced, and the duration of the respective pre- and post-synaptic action potentials increased (Blosa et al., 2015). A significant prolongation of transmission speed at the calyx of Held has been reported in neurocan-deficient mice (Schmidt et al., 2020).

Perineuronal nets have been implicated in a number of psychiatric disorders (Fawcett et al., 2019). Recently, the *HAPLN4* gene has been included as a significant gene according to the transcriptome-wide association study FUSION in its analysis of 13,435 genes using gene expression data from the PsychENCODE Consortium (1,321 brain samples) (Gandal et al., 2018; Mullins et al., 2021). Furthermore, the Schizophrenia Working Group of the Psychiatric Genomics Consortium identified 108 schizophrenia-related loci (Schizophrenia Working Group of the Psychiatric Genomics Consortium, 2014). Although gray matter volume (GMV) reduction is a common neuroimaging finding of schizophrenia, little is known about the underlying mechanism for the GMV reduction. Ji et al. (2021) applied transcription (196 schizophrenia risk genes)—a neuroimaging analysis to test which of these genes were associated with GMV alterations in patients with schizophrenia. Finally, they identified 98 genes associated with GMV alterations in patients with schizophrenia. Of note is that the 98 identified genes showed a significant enrichment

on eight gene ontology terms for molecular functions, including CSPG binding and hyaluronan binding. Among them, *HAPLN4* showed the largest negative correlation: the expression of this gene was lower in the brain regions with more GMV reduction in patients with schizophrenia. The authors suggested that the low expression level of *HAPLN4* might lead to GMV reduction by influencing the ECM and PNNs. This result is in line with our previous findings that HAPLN4 deficiency in mice led to a decrease in the extracellular space volume fraction but only in the aged brain (Cicanic et al., 2018; Sucha et al., 2020).

Hyaluronan and proteoglycan binding link proteins play an important role as organizers of PNNs. Moreover, the current study indicated that each HAPLN may contribute to the formation of distinct PNNs with different functional relevance. The main limitation to this study is the lack of functional studies on aberrant PNN at the calyx of Held in *Hapln4*-KO mice. Regarding the direct evaluation of the developmental and physiological role of HAPLN4, electrophysiological studies on the calyx of Held–MNTB synapses in *Hapln4*-KO would be a powerful approach.

## CONCLUSION

Our results demonstrated a clear ectopic shift of brevican localization from the perisynaptic space between the calyx of Held terminals and principal neurons to the surrounding neuropil. In contrast, aggrecan expression showed a consistent localization at the surrounding neuropil together with HAPLN1 and tenascin-R in both KO and WT mice.

## DATA AVAILABILITY STATEMENT

The original contributions presented in the study are included in the article/**Supplementary Material**, further inquiries can be directed to the corresponding author.

## ETHICS STATEMENT

The animal study was reviewed and approved by the Animal Care and Use Committee of Okayama University.

## AUTHOR CONTRIBUTIONS

TO, TH, and LV contributed to the study concept and design. KN and HM contributed to the performance of the experiments. KN, HM, TH, LV, and TO contributed to the analysis and interpretation of data. TO, HM, and KN prepared the manuscript initial draft. All authors participated in the critical correction of the manuscript and approved the final version.

## FUNDING

This study was funded by the Ministry of Education, Culture, Sports, Science, and Technology, Japan (Grant Numbers 26110713 and 19H04754 to TO), and the Operational Programme Research, Development, and Education in the framework of the project "Center of Reconstructive Neuroscience," registration number CZ.02.1.01/0.0./0.0/15_003/0000419, to LV.

## ACKNOWLEDGMENTS

We acknowledge Midori Edamatsu, Koichi Nosaka, and Takahiro Ishii for their excellent technical support and Mitsuaki Ono, Tomoko Yonezawa, and other members of our laboratory who provided discussion and comments on this manuscript. We also acknowledge Takako Sasaki (Oita University) for providing antibodies against brevican and Reinhard Fässler (Max Planck Institute of Biochemistry) for their support in generating the knockout mice, and Editage (www.editage.com) for the English language editing.

## SUPPLEMENTARY MATERIAL

The Supplementary Material for this article can be found online at: https://www.frontiersin.org/articles/10.3389/fcell.2021.730550/full#supplementary-material

## REFERENCES

Aspberg, A. (2012). The different roles of aggrecan interaction domains. *J. Histochem. Cytochem.* 60, 987–996. doi: 10.1369/0022155412464376

Balmer, T. S. (2016). Perineuronal nets enhance the excitability of fast-spiking neurons. *eNeuro* 3:ENEURO.0112-16.2016. doi: 10.1523/ENEURO.0112-16.2016

Bekku, Y., Saito, M., Moser, M., Fuchigami, M., Maehara, A., Nakayama, M., et al. (2012). Bral2 is indispensable for the proper localization of brevican and the structural integrity of the perineuronal net in the brainstem and cerebellum. *J. Comp. Neurol.* 520, 1721–1736. doi: 10.1002/cne.23009

Bekku, Y., Su, W. D., Hirakawa, S., Fässler, R., Ohtsuka, A., Kang, J. S., et al. (2003). Molecular cloning of Bral2, a novel brain-specific link protein, and immunohistochemical colocalization with brevican in perineuronal nets. *Mol. Cell. Neurosci.* 24, 148–159. doi: 10.1016/s1044-7431(03)00133-7

Bekku, Y., Vargová, L., Goto, Y., Vorísek, I., Dmytrenko, L., Narasaki, M., et al. (2010). Bral1: its role in diffusion barrier formation and conduction velocity in the CNS. *J. Neurosci.* 30, 3113–3123. doi: 10.1523/jneurosci.5598-09.2010

Blosa, M., Bursch, C., Weigel, S., Holzer, M., Jäger, C., Janke, C., et al. (2016). Reorganization of synaptic connections and perineuronal nets in the deep cerebellar nuclei of purkinje cell degeneration mutant mice. *Neural. Plast.* 2016:2828536. doi: 10.1155/2016/2828536

Blosa, M., Sonntag, M., Brückner, G., Jäger, C., Seeger, G., Matthews, R. T., et al. (2013). Unique features of extracellular matrix in the mouse medial nucleus of trapezoid body–implications for physiological functions. *Neuroscience* 228, 215–234. doi: 10.1016/j.neuroscience.2012.10.003

Blosa, M., Sonntag, M., Jäger, C., Weigel, S., Seeger, J., Frischknecht, R., et al. (2015). The extracellular matrix molecule brevican is an integral component of the machinery mediating fast synaptic transmission at the calyx of Held. *J. Physiol.* 593, 4341–4360. doi: 10.1113/jp270849

Borst, J. G., and Soria van Hoeve, J. (2012). The calyx of Held synapse: from model synapse to auditory relay. *Annu. Rev. Physiol.* 74, 199–224. doi: 10.1146/annurev-physiol-020911-153236

Carulli, D., and Verhaagen, J. (2021). An extracellular perspective on CNS maturation: perineuronal nets and the control of plasticity. *Int. J. Mol. Sci.* 22:2434. doi: 10.3390/ijms22052434

Carulli, D., Pizzorusso, T., Kwok, J. C., Putignano, E., Poli, A., Forostyak, S., et al. (2010). Animals lacking link protein have attenuated perineuronal nets and persistent plasticity. *Brain* 133, 2331–2347. doi: 10.1093/brain/awq145

Carulli, D., Rhodes, K. E., and Fawcett, J. W. (2007). Upregulation of aggrecan, link protein 1, and hyaluronan synthases during formation of perineuronal nets in the rat cerebellum. *J. Comp. Neurol.* 501, 83–94. doi: 10.1002/cne.21231

Cicanic, M., Edamatsu, M., Bekku, Y., Vorisek, I., Oohashi, T., and Vargova, L. (2018). A deficiency of the link protein Bral2 affects the size of the extracellular space in the thalamus of aged mice. *J. Neurosci. Res.* 96, 313–327. doi: 10.1002/jnr.24136

Edamatsu, M., Miyano, R., Fujikawa, A., Fujii, F., Hori, T., Sakaba, T., et al. (2018). Hapln4/Bral2 is a selective regulator for formation and transmission of GABAergic synapses between Purkinje and deep cerebellar nuclei neurons. *J. Neurochem.* 147, 748–763. doi: 10.1111/jnc.14571

Fawcett, J. W., Oohashi, T., and Pizzorusso, T. (2019). The roles of perineuronal nets and the perinodal extracellular matrix in neuronal function. *Nat. Rev. Neurosci.* 20, 451–465. doi: 10.1038/s41583-019-0196-3

Gandal, M. J., Zhang, P., Hadjimichael, E., Walker, R. L., Chen, C., Liu, S., et al. (2018). Transcriptome-wide isoform-level dysregulation in ASD, schizophrenia, and bipolar disorder. *Science* 362:eaat8127. doi: 10.1126/science.aat8127

Ji, Y., Zhang, X., Wang, Z., Qin, W., Liu, H., Xue, K., et al. (2021). Genes associated with gray matter volume alterations in schizophrenia. *Neuroimage* 225:117526. doi: 10.1016/j.neuroimage.2020.117526

Joris, P. X., and Trussell, L. O. (2018). The calyx of held: a hypothesis on the need for reliable timing in an intensity-difference encoder. *Neuron* 100, 534–549. doi: 10.1016/j.neuron.2018.10.026

Kwok, J. C., Carulli, D., and Fawcett, J. W. (2010). *In vitro* modeling of perineuronal nets: hyaluronan synthase and link protein are necessary for their formation and integrity. *J. Neurochem.* 114, 1447–1459.

Morawski, M., Dityatev, A., Hartlage-Rübsamen, M., Blosa, M., Holzer, M., Flach, K., et al. (2014). Tenascin-R promotes assembly of the extracellular matrix of perineuronal nets via clustering of aggrecan. *Philos. Trans. R. Soc. Lond. B. Biol. Sci.* 369:20140046. doi: 10.1098/rstb.2014.0046

Mullins, N., Forstner, A. J., O'Connell, K. S., Coombes, B., Coleman, J. R. I., Qiao, Z., et al. (2021). Genome-wide association study of more than 40,000 bipolar disorder cases provides new insights into the underlying biology. *Nat. Genet.* 53, 817–829.

Nakakubo, Y., Abe, S., Yoshida, T., Takami, C., Isa, M., Wojcik, S. M., et al. (2020). Vesicular glutamate transporter expression ensures high-fidelity synaptic transmission at the calyx of held synapses. *Cell Rep.* 32:108040. doi: 10.1016/j.celrep.2020.108040

Oohashi, T., Edamatsu, M., Bekku, Y., and Carulli, D. (2015). The hyaluronan and proteoglycan link proteins: organizers of the brain extracellular matrix and key molecules for neuronal function and plasticity. *Exp. Neurol.* 274, 134–144. doi: 10.1016/j.expneurol.2015.09.010

Popelář, J., Díaz Gómez, M., Lindovský, J., Rybalko, N., Burianová, J., Oohashi, T., et al. (2017). The absence of brain-specific link protein Bral2 in perineuronal nets hampers auditory temporal resolution and neural adaptation in mice. *Physiol. Res.* 66, 867–880. doi: 10.33549/physiolres.933605

Schizophrenia Working Group of the Psychiatric Genomics Consortium (2014). Biological insights from 108 schizophrenia-associated genetic loci. *Nature* 511, 421–427. doi: 10.1038/nature13595

Schmidt, S., Arendt, T., Morawski, M., and Sonntag, M. (2020). Neurocan contributes to perineuronal net development. *Neuroscience.* 442, 69–86. doi: 10.1016/j.neuroscience.2020.06.040

Sonntag, M., Blosa, M., Schmidt, S., Rübsamen, R., and Morawski, M. (2015). Perineuronal nets in the auditory system. *Hear. Res.* 329, 21–32. doi: 10.1016/j.heares.2014.12.012

Sonntag, M., Englitz, B., Typlt, M., and Rübsamen, R. (2011). The calyx of Held develops adult-like dynamics and reliability by hearing onset in the mouse in vivo. *J. Neurosci.* 31, 6699–6709.

Sucha, P., Chmelova, M., Kamenicka, M., Bochin, M., Oohashi, T., and Vargova, L. (2020). The effect of Hapln4 link protein deficiency on extracellular space diffusion parameters and perineuronal nets in the auditory system during aging. *Neurochem. Res.* 45, 68–82. doi: 10.1007/s11064-019-02894-2

Thon, N., Haas, C. A., Rauch, U., Merten, T., Fässler, R., Frotscher, M., et al. (2000). The chondroitin sulphate proteoglycan brevican is upregulated by astrocytes after entorhinal cortex lesions in adult rats. *Eur. J. Neurosci.* 12, 2547–2558. doi: 10.1046/j.1460-9568.2000.00109.x

**Conflict of Interest:** The authors declare that the research was conducted in the absence of any commercial or financial relationships that could be construed as a potential conflict of interest.

**Publisher's Note:** All claims expressed in this article are solely those of the authors and do not necessarily represent those of their affiliated organizations, or those of the publisher, the editors and the reviewers. Any product that may be evaluated in this article, or claim that may be made by its manufacturer, is not guaranteed or endorsed by the publisher.

frontiers in Cell and Developmental Biology

BRIEF RESEARCH REPORT
published: 23 September 2021
doi: 10.3389/fcell.2021.733964

# Dermatan-4-*O*-Sulfotransferase-1 Contributes to the Undifferentiated State of Mouse Embryonic Stem Cells

*Chika Ogura*[1] *and Shoko Nishihara*[1,2]*

[1] *Department of Bioinformatics, Graduate School of Engineering, Soka University, Hachioji, Japan,* [2] *Glycan and Life System Integration Center (GaLSIC), Soka University, Hachioji, Japan*

Mouse embryonic stem cells (mESCs) have the properties of self-renewal and pluripotency. Various signals and growth factors maintain their undifferentiated state and also regulate their differentiation. Glycosaminoglycans are present on the cell surface and in the cell matrix as proteoglycans. Previously, we and other groups reported that the glycosaminoglycan heparan sulfate contributes to both maintenance of undifferentiated state and regulation of mESC differentiation. It has been shown that chondroitin sulfate is needed for pluripotency and differentiation of mESCs, while keratan sulfate is a known marker of human ESCs or induced pluripotent stem cells. We also found that DS promotes neuronal differentiation from mESCs and human neural stem cells; however, the function of DS in the maintenance of mESCs has not yet been revealed. Here, we investigated the role of DS in mESCs by knockdown (KD) or overexpression (O/E) of the *dermatan-4-O-sulfotransferase-1* (*D4ST1*) gene. We found that the activity of the ESC self-renewal marker alkaline phosphatase was reduced in *D4ST1* KD mESCs, but, in contrast, increased in *D4ST1* O/E mESCs. *D4ST1* KD promoted endodermal differentiation, as indicated by an increase in *Cdx2* expression. Conversely, *Cdx2* expression was decreased by *D4ST1* O/E. Wnt signaling, which is also involved in endodermal differentiation, was activated by *D4ST1* KD and suppressed by *D4ST1* O/E. Collectively, these results demonstrate that D4ST1 contributes to the undifferentiated state of mESCs. Our findings provide new insights into the function of DS in mESCs.

**Keywords: mouse embryonic stem cells, *D4ST1*, self-renewal, *Cdx2*, endodermal differentiation**

OPEN ACCESS

***Edited by:***
*Fuchuan Li,*
*Shandong University, China*

***Reviewed by:***
*Inmaculada Navarro-Lérida,*
*Autonomous University of Madrid, Spain*
*Yong Fan,*
*Guangzhou Medical University, China*

***Correspondence:**
*Shoko Nishihara*
*shoko@soka.ac.jp*

***Specialty section:***
*This article was submitted to Signaling, a section of the journal Frontiers in Cell and Developmental Biology*

***Received:*** *30 June 2021*
***Accepted:*** *01 September 2021*
***Published:*** *23 September 2021*

***Citation:***
*Ogura C and Nishihara S (2021) Dermatan-4-O-Sulfotransferase-1 Contributes to the Undifferentiated State of Mouse Embryonic Stem Cells. Front. Cell Dev. Biol. 9:733964. doi: 10.3389/fcell.2021.733964*

## INTRODUCTION

Mouse embryonic stem cells (mESCs) are established from the inner cell mass at the blastocyst stage (Evans and Kaufman, 1981; Martin, 1981). They have the properties of self-renewal and pluripotency, which means that they are capable of differentiation into the three primary germ layers, endoderm, mesoderm, and ectoderm, via the epiblast and primitive endoderm. There are many studies showing that various signals and growth factors contribute to maintenance of undifferentiated state and regulation of differentiation in mESCs. Because the role of glycans in these processes has not been fully elucidated, we previously performed an RNA interference (RNAi) screen to identify glycosyltransferases essential for self-renewal and pluripotency in mESCs.

To date, we have identified four glycan structures that are required to maintain the naïve pluripotent state: (1) LacdiNAc structure (GalNAcβ1-4GlcNAc) (Sasaki et al., 2011), (2) heparan sulfate (HS) (Sasaki et al., 2008, 2009; Hirano et al., 2012, 2013), (3) *O*-GlcNAc (Miura and Nishihara, 2016; Miura et al., 2018; Pecori et al., 2021), and (4) T antigen (Galβ1-3GalNAc) (Pecori et al., 2020).

Glycosaminoglycans (GAGs) such as HS are present on the cell surface and in the cell matrix as proteoglycans, consisting of GAG and a core protein. GAGs show diverse structures due to sulfation and have a characteristic disaccharide repeating structure. In addition to HS, keratan sulfate (KS), and chondroitin sulfate (CS)/dermatan sulfate (DS) are well-known GAGs. HS and CS/DS bind to the Ser residue of core proteins through a common linkage region, namely GlcAβ1-3Galβ1-3Galβ1-4Xylβ-*O*-ser (Sugahara and Kitagawa, 2000), while KS binds to core proteins via an *N*-linked or *O*-linked oligosaccharide (Funderburgh, 2002). Previously, we and other groups showed that HS contributes to maintenance of undifferentiated state and regulation of differentiation in mESCs by promoting Wnt, BMP, FGF, and Fas signaling (Johnson et al., 2007; Sasaki et al., 2008, 2009; Kraushaar et al., 2010, 2012; Lanner et al., 2010; Fico et al., 2012; Hirano et al., 2012, 2013). In addition, Izumikawa et al. (2014) reported that CS is required for pluripotency and differentiation of mESCs, while KS is known as a marker of human ESCs or induced pluripotent stem cells (Andrews et al., 1984; Pera et al., 1988; Adewumi et al., 2007; Kawabe et al., 2013). To our knowledge, however, the function of DS in mESCs has not been revealed yet.

In the synthesis of DS, epimerization from glucuronic acid (GlcA) to iduronic acid (IdoA) is initially carried out by dermatan sulfate epimerase (Maccarana et al., 2006) or dermatan sulfate epimerase-like (Pacheco et al., 2009) after synthesis of the CS chain (i.e., GlcA-GalNAc repeating disaccharide structure). Subsequently, dermatan-4-*O*-sulfotransferase-1 (D4ST1) (Evers et al., 2001) transfers sulfate to the C-4 hydroxyl group of GalNAc. Lastly, sulfate is transferred to the C-6-hydroxyl group of GalNAc and the C-2 hydroxyl group of IdoA by *N*-acetylgalactosamine-4-sulfate 6-*O*-sulfotransferase (GalNAc4S-6ST) (Ito and Habuchi, 2000) and uronyl-2-sulfotransferase (UST) (Kobayashi et al., 1999), respectively. While the GalNAc4S-6ST and UST sulfotransferases are common to both CS and DS, D4ST1 is specific to DS.

We previously reported that DS promotes neuronal differentiation from mESCs and human neural stem cells (Ogura et al., 2020). It is also known that D4ST1 is needed for neuronal differentiation from mouse neural stem cells (Bian et al., 2011). Moreover, *D4ST1* deficiency is the cause of Ehlers-Danlos syndrome (EDS), a genetic connective tissue disorder with defects in skin, ligaments, articulation, internal organs, and blood vessels (Kosho, 2016; Malfait et al., 2017).

Here, therefore, we investigated the role of DS in the undifferentiated state of mESCs by knockdown or overexpression of *D4ST1*. We found that D4ST1 contributes to self-renewal of mESCs and *D4ST1* knockdown induces endodermal differentiation by activating Wnt signaling. Our results provide new insights into function of DS in mESCs.

# MATERIALS AND METHODS

## Cell Culture

The R1 mESC line (Nagy et al., 1993) was cultured on mouse embryonic fibroblasts (MEFs) in mESC culture medium [DMEM (Gibco), 15% FBS (Nichirei Bioscience, Inc.), 1% penicillin/streptomycin (Gibco), 0.1 mM 2-mercaptoethanol (Gibco), 1 mM non-essential amino acids (Gibco), and 1,000 units/ml of LIF (Oriental Yeast)]. MEFs were isolated from embryos at E14.5 and inactivated by the addition of 10 μg/ml of mitomycin C (Sigma).

## Transfection

For transient knockdown (KD) of *D4ST1* in mESCs, we generated siRNA expression vectors using pSilencer 3.1-H1 (Ambion). The siRNA sequences used for RNAi were designed as described previously (Ui-Tei et al., 2004) by using siDirect[1]:

E*gfp*, 5′-GATCCCGCCACAACGTCTATATCATGGGGAAA ATCCATGATATAGACGTTGTGGCTTTTTTGGAAA-3′; *D4S T1* KD1, 5′-GATCCCCAGCACTACTTCAAGTTCCTGTTTGG CTTCCTGTCACCAAACAGGAACTTGAAGTAGTGCTGTTT TTTA-3′; *D4ST1* KD2, 5′-GATCCCTCCTCTTGCTAGGTCTGA ATCATTTGCTTCCTGTCACAAATGATTCAGACCTAGCAAG AGGATTTTTTA-3′; *D4ST1* KD3, 5′-GATCCCCTTCAAGAT GTGCTACCTAAGGCTTCCTGTCACCTTAGGTAGCACATCT TGAAGTTTTTTA-3′. *Egfp* was used as a negative control.

We also generated a *D4ST1* overexpression (O/E) vector using pCAGI-Puro (a kind gift of Professor Kumiko Ui-Tei). The vector was produced by using the pGEM®-T Easy Vector Systems (Promega) as described previously (Kamiyama et al., 2006). We used an empty vector as a control for the O/E experiments.

Before transfection, we replated the mESCs at $1 \times 10^6$ cells on gelatin-coated 60-mm culture dishes (NIPPON Genetics) containing LIF. After 16 h, the cells were transfected with 4 μg of siRNA expression vectors targeting *D4ST1* (*D4ST1* KD1 and *D4ST1* KD2) or *Egfp*, or the *D4ST1* O/E vector by using Lipofectamine 2000 (Invitrogen). At 1 day after transfection (TF day 1), transfected cells were selected by adding 2 μg/ml of puromycin (Sigma). We harvested the cells at TF day 2 for the *D4ST1* O/E experiments or TF day 4 for the *D4ST1* KD experiments.

## Cell Proliferation Assay

*D4ST1* KD mESCs at TF day 4 were replated at $8 \times 10^3$ cells per well on gelatin-coated 96-well plates (IWAKI) containing LIF. After 24 h, we counted the number of viable cells by using microscopy.

## Alkaline Phosphatase Staining

The transfected mESCs were replated at $1.25 \times 10^5$ cells per well on gelatin-coated 24-well plates (NIPPON Genetics) containing LIF. After 5 days, we carried out ALP staining with a StemTAG™ Alkaline Phosphatase Staining Kit (Cell Biolabs, Inc.). ALP-positive colonies were counted by using microscopy.

[1]http://sidirect2.rnai.jp/

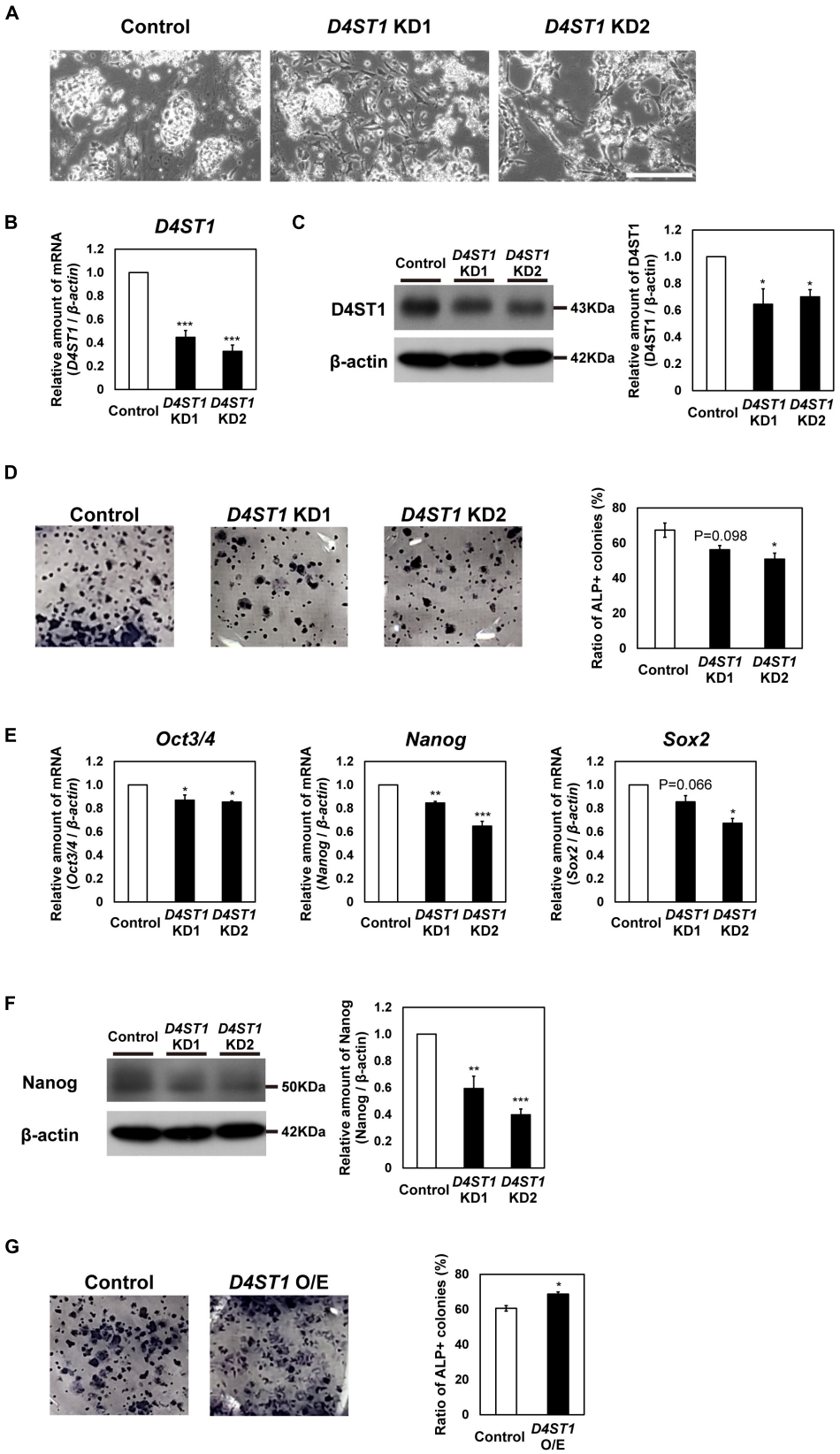


**FIGURE 1 |** (Continued)

**FIGURE 1 |** *D4ST1* contributes to self-renewal of mESCs. **(A)** Morphological observation of *D4ST1* KD mESCs at day 4 after transfection (TF day 4). Scale bar: 200 μm. **(B)** Real-time PCR analysis of *D4ST1* in *D4ST1* KD mESCs at TF day 4. The amount of *D4ST1* mRNA was normalized to that of *β-actin* mRNA and is shown relative to the control (set to 1). **(C)** Western blotting analysis of D4ST1 in *D4ST1* KD mESCs at TF day 4. Histogram shows the mean densitometric readings of bands, which were normalized to β-actin and are shown relative to the control (set to 1). **(D)** Alkaline phosphatase (ALP) staining of *D4ST1* KD mESCs at TF day 4. (Left) Representative images of ALP staining. (Right) Histogram showing the ratio of ALP-positive colonies. **(E)** Real-time PCR analysis of pluripotent markers in *D4ST1* KD mESCs at TF day 4. The amounts of pluripotent marker mRNAs (*Oct3/4*, *Nanog*, and *Sox2*) were normalized to that of *β-actin* mRNA and are shown relative to the control (set to 1). **(F)** Western blotting analysis of Nanog in *D4ST1* KD mESCs at TF day 4. Histogram shows the mean densitometric readings of bands, which were normalized to β-actin and are shown relative to the control (set to 1). The representative bands of the loading control (β-actin) are the same as those in **(C)** because the same samples were used for these analyses. **(G)** ALP staining of *D4ST1* O/E mESCs at TF day 2. (Left) Representative images of ALP staining. (Right) Histogram showing the ratio of ALP-positive colonies. The values shown are means ± SD ($N = 3$). Those significantly different to the control by Dunnett test **(B–F)** or unpaired two-tailed Student's *t*-test **(G)** are indicated as follows: $^{***}p < 0.001$; $^{**}p < 0.01$; $^{*}p < 0.05$.

## Real-Time PCR

Total RNA was extracted from cells by using TRI Reagent® (Molecular Research Center, Inc.) and reverse-transcribed by using SuperScript™ VILO™ Master Mix (Invitrogen). Real-time PCR was performed by using Quant Studio 12K Flex (Applied Biosystems). The relative amount of each mRNA was normalized against the amount of *β-actin* mRNA in the same sample. The primer sets for real-time PCR are listed in **Supplementary Table 1**.

## Western Blotting Analysis

The transfected mESCs were lysed with lysis buffer (50 mM Tris–HCl pH 7.4, 150 mM NaCl, 1% Triton X-100, 5 mM EDTA, 1 mM $Na_3VO_4$, 10 mM NaF, and protease inhibitors). The protein samples (5–10 μg) were separated by 8% SDS-PAGE and transferred to PVDF membranes (Millipore). After blocking with 1% BSA/TBST, the membranes were incubated with primary antibodies. The membranes were then incubated with secondary antibodies and Amersham ECL Prime Western Blotting Detection Reagent (GE Healthcare Life Science) was used for detection. The antibodies are listed in **Supplementary Table 2**.

## Statistical Analysis

Data were compared with unpaired two-tailed Student's *t*-test or Dunnett test. Asterisks denote statistical significance (n.s., $p > 0.05$; $^{*}p < 0.05$; $^{**}p < 0.01$; and $^{***}p < 0.001$).

# RESULTS

## *D4ST1* Contributes to Self-Renewal of mESCs

To investigate function of DS in mESCs, we performed knockdown (KD) of *D4ST1*, which is the first sulfotransferase in the DS synthesis pathway (**Figure 1A**). We designed two constructs (*D4ST1* KD1 and *D4ST1* KD2), which expressed different siRNAs targeting *D4ST1* mRNA, and one construct targeting *Egfp* as a negative control. After transfection of mESCs with these constructs, the decreased expression of *D4ST1* mRNA and D4ST1 was confirmed by real-time PCR and western blotting, respectively (**Figures 1B,C**). Proliferation in *D4ST1* KD mESCs was not changed as compared with control cells (**Supplementary Figure 1**). To determine self-renewal potential, ALP staining was performed for the *D4ST1* KD1 and KD2 transfected mESCs. The number of ALP-positive colonies was reduced by *D4ST1* KD, indicating that D4ST1 contributes to self-renewal of mESCs (**Figure 1D**). Furthermore, the expression of three pluripotent markers, *Oct3/4*, *Nanog* and *Sox2*, were decreased in *D4ST1* KD mESCs (**Figure 1E** and **Supplementary Figure 2**). The expression of *Klf2* was decreased, while that of *Klf4* and *Rex1* did not change significantly (**Supplementary Figure 3**). The amount of Nanog was also significantly decreased in *D4ST1* KD mESCs (**Figure 1F**).

We also examined the effect of overexpression (O/E) of *D4ST1* in mESCs (**Supplementary Figure 4A**). The increased expression of *D4ST1* mRNA and D4ST1 after transfection with the O/E vector was confirmed by real-time PCR and western blotting, respectively (**Supplementary Figures 4B,C**). In contrast to *D4ST1* KD, *D4ST1* O/E increased the number of ALP-positive colonies (**Figure 1G**), confirming that D4ST1 contributes to self-renewal of mESCs.

## Endodermal Differentiation of mESCs Is Induced by *D4ST1* KD

Next, we examined the expression of differentiation markers to determine which lineages are induced from mESCs by *D4ST1* KD (**Figure 2A** and **Supplementary Figure 2**). In *D4ST1* KD mESCs, the expression of two epiblast markers, *Fgf5* and *Otx2*, was decreased. The expression of two mesoderm markers, *T* and *Mixl*, was also significantly decreased. In contrast to mesodermal markers, the expression of two endoderm markers, *Sox17* and *Cdx2*, was significantly increased in *D4ST1* KD mESCs, indicating that the endodermal differentiation was induced in *D4ST1* KD mESCs. Expression of the primitive endoderm marker *Gata6* was significantly increased, indicating that the differentiation to primitive endoderm was also induced in *D4ST1* KD mESCs. However, expression of the ectoderm marker *Mash1* was not changed by *D4ST1* KD. Collectively, these results suggest that D4ST1 contributes to the pluripotency of mESCs.

We also analyzed the expression of *Cdx2*, a marker of hindgut (Beck et al., 1995; Sherwood et al., 2007), in *D4ST1* O/E mESCs. The expression of *Cdx2* was significantly decreased in *D4ST1* O/E mESCs (**Figure 2B**). It has been reported that *Cdx2* expression is required for differentiation of hindgut (Stringer et al., 2008). Thus, the significantly increased or decreased expression of *Cdx2* in the respective *D4ST1* KD or *D4ST1* O/E mESCs indicates

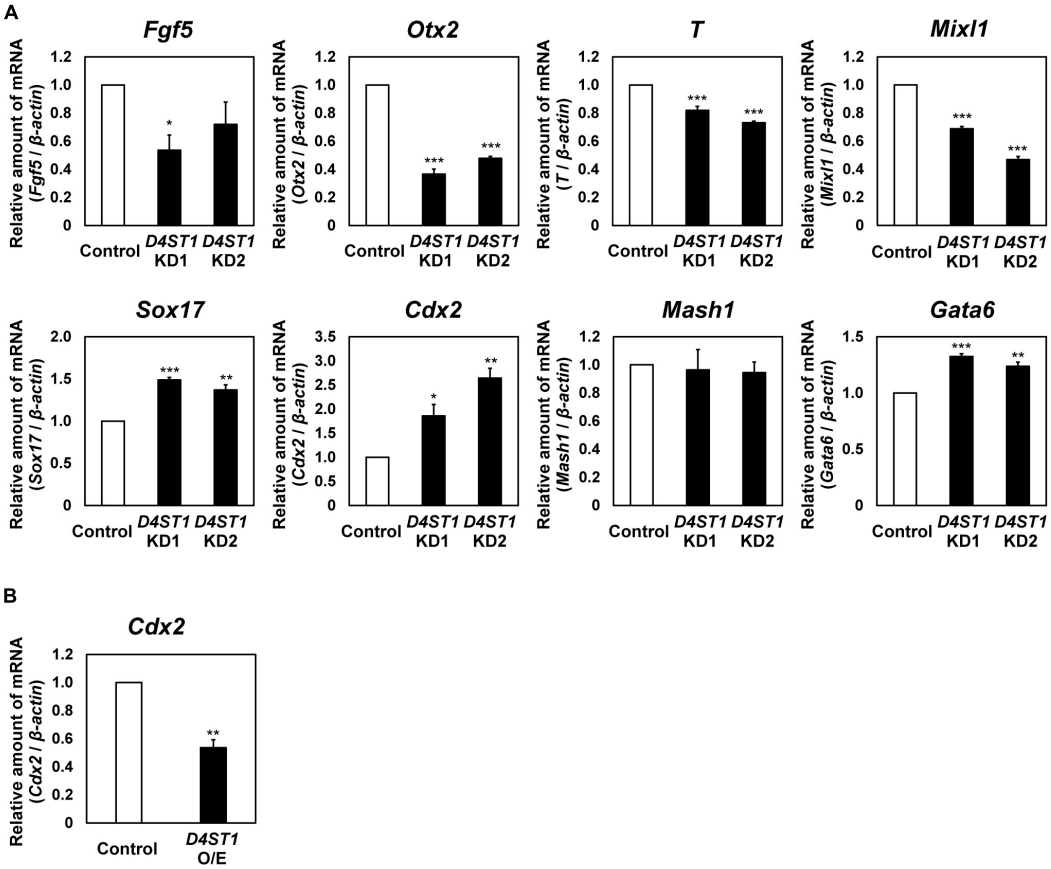


**FIGURE 2 |** Endodermal differentiation of mESCs is induced by *D4ST1* KD. **(A)** Real-time PCR analysis of differentiation markers in *D4ST1* KD at TF day 4. The amounts of differentiation marker mRNAs (*Fgf5*, *Otx2*, *T*, *Mixl1*, *Sox17*, *Cdx2*, *Mash1*, and *Gata6*) were normalized to that of *β-actin* mRNA and are shown relative to the control (set to 1). **(B)** Real-time PCR analysis of *Cdx2* in *D4ST1* O/E at TF day 2. The amount of *Cdx2* mRNA was normalized to that of *β-actin* mRNA and is shown relative to the control (set to 1). The values shown are means ± SD ($N = 3$). Those significantly different to the control by Dunnett test **(A)** or unpaired two-tailed Student's *t*-test **(B)** are indicated as follows: $^{***}p < 0.001$; $^{**}p < 0.01$; $^{*}p < 0.05$.

that D4ST1 might regulate endodermal differentiation, including differentiation to hindgut.

## BMP Signaling Is Suppressed and Wnt Signaling Is Activated by *D4ST1* KD

To analyze effect of *D4ST1* KD on signaling pathways, we used western blotting to analyze several signaling components in *D4ST1* KD mESCs. First, we examined the BMP/Smad1/5/8 signal, which contributes to self-renewal in mESCs by suppressing neural determination (Ying et al., 2003) and by up-regulating ERK-specific dual-specificity phosphatase 9 to reduce extracellular signal-regulated kinase activity, which is required for cell fate commitment (Li et al., 2012). Phosphorylated Smad1/5/8 was significantly decreased by *D4ST1* KD (**Figure 3A**). Thus, the reduced activity of the ESC self-renewal marker ALP (**Figure 1D**) is caused by a decrease in BMP signal.

Second, we examined the Wnt/β-catenin signal which induces endodermal differentiation (Zhong et al., 2017) and subsequently the hindgut domain during primitive gut tube formation in mouse (Engert et al., 2013). Whereas the relative amount of Active-β-catenin was significantly decreased by *D4ST1* O/E (**Figure 3C**), it was significantly increased (**Figure 3B**) by *D4ST1* KD. We also analyzed the expression of Wnt signaling target genes in *D4ST1* O/E mESCs; *Lef1* was significantly decreased, while that of *Axin2* and *Cdx1* tended to be decreased (**Supplementary Figure 5**). These results demonstrate that *D4ST1* KD induces endodermal differentiation and subsequent regionalization of the hindgut domain by activating Wnt signaling.

## DISCUSSION

In this study, we found that self-renewal and the undifferentiated state of mESCs were compromised by *D4ST1* KD. In *D4ST1* KD mESCs, self-renewal of mESCs was reduced and endodermal differentiation was induced. In particular, the expression of *Cdx2*, which is a hindgut marker, was significantly increased by *D4ST1* KD and significantly decreased by *D4ST1* O/E. Similarly, Wnt signal was activated by *D4ST1* KD and suppressed by *D4ST1* O/E.

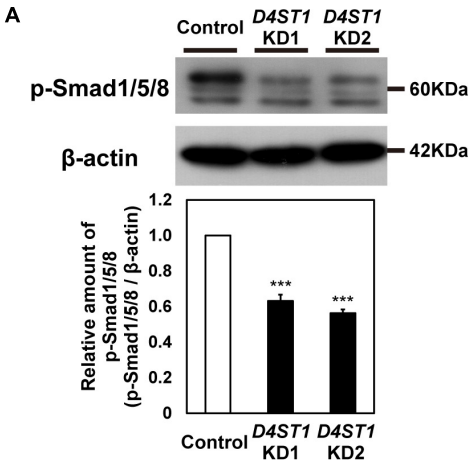


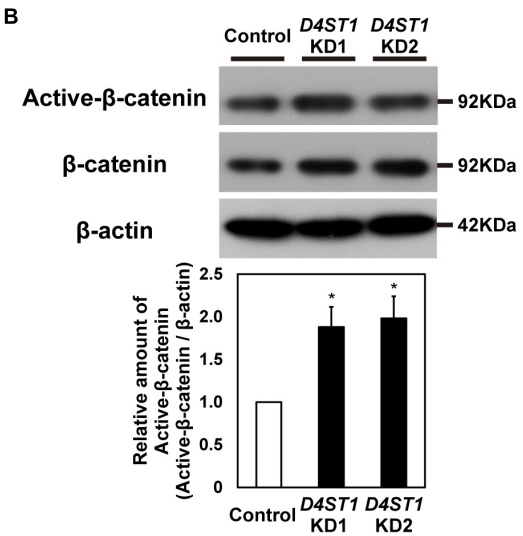


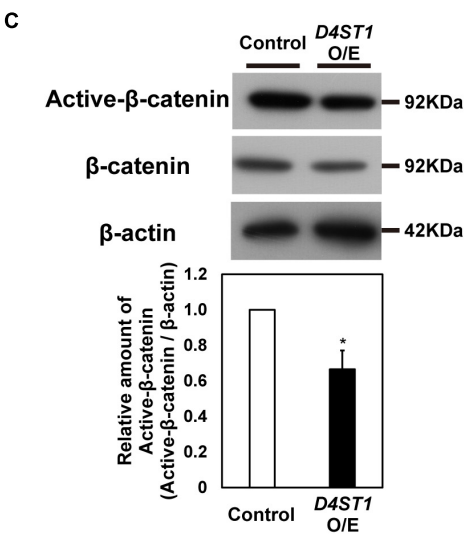


**FIGURE 3 |** (Continued)

**FIGURE 3 |** Wnt signaling is activated by *D4ST1* KD. **(A,B)** Western blotting analysis of p-Smad1/5/8 and Active-β-catenin in *D4ST1* KD mESCs at TF day 4. Histogram shows the mean densitometric readings of bands normalized to β-actin, and was shown relative to the control (set to 1). The representative bands of the loading control (β-actin) are the same as those in **Figure 1C** because the same samples were used for these analyses. **(C)** Western blotting analysis of Active-β-catenin in *D4ST1* O/E mESCs at TF day 2. Histogram shows the mean densitometric readings of bands, which were normalized to β-catenin and are shown relative to the control (set to 1). The values shown are means ± SD ($N = 3$). Those significantly different to the control by Dunnett test **(A,B)** or unpaired two-tailed Student's *t*-test **(C)** are indicated as follows: $^{***}p < 0.001$; $^{*}p < 0.05$.

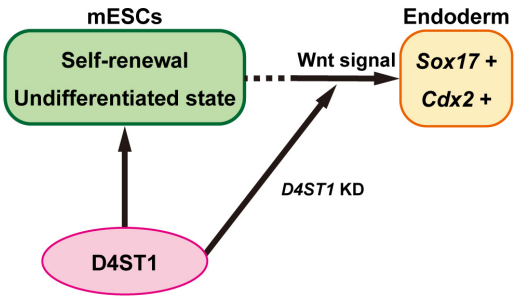


**FIGURE 4 |** *D4ST1* contributes to the undifferentiated state of mESCs. *D4ST1* contributes to self-renewal and the undifferentiated state of mESCs. Knockdown of *D4ST1* causes promotion of endodermal differentiation by activation of Wnt signaling.

It has been reported that *Cdx2* is essential for determination of intestinal mesoderm or endoderm differentiation (Stringer et al., 2008). The endoderm and mesoderm arise from a transient common precursor cell population referred to as "mesendoderm." The specification of endoderm requires Wnt/β-catenin signaling, which maintains the expression of Nodal, which in turn promotes the expression of a network of transcription factors within the endodermal lineage including Sox17 (Zorn and Wells, 2009). After endodermal linage determination, the gut tube is formed. The gut tube then becomes regionalized along the dorsal-ventral and anterior-posterior axes into broad foregut, midgut, and hindgut domains (Zorn and Wells, 2009). The Wnt/β-catenin signal also specifies the hindgut domain by inducing *Cdx2* expression, which is required for both the hindgut and positioning of the foregut-hindgut boundary in mouse development (Sherwood et al., 2011). Therefore, our results demonstrate that D4ST1 contributes to the undifferentiated state of mESCs, and *D4ST1* KD induces endodermal and subsequent hindgut differentiation by activating Wnt signaling (**Figure 4**).

*CDX2* is also required for intestinal development in human pluripotent stem cells, and WNT signaling similarly promotes endoderm-hindgut differentiation (Kumar et al., 2019). Although further investigation is needed to elucidate the function of D4ST1 in human development, *D4ST1* deficiency is known to be one of the causes of EDS (Kosho, 2016). *D4ST1*-deficient EDS presents characteristic craniofacial features, multiple congenital contractures, and progressive joint and skin laxity. Of note,

joints and dermis are tissues derived from mesoderm. In the present study, in contrast to endodermal markers, mesodermal markers were suppressed by *D4ST1* KD. Thus, D4ST1 may contribute to mesodermal differentiation in humans. In addition, it has been reported that skin complaints are caused by disorganization of collagen networks due to decorin, a dermatan sulfate proteoglycan (DSPG) (Hirose et al., 2018). There are several DSPGs, including decorin, biglycan, and fibromodulin. Determination of the DSPG that contributes to differentiation of mESCs will be an interesting issue for future study.

Because D4ST1 is a sulfotransferase involved in DS synthesis, it is possible that DS regulates Wnt signaling. GAGs such as HS and CS play a key role in signal transduction as co-receptors or as trappers by binding signal ligands (Wang et al., 2017). For example, DS has been reported to interact with bFGF, FGF7, and EGF (Taylor et al., 2005; Bian et al., 2011). To our knowledge, however, binding of DS to Wnt has not been demonstrated. This is also an interesting issue for future analysis.

In conclusion, we have shown that D4ST1 is required for self-renewal and the undifferentiated state in mESCs and *D4ST* KD induces endoderm differentiation and subsequent hindgut differentiation by activating Wnt signals. This study provides new insights into function of DS in mESCs.

## DATA AVAILABILITY STATEMENT

The original contributions presented in the study are included in the article/**Supplementary Material**, further inquiries can be directed to the corresponding author.

## AUTHOR CONTRIBUTIONS

CO and SN: conceptualization. CO: methodology, validation, formal analysis, investigation, data curation, writing – original draft, and visualization. SN: resources, writing – review and editing, supervision, project administration, and funding acquisition. Both authors contributed to the article and approved the submitted version.

## FUNDING

This work was supported by Japan Society for the Promotion of Science (JSPS) KAKENHI Grant Number JP18K06139 (to SN) and Japan Science and Technology Agency (JST)-Mirai Program Grant Number JPMJMI18GB (to SN).

## ACKNOWLEDGMENTS

We thank Kumiko Ui-Tei for providing pCAGI-Puro. We also thank Taichi Miura for the constructive discussion and advice.

## SUPPLEMENTARY MATERIAL

The Supplementary Material for this article can be found online at: https://www.frontiersin.org/articles/10.3389/fcell.2021.733964/full#supplementary-material

## REFERENCES

Adewumi, O., Aflatoonian, B., Ahrlund-Richter, L., Amit, M., Andrews, P. W., Beighton, G., et al. (2007). Characterization of human embryonic stem cell lines by the International Stem Cell Initiative. *Nat. Biotechnol.* 25, 803–816. doi: 10.1038/nbt1318

Andrews, P. W., Banting, G., Damjanov, I., Arnaud, D., and Avner, P. (1984). Three monoclonal antibodies defining distinct differentiation antigens associated with different high molecular weight polypeptides on the surface of human embryonal carcinoma cells. *Hybridoma* 3, 347–361.

Beck, F., Erler, T., Russell, A., and James, R. (1995). Expression of Cdx−2 in the mouse embryo and placenta: possible role in patterning of the extra−embryonic membranes. *Dev. Dynam.* 204, 219–227. doi: 10.1002/aja.1002040302

Bian, S., Akyüz, N., Bernreuther, C., Loers, G., Laczynska, E., Jakovcevski, I., et al. (2011). Dermatan sulfotransferase Chst14/D4st1, but not chondroitin sulfotransferase Chst11/C4st1, regulates proliferation and neurogenesis of neural progenitor cells. *J. Cell Sci.* 124, 4051–4063. doi: 10.1242/jcs.088120

Engert, S., Burtscher, I., Liao, W. P., Dulev, S., Schotta, G., and Lickert, H. (2013). Wnt/β-catenin signalling regulates Sox17 expression and is essential for organizer and endoderm formation in the mouse. *Development* 140, 3128–3138. doi: 10.1242/dev.088765

Evans, M. J., and Kaufman, M. H. (1981). Establishment in culture of pluripotential cells from mouse embryos. *Nature* 292, 154–156. doi: 10.1038/292154a0

Evers, M. R., Xia, G., Kang, H.-G., Schachner, M., and Baenziger, J. U. (2001). Molecular cloning and characterization of a dermatan-specific *N*-acetylgalactosamine 4-*O*-sulfotransferase. *J. Biol. Chem.* 276, 36344–36353. doi: 10.1074/jbc.m105848200

Fico, A., Chevigny, A. D., Egea, J., Bösl, M. R., Cremer, H., Maina, F., et al. (2012). Modulating glypican4 suppresses tumorigenicity of embryonic stem cells while preserving self−renewal and pluripotency. *Stem Cells* 30, 1863–1874. doi: 10.1002/stem.1165

Funderburgh, J. L. (2002). Keratan sulfate biosynthesis. *Iubmb Life* 54, 187–194. doi: 10.1080/15216540214932

Hirano, K., Kuppevelt, T. H. V., and Nishihara, S. (2013). The transition of mouse pluripotent stem cells from the naïve to the primed state requires Fas signaling through 3-O sulfated heparan sulfate structures recognized by the HS4C3 antibody. *Biochem. Bioph. Res. Co.* 430, 1175–1181. doi: 10.1016/j.bbrc.2012.12.005

Hirano, K., Sasaki, N., Ichimiya, T., Miura, T., Kuppevelt, T. H. V., and Nishihara, S. (2012). 3-*O*-sulfated heparan sulfate recognized by the antibody HS4C3 contribute to the differentiation of mouse embryonic stem cells via Fas signaling. *PLoS One* 7:e43440. doi: 10.1371/journal.pone.0043440

Hirose, T., Takahashi, N., Tangkawattana, P., Minaguchi, J., Mizumoto, S., Yamada, S., et al. (2018). Structural alteration of glycosaminoglycan side chains and spatial disorganization of collagen networks in the skin of patients with mcEDS-CHST14. *Biochimica Et Biophysica Acta Bba - Gen Subj* 1863, 623–631. doi: 10.1016/j.bbagen.2018.12.006

Ito, Y., and Habuchi, O. (2000). Purification and characterization of *N*-acetylgalactosamine 4-sulfate 6-*O*-sulfotransferase from the squid cartilage. *J. Biol. Chem.* 275, 34728–34736. doi: 10.1074/jbc.m909633199

Izumikawa, T., Sato, B., and Kitagawa, H. (2014). Chondroitin sulfate is indispensable for pluripotency and differentiation of mouse embryonic stem cells. *Sci. Rep.* 4:3701. doi: 10.1038/srep03701

Johnson, C. E., Crawford, B. E., Stavridis, M., Dam, G., Wat, A. L., Rushton, G., et al. (2007). Essential alterations of heparan sulfate during the differentiation of embryonic stem cells to Sox1−enhanced green fluorescent protein−expressing neural progenitor cells. *Stem Cells* 25, 2389–2389. doi: 10.1634/stemcells.2006-0445erratum

Kamiyama, S., Sasaki, N., Goda, E., Ui-Tei, K., Saigo, K., Narimatsu, H., et al. (2006). Molecular cloning and characterization of a novel 3′-phosphoadenosine 5′-phosphosulfate transporter, PAPST2. *J. Biol. Chem.* 281, 10945–10953. doi: 10.1074/jbc.m508991200

Kawabe, K., Tateyama, D., Toyoda, H., Kawasaki, N., Hashii, N., Nakao, H., et al. (2013). A novel antibody for human induced pluripotent stem cells and embryonic stem cells recognizes a type of keratan sulfate lacking oversulfated structures. *Glycobiology* 23, 322–336. doi: 10.1093/glycob/cws159

Kobayashi, M., Sugumaran, G., Liu, J., Shworak, N. W., Silbert, J. E., and Rosenberg, R. D. (1999). Molecular cloning and characterization of a human uronyl 2-sulfotransferase that sulfates iduronyl and glucuronyl residues in dermatan/chondroitin sulfate. *J. Biol. Chem.* 274, 10474–10480. doi: 10.1074/jbc.274.15.10474

Kosho, T. (2016). CHST14/D4ST1 deficiency: new form of Ehlers–Danlos syndrome. *Pediatr. Int.* 58, 88–99. doi: 10.1111/ped.12878

Kraushaar, D. C., Rai, S., Condac, E., Nairn, A., Zhang, S., Yamaguchi, Y., et al. (2012). Heparan sulfate facilitates FGF and BMP signaling to drive mesoderm differentiation of mouse embryonic stem cells. *J. Biol. Chem.* 287, 22691–22700. doi: 10.1074/jbc.m112.368241

Kraushaar, D. C., Yamaguchi, Y., and Wang, L. (2010). Heparan sulfate is required for embryonic stem cells to exit from self-renewal. *J. Biol. Chem.* 285, 5907–5916. doi: 10.1074/jbc.m109.066837

Kumar, N., Tsai, Y.-H., Chen, L., Zhou, A., Banerjee, K. K., Saxena, M., et al. (2019). The lineage-specific transcription factor CDX2 navigates dynamic chromatin to control distinct stages of intestine development. *Development* 146:dev172189. doi: 10.1242/dev.172189

Lanner, F., Lee, K. L., Sohl, M., Holmborn, K., Yang, H., Wilbertz, J., et al. (2010). Heparan sulfation–dependent fibroblast growth factor signaling maintains embryonic stem cells primed for differentiation in a heterogeneous state. *Stem Cells* 28, 191–200. doi: 10.1002/stem.265

Li, Z., Fei, T., Zhang, J., Zhu, G., Wang, L., Lu, D., et al. (2012). BMP4 signaling acts via dual-specificity phosphatase 9 to control ERK activity in mouse embryonic stem cells. *Cell Stem Cell* 10, 171–182. doi: 10.1016/j.stem.2011.12.016

Maccarana, M., Olander, B., Malmström, J., Tiedemann, K., Aebersold, R., Lindahl, U., et al. (2006). Biosynthesis of dermatan sulfate chondroitin-glucuronate C5-epimerase is identical to SART2. *J. Biol. Chem.* 281, 11560–11568. doi: 10.1074/jbc.m513373200

Malfait, F., Francomano, C., Byers, P., Belmont, J., Berglund, B., Black, J., et al. (2017). The 2017 international classification of the Ehlers–Danlos syndromes. *Am. J. Med. Genet. Part C Semin. Med. Genet.* 175, 8–26. doi: 10.1002/ajmg.c.31552

Martin, G. R. (1981). Isolation of a pluripotent cell line from early mouse embryos cultured in medium conditioned by teratocarcinoma stem cells. *Proc. Natl. Acad. Sci.* 78, 7634–7638. doi: 10.1073/pnas.78.12.7634

Miura, T., Kume, M., Kawamura, T., Yamamoto, K., Hamakubo, T., and Nishihara, S. (2018). *O*-GlcNAc on PKCζ inhibits the FGF4-PKCζ-MEK-ERK1/2 pathway via inhibition of PKCζ phosphorylation in mouse embryonic stem cells. *Stem Cell Rep.* 10, 272–286. doi: 10.1016/j.stemcr.2017.11.007

Miura, T., and Nishihara, S. (2016). *O*-GlcNAc is required for the survival of primed pluripotent stem cells and their reversion to the naïve state. *Biochem. Bioph. Res. Co.* 480, 655–661. doi: 10.1016/j.bbrc.2016.10.111

Nagy, A., Rossant, J., Nagy, R., Abramow-Newerly, W., and Roder, J. C. (1993). Derivation of completely cell culture-derived mice from early-passage embryonic stem cells. *Proc. Natl. Acad. Sci.* 90, 8424–8428. doi: 10.1073/pnas.90.18.8424

Ogura, C., Hirano, K., Mizumoto, S., Yamada, S., and Nishihara, S. (2020). Dermatan sulphate promotes neuronal differentiation in mouse and human stem cells. *J. Biochem.* 169, 55–64. doi: 10.1093/jb/mvaa087

Pacheco, B., Malmström, A., and Maccarana, M. (2009). Two dermatan sulfate epimerases form iduronic acid domains in dermatan sulfate. *J. Biol. Chem.* 284, 9788–9795. doi: 10.1074/jbc.m809339200

Pecori, F., Akimoto, Y., Hanamatsu, H., Furukawa, J., Shinohara, Y., Ikehara, Y., et al. (2020). Mucin-type *O*-glycosylation controls pluripotency in mouse embryonic stem cells via Wnt receptor endocytosis. *J. Cell Sci.* 133:jcs245845. doi: 10.1242/jcs.245845

Pecori, F., Kondo, N., Ogura, C., Miura, T., Kume, M., Minamijima, Y., et al. (2021). Site-specific *O*-GlcNAcylation of Psme3 maintains mouse stem cell pluripotency by impairing P-body homeostasis. *Cell Rep.* 36, 109361. doi: 10.1016/j.celrep.2021.109361

Pera, M. F., Blasco−Lafita, M. J., Cooper, S., Mason, M., Mills, J., and Monaghan, P. (1988). Analysis of cell−differentiation lineage in human teratomas using new monoclonal antibodies to cytostructural antigens of embryonal carcinoma cells. *Differentiation* 39, 139–149. doi: 10.1111/j.1432-0436.1988.tb00089.x

Sasaki, N., Hirano, T., Ichimiya, T., Wakao, M., Hirano, K., Kinoshita-Toyoda, A., et al. (2009). The 3′-phosphoadenosine 5′-phosphosulfate transporters, PAPST1 and 2, contribute to the maintenance and differentiation of mouse embryonic stem cells. *PLoS One* 4:e8262. doi: 10.1371/journal.pone.0008262

Sasaki, N., Okishio, K., Ui-Tei, K., Saigo, K., Kinoshita-Toyoda, A., Toyoda, H., et al. (2008). Heparan sulfate regulates self-renewal and pluripotency of embryonic stem cells. *J. Biol. Chem.* 283, 3594–3606. doi: 10.1074/jbc.m705621200

Sasaki, N., Shinomi, M., Hirano, K., Ui−Tei, K., and Nishihara, S. (2011). LacdiNAc (GalNAcβ1−4GlcNAc) contributes to self−renewal of mouse embryonic stem cells by regulating leukemia inhibitory factor/STAT3 signaling. *Stem Cells* 29, 641–650. doi: 10.1002/stem.615

Sherwood, R. I., Jitianu, C., Cleaver, O., Shaywitz, D. A., Lamenzo, J. O., Chen, A. E., et al. (2007). Prospective isolation and global gene expression analysis of definitive and visceral endoderm. *Dev. Biol.* 304, 541–555. doi: 10.1016/j.ydbio.2007.01.011

Sherwood, R. I., Maehr, R., Mazzoni, E. O., and Melton, D. A. (2011). Wnt signaling specifies and patterns intestinal endoderm. *Mech. Dev.* 128, 387–400. doi: 10.1016/j.mod.2011.07.005

Stringer, E. J., Pritchard, C. A., and Beck, F. (2008). Cdx2 initiates histodifferentiation of the midgut endoderm. *Febs. Lett.* 582, 2555–2560. doi: 10.1016/j.febslet.2008.06.024

Sugahara, K., and Kitagawa, H. (2000). Recent advances in the study of the biosynthesis and functions of sulfated glycosaminoglycans. *Curr. Opin. Struc. Biol.* 10, 518–527. doi: 10.1016/s0959-440x(00)00125-1

Taylor, K. R., Rudisill, J. A., and Gallo, R. L. (2005). Structural and sequence motifs in dermatan sulfate for promoting fibroblast growth factor-2 (FGF-2) and FGF-7 activity. *J. Biol. Chem.* 280, 5300–5306. doi: 10.1074/jbc.m410412200

Ui-Tei, K., Naito, Y., Takahashi, F., Haraguchi, T., Ohki−Hamazaki, H., Juni, A., et al. (2004). Guidelines for the selection of highly effective siRNA sequences for mammalian and chick RNA interference. *Nucleic Acids Res.* 32, 936–948. doi: 10.1093/nar/gkh247

Wang, M., Liu, X., Lyu, Z., Gu, H., Li, D., and Chen, H. (2017). Glycosaminoglycans (GAGs) and GAG mimetics regulate the behavior of stem cell differentiation. *Coll. Surf. B Biointerf.* 150, 175–182. doi: 10.1016/j.colsurfb.2016.11.022

Ying, Q. L., Nichols, J., Chambers, I., and Smith, A. (2003). BMP induction of Id proteins suppresses differentiation and sustains embryonic stem cell self-renewal in collaboration with STAT3. *Cell* 115, 281–292. doi: 10.1016/s0092-8674(03)00847-x

Zhong, W., Lai, Y., Yu, T., Xia, Z. S., Yuan, Y. H., Ouyang, H., et al. (2017). Wnt and Nodal signaling simultaneously induces definitive endoderm differentiation of mouse embryonic stem cells. *Romanian J. Morphol. Embryology Revue Roumaine De Morphol Et Embryologie* 58, 527–535.

Zorn, A. M., and Wells, J. M. (2009). Vertebrate endoderm development and organ formation. *Cell Dev. Biol.* 25, 221–251. doi: 10.1146/annurev.cellbio.042308.113344

**Conflict of Interest:** The authors declare that the research was conducted in the absence of any commercial or financial relationships that could be construed as a potential conflict of interest.

**Publisher's Note:** All claims expressed in this article are solely those of the authors and do not necessarily represent those of their affiliated organizations, or those of the publisher, the editors and the reviewers. Any product that may be evaluated in this article, or claim that may be made by its manufacturer, is not guaranteed or endorsed by the publisher.

frontiers in Cell and Developmental Biology

BRIEF RESEARCH REPORT
published: 11 October 2021
doi: 10.3389/fcell.2021.695021

# Myopathy Associated With Dermatan Sulfate-Deficient Decorin and Myostatin in Musculocontractural Ehlers-Danlos Syndrome: A Mouse Model Investigation

*Yuko Nitahara-Kasahara[1,2]*, Guillermo Posadas-Herrera[2], Shuji Mizumoto[3], Aki Nakamura-Takahashi[4], Yukiko U. Inoue[5], Takayoshi Inoue[5], Yoshihiro Nomura[6], Shin'ichi Takeda[7], Shuhei Yamada[3], Tomoki Kosho[8,9,10,11] and Takashi Okada[2]**

[1] Department of Biochemistry and Molecular Biology, Nippon Medical School, Tokyo, Japan, [2] Division of Molecular and Medical Genetics, Center for Gene and Cell Therapy, The Institute of Medical Science, The University of Tokyo, Tokyo, Japan, [3] Department of Pathobiochemistry, Faculty of Pharmacy, Meijo University, Nagoya, Japan, [4] Department of Pharmacology, Tokyo Dental College, Tokyo, Japan, [5] Department of Biochemistry and Cellular Biology, National Center of Neurology and Psychiatry, National Institute of Neuroscience, Kodaira, Japan, [6] Faculty of Agriculture, Tokyo University of Agriculture and Technology, Fuchu, Japan, [7] National Institute of Neuroscience, National Center of Neurology and Psychiatry, Kodaira, Japan, [8] Department of Medical Genetics, Shinshu University School of Medicine, Matsumoto, Japan, [9] Center for Medical Genetics, Shinshu University Hospital, Matsumoto, Japan, [10] Division of Clinical Sequencing, Shinshu University School of Medicine, Matsumoto, Japan, [11] Research Center for Supports to Advanced Science, Shinshu University, Matsumoto, Japan

OPEN ACCESS

**Edited by:**
*Juan Jose Sanz-Ezquerro, Centro Nacional de Biotecnología, Consejo Superior de Investigaciones Científicas (CSIC), Spain*

**Reviewed by:**
*Anders Malmström, Lund University, Sweden*
*Fransiska Malfait, Ghent University, Belgium*

***Correspondence:**
*Yuko Nitahara-Kasahara*
*y-kasahara@ims.u-tokyo.ac.jp*
*Takashi Okada*
*t-okada@ims.u-tokyo.ac.jp*

**Specialty section:**
*This article was submitted to Signaling, a section of the journal Frontiers in Cell and Developmental Biology*

**Received:** *14 April 2021*
**Accepted:** *20 September 2021*
**Published:** *11 October 2021*

**Citation:**
*Nitahara-Kasahara Y, Posadas-Herrera G, Mizumoto S, Nakamura-Takahashi A, Inoue YU, Inoue T, Nomura Y, Takeda S, Yamada S, Kosho T and Okada T (2021) Myopathy Associated With Dermatan Sulfate-Deficient Decorin and Myostatin in Musculocontractural Ehlers-Danlos Syndrome: A Mouse Model Investigation. Front. Cell Dev. Biol. 9:695021. doi: 10.3389/fcell.2021.695021*

*Carbohydrate sulfotransferase 14* (*CHST14*) encodes dermatan 4-*O*-sulfotransferase 1, a critical enzyme for dermatan sulfate (DS) biosynthesis. Musculocontractural Ehlers-Danlos syndrome (mcEDS) is associated with biallelic pathogenic variants of *CHST14* and is characterized by malformations and manifestations related to progressive connective tissue fragility. We identified myopathy phenotypes in *Chst14*-deficient mice using an mcEDS model. Decorin is a proteoglycan harboring a single glycosaminoglycan chain containing mainly DS, which are replaced with chondroitin sulfate (CS) in mcEDS patients with CHST14 deficiency. We studied the function of decorin in the skeletal muscle of *Chst14*-deficient mice because decorin is important for collagen-fibril assembly and has a myokine role in promoting muscle growth. Although decorin was present in the muscle perimysium of wild-type ($Chst14^{+/+}$) mice, decorin was distributed in the muscle perimysium as well as in the endomysium of $Chst14^{-/-}$ mice. $Chst14^{-/-}$ mice had small muscle fibers within the spread interstitium; however, histopathological findings indicated milder myopathy in $Chst14^{-/-}$ mice. Myostatin, a negative regulator of protein synthesis in the muscle, was upregulated in $Chst14^{-/-}$ mice. In the muscle of $Chst14^{-/-}$ mice, decorin was downregulated compared to that in $Chst14^{+/+}$ mice. $Chst14^{-/-}$ mice showed altered cytokine/chemokine balance and increased fibrosis, suggesting low myogenic activity in DS-deficient muscle. Therefore, DS deficiency in mcEDS causes pathological localization and functional abnormalities of decorin, which causes disturbances in skeletal muscle myogenesis.

**Keywords: Ehlers-Danlos syndrome, dermatan sulfate, dermatan 4-*O*-sulfotransferase 1, decorin, chst14 mutant mouse, myostatin, myopathy**

## INTRODUCTION

The musculocontractural Ehlers-Danlos syndrome (mcEDS) subtype is caused by defective biosynthesis of dermatan sulfate (DS). Most patients with mcEDS have biallelic pathogenic variants in the gene for *carbohydrate sulfotransferase 14* (*CHST14*), which encodes dermatan 4-*O*-sulfotransferase 1 (D4ST1) (mcEDS-*CHST14*), whereas the remaining patients have biallelic pathogenic variants in the DS epimerase gene (Dündar et al., 2009; Miyake et al., 2010; Müller et al., 2013; Brady et al., 2017; Kosho et al., 2020). mcEDS is clinically characterized by craniofacial features, multiple congenital contractures, ocular and visceral malformations, and progressive connective tissue fragility-related manifestations, such as skin hyperextensibility and fragility, joint hypermobility with luxation, progressive spinal and foot deformities, large subcutaneous hematomas, and visceral ruptures (Kosho et al., 2011, 2020; Kosho, 2016). The myopathic process has been suggested in mcEDS because of a reduced amplitude of muscle action potential with normal distal latency time and nerve conduction velocity (Dundar et al., 1997); the muscle phenotypes of a patient with mcEDS-*CHST14* have also been reported (Voermans et al., 2012).

Proteoglycans are the most abundant components of the non-fibrillar extracellular matrix (ECM). They are composed of a protein core to which long, linear, highly sulfated glycosaminoglycan (GAG) chains are covalently attached. Proteoglycans display different functions that are principally mediated by GAG chains (Sugahara et al., 2003). The main sulfated GAG families in muscles are chondroitin sulfate (CS)/DS, heparan sulfate, and keratan sulfate (Handel et al., 2005; Fadic et al., 2006; Hannesson et al., 2007; Zhang, 2010; Negroni et al., 2014). Decorin is a proteoglycan that contains a single GAG chain and plays an important role in the assembly of collagen fibrils, possibly via electrostatic interaction between decorin-DS chains and adjacent collagen fibrils (Iozzo, 1998; Nomura, 2006). The GAG side chain of decorin from the skin fibroblasts of mcEDS-*CHST14* patients contained CS instead of DS (Miyake et al., 2010). Collagen fibrils normally aggregate in line and form collagen fibers, which are round and uniform. Although there were no significant differences in the diameter of collagen fibrils as well as the circularity as an index of shape between *Chst14*$^{+/+}$ and *Chst14*$^{-/-}$ mice, collagen fibrils were scattered and oriented in various directions (Hirose et al., 2021). Furthermore, irregular shapes and sizes of collagen fibrils were detected in decorin-null mice (Danielson et al., 1997), being partially different from those in *Chst14*$^{-/-}$ mice.

Decorin is also characterized as a myokine, which is elevated following exercise in normal muscle, and promotes muscle fiber hypertrophy by competitively binding to inhibit myostatin, a negative regulator of muscle protein synthesis (Ostrowski et al., 1998; Lightfoot and Cooper, 2016). In transgenic models, decorin has been shown to induce upregulation of factors associated with myogenesis, such as MyoD and follistatin (Lightfoot and Cooper, 2016). In addition, transforming growth factor type β (TGF-β), a potent inhibitor of myogenesis like myostatin, is also regulated by complexing with decorin (Florini et al., 1991). Decorin requirement seems to be necessary for myogenesis as decorin expression accelerates skeletal muscle differentiation (Cabello-Verrugio and Brandan, 2007; Brandan and Gutierrez, 2013).

We developed CRISPR/Cas9-genome engineered *Chst14* mutant (*Chst14*$^{-/-}$) mice, which showed a pathological phenotype and shared the typical mcEDS phenotype features, including loss of DS, growth delay, skin fragility, myopathy, reduced muscle function, and thoracic kyphosis. In the present study, we investigated the effects of decorin on spatial distribution and expression in myopathy using *Chst14*$^{-/-}$ mice as an mcEDS model.

## MATERIALS AND METHODS

All experimental procedures were approved by the Experimental Animal Care and Use Committee at the National Center of Neurology and Psychiatry (NCNP) and Nippon Medical School. *Chst*14$^{-/-}$ mice with a 6 base pair (bp) insertion/10 bp deletion (31_40delinsCCACTG) and 1 bp deletion (–1 bp mutant; c.57delG) were developed by CRISPR/Cas9-genome engineering at NCNP (Nitahara-Kasahara et al., 2021b) and were maintained according to the standard protocol for animal care at the NCNP and Nippon Medical School. *Chst*14$^{-/-}$ mice were inbred as C57BL/6 and 129svj mixed backgrounds. 129S1/SvImJ and B6C3F1 mice were purchased from Nihon CLEA (Tokyo, Japan) and Japan SLC, Inc. (Shizuoka, Japan), respectively. Age-matched littermate mice were used in all the experiments. Each mouse group contained sex-matched mice (females, $n$ = 2; males, $n$ = 2).

### Histopathology and Immunohistochemistry

The tibialis anterior (TA) muscle obtained from age- and sex-matched mice was immediately frozen in liquid nitrogen-cooled isopentane. Transverse cryosections (10 μm thickness) were prepared from frozen muscle tissues, stained with hematoxylin and eosin (H&E) using standard procedures, and immunostained for decorin. Muscle cryosections fixed with 1% paraformaldehyde were treated with anti-decorin antibody (monoclonal mouse IgG1 clone 115402, R&D Systems, Minneapolis, MN) or anti-laminin β-1 antibody (Abcam, Cambridge, United Kingdom) as the primary antibody, followed by Alexa 488-conjugated anti-rat IgG antibody (Thermo Fisher Scientific, Waltham, MA) or Alexa 594-conjugated anti-mouse IgG antibody (Thermo Fisher Scientific) as the secondary antibody. The sections were mounted in Vectashield with 4, 6-diamidino-2-phenylindole (Vector Laboratories). Immunofluorescence and H&E staining were visualized using an IX81 fluorescence microscope (Olympus, Tokyo, Japan). For quantification analysis of myofiber size distribution, the myofiber area in H&E images (95-100 fibers) was measured using CellSence software (Olympus). For collagen staining, sirius red staining of cryosections from the TA muscle was performed using a general protocol (Morphotechnology, Sapporo, Japan). Quantitative analysis of the sirius red staining area was performed using CellSence software (Olympus).

## Enzyme-Linked Immunosorbent Assay

Protein expression levels were measured in TA muscle lysate obtained from each mouse using a Quantikine enzyme-linked immunosorbent assay (ELISA), such as mouse myostatin Immunoassay (Thermo Fisher Scientific), mouse collagen type I, and type III Immunoassay (Cloud-clone Corp., Katy, TX), and mouse transforming growth factor-β1 (TGF-β1) Immunoassay (R&D Systems), according to the manufacturer's recommendations. The final values were normalized to protein concentrations and measured using a Pierce® BCA Protein Assay Kit (Thermo Fisher Scientific).

## Reverse Transcription Polymerase Chain Reaction

Total RNA was isolated from muscle samples disrupted in a Multi-Bead Shocker (M&S Instruments, Osaka, Japan) using an RNeasy Micro Kit (Qiagen). First-strand cDNA was synthesized using a Super Script III First Strand Synthesis System for RT-PCR (Thermo Fisher Scientific). For each PCR assay, 500 ng –1 μg cDNA was used. The primers used in the present study were as follows: *decorin*, forward, 5′-TGCTGCTGCCGTC CATGCTGAT-3′, and reverse, 5′-CATGCCTGGCTGTCCGCA CA-3′; *MyoD*, forward, 5′-GCCGCCTGAGCAAAGTGAATG-3′, and reverse, 5′-CAGCGGTCCAGGTGCGTAGAAG-3′. As an internal control, the primer set used for the housekeeping gene, glyceraldehyde-3-phosphate dehydrogenase (*Gapdh*) was as follows: mouse, forward, 5′- GATGACATCAAGAAGGT GGTGA-3′, and reverse, 5′-TGCTGTAGCCGTATTCATTGTC-3′. Quantitative PCR was performed using SYBR® Premix Ex Taq™ II (Perfect Real Time, Takara Bio Inc., Ohtsu, Japan). SYBR green detection of PCR products was conducted in real time using the MyiQ single-color detection system (Bio-Rad, Hercules, CA).

## Western Blotting Analysis

The proteins were separated by electrophoresis using precast NuPAGE 4–12% Bis-Tris gels (Thermo Fisher Scientific) in NuPAGE™ 3-(*N*-morpholino) propanesulfonic acid buffer (pH 7.7) containing sodium dodecyl sulfate, and then transferred to a polyvinylidene difluoride membrane. The membranes were blocked for 60 min at room temperature in Tris-buffered saline containing 0.1% Tween 20 and 5% skim milk. The blots were probed with the primary antibody: mouse monoclonal antibody to decorin (R&D Systems, clone 115402) or GAPDH (Santa Cruz, Dallas, TX, clone G-4) at 1:1,000 dilution overnight at 4°C or for 60 min at room temperature and then incubated with horseradish peroxidase (HRP)-conjugated goat anti-mouse IgG (Cytiva, Marlborough, MA) at 1:2,000 dilution for 45 min. Immunoreactive proteins were detected and quantified using an enhanced chemiluminescence system, Image Quant LAS 4000 coupled with Image Quant TL software (GE Healthcare, Chicago, IL).

## Proteome Cytokine/Chemokine Array

The relative expression of cytokines and chemokines in muscle lysate was quantified using the Proteome Profiler™ Array (Mouse Cytokine/chemokine Array, Panel A; R&D Systems), as previously described (Nitahara-Kasahara et al., 2014, 2021a). To achieve maximum assay sensitivity, the blots were incubated overnight with the lysate. Enhanced chemiluminescence incubation was performed for 5 min using a Super Signal West Femto Chemiluminescence Kit (Thermo Scientific Pierce), and the samples were imaged and analyzed using Image Quant LAS 4000 coupled with Image Quant TL software (GE Healthcare).

## Quantitative Analysis of Chondroitin Sulfate and Dermatan Sulfate Disaccharides

The disaccharide compositions of the CS and DS moieties of CS/DS hybrid chains in the skeletal muscle of mice were assessed as described previously (Mizumoto and Sugahara, 2012). Briefly, the GAG fraction was crudely purified from the tissue and then digested with a mixture of chondroitinase AC-I and AC-II, or chondroitinase B. Each digest was labeled with a fluorophore, 2-aminobenzamide, and then analyzed using anion-exchange high-performance liquid chromatography (HPLC) on a PA-G silica column (4.6 × 150 mm; YMC Co., Kyoto, Japan). Identification and quantification of the resulting disaccharides were achieved by comparing with the elution positions of the CS- or DS-derived authentic unsaturated disaccharides. The amount of disaccharides in each sample was calculated by comparing the peak areas of standard unsaturated disaccharides.

## Statistical Analyses

Data are presented as the mean ± standard deviation. Differences between two groups were assessed using unpaired two-tailed *t*-tests. Multiple comparisons between three or more groups were performed using a one-way or two-way analysis of variance. Statistical differences were defined as $^{*}p < 0.05$, $^{**}p < 0.01$, $^{***}p < 0.001$, and $^{****}p < 0.0001$, and were calculated using Excel (Microsoft, Redmond, WA, United States) and GraphPad Prism 8 (GraphPad, La Jolla, CA).

# RESULTS

## Decorin Expression and Localization in the Dermatan Sulfate Deficiency Muscle

To confirm D4ST1 inactivation for DS biosynthesis in *Chst14*$^{-/-}$mice, we analyzed the amount of CS and DS disaccharides in the skeletal muscle (**Figure 1A**). Largely suppressed DS disaccharides and an increase in CS disaccharides were observed in *Chst14*$^{-/-}$ mice compared to the wild type (*Chst14*$^{+/+}$) mice, suggesting DS deficiency due to D4ST1 inactivation (**Supplementary Table 1**). To investigate the expression levels and localization of decorin in skeletal muscle, quantitative reverse-transcription PCR, western blotting, and immunohistological analysis were performed using the TA muscle from *Chst14*$^{-/-}$ mice. We confirmed that the mRNA expression of decorin was downregulated in the *Chst14*$^{-/-}$ mice compared to that in the *Chst14*$^{+/+}$ mice (**Figure 1B**). The expression of glycanated decorin was also downregulated in *Chst14*$^{-/-}$ mice compared to that in *Chst14*$^{+/+}$ mice, whereas

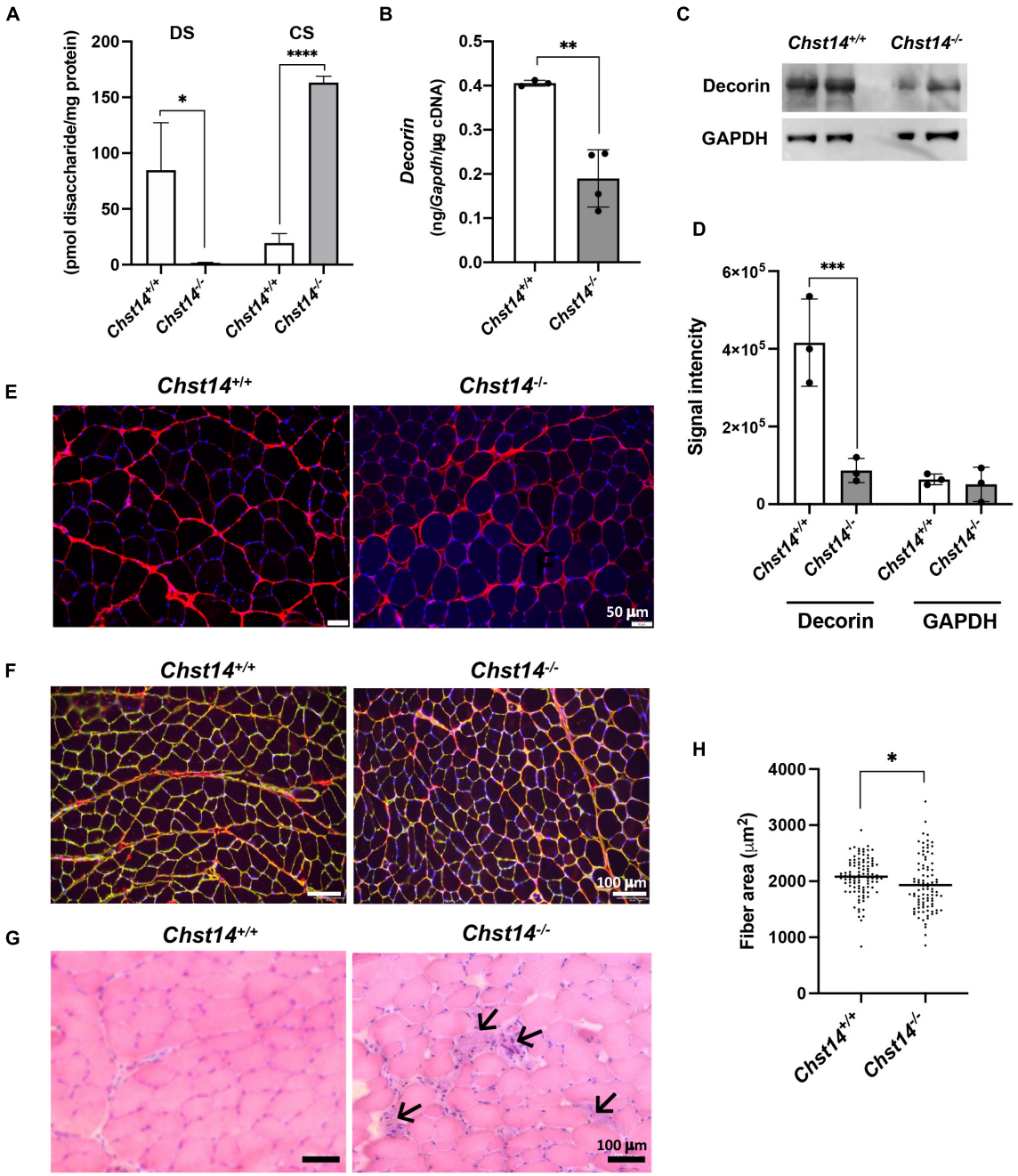


**FIGURE 1 |** Decorin expression and localization in dermatan sulfate (DS) deficient muscle. **(A)** Total amounts of chondroitin sulfate (CS) and DS disaccharides derived from the tibialis anterior (TA) muscle of *Chst14*$^{+/+}$ and *Chst14*$^{-/-}$ mice, analyzed by anion-exchange HPLC after enzymatic digestion. **(B)** *Decorin* mRNA in the TA muscle from *Chst14*$^{+/+}$ ($n$ = 3) and *Chst14*$^{-/-}$ ($n$ = 4) mice was quantified by reverse transcription polymerase chain reaction (RT-PCR). Quantitative data were normalized using the glyceraldehyde 3-phosphate dehydrogenase (*Gapdh*) signal. **(C)** The protein level of decorin in the TA muscle were analyzed by western blotting using anti-decorin antibody and anti-glyceraldehyde 3-phosphate dehydrogenase (GAPDH) antibodies. **(D)** Signal intensity quantified using blotting band images using Image Quant TL software. **(E)** Immunofluorescence staining of TA muscle from *Chst14*$^{+/+}$and *Chst14*$^{-/-}$ mice was performed using anti-decorin antibody (red signals). Nuclear staining was detected using 4,6-diamidino-2-phenylindole (blue signals). Bars, 50 µm. **(F)** Dual staining of the TA muscle from *Chst14*$^{+/+}$ and *Chst14*$^{-/-}$ mice for the detection of decorin (red signals) and laminin (green signals) with nuclear staining (blue signals). Bars, 100 µm. **(G)** Hematoxylin and eosin (H&E) staining of the TA muscle from *Chst14*$^{+/+}$ and *Chst14*$^{-/-}$ mice. Arrows show the nuclear accumulation and spread of muscle fiber stroma. Bars, 100 µm. **(H)** Muscle fiber areas (µm$^2$) measured from the TA muscle of *Chst14*$^{+/+}$ and *Chst14*$^{-/-}$ mice using H&E staining. Each fiber area is indicated by a dot, and the average fiber area is described as a bar for each muscle. In total, 1931 fibers are represented in the dot plot. Median values are indicated by red bars. Statistical differences between *Chst14*$^{+/+}$ and *Chst14*$^{-/-}$ (*$P$ < 0.05, **$P$ < 0.01. ***$P$ < 0.001, and ****$P$ < 0.0001), $t$-test. All data were analyzed using the TA muscle of 1-year-old sex-matched *Chst14*$^{+/+}$ ($n$ = 3) and *Chst14*$^{-/-}$ ($n$ = 3) mice.

the expression levels of the internal control, GAPDH protein, were not changed based on western blot and quantitative data (**Figures 1C,D**). In healthy muscle, histochemical images showed that most of the decorin was localized in the perimysium, which is the sheath of connective tissue that covers a bundle of muscle fibers, whereas a small amount was found in the endomysium, a layer of connective tissue that surrounds individual muscle fibers (**Figure 1E**). In contrast, decorin in the muscle of *Chst14*$^{-/-}$ mice was localized in the perimysium around packages of muscle fibers and was augmented around individual muscle fibers in the endomysium (**Figure 1E**). The decorin in the *Chst14*$^{-/-}$ mice was co-localized with laminin in the endomysium, whereas decorin did not co-localization with laminin in the perimysium of muscle from *Chst14*$^{+/+}$ mice, as shown in **Figure 1F**. A cross-section of the TA muscle from *Chst14*$^{-/-}$ mice revealed the spreading of the muscle fiber interstitium and cell infiltration by H&E staining (**Figure 1G**). The histopathological findings observed in *Chst14*$^{-/-}$ mice indicated high myofiber size variability due to a higher number of smaller fibers (**Figure 1H**). Furthermore, central nuclear fibers, which are regenerated fibers that have undergone degeneration, were observed in *Chst14*$^{-/-}$ mice (0.96% per total number of fibers), whereas only a small percentage were found in *Chst14*$^{+/+}$ mice (0.28%).

## Effect of Chst14 on Myogenesis and Myokine/Chemokine Expression in the Muscle

mcEDS showed a smaller area of muscle fibers compared to healthy muscle; therefore, we investigated the possibility of muscle formation in the mcEDS and myokine environments. Myostatin, a negative regulator, was upregulated in the muscle of *Chst14*$^{-/-}$ mice compared to that in the muscle of *Chst14*$^{+/+}$ mice (**Figure 2A**). We assessed expression of MyoD, which is a muscle-growth-associating factor that maintains a regulated signal pathway toward muscle growth, but did not find a significant difference in *MyoD* mRNA expression in the muscle between *Chst14*$^{+/+}$ and *Chst14*$^{-/-}$ mice (**Figure 2B**).

To investigate the changes in the myokine and chemokine expression in the DS-deficient muscle, we performed a cytokine/chemokine array using the muscle lysate (**Figures 2C,D**). Quantitative results demonstrated that soluble intercellular adhesion molecule-1 (sICAM-1) showed strong signals in the muscles of both *Chst14*$^{+/+}$ and *Chst14*$^{-/-}$ mice. Stromal cell-derived factor 1 (SDF1), complement component C5a, and pro-inflammatory cytokines, interferon-γ (IFN-γ) as well as IL-1β, was found to be reduced in *Chst14*$^{-/-}$ mice. In contrast, IL-1ra, an antagonist of IL-1, was slightly increased compared to that in the *Chst14*$^{+/+}$ mice (**Figures 2C,D**), suggesting an altered cytokine/chemokine balance in DS-deficient muscles.

## Enhanced Fibrosis in the Dermatan Sulfate-Deficient Muscle

Decorin can interact with fibrillar collagens and is assumed to play a role in fibril formation and the maintenance of the fibrillar network, organizing the ECM (Toole and Lowther, 1968; Weber et al., 1996). To examine disease-associated fibrosis in DS-deficient muscle, we performed sirius red staining (**Figures 3A,B**). *Chst14*$^{-/-}$ mice showed a higher fibrotic area in the muscle compared to that in *Chst14*$^{+/+}$ mice. To further characterize fibrosis in mcEDS, the expression of TGF-β1 and collagen type I and III, which are classically upregulated in fibrotic processes, was measured by ELISA. We confirmed the upregulation of TGF-β1 and collagen type III, but not of collagen type I (**Figures 3C–E**). These results suggest that fibrosis is enhanced in DS-deficient muscle.

# DISCUSSION

In the present study, we investigated the effects of DS deficiency on myogenesis and the potential cause of myopathy. We demonstrated that the pathological decorin localization and functional abnormalities of decorin with the CS side chain were caused by DS deficiency in mcEDS, which causes disturbances in myogenesis of skeletal muscle, suggesting disease-specific phenotypes in myogenesis. **Figure 4** summarizes the hypotheses proposed in this study.

We focused on the pathology analysis to eliminate the effects of decreased motor function in mcEDS mice in the present study (Nitahara-Kasahara et al., 2021b), even though decorin has been reported to act as a myokine after exercise (Kanzleiter et al., 2014). In *Chst14*$^{-/-}$ mice, a decrease of DS accompanied with an increase of CS was observed in TA muscle (**Figure 1**). Furthermore, total CS/DS was also increased in the *Chst14*-deficient mice, indicating that the chain length as well as number of CS may be increased in the mice. Most of the decorin with DS chains was localized in the perimysium of normal muscle; however, decorin with the CS chain showed co-localization with laminin and was diffused in the perimysium and endomysium (**Figure 1**). In the muscle of *Chst14*$^{-/-}$ mice, decreased expression and altered localization of decorin core protein may affect the conventional functions of decorin. We previously reported the structural and conformational alteration of GAG chains of decorin-proteoglycan in the skin of patients with mcEDS-*CHST14* (Hirose et al., 2019). By electron microscopy staining, rod-shaped linear GAG chains were found to be attached at one end to collagen fibrils and protruded outside the fibrils in the skin of mcEDS-*CHST14*, in contrast to those in wild type mice where they surround and wrap the collagen fibrils. The structure of the GAG chain from *Chst14*$^{-/-}$ mice also exhibited similar abnormalities of collagen networks in the skin (Hirose et al., 2021). Similar to these findings observed in skin tissue, structural and conformational abnormalities in the GAG chain on decorin may affect the formation of collagen fibrils in the muscle tissue. Decorin-null mice exhibit dermal collagen fibrils with a large variety of sizes and shapes (Danielson et al., 1997). These findings suggest that the decorin-proteoglycan is important for collagen fibril formation, and regulates the space between collagen fibrils as well as bundles, as reported previously (Scott et al., 1995). DS and CS/DS hybrid chains are conformationally more flexible than CS chains (Casu et al., 1988; Hirose et al., 2021). Thus, collagen bundles bound by CS chains,

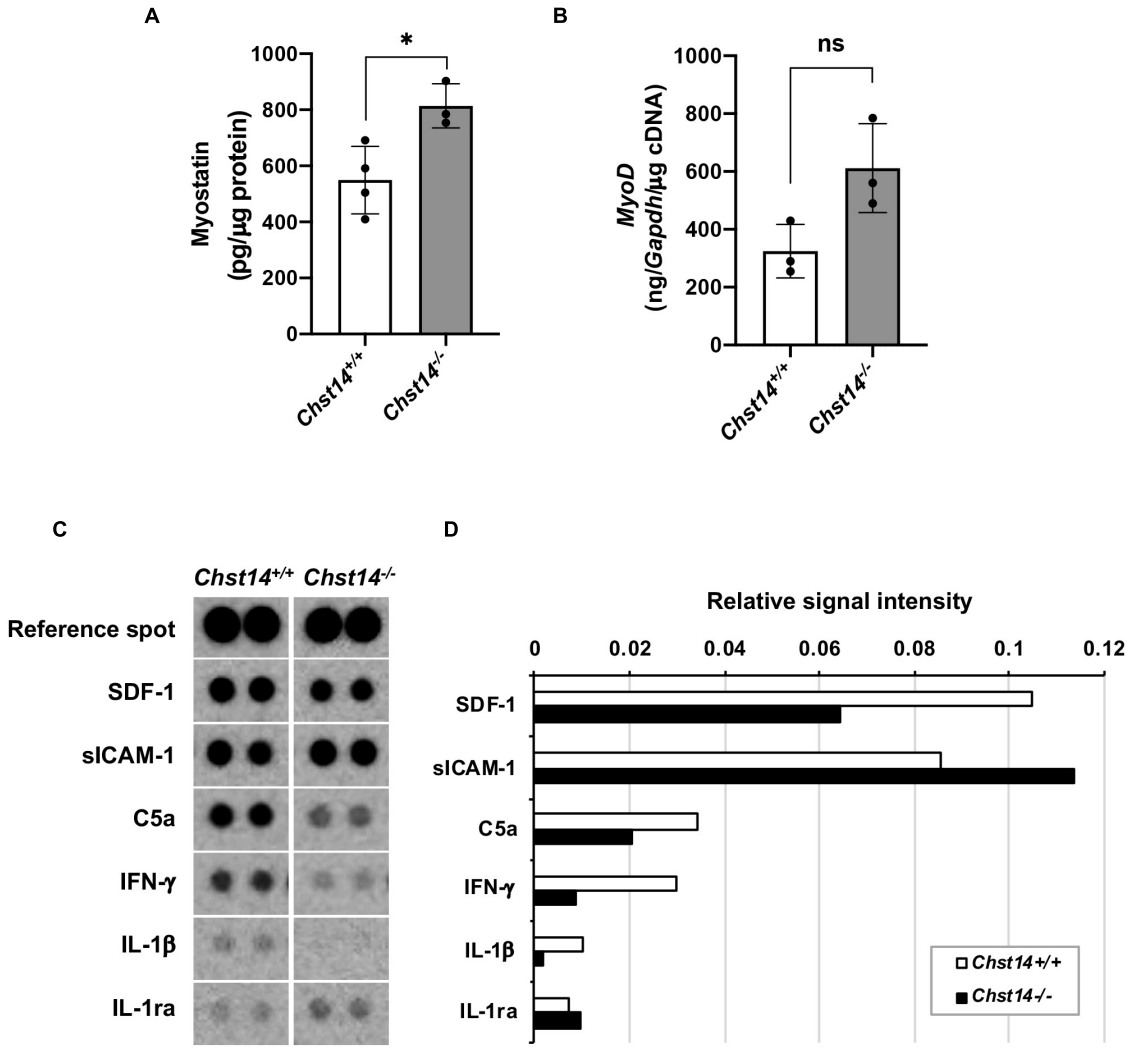


**FIGURE 2 |** Expression of myogenesis-associated factors and myokines/chemokines in DS-deficient muscle. **(A)** Quantitative measurement of myostatin expression (pg/μg protein) in the muscle lysate using an enzyme-linked immunosorbent assay (ELISA) (*$p < 0.05$). **(B)** Quantitative measurement of *MyoD* mRNA in the muscle from 1-year-old sex-matched *Chst14*$^{+/+}$ ($n = 8$) and *Chst14*$^{-/-}$ ($n = 4$) mice by quantitative real-time PCR were normalized with *Gapdh* (ng/*Gapdh*/μg cDNA). Data are presented as mean ± standard deviation, and there was no statistical difference between *Chst14*$^{+/+}$ and *Chst14*$^{-/-}$ by *t*-test. (ns, not significant). **(C)** Cytokine and chemokine expression in the muscle from 1-year-old sex-matched *Chst14*$^{+/+}$ ($n = 3$) and *Chst14*$^{-/-}$ ($n = 3$) mice were analyzed using the Proteome profiler™ array. Images of dot signals showed changes in the expression levels of stromal cell-derived factor 1 (SDF-1), soluble intercellular adhesion molecule-1 (sICAM-1), complement component 5a (C5a), interferon-γ (IFN-γ), IL-1β, and IL-1ra, compared to the reference spot signals. **(D)** Relative signal intensity correlated by reference spot signals in the array images were quantified using Image Quant TL software.

instead of DS chains, on decorin in mcEDS-*CHST14* patients as well as *Chst14*$^{-/-}$ mice may be more fragile than those in healthy and wild-type controls, respectively.

The diffused decorin localization in the spread of the endomysium and perimysium of DS-deficient muscle was similar to that of the dystrophic muscle (Caceres et al., 2000). In dystrophic skeletal muscle, the biosynthesis and accumulation of decorin around individual muscle fibers are enhanced in the endomysium and exomysium (Caceres et al., 2000). The histopathological findings observed in the *Chst14*$^{-/-}$ mice indicated that several central nuclear fibers, nuclear infiltration, and fibrosis were not as high as in severe myopathy and dystrophy (**Figure 1**; Coulton et al., 1988). Although dystrophic muscles showed a larger number of smaller fibers, occurrence of hypertrophic fibers, and high levels of creatine kinase, a marker of muscle damage, this was not confirmed in *Chst14*$^{-/-}$ mice, suggesting milder phenotypes of myopathy in mcEDS.

Altered localization of decorin indicates structural modification of the ECM in the spreading interstitium of the DS-deficient muscles. Expression of decorin mRNA was confirmed in the connective tissue cells, that is, in the mesenchymal and satellite cells, suggesting that decorin plays an important role in organizing the fibrillar network of the ECM (Caceres et al., 2000; Fadic et al., 2006). In the muscle of *Chst14*$^{-/-}$mice, upregulated

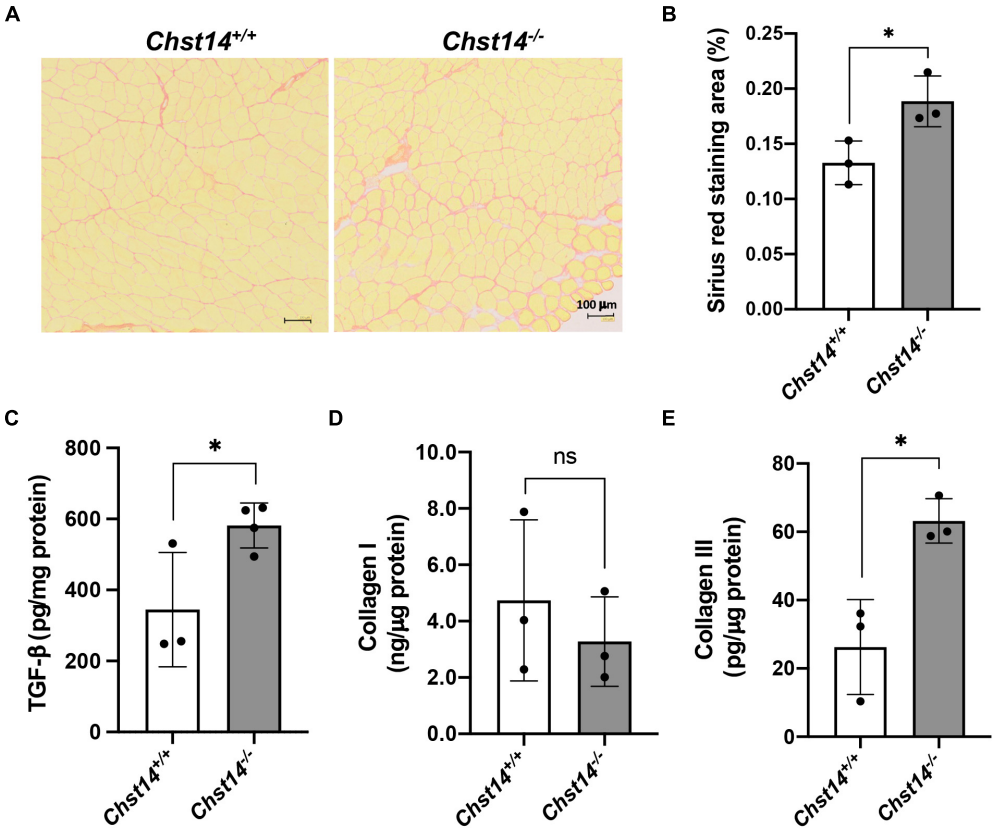


**FIGURE 3 |** Fibrosis in DS-deficient muscles. **(A)** Sirius red staining of the tibialis anterior (TA) muscle of 1-year-old sex-matched *Chst14*$^{+/+}$ and *Chst14*$^{-/-}$ mice. Bars, 100 µm. **(B)** Quantification of sirius red staining area of the cross-section (% of total area) from 1-year-old sex-matched *Chst14*$^{+/+}$ and *Chst14*$^{-/-}$ mice ($n$ = 3, each). **(C–E)** Quantitative measurement of TGF-β **(C)**, collagen type I **(D)**, and collagen type III **(E)** in the muscle lysate from 1-year-old sex-matched *Chst14*$^{+/+}$ and *Chst14*$^{-/-}$ ($n$ = 3, each) mice using ELISA. All data are presented as mean ± standard deviation, and statistical differences between *Chst14*$^{+/+}$ and *Chst14*$^{-/-}$ (*$P$ < 0.05), $t$-test. ns, not significant.

myostatin appears to induce muscle growth delay and muscle dystrophy. MyoD and follistatin have also been reported to increase in response to decorin overexpression (Kanzleiter et al., 2014). *Chst14*$^{-/-}$ mice had decorin with a CS side chain and showed lower activity of myogenesis and muscle formation in the DS-deficient muscle, supported by a larger number of smaller fibers, while the significant difference of *MyoD* expression was not detected between *Chst14*$^{-/-}$ and *Chst14*$^{+/+}$ mice.

Besides function as a matrix component, biglycan-proteoglycan can be either proteolytically released from the ECM upon tissue stress and injury or synthesized by activated macrophages (Schaefer et al., 2005). Biglycan protein core together with GAG side chain(s), triggers a proinflammatory response by acting as a signaling molecule and an endogenous ligand of Toll-like receptors (TLR)-2 and -4 on the surface of macrophages. It then induces the synthesis and secretion of pro-inflammatory cytokines and chemokines, such as IL-1β, tumor necrosis factor (TNF)-α, chemokine (C-C motif) ligand (CCL) 2 and 5, and chemokine (C-X-C motif) ligand (CXCL)1, -2, and -13 (Schaefer et al., 2017). These processes initiate modulation of the immune environment. Pathogenic muscle-derived cytokines are thought to be produced by infiltrating inflammatory cells. Cytokine and chemokine arrays demonstrated that the expression pattern of SDF-1, IFN-γ, C5a, IL-1β, and IL-1ra was altered in *Chst14*$^{-/-}$ mice (**Figure 2**). Thus, the reduction of DS in *Chst14*$^{-/-}$ mice might affect the expression and/or stability of cytokines as well as chemokines in the ECM or on the cell surface. SDF-1 and its receptor CXCR4 and CXCR7, stimulate the production of paracrine mediators, including some of growth factors such as vascular endothelial growth factor, fibroblast growth factor, and hepatocyte growth factor (Liu et al., 2012) associated muscle growth. Thus, the reduction of SDF-1 may indicate lower activity of growth factors in *Chst14*$^{-/-}$ mice. C5a, which is known to play recruitment of inflammatory cells, and lead to pro-inflammatory cytokines. Thus, low expression of C5a may suppress pro-inflammatory activation in *Chst14*$^{-/-}$ mice. The *IL-1ra* gene has been associated with various human diseases, primarily epithelial and endothelial cells. This may indirectly lead to an imbalance in the IL-1 system with enhanced production of IL-1β and reduced production of IL-1ra (Arend, 2002). In DS-deficient muscle, disease-specific changes in cytokine balance could affect myogenesis

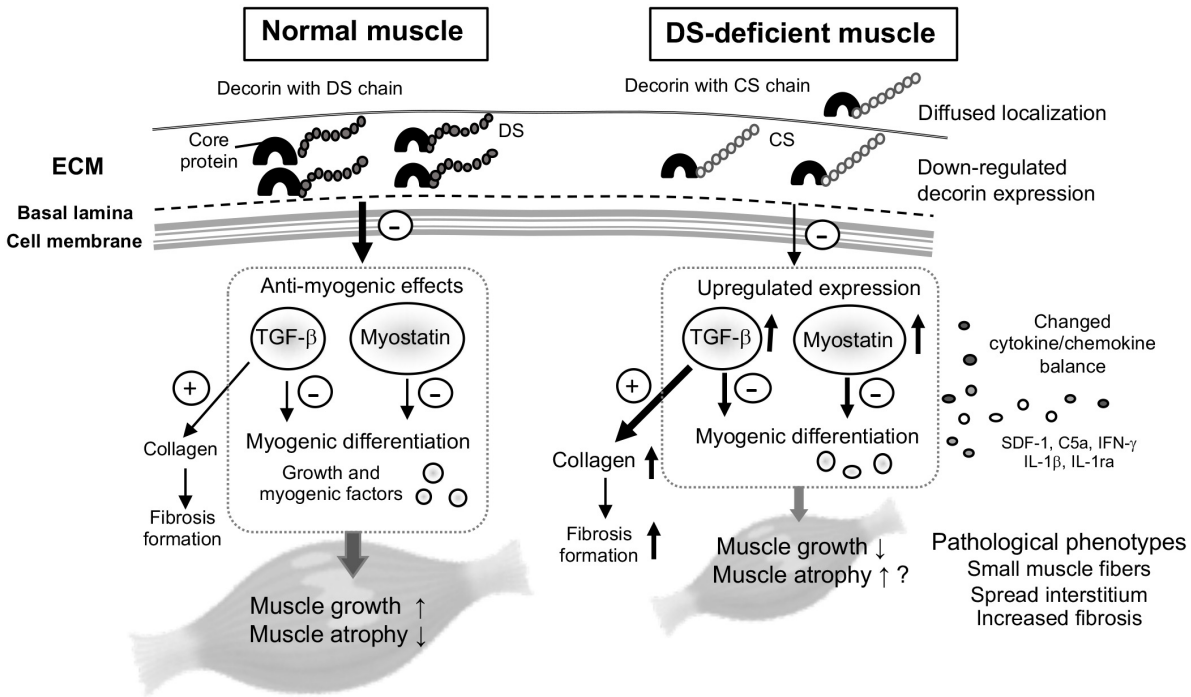


**FIGURE 4 |** Schematic for the proposed hypothesis of this study. Decorin is one of the most abundant proteoglycans in the skeletal muscle, mainly associated with ECM surrounding bundles of myofibers. In normal muscle, decorin acts as a myokine through the pathway: inhibition of transforming growth factor (TGF)-β, and down-regulation of myostatin expression, by competitively binding to TGF-β or myostatin. The inhibitory effects on TGF-β or myostatin (arrow with minus mark) might be reduced in DS-deficient muscle, because down-regulation of decorin core protein as well as its modification by CS instead of DS lead to diffused localization and induced up-regulated expression of myostatin and TGF-β, with the resulting collagen production leading to fibrosis. Decorin with CS also leaded to changes in the cytokine/chemokine environment, and might result in delayed muscle growth and pathological phenotypes, but had no effect on expression levels of myogenic factors.

and induce disease progression. Functional changes in CS-containing decorin may induce a modified environment for some myokines.

The ECM is essential for normal myogenesis, which includes interactions between myoblasts and their environment (Osses and Brandan, 2002). Decorin plays an important role in organizing the fibrillar network of the ECM (Caceres et al., 2000; Fadic et al., 2006). Various proteoglycans in the ECM have been reported to play a role in the differentiation process by regulating growth factor activity (Villena and Brandan, 2004). DS is an enhancer of growth factor-dependent proliferation of satellite cells and migration during skeletal muscle formation (Villena and Brandan, 2004). Therefore, DS depletion in the skeletal muscle of *Chst14*$^{-/-}$ mice and mcEDS may induce disease-specific myogenesis, including delayed muscle growth and reduced structural stability.

CS/DS-proteogrycans regulate cell signaling on the cell surface through binding with various growth factors (Mizumoto et al., 2015). Both the amount and distribution of iduronic acid (IdoUA) are subjected to physiological regulation; for example, TGF-β considerably affects IdoUA in decorin (Tiedemann et al., 2005). The conformational flexibility of IdoUA-containing CS/DS hybrid as well as DS chains is thought to facilitate the binding activity to proteins (Casu et al., 1988). For instance, the interaction of hepatocyte growth factor with CS/DS requires IdoUA residue flanked by 4-*O*-sulfated *N*-acetylgalactosamine (Deakin et al., 2009). The IdoUA-containing domains of CS/DS have also been shown to interact with the fibroblast growth factor family, thereby regulating cell migration (Trowbridge et al., 2002). Considering these facts, the IdoA residue seems to effects of the replacement of DS by CS migration and proliferation of muscle cells in *Chst14*$^{-/-}$ mice.

Decorin shows high affinity for TGF-β by binding to decorin core protein (Hildebrand et al., 1994), allowing decorin to function as a reservoir for TGF-β in the ECM. We demonstrated enhanced fibrosis in *Chst14*$^{-/-}$ mice supported by histopathological staining and upregulated expression of collagen and TGF-β (**Figure 3**). Decorin with the CS chain in *Chst14*$^{-/-}$ mice led to enhanced fibrosis and resulted in connective tissue fragility, as observed in dystrophic muscle. In patients with dystrophy, selective accumulation of CS, increase in 4-*O*-sulfation of CS accompanied by upregulation of *CHST11*, which encodes chondroitin 4-*O*-sulfotransferase-1, and reduction in expression of CS-degrading enzyme, hyaluronidase-4, in the muscles (Negroni et al., 2014). In this study, we demonstrated that DS chain of decorin-proteoglycan was replaced with CS, and that its protein expression was reduced in *Chst14*$^{-/-}$ mice (**Figure 1**). The functional alteration by decorin-proteoglycan

in *Chst14*$^{-/-}$ mice might lead the myopathy phenotype in the muscle. Further investigation may be required for more understanding of the mechanisms of myopathy phenotype caused by decorin-proteoglycan with CS side chain.

Abnormal collagen bundle formation was associated with decorin GAG abnormalities. Decorin interacts with collagen I as well as with collagens II, III, IV, V, VI, XII, and XIV (Gubbiotti et al., 2016). The fibril-forming of types I and III are by far the most abundant by proteomic studies, suggesting that they jointly account for approximately 75% of total muscle collagen (McKee et al., 2019). The strong parallel fibers of collagen I, which are present in the endo-, peri-, and epimysium, are assumed to confer tensile strength and rigidity to the muscle, whereas collagen III forms a loose meshwork of fibers that bestows elasticity to the endo- and perimysium (Kovanen, 2002). Our data showed downregulation of collagen III in the muscle of *Chst14*$^{-/-}$ mice. Therefore, the loose meshwork of fibers might be associated with the myopathy phenotype in *Chst14*$^{-/-}$ mice, and mcEDS may be caused by connective tissue fragility in the skeletal muscle, associated with ECM functional changes including ectopic localization of decorin. These findings will facilitate future research on the disease-specific mechanisms of decorin with DS or CS chains in muscle maintenance and potential therapeutic approaches for myopathy.

## DATA AVAILABILITY STATEMENT

The datasets presented in this study can be found in online repositories. The names of the repository/repositories and accession number(s) can be found below: Gene ID: 16176, https://www.ncbi.nlm.nih.gov/gene/16176; Gene ID: 16181, https://www.ncbi.nlm.nih.gov/gene/16181; Gene ID: 14433, https://www.ncbi.nlm.nih.gov/gene/14433; Gene ID: 17927, https://www.ncbi.nlm.nih.gov/gene/17927; and Gene ID: 13179, https://www.ncbi.nlm.nih.gov/gene/13179.

## ETHICS STATEMENT

The animal study was reviewed and approved by the Experimental Animal Care and Use Committee at the National Center of Neurology and Psychiatry (NCNP) and the Nippon Medical School.

## AUTHOR CONTRIBUTIONS

YN-K and TK conceived and planned the experiments. YN-K, SM, YI, GP-H, and AN-T performed the experiments, derived the models, contributed to sample preparation, assisted with experiments involving animal models, and analyzed the data. SM, TI, SY, YN, and ST provided advice and suggestions for the discussion. YN-K wrote the manuscript in consultation. TO and TK supervised the project. All authors contributed to the article and approved the submitted version.

## FUNDING

This work was supported by a research grant from the Health Sciences Research Grants for Research on Human Genome and Gene Therapy from the Ministry of Health, Labor and Welfare of Japan, and a Grant-in-Aid for Scientific Research (B) from the Japan Society for the Promotion of Science (19H03616 to TK, SM, YN-K, TO, TY, YN and SY); Grant-in-Aid for Scientific Research (C) from the Japan Society for the Promotion of Science (19K07054 to SM), the Practical Research Project for Rare/Intractable Diseases, the Japan Agency for Medical Research and Development (AMED) (17ek0109105h0003 to TK, SM, YN-K, KT, TO and SY). Grant-in Aid for Research Center for Pathogenesis of Intractable Diseases from the Research Institute of Meijo University (SM and SY).

## ACKNOWLEDGMENTS

We express their gratitude to Nana Tsumita, Yuki Oda, Jun Tanihata, and Chiaki Masuda for their technical advice, support, and helpful discussions. We would also like to thank Sonoko Shimazu, Tomomi Fukatsu, Maya Kawamura, and Yuko Kakiuchi for their technical assistance. We thank Editage (www.editage.jp) for editing the English text of the draft of this manuscript.

## SUPPLEMENTARY MATERIAL

The Supplementary Material for this article can be found online at: https://www.frontiersin.org/articles/10.3389/fcell.2021.695021/full#supplementary-material

## REFERENCES

Arend, W. P. (2002). The balance between IL-1 and IL-1Ra in disease. *Cytokine Growth Factor Rev.* 13, 323–340. doi: 10.1016/s1359-6101(02)00020-5

Brady, A. F., Demirdas, S., Fournel-Gigleux, S., Ghali, N., Giunta, C., Kapferer-Seebacher, I., et al. (2017). The Ehlers-Danlos syndromes, rare types. *Am. J. Med. Genet. C Semin. Med. Genet.* 175, 70–115. doi: 10.1002/ajmg.c.31550

Brandan, E., and Gutierrez, J. (2013). Role of skeletal muscle proteoglycans during myogenesis. *Matrix Biol.* 32, 289–297. doi: 10.1016/j.matbio.2013.03.007

Cabello-Verrugio, C., and Brandan, E. (2007). A novel modulatory mechanism of transforming growth factor-beta signaling through decorin and LRP-1. *J. Biol. Chem.* 282, 18842–18850. doi: 10.1074/jbc.M700243200

Caceres, S., Cuellar, C., Casar, J. C., Garrido, J., Schaefer, L., Kresse, H., et al. (2000). Synthesis of proteoglycans is augmented in dystrophic mdx mouse skeletal muscle. *Eur. J. Cell Biol.* 79, 173–181. doi: 10.1078/S0171-9335(04)70020-5

Casu, B., Petitou, M., Provasoli, M., and Sinaÿ, P. (1988). Conformational flexibility: a new concept for explaining binding and biological properties of iduronic acid-containing glycosaminoglycans. *Trends Biochem. Sci.* 13, 221–225. doi: 10.1016/0968-0004(88)90088-6

Coulton, G. R., Morgan, J. E., Partridge, T. A., and Sloper, J. C. (1988). The mdx mouse skeletal muscle myopathy: I. A histological, morphometric and biochemical investigation. *Neuropathol. Appl. Neurobiol.* 14, 53–70. doi: 10.1111/j.1365-2990.1988.tb00866.x

Danielson, K. G., Baribault, H., Holmes, D. F., Graham, H., Kadler, K. E., and Iozzo, R. V. (1997). Targeted disruption of decorin leads to abnormal collagen fibril morphology and skin fragility. *J. Cell Biol.* 136, 729–743. doi: 10.1083/jcb.136.3.729

Deakin, J. A., Blaum, B. S., Gallagher, J. T., Uhrín, D., and Lyon, M. (2009). The binding properties of minimal oligosaccharides reveal a common heparan sulfate/dermatan sulfate-binding site in hepatocyte growth factor/scatter factor that can accommodate a wide variety of sulfation patterns. *J. Biol. Chem.* 284, 6311–6321. doi: 10.1074/jbc.M807671200

Dundar, M., Demiryilmaz, F., Demiryilmaz, I., Kumandas, S., Erkilic, K., Kendirci, M., et al. (1997). An autosomal recessive adducted thumb-club foot syndrome observed in Turkish cousins. *Clin. Genet.* 51, 61–64. doi: 10.1111/j.1399-0004.1997.tb02417.x

Dündar, M., Müller, T., Zhang, Q., Pan, J., Steinmann, B., Vodopiutz, J., et al. (2009). Loss of dermatan-4-sulfotransferase 1 function results in adducted thumb-clubfoot syndrome. *Am. J. Hum. Genet.* 85, 873–882. doi: 10.1016/j.ajhg.2009.11.010

Fadic, R., Mezzano, V., Alvarez, K., Cabrera, D., Holmgren, J., and Brandan, E. (2006). Increase in decorin and biglycan in Duchenne Muscular Dystrophy: role of fibroblasts as cell source of these proteoglycans in the disease. *J. Cell. Mol. Med.* 10, 758–769. doi: 10.1111/j.1582-4934.2006.tb00435.x

Florini, J. R., Ewton, D. Z., and Magri, K. A. (1991). Hormones, growth factors, and myogenic differentiation. *Annu. Rev. Physiol.* 53, 201–216. doi: 10.1146/annurev.ph.53.030191.001221

Gubbiotti, M. A., Vallet, S. D., Ricard-Blum, S., and Iozzo, R. V. (2016). Decorin interacting network: a comprehensive analysis of decorin-binding partners and their versatile functions. *Matrix Biol.* 55, 7–21. doi: 10.1016/j.matbio.2016.09.009

Handel, T. M., Johnson, Z., Crown, S. E., Lau, E. K., and Proudfoot, A. E. (2005). Regulation of protein function by glycosaminoglycans–as exemplified by chemokines. *Annu. Rev. Biochem.* 74, 385–410. doi: 10.1146/annurev.biochem.72.121801.161747

Hannesson, K. O., Tingbo, M. G., Olsen, R. L., Enersen, G., Baevre, A. B., and Ofstad, R. (2007). An immunological study of glycosaminoglycans in the connective tissue of bovine and cod skeletal muscle. *Comp. Biochem. Physiol. B Biochem. Mol. Biol.* 146, 512–520. doi: 10.1016/j.cbpb.2006.11.024

Hildebrand, A., Romarís, M., Rasmussen, L. M., Heinegård, D., Twardzik, D. R., Border, W. A., et al. (1994). Interaction of the small interstitial proteoglycans biglycan, decorin and fibromodulin with transforming growth factor beta. *Biochem. J.* 302, 527–534. doi: 10.1042/bj3020527

Hirose, T., Mizumoto, S., Hashimoto, A., Takahashi, Y., Yoshizawa, T., Nitahara-Kasahara, Y., et al. (2021). Systematic investigation of the skin in Chst14-/- mice: a model for skin fragility in musculocontractural Ehlers-Danlos syndrome caused by CHST14 variants (mcEDS-CHST14). *Glycobiology* 31, 137–150. doi: 10.1093/glycob/cwaa058

Hirose, T., Takahashi, N., Tangkawattana, P., Minaguchi, J., Mizumoto, S., Yamada, S., et al. (2019). Structural alteration of glycosaminoglycan side chains and spatial disorganization of collagen networks in the skin of patients with mcEDS-CHST14. *Biochim. Biophys. Acta Gen. Subj.* 1863, 623–631. doi: 10.1016/j.bbagen.2018.12.006

Iozzo, R. V. (1998). Matrix proteoglycans: from molecular design to cellular function. *Annu. Rev. Biochem.* 67, 609–652. doi: 10.1146/annurev.biochem.67.1.609

Kanzleiter, T., Rath, M., Görgens, S. W., Jensen, J., Tangen, D. S., Kolnes, A. J., et al. (2014). The myokine decorin is regulated by contraction and involved in muscle hypertrophy. *Biochem. Biophys. Res. Commun.* 450, 1089–1094. doi: 10.1016/j.bbrc.2014.06.123

Kosho, T. (2016). CHST14/D4ST1 deficiency: new form of Ehlers-Danlos syndrome. *Pediatr. Int.* 58, 88–99. doi: 10.1111/ped.12878

Kosho, T., Miyake, N., Mizumoto, S., Hatamochi, A., Fukushima, Y., Yamada, S., et al. (2011). A response to: loss of dermatan-4-sulfotransferase 1 (D4ST1/CHST14) function represents the first dermatan sulfate biosynthesis defect, "dermatan sulfate-deficient Adducted Thumb-Clubfoot Syndrome". Which name is appropriate, "Adducted Thumb-Clubfoot Syndrome" or "Ehlers-Danlos syndrome"? *Hum. Mutat.* 32, 1507–1509. doi: 10.1002/humu.21586

Kosho, T., Mizumoto, S., Watanabe, T., Yoshizawa, T., Miyake, N., and Yamada, S. (2020). Recent advances in the pathophysiology of musculocontractural Ehlers-Danlos syndrome. *Genes (Basel)* 11, 43. doi: 10.3390/genes11010043

Kovanen, V. (2002). Intramuscular extracellular matrix: complex environment of muscle cells. *Exerc. Sport Sci. Rev.* 30, 20–25. doi: 10.1097/00003677-200201000-00005

Lightfoot, A. P., and Cooper, R. G. (2016). The role of myokines in muscle health and disease. *Curr. Opin. Rheumatol.* 28, 661–666. doi: 10.1097/BOR.0000000000000337

Liu, H., Liu, S., Li, Y., Wang, X., Xue, W., Ge, G., et al. (2012). The role of SDF-1-CXCR4/CXCR7 axis in the therapeutic effects of hypoxia-preconditioned mesenchymal stem cells for renal ischemia/reperfusion injury. *PLoS One* 7, e34608. doi: 10.1371/journal.pone.0034608

McKee, T. J., Perlman, G., Morris, M., and Komarova, S. V. (2019). Extracellular matrix composition of connective tissues: a systematic review and meta-analysis. *Sci. Rep.* 9, 10542. doi: 10.1038/s41598-019-46896-0

Miyake, N., Kosho, T., Mizumoto, S., Furuichi, T., Hatamochi, A., Nagashima, Y., et al. (2010). Loss-of-function mutations of CHST14 in a new type of Ehlers-Danlos syndrome. *Hum. Mutat.* 31, 966–974. doi: 10.1002/humu.21300

Mizumoto, S., and Sugahara, K. (2012). Glycosaminoglycan chain analysis and characterization (glycosylation/epimerization). *Methods Mol. Biol.* 836, 99–115. doi: 10.1007/978-1-61779-498-8_7

Mizumoto, S., Yamada, S., and Sugahara, K. (2015). Molecular interactions between chondroitin-dermatan sulfate and growth factors/receptors/matrix proteins. *Curr. Opin. Struct. Biol.* 34, 35–42. doi: 10.1016/j.sbi.2015.06.004

Müller, T., Mizumoto, S., Suresh, I., Komatsu, Y., Vodopiutz, J., Dundar, M., et al. (2013). Loss of dermatan sulfate epimerase (DSE) function results in musculocontractural Ehlers-Danlos syndrome. *Hum. Mol. Genet.* 22, 3761–3772. doi: 10.1093/hmg/ddt227

Negroni, E., Henault, E., Chevalier, F., Gilbert-Sirieix, M., Van Kuppevelt, T. H., Papy-Garcia, D., et al. (2014). Glycosaminoglycan modifications in Duchenne muscular dystrophy: specific remodeling of chondroitin sulfate/dermatan sulfate. *J. Neuropathol. Exp. Neurol.* 73, 789–797. doi: 10.1097/NEN.0000000000000098

Nitahara-Kasahara, Y., Hayashita-Kinoh, H., Chiyo, T., Nishiyama, A., Okada, H., Takeda, S., et al. (2014). Dystrophic mdx mice develop severe cardiac and respiratory dysfunction following genetic ablation of the anti-inflammatory cytokine IL-10. *Hum. Mol. Genet.* 23, 3990–4000. doi: 10.1093/hmg/ddu113

Nitahara-Kasahara, Y., Kuraoka, M., Oda, Y., Hayashita-Kinoh, H., Takeda, S., and Okada, T. (2021a). Enhanced cell survival and therapeutic benefits of IL-10-expressing multipotent mesenchymal stromal cells for muscular dystrophy. *Stem Cell Res. Ther.* 12, 105. doi: 10.1186/s13287-021-02168-1

Nitahara-Kasahara, Y., Mizumoto, S., Inoue, Y. U., Saka, S., Posadas-Herrera, G., Nakamura-Takahashi, A., et al. (2021b). Muscle pathophysiology in mouse models of musculocontractural ehlers-danlos syndrome due to CHST14 mutations (mcEDS-CHST14), generated through CRISPR/Cas9-mediated genomic editing. *Dis. Model. Mech.*

Nomura, Y. (2006). Structural change in decorin with skin aging. *Connect. Tissue Res.* 47, 249–255. doi: 10.1080/03008200600846606

Osses, N., and Brandan, E. (2002). ECM is required for skeletal muscle differentiation independently of muscle regulatory factor expression. *Am. J. Physiol. Cell Physiol.* 282, 383–394. doi: 10.1152/ajpcell.00322.2001

Ostrowski, K., Rohde, T., Zacho, M., Asp, S., and Pedersen, B. K. (1998). Evidence that interleukin-6 is produced in human skeletal muscle during prolonged running. *J. Physiol.* 508, 949–953. doi: 10.1111/j.1469-7793.1998.949bp.x

Schaefer, L., Babelova, A., Kiss, E., Hausser, H. J., Baliova, M., Krzyzankova, M., et al. (2005). The matrix component biglycan is proinflammatory and signals through Toll-like receptors 4 and 2 in macrophages. *J. Clin. Invest.* 115, 2223–2233. doi: 10.1172/JCI23755

Schaefer, L., Tredup, C., Gubbiotti, M. A., and Iozzo, R. V. (2017). Proteoglycan neofunctions: regulation of inflammation and autophagy in cancer biology. *FEBS J.* 284, 10–26. doi: 10.1111/febs.13963

Scott, P. G., Dodd, C. M., Tredget, E. E., Ghahary, A., and Rahemtulla, F. (1995). Immunohistochemical localization of the proteoglycans decorin, biglycan and versican and transforming growth factor-beta in human post-burn hypertrophic and mature scars. *Histopathology* 26, 423–431. doi: 10.1111/j.1365-2559.1995.tb00249.x

Sugahara, K., Mikami, T., Uyama, T., Mizuguchi, S., Nomura, K., and Kitagawa, H. (2003). Recent advances in the structural biology of chondroitin sulfate and dermatan sulfate. *Curr. Opin. Struct. Biol.* 13, 612–620. doi: 10.1016/j.sbi.2003.09.011

Tiedemann, K., Olander, B., Eklund, E., Todorova, L., Bengtsson, M., Maccarana, M., et al. (2005). Regulation of the chondroitin/dermatan fine structure by transforming growth factor-beta1 through effects on polymer-modifying enzymes. *Glycobiology* 15, 1277–1285. doi: 10.1093/glycob/cwj027

Toole, B. P., and Lowther, D. A. (1968). Dermatan sulfate-protein: isolation from and interaction with collagen. *Arch. Biochem. Biophys.* 128, 567–578. doi: 10.1016/0003-9861(68)90064-7

Trowbridge, J. M., Rudisill, J. A., Ron, D., and Gallo, R. L. (2002). Dermatan sulfate binds and potentiates activity of keratinocyte growth factor (FGF-7). *J. Biol. Chem.* 277, 42815–42820. doi: 10.1074/jbc.M204959200

Villena, J., and Brandan, E. (2004). Dermatan sulfate exerts an enhanced growth factor response on skeletal muscle satellite cell proliferation and migration. *J. Cell. Physiol.* 198, 169–178. doi: 10.1002/jcp.10422

Voermans, N. C., Kempers, M., Lammens, M., van Alfen, N., Janssen, M. C., Bönnemann, C., et al. (2012). Myopathy in a 20-year-old female patient with D4ST-1 deficient Ehlers-Danlos syndrome due to a homozygous CHST14 mutation. *Am. J. Med. Genet. A* 158A, 850–855. doi: 10.1002/ajmg.a.35232

Weber, I. T., Harrison, R. W., and Iozzo, R. V. (1996). Model structure of decorin and implications for collagen fibrillogenesis. *J. Biol. Chem.* 271, 31767–31770. doi: 10.1074/jbc.271.50.31767

Zhang, L. (2010). Glycosaminoglycan (GAG) biosynthesis and GAG-binding proteins. *Prog. Mol. Biol. Transl. Sci.* 93, 1–17. doi: 10.1016/S1877-1173(10)93001-9

**Conflict of Interest:** The authors declare that the research was conducted in the absence of any commercial or financial relationships that could be construed as a potential conflict of interest.

The reviewer FM declared a past co-authorship with several of the authors SM, SY, TK to the handling editor.

frontiers in Cell and Developmental Biology

MINI REVIEW
published: 20 October 2021
doi: 10.3389/fcell.2021.767924

# New Insights Into Human Hyaluronidase 4/Chondroitin Sulphate Hydrolase

*Marissa L. Maciej-Hulme**

*Department of Nephrology, Radboud University Medical Center, Nijmegen, Netherlands*

In this review, the current experimental evidence, literature and hypotheses surrounding hyaluronidase 4 [HYAL4, also known as chondroitin sulphate hydrolase (CHSE)] and chondroitin sulphate (CS) are explored. Originally named for its sequence similarity to other members of the hyaluronidase family, HYAL4 is actually a relatively distinct member of the family, particularly for its unique degradation of CS-D (2-*O*-, 6-*O*-sulphated CS) motifs and specific expression. Human HYAL4 protein expression and structural features are discussed in relation to different isoforms, activities, potential localisations and protein-protein interaction partners. CS proteoglycan targets of HYAL4 activity include: serglycin, aggrecan, CD44 and sulfatase 2, with other potential proteoglycans yet to be identified. Importantly, changes in HYAL4 expression changes in human disease have been described for testicular, bladder and kidney cancers, with gene mutations reported for several others including: leukaemia, endometrial, ovarian, colorectal, head and neck, stomach, lung and breast cancers. The HYAL4 gene also plays a role in P53 negative human cancer cell proliferation and is linked to stem cell naivety. However, its role in cancer remains relatively unexplored. Finally, current tools and techniques for the detection of specific HYAL4 activity in biological samples are critically assessed. Understanding the role of HYAL4 in human diseases will fortify our understanding of developmental processes and disease manifestation, ultimately providing novel diagnostic opportunities and therapeutic targets for drug discovery.

**Keywords: chondroitin sulphate, proteoglycan, hydrolase, cancer, stem cell, spinal cord injury, osteoarthritis, catabolism**

OPEN ACCESS

***Edited by:***
*John Whitelock,*
*University of New South Wales, Sydney, Australia*

***Reviewed by:***
*Brooke Farrugia,*
*The University of Melbourne, Australia*
*Shuhei Yamada,*
*Meijo University, Japan*

***Correspondence:**
*Marissa L. Maciej-Hulme*
*marissa.maciej-hulme@radboudumc.nl*

***Specialty section:***
*This article was submitted to Signaling, a section of the journal Frontiers in Cell and Developmental Biology*

***Received:*** *31 August 2021*
***Accepted:*** *27 September 2021*
***Published:*** *20 October 2021*

***Citation:***
*Maciej-Hulme ML (2021) New Insights Into Human Hyaluronidase 4/Chondroitin Sulphate Hydrolase. Front. Cell Dev. Biol. 9:767924. doi: 10.3389/fcell.2021.767924*

## INTRODUCTION

### Structure of Chondroitin Sulphate/Dermatan Sulphate (CSPGs)

The glycosaminoglycan, chondroitin sulphate (CS), is a long, linear polysaccharide comprised of repeating glucuronic acid-*N*-acetylgalactosamine (GlcA-GalNAc) disaccharides that adorn a subset of glycosylated proteins, termed CS proteoglycans (CSPGs). Members of the family play diverse roles in tissue architecture, cell signalling, cell migration and growth, as well as in disease manifestation including: inflammation, cancer, neurological diseases and osteoarthritis (Bautch et al., 2000; Kim et al., 2011; Chi et al., 2012; Mikami and Kitagawa, 2013; Mizumoto et al., 2015; Hayes et al., 2016; Stephenson and Yong, 2018; Shida et al., 2019; Lokeshwar et al., 2020). The CSPG family has recently expanded to include 19 newly identified CS attachment sites in the human

proteome (Noborn et al., 2021). CS chains are built on to a common tetrasaccharide linker (xylose-galactose-galactose-GlcA) in the endoplasmic reticulum and Golgi apparatus, and are tethered to the protein core via a serine residue. A myriad of enzymes construct CS chains [reviewed extensively in Mikami and Kitagawa (2013)] and multiple sulphate groups may be positioned along the CS polymer, namely 2-*O*-sulphation on the GlcA, and/or 4-*O*- and 6-*O*-sulphation on the GalNAc, respectively. These sulphation modifications give rise to great structural diversity, forming functional motifs that participate in CS-ligand interactions. In addition, epimerisation of GlcA to iduronic acid within the chain creates hybrid CS/dermatan sulphate (DS) chains, altering the flexibility of the polymer and consequentially potential ligand interactions (Thelin et al., 2013; Mizumoto et al., 2015). Classification of unsulphated chondroitin, CS and DS chains is defined by the chemical structure of the polymer, with CS split into subtypes: CS-A (4-*O*-sulphated), CS-C (6-*O*-sulphated), CS-D (2-*O*-, 6-*O*-sulphated), and CS-E (4-*O*-, 6-*O*-sulphated). The latter two subtypes represent rarer sulphation modifications present within CS/DS chains. CS bioactivity is often described for CS/DS hybrid chains, and CS enriched in rarer sulphation types, such as CS-D and CS-E (Bao et al., 2004; Kim et al., 2011; Beurdeley et al., 2012; Mizumoto et al., 2015; Shida et al., 2019).

After biosynthesis is complete, further modification of CS chains can occur via degradation enzymes that cleave the glycosidic bonds between the saccharide units and release CS fragments from the parent polymer. Three human extra-lysosomal CS hydrolases have been identified: PH20 (SPAM1), hyaluronidase 1 (HYAL1) and hyaluronidase 4 [HYAL4, also known as chondroitin sulphate hydrolase (CHSE)] (Kaneiwa et al., 2010; Honda et al., 2012; Yamada, 2015). Unlike the first two that can degrade hyaluronic acid and CS substrates to a similar degree (Honda et al., 2012), HYAL4 is predominantly an endo-β-*N*-acetylgalactosaminidase with a strong preference for CS-D (2-*O*-, 6-*O*-sulphated CS) (Kaneiwa et al., 2010; Wu and Ertelt, 2021). Although HYAL4 CHSE activity was only discovered in 2010, a few CSPGs have already been identified to be modified by HYAL4 degradation including serglycin, aggrecan (Farrugia et al., 2019), CD-44 (Lokeshwar et al., 2020) and likely Sulfatase 2 too (El Masri et al., 2021). HYAL4 cleavage of CSPGs produces smaller [tetra- to dodecasaccharide (Bautch et al., 2000; Bao et al., 2004; Kim et al., 2011; Mikami and Kitagawa, 2013; Thelin et al., 2013; Mizumoto et al., 2015; Hayes et al., 2016; Shida et al., 2019; Noborn et al., 2021) sized] fragments (Farrugia et al., 2019) with a common structure [GlcA-GalNAc(6S)-GlcA, also known as 3B3- motifs] located proximally at the non-reducing end of the chain (**Figure 1**).

## HUMAN HYALURONIDASE 4 PROTEIN EXPRESSION AND STRUCTURE

The HYAL4 gene is located on chromosome locus 7q31.3. Several tissues and cell types have been identified to express HYAL4, particularly placenta, skeletal muscle tissue and neutrophils (granulocytes) (Farrugia et al., 2019; Quirós et al., 2019). Northern blot analysis showed that expression of HYAL4 exists as 2.4- and 4.0-kb transcripts in placenta as well as a 2.1-kb transcript in skeletal muscle, suggesting differential splicing of the gene may occur in different cell types and/or contexts (Csoka et al., 1999). HYAL4 protein expression has also been identified for several tissues of which testes and skeletal muscle are enriched (Bastow et al., 2008; Elbein et al., 2011; Quirós et al., 2019). Immunohistochemical staining of human tissues showed HYAL4 in the cytoplasm and membrane of cells and indicated the presence of HYAL4 in neuronal cell nuclei (Uhlen et al., 2015). Flow cytometry of non-permeabilised mast cells showed HYAL4 to be associated with the cell surface (Farrugia et al., 2019). *In vitro* experiments have demonstrated that at least one protein isoform is released into the extracellular milieu (Lokeshwar et al., 2020). However, the habitual location(s) of HYAL4 remains to be established.

Four proteins have been predicted from the human gene, two of which have been confirmed experimentally. The full-length variant (481 amino acids, UniProt Q2M3T9) is currently predicted to be a transmembrane protein, with cytoplasmic N- and C-termini and an extracellular catalytic domain followed by a peptide linker. However, unlike HYAL1, HYAL2, and HYAL3, no obvious canonical signal sequence has been identified for targeting to the membrane. Furthermore, a putative GPI-anchor at the C-terminus (position 455) is predicted (Kaneiwa et al., 2010, 2012), which would subsequently remove the C-terminal transmembrane domain. In several ape species, pig and mouse, HYAL4 orthologs also have predicted GPI-anchors but in rats and *Caenorhabditis elegans* the protein is probably secreted. Interestingly, human HYAL2, and PH20 also have consensus GPI anchor sites, but HYAL1 and HYAL3 do not. The shorter 349 amino acid human v1 variant of HYAL4 (UniProt, F8WDH9) is a truncated version, omitting the C-terminal peptide linker, predicted transmembrane and cytoplasmic peptide domains, which suggests that this protein form is secreted.

Both identified HYAL4 variants possess catalytic activity. For the full-length version, CS-D motifs are the preferred substrate with an optimum pH of 4.5–5 (Kaneiwa et al., 2010). In contrast, the v1 variant preferred cleaving CS-C over CS-D and enzyme activity had an optimum pH of 5–5.5 (Lokeshwar et al., 2020), suggesting that some catalytic specificity of the substrate preference is encoded within the peptide linker, even though the mutation was not directly adjacent to the catalytic residue (E147). A single mutation in the positioning residue Y247 in human HYAL4 (equivalent to Y219 in TsHyal-1) results in altered substrate specificity of full length HYAL4 (Jedrzejas and Stern, 2005). The differences in CS catalytic specificities in the splice variants may act as an additional layer of regulation to CS biology in tandem with enzyme localisation (membrane bound/anchored vs. secretion) for diverse control of multiple CSPG targets. Other methods of catalytic control may lie in the post translational modifications of the protein. Phosphorylation and acetylation mechanisms for enzyme activation or deactivation have been described for many enzymes (Guan and Xiong, 2011; Ardito et al., 2017). Three potential phosphorylation sites (Y43, T88, and Y296) and one acetylation site (E193) close to the catalytic residue (E147) have been predicted, all located within the catalytic

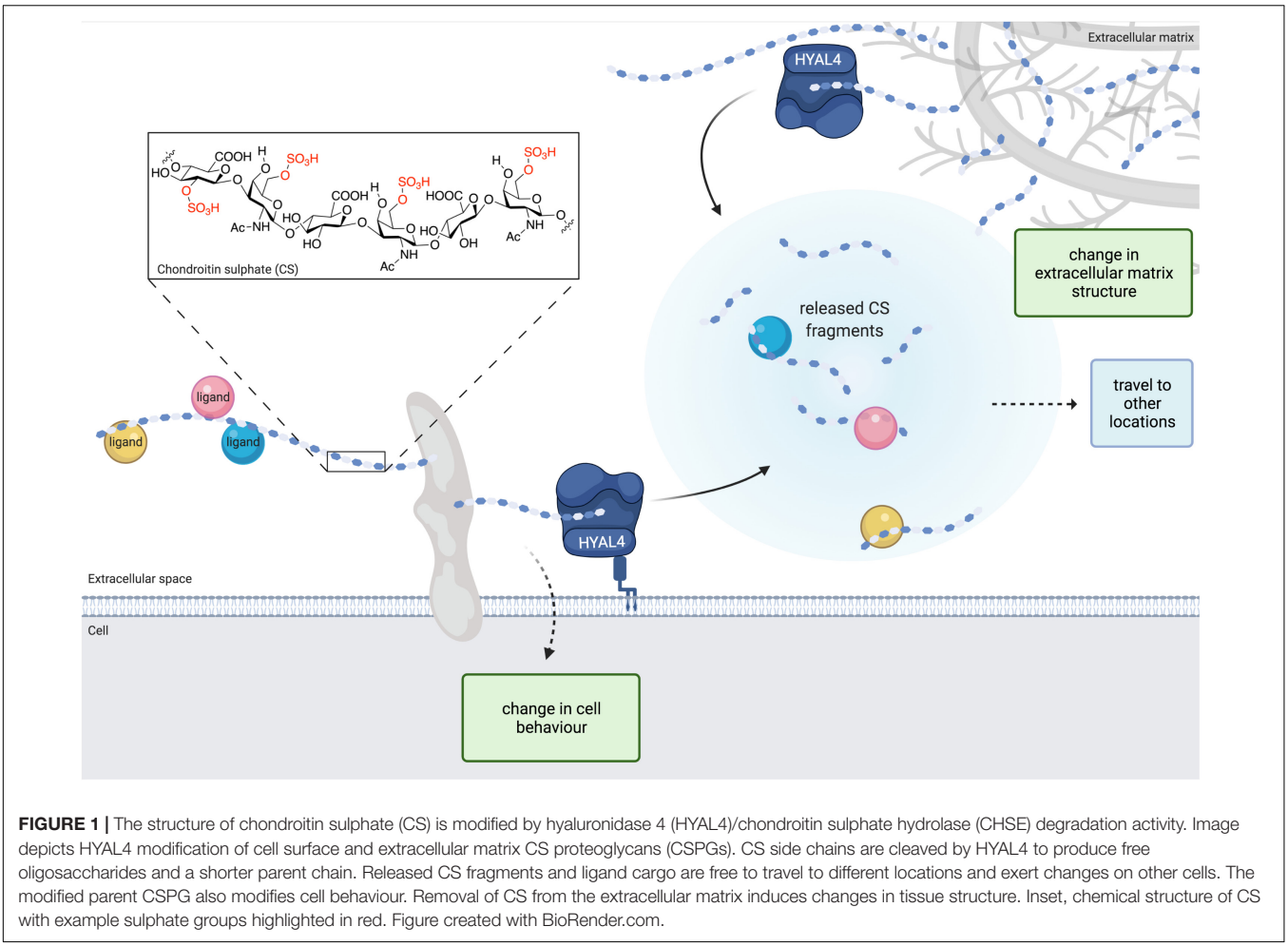


**FIGURE 1 |** The structure of chondroitin sulphate (CS) is modified by hyaluronidase 4 (HYAL4)/chondroitin sulphate hydrolase (CHSE) degradation activity. Image depicts HYAL4 modification of cell surface and extracellular matrix CS proteoglycans (CSPGs). CS side chains are cleaved by HYAL4 to produce free oligosaccharides and a shorter parent chain. Released CS fragments and ligand cargo are free to travel to different locations and exert changes on other cells. The modified parent CSPG also modifies cell behaviour. Removal of CS from the extracellular matrix induces changes in tissue structure. Inset, chemical structure of CS with example sulphate groups highlighted in red. Figure created with BioRender.com.

domain. The protein has four potential *N*-glycosylation sites (86, 115, 177, and 343 amino acid positions), with the presence of a complex *N*-glycan confirmed at 177 (Jia et al., 2009). Curiously, the peptide linker (and C-terminus) is what sets HYAL4 apart from other HYALs, and is a conserved feature in other species, including mice and the single CSHY present in *C. elegans* (Kaneiwa et al., 2008). This raises questions about its purpose for HYAL4 function via non-enzymatic mechanisms that have been described for other enzymes such as transportation of molecules, regulation and structural support (Kung and Jura, 2016).

In short, there are many unanswered questions surrounding HYAL4 protein structure. Whilst the structural features of the protein(s) remain unsolved, so do their functions. Hence the deduction of HYAL4 protein structure and the characterisation of post translational modifications of the protein will be an important corner stone for future studies in HYAL4 and CS/DS biology.

## Hyaluronidase 4 Protein-Protein Interactions

Interestingly, three distinct proteins have been identified as interaction partners of HYAL4: Glyceraldehyde-3-phosphate dehydrogenase, spermatogenic (GAPDHS; Huttlin et al., 2017), Isoleucine tRNA Synthetase 2 (IARS2; Wan et al., 2015) and NIMA Related Kinase 4 (NEK4; Basei et al., 2015). GAPDHS (also known as GAPDH-2) is an enzyme belonging to the Glyceraldehyde-3-phosphate dehydrogenase family that generates 1,3-diphosphoglycerate from glyceraldehyde-3-phosphate, and is thought to act as a switch between pathways for energy production. It is highly expressed in elongated (late) spermatids but has also been detected in malignant melanoma (Hoek et al., 2008), suggesting that its role is not confined to spermiogenesis as implied by its name. IARS2 is a ubiquitously expressed mitochondrial tRNA synthase that catalyses the aminoacylation of tRNA with isoleucine. Knockdown of IARS2 has been shown to promote apoptosis and inhibit proliferation in melanoma cells (Ma et al., 2020). NEK4 is a serine/threonine kinase involved in replicative senescence and for normal cell cycle arrest in response to double-stranded DNA damage (Nguyen et al., 2012). There are two splice variants of NEK4 (NEK4.1 and NEK4.2) (Basei et al., 2015) both with a nuclear localisation sequence in the regulatory domain (Hayashi et al., 1999) but cell cytoplasmic expression has also been observed. Expression of NEK4 is particularly abundant in Leydig cells of the testes as well as exocrine glandular cells of the pancreas, adrenal glandular cells

of the stomach and adrenal gland. GAPDHS, IARS2, and NEK4 have no known links between each other and none have been previously associated with CS. Thus, until further experimental evidence is reported, their roles in HYAL4 (and CS) biology remain intriguing but speculative.

# ASSAYS AND TOOLS FOR THE DETECTION OF HYALURONIDASE 4 ACTIVITY AND FUNCTION

## Degradation Activity Assays

Since the discovery of HYAL4 activity on CS, several new antibodies and quantitation kits became commercially available for the protein, which will greatly support future HYAL4 research. However, detection and quantification of HYAL4 enzyme activity remains challenging, as it is not always straightforward to delineate specific enzyme CHSE activity from biological samples. Although PH20 expression appears to be largely restricted to testes, HYAL1 is more widely expressed and possesses CHSE activity for CS-A. Unfortunately, natural sources of CS are typically a mixture of sulphation types classified on their predominant species i.e., CS-A is predominantly 4-sulphated but also contains a small amount of other rarer CS unit types, such as CS-D. Furthermore, CS-D preparations are usually a type of CS-A enriched with CS-D units (e.g., 16% CS-D units from shark cartilage produced by Iduron, United Kingdom). So for determining HYAL1 CHSE activity, one could simply use CS-A as an optimal substrate with relative ease. But for HYAL4, the CS-D preparations have cleavable sites for both HYAL4 and HYAL1, meaning that both HYALs could degrade significant portions of CS-D and produce a positive result in the assay. To untangle this, (1) a parallel assay must be performed with CS-A to deduce whether HYAL1 CHSE activity is present in the sample, (2) careful consideration of the detection strategy (biotinylation, antibodies) is important to maximise detection of removed CS and therefore detection of desired activity, (3) in the case that HYAL1 CHSE activity is detected, other evidence (e.g., qPCR for gene expression, western blot, protein quantification ELISA) is necessary to verify the enzymes responsible. For situations where both HYAL1 and HYAL4 activity is detected, quantification of HYAL4 activity will not be possible until assays with specific substrates exclusive for HYAL4 activity can be developed. Therefore, new chemically synthesised substrates designed specifically for HYAL4 activity and tailored antibodies for CS-D units are much-needed tools to facilitate the measurement of HYAL4 activity in biological samples.

## Antibodies

The monoclonal antibody (mab) 3B3 was originally created to recognise the neoepitope of CS chains following bacterial lyase (cABCase) digestion (designated 3B3+, i.e., +cABCase digestion) (Couchman et al., 1984). However, native 3B3 (i.e., without cABCase digestion) motifs were also detected in subpopulations of proteoglycans in chick embryos (Sorrell et al., 1988), subsequently termed 3B3-. Indeed, other CSPG 3B3- motifs have been studied including: serglycin, aggrecan (Farrugia et al., 2019, 2020), and CSPGs in the synovial fluid of elderly osteoarthritic patients (Bautch et al., 2000), where a significant decline in 3B3 and CS is associated with aging and articular cartilage progenitor CSPG(s) (Hayes et al., 2008). In addition to 3B3, MO-225 specifically recognises 2-*O*-sulphation in CS-D (Ito et al., 2005) and thus may be a useful antibody for the identification of HYAL4 modulated CSPGs.

# HYALURONIDASE 4 IN HUMAN DEVELOPMENT AND DISEASE

## Stem Cells and Differentiation

As mentioned earlier, the expression of human HYAL4 is somewhat limited in adult tissues. Beguilingly though, HYAL4 expression has been associated with stem cell naivety in human embryonic stem cells, suggesting a fundamental role in the delicate balance of cell cycle regulation, pluripotency and priming for differentiation (Messmer et al., 2019). 3B3- motifs decorate stem cell/progenitor cell proteoglycans (Hayes et al., 2018) and are located in discrete zones of foetal human knee joint during bone and cartilage development (Hayes et al., 2016). Specifically, HYAL4 expression increases during bone mineralisation, along with an increase in CS/DS chains and sulphation content of the chains (Adams et al., 2006). Expression of HYAL4 is also located distinctively at the epidermal-dermal junction in the skin (Sorrell et al., 1990), as well as being expressed following rat spinal cord injury and in a sheep intervertebral disc regeneration model, indicating its involvement in CSPG remodelling for tissue development and regeneration (Tachi et al., 2015; Farrugia et al., 2020). When taken in tandem with its limited constitutive adult tissue expression, the association of HYAL4 expression with naïve human embryonic stem cells and its temporal and/or localised expression in tissues, implies that HYAL4 activity may play transient, but important roles during organismal development.

## Cancer

In the Cancer Genome Atlas project database, HYAL4 gene mutations were associated with 12 out of the 15 cancer types analysed. In particular, roughly 4% of endometrial tumours had some kind of mutation in the HYAL4 gene that resulted in a disruption of protein structure. Other cancers with HYAL4 gene mutations included: colorectal, stomach, lung (adenocarcinoma, squamous), bladder, glioblastoma, leukaemia, head/neck, ovarian, breast and kidney (clear cell) cancers (∼0.25–1.8% prevalence) (Chi et al., 2012; Li et al., 2013; Lokeshwar et al., 2020; Hasanali et al., 2021). In addition, upregulation of HYAL4 protein was observed in testicular cancer (Lokeshwar et al., 2020) and the HYAL4 gene was preferentially required for the proliferation of P53 negative human cancer cells (Xie et al., 2012). On a protein level, interaction of HYAL4 with NEK4 may play an important part in the epithelial-to-mesenchymal transition of cells during the development of cancer. NEK4 is present in most primary

carcinomas where it acts as a positive regulator for EMT, resulting in an increased potential for cancer cell migration and invasion (Ding et al., 2018). So far, only two of the HYAL4 mutated cancer types identified have been investigated in more detail. In kidney cancer tissue, HYAL4 mRNA expression was significantly increased in clear cell renal cell carcinomas, papillary tumours and chromophobe renal cell carcinomas when compared with oncocytomas and HYAL4 upregulation was increased in patients with metastasis (Chi et al., 2012). In bladder cancer, HYAL4 activity increased the release of CD44, MMP-9 and Akt signalling and corresponded with metastasis and/or death of the patient after follow up. The v1 protein variant also showed chemotherapeutic resistance to Gemcitabine in preclinical models, suggesting HYAL4 drives chemoresistance in bladder cancer (Lokeshwar et al., 2020; Hasanali et al., 2021). Transfection of the v1 isoform in normal bladder cells resulted in an increase in aldehyde dehydrogenase-1, cell motility in wound healing assays and upregulation of EMT invasive phenotype markers that are hallmarks of cancer stem cells, invasiveness and EMT, respectively (Lokeshwar et al., 2020). Notably, the commonality of HYAL4 shared between cancer proliferation and stem cell naivety points toward a function for HYAL4 in the development and/or maintenance of cancer stem cells, which often cause therapeutic resistance and tumour relapse. Thus, swift investigation of HYAL4 in more cancers could provide beneficial insight and a novel, specific treatment target for a variety of cancer patients. Together, these data suggest that a defective HYAL4 mechanism may underlie the formation of various cancers.

## DISCUSSION

It is clear that many secrets of HYAL4 biology await discovery. A few clues buried within large data sets are beginning to emerge, demonstrating the usefulness of open access data repositories and predictive software programmes of modern science alongside traditional data publication. However, many annotations of human HYAL4 still report that the protein(s) only have hyaluronidase activity, which like the name HYAL4, is misleading and may have contributed to the slow connection of HYAL4 to CS-mediated diseases. Others have proposed new names to combat this, namely chondroitin sulphate hydrolase (CSHY; Kaneiwa et al., 2010), but unfortunately the abbreviation looks too similar to CHSY that is already used for CS synthesis enzymes. Another abbreviated name, Chase (from chondroitinase), has also been used (Lokeshwar et al., 2020) but as no sulphate reference is mentioned, it implies that HYAL4 has unsulphated chondroitin degradation activity, which is not accurate. Using "CSase" is also not advised since this abbreviation has been used historically for bacterial CS lyases. Therefore going forward, an abbreviation similar to HPSE, which is a well known GAG hydrolase, might be optimal: CHSE.

Multiple mechanisms may orchestrate the localisation and activity of human HYAL4 via expression of alternative splice variants by different cell types, although which cell types express which variants(s) remains to be investigated. The missing C-terminus of the v1 variant infers that the truncated version may be solely secreted and that the full length protein is associated with the cell surface. However, release of the putative GPI-anchor in the full length protein might also be possible via lytic cleavage or by other GPI-mitigated mechanisms (Muller, 2018). Aside from this, it is logical to assume that the full length version is primarily located on the cell surface to modulate cell surface CSPGs and the secreted version(s) are free to cleave CS in the extracellular milieu, matrices and on other cells. Close investigation of the protein structure and comparison of different variants would quickly detail which hypotheses are true, and provide leads for uncovering the mechanism(s) behind HYAL4 functions.

A limited number of useful methods and tools exist for HYAL4. The link between HYAL4 activity and expression of the mab 3B3- motif provides an effective screening tool for HYAL4 modification of CSPGs in new contexts and an anchor point to begin more specific analyses on a cell type or disease situation of interest. For example, 3B3-associated diseases such as osteoarthritis, development and aging warrant HYAL4 investigation. In addition, CSPGs (e.g., lubricin/proteoglycan 4), which display 3B3+ after cABCase digestion may also contain HYAL4 cleavage sites within the CS chains (Lord et al., 2012), meaning a wealth of knowledge may await in the literature for CSPGs modulated by HYAL4. Unfortunately, the same is not true for HYAL4 activity assays, where the lack of specific tools continues to complicate analyses due to overlapping activities for HYAL1 within CS substrates. However, as the interest in HYAL4 research grows, the production of new knockout models, antibodies, specific detection tools and assays for HYAL4 activity will enhance our knowledge of this CS degradation enzyme and will hasten its identification in organismal processes and reveal its role in cancers (and other human diseases). Understanding the role of HYAL4 in human diseases will undoubtedly provide novel diagnostic opportunities and therapeutic targets for drug discovery.

## AUTHOR CONTRIBUTIONS

MM-H conceived the idea, wrote the review, and produced **Figure 1**.

## ACKNOWLEDGMENTS

The results discussed here are in whole or part based upon data generated by the TCGA Research Network: https://www.cancer.gov/tcga and the Human Protein Atlas available from https://www.proteinatlas.org/ENSG00000106302-HYAL4/tissue. **Figure 1** was created with BioRender.com. I would like to thank David Briggs (Francis Crick Institute, United Kingdom) for helpful discussions on protein structure and Aurijit Sarkar (High Point University, United States) for the chemical structure of CS in the inset of **Figure 1**.

## REFERENCES


Adams, J. R., Sander, G., and Byers, S. (2006). Expression of hyaluronan synthases and hyaluronidases in the MG63 osteoblast cell line. *Matrix Biol.* 25, 40–46. doi: 10.1016/j.matbio.2005.08.007

Ardito, F., Giuliani, M., Perrone, D., Troiano, G., and Lo Muzio, L. (2017). The crucial role of protein phosphorylation in cell signaling and its use as targeted therapy (Review). *Int. J. Mol. Med.* 40, 271–280. doi: 10.3892/ijmm.2017.3036

Bao, X., Nishimura, S., Mikami, T., Yamada, S., Itoh, N., anrrrrrrd Sugahara, K. (2004). Chondroitin sulfate/dermatan sulfate hybrid chains from embryonic pig brain, which contain a higher proportion of L-iduronic acid than those from adult pig brain, exhibit neuritogenic and growth factor binding activities. *J. Biol. Chem.* 279, 9765–9776. doi: 10.1074/jbc.m310877200

Basei, F. L., Meirelles, G. V., Righetto, G. L., Dos Santos Migueleti, D. L., Smetana, J. H., and Kobarg, J. (2015). New interaction partners for Nek4.1 and Nek4.2 isoforms: from the DNA damage response to RNA splicing. *Proteome Sci.* 13:11.

Bastow, E. R., Byers, S., Golub, S. B., Clarkin, C. E., Pitsillides, A. A., and Fosang, A. J. (2008). Hyaluronan synthesis and degradation in cartilage and bone. *Cell. Mol. Life Sci.* 65, 395–413. doi: 10.1007/s00018-007-7360-z

Bautch, J. C., Clayton, M. K., Chu, Q., and Johnson, K. A. (2000). Synovial fluid chondroitin sulphate epitopes 3B3 and 7D4, and glycosaminoglycan in human knee osteoarthritis after exercise. *Ann. Rheum. Dis.* 59, 887–891. doi: 10.1136/ard.59.11.887

Beurdeley, M., Spatazza, J., Lee, H. H., Sugiyama, S., Bernard, C., Di Nardo, A. A., et al. (2012). Otx2 binding to perineuronal nets persistently regulates plasticity in the mature visual cortex. *J. Neurosci.* 32, 9429–9437. doi: 10.1523/jneurosci.0394-12.2012

Chi, A., Shirodkar, S. P., Escudero, D. O., Ekwenna, O. O., Yates, T. J., Ayyathurai, R., et al. (2012). Molecular characterization of kidney cancer: association of hyaluronic acid family with histological subtypes and metastasis. *Cancer* 118, 2394–2402. doi: 10.1002/cncr.26520

Couchman, J. R., Caterson, B., Christner, J. E., and Baker, J. R. (1984). Mapping by monoclonal antibody detection of glycosaminoglycans in connective tissues. *Nature* 307, 650–652. doi: 10.1038/307650a0

Csoka, A. B., Scherer, S. W., and Stern, R. (1999). Expression analysis of six paralogous human hyaluronidase genes clustered on chromosomes 3p21 and 7q31. *Genomics* 60, 356–361. doi: 10.1006/geno.1999.5876

Ding, N. H., Zhang, L., Xiao, Z., Rong, Z. X., Li, Z., He, J., et al. (2018). NEK4 kinase regulates EMT to promote lung cancer metastasis. *J. Cell. Mol. Med.* 22, 5877–5887. doi: 10.1111/jcmm.13857

El Masri, R., Seffouh, A., Roelants, C., Seffouh, I., Gout, E., Pérard, J., et al. (2021). Extracellular endosulfatase Sulf-2 harbours a chondroitin/dermatan sulfate chain that modulates its enzyme activity. *BioRxiv* [Preprint]. doi: 10.1101/2021.01.04.425218

Elbein, S. C., Kern, P. A., Rasouli, N., Yao-Borengasser, A., Sharma, N. K., and Das, S. K. (2011). Global gene expression profiles of subcutaneous adipose and muscle from glucose-tolerant, insulin-sensitive, and insulin-resistant individuals matched for BMI. *Diabetes* 60, 1019–1029. doi: 10.2337/db10-1270

Farrugia, B., Smith, S. M., Shu, C. C., and Melrose, J. (2020). Spatiotemporal Expression of 3-B-3(−) and 7-D-4 chondroitin sulfation, tissue remodeling, and attempted repair in an ovine model of intervertebral disc degeneration. *Cartilage* 11, 234–250. doi: 10.1177/1947603519876354

Farrugia, B. L., Mizumoto, S., Lord, M. S., O'Grady, R. L., Kuchel, R. P., Yamada, S., et al. (2019). Hyaluronidase-4 is produced by mast cells and can cleave serglycin chondroitin sulfate chains into lower molecular weight forms. *J. Biol. Chem.* 294, 11458–11472. doi: 10.1074/jbc.ra119.008647

Guan, K. L., and Xiong, Y. (2011). Regulation of intermediary metabolism by protein acetylation. *Trends Biochem. Sci.* 36, 108–116. doi: 10.1016/j.tibs.2010.09.003

Hasanali, S. L., Morera, D. S., Racine, R. R., Hennig, M., Ghosh, S., Lopez, L. E., et al. (2021). HYAL4-V1/Chondroitinase (Chase) drives gemcitabine resistance and predicts chemotherapy failure in patients with bladder cancer. *Clin. Cancer Res.* 27, 4410–4421. doi: 10.1158/1078-0432.ccr-21-0422

Hayashi, K., Igarashi, H., Ogawa, M., and Sakaguchi, N. (1999). Activity and substrate specificity of the murine STK2 Serine/Threonine kinase that is structurally related to the mitotic regulator protein NIMA of Aspergillus nidulans. *Biochem. Biophys. Res. Commun.* 264, 449–456. doi: 10.1006/bbrc.1999.1536

Hayes, A. J., Hughes, C. E., Smith, S. M., Caterson, B., Little, C. B., and Melrose, J. (2016). The CS sulfation motifs 4C3, 7D4, 3B3[−]; and perlecan identify stem cell populations and their niches, activated progenitor cells and transitional areas of tissue development in the fetal human elbow. *Stem Cells Dev.* 25, 836–847. doi: 10.1089/scd.2016.0054

Hayes, A. J., Smith, S. M., Caterson, B., and Melrose, J. (2018). Concise review: stem/progenitor cell proteoglycans decorated with 7-D-4, 4-C-3, and 3-B-3(−) chondroitin sulfate motifs are morphogenetic markers of tissue development. *Stem Cells* 36, 1475–1486. doi: 10.1002/stem.2860

Hayes, A. J., Tudor, D., Nowell, M. A., Caterson, B., and Hughes, C. E. (2008). Chondroitin sulfate sulfation motifs as putative biomarkers for isolation of articular cartilage progenitor cells. *J. Histochem. Cytochem.* 56, 125–138. doi: 10.1369/jhc.7a7320.2007

Hoek, K. S., Schlegel, N. C., Eichhoff, O. M., Widmer, D. S., Praetorius, C., Einarsson, S. O., et al. (2008). Novel MITF targets identified using a two-step DNA microarray strategy. *Pigment Cell Melanoma Res.* 21, 665–676. doi: 10.1111/j.1755-148x.2008.00505.x

Honda, T., Kaneiwa, T., Mizumoto, S., Sugahara, K., and Yamada, S. (2012). Hyaluronidases have strong hydrolytic activity toward chondroitin 4-sulfate comparable to that for hyaluronan. *Biomolecules* 2, 549–563. doi: 10.3390/biom2040549

Huttlin, E. L., Bruckner, R. J., Paulo, J. A., Cannon, J. R., Ting, L., Baltier, K., et al. (2017). Architecture of the human interactome defines protein communities and disease networks. *Nature* 545, 505–509. doi: 10.1038/nature22366

Ito, Y., Hikino, M., Yajima, Y., Mikami, T., Sirko, S., von Holst, A., et al. (2005). Structural characterization of the epitopes of the monoclonal antibodies 473HD, CS-56, and MO-225 specific for chondroitin sulfate D-type using the oligosaccharide library. *Glycobiology* 15, 593–603. doi: 10.1093/glycob/cwi036

Jedrzejas, M. J., and Stern, R. (2005). Structures of vertebrate hyaluronidases and their unique enzymatic mechanism of hydrolysis. *Proteins* 61, 227–238. doi: 10.1002/prot.20592

Jia, W., Lu, Z., Fu, Y., Wang, H. P., Wang, L. H., Chi, H., et al. (2009). A strategy for precise and large scale identification of core fucosylated glycoproteins. *Mol. Cell. Proteomics* 8, 913–923. doi: 10.1074/mcp.m800504-mcp200

Kaneiwa, T., Miyazaki, A., Kogawa, R., Mizumoto, S., Sugahara, K., and Yamada, S. (2012). Identification of amino acid residues required for the substrate specificity of human and mouse chondroitin sulfate hydrolase (conventional hyaluronidase-4). *J. Biol. Chem.* 287, 42119–42128. doi: 10.1074/jbc.m112.360693

Kaneiwa, T., Mizumoto, S., Sugahara, K., and Yamada, S. (2010). Identification of human hyaluronidase-4 as a novel chondroitin sulfate hydrolase that preferentially cleaves the galactosaminidic linkage in the trisulfated tetrasaccharide sequence. *Glycobiology* 20, 300–309. doi: 10.1093/glycob/cwp174

Kaneiwa, T., Yamada, S., Mizumoto, S., Montano, A. M., Mitani, S., and Sugahara, K. (2008). Identification of a novel chondroitin hydrolase in *Caenorhabditis elegans*. *J Biol Chem.* 283, 14971–14979.

Kim, E., Okumura, M., Sawa, H., Miyazaki, T., Fujikura, D., Yamada, S., et al. (2011). Paradoxical effects of chondroitin sulfate-E on Japanese encephalitis viral infection. *Biochem. Biophys. Res. Commun.* 409, 717–722. doi: 10.1016/j.bbrc.2011.05.072

Kung, J. E., and Jura, N. (2016). Structural basis for the non-catalytic functions of protein kinases. *Structure* 24, 7–24. doi: 10.1016/j.str.2015.10.020

Li, Y., Wang, D., Wang, L., Yu, J., Du, D., Chen, Y., et al. (2013). Distinct genomic aberrations between low-grade and high-grade gliomas of Chinese patients. *PLoS One* 8:e57168. doi: 10.1371/journal.pone.0057168

Lokeshwar, V. B., Morera, D. S., Hasanali, S. L., Yates, T. J., Hupe, M. C., Knapp, J., et al. (2020). A novel splice variant of HYAL-4 drives malignant transformation and predicts outcome in patients with bladder cancer. *Clin. Cancer Res.* 26, 3455–3467. doi: 10.1158/1078-0432.ccr-19-2912

Lord, M. S., Estrella, R. P., Chuang, C. Y., Youssef, P., Karlsson, N. G., Flannery, C. R., et al. (2012). Not all lubricin isoforms are substituted with a glycosaminoglycan chain. *Connect. Tissue Res.* 53, 132–141. doi: 10.3109/03008207.2011.614364

Ma, D., Li, S., Nie, X., Chen, L., Chen, N., Hou, D., et al. (2020). RNAi-mediated IARS2 knockdown inhibits proliferation and promotes apoptosis in human melanoma A375 cells. *Oncol. Lett.* 20, 1093–1100. doi: 10.3892/ol.2020.11688

Messmer, T., von Meyenn, F., Savino, A., Santos, F., Mohammed, H., Lun, A. T. L., et al. (2019). Transcriptional heterogeneity in naive and primed human pluripotent stem cells at single-cell resolution. *Cell Rep.* 26, 815–24.e4.

Mikami, T., and Kitagawa, H. (2013). Biosynthesis and function of chondroitin sulfate. *Biochim. Biophys. Acta* 1830, 4719–4733. doi: 10.1016/j.bbagen.2013.06.006

Mizumoto, S., Yamada, S., and Sugahara, K. (2015). Molecular interactions between chondroitin-dermatan sulfate and growth factors/receptors/matrix proteins. *Curr. Opin. Struct. Biol.* 34, 35–42. doi: 10.1016/j.sbi.2015.06.004

Muller, G. A. (2018). The release of glycosylphosphatidylinositol-anchored proteins from the cell surface. *Arch. Biochem. Biophys.* 656, 1–18. doi: 10.1016/j.abb.2018.08.009

Nguyen, C. L., Possemato, R., Bauerlein, E. L., Xie, A., Scully, R., and Hahn, W. C. (2012). Nek4 regulates entry into replicative senescence and the response to DNA damage in human fibroblasts. *Mol. Cell. Biol.* 32, 3963–3977. doi: 10.1128/mcb.00436-12

Noborn, F., Nikpour, M., Persson, A., Nilsson, J., and Larson, G. (2021). Expanding the chondroitin sulfate glycoproteome — but how far? *Front. Cell Dev. Biol.* 9:695970. doi: 10.3389/fcell.2021.695970

Quirós, L. M., Merayo-Lloves, J., Alcalde, I., Martín, C., Vázquez, F., Alfonso, J., et al. (2019). HYAL4 and PH20, involved in the hydrolysis of chondroitin sulfate chains, undergo a subexpression in the cornea of keratoconus patients. *ARVO Annu. Meet. Abstr.* 60:5107.

Shida, M., Mikami, T., Tamura, J. I., and Kitagawa, H. (2019). Chondroitin sulfate-D promotes neurite outgrowth by acting as an extracellular ligand for neuronal integrin alphaVbeta3. *Biochim. Biophys. Acta Gen. Subj.* 1863, 1319–1331. doi: 10.1016/j.bbagen.2019.06.004

Sorrell, J. M., Lintala, A. M., Mahmoodian, F., and Caterson, B. (1988). Epitope-specific changes in chondroitin sulfate/dermatan sulfate proteoglycans as markers in the lymphopoietic and granulopoietic compartments of developing bursae of Fabricius. *J. Immunol.* 140, 4263–4270.

Sorrell, J. M., Mahmoodian, F., Schafer, I. A., Davis, B., and Caterson, B. (1990). Identification of monoclonal antibodies that recognize novel epitopes in native chondroitin/dermatan sulfate glycosaminoglycan chains: their use in mapping functionally distinct domains of human skin. *J. Histochem. Cytochem.* 38, 393–402. doi: 10.1177/38.3.1689338

Stephenson, E. L., and Yong, V. W. (2018). Pro-inflammatory roles of chondroitin sulfate proteoglycans in disorders of the central nervous system. *Matrix Biol.* 71-72, 432–442. doi: 10.1016/j.matbio.2018.04.010

Tachi, Y., Okuda, T., Kawahara, N., Kato, N., Ishigaki, Y., and Matsumoto, T. (2015). Expression of hyaluronidase-4 in a rat spinal cord hemisection model. *Asian Spine J.* 9, 7–13. doi: 10.4184/asj.2015.9.1.7

Thelin, M. A., Bartolini, B., Axelsson, J., Gustafsson, R., Tykesson, E., Pera, E., et al. (2013). Biological functions of iduronic acid in chondroitin/dermatan sulfate. *FEBS J.* 280, 2431–2446. doi: 10.1111/febs.12214

Uhlen, M., Fagerberg, L., Hallstrom, B. M., Lindskog, C., Oksvold, P., Mardinoglu, A., et al. (2015). Proteomics. Tissue-based map of the human proteome. *Science* 347:1260419.

Wan, C., Borgeson, B., Phanse, S., Tu, F., Drew, K., Clark, G., et al. (2015). Panorama of ancient metazoan macromolecular complexes. *Nature* 525, 339–344. doi: 10.1038/nature14877

Wu, Z. L., and Ertelt, J. M. (2021). Assays for hyaluronidases and heparanase using nonreducing end fluorophore-labeled hyaluronan and heparan sulfate proteoglycan. *Glycobiology* doi: 10.1093/glycob/cwab061

Xie, L., Gazin, C., Park, S. M., Zhu, L. J., Debily, M. A., Kittler, E. L., et al. (2012). A synthetic interaction screen identifies factors selectively required for proliferation and TERT transcription in p53-deficient human cancer cells. *PLoS Genet.* 8:e1003151. doi: 10.1371/journal.pgen.1003151

Yamada, S. (2015). Role of hyaluronidases in the catabolism of chondroitin sulfate. *Adv. Exp. Med. Biol.* 842, 185–197.

**Conflict of Interest:** The author declares that the research was conducted in the absence of any commercial or financial relationships that could be construed as a potential conflict of interest.

**Publisher's Note:** All claims expressed in this article are solely those of the authors and do not necessarily represent those of their affiliated organizations, or those of the publisher, the editors and the reviewers. Any product that may be evaluated in this article, or claim that may be made by its manufacturer, is not guaranteed or endorsed by the publisher.

frontiers in Cell and Developmental Biology

REVIEW
published: 24 November 2021
doi: 10.3389/fcell.2021.764781

# An Overview of *in vivo* Functions of Chondroitin Sulfate and Dermatan Sulfate Revealed by Their Deficient Mice

*Shuji Mizumoto* and Shuhei Yamada*

*Department of Pathobiochemistry, Faculty of Pharmacy, Meijo University, Nagoya, Japan*

OPEN ACCESS

**Edited by:**
*Ana Cuenda,*
*Consejo Superior de Investigaciones Científicas (CSIC), Spain*

**Reviewed by:**
*Krishna Mohan Sepuru,*
*Howard Hughes Medical Institute (HHMI), United States*
*Mauro Sergio Pavao,*
*Federal University of Rio de Janeiro, Brazil*
*Hiroshi Kitagawa,*
*Kobe Pharmaceutical University, Japan*
*Göran Larson,*
*University of Gothenburg, Sweden*
*Chiara Schiraldi,*
*Università della Campania Luigi Vanvitelli, Italy*

***Correspondence:**
*Shuji Mizumoto*
*mizumoto@meijo-u.ac.jp*

**Specialty section:**
*This article was submitted to Signaling, a section of the journal Frontiers in Cell and Developmental Biology*

**Received:** *26 August 2021*
**Accepted:** *09 November 2021*
**Published:** *24 November 2021*

**Citation:**
*Mizumoto S and Yamada S (2021) An Overview of in vivo Functions of Chondroitin Sulfate and Dermatan Sulfate Revealed by Their Deficient Mice. Front. Cell Dev. Biol. 9:764781. doi: 10.3389/fcell.2021.764781*

Chondroitin sulfate (CS), dermatan sulfate (DS) and heparan sulfate (HS) are covalently attached to specific core proteins to form proteoglycans in their biosynthetic pathways. They are constructed through the stepwise addition of respective monosaccharides by various glycosyltransferases and maturated by epimerases as well as sulfotransferases. Structural diversities of CS/DS and HS are essential for their various biological activities including cell signaling, cell proliferation, tissue morphogenesis, and interactions with a variety of growth factors as well as cytokines. Studies using mice deficient in enzymes responsible for the biosynthesis of the CS/DS and HS chains of proteoglycans have demonstrated their essential functions. Chondroitin synthase 1-deficient mice are viable, but exhibit chondrodysplasia, progression of the bifurcation of digits, delayed endochondral ossification, and reduced bone density. DS-epimerase 1-deficient mice show thicker collagen fibrils in the dermis and hypodermis, and spina bifida. These observations suggest that CS/DS are essential for skeletal development as well as the assembly of collagen fibrils in the skin, and that their respective knockout mice can be utilized as models for human genetic disorders with mutations in chondroitin synthase 1 and DS-epimerase 1. This review provides a comprehensive overview of mice deficient in CS/DS biosyntheses.

**Keywords: chondroitin sulfate, dermatan sulfate, epimerase, glycosyltransferase, knockout mouse, proteoglycan, sulfotransferase, transporter**

## INTRODUCTION

Chondroitin sulfate (CS) and dermatan sulfate (DS) are covalently attached to core proteins to form proteoglycans (PGs). CS-PGs and DS-PGs are ubiquitously distributed in the extracellular matrix as well as on the cell surface (Rodén, 1980; Kjellén and Lindahl, 1991; Iozzo, 1998). Both glycosaminoglycans (GAGs) are linear polysaccharides. CS-PGs is abundantly distributed in cartilage (Rodén, 1980), whereas DS-PGs is predominantly distributed in skin, aorta, and blood vessel (Fransson et al., 1993). The backbone of CS is composed of repeating disaccharide units of D-glucuronic acid (GlcA) and *N*-acetyl-D-galactosamine (GalNAc) (**Figure 1**). DS is a stereoisomer of CS and consists of L-iduronic acid (IdoA) instead of GlcA and GalNAc (**Figure 1**). CS/DS chains are modified by sulfation at various hydroxy groups, which gives rise to structural diversity, thereby playing an important role in a variety of biological processes including interactions with various growth factors, cytokines, and morphogens, cell proliferation, tissue morphogenesis, and infections

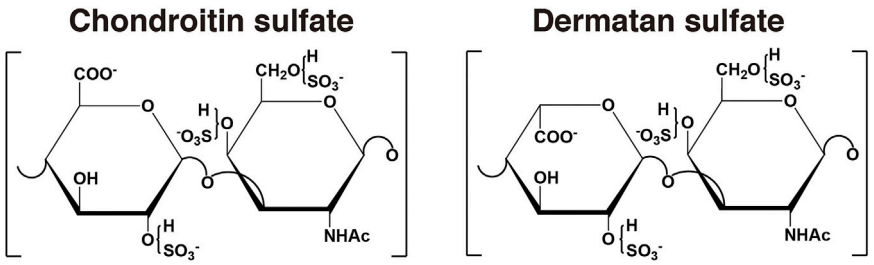


| Unit | Sequence |
|---|---|
| O unit | GlcA-GalNAc |
| A unit | GlcA-GalNAc(4S) |
| C unit | GlcA-GalNAc(6S) |
| B unit | GlcA(2S)-GalNAc(4S) |
| D unit | GlcA(2S)-GalNAc(6S) |
| E unit | GlcA-GalNAc(4S,6S) |

| Unit | Sequence |
|---|---|
| iO unit | IdoA-GalNAc |
| iA unit | IdoA-GalNAc(4S) |
| iC unit | IdoA-GalNAc(6S) |
| iB unit | IdoA(2S)-GalNAc(4S) |
| iD unit | IdoA(2S)-GalNAc(6S) |
| iE unit | IdoA-GalNAc(4S,6S) |

**FIGURE 1 |** Typical repeating disaccharide units in CS and DS. CS consists of GlcA and GalNAc, whereas DS is a stereoisomer of CS including IdoA instead of GlcA. These sugar moieties are esterified by sulfate at various positions, as indicated in the figures.

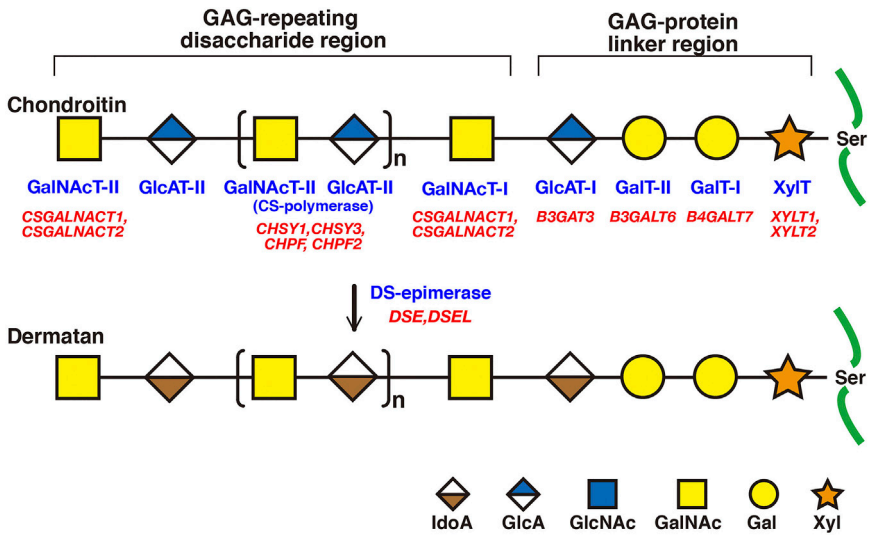


**FIGURE 2 |** Biosynthetic assembly of CS and DS backbones by various glycosyltransferases. Schematic presentation of the biosynthesis of CS and DS backbones. All glycosyltransferases require a corresponding UDP-sugar, such as UDP-Xyl, -Gal, -GlcA, and -GalNAc, as a donor substrate. After specific core proteins have been translated, synthesis of the common GAG-protein linkage region, GlcAβ1-3Galβ1-3Galβ1-4Xylβ1-, is evoked by XylT, which transfers a Xyl residue from UDP-Xyl to the specific serine residue(s) at the GAG attachment sites. The linker region tetrasaccharide is subsequently constructed by GalT-I, GalT-II, and GlcAT-I. The first β1-4-linked GalNAc residue is then transferred to the GlcA residue in the linker region by GalNAcT-I, which initiates the assembly of the chondroitin backbone, thereby resulting in the formation of the repeating disaccharide region, $[-4GlcA\beta1\text{-}3GalNAc\beta1\text{-}]_n$, by CS-polymerase. DS-epimerase converts GlcA into IdoA by epimerizing the C-5 carboxy group in the chondroitin precursor, thereby resulting in the formation of the repeating disaccharide region of dermatan precusor, $[-4IdoA\alpha1\text{-}3GalNAc\beta1\text{-}]_n$. Each enzyme and its coding gene are described under the respective sugar symbols.

by viruses (Trowbridge and Gallo, 2002; Sugahara et al., 2003; Sugahara and Mikami, 2007; Malavaki et al., 2008; Yamada and Sugahara, 2008; Malmström et al., 2012; Thelin et al., 2013; Mizumoto et al., 2015; 2013; 2017; Mizumoto and Sugahara, 2013; Schaefer et al., 2017; Kosho et al., 2019). A variety of functions of CS/DS are thought to be dependent on sulfation modification (Sugahara and Mikami, 2007; Mizumoto et al., 2015). A, C, B, D, and E disaccharide units stand for the disaccharide (GlcA-GalNAc) units containing one or two sulfate groups in different combinations (**Figure 1**). If the GlcA residue has been epimerized to IdoA in each disaccharide unit, "i" is added to the codes, such as iA, iC, iB,

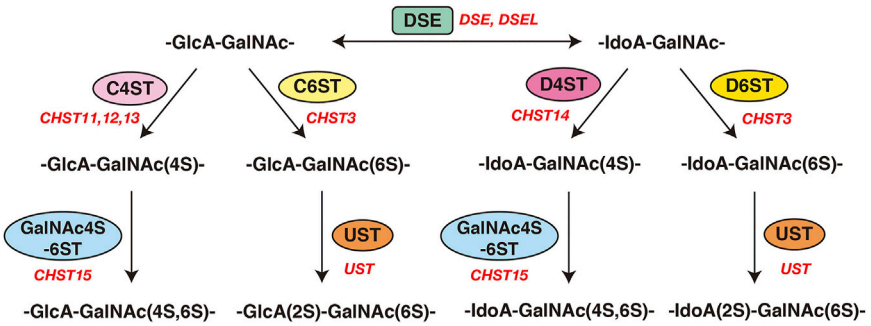


**FIGURE 3 |** Modification of CS and DS by sulfotransferases and epimerases. Modification pathways of CS and DS. After formation of the CS/DS backbones, each sugar residue is modified by sulfation, catalyzed by sulfotransferases, as indicated in the figure. C4ST or C6ST transfers a sulfate group from PAPS to the C-4 or C-6 position of the GalNAc residues in the chondroitin chain, respectively. D4ST transfers a sulfate group from PAPS to the C-4 position of the GalNAc residues in dermatan. Further sulfation reactions are catalyzed by GalNAc4S-6ST or UST, which is required for formation of the disulfated disaccharide units indicated, respectively.

iD, and iE (**Figure 1**). The A, iA, D, and E units are involved in infection of malaria, binding with heparin cofactor II, neurite outgrowth, and infection of herpes simplex virus, respectively (Maimone and Tollefsen 1991; Clement et al., 1998; Buffet et al., 1999; Bergefall et al., 2005). However, the functional domain in CS/DS does not appear to be composed of a single distinct saccharide sequence, but rather several heterogeneous sulfation patterns, the "wobble CS-DS motifs" (Purushothaman et al., 2012).

Various glycosyltransferases, epimerases, sulfotransferases, and related enzymes in the biosynthesis of CS and DS have been identified and characterized (**Figures 2**, **3**) (Kusche-Gullberg and Kjellén, 2003; Mikami and Kitagawa, 2013; Mizumoto, 2018). Moreover, functional analyses of CS and DS using model organisms such as nematodes, fruit flies, zebrafish, and mice have revealed that both are indispensable for normal development (Sugahara and Schwartz, 1979; Bernhardt and Schachner, 2000; Hwang et al., 2003; Mizuguchi et al., 2003; Sugahara et al., 2003; Takemae et al., 2003; Olson et al., 2006; Maccarana et al., 2009; Mizumoto et al., 2009; Li et al., 2010; Tian et al., 2010; Watanabe et al., 2010; Wilson et al., 2012; Takemura et al., 2020). Genetic disorders related to mutations in biosynthetic enzymes for CS/DS-biosynthesis were described in another review article (Mizumoto and Yamada, 2021). This review focuses on recent advances in studies on mice deficient in CS and DS biosynthetic enzymes.

## BIOSYNTHESES OF CS AND DS

### Biosyntheses of Donor Substrates for GAGs and Transporters of Uridine 5′-Diphosphate -Sugars, Sulfate Ions, and 3′-Phosphoadenosine 5′-Phosphosulfate

Most glycosyltransferases utilize uridine 5′-diphosphate (UDP)-sugars as the donor substrates, including: UDP-Glc, UDP-GlcNAc, UDP-GlcA, UDP-Gal, UDP-GalNAc, and UDP-Xyl, where Glc, GlcNAc, GlcA, Gal, GalNAc, and Xyl, represent D-glucose, *N*-acetyl-D-glucosamine, D-glucuronic acid, D-galactose, *N*-acetyl-D-galactosamine, and D-xylose, respectively. UDP-GlcA is formed by the action of UDP-Glc dehydrogenase on UDP-Glc in the cytosol (**Table 1**) (Spicer et al., 1998). UDP-Xyl is formed by the action of UDP-GlcA decarboxylase/UDP-xylose synthase in the endoplasmic reticulum and Golgi apparatus (Moriarity et al., 2002). These UDP-sugars mainly synthesized in the cytosol, except for UDP-Xyl, are incorporated into the endoplasmic reticulum and Golgi lumen through the corresponding nucleotide sugar transporters (Berninsone and Hirschberg, 2000; Orellana et al., 2016; Parker and Newstead, 2019).

Various GAG sulfotransferases catalyze the transfer of a sulfate group from 3′-phosphoadenosine 5′-phosphosulfate (PAPS), as a donor substrate, to respective acceptor substrates (Kusche-Gullberg and Kjellén, 2003). PAPS synthase (PAPSS) has two enzymatic domains, adenosine 5′-phosphosulfate kinase and ATP sulfurylase domains, in N- and C-terminals, respectively (Venkatachalam, 2003) (**Table 1**). PAPS is formed from inorganic sulfate, which is incorporated into the cytosol through the sulfate transporter at the plasma membrane and ATP (Hästbacka et al., 1994).

### Backbones of CS and DS

CS and DS polysaccharides are covalently attached to specific serine residues in core proteins through the common GAG-protein linker region tetrasaccharide GlcAβ1-3Galβ1-3Galβ1-4xylose(Xyl)β1-*O*- (**Figure 2**) (Lindahl and Rodén, 1972; Kjellén and Lindahl, 1991; Sugahara and Kitagawa 2000). The transfer of a Xyl residue from UDP-Xyl to specific serine residues in the newly synthesized core proteins of PGs in the endoplasmic reticulum and/or cis-Golgi compartments is initiated by β-xylosyltransferase (XylT) encoded by *XYLT1* or *XYLT2* (**Figure 2**; **Table 2**) (Götting et al., 2000; Pönighaus et al., 2007). It should be noted that human genes, which were described by all upper capital, were utilized in this section, because enzymatic activity of glycosyltransferases, epimerase, and sulfotransferases, which are responsible for biosynthesis of CS/DS, had been measured using recombinant human enzymes.

**TABLE 1 |** Transporters for UDP-sugars and sulfate, biosynthetic enzymes for PAPS and UDP-GlcA, and related proteins. Among the several transporters and biosynthetic enzymes involved in PAPS and UDP-sugars, GAG biosynthesis-related genes are listed here.

| Transporters and enzymes | Coding genes | mRNA accession no | Phenotypes of KO or mutant mouse | Human genetic disorders | MIM number | Refs. For knockout mouse |
|---|---|---|---|---|---|---|
| UDP-glucose dehydrogenase | *Ugdh* | NM_009466 | Defects in migration of mesoderm and endoderm, and disturbance of FGF signaling | Developmental and epileptic encephalopathy 84 | 603370<br>618792 | García-García and Anderson, (2003) |
| PAPS synthase 2 | *Papss2* | NM_001201470<br>NM_001360403<br>NM_011864 | A dome-shaped skull, reductions in limb size and axial skeletons, and disturbance of Indian hedgehog signaling | Brachyolmia 4 with mild epiphyseal and metaphyseal changes;<br>Spondyloepimetaphyseal dysplasia Pakistani type (PAPSS2 type);<br>Hyperandrogenism | 612847<br><br>603005 | Orkin et al. (1976), Schwartz et al. (1978), Sugahara and Schwartz (1979), Sugahara and Schwartz (1982a), Sugahara and Schwartz (1982b), Pennypacker et al. (1981), Cortes et al. (2009) |
| Diastrophic dysplasia sulfate transporter (Solute carrier family 26 member A2) | *Slc26a2* | NM_007885 | Growth retardation, joint contractures, and skeletal dysplasia including irregular size of chondrocytes, delay in the formation of the secondary osscification center, osteoporosis of long bone, severe thoracic kyphosis, bite overclosure, and hip dysplasia with pelvic deformity | Achondrogenesis type IB; Atelosteogenesis type II; De la Chapelle dysplasia; Diastrophic dysplasia; Diastrophic dysplasia, broad bone-platyspondylic variant; Epiphyseal dysplasia multiple 4 | 600972<br>256050<br>222600<br>226900<br>606718 | Forlino et al. (2005) |
| UDP-GlcA/UDP-GalNAc dual transporter (Solute carrier family 35 member D1) | *Slc35d1* | NM_001356276<br>NM_177732 | A lethal form of skeletal dysplasia including severe shortening of limbs, a decreased proliferating zone with round chondrocytes in the face, and scarce matrices | Schneckenbecken dysplasia | 610804<br>269250 | Hiraoka et al. (2007) |
| UDP 5′-diphosphatase | *Cant1* | NM_001025617<br>NM_001025618<br>NM_001267591<br>NM_001267592<br>NM_029502 | A moderate kyphosis, decrease in both length and width of tibiae, femurs, and ilium, delta phalanx, and a defect in endochondral ossification | Desbuquois dysplasia 1<br>Epiphyseal dysplasia multiple 7<br>Pseudodiastrophic dysplasia | 617719<br>251450<br>613165<br>264180 | Paganini et al. (2019), Kodama et al. (2020) |
| 3′-phosphoadenosine 5′-phosphate 3′-phosphatase | *Bpnt2/ Impad1* | NM_177730 | Either neonatal or embryonic lethality, reductions of limb length, shortening of the snout and lower limbs, and reduced sternal length | Chondrodysplasia with joint dislocations GRAPP type | 614078<br>614010 | Frederick et al. (2008) |
| Golgin, Rab6-interacting protein | *Gorab* | NM_001313738<br>NM_178883 | Neonatal lethal. Abnormal collagen fibrils, thinned and porous cortical bone, and spontaneous fractures | Geroderma osteodysplasticum | 607983<br>231070 | Chan et al. (2018) |

*Cant1, calcium activated nucleotidase 1; Bpnt2, 3′(2′), 5′-bisphosphate nucleotidase 2; Impad1, inositol monophosphatase domain-containing protein 1; GRAPP, Golgi-resident phosphoadenosine phosphate phosphatase; MIM, mendelian inheritance in man.*

β4-Galactosyltransferase-I (GalT-I) encoded by *B4GALT7*, then transfers a Gal residue from UDP-Gal to Xyl-*O*-serine in the core proteins (Almeida et al., 1999; Okajima et al., 1999). β3-Galactosyltransferase-II (GalT-II) encoded by *B3GALT6* transfers the second Gal residue from UDP-Gal to Gal-Xyl-*O*-serine (Bai et al., 2001). Thereafter, β3-glucuronyltransferase-I (GlcAT-I) encoded by *B3GAT3*, transfers a GlcA residue from UDP-GlcA to Gal-Gal-Xyl-*O*-serine (**Figure 2**; **Table 2**) (Kitagawa et al., 1998).

Several modifications occur such as 2-*O*-phosphorylation and 2-*O*-dephosphorylation of Xyl and Xyl-2-*O*-phosphate residues by Xyl kinase and Xyl-2-*O*-phosphate phosphatase encoded by *FAM20B* and *PXYLP1*, respectively (Koike et al., 2009; 2014). Furthermore, sulfation at the C6 position of the first Gal and at

**TABLE 2 |** Biosynthetic enzymes of the GAG-linkage region tetrasaccharide.

| Enzymes | Coding genes | mRNA accession no | Phenotypes of KO or mutant mouse | Human genetic disorders | MIM numbers | Refs. For knockout mouse |
|---|---|---|---|---|---|---|
| Xylosytransferase | *Xylt1* | NM_175645 | Reduced lengths of limb, humerus, femur, radius, ulna, tibia, and fibula, promotion of premature chondrocytes, and defect in endochondral ossification | Desbuquios dysplasia type 2; Short stature syndrome; Baratela-Scott syndrome | 615777<br>608124<br>300881 | Mis et al. (2014) |
| | *Xylt2* | NM_145828 | Liver abnormalities including biliary tract hyperplasia, liver fibrosis, and biliary cysts, as well as renal abnormalities including dilated tubules, intestinal fibrosis, increase of renal weight, and hydronephrosis. Reductions in size and number of adipocytes, glucose intolerance, insulin resistance, and an increase in serum triglycerides | Spondyloocular syndrome | 605822<br>608125 | Condac et al. (2007), Sivasami et al. (2019) |
| β4Galactosyltransferase-I | *B4galt7* | NM_001311137<br>NM_146045 | — | Ehlers-Danlos syndrome spondylodysplastic type 1; Ehlers-Danlos syndrome progeroid type 1; Ehlers-Danlos syndrome with a short stature and limb anomalies; Larsen of Reunion Island syndrome | 130070<br>604327 | — |
| β3Galactosyltransferase-II | *B3galt6* | NM_080445 | — | Ehlers-Danlos syndrome spondylodysplastic type 2; Ehlers-Danlos syndrome progeroid type 2; Spondyloepimetaphyseal dysplasia with joint laxity type 1 | 615349<br>615291<br>271640 | — |
| β3Glucuronyltransferase-I | *B3gat3* | NM_024256 | An embryonic lethality before 8-cell stage | Multiple joint dislocations, a short stature, craniofacial dysmorphism with or without congenital heart defects | 245600 | Izumikawa et al. (2010), (2014) |
| | | | | Larsen-like syndrome B3GAT3 type B3GAT3-related disorder with dislocation and congenital heart defects; B3GAT3-related disorder with cutis laxa and bone fragility; B3GAT3-related disorder with craniosynostosis and bone fragility; Pseudodiastrophic dysplasia | 606374<br>264180 | |
| Glycosaminoglycan xylosylkinase | *Fam20b* | NM_145413 | Underdifferentiation and overproliferation of chondrocytes, failure to initiate ossification on the popliteal side of the secondary ossification center, tongue elevation, micrognathia, microcephaly, suture widening, reduced mineralization in the calvaria, facial bones, and temporomandibular joint, death immediately after birth, marked intervertebral disc defects, and abnormal tooth development | Severe (lethal) neonatal short limb dysplasia with multiple dislocations | 611063 | Ma et al. (2016), Liu et al. (2018), Saiyin et al. (2019), Wu et al. (2020) |
| 2-Phosphoxylose phosphatase 1 | *Pxylp1* | NM_001289645<br>NM_001289646<br>NM_001289647<br>NM_153420 | — | — | — | — |

*—, not reported; B4galt7, beta 1,4-galactosyltransferase 7; B3galt6, beta 1,3-galactosyltransferase 6; B3gat3, beta 1,3-glucuronyltransferase 3; Fam20b, Family with sequence similarity 20 member B.*

**TABLE 3 |** Biosynthetic enzymes of CS and DS chains.

| Enzymes (transferase activity) | Coding genes | mRNA accession no | Phenotypes of KO or mutant mouse | Human genetic disorders | MIM number | Refs. For knockout or transgenic mouse |
|---|---|---|---|---|---|---|
| Chondroitin sulfate synthase (GalNAcT-II, CS-GlcAT-II) | *Chsy1* | NM_001081163 | Chondrodysplasia, progression of the bifurcation of digits, delayed endochondral ossification, reduced bone density, retinal stress, and decreased neutrophils in the bone marrow and spleen | Temtamy preaxial brachydactyly syndrome | 605282<br>608183 | Wilson et al., 2012), Macke et al. (2020) |
| | *Chsy3* | NM_001081328 | A short body length and intervertebral disc degeneration | — | 609963 | Wei et al. (2020) |
| Chondroitin polymerizing factor | *Chpf* | NM_001001565<br>NM_001001566 | No obvious abnormalities, and slightly reduced length of femur and tibia | — | 610405 | Ogawa et al. (2012) |
| | *Chpf2* | NM_133913 | Anomalies of the bone and heart | — | 608037 | Tang et al. (2010) |
| Chondroitin sulfate *N*-acetylgalactosaminyltransferase (GalNAcT-I, GalNAcT-II) | *Csgalnact1* | NM_001252623<br>NM_001364256<br>NM_172753 | A short body length and small body weight caused by shorter limbs and axial skeleton, and a thinner growth plate in cartilage, impaired intramembranous ossification, malocclusion, abnormal eyes, skin hyperextension, severe scoliosis, joint laxity, and promotion of axonal regeneration after the spinal cord injury | Skeletal dysplasia, mild, with joint laxity and advanced bone age | 616615 | Watanabe et al. (2010), Sato et al. (2011), Takeuchi et al. (2013), Yoshioka et al. (2017), Hou et al. (2017), Ida-Yonemochi et al. (2018), Inada et al. (2021) |
| | *Csgalnact2* | NM_172753<br>NM_030165 | Normal development, fertility, growth rates, and skeletal formation | — | 616616 | Shimbo et al. (2017) |
| Dermatan sulfate epimerase | *Dse* | NM_172508 | A smaller body weight, thicker collagen fibrils in the dermis and hypodermis, kinked tail, impairment of directional migration of aortic smooth muscle cells, defects in fetal abdominal wall, exencephaly, and spina bifida | Ehlers-Danlos syndrome musculocontractural type 2 | 615539<br>605942 | Maccarana et al. (2009), Gustafsson et al. (2014), Bartolini et al. (2013), Stachtea et al. (2015) |
| | *Dsel* | NM_001081316 | Normal extracellular matrix features | Bipolar disorder; Depressive disorder; Diaphragmatic hernia; Microphthalmia | 611125 | Bartolini et al. (2012), Stachtea et al. (2015) |
| Chondroitin 6-*O*-sulfotransferase | *Chst3* | NM_016803 | Decreased number of naive T-lymphocytes, hyperthickened *epidermis*, enhanced proliferation and altered differentiation of basal keratinocytes, few regenerating axons, and more axonal retraction after axotomy of nigrostriatal axons | Spondyloepiphyseal dysplasia with congenital joint dislocations; Spondyloepiphyseal dysplasia Omani type; Chondrodysplasia with multiple dislocations Megarbane type; Humerospinal dysostosis; Larsen syndrome autosomal recessive type; Desbuquois syndrome | 143095<br>603799 | Uchimura et al. (2002), Lin et al. (2011), Properzi et al. (2005), Miyata et al. (2012), Kitazawa et al. (2021) |

(Continued on following page)

**TABLE 3 |** (*Continued*) Biosynthetic enzymes of CS and DS chains.

| Enzymes (transferase activity) | Coding genes | mRNA accession no | Phenotypes of KO or mutant mouse | Human genetic disorders | MIM number | Refs. For knockout or transgenic mouse |
|---|---|---|---|---|---|---|
| Chondroitin 4-*O*-sulfotransferase | *Chst11* | NM_021439 | Severe dwarfism, multiple skeletal abnormalities including a small rib cage, a kinked vertebral column, severely shortened limbs, and a dome-shaped skull, reduction in Alcian blue staining in cartilage, and died within 6 h of birth with severe respiratory distress | Osteochondrodysplasia, brachydactyly, and overlapping malformed digits | 610128<br>618167 | Klüppel et al., 2005, Bian et al. (2011) |
| Dermatan 4-*O*-sulfotransferase | *Chst14* | NM_028117 | A smaller body mass, reduced fertility, kinked tail, increased skin fragility, disorganized collagen fibers, thoracic kyphosis, myopathy-related phenotypes including variation in fiber size and spread of the muscle interstitium, alterations in the vascular structure of the placenta, an abnormal structure of the basement membrane of capillaries in the placental villus, an increase of proliferation of Schwann cells, better recovery after femoral nerve injury, and a small number and large diameter of neurospheres | Ehlers-Danlos syndrome musculocontractural type 1; Ehlers-Danlos syndrome, type VIB; Adducted thumb-clubfoot syndrome | 601776<br>608429 | Bian et al. (2011), Akyüz et al. (2013), Yoshizawa et al. (2018), Hirose et al. (2021), Nitahara-Kasahara et al. (2021a) |
| *N*-Acetylgalactosamine-4-sulfate-6-*O*-sulfotransferase | *Chst15* | NM_001360768<br>NM_029935 | Weak staining of bone marrow-derived mast cells with May Grünwald-Giemsa, increase in empty granules in bone marrow-derived mast cells, lower activities of carboxypeptidase A and tryptase from bone marrow-derived mast cells, low bone mass, impairment of osteoblast differentiation, and enhanced liver fibrosis induced by $CCl_4$ | — | 608277 | Ohtake-Niimi et al. (2010), Koike et al., (2015), Habuchi et al. (2016), Nadanaka et al. (2020) |
| Uronyl 2-*O*-sulfotransferase | *Ust* | NM_177387 | — | Multiple congenital anomalies of the heart and central nervous system | 610752 | — |

—, *not reported; CHST, carbohydrate sulfotransferase.*

C4 or C6 of the second Gal residues has been identified (Sugahara and Kitagawa, 2000). Chondroitin 6-*O*-sulfotransferase 1 (C6ST1) encoded by *CHST3* transfers a sulfate group from PAPS to Gal residues on the linker region tetrasaccharide GlcA-Gal-Gal-Xyl *in vitro* (Kitagawa et al., 2008). These modifications affect the glycosyltransferase reactions of GalT-I, GlcAT-I, CSGALNACT1, and may regulate the formation of CS/DS chains (Gulberti et al., 2005; Tone et al., 2008; Izumikawa et al., 2015).

Initiation of the repeating disaccharide region in the CS chain, $[-4GlcA\beta1-3GalNAc\beta1-]_n$, is evoked by the transfer of

the first GalNAc residue from UDP-GalNAc to the GlcA residue in the linker region tetrasaccharide, GlcA-Gal-Gal-Xyl-*O*-, by β4-*N*-acetylgalactosaminyltransferase-I (GalNAcT-I) encoded by *CSGALNACT1* or *CSGALNACT2* (**Figure 2**; **Table 3**) (Uyama et al., 2002; 2003). Chain elongation of CS occurs by the alternative addition of GlcA and GalNAc residues by CS-β3-glucuronyltransferase-II (CS-GlcAT-II) and GalNAcT-II, respectively (**Figure 2**; **Table 3**) (Mikami and Kitagawa, 2013). Chondroitin synthase (CHSY) encoded by *CHSY1* or *CHSY3* has a dual enzymatic activity of both CS-GlcAT-II and GalNAcT-II, which may be exerted in N- and C-terminal domains, respectively (Kitagawa et al., 2001b; Izumikawa et al., 2007). Chondroitin-polymerizing factor (CHPF) encoded by *CHPF* or *CHPF2* is able to construct the repeating disaccharide region of CS by forming an enzyme complex with CHSY (Kitagawa et al., 2003; Izumikawa et al., 2008). CHPF2 has both CS-GlcAT-II and GalNAcT-II activities; thereby, CHPF2 was designated as CHSY (Izumikawa et al., 2008). After or during construction of the non-sulfated disaccharide region of CS, the chondroitin backbone, it is modified by sulfation by the respective sulfotransferase including uronyl 2-*O*-sulfotransferase (UST) encoded by *UST* (Kobayashi et al., 1999), chondroitin 4-*O*-sulfotransferase (C4ST) encoded by *CHST11*, *CHST12*, or *CHST13* (Hiraoka et al., 2000; Yamauchi et al., 2000; Kang et al., 2002), C6ST encoded by *CHST3* (Fukuta et al., 1995; 1998), and GalNAc 4-*O*-sulfate 6-*O*-sulfotransferase (GalNAc4S-6ST) encoded by *CHST15* (Ohtake et al., 2001) (**Figure 3**; **Table 3**).

Formation of the repeating disaccharide region, $[-4\text{IdoA}\beta1-3\text{GalNAc}\beta1-]_n$, of DS chains occurs by epimerization of the C5 position of GlcA residues in a chondroitin precursor backbone, which is catalyzed by DS-epimerase encoded by *DSE* or *DSEL* (**Figure 2**) (Maccarana et al., 2006; Pacheco et al., 2009). The dermatan chains are modified by sulfation catalyzed by UST and dermatan 4-*O*-sulfotransferase (D4ST) encoded by *UST* and *CHST14*, which transfer the sulfate from PAPS to the C2 position of IdoA and C4 position of GalNAc residues, respectively (Kobayashi et al., 1999; Evers et al., 2001; Mikami et al., 2003) (**Figure 3**; **Table 3**).

## Catabolism of Donor Substrates for CS/DS Biosynthesis

After glycosyltransferase reaction, the reaction product, UDP, derived from UDP-sugar is hydrolyzed into uridine 5′-monophosphate (UMP) by nucleoside 5′-diphosphatase, which is encoded by *calcium-activated nucleotidase 1* (*CANT1*), in the endoplasmic reticulum and Golgi apparatus (**Table 1**) (Failer et al., 2002; Smith et al., 2002). UMP is exported to the cytosol by nucleotide sugar transporters, which are antiporters for UDP-sugars and UMP, from the Golgi apparatus and/or endoplasmic reticulum (Parker and Newstead, 2019).

After the sulfotransferase reaction, the reaction product, adenosine-3′, 5′-bisphosphate (PAP), derived from PAPS is hydrolyzed into adenosine 5′-phosphate (5′-AMP) by the Golgi-resident PAP 3′-phosphatase, which is encoded by *3′(2′), 5′-bisphosphate nucleotidase 2* (*BPNT2*)*/inositol monophosphatase domain containing 1* (*IMPAD1*) (**Table 1**) (Frederick et al., 2008). The 5′-AMP may be exported to the cytosol by unidentified transporters from the Golgi apparatus and/or endoplasmic reticulum.

# KNOCKOUT AND MUTANT MICE OF BIOSYNTHETIC ENZYMES OF CS/DS AND ITS DONOR SUBSTRATES AS WELL AS NUCLEOTIDE SUGAR TRANSPORTERS

## Ugdh

UDP-Glc dehydrogenase (UGDH) is an oxidoreductase that converts UDP-Glc to UDP-GlcA in the cytosol (Spicer et al., 1998). The mutant mice *lazy mesoderm* have a mutation in *Ugdh*, which was introduced by ethyl-nitrosourea, and show a phenotype of embryogenesis arrest during gastrulation with defects in migration of the mesoderm and endoderm (García-García and Anderson, 2003). Furthermore, no CS or heparan sulfate (HS) were detected in the mutant using respective antibodies against them (García-García and Anderson, 2003). HS is also linear polysaccharide of GAG family, and composed of repeating disaccharide unit, $[-4\text{GlcA}\beta1-4\text{GlcNAc}\alpha1-]_n$, which is covalently attached to the specific core proteins, forming PGs (**Supplemental Figure S1**) (Kjellén and Lindahl, 1991). HS and HS-PGs play essential roles in signal transduction, tissue morphogenesis, early development, and tumor progression (Bishop et al., 2007). The disturbance of FGF signaling has been demonstrated in the *Ugdh* mutant, resulting in a similar phenotype to those of *Fgf8* and *Fgfr1* mutants (Yamaguchi et al., 1994; Sun et al., 1999). The interaction of not only HS but also CS with FGFs and their receptors has been shown to be required for signal transduction (Esko and Selleck, 2002; Bishop et al., 2007; Mizumoto et al., 2015). Thus, the phenotype of the *Ugdh* mutant might be caused by defects in HS and/or CS.

## Papss2

PAPS synthase (PAPSS) is a dual enzyme with both adenosine 5′-phosphosulfate kinase and ATP sulfurylase activities, catalyzed by its N- and C-terminal domains, respectively (Fuda et al., 2002; Venkatachalam, 2003). The *Papss2* mutant, brachymorphic mouse, which is generated by *N*-ethyl-*N*-nitrosourea, and has the substitution Gly79Arg, shows a normal life span, a dome-shaped skull, and reductions in limb as well as axial skeletons, thereby leading to brachymorphism (Schwartz et al., 1978; Sugahara and Schwartz, 1979, 1982a, 1982b; Pennypacker et al., 1981). Moreover, the mutant mice produce lower sulfated CS but not HS in the growth plate cartilage, and show disturbed Indian hedgehog signaling due to abnormal distribution in the extracellular matrix, which results in a reduction in chondrocyte proliferation (Orkin et al., 1976; Cortes et al., 2009). These findings suggest that the sulfation in CS side chains of PG(s), such as aggrecan, modulates Indian hedgehog signaling.

### Slc26a2

The sulfate transporter is encoded by *SLC26A2*, which incorporates a sulfate anion into the cytosol at the plasma membrane (Hästbacka et al., 1994; Satoh et al., 1998; Seidler and Nikolovska, 2019). The incorporated sulfate is activated to adenosine-phosphosulfate and then to PAPS by PAPS synthase (Venkatachalam, 2003). An *Slc26a2* knock-in mouse with an Ala386Val substitution in the eighth transmembrane domain of *Slc26a2*, whose mutation was detected in a patient with diastrophic dysplasia characterized by a short stature, cleft plate, and deformity of the external ear and thumb (Rossi and Superti-Furga, 2001), was characterized by growth retardation, joint contracture, and skeletal dysplasia including an irregular size of chondrocytes, delay in the formation of the secondary osscification center and osteoporosis of long bones, severe thoracic kyphosis, bite overclosure, and hip dysplasia with pelvic deformity (Forlino et al., 2005). Furthermore, the proportion of a non-sulfated disaccharide unit, GlcA-GalNAc, was higher than that of the wild-type in cartilage and bone, but not skin (Forlino et al., 2005). These findings suggest that abnormalities of proliferation and differentiation of chondrocytes contribute to reduced bone growth, and lead to similar phenotypes to probands of human diastrophic dysplasia. Thus, this mutant mouse is a useful model to explore the pathogenic and therapeutic approaches for human diastrophic dysplasia.

### Slc35d1

UDP-GlcA/UDP-GalNAc dual transporter encoded by solute carrier family 35 member D1 (*SLC35D1*) incorporates both UDP-GlcA and UDP-GalNAc from the cytosol into endoplasmic reticulum (Muraoka et al., 2001). The *Slc35d1*-deficient mouse showed a lethal form of skeletal dysplasia associated with severe shortening of limbs, abnormal facial structures, a decreased proliferating zone with round chondrocytes, scarce matrices, and reduced CS but not HS in long bones (Hiraoka et al., 2007). Furthermore, schneckenbecken dysplasia characterized by perinatally lethal skeletal dysplasia is caused by mutations in *SLC35D1* (Hiraoka et al., 2007). These findings indicate that CS chains and/or CS-PGs are indispensable for early embryonic as well as skeletal development, and that the mutant mouse can be utilized to explore the pathogenic and therapeutic approaches for human schneckenbecken dysplasia.

## KNOCKOUT AND MUTANT MICE OF BIOSYNTHETIC ENZYMES FOR CS/DS BACKBONES

### Xylt1 and Xylt2

XYLT1 encoded by *XYLT1* transfers Xyl to specific serine residues in core proteins of PGs from UDP-Xyl as a donor substrate in the Golgi apparatus (**Figure 2**) (Götting et al., 2000; Schön et al., 2006; Pönighaus et al., 2007). The *Xylt1* mutant *pug*, which is generated by *N*-ethyl-*N*-nitrosourea, and has the substitution Trp932Arg, showed lower XYLT activity in chondrocytes from the mutant than the wild-types, thereby decreasing the production of GAGs in cartilage (Mis et al., 2014). It should be noted that a defect in XYLT1 may affect the biosyntheses of not only CS/DS but also HS, because the linker region tetrasaccharide GlcA-Gal-Gal-Xyl- is common to CS, DS, and HS (**Supplemental Figure S1**). Moreover, *pug* mutants showed phenotypes including reduced limb, humerus, femur, radius, ulna, tibia, and fibula lengths, and the normal proliferation as well as promotion of premature maturation of chondrocytes, which suggests a general defect in endochondral ossification, resulting in dwarfism. These skeletal abnormalities may be caused by an up-regulation of Indian hedgehog signaling but not FGF signaling (Mis et al., 2014). In fact, mutations in human *XYLT1* cause Desbuquois dysplasia type 2 characterized by severe pre- and postnatal growth retardation, a short stature, joint laxity, and the dislocation of large joints (Bui et al., 2014). Thus, the *pug* mutant mouse is available to help understand the pathogenic mechanism and development of treatment for human Desbuquois dysplasia type 2.

XYLT2 encoded by *XYLT2* also transfers Xyl to specific serine residues in core proteins of PGs from UDP-Xyl as a donor substrate in the Golgi apparatus (Götting et al., 2000; Schön et al., 2006; Pönighaus et al., 2007). The *Xylt2*-deficient mouse exhibited liver abnormalities including biliary tract hyperplasia, liver fibrosis, and biliary cysts, as well as renal abnormalities including dilated tubules, intestinal fibrosis, increase of the renal weight, and hydronephrosis (Condac et al., 2007). Furthermore, it was demonstrated that there is an 86% reduction in HS disaccharides from the liver of *Xylt2*-deficient mice compared with wild-type mice, and a lack of the GAG side chain of decorin, which is a DSPG, in both the liver and kidney of *Xylt2*-deficient mice. The defect in XYLT2 may affect the biosyntheses of not only CS/DS but also HS, because the linker region tetrasaccharide, GlcA-Gal-Gal-Xyl-, is common to CS, DS, and HS (**Supplemental Figure S1**). However, normal levels of renal CS as well as HS in *Xylt2*-deficient mice were detedcted (Condac et al., 2007). These findings suggest that the residual HS observed in liver from *Xylt2*-deficient mice may be sufficient for hepatocellular differentiation as well as proliferation, but not maturation, and that renal development requires decorin, the DS side chain, or other DSPGs. Homozygous mutations in *XYLT2* cause spondyloocular syndrome that is characterized by retinal detachment, amblyopia, nystagmus, hearing loss, heart septal defects, bone fragility, and mild learning difficulties (Munns et al., 2015). However, patients with predicted null mutations in *XYLT2* did not show polycystic disease. Hence, XYLT1 may compensate for the loss-of-function mutation of XYLT2 in the human liver as well as kidney.

The *Xylt2*-deficient mouse also showed reductions in the size and number of adipocytes, glucose intolerance, and insulin resistance, as well as an increase in serum triglycerides as compared with wild-type mice (Sivasami et al., 2019). Moreover, elevations of interleukin-6 and interleukin-1β, which are proinflammatory M1 cytokines, and the upregulation of TGFβ signaling that inhibits adipogenesis in preadipocyte cells, result in the inflammation of adipose tissues. It was demonstrated that adipose-derived stem cells

showed impaired adipogenic differentiation in *Xylt2*-deficient mice, and that maturation of endothelium from gonadal fat tissue was reduced, thereby increasing adipogenic precursors. These findings suggest that the GAG decrease caused by a defect in XYLT2 leads to reduced steady state adipose tissue stores, which is a unique lipodystrophic model.

## Fam20b

Xyl 2-*O*-kinase encoded by *FAM20B* transfers a phosphate group to the Xyl residue in the linkage region from ATP as a donor substrate in the Golgi apparatus (Koike et al., 2009). Conditional knockout (cKO) of *Fam20b* (*Osr2-Cre;Fam20B*$^{flox/flox}$) in the joint cartilage, palate mesenchyme, and metanephric mesenchyme-derived glomeruli tissues, showed that chondrocytes overproliferated but underdifferentiated, and failed to initiate ossification on the popliteal side of the secondary ossification center (Ma et al., 2016). Furthermore, the gain-of-functions of bone morphogenetic protein (BMP) as well as WNT, and the down-regulation of Indian hedgehog, which coordinates chondrocyte proliferation and maturation, were detected in the cartilage of *Fam20b* cKO (Ma et al., 2016). These phenotypes lead to chondrosarcoma in the knee joint and marked defects of postnatal ossification in long bones. However, no significant changes in FGF and TGF-β signaling in *Fam20b* cKO mice were detected. Taken together, the FAM20B-catalyzed PGs are essential for chondrocyte differentiation and maturation, as well as subsequent ossification.

*Wnt1-Cre;Fam20b*$^{flox/flox}$ cKO mice, which were deficient in *Fam20b* in the neural crest and midbrain, died immediately after birth due to complete cleft palates (Liu et al., 2018). Moreover, the *Fam20b* cKO mice showed tongue elevation, micrognathia, microcephaly, suture widening, and reduced mineralization in the calvaria, facial bones, and temporomandibular joint (Liu et al., 2018). These findings suggest that GAG side chains of PGs formed by catalysis of FAM20B are necessary for the morphogenesis and mineralization of the craniofacial complex.

*Col1a1-Cre;Fam20B*$^{flox/flox}$ cKO mice, which were deficient in *Fam20b* in osteoblasts, showed apparent postnatal growth retardation, a shorter tail and spine, and the spinal curvature, resulting in severe kyphosis (Saiyin et al., 2019). Furthermore, *Fam20B* cKO mice showed marked intervertebral disc defects associated with malformation of the peripheral annulus fibrosus, which resulted from the fibrosus tissue transforming to cartilage-like tissue. Not only CS but also HS were reduced in the annulus fibrosus from *Fam20B* cKO mice. TGF-β signaling required for the development and maintenance of the annulus fibrosus and intervertebral disc, was not activated in *Fam20B* cKO mice. MAPK signaling was also modified in cKO mice, *i.e.*, increases in phospho-P38 and phospho-ERK but decreases in phospho-JNK (Saiyin et al., 2019). These findings indicate that FAM20B-mediated PGs may play an essential role in annulus fibrosus development through regulating TGF-β and MAPK signaling pathways.

*K14-Cre;Fam20B*$^{flox/flox}$ cKO mice, which were deficient in *Fam20b* in the dental epithelium, showed supernumerary tooth formation. Reductions in CS and HS in the dental epithelium attenuated FGFR2b as well as WNT signalings in the initial stage and later cap stage, respectively, of tooth development (Wu et al., 2020). These findings suggest that FAM20B-catalyzed GAG biosynthesis on PGs regulates the number of murine teeth through FGFR2b signaling in the initial stage of tooth development.

## B3gat3

GlcAT-I encoded by *B3GAT3* transfers the 4th sugar residue in the linker region tetrasaccharide GlcA-Gal-Gal-Xyl from UDP-GlcA to Gal-Gal-Xyl-*O*-serine (**Figure 2**) (Kitagawa et al., 1998). The *B3gat3*-deficient mice showed embryonic lethality before the 8-cell stage due to the failure of cytokinesis (Izumikawa et al., 2010). Moreover, neither CS nor HS was detected in blastocysts from *B3gat3*-deficient mice (Izumikawa et al., 2010). The defect in B3GAT3 may affect the biosynthesis of not only CS/DS but also HS, because the linker region tetrasaccharide GlcA-Gal-Gal-Xyl- is common to CS, DS, and HS (**Supplemental Figure S1**). Interestingly, treatment of 2-cell embryos with chondroitinase, which is a bacterial eliminase acting specifically on CS, resulted in embryonic lethality between 2- and 8-cell stages, but treatment with heparitinase, a bacterial eliminase acting specifically on HS, showed no lethality (Izumikawa et al., 2010). *Ext1*- or *Ext2*-deficient mice that lack HS developed normally until embryonic day 6.5 (Lin et al., 2000; Stickens et al., 2005). EXT1 and EXT2 have both HS-GlcAT-II and α-1,4*N*-acetylglucosaminyltransferase-II activities, which are required for biosynthesis of HS chains (Lind et al., 1998; McCormick et al., 1998) (**Supplemental Figure S1**). *Caenorhabditis elegans* synthesizes chondroitin, non-sulfated CS, which is required for normal cell division and cytokinesis in an early developmental stage (Mizuguchi et al., 2003; Izumikawa et al., 2004). These findings suggest that abnormal cytokinesis in *B3gat3*-deficient mice may be attributed to deficiency in CS, but not HS.

Embryonic stem cells derived from *B3gat3*-deficient mice completely lost both CS and HS, and failed to differentiate into multiple lineages (Izumikawa et al., 2014). Degradation of CS on wild-type embryonic stem cells by treatment with chondroitinase had effects on the formation of embryonic bodies, which is *in vitro* differentiation by free-floating aggregates of the embryonic stem cells, whereas treatment with heparitinase showed no effects on the development of embryonic bodies. Furthermore, the exogeneous addition of CS-A or CS-E polysaccharides to embryonic bodies derived from *B3gat3*-deficient mice rescued the differentiation of these cells into primitive endodermal cells in a culture assay (Izumikawa et al., 2014). The interaction of CS with E-cadherin regulates the Rho signaling pathway, which leads to the control of differentiation of embryonic stem cells (Izumikawa et al., 2014). These findings suggest that CS contributes to the integrity of embryonic stem cells via interaction with E-cadherin.

## Csgalnact1 and Csgalnact2

*N*-Acetylgalactosaminyltransferase (GalNAcT) encoded by *CSGALNACT1* or *CSGALNACT2* transfers a GalNAc residue from UDP-GalNAc to GlcA-Gal-Gal-Xyl-*O*-serine and [GlcA-

GalNAc]$_n$ (**Figure 2**) (Uyama et al., 2002; 2003). *Csgalnact1*-deficient mice showed a short body length and small body weight, caused by shortening of the limbs and axial skeleton, and a thinner growth plate in cartilage than wild-type mice (Watanabe et al., 2010; Sato et al., 2011). The level of CS disaccharides in the cartilage from the *Csgalnact1*-deficient mice was reduced to half of that in the wild-type (Watanabe et al., 2010; Sato et al., 2011). These findings indicate that CSGALNACT1 and/or CS-PG is necessary for the differentiation and maturation of cartilage.

*Csgalnact1*-deficient mice also showed impaired intramembranous ossification, resulting in a shorter face, and higher and broader calvaria (Ida-Yonemochi et al., 2018). Protein levels of Wnt3a and β-catenin were decreased in the mesenchymal tissues of calvaria, and collagen fibers were irregular, thick, and aggregated in the calvaria and scalp from *Csgalnact1*-deficient mice, which causes skull abnormalities (Ida-Yonemochi et al., 2018). Furthermore, *Csgalnact1*-deficient mice were characterized by malocclusion, abnormal eyes, skin hyperextension, severe scoliosis, joint laxity, and reduction of CS in skin, muscle, tendon, and bone, which are similar to the hallmarks of Ehlers-Danlos syndrome in humans. Loss of CSGALNACT1 may cause disturbance of DS biosynthesis, because chondroitin is a precursor for DS. Musculocontractural Ehlers-Danlos syndrome is caused by a defect in DS (Malfait et al., 2017; 2020).

*Csgalnact1*-deficient mice showed better recovery after spinal cord injury than wild-type mice, based on a footfall test, footprint test, and electromyography, because of the promotion of axonal regeneration (Takeuchi et al., 2013). On the other hand, *Csgalnact2*-deficient mice have not been demonstrated to show such promotional activity. After spinal cord injury, the biosynthesis of CS is promoted and resultant CS inhibits axonal regeneration as a barrier-forming molecule (Carulli et al., 2005). However, the promotion of CS biosynthesis is lower in *Csgalnact1*-deficient mice than in wild-type mice (Takeuchi et al., 2013). Interestingly, an increase of HS was detected in association with up-regulations of *Ext1*, *Ext2*, and *Extl3* mRNAs that encode glycosyltransferases responsible for HS biosynthesis (Takeuchi et al., 2013). HS has been reported to promote axonal growth and regulate axon guidance (Yamaguchi, 2001). Thus, the decrease and increase of CS and HS, respectively, in *Csgalnact1*-deficient mice resulted in better recovery from spinal cord injury than in wild-type mice.

CS-PG is a major component in perineuronal nets, which are unique extracellular matrix structures that wrap around neurons during development and control plasticity in the central nervous system (Sorg et al., 2016). *Csgalnact1*-deficient mice showed a significant decrease in CS in the cerebrum, diencephalon, spinal cord, and visual cortex (Yoshioka et al., 2017). Furthermore, *Csgalnact1*-deficient mice showed a significantly greater total distance traveled than wild-type mice in the open field test, which measures voluntary activity in a novel environment. *Csgalnact1*-deficient mice manifested much larger responses than wild-type mice in an acoustic startle test, which can measure reflex movement in response to a sudden loud sound stimulus (Yoshioka et al., 2017). These findings suggest that CS generated by CSGALNACT1 may affect the formation of perineuronal nets as well as behaviors of mice.

*Csgalnact1*-deficient mice were characterized by a reduction in CS in the visual cortical area and impaired ocular plasticity, which is caused by a decrease of Otx2 accumulation (Hou et al., 2017). CS binds to Otx2 in perineuronal nets, and promotes uptake of Otx2 into parvalbumin-expressing basket cells, thereby terminating the critical period for plasticity (Miyata and Kitagawa, 2015). These findings indicate that CS and CS-PGs are required for the critical period for plasticity in the visual cortex.

*Csgalnact1*-deficient mice with experimentally induced autoimmune encephalomyelitis showed milder symptoms including lower cell infiltration, proliferation, and productions of interleukin-6 and interferon-$\gamma$ than those in the wild-type (Inada et al., 2021). These findings suggest that CS side chains of PGs may be associated with autoimmune encephalomyelitis and potential therapeutic targets for neuroimmunological diseases.

*Csgalnact2*-deficient mice exhibited normal development, fertility, growth rates, and skeletal formation (Shimbo et al., 2017). These findings suggest that loss of functions of CSGALNACT2 might be compensated for by CSGALNACT1.

Mice with double KO of *Csgalnact1* and *Csgalnact2* died during the postnatal stage due to respiratory failure (Shimbo et al., 2017). Furthermore, the double KO mice exhibited severer phenotypes including short humeral and tibial lengths compared with *Csgalnact1*-or *Csgalnact2*-deficient mice. The total CS disaccharides in rib cartilage from *Csgalnact1*-KO, *Csgalnact2*-KO, and double KO mice were reduced to ~74, ~99, and ~40%, compared with that of the wild-type, respectively (Shimbo et al., 2017).

Approximately 80% of *Col2a1-Cre; Csgalnact1$^{flox/-}$; Csgalnact2$^{flox/-}$* double cKO mice, which were deficient in both *Csgalnact1* and *Csgalnact2* in chondrocytes, immediately died after birth because of respiratory failure, and the remaining ~20% of the double KO mice could start spontaneous respiration (Shimbo et al., 2017). They were characterized by a lower body weight, severer dwarfism, and lower proliferation of chondrocytes than control mice.

These data indicate that CS synthesized by CSGALNACT1 and CSGALNACT2, may be required for pulmonary and skeletal development during embryogenesis.

## Chsy1

GalNAcT-II and glucuronyltransferase-II (GlcAT-II) encoded by *CHSY1* transfer GalNAc and GlcA residues from UDP-GalNAc and UDP-GlcA to [GlcA-GalNAc]$_n$ or [GalNAc-GlcA]$_n$, respectively (**Figure 2**) (Kitagawa et al., 2001b). *Chsy1*-deficient mice were characterized by chondrodysplasia, progression of the bifurcation of digits, delayed endochondral ossification, and reduced bone density (Wilson et al., 2012). Furthermore, a decrease in 4-*O*-sulfation and increases in 6-*O*-sulfation as well as non-sulfated GalNAc residues were detected in the cartilage of *Chsy1*-deficient mice. The up-regulation of transcriptional target of Hedgehog, *Gli1*, was detected in embryonic

fibroblast cultures from *Chsy1*-deficient mice (Wilson et al., 2012). Moreover, a brachymorphic mouse with mutation in *Papss2* also showed low sulfated CS in the cartilage, and its Hedgehog signaling was attenuated (Orkin et al., 1976; Cortes et al., 2009). These findings indicate that CS and Hedgehog protein may coordinately modulate bone development.

Small with kinky tail (*skt*) mutant mice spontaneously arose at the Jackcon Laboratory with recessive mutation (Lane, 1988). The *skt* mutant was caused by a 27-kb deletion containing *Chsy1* (Macke et al., 2020). The *skt* mutant mice showed reduced CS in the retina as well as hippocampus compared with heterozygous deficient mice, an increase in a number of empty spaces surrounding cells in the cornu ammonis 1, 2, and 3 hippocampal subfields compared with control mice, decreased neutrophils in bone marrow as well as macrophages in both the bone marrow and spleen, and age-dependent retinal changes including progressive photoreceptor cell degeneration with an increase of glial fibrillary acidic protein, considered to be a sign of retinal stress (Macke et al., 2020). In contrast, frequencies of monocytic cells and lymphocytic cells such as T-cells, B-cells, and natural killer cells, did not appear to be consistently altered in the *skt* mutant mice compared with heterozygous controls. These findings suggest that CS constructed by CHSY1 regulates the development of the hippocampus, retina, neutrophils, and macrophages.

## Chsy3

CHSY3 also has a dual enzymatic activity with β1,3-GlcA transferase and β1,4-GalNAc transferase on its amino- and carboxy-terminal sides, respectively (Yada et al., 2003a; Izumikawa et al., 2007). *Chsy3*-deficient mice showed a shorter body length than the wild-type after 4 weeks old, a reduction of CS in disc tissues, and intervertebral disc degeneration such as a narrowed disc height, loss of the nucleus pulposus, and unclear demarcation between the nucleus pulposus and annulus fibrosus (Wei et al., 2020). Furthermore, the Hippo signaling pathway, which is regulated by a kinase of the Sterile-20 family and activates the suppressor Warts (Zheng and Pan, 2019), was significantly downregulated. The activation of Yap1, which is a transcriptional coactivator as well as a negative regulator of the Hippo pathway, and is involved in intervertebral disc degeneration (Chen et al., 2019), was mainly affected in nucleus pulposus cells from *Chsy3*-deficient mice (Wei et al., 2020). These findings suggest that CS activates Yap signaling and spontaneous intervertebral disc degeneration.

## Chpf

Chondroitin polymerizing factor encoded by *CHPF* exhibits an enzymatic activity to polymerize the disaccharide region of CS in concert with CHSY1 *in vitro* (Kitagawa et al., 2003). Since CHPF has a dual enzymatic activity of β1,3-GlcA transferase and β1,4-GalNAc transferase, it was also designated as CHSY2 (Yada et al., 2003b). Although *Chpf*-deficient mice showed no obvious abnormalities, the femur and tibia lengths were slightly reduced, and the chain length of CS was shorter in cartilage than in wild-type mice (Ogawa et al., 2012). These findings indicate that other CHSY family proteins, CHPF2, CHSY1, and/or CHSY3, might compensate for the activity of CHPF.

## Chpf2

CHPF2 also has a dual enzymatic activity of β1,3-GlcA transferase and β1,4-GalNAc transferase, and has been designated as CHSY3 or CSGlcA-T (Gotoh et al., 2002; Izumikawa et al., 2008). *Chpf2*-deficient mice have been registered in the knockout mouse library, and their anomalies in the bone and heart were reported without detailed analyses (Tang et al., 2010). Further investigation is required for elucidation of the *in vivo* function of CHPF2.

## Chst3

C6ST1 encoded by *carbohydrate sulfotransferase 3* (*CHST3*) transfers a sulfate group from PAPS to the C-6 hydroxy group of GalNAc residues in the CS repeating disaccharide region, $[GlcA\text{-}GalNAc]_n$ (**Figure 3**) (Fukuta et al., 1995, 1998; Uchimura et al., 1998). *Chst3*-deficient mice showed a loss of 6-*O*-sulfated disaccharide units such as the C-unit, GlcA–GalNAc(6-*O*-sulfate), and D-unit, GlcA(2-*O*-sulfate)–GalNAc(6-*O*-sulfate), in the spleen, cartilage, and brain (Uchimura et al., 2002), although brain development seems to be normal in *Chst3*-deficient mice. *Chst3* was not expressed in the thymus (Uchimura et al., 1998), where naive T-cells differentiate, and the proportion of $CD4^+/CD8^-$ and $CD4^-/CD8^+$ cells in the thymus from *Chst3*-deficient mice did not change (Uchimura et al., 2002). However, the number of naive T-lymphocytes decreased (Uchimura et al., 2002). These findings indicate that survival, retention, and/or emigration of naive T lymphocytes was affected in the spleen of the *Chst3*-deficient mice, rather than that of thymocytes.

After axotomy of nigrostriatal axons, *Chst3*-deficient mice exhibited fewer regenerating axons and more axonal retraction than wild-type mice (Lin et al., 2011), although repair of the median and ulnar nerves was similar between wild-type and *Chst3*-deficient mice after peripheral nerve injury. Increases in the expression of *Chst3* and proportion of the 6-*O*-sulfated structure have been demonstrated in glial scars after cortical injury (Properzi et al., 2005). These findings suggest that the suppression of 6-*O*-sulfation in CS after injury of the central nervous system prevents axons to regenerate.

*Chst3*-transgenic mice with an increase in 6-*O*-sulfation of the brain CS showed loss of perineuronal nets in the brain, leading to the continuance of the critical period for cortical plasticity (Miyata et al., 2012). Furthermore, Otx2, which is a homeoprotein and regulates ocular dominance plasticity via its effects on maturation of parvalbumin-expressing interneurons (Sugiyama et al., 2008), diffused and reduced at the surrounding parvalbumin-expressing interneurons in *Chst3*-transgenic mice (Miyata et al., 2012). These findings indicate that 6-*O*-sulfation of CS at perineuronal nets in the brain regulates the critical period for cortical plasticity by maturation of parvalbumin-expressing interneurons.

*Chst3*-deficient mice presented with a hyperthickened epidermis, enhanced proliferation, and altered differentiation of basal keratinocytes, thereby impairing the epidermal

permeability barrier function (Kitazawa et al., 2021). Furthermore, the 6-*O*-sulfated CS directly binds to epidermal growth factor receptor (EGFR), leading to the blockade of EGFR signaling (Kitazawa et al., 2021). The *Chst3*-deficient mice had a thicker epidermis and increased levels of acute inflammation including erythema, scaling, and skin induration, compared with wild-type mice when psoriasis was induced by imiquimod (Kitazawa et al., 2021). These findings indicate that the 6-*O*-sulfated CS repress proliferation of keratinocytes and progression of psoriasis in the skin.

## Chst11

C4ST1 encoded by *carbohydrate sulfotransferase 11* (*CHST11*) transfers a sulfate group from PAPS to the C-4 hydroxy group of GalNAc residues in the CS repeating disaccharide region, $[GlcA\text{-}GalNAc]_n$ (**Figure 3**) (Hiraoka et al., 2000; Yamauchi et al., 2000). *Chst11*-deficient mice showed a more than 90% reduction of the 4-*O*-sulfated disaccharide unit in the growth plate compared with the wild-type (Klüppel et al., 2005). Furthermore, they exhibited severe dwarfism, multiple skeletal abnormalities including a small rib cage, a kinked vertebral column, severely shortened limbs, a dome-shaped skull, reduction in Alcian blue staining in cartilage, and fatality within 6 h of birth with severe respiratory distress (Klüppel et al., 2005). In the *Chst11*-deficient embryos, chondrocyte differentiation was affected during morphogenesis of the cartilage growth plate because of upregulation of TGFβ signaling with concomitant downregulation of BMP signaling, but not Indian hedgehog signaling (Klüppel et al., 2005), although mesenchymal aggregation and cartilage primordium formation were normal. These findings suggest that CS 4-*O*-sulfation and C4ST1 are required for embryonic development and morphogenesis of the cartilage growth plate by modulation of signaling pathways.

## Chst15

GalNAc4S-6ST encoded by *carbohydrate sulfotransferase 15* (*CHST15*) transfers a sulfate group from PAPS to the C-6 hydroxy group of GalNAc4-*O*-sulfate residues in the CS repeating disaccharide region, $[GlcA\text{-}GalNAc(4\text{-}O\text{-}sulfate)]_n$ (**Figure 3**) (Ohtake et al., 2001). *Chst15*-deficient mice showed complete loss of GalNAc 4- and 6-*O*-disulfated structure (E-unit) in CS/DS from the tissues examined, including the cerebrum, cerebellum, heart, lung, liver, spleen, kidney, thymus, stomach, small intestine, large intestine, mesentery, testis, whole embryo, and bone marrow-derived mast cells, suggesting that GalNAc4S-6ST encoded by *Chst15* is the sole enzyme responsible for the biosynthesis of GalNAc 4- and 6-*O*-disulfated structure (Ohtake-Niimi et al., 2010). Furthermore, *Chst15*-deficient mice were fertile, showed normal development, exhibited weak staining of bone marrow-derived mast cells with May Grünwald-Giemsa, showed an increase of empty granules in bone marrow-derived mast cells, and presented lower activities of carboxypeptidase A as well as tryptase from bone marrow-derived mast cells (Ohtake-Niimi et al., 2010). These findings suggest that GalNAc 4- and 6-*O*-disulfated structure in CS/DS-PGs may be involved in the storage of these proteases in the granules of mast cells.

*Chst15*-deficient mice also exhibited impairment of osteoblast differentiation leading to be low bone mass (Koike et al., 2015). Liver fibrosis induced by $CCl_4$ was enhanced in these mice (Habuchi et al., 2016). These findings indicate that GalNAc4S-6ST and/or E-disaccharide unit-containing CS, [GlcA-GalNAc(4-, 6-*O*-disulfates)], may be a therapeutic target for osteopenia, osteoporosis, and fibrosis. However, GalNAc 4- and 6-*O*-disulfated structure was not necessary for binding with semaphoring 3A in the perineuronal nets of brain (Nadanaka et al., 2020).

## Dse and Dsel

DS-epimerase encoded by *DSE* or *DSEL* converts GlcA into IdoA by C5-epimerization of GlcA residues in the CS repeating disaccharide region, $[GlcA\text{-}GalNAc]_n$ (**Figure 2**) (Maccarana et al., 2006; Pacheco et al., 2009). *Dse*-deficient mice exhibited a smaller body weight, reductions in IdoA-containing structures in the skin, thicker collagen fibrils in the dermis and hypodermis, kinked tails, impairment of directional migration of aortic smooth muscle cells, and defects in the fetal abdominal wall, exencephaly, and spina bifida (Maccarana et al., 2009; Bartolini et al., 2013; Gustafsson et al., 2014). Dse and/or DS may be indispensable for normal development and formation of collagen fibrils.

*Dsel*-deficient mice had no anatomical, histological, or morphological abnormalities (Bartolini et al., 2012). Furthermore, *Dsel*-deficient mice exhibited reduced epimerase activity in the skin (24% reduction), lung (34%), liver (38%), spleen (44%), kidney (55%), and brain (89%) compared with those in the wild-type mouse tissues (Bartolini et al., 2012). Consistent with this result, IdoA contents of CS/DS chains from the neonatal brain and kidney were reduced to 87 and 62% of wild-type mice, respectively (Bartolini et al., 2012). Brain from *Dsel*-deficient mice showed normal extracellular matrix features by immunohistological staining. DSE may compensate for the function of DSEL.

Double knockout mice of *Dse* and *Dsel* exhibited perinatal lethality with an umbilical hernia, exencephaly, a kinked tail, and complete loss of DS, suggesting that DS plays an important role in embryonic development as well as perinatal survival (Stachtea et al., 2015).

## Chst14

D4ST1 encoded by *carbohydrate sulfotransferase 14* (*CHST14*) transfers a sulfate group from PAPS to the C-4 hydroxy group of GalNAc residues in the repeating disaccharide region of DS, $[IdoA\text{-}GalNAc]_n$ (**Figure 3**) (Evers et al., 2001; Mikami et al., 2003). *Chst14*-deficient mice showed a smaller body mass, reduced fertility, kinked tail, and increased skin fragility compared with wild-type littermates (Akyüz et al., 2013). Moreover, in *Chst14*-deficient mouse skin, the amount of DS was markedly decreased with elevation of the level of CS, which is a precursor chain of DS. These phenotypes of *Chst14*-deficient mice were considerably similar to those of *Dse*-deficient mice (Maccarana et al., 2006). In addition to both enzymes involving the biosynthesis of DS, it has been reported that 4-*O*-sulfated GalNAc residues in DS chains prevent back-epimerization by

DSE *in vitro* (Malmström, 1984). Furthermore, DSE and CHST14 forms heterocomplex, but not DSEL, which is necessary to build longer IdoA-containing chains (Tykesson et al., 2018). Therefore, the cooperation of both enzymes by heterocomplex is required for the formation of repeating disaccharide, [GalNAc(4S)–IdoA], in DS.

Its skin tensile strength was significantly decreased compared with that in wild-type mice, and the collagen fibrils were oriented in various directions to form disorganized collagen fibers in the reticular layer (Hirose et al., 2021). Rod-shaped linear GAG chains were found to be attached at one end to collagen fibrils and protruded outside of the fibrils in the *Chst14*-deficient mice, in contrast to those being round and wrapping the collagen fibrils in wild-type mice (Hirose et al., 2021). These findings suggest that the DS side chain of decorin is necessary for assembly of decorin-PG with collagen, and maintenance of the skin strength.

CRISPR/Cas9-genome engineered *Chst14*-deficient mice exhibited common growth impairment and skin fragility similar to the conventional knockout mice of *Chst14* (Nitahara-Kasahara et al., 2021a). In addition, CRISPR/Cas9-genome engineered *Chst14*-deficient mice showed decreased DS in muscle, thoracic kyphosis, and myopathy-related phenotypes including variation in fiber size and spread of the muscle interstitium, as well as diffuse localization of decorin in the spread endomysium of skeletal muscle, which caused the lower grip strength and decreased exercise capacity, compared with wild-type and heterozygous mutant mice (Nitahara-Kasahara et al., 2021a; 2021b). The CRISPR/Cas9-engineered *Chst14*-mutant mouse is a useful model for musculocontractural Ehlers-Danlos syndrome caused by mutations in CHST14 (Dündar et al., 2009; Malfait et al., 2010; Miyake et al., 2010; Voermans et al., 2012; Kosho et al., 2019; Malfait et al., 2020).

*Chst14*-deficient mice are sometimes perinatally lethal (Yoshizawa et al., 2018). Their placenta showed immaturity such as a reduced weight of the placenta, alteration in the vascular structure with ischemic and/or necrotic-like change, an abnormal structure of the basement membrane of capillaries in the placental villus, and significantly decreased DS (Yoshizawa et al., 2018). These findings suggest that DS may be essential for placental vascular development.

Cultured Schwann cells from dorsal roots and nerves, cerebellar neurons, and motoneurons of *Chst14*-deficient mice exhibited longer cell processes compared with those from wild-type cells (Akyüz et al., 2013). Schwann cells from *Chst14*-deficient mice had a higher proliferation rate. Moreover, the values for the foot-base and heel-tail angles in *Chst14*-deficient mice showed better recovery than those in wild-type mice at each time-point between 1 and 12 weeks after femoral nerve injury (Akyüz et al., 2013). These findings indicate that *Chst14* partially controls inhibitory functions during neural development and recovery from nerve injury.

Neurospheres from *Chst14*-deficient, but not *Chst11*-deficient mice exhibited fewer numbers and larger diameters than those from wild-types (Bian et al., 2011). This was caused by impairments of self-renewal and proliferation, but neither apotosis nor migration, of neural stem cells *in vitro* as well as *in vivo* (Bian et al., 2011). The expression level of GLAST but not Nestin, which are markers of radial glial cells and neurons, respectively, was increased in neurospheres from *Chst14*-deficient mice. These findings suggest that DS-PGs play important roles in the proliferation and differentiation of neural stem cells.

# KNOCKOUT AND MUTANT MICE OF CATABOLISM OF THE REACTION PRODUCTS OF DONOR SUBSTRATES, UDP AND PAP

## Cant1

Most glycosyltransferases utilize UDP-sugar as a donor substrate, which is converted to UDP after the reaction in the endoplasmic reticulum or Golgi apparatus. The UDP is hydrolyzed to UMP by 5′-diphosphatase encoded by *CANT1* (Failer et al., 2002; Smith et al., 2002). *Cant1*-deficient mice exhibited moderate kyphosis, a decrease in both the length and width of tibiae, femurs, and ilium, delta phalanx, a defect in endochondral ossification, and reduction in GAGs in chondrocytes (Paganini et al., 2019). Furthermore, the phenotypes of the *Cant1*-knockout mouse were similar to those of a *Cant1* knock-in mouse with an Arg302His substitution in the catalytic domain (Huber et al., 2009), which corresponds to the human mutation in patients with Desbuquois dysplasia characterized by a short stature, round face, progressive scoliosis, and joint laxity (Paganini et al., 2019). *Cant1*-deficient mice generated by the CRISPR/Cas9 system also exhibited a lower body weight, short stature, thoracic kyphosis, delta phalanx, reduction in GAG content in growth plate cartilage, and impairment of differentiation of chondrocytes (Kodama et al., 2020).

These findings suggest that CANT1 and/or hydrolysis of UDP to UMP may be necessary for the metabolism of GAGs and that it affects the maturation of chondrocytes in the cartilage growth plate. Accumulation of UDP may inhibit the activity of glycosyltransferases involved in the biosynthesis of GAGs. The lack of UMP may inhibit the incorporation of UDP-sugars from the cytosol into the endoplasmic reticulum and Golgi apparatus through antiporters, nucleotide sugar transporters. Further biochemical analyses of the cellular pathways will be crucial in order to elucidate the molecular basis of CANT1 deficiency as well as Desbuquois dysplasia.

## Bpnt2

Most sulfotransferases utilize PAPS as a donor substrate, which is converted to PAP after the reaction in the cytosol as well as Golgi apparatus. PAP is hydrolyzed to 5′-AMP by PAP 3′-phosphatase encoded by *BPNT1* and *BPNT2/IMPAD1* in the cytosol and Golgi apparatus, respectively (Frederick et al., 2008; Hudson et al., 2013). The gene trap *Bpnt2*-deficient mice are neonatally or embryonically lethal, and showed reduction of the limb length, shortening of the snout and lower limbs, reduced sternal length, and diminished rib spacing (Frederick et al., 2008). Furthermore, a marked decrease in chondroitin 4-*O*-sulfate and an increase in

**TABLE 4 |** Outstanding questions and perspectives for functions of glycosyltransferases, sulfotransferases, and epimerase involving CS/DS-biosynthesis.

| Questions | Related enzymes | Related references |
|---|---|---|
| How XYLTs recognize serine residues on core proteins? | XYLT1, XYLT2 | Götting et al. (2000), Pönighaus et al. (2007) |
| What sorting mechanism of CS/DS and HS? | CSGALNACT1, CSGALNACT2, EXTL2, EXTL3 | Izumikawa and Kitagawa (2015), Izumikawa et al. (2015), Koike et al. (2009), Koike et al. (2014), Sugahara and Kitagawa, (2000) |
| Which GalTs compensate GalT-I and GalT-II-deficiencies? | B4GALTs, B3GALTs | Almeida et al. (1999), Okajima et al. (1999), Bai et al. (2001), Mizumoto and Yamada (2021) |
| How three dimensional structures of glycosyltransferases and sulfotransferases? | CHSY1, CHPF, DSE, CHST14 | Kitagawa et al. (2001a), Kitagawa et al. (2003), Maccarana et al. (2006), Evers et al. (2001), Mikami et al. (2003) |
| What is the differential roles of the respective isoforms? | XYLTs, CHSYs, CHPFs, CSGALNACTs, C4STs, DSEs | Götting et al. (2000), Kitagawa et al. (2001b), Kitagawa et al., 2003, Uyama et al. (2002), Hiraoka et al. (2000), Maccarana et al. (2006) |
| What is the roles of 2-O-sulfation in CS/DS? | UST | Kobayashi et al. (1999) |
| What is the roles of CS/DS in tumor metastasis and development? | All CS/DS-biosynthetic enzymes | ten Dam et al. (2007), Bi et al., (2008), Li et al. (2008), Sugahara et al. (2008), Mizumoto et al. (2012) |
| Which golgin(s) regurate GAG biosynthesis? | All CS/DS-biosynthetic enzymes | Chan et al. (2018), Ferreira et al. (2018) |
| Regulation of gene expression and related transcriptional factors | All genes encoding CS/DS-biosynthetic enzymes | Kitagawa et al. (2001a) |

non-sulfated chondroitin were detected in the cartilage, lung, and embryos of *Bpnt2*-deficient mice. Although significant changes in the amount and sulfation modification of HS were not observed in the embryos from mutant mice, the degree of sulfation of HS was slightly decreased in the lung (Frederick et al., 2008). These findings indicate that BPNT2 and/or hydrolysis of PAP to 5′-AMP may be necessary for the metabolism of sulfation of GAGs and that it affects skeletal development. The accumulation of PAP may inhibit sulfotransferases involved in the biosynthesis of GAGs. The lack of 5′-AMP may inhibit the incorporation of PAPS from the cytosol into Golgi apparatus through an unidentified antiporter(s).

## KNOCKOUT MICE OF GOLGINS

### Gorab

Golgins comprise a family of vesicle-tethering proteins at the Golgi apparatus (Witkos and Lowe, 2017; Lowe, 2019). The vesicle-bound cargo tethers to the Golgi apparatus, which triggers membrane fusion. Various golgins are localized to distinct regions of the Golgi apparatus, and their ability to tether transported vesicles selectively is necessary for the specificity of vesicle traffic in the secretory pathway. Because the biosynthesis of GAG side chains on PGs is achieved in the endoplasmic reticulum and Golgi apparatus, some golgins are most likely involved in the transport of PGs.

*GORAB* encodes a Rab6-interacting Golgi protein, and its mutations cause human genetic disorder, gerodermia osteodysplastica, which is characterized by skin laxity and early-onset osteoporosis (Hennies et al., 2008). Mutant mice of *Gorab* have been generated, with fully and conditionally inactivated mesenchymal progenitor cells (*Prx1*-cre), pre-osteoblasts (*Runx2*-cre), and late osteoblasts/osteocytes (*Dmp1*-cre), respectively (Chan et al., 2018). The *Gorab* full-knockout mice ($Gorab^{Null}$) were neonatal lethal, and showed disorganized collagen fibrils (Chan et al., 2018). The *Gorab* conditional-knockout mice, $Gorab^{Prx1}$ and $Gorab^{Runx2}$, exhibited thinned, porous cortical bone and spontaneous fractures (Chan et al., 2018), which were also observed in a patient with gerodermia osteodysplastica (Hennies et al., 2008). Furthermore, the level of DS, but not CS or HS, was decreased in skin and cartilage from $Gorab^{Null}$ mutants. The glycanation of DS-proteoglycans, biglycan and decorin, in skin and bone may be reduced (Chan et al., 2018). The Golgi apparatus compartment of cultured fibroblasts from $Gorab^{Null}$ mutants showed the accumulation of decorin core protein, but a reduced level of DS, indicating that the newly synthesized decorin core protein accumulates within the Golgi apparatus due to the impairment of DS biosynthesis. However, it remains unclear whether there are anomalies in the transport of decorin core protein or DS-biosynthetic enzymes including DSE as well as D4ST1 to the Golgi apparatus. Taken together, these findings suggest that mutation and/or deficiency of *Gorab* primarily perturbs pre-osteoblasts, and that gerodermia osteodysplastica might be affected by biosynthesis of the DS side chain in proteoglycans and/or transport of decorin core protein in the Golgi compartment.

## CONCLUSIONS AND PERSPECTIVES

Mice deficient in glycosyltransferases or sulfotransferases involved in the biosynthesis of CS/DS demonstrated abnormalities of bone, skin, and nervous systems. These knockout mice with deficiency of *Chst11*, *Chst3*, and *Chst15* have revealed that A, C, and E units in CS chains play essential roles in chondrocyte differentiation, T-cell differentiation, and storage of proteases in mast cells, respectively. Furthermore, *Chst14*-knockout mice revealed that DS-containing iA unit, but not CS-containing A unit, bundles collagen fibrils in skin, which might be dependent on the structural and conformational alteration of CS and DS chains (Casu et al., 1988; Hirose et al., 2021). These findings indicate that specific sulfation modifications as well as conformation of uronic acid in CS/DS are essential for connective tissue and neuronal development.

Recent advances in studies on human genetic disorders in connective tissues have also clarified the biological significance of CS/DS side chains of PGs (Mizumoto et al., 2013, 2017; Mizumoto, 2018; Kosho et al., 2019; Malfait et al., 2020). The clinical halmarks in human diseases caused by deficiency in the biosynthetic enzymes of CS/DS are not always consistent with the phenotypes of knockout mice with deficiency of the corresponding enzymes. This contradiction may be due to residual enzymatic activity in human patients. However, the phenotypes of some null-mutant mice are consistent with human clinical symptoms in patients with mutations in the corresponding gene. Further studies on molecular pathogeneses involving CS and DS chains of PGs are necessary to develop therapeutics and new drugs against these diseases (**Table 4**).

The biosynthesis of CS/DS-PGs is up-regulated in both tumor stroma and neoplastic cells, resulting in the abundant accumulation of these components in the tumor stroma adjacent to neoplastic cells (Fukatsu et al., 1988; Iozzo et al., 1989; ten Dam et al., 2009; Thelin et al., 2012). Consistent with these observations, up-regulations of gene expressions including glycosyltransferases, epimerases, and sulfotransferases responsible for the biosynthesis of CS/DS (Huang et al., 2021). These findings indicate that CS/DS-PGs contribute to the functions and phenotypes of tumor cells as effectors or modulator macromolecules (ten Dam et al., 2007; Bi et al., 2008; Li et al., 2008; Sugahara et al., 2008; Mizumoto et al., 2012). However, there is little or no report regarding tumor biology of CS/DS using the knockout mice. Further studies on the molecular mechanisms underlying pathological conditions involving CS/DS-PGs using the knockout mice will provide insights into new therapeutic approaches for tumor development (**Table 4**).

## AUTHOR CONTRIBUTIONS

All authors listed have made a substantial, direct, and intellectual contribution to the work and approved it for publication.

## FUNDING

This work was supported in part by a Grant-in Aid for Scientific Research (C) from the Japan Society for the Promotion of Science, Japan (19K07054 to SM; 21K06552 to SY). Grant-in Aid for Research Center for Pathogenesis of Intractable Diseases from the Research Institute of Meijo University (SM and SY).

## ACKNOWLEDGMENTS

The authors thank Medical English Service for editing the English text of the draft of this manuscript.

## SUPPLEMENTARY MATERIAL

The Supplementary Material for this article can be found online at: https://www.frontiersin.org/articles/10.3389/fcell.2021.764781/full#supplementary-material

## REFERENCES

Akyüz, N., Rost, S., Mehanna, A., Bian, S., Loers, G., Oezen, I., et al. (2013). Dermatan 4-*O*-Sulfotransferase1 Ablation Accelerates Peripheral Nerve Regeneration. *Exp. Neurol.* 247, 517–530. doi:10.1016/j.expneurol.2013.01.025

Almeida, R., Levery, S. B., Mandel, U., Kresse, H., Schwientek, T., Bennett, E. P., et al. (1999). Cloning and Expression of a Proteoglycan UDP-Galactose: β-Xylose β1,4-Galactosyltransferase I. *J. Biol. Chem.* 274, 26165–26171. doi:10.1074/jbc.274.37.26165

Bai, X., Zhou, D., Brown, J. R., Crawford, B. E., Hennet, T., and Esko, J. D. (2001). Biosynthesis of the Linkage Region of Glycosaminoglycans. *J. Biol. Chem.* 276, 48189–48195. doi:10.1074/jbc.M107339200

Bartolini, B., Thelin, M. A., Rauch, U., Feinstein, R., Oldberg, A., Malmström, A., et al. (2012). Mouse Development Is Not Obviously Affected by the Absence of Dermatan Sulfate Epimerase 2 in Spite of a Modified Brain Dermatan Sulfate Composition. *Glycobiology* 22, 1007–1016. doi:10.1093/glycob/cws065

Bartolini, B., Thelin, M. A., Svensson, L., Ghiselli, G., van Kuppevelt, T. H., Malmström, A., et al. (2013). Iduronic Acid in Chondroitin/dermatan Sulfate Affects Directional Migration of Aortic Smooth Muscle Cells. *PLoS One* 8, e66704. doi:10.1371/journal.pone.0066704

Bergefall, K., Trybala, E., Johansson, M., Uyama, T., Naito, S., Yamada, S., et al. (2005). Chondroitin Sulfate Characterized by the E-Disaccharide Unit Is a Potent Inhibitor of Herpes Simplex Virus Infectivity and Provides the Virus Binding Sites on gro2C Cells. *J. Biol. Chem.* 280, 32193–32199. doi:10.1074/jbc.M503645200

Bernhardt, R. R., and Schachner, M. (2000). Chondroitin Sulfates Affect the Formation of the Segmental Motor Nerves in Zebrafish Embryos. *Dev. Biol.* 221, 206–219. doi:10.1006/dbio.2000.9673

Berninsone, P. M., and Hirschberg, C. B. (2000). Nucleotide Sugar Transporters of the Golgi Apparatus. *Curr. Opin. Struct. Biol.* 10, 542–547. doi:10.1016/s0959-440x(00)00128-7

Bi, X., Tong, C., Dockendorff, A., Bancroft, L., Gallagher, L., Guzman, G., et al. (2008). Genetic Deficiency of Decorin Causes Intestinal Tumor Formation through Disruption of Intestinal Cell Maturation. *Carcinogenesis* 29, 1435–1440. doi:10.1093/carcin/bgn141

Bian, S., Akyüz, N., Bernreuther, C., Loers, G., Laczynska, E., Jakovcevski, I., et al. (2011). Dermatan Sulfotransferase Chst14/D4st1, but Not Chondroitin Sulfotransferase Chst11/C4st1, Regulates Proliferation and Neurogenesis of Neural Progenitor Cells. *J. Cell Sci.* 124, 4051–4063. doi:10.1242/jcs.088120

Bishop, J. R., Schuksz, M., and Esko, J. D. (2007). Heparan Sulphate Proteoglycans fine-tune Mammalian Physiology. *Nature* 446, 1030–1037. doi:10.1038/nature05817

Buffet, P. A., Gamain, B., Scheidig, C., Baruch, D., Smith, J. D., Hernandez-Rivas, R., et al. (1999). *Plasmodium Falciparum* Domain Mediating Adhesion to Chondroitin Sulfate A: a Receptor for Human Placental Infection. *Proc. Natl. Acad. Sci.* 96, 12743–12748. doi:10.1073/pnas.96.22.12743

Bui, C., Huber, C., Tuysuz, B., Alanay, Y., Bole-Feysot, C., Leroy, J. G., et al. (2014). *XYLT1* Mutations in Desbuquois Dysplasia Type 2. *Am. J. Hum. Genet.* 94, 405–414. doi:10.1016/j.ajhg.2014.01.020

Carulli, D., Laabs, T., Geller, H. M., and Fawcett, J. W. (2005). Chondroitin Sulfate Proteoglycans in Neural Development and Regeneration. *Curr. Opin. Neurobiol.* 15, 116–120. doi:10.1016/j.conb.2005.01.014

Casu, B., Petitou, M., Provasoli, M., and Sinaÿ, P. (1988). Conformational Flexibility: a New Concept for Explaining Binding and Biological Properties of Iduronic Acid-Containing Glycosaminoglycans. *Trends Biochem. Sci.* 13, 221–225. doi:10.1016/0968-0004(88)90088-6

Chan, W. L., Steiner, M., Witkos, T., Egerer, J., Busse, B., Mizumoto, S., et al. (2018). Impaired Proteoglycan Glycosylation, Elevated TGF-β Signaling, and Abnormal Osteoblast Differentiation as the Basis for Bone Fragility in a Mouse Model for

Gerodermia Osteodysplastica. *Plos Genet.* 14, e1007242. doi:10.1371/journal.pgen.1007242

Chen, J., Mei, Z., Huang, B., Zhang, X., Liu, J., Shan, Z., et al. (2019). IL-6/YAP1/β-catenin Signaling Is Involved in Intervertebral Disc Degeneration. *J. Cell. Physiol.* 234, 5964–5971. doi:10.1002/jcp.27065

Clement, A. M., Nadanaka, S., Masayama, K., Mandl, C., Sugahara, K., and Faissner, A. (1998). The DSD-1 Carbohydrate Epitope Depends on Sulfation, Correlates with Chondroitin Sulfate D Motifs, and Is Sufficient to Promote Neurite Outgrowth. *J. Biol. Chem.* 273, 28444–28453. doi:10.1074/jbc.273.43.28444

Condac, E., Silasi-Mansat, R., Kosanke, S., Schoeb, T., Towner, R., Lupu, F., et al. (2007). Polycystic Disease Caused by Deficiency in Xylosyltransferase 2, an Initiating Enzyme of Glycosaminoglycan Biosynthesis. *Proc. Natl. Acad. Sci.* 104, 9416–9421. doi:10.1073/pnas.0700908104

Cortes, M., Baria, A. T., and Schwartz, N. B. (2009). Sulfation of Chondroitin Sulfate Proteoglycans Is Necessary for Proper Indian Hedgehog Signaling in the Developing Growth Plate. *Development* 136, 1697–1706. doi:10.1242/dev.030742

Dündar, M., Müller, T., Zhang, Q., Pan, J., Steinmann, B., Vodopiutz, J., et al. (2009). Loss of Dermatan-4-Sulfotransferase 1 Function Results in Adducted Thumb-Clubfoot Syndrome. *Am. J. Hum. Genet.* 85, 873–882. doi:10.1016/j.ajhg.2009.11.010

Esko, J. D., and Selleck, S. B. (2002). Order Out of Chaos: Assembly of Ligand Binding Sites in Heparan Sulfate. *Annu. Rev. Biochem.* 71, 435–471. doi:10.1146/annurev.biochem.71.110601.135458

Evers, M. R., Xia, G., Kang, H.-G., Schachner, M., and Baenziger, J. U. (2001). Molecular Cloning and Characterization of a Dermatan-specific *N*-Acetylgalactosamine 4-*O*-Sulfotransferase. *J. Biol. Chem.* 276, 36344–36353. doi:10.1074/jbc.M105848200

Failer, B. U., Braun, N., and Zimmermann, H. (2002). Cloning, Expression, and Functional Characterization of a Ca2+-dependent Endoplasmic Reticulum Nucleoside Diphosphatase. *J. Biol. Chem.* 277, 36978–36986. doi:10.1074/jbc.M201656200

Ferreira, C. R., Xia, Z.-J., Clément, A., Parry, D. A., Davids, M., Taylan, F., et al.Undiagnosed Diseases Network, Scottish Genome Partnership (2018). A Recurrent De Novo Heterozygous COG4 Substitution Leads to Saul-Wilson Syndrome, Disrupted Vesicular Trafficking, and Altered Proteoglycan Glycosylation. *Am. J. Hum. Genet.* 103, 553–567. doi:10.1016/j.ajhg.2018.09.003

Forlino, A., Piazza, R., Tiveron, C., Della Torre, S., Tatangelo, L., Bonafè, L., et al. (2005). A Diastrophic Dysplasia Sulfate Transporter (SLC26A2) Mutant Mouse: Morphological and Biochemical Characterization of the Resulting Chondrodysplasia Phenotype. *Hum. Mol. Genet.* 14, 859–871. doi:10.1093/hmg/ddi079

Fransson, L-. A., Cheng, F., Yoshida, K., Heinegård, D., Malmström, A., and Schmidtchen, A. (1993). "Patterns of Epimerization and Sulphation in Dermatan Sulphate Chains," in *Dermatan Sulphate Proteoglycans: Chemistry, Biology, Chemical Pathology*. Editor J. E. Scott (London: Portland Press), 11–25.

Frederick, J. P., Tafari, A. T., Wu, S.-M., Megosh, L. C., Chiou, S.-T., Irving, R. P., et al. (2008). A Role for a Lithium-Inhibited Golgi Nucleotidase in Skeletal Development and Sulfation. *Proc. Natl. Acad. Sci.* 105, 11605–11612. doi:10.1073/pnas.0801182105

Fuda, H., Shimizu, C., Lee, Y. C., Akita, H., and Strott, C. A. (2002). Characterization and Expression of Human Bifunctional 3′-phosphoadenosine 5′-phosphosulphate Synthase Isoforms. *Biochem. J.* 365, 497–504. doi:10.1042/BJ20020044

Fukatsu, T., Sobue, M., Nagasaka, T., Ohiwa, N., Fukata, S., Nakashima, N., et al. (1988). Immunohistochemical Localization of Chondroitin Sulphate and Dermatan Sulphate Proteoglycans in Tumour Tissues. *Br. J. Cancer* 57, 74–78. doi:10.1038/bjc.1988.12

Fukuta, M., Kobayashi, Y., Uchimura, K., Kimata, K., and Habuchi, O. (1998). Molecular Cloning and Expression of Human Chondroitin 6-sulfotransferase. *Biochim. Biophys. Acta (Bba) - Gene Struct. Expr.* 1399, 57–61. doi:10.1016/s0167-4781(98)00089-x

Fukuta, M., Uchimura, K., Nakashima, K., Kato, M., Kimata, K., Shinomura, T., et al. (1995). Molecular Cloning and Expression of Chick Chondrocyte Chondroitin 6-sulfotransferase. *J. Biol. Chem.* 270, 18575–18580. doi:10.1074/jbc.270.31.18575

García-García, M. J., and Anderson, K. V. (2003). Essential Role of Glycosaminoglycans in Fgf Signaling during Mouse Gastrulation. *Cell* 114, 727–737. doi:10.1016/s0092-8674(03)00715-3

Gotoh, M., Yada, T., Sato, T., Akashima, T., Iwasaki, H., Mochizuki, H., et al. (2002). Molecular Cloning and Characterization of a Novel Chondroitin Sulfate Glucuronyltransferase that Transfers Glucuronic Acid toN-Acetylgalactosamine. *J. Biol. Chem.* 277, 38179–38188. doi:10.1074/jbc.M202601200

Götting, C., Kuhn, J., Zahn, R., Brinkmann, T., and Kleesiek, K. (2000). Molecular Cloning and Expression of Human UDP-D-Xylose:Proteoglycan Core Protein β-d-Xylosyltransferase and its First Isoform XT-II. *J. Mol. Biol.* 304, 517–528. doi:10.1006/jmbi.2000.4261

Gulberti, S., Lattard, V., Fondeur, M., Jacquinet, J.-C., Mulliert, G., Netter, P., et al. (2005). Phosphorylation and Sulfation of Oligosaccharide Substrates Critically Influence the Activity of Human β1,4-Galactosyltransferase 7 (GalT-I) and β1,3-Glucuronosyltransferase I (GlcAT-I) Involved in the Biosynthesis of the Glycosaminoglycan-Protein Linkage Region of Proteoglycans. *J. Biol. Chem.* 280, 1417–1425. doi:10.1074/jbc.M411552200

Gustafsson, R., Stachtea, X., Maccarana, M., Grottling, E., Eklund, E., Malmström, A., et al. (2014). Dermatan Sulfate Epimerase 1 Deficient Mice as a Model for Human Abdominal wall Defects. *Birth Defects Res. A: Clin. Mol. Teratology* 100, 712–720. doi:10.1002/bdra.23300

Habuchi, H., Ushida, T., and Habuchi, O. (2016). Mice Deficient in N-Acetylgalactosamine 4-sulfate 6-*O*-Sulfotransferase Exhibit Enhanced Liver Fibrosis and Delayed Recovery from Fibrosis in Carbon Tetrachloride-Treated Mice. *Heliyon* 2, e00138. doi:10.1016/j.heliyon.2016.e00138

Hästbacka, J., de la Chapelle, A., Mahtani, M. M., Clines, G., Reeve-Daly, M. P., Daly, M., et al. (1994). The Diastrophic Dysplasia Gene Encodes a Novel Sulfate Transporter: Positional Cloning by fine-structure Linkage Disequilibrium Mapping. *Cell* 78, 1073–1087. doi:10.1016/0092-8674(94)90281-x

Hennies, H. C., Kornak, U., Zhang, H., Egerer, J., Zhang, X., Seifert, W., et al. (2008). Gerodermia Osteodysplastica Is Caused by Mutations in *SCYL1BP1*, a Rab-6 Interacting Golgin. *Nat. Genet.* 40, 1410–1412. doi:10.1038/ng.252

Hiraoka, N., Nakagawa, H., Ong, E., Akama, T. O., Fukuda, M. N., and Fukuda, M. (2000). Molecular Cloning and Expression of Two Distinct Human Chondroitin 4-*O*-Sulfotransferases that Belong to the HNK-1 Sulfotransferase Gene Family. *J. Biol. Chem.* 275, 20188–20196. doi:10.1074/jbc.M002443200

Hiraoka, S., Furuichi, T., Nishimura, G., Shibata, S., Yanagishita, M., Rimoin, D. L., et al. (2007). Nucleotide-sugar Transporter SLC35D1 Is Critical to Chondroitin Sulfate Synthesis in Cartilage and Skeletal Development in Mouse and Human. *Nat. Med.* 13, 1363–1367. doi:10.1038/nm1655

Hirose, T., Mizumoto, S., Hashimoto, A., Takahashi, Y., Yoshizawa, T., Nitahara-Kasahara, Y., et al. (2021). Systematic Investigation of the Skin in Chst14−/− Mice: A Model for Skin Fragility in Musculocontractural Ehlers-Danlos Syndrome Caused by CHST14 Variants (mcEDS-CHST14). *Glycobiology* 31, 137–150. doi:10.1093/glycob/cwaa058

Hou, X., Yoshioka, N., Tsukano, H., Sakai, A., Miyata, S., Watanabe, Y., et al. (2017). Chondroitin Sulfate Is Required for Onset and Offset of Critical Period Plasticity in Visual Cortex. *Sci. Rep.* 7, 12646. doi:10.1038/s41598-017-04007-x

Huang, Y.-F., Mizumoto, S., and Fujita, M. (2021). Novel Insight into Glycosaminoglycan Biosynthesis Based on Gene Expression Profiles. *Front. Cel Dev. Biol.* 9, 709018. doi:10.3389/fcell.2021.709018

Huber, C., Oulès, B., Bertoli, M., Chami, M., Fradin, M., Alanay, Y., et al. (2009). Identification of *CANT1* Mutations in Desbuquois Dysplasia. *Am. J. Hum. Genet.* 85, 706–710. doi:10.1016/j.ajhg.2009.10.001

Hudson, B. H., Frederick, J. P., Drake, L. Y., Megosh, L. C., Irving, R. P., and York, J. D. (2013). Role for Cytoplasmic Nucleotide Hydrolysis in Hepatic Function and Protein Synthesis. *Proc. Natl. Acad. Sci.* 110, 5040–5045. doi:10.1073/pnas.1205001110

Hwang, H.-Y., Olson, S. K., Esko, J. D., and Robert Horvitz, H. (2003). *Caenorhabditis elegans* Early Embryogenesis and Vulval Morphogenesis Require Chondroitin Biosynthesis. *Nature* 423, 439–443. doi:10.1038/nature01634

Ida-Yonemochi, H., Morita, W., Sugiura, N., Kawakami, R., Morioka, Y., Takeuchi, Y., et al. (2018). Craniofacial Abnormality with Skeletal Dysplasia in Mice Lacking Chondroitin Sulfate *N*-Acetylgalactosaminyltransferase-1. *Sci. Rep.* 8, 17134. doi:10.1038/s41598-018-35412-5

Inada, R., Miyamoto, K., Tanaka, N., Moriguchi, K., Kadomatsu, K., Takeuchi, K., et al. (2021). Chondroitin Sulfate *N*-Acetylgalactosyltransferase-1 Knockout Shows Milder Phenotype in Experimental Autoimmune Encephalomyelitis Than in Wild Type. *Glycobiology* 31, 260–265. doi:10.1093/glycob/cwaa072

Iozzo, R. V. (1998). Matrix Proteoglycans: from Molecular Design to Cellular Function. *Annu. Rev. Biochem.* 67, 609–652. doi:10.1146/annurev.biochem.67.1.609

Iozzo, R. V., Sampson, P. M., and Schmitt, G. K. (1989). Neoplastic Modulation of Extracellular Matrix: Stimulation of Chondroitin Sulfate Proteoglycan and Hyaluronic Acid Synthesis in Co-cultures of Human colon Carcinoma and Smooth Muscle Cells. *J. Cell. Biochem.* 39, 355–378. doi:10.1002/jcb.240390403

Izumikawa, T., Kanagawa, N., Watamoto, Y., Okada, M., Saeki, M., Sakano, M., et al. (2010). Impairment of Embryonic Cell Division and Glycosaminoglycan Biosynthesis in Glucuronyltransferase-I-Deficient Mice. *J. Biol. Chem.* 285, 12190–12196. doi:10.1074/jbc.M110.100941

Izumikawa, T., and Kitagawa, H. (2015). Amino Acid Sequence Surrounding the Chondroitin Sulfate Attachment Site of Thrombomodulin Regulates Chondroitin Polymerization. *Biochem. Biophysical Res. Commun.* 460, 233–237. doi:10.1016/j.bbrc.2015.03.016

Izumikawa, T., Kitagawa, H., Mizuguchi, S., Nomura, K. H., Nomura, K., Tamura, J.-i., et al. (2004). Nematode Chondroitin Polymerizing Factor Showing Cell-/organ-specific Expression Is Indispensable for Chondroitin Synthesis and Embryonic Cell Division. *J. Biol. Chem.* 279, 53755–53761. doi:10.1074/jbc.M409615200

Izumikawa, T., Koike, T., Shiozawa, S., Sugahara, K., Tamura, J.-i., and Kitagawa, H. (2008). Identification of Chondroitin Sulfate Glucuronyltransferase as Chondroitin Synthase-3 Involved in Chondroitin Polymerization. *J. Biol. Chem.* 283, 11396–11406. doi:10.1074/jbc.M707549200

Izumikawa, T., Sato, B., and Kitagawa, H. (2014). Chondroitin Sulfate Is Indispensable for Pluripotency and Differentiation of Mouse Embryonic Stem Cells. *Sci. Rep.* 4, 3701. doi:10.1038/srep03701

Izumikawa, T., Sato, B., Mikami, T., Tamura, J.-i., Igarashi, M., and Kitagawa, H. (2015). GlcUAβ1-3Galβ1-3Galβ1-4Xyl(2-O-phosphate) Is the Preferred Substrate for Chondroitin N-Acetylgalactosaminyltransferase-1. *J. Biol. Chem.* 290, 5438–5448. doi:10.1074/jbc.M114.603266

Izumikawa, T., Uyama, T., Okuura, Y., Sugahara, K., and Kitagawa, H. (2007). Involvement of Chondroitin Sulfate Synthase-3 (Chondroitin Synthase-2) in Chondroitin Polymerization through its Interaction with Chondroitin Synthase-1 or Chondroitin-Polymerizing Factor. *Biochem. J.* 403, 545–552. doi:10.1042/BJ20061876

Kang, H.-G., Evers, M. R., Xia, G., Baenziger, J. U., and Schachner, M. (2002). Molecular Cloning and Characterization of Chondroitin-4-O-Sulfotransferase-3. *J. Biol. Chem.* 277, 34766–34772. doi:10.1074/jbc.M204907200

Kitagawa, H., Izumikawa, T., Uyama, T., and Sugahara, K. (2003). Molecular Cloning of a Chondroitin Polymerizing Factor that Cooperates with Chondroitin Synthase for Chondroitin Polymerization. *J. Biol. Chem.* 278, 23666–23671. doi:10.1074/jbc.M302493200

Kitagawa, H., Taoka, M., Tone, Y., and Sugahara, K. (2001a). Human Glycosaminoglycan Glucuronyltransferase I Gene and a Related Processed Pseudogene: Genomic Structure, Chromosomal Mapping and Characterization. *Biochem. J.* 358, 539–546. doi:10.1042/0264-6021:358053910.1042/bj3580539

Kitagawa, H., Tone, Y., Tamura, J.-i., Neumann, K. W., Ogawa, T., Oka, S., et al. (1998). Molecular Cloning and Expression of Glucuronyltransferase I Involved in the Biosynthesis of the Glycosaminoglycan-Protein Linkage Region of Proteoglycans. *J. Biol. Chem.* 273, 6615–6618. doi:10.1074/jbc.273.12.6615

Kitagawa, H., Tsutsumi, K., Ikegami-Kuzuhara, A., Nadanaka, S., Goto, F., Ogawa, T., et al. (2008). Sulfation of the Galactose Residues in the Glycosaminoglycan-Protein Linkage Region by Recombinant Human Chondroitin 6-*O*-Sulfotransferase-1. *J. Biol. Chem.* 283, 27438–27443. doi:10.1074/jbc.M803279200

Kitagawa, H., Uyama, T., and Sugahara, K. (2001b). Molecular Cloning and Expression of a Human Chondroitin Synthase. *J. Biol. Chem.* 276, 38721–38726. doi:10.1074/jbc.M106871200

Kitazawa, K., Nadanaka, S., Kadomatsu, K., and Kitagawa, H. (2021). Chondroitin 6-sulfate Represses Keratinocyte Proliferation in Mouse Skin, Which Is Associated with Psoriasis. *Commun. Biol.* 4, 114. doi:10.1038/s42003-020-01618-5

Kjellén, L., and Lindahl, U. (1991). Proteoglycans: Structures and Interactions. *Annu. Rev. Biochem.* 60, 443–475. doi:10.1146/annurev.bi.60.070191.002303

Klüppel, M., Wight, T. N., Chan, C., Hinek, A., and Wrana, J. L. (2005). Maintenance of Chondroitin Sulfation Balance by Chondroitin-4-Sulfotransferase 1 Is Required for Chondrocyte Development and Growth Factor Signaling during Cartilage Morphogenesis. *Development* 132, 3989–4003. doi:10.1242/dev.01948

Kobayashi, M., Sugumaran, G., Liu, J., Shworak, N. W., Silbert, J. E., and Rosenberg, R. D. (1999). Molecular Cloning and Characterization of a Human Uronyl 2-sulfotransferase that Sulfates Iduronyl and Glucuronyl Residues in Dermatan/chondroitin Sulfate. *J. Biol. Chem.* 274, 10474–10480. doi:10.1074/jbc.274.15.10474

Kodama, K., Takahashi, H., Oiji, N., Nakano, K., Okamura, T., Niimi, K., et al. (2020). *CANT1* Deficiency in a Mouse Model of Desbuquois Dysplasia Impairs Glycosaminoglycan Synthesis and Chondrocyte Differentiation in Growth Plate Cartilage. *FEBS Open Bio* 10, 1096–1103. doi:10.1002/2211-5463.12859

Koike, T., Izumikawa, T., Sato, B., and Kitagawa, H. (2014). Identification of Phosphatase that Dephosphorylates Xylose in the Glycosaminoglycan-Protein Linkage Region of Proteoglycans. *J. Biol. Chem.* 289, 6695–6708. doi:10.1074/jbc.M113.520536

Koike, T., Izumikawa, T., Tamura, J.-I., and Kitagawa, H. (2009). FAM20B Is a Kinase that Phosphorylates Xylose in the Glycosaminoglycan-Protein Linkage Region. *Biochem. J.* 421, 157–162. doi:10.1042/BJ20090474

Koike, T., Mikami, T., Shida, M., Habuchi, O., and Kitagawa, H. (2015). Chondroitin Sulfate-E Mediates Estrogen-Induced Osteoanabolism. *Sci. Rep.* 5, 8994. doi:10.1038/srep08994

Kosho, T., Mizumoto, S., Watanabe, T., Yoshizawa, T., Miyake, N., and Yamada, S. (2019). Recent Advances in the Pathophysiology of Musculocontractural Ehlers-Danlos Syndrome. *Genes* 11, 43. doi:10.3390/genes11010043

Kusche-Gullberg, M., and Kjellén, L. (2003). Sulfotransferases in Glycosaminoglycan Biosynthesis. *Curr. Opin. Struct. Biol.* 13, 605–611. doi:10.1016/j.sbi.2003.08.002

Lane, P. (1988). Subtle gray (Sut); Small with Kinky Tail (Skt). *Mouse News Lett.* 165.

Li, F., ten Dam, G. B., Murugan, S., Yamada, S., Hashiguchi, T., Mizumoto, S., et al. (2008). Involvement of Highly Sulfated Chondroitin Sulfate in the Metastasis of the Lewis Lung Carcinoma Cells. *J. Biol. Chem.* 283, 34294–34304. doi:10.1074/jbc.M806015200

Li, Y., Laue, K., Temtamy, S., Aglan, M., Kotan, L. D., Yigit, G., et al. (2010). Temtamy Preaxial Brachydactyly Syndrome Is Caused by Loss-Of-Function Mutations in Chondroitin Synthase 1, a Potential Target of BMP Signaling. *Am. J. Hum. Genet.* 87, 757–767. doi:10.1016/j.ajhg.2010.10.003

Lin, R., Rosahl, T. W., Whiting, P. J., Fawcett, J. W., and Kwok, J. C. F. (2011). 6-Sulphated Chondroitins Have a Positive Influence on Axonal Regeneration. *PLoS One* 6, e21499. doi:10.1371/journal.pone.0021499

Lin, X., Wei, G., Shi, Z., Dryer, L., Esko, J. D., Wells, D. E., et al. (2000). Disruption of Gastrulation and Heparan Sulfate Biosynthesis in EXT1-Deficient Mice. *Dev. Biol.* 224, 299–311. doi:10.1006/dbio.2000.9798

Lind, T., Tufaro, F., McCormick, C., Lindahl, U., and Lidholt, K. (1998). The Putative Tumor Suppressors EXT1 and EXT2 Are Glycosyltransferases Required for the Biosynthesis of Heparan Sulfate. *J. Biol. Chem.* 273, 26265–26268. doi:10.1074/jbc.273.41.26265

Lindahl, U., and Rodén, L. (1972). in *Carbohydrate-protein Linkages in Proteoglycans of Animal, Plant and Bacterial Origin* in Glycoproteins: Their Composition, Structure And Function. Editor A. Gottschalk (Amsterdam: Elsevier), 491–517.

Liu, X., Li, N., Zhang, H., Liu, J., Zhou, N., Ran, C., et al. (2018). Inactivation of Fam20b in the Neural Crest-Derived Mesenchyme of Mouse Causes Multiple Craniofacial Defects. *Eur. J. Oral Sci.* 126, 433–436. doi:10.1111/eos.12563

Lowe, M. (2019). The Physiological Functions of the Golgin Vesicle Tethering Proteins. *Front. Cell Dev. Biol.* 7, 94. doi:10.3389/fcell.2019.00094

Ma, P., Yan, W., Tian, Y., Wang, J., Feng, J. Q., Qin, C., et al. (20162016). Inactivation of Fam20b in Joint Cartilage Leads to Chondrosarcoma and Postnatal Ossification Defects. *Sci. Rep.* 6, 29814. doi:10.1038/srep29814

Maccarana, M., Kalamajski, S., Kongsgaard, M., Magnusson, S. P., Oldberg, A., and Malmström, A. (2009). Dermatan Sulfate Epimerase 1-deficient Mice Have Reduced Content and Changed Distribution of Iduronic Acids in

Dermatan Sulfate and an Altered Collagen Structure in Skin. *Mol. Cell. Biol.* 29, 5517–5528. doi:10.1128/MCB.00430-09

Maccarana, M., Olander, B., Malmström, J., Tiedemann, K., Aebersold, R., Lindahl, U., et al. (2006). Biosynthesis of Dermatan Sulfate. *J. Biol. Chem.* 281, 11560–11568. doi:10.1074/jbc.M513373200

Macke, E. L., Henningsen, E., Jessen, E., Zumwalde, N. A., Landowski, M., Western, D. E., et al. (2020). Loss of Chondroitin Sulfate Modification Causes Inflammation and Neurodegeneration in Skt Mice. *Genetics* 214, 121–134. doi:10.1534/genetics.119.302834

Maimone, M. M., and Tollefsen, D. M. (1991). Structure of a Dermatan Sulfate Hexasaccharide that Binds to Heparin Cofactor II with High Affinity. *J. Biol. Chem.* 265, 18263–18271. doi:10.1016/s0021-9258(18)98760-0

Malavaki, C., Mizumoto, S., Karamanos, N., and Sugahara, K. (2008). Recent Advances in the Structural Study of Functional Chondroitin Sulfate and Dermatan Sulfate in Health and Disease. *Connect. Tissue Res.* 49, 133–139. doi:10.1080/03008200802148546

Malfait, F., Castori, M., Francomano, C. A., Giunta, C., Kosho, T., and Byers, P. H. (2020). The Ehlers-Danlos Syndromes. *Nat. Rev. Dis. Primers* 6, 64. doi:10.1038/s41572-020-0194-9

Malfait, F., Francomano, C., Byers, P., Belmont, J., Berglund, B., Black, J., et al. (2017). The 2017 International Classification of the Ehlers-Danlos Syndromes. *Am. J. Med. Genet.* 175, 8–26. doi:10.1002/ajmg.c.31552

Malfait, F., Syx, D., Vlummens, P., Symoens, S., Nampoothiri, S., Hermanns-Lê, T., et al. (2010). Musculocontractural Ehlers-Danlos Syndrome (Former EDS Type VIB) and Adducted Thumb Clubfoot Syndrome (ATCS) Represent a Single Clinical Entity Caused by Mutations in the Dermatan-4-Sulfotransferase 1 Encoding *CHST14* Gene. *Hum. Mutat.* 31, 1233–1239. doi:10.1002/humu.21355

Malmström, A., Bartolini, B., Thelin, M. A., Pacheco, B., and Maccarana, M. (2012). Iduronic Acid in Chondroitin/Dermatan Sulfate. *J. Histochem. Cytochem.* 60, 916–925. doi:10.1369/0022155412459857

Malmström, A. (1984). Biosynthesis of Dermatan Sulfate. II. Substrate Specificity of the C-5 Uronosyl Epimerase. *J. Biol. Chem.* 259, 161–165. doi:10.1016/s0021-9258(17)43635-0

McCormick, C., Leduc, Y., Martindale, D., Mattison, K., Esford, L., Dyer, A., et al. (1998). The Putative Tumour Suppressor EXT1 Alters the Expression of Cell-Surface Heparan Sulfate. *Nat. Genet.* 19, 158–161. doi:10.1038/514

Mikami, T., and Kitagawa, H. (2013). Biosynthesis and Function of Chondroitin Sulfate. *Biochim. Biophys. Acta (Bba) - Gen. Subjects* 1830, 4719–4733. doi:10.1016/j.bbagen.2013.06.006

Mikami, T., Mizumoto, S., Kago, N., Kitagawa, H., and Sugahara, K. (2003). Specificities of Three Distinct Human Chondroitin/Dermatan N-Acetylgalactosamine 4-O-Sulfotransferases Demonstrated Using Partially Desulfated Dermatan Sulfate as an Acceptor. *J. Biol. Chem.* 278, 36115–36127. doi:10.1074/jbc.M306044200

Mis, E. K., Liem, K. F., Jr., Kong, Y., Schwartz, N. B., Domowicz, M., and Weatherbee, S. D. (2014). Forward Genetics Defines Xylt1 as a Key, Conserved Regulator of Early Chondrocyte Maturation and Skeletal Length. *Dev. Biol.* 385, 67–82. doi:10.1016/j.ydbio.2013.10.014

Miyake, N., Kosho, T., Mizumoto, S., Furuichi, T., Hatamochi, A., Nagashima, Y., et al. (2010). Loss-of-function Mutations of *CHST14* in a New Type of Ehlers-Danlos Syndrome. *Hum. Mutat.* 31, 966–974. doi:10.1002/humu.21300

Miyata, S., and Kitagawa, H. (2015). Mechanisms for Modulation of Neural Plasticity and Axon Regeneration by Chondroitin Sulphate. *J. Biochem.* 157, 13–22. doi:10.1093/jb/mvu067

Miyata, S., Komatsu, Y., Yoshimura, Y., Taya, C., and Kitagawa, H. (2012). Persistent Cortical Plasticity by Upregulation of Chondroitin 6-sulfation. *Nat. Neurosci.* 15, 414–422. doi:10.1038/nn.3023

Mizuguchi, S., Uyama, T., Kitagawa, H., Nomura, K. H., Dejima, K., Gengyo-Ando, K., et al. (2003). Chondroitin Proteoglycans Are Involved in Cell Division of *Caenorhabditis elegans*. *Nature* 423, 443–448. doi:10.1038/nature01635

Mizumoto, S. (2018). Defects in Biosynthesis of Glycosaminoglycans Cause Hereditary Bone, Skin, Heart, Immune, and Neurological Disorders. *Trends Glycosci. Glycotechnol.* 30, E67–E89. doi:10.4052/tigg.1812.2e

Mizumoto, S., Ikegawa, S., and Sugahara, K. (2013). Human Genetic Disorders Caused by Mutations in Genes Encoding Biosynthetic Enzymes for Sulfated Glycosaminoglycans. *J. Biol. Chem.* 288, 10953–10961. doi:10.1074/jbc.R112.437038

Mizumoto, S., Kosho, T., Yamada, S., and Sugahara, K. (2017). Pathophysiological Significance of Dermatan Sulfate Proteoglycans Revealed by Human Genetic Disorders. *Pharmaceuticals* 10, 34. doi:10.3390/ph10020034

Mizumoto, S., Mikami, T., Yasunaga, D., Kobayashi, N., Yamauchi, H., Miyake, A., et al. (2009). Chondroitin 4-*O*-Sulfotransferase-1 Is Required for Somitic Muscle Development and Motor Axon Guidance in Zebrafish. *Biochem. J.* 419, 387–399. doi:10.1042/BJ20081639

Mizumoto, S., and Sugahara, K. (2013). Glycosaminoglycans Are Functional Ligands for Receptor for Advanced Glycation End-Products in Tumors. *FEBS J.* 280, 2462–2470. doi:10.1111/febs.12156

Mizumoto, S., Takahashi, J., and Sugahara, K. (2012). Receptor for Advanced Glycation End Products (RAGE) Functions as Receptor for Specific Sulfated Glycosaminoglycans, and Anti-RAGE Antibody or Sulfated Glycosaminoglycans Delivered *In Vivo* Inhibit Pulmonary Metastasis of Tumor Cells. *J. Biol. Chem.* 287, 18985–18994. doi:10.1074/jbc.M111.313437

Mizumoto, S., and Yamada, S. (2021). Congenital Disorders of Deficiency in Glycosaminoglycan Biosynthesis. *Front. Genet.* 12, 717535. doi:10.3389/fgene.2021.717535

Mizumoto, S., Yamada, S., and Sugahara, K. (2015). Molecular Interactions between Chondroitin-Dermatan Sulfate and Growth Factors/receptors/matrix Proteins. *Curr. Opin. Struct. Biol.* 34, 35–42. doi:10.1016/j.sbi.2015.06.004

Moriarity, J. L., Hurt, K. J., Resnick, A. C., Storm, P. B., Laroy, W., Schnaar, R. L., et al. (2002). UDP-glucuronate Decarboxylase, a Key Enzyme in Proteoglycan Synthesis. *J. Biol. Chem.* 277, 16968–16975. doi:10.1074/jbc.M109316200

Munns, C. F., Fahiminiya, S., Poudel, N., Munteanu, M. C., Majewski, J., Sillence, D. O., et al. (2015). Homozygosity for Frameshift Mutations in *XYLT2* Result in a Spondylo-Ocular Syndrome with Bone Fragility, Cataracts, and Hearing Defects. *Am. J. Hum. Genet.* 96, 971–978. doi:10.1016/j.ajhg.2015.04.017

Muraoka, M., Kawakita, M., and Ishida, N. (2001). Molecular Characterization of Human UDP-Glucuronic acid/UDP-*N*-Acetylgalactosamine Transporter, a Novel Nucleotide Sugar Transporter with Dual Substrate Specificity. *FEBS Lett.* 495, 87–93. doi:10.1016/s0014-5793(01)02358-4

Nadanaka, S., Miyata, S., Yaqiang, B., Tamura, J.-i., Habuchi, O., and Kitagawa, H. (2020). Reconsideration of the semaphorin-3A Binding Motif Found in Chondroitin Sulfate Using Galnac4s-6st-Knockout Mice. *Biomolecules* 10, 1499. doi:10.3390/biom10111499

Nitahara-Kasahara, Y., Mizumoto, S., Inoue, Y. U., Saka, S., Posadas-Herrera, G., Nakamura-Takahashi, A., et al. (2021a). Muscle Pathophysiology in Mouse Models of Musculocontractural Ehlers-Danlos Syndrome Due to CHST14 Mutations (mcEDS-CHST14), Generated through CRISPR/Cas9-mediated Genomic Editing. *Dis. Model. Mech.* In press.

Nitahara-Kasahara, Y., Posadas-Herrera, G., Mizumoto, S., Nakamura-Takahashi, A., Inoue, Y. U., Inoue, T., et al. (2021b). Myopathy Associated with Dermatan Sulfate-Deficient Decorin and Myostatin in Musculocontractural Ehlers-Danlos Syndrome: a Mouse Model Investigation. *Front. Cell Dev. Biol.* 9, 695021. doi:10.3389/fcell.2021.695021

Ogawa, H., Hatano, S., Sugiura, N., Nagai, N., Sato, T., Shimizu, K., et al. (2012). Chondroitin Sulfate Synthase-2 Is Necessary for Chain Extension of Chondroitin Sulfate but Not Critical for Skeletal Development. *PLoS One* 7, e43806. doi:10.1371/journal.pone.0043806

Ohtake, S., Ito, Y., Fukuta, M., and Habuchi, O. (2001). Human *N*-Acetylgalactosamine 4-sulfate 6-*O*-Sulfotransferase cDNA Is Related to Human B Cell Recombination Activating Gene-Associated Gene. *J. Biol. Chem.* 276, 43894–43900. doi:10.1074/jbc.M104922200

Ohtake-Niimi, S., Kondo, S., Ito, T., Kakehi, S., Ohta, T., Habuchi, H., et al. (2010). Mice Deficient in *N*-Acetylgalactosamine 4-sulfate 6-*O*-Sulfotransferase Are Unable to Synthesize Chondroitin/dermatan Sulfate Containing *N*-Acetylgalactosamine 4,6-bissulfate Residues and Exhibit Decreased Protease Activity in Bone Marrow-Derived Mast Cells. *J. Biol. Chem.* 285, 20793–20805. doi:10.1074/jbc.M109.084749

Okajima, T., Yoshida, K., Kondo, T., and Furukawa, K. (1999). Human Homolog of *Caenorhabditis elegans Sqv-3* Gene Is Galactosyltransferase I Involved in the Biosynthesis of the Glycosaminoglycan-Protein Linkage Region of Proteoglycans. *J. Biol. Chem.* 274, 22915–22918. doi:10.1074/jbc.274.33.22915

Olson, S. K., Bishop, J. R., Yates, J. R., Oegema, K., and Esko, J. D. (2006). Identification of Novel Chondroitin Proteoglycans in *Caenorhabditis elegans*: Embryonic Cell Division Depends on CPG-1 and CPG-2. *J. Cell Biol.* 173, 985–994. doi:10.1083/jcb.200603003

Orellana, A., Moraga, C., Araya, M., and Moreno, A. (2016). Overview of Nucleotide Sugar Transporter Gene Family Functions across Multiple Species. *J. Mol. Biol.* 428, 3150–3165. doi:10.1016/j.jmb.2016.05.021

Orkin, R. W., Pratt, R. M., and Martin, G. R. (1976). Undersulfated Chondroitin Sulfate in the Cartilage Matrix of Brachymorphic Mice. *Dev. Biol.* 50, 82–94. doi:10.1016/0012-1606(76)90069-5

Pacheco, B., Malmström, A., and Maccarana, M. (2009). Two Dermatan Sulfate Epimerases Form Iduronic Acid Domains in Dermatan Sulfate. *J. Biol. Chem.* 284, 9788–9795. doi:10.1074/jbc.M809339200

Paganini, C., Monti, L., Costantini, R., Besio, R., Lecci, S., Biggiogera, M., et al. (2019). Calcium Activated Nucleotidase 1 (CANT1) Is Critical for Glycosaminoglycan Biosynthesis in Cartilage and Endochondral Ossification. *Matrix Biol.* 81, 70–90. doi:10.1016/j.matbio.2018.11.002

Parker, J. L., and Newstead, S. (2019). Gateway to the Golgi: Molecular Mechanisms of Nucleotide Sugar Transporters. *Curr. Opin. Struct. Biol.* 57, 127–134. doi:10.1016/j.sbi.2019.03.019

Pennypacker, J. P., Kimata, K., and Brown, K. S. (1981). Brachymorphic Mice (Bm/bm): A Generalized Biochemical Defect Expressed Primarily in Cartilage. *Dev. Biol.* 81, 280–287. doi:10.1016/0012-1606(81)90291-8

Poönighaus, C., Ambrosius, M., Casanova, J. C., Prante, C., Kuhn, J., Esko, J. D., et al. (2007). Human Xylosyltransferase II Is Involved in the Biosynthesis of the Uniform Tetrasaccharide Linkage Region in Chondroitin Sulfate and Heparan Sulfate Proteoglycans. *J. Biol. Chem.* 282, 5201–5206. doi:10.1074/jbc.M611665200

Properzi, F., Carulli, D., Asher, R. A., Muir, E., Camargo, L. M., van Kuppevelt, T. H., et al. (2005). Chondroitin 6-sulphate Synthesis Is Up-Regulated in Injured CNS, Induced by Injury-Related Cytokines and Enhanced in Axon-Growth Inhibitory Glia. *Eur. J. Neurosci.* 21, 378–390. doi:10.1111/j.1460-9568.2005.03876.x

Purushothaman, A., Sugahara, K., and Faissner, A. (2012). Chondroitin Sulfate "wobble Motifs" Modulate Maintenance and Differentiation of Neural Stem Cells and Their Progeny. *J. Biol. Chem.* 287, 2935–2942. doi:10.1074/jbc.R111.298430

Rodén, L. (1980). "Structure and Metabolism of Connective Tissue Proteoglycans," in *The Biochemistry Of Glycoproteins And Proteoglycans*. Editor W. J. Lennarz (New York: Plenum Press), 267–371. doi:10.1007/978-1-4684-1006-8_7

Rossi, A., and Superti-Furga, A. (2001). Mutations in the Diastrophic Dysplasia Sulfate Transporter (DTDST) Gene (SLC26A2): 22 Novel Mutations, Mutation Review, Associated Skeletal Phenotypes, and Diagnostic Relevance. *Hum. Mutat.* 17, 159–171. doi:10.1002/humu.1

Saiyin, W., Li, L., Zhang, H., Lu, Y., and Qin, C. (2019). Inactivation of FAM20B Causes Cell Fate Changes in Annulus Fibrosus of Mouse Intervertebral Disc and Disc Defects via the Alterations of TGF-β and MAPK Signaling Pathways. *Biochim. Biophys. Acta (Bba) - Mol. Basis Dis.* 1865, 165555. doi:10.1016/j.bbadis.2019.165555

Sato, T., Kudo, T., Ikehara, Y., Ogawa, H., Hirano, T., Kiyohara, K., et al. (2011). Chondroitin Sulfate *N*-Acetylgalactosaminyltransferase 1 Is Necessary for normal Endochondral Ossification and Aggrecan Metabolism. *J. Biol. Chem.* 286, 5803–5812. doi:10.1074/jbc.M110.159244

Satoh, H., Susaki, M., Shukunami, C., Iyama, K.-I., Negoro, T., and Hiraki, Y. (1998). Functional Analysis of Diastrophic Dysplasia Sulfate Transporter. *J. Biol. Chem.* 273, 12307–12315. doi:10.1074/jbc.273.20.12307

Schaefer, L., Tredup, C., Gubbiotti, M. A., and Iozzo, R. V. (2017). Proteoglycan Neofunctions: Regulation of Inflammation and Autophagy in Cancer Biology. *FEBS J.* 284, 10–26. doi:10.1111/febs.13963

Schön, S., Prante, C., Bahr, C., Kuhn, J., Kleesiek, K., and Götting, C. (2006). Cloning and Recombinant Expression of Active Full-Length Xylosyltransferase I (XT-I) and Characterization of Subcellular Localization of XT-I and XT-II. *J. Biol. Chem.* 281, 14224–14231. doi:10.1074/jbc.M510690200

Schwartz, N. B., Ostrowski, V., Brown, K. S., and Pratt, R. M. (1978). Defective PAPS-Synthesis in Epiphyseal Cartilage from Brachymorphic Mice. *Biochem. Biophysical Res. Commun.* 82, 173–178. doi:10.1016/0006-291x(78)90592-2

Seidler, U., and Nikolovska, K. (2019). Slc26 Family of Anion Transporters in the Gastrointestinal Tract: Expression, Function, Regulation, and Role in Disease. *Compr. Physiol.* 9, 839–872. doi:10.1002/cphy.c180027

Shimbo, M., Suzuki, R., Fuseya, S., Sato, T., Kiyohara, K., Hagiwara, K., et al. (2017). Postnatal Lethality and Chondrodysplasia in Mice Lacking Both Chondroitin Sulfate *N*-Acetylgalactosaminyltransferase-1 and -2. *PLoS One* 12, e0190333. doi:10.1371/journal.pone.0190333

Sivasami, P., Poudel, N., Munteanu, M. C., Hudson, J., Lovern, P., Liu, L., et al. (2019). Adipose Tissue Loss and Lipodystrophy in Xylosyltransferase II Deficient Mice. *Int. J. Obes.* 43, 1783–1794. doi:10.1038/s41366-019-0324-1

Smith, T. M., Hicks-Berger, C. A., Kim, S., and Kirley, T. L. (2002). Cloning, Expression, and Characterization of a Soluble Calcium-Activated Nucleotidase, a Human Enzyme Belonging to a New Family of Extracellular Nucleotidases. *Arch. Biochem. Biophys.* 406, 105–115. doi:10.1016/s0003-9861(02)00420-4

Sorg, B. A., Berretta, S., Blacktop, J. M., Fawcett, J. W., Kitagawa, H., Kwok, J. C. F., et al. (2016). Casting a Wide Net: Role of Perineuronal Nets in Neural Plasticity. *J. Neurosci.* 36, 11459–11468. doi:10.1523/JNEUROSCI.2351-16.2016

Spicer, A. P., Kaback, L. A., Smith, T. J., and Seldin, M. F. (1998). Molecular Cloning and Characterization of the Human and Mouse UDP-Glucose Dehydrogenase Genes. *J. Biol. Chem.* 273, 25117–25124. doi:10.1074/jbc.273.39.25117

Stachtea, X. N., Tykesson, E., van Kuppevelt, T. H., Feinstein, R., Malmström, A., Reijmers, R. M., et al. (2015). Dermatan Sulfate-free Mice Display Embryological Defects and Are Neonatal Lethal Despite normal Lymphoid and Non-lymphoid Organogenesis. *PLoS One* 10, e0140279. doi:10.1371/journal.pone.0140279

Stickens, D., Zak, B. M., Rougier, N., Esko, J. D., and Werb, Z. (2005). Mice Deficient in Ext2 Lack Heparan Sulfate and Develop Exostoses. *Development* 132, 5055–5068. doi:10.1242/dev.02088

Sugahara, K., and Kitagawa, H. (2000). Recent Advances in the Study of the Biosynthesis and Functions of Sulfated Glycosaminoglycans. *Curr. Opin. Struct. Biol.* 10, 518–527. doi:10.1016/s0959-440x(00)00125-1

Sugahara, K., and Mikami, T. (2007). Chondroitin/dermatan Sulfate in the central Nervous System. *Curr. Opin. Struct. Biol.* 17, 536–545. doi:10.1016/j.sbi.2007.08.015

Sugahara, K., Mikami, T., Uyama, T., Mizuguchi, S., Nomura, K., and Kitagawa, H. (2003). Recent Advances in the Structural Biology of Chondroitin Sulfate and Dermatan Sulfate. *Curr. Opin. Struct. Biol.* 13, 612–620. doi:10.1016/j.sbi.2003.09.011

Sugahara, K. N., Hirata, T., Tanaka, T., Ogino, S., Takeda, M., Terasawa, H., et al. (2008). Chondroitin Sulfate E Fragments Enhance CD44 Cleavage and CD44-dependent Motility in Tumor Cells. *Cancer Res.* 68, 7191–7199. doi:10.1158/0008-5472.CAN-07-6198

Sugahara, K., and Schwartz, N. B. (1979). Defect in 3'-phosphoadenosine 5'-phosphosulfate Formation in Brachymorphic Mice. *Proc. Natl. Acad. Sci.* 76, 6615–6618. doi:10.1073/pnas.76.12.6615

Sugahara, K., and Schwartz, N. B. (1982b). Defect in 3'-phosphoadenosine 5'-phosphosulfate Synthesis in Brachymorphic Mice. II. Tissue Distribution of the Defect. *Arch. Biochem. Biophys.* 214, 602–609. doi:10.1016/0003-9861(82)90065-0

Sugahara, K., and Schwartz, N. B. (1982a). Defect in 3′-phosphoadenosine 5′-phosphosulfate Synthesis in Brachymorphic Mice. *Arch. Biochem. Biophys.* 214, 589–601. doi:10.1016/0003-9861(82)90064-9

Sugiyama, S., Di Nardo, A. A., Aizawa, S., Matsuo, I., Volovitch, M., Prochiantz, A., et al. (2008). Experience-dependent Transfer of Otx2 Homeoprotein into the Visual Cortex Activates Postnatal Plasticity. *Cell* 134, 508–520. doi:10.1016/j.cell.2008.05.054

Sun, X., Meyers, E. N., Lewandoski, M., and Martin, G. R. (1999). Targeted Disruption of Fgf8 Causes Failure of Cell Migration in the Gastrulating Mouse Embryo. *Genes Dev.* 13, 1834–1846. doi:10.1101/gad.13.14.1834

Takemae, H., Ueda, R., Okubo, R., Nakato, H., Izumi, S., Saigo, K., et al. (2003). Proteoglycan UDP-Galactose:β-Xylose β1,4-Galactosyltransferase I Is Essential for Viability in Drosophila Melanogaster. *J. Biol. Chem.* 278, 15571–15578. doi:10.1074/jbc.M301123200

Takemura, M., Noborn, F., Nilsson, J., Bowden, N., Nakato, E., Baker, S., et al. (2020). Chondroitin Sulfate Proteoglycan Windpipe Modulates Hedgehog Signaling in Drosophila. *Mol. Biol. Cell* 31, 813–824. doi:10.1091/mbc.E19-06-0327

Takeuchi, K., Yoshioka, N., Higa Onaga, S., Watanabe, Y., Miyata, S., Wada, Y., et al. (2013). Chondroitin Sulphate *N*-Acetylgalactosaminyl-Transferase-1 Inhibits Recovery from Neural Injury. *Nat. Commun.* 4, 2740. doi:10.1038/ncomms3740

Tang, T., Li, L., Tang, J., Li, Y., Lin, W. Y., Martin, F., et al. (2010). A Mouse Knockout Library for Secreted and Transmembrane Proteins. *Nat. Biotechnol.* 28, 749–755. doi:10.1038/nbt.1644

ten Dam, G. B., van de Westerlo, E. M. A., Purushothaman, A., Stan, R. V., Bulten, J., Sweep, F. C. G. J., et al. (2007). Antibody GD3G7 Selected against Embryonic Glycosaminoglycans Defines Chondroitin Sulfate-E Domains Highly Up-Regulated in Ovarian Cancer and Involved in Vascular Endothelial Growth Factor Binding. *Am. J. Pathol.* 171, 1324–1333. doi:10.2353/ajpath.2007.070111

ten Dam, G. B., Yamada, S., Kobayashi, F., Purushothaman, A., Westerlo, E. M. A., Bulten, J., et al. (2009). Dermatan Sulfate Domains Defined by the Novel Antibody GD3A12, in normal Tissues and Ovarian Adenocarcinomas. *Histochem. Cell Biol.* 132, 117–127. doi:10.1007/s00418-009-0592-2

Thelin, M. A., Bartolini, B., Axelsson, J., Gustafsson, R., Tykesson, E., Pera, E., et al. (2013). Biological Functions of Iduronic Acid in Chondroitin/dermatan Sulfate. *FEBS J.* 280, 2431–2446. doi:10.1111/febs.12214

Thelin, M. A., Svensson, K. J., Shi, X., Bagher, M., Axelsson, J., Isinger-Ekstrand, A., et al. (2012). Dermatan Sulfate Is Involved in the Tumorigenic Properties of Esophagus Squamous Cell Carcinoma. *Cancer Res.* 72, 1943–1952. doi:10.1158/0008-5472.CAN-11-1351

Tian, J., Ling, L., Shboul, M., Lee, H., O'Connor, B., Merriman, B., et al. (2010). Loss of CHSY1, a Secreted FRINGE Enzyme, Causes Syndromic Brachydactyly in Humans via Increased NOTCH Signaling. *Am. J. Hum. Genet.* 87, 768–778. doi:10.1016/j.ajhg.2010.11.005

Tone, Y., Pedersen, L. C., Yamamoto, T., Izumikawa, T., Kitagawa, H., Nishihara, J., et al. (2008). 2-*O*-phosphorylation of Xylose and 6-*O*-Sulfation of Galactose in the Protein Linkage Region of Glycosaminoglycans Influence the Glucuronyltransferase-I Activity Involved in the Linkage Region Synthesis. *J. Biol. Chem.* 283, 16801–16807. doi:10.1074/jbc.M709556200

Trowbridge, J. M., and Gallo, R. L. (2002). Dermatan Sulfate: New Functions from an Old Glycosaminoglycan. *Glycobiology* 12, 117R–125R. doi:10.1093/glycob/cwf066

Tykesson, E., Hassinen, A., Zielinska, K., Thelin, M. A., Frati, G., Ellervik, U., et al. (2018). Dermatan Sulfate Epimerase 1 and Dermatan 4-*O*-Sulfotransferase 1 Form Complexes that Generate Long Epimerized 4-*O*-Sulfated Blocks. *J. Biol. Chem.* 293, 13725–13735. doi:10.1074/jbc.RA118.003875

Uchimura, K., Kadomatsu, K., Fan, Q.-W., Muramatsu, H., Kurosawa, N., Kaname, T., et al. (1998). Mouse Chondroitin 6-sulfotransferase: Molecular Cloning, Characterization and Chromosomal Mapping. *Glycobiology* 8, 489–496. doi:10.1093/glycob/8.5.489

Uchimura, K., Kadomatsu, K., Nishimura, H., Muramatsu, H., Nakamura, E., Kurosawa, N., et al. (2002). Functional Analysis of the Chondroitin 6-sulfotransferase Gene in Relation to Lymphocyte Subpopulations, Brain Development, and Oversulfated Chondroitin Sulfates. *J. Biol. Chem.* 277, 1443–1450. doi:10.1074/jbc.M104719200

Uyama, T., Kitagawa, H., Tamura, J.-i., and Sugahara, K. (2002). Molecular Cloning and Expression of Human ChondroitinN-Acetylgalactosaminyltransferase. *J. Biol. Chem.* 277, 8841–8846. doi:10.1074/jbc.M111434200

Uyama, T., Kitagawa, H., Tanaka, J., Tamura, J.-i., Ogawa, T., and Sugahara, K. (2003). Molecular Cloning and Expression of a Second Chondroitin *N*-Acetylgalactosaminyltransferase Involved in the Initiation and Elongation of Chondroitin/dermatan Sulfate. *J. Biol. Chem.* 278, 3072–3078. doi:10.1074/jbc.M209446200

Venkatachalam, K. V. (2003). Human 3′-phosphoadenosine 5′-phosphosulfate (PAPS) Synthase: Biochemistry, Molecular Biology and Genetic Deficiency. *IUBMB Life (International Union Biochem. Mol. Biol. Life)* 55, 1–11. doi:10.1080/1521654031000072148

Voermans, N. C., Kempers, M., Lammens, M., van Alfen, N., Janssen, M. C., Bönnemann, C., et al. (2012). Myopathy in a 20-Year-Old Female Patient with D4ST-1 Deficient Ehlers-Danlos Syndrome Due to a Homozygous CHST14 Mutation. *Am. J. Med. Genet.* 158A, 850–855. doi:10.1002/ajmg.a.35232

Watanabe, Y., Takeuchi, K., Higa Onaga, S., Sato, M., Tsujita, M., Abe, M., et al. (2010). Chondroitin Sulfate *N*-Acetylgalactosaminyltransferase-1 Is Required for normal Cartilage Development. *Biochem. J.* 432, 47–55. doi:10.1042/BJ20100847

Wei, L., Cao, P., Xu, C., Zhong, H., Wang, X., Bai, M., et al. (2020). Chondroitin Synthase-3 Regulates Nucleus Pulposus Degeneration through Actin-induced YAP Signaling. *FASEB J.* 34, 16581–16600. doi:10.1096/fj.202001021R

Wilson, D. G., Phamluong, K., Lin, W. Y., Barck, K., Carano, R. A. D., Diehl, L., et al. (2012). Chondroitin Sulfate Synthase 1 (Chsy1) Is Required for Bone Development and Digit Patterning. *Dev. Biol.* 363, 413–425. doi:10.1016/j.ydbio.2012.01.005

Witkos, T. M., and Lowe, M. (2017). Recognition and Tethering of Transport Vesicles at the Golgi Apparatus. *Curr. Opin. Cell Biol.* 47, 16–23. doi:10.1016/j.ceb.2017.02.003

Wu, J., Tian, Y., Han, L., Liu, C., Sun, T., Li, L., et al. (2020). FAM20B-catalyzed Glycosaminoglycans Control Murine Tooth Number by Restricting FGFR2b Signaling. *BMC Biol.* 18, 87. doi:10.1186/s12915-020-00813-4

Yada, T., Gotoh, M., Sato, T., Shionyu, M., Go, M., Kaseyama, H., et al. (2003a). Chondroitin Sulfate Synthase-2. *J. Biol. Chem.* 278, 30235–30247. doi:10.1074/jbc.M303657200

Yada, T., Sato, T., Kaseyama, H., Gotoh, M., Iwasaki, H., Kikuchi, N., et al. (2003b). Chondroitin Sulfate Synthase-3. *J. Biol. Chem.* 278, 39711–39725. doi:10.1074/jbc.M304421200

Yamada, S., and Sugahara, K. (2008). Potential Therapeutic Application of Chondroitin Sulfate/dermatan Sulfate. *Curr. Drug Discov. Technol.* 5, 289–301. doi:10.2174/157016308786733564

Yamaguchi, T. P., Harpal, K., Henkemeyer, M., and Rossant, J. (1994). Fgfr-1 Is Required for Embryonic Growth and Mesodermal Patterning during Mouse Gastrulation. *Genes Dev.* 8, 3032–3044. doi:10.1101/gad.8.24.3032

Yamaguchi, Y. (2001). Heparan Sulfate Proteoglycans in the Nervous System: Their Diverse Roles in Neurogenesis, Axon Guidance, and Synaptogenesis. *Semin. Cell Dev. Biol.* 12, 99–106. doi:10.1006/scdb.2000.0238

Yamauchi, S., Mita, S., Matsubara, T., Fukuta, M., Habuchi, H., Kimata, K., et al. (2000). Molecular Cloning and Expression of Chondroitin 4-sulfotransferase. *J. Biol. Chem.* 275, 8975–8981. doi:10.1074/jbc.275.12.8975

Yoshioka, N., Miyata, S., Tamada, A., Watanabe, Y., Kawasaki, A., Kitagawa, H., et al. (2017). Abnormalities in Perineuronal Nets and Behavior in Mice Lacking CSGalNAcT1, a Key Enzyme in Chondroitin Sulfate Synthesis. *Mol. Brain* 10, 47. doi:10.1186/s13041-017-0328-5

Yoshizawa, T., Mizumoto, S., Takahashi, Y., Shimada, S., Sugahara, K., Nakayama, J., et al. (2018). Vascular Abnormalities in the Placenta of Chst14−/− Fetuses: Implications in the Pathophysiology of Perinatal Lethality of the Murine Model and Vascular Lesions in Human CHST14/D4ST1 Deficiency. *Glycobiology* 28, 80–89. doi:10.1093/glycob/cwx099

Zheng, Y., and Pan, D. (2019). The Hippo Signaling Pathway in Development and Disease. *Dev. Cell* 50, 264–282. doi:10.1016/j.devcel.2019.06.003

**Conflict of Interest:** The authors declare that the research was conducted in the absence of any commercial or financial relationships that could be construed as a potential conflict of interest.

**Publisher's Note:** All claims expressed in this article are solely those of the authors and do not necessarily represent those of their affiliated organizations, or those of the publisher, the editors and the reviewers. Any product that may be evaluated in this article, or claim that may be made by its manufacturer, is not guaranteed or endorsed by the publisher.

frontiers | Frontiers in Cell and Developmental Biology

REVIEW
published: 08 April 2022
doi: 10.3389/fcell.2022.745372

# Roles of Chondroitin Sulfate Proteoglycans as Regulators of Skeletal Development

*Nancy B. Schwartz*[1,2]* *and Miriam S. Domowicz*[1]

[1]Department of Pediatrics, Biological Sciences Division, The University of Chicago, Chicago, IL, United States, [2]Department of Biochemistry and Molecular Biology, Biological Sciences Division, The University of Chicago, Chicago, IL, United States

The extracellular matrix (ECM) is critically important for most cellular processes including differentiation, morphogenesis, growth, survival and regeneration. The interplay between cells and the ECM often involves bidirectional signaling between ECM components and small molecules, i.e., growth factors, morphogens, hormones, etc., that regulate critical life processes. The ECM provides biochemical and contextual information by binding, storing, and releasing the bioactive signaling molecules, and/or mechanical information that signals from the cell membrane integrins through the cytoskeleton to the nucleus, thereby influencing cell phenotypes. Using these dynamic, reciprocal processes, cells can also remodel and reshape the ECM by degrading and re-assembling it, thereby sculpting their environments. In this review, we summarize the role of chondroitin sulfate proteoglycans as regulators of cell and tissue development using the skeletal growth plate model, with an emphasis on use of naturally occurring, or created mutants to decipher the role of proteoglycan components in signaling paradigms.

**Keywords: growth plate, signaling factors, chondrogenesis, degradation, regeneration, proteoglycans**

OPEN ACCESS

***Edited by:***
*Jesus Chimal-Monroy, Universidad Nacional Autónoma de México, Mexico*

***Reviewed by:***
*X. Lucas Lu, University of Delaware, United States*
*Shinji Miyata, Tokyo University of Agriculture and Technology, Japan*
*Achilleas D. Theocharis, University of Patras, Greece*
*Hiroshi Kitagawa, Kobe Pharmaceutical University, Japan*

***Correspondence:**
*Nancy B. Schwartz*
*n-schwartz@uchicago.edu*

***Specialty section:***
*This article was submitted to Signaling, a section of the journal Frontiers in Cell and Developmental Biology*

***Received:*** *22 July 2021*
***Accepted:*** *21 March 2022*
***Published:*** *08 April 2022*

***Citation:***
*Schwartz NB and Domowicz MS (2022) Roles of Chondroitin Sulfate Proteoglycans as Regulators of Skeletal Development. Front. Cell Dev. Biol. 10:745372. doi: 10.3389/fcell.2022.745372*

## INTRODUCTION

Proteoglycans, complex macromolecules that are prominent constituents of the ECM composed of a protein core to which are covalently attached variable length and composition glycosaminoglycan (GAG) chains (Schwartz, 2000). Because of their complex structure and chemistry, proteoglycans have been classified based on function, localization, and protein cores. To date, forty-three distinct proteoglycan-encoding genes have been identified, and are organized into four families based on their cellular and subcellular location, protein and genomic homologies, and unique protein modules shared by members of each specific family (Iozzo and Schaefer, 2015). Most proteoglycans interact with signaling molecules in multiple biological processes i.e., tissue development, wound healing and disease progression. These interactions are complex and often multivalent involving contributions by nonionic (hydrogen-bonding, Van der Waals and hydrophobic) forces, conformational changes, or clustering of binding complexes (Soares da Costa et al., 2017), or the ability of signaling factors to multimerize (Whalen et al., 2013). Among the families of sulfated proteoglycans, the heparan sulfate proteoglycans (HSPGs) are the best studied in terms of biointeractions with diverse ligands and various signaling molecules affecting cell behavior. A major ionic interaction is that between the carboxyl and sulfate groups in the GAG chains and positively charged amino acid (lysine and arginine) residues (Cardin-Weintraub sequence) in the N-terminal region of all hedgehog (HH) signaling molecules (Cardin and Weintraub, 1989) including sonic (SHH), indian (IHH) and desert (DHH). In addition to the HHs, proteoglycans with different modification patterns also function in

fibroblast growth factor (FGF), wingless (WNT), transforming growth factor (TGFβ), chemokines and Slit/Robo signaling (Townley and Bulow, 2018).

## CHONDROITIN SULFATE PROTEOGLYCANS

In contrast to the HSPGs, the interactions of signaling molecules with chondroitin sulfate and dermatan sulfate proteoglycans (CSPG and DSPG), which are the focus of this review and are often the most abundant proteoglycans in tissues, are not as well understood. Chondroitin sulfate (CS) chains are found on multiple proteoglycans; the most common are the hyaluronan- and lectin-binding proteoglycans (hyalectans) which have structural similarity at both the protein and genomic levels. The hyalectan family consists of four members: aggrecan, versican, neurocan, and brevican, which all share a tri-domain structure: an N-terminal globular domain that binds hyaluronan, a central domain bearing the CS chains and a C-terminal region that binds lectins. The CS chains consist of repeating disaccharides of N-acetylgalactosamine (GalNAc) and glucuronic acid (GlcA) decorated with different degrees and patterns of sulfation on the disaccharides: GalNAc may have sulfate on C4 (CS-A), C6 (CS-C) or both C4 and C6 (CS-E), all catalyzed by specific sulfotransferases. The GlcA unit may also be sulfated on the C2 position (CS-B or CS-D) depending on where the sulfate residue is on GalNAc. Dermatan sulfate (DS) derives from chondroitin sulfate by inversion of GlcA to iduronic acid (IdA), catalyzed by an epimerase enzyme.

## DEFINING THE ROLE OF PROTEOGLYCANS IN SIGNALING PATHWAYS DURING DEVELOPMENT

Determining direct relationships between proteoglycan structure/function and the bi-directional signaling that regulates development remains challenging, mainly because few tools exist that allow alteration or removal of specific GAG motifs or sulfate substitutions. However, some progress has been made using *in vitro* and *in vivo* approaches. Although general principles of CSPG interaction with signaling molecules have been shown in several developing tissue systems, we use as example the formation of skeletal structures with a focus on the growth plate of long bones, a transient cartilage template that is, replaced by bone. A complex and highly orchestrated program regulates growth plate cartilage morphogenesis in which chondroblasts proliferate, differentiate to chondrocytes, alter their shape, proliferate in stacks along the longitudinal axis, terminally differentiate to hypertrophic chondrocytes, and elaborate a mineralized vascularized matrix, which is then replaced by osteocytes (Karsenty and Wagner, 2002; Kozhemyakina et al., 2015). Multiple signaling pathways control the growth plate morphogenesis process including: IHH, FGF, TGFβ, bone morphogenic protein (BMP), parathyroid hormone-related peptide (PTHrP), SMAD6 and SMURF, all of which play unique and sometimes interacting roles in growth plate morphogenesis (Wang et al., 2021) (**Figure 1A**).

Some well documented examples of the mechanisms by which signaling pathways are necessary for cartilage morphogenesis are illustrated in **Figure 1A** and include the IHH-PTHrP negative feedback loop which regulates the size of the proliferative zone and onset of hypertrophy (Vortkamp, 2001). PTHrP, secreted by the resting zone, preserves the reservoir of progenitor cells and promotes chondrocyte proliferation by interacting with IHH secreted by hypertrophic chondrocytes (Mizuhashi et al., 2018). Conversely, IHH antagonizes PTHrP signaling and promotes chondrocyte hypertrophy in the lower segment of the growth plate (Lee et al., 2019). Members of the TGFβ family promote chondrogenesis in undifferentiated mesenchyme cultures (Karsenty and Wagner, 2002), while long bone chondrocyte proliferation and hypertrophy is inhibited by TGFβ (Serra and Chang, 2003). Targeted deletion of the TGFβ2 gene product alters the overall size and shape of limb rudiments (Sanford et al., 1997), and naturally occurring mutations in the TGFβ2 gene cause Camurati-Engelmann Disease, characterized by thickening of the long bone collar (Campos-Xavier et al., 2001). Another major signaling family, the BMPs, positively regulate both chondrocyte proliferation and hypertrophy (Horiki et al., 2004), as shown in mice with mutations in the BMP receptor type 1B that develop brachyactyly (Baur et al., 2000), and in mice which over-express SMAD and SMURF (negative regulators of BMP signaling), leading to chondrocyte hypertrophy and dwarfism (Horiki et al., 2004). The patterning of bone and joints also requires the interaction of multiple signaling pathways, including BMP members, HH, WNT, and FGF families (Archer et al., 2003; Baldridge et al., 2010). Thus, as these examples illustrate, the processes of cartilage, bone, and joint development is dependent on multiple morphogens, growth factors, and cytokines. However, understanding the role of CSPGs, the major proteoglycans in the growth plate, in influencing the functions of these signaling molecules and pathways during skeletal development remains limited. In this review we provide evidence of the roles by which each major feature (core protein, GAG chains, sulfation) of proteoglycans contribute to regulation of chondrogenesis (**Figure 2**).

## ROLE OF CSPG CORE PROTEIN

Several studies have described critical roles for CSPGs such as aggrecan, which is broadly expressed by chondrocytes, and versican, which is transiently expressed in undifferentiated mesenchyme, in chondrogenesis and joint morphogenesis (Schwartz and Domowicz, 2002; Snow et al., 2005; Shepard et al., 2007; Domowicz et al., 2009; Choocheep et al., 2010; Lauing et al., 2014). For most of these studies, mutant models of proteoglycan biosynthesis and metabolism have helped to unravel the role of proteoglycans in skeletal formation and maintenance. In fact, the strongest evidence that CSPGs are essential during differentiation of chondrocytes and

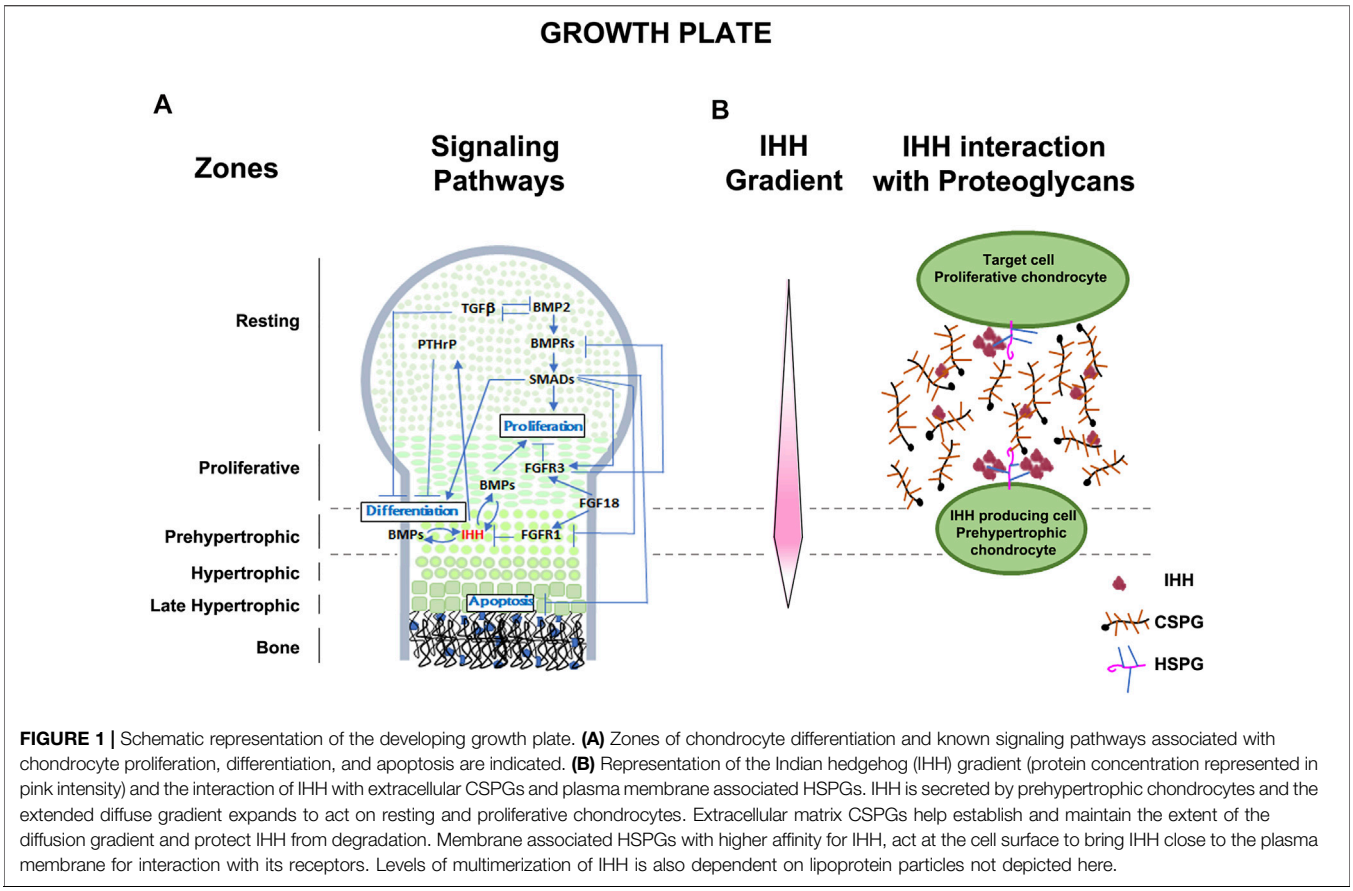


**FIGURE 1 |** Schematic representation of the developing growth plate. **(A)** Zones of chondrocyte differentiation and known signaling pathways associated with chondrocyte proliferation, differentiation, and apoptosis are indicated. **(B)** Representation of the Indian hedgehog (IHH) gradient (protein concentration represented in pink intensity) and the interaction of IHH with extracellular CSPGs and plasma membrane associated HSPGs. IHH is secreted by prehypertrophic chondrocytes and the extended diffuse gradient expands to act on resting and proliferative chondrocytes. Extracellular matrix CSPGs help establish and maintain the extent of the diffusion gradient and protect IHH from degradation. Membrane associated HSPGs with higher affinity for IHH, act at the cell surface to bring IHH close to the plasma membrane for interaction with its receptors. Levels of multimerization of IHH is also dependent on lipoprotein particles not depicted here.

maintenance of skeletal elements rests on the demonstration of abnormalities in CSPGs concomitant with aberrant growth patterns in human and animal models (Melvin and Schwartz, 1988; Schwartz and Domowicz, 1998). In particular, mutations in the aggrecan gene are the cause of several chondrodysplasias and inherited skeletal disorders in humans and animals (Schwartz and Domowicz, 2002; Schwartz and Domowicz, 2014). Mutations in the aggrecan core protein gene have been identified in human skeletal disorders including: spondyloepimetaphyseal dysplasia with premature and severe osteoarthritis and osteochondritis (Gleghorn et al., 2005) and the recessive skeletal dysplasia EMD aggrecan-type which results from a missence mutation affecting the C-type lectin domain of aggrecan (Tompson et al., 2009; Stattin et al., 2010). To date, eight human genetic diseases involving defects in aggrecan, now coined the aggrecanopathies (Gibson and Briggs, 2016) have been identified, but the impact of these aggrecan defects on signaling in humans has not yet been fully explored.

One of the earliest studied animal models was nanomelia (*nm*), a lethal chondrodystrophy of fowl (Landauer, 1965). The *nanomelic* chick cartilage can synthesize CS chains, but aggrecan core protein is absent due to a single nucleotide change that results in a premature stop codon in the aggrecan gene (Argraves et al., 1981; Li et al., 1993; Schwartz et al., 1993; Vertel et al., 1994). This severely truncated core protein is not glycosylated or transported through the secretory pathway leading to an altered cytoarchitecture (densely packed cellular growth plate devoid of matrix) and homeostasis (increased proliferation of hypertrophic chondrocytes and increased cell death in the proliferative zone) (Domowicz et al., 2000). Since all of these phenotypes are regulated by signaling pathways, these aggrecan mutants present ideal models for investigating the core protein interactions with growth plate regulators. Thus, further studies documented that loss of aggrecan results in defects in morphogen gradient distribution and gene expression profiles of the critical chondrocyte regulators (IHH, BMP, and FGF) (Domowicz et al., 2009; Schwartz and Domowicz, 2014).

A similar lethal mutation in the aggrecan genes of the cartilage-matrix deficiency (*cmd*) mouse is due to a 7-bp deletion in exon 5, resulting in a premature stop codon and no aggrecan product (Watanabe et al., 1994). A second mutation within the same locus and generating a similar phenotype, $cmd^{bc}$, has been identified as the complete loss of exon 2 to 18, resulting in a significantly shortened mRNA and production of no aggrecan core protein (Krueger et al., 1999). In a landmark study, a novel transgenic mouse line (Tg COL2A1-ACAN) expressing a chick ACAN coding sequence driven by the mouse *Col2A1* promoter has enabled the generation of cmdbc/cmdbc; Tg (COL2A1-ACAN) rescue embryos (Lauing et al., 2014). Robust re-expression of aggrecan in rescue embryos reversed the defects in different skeletal elements to varying degrees, most notably the reappearance of a hypertrophic zone

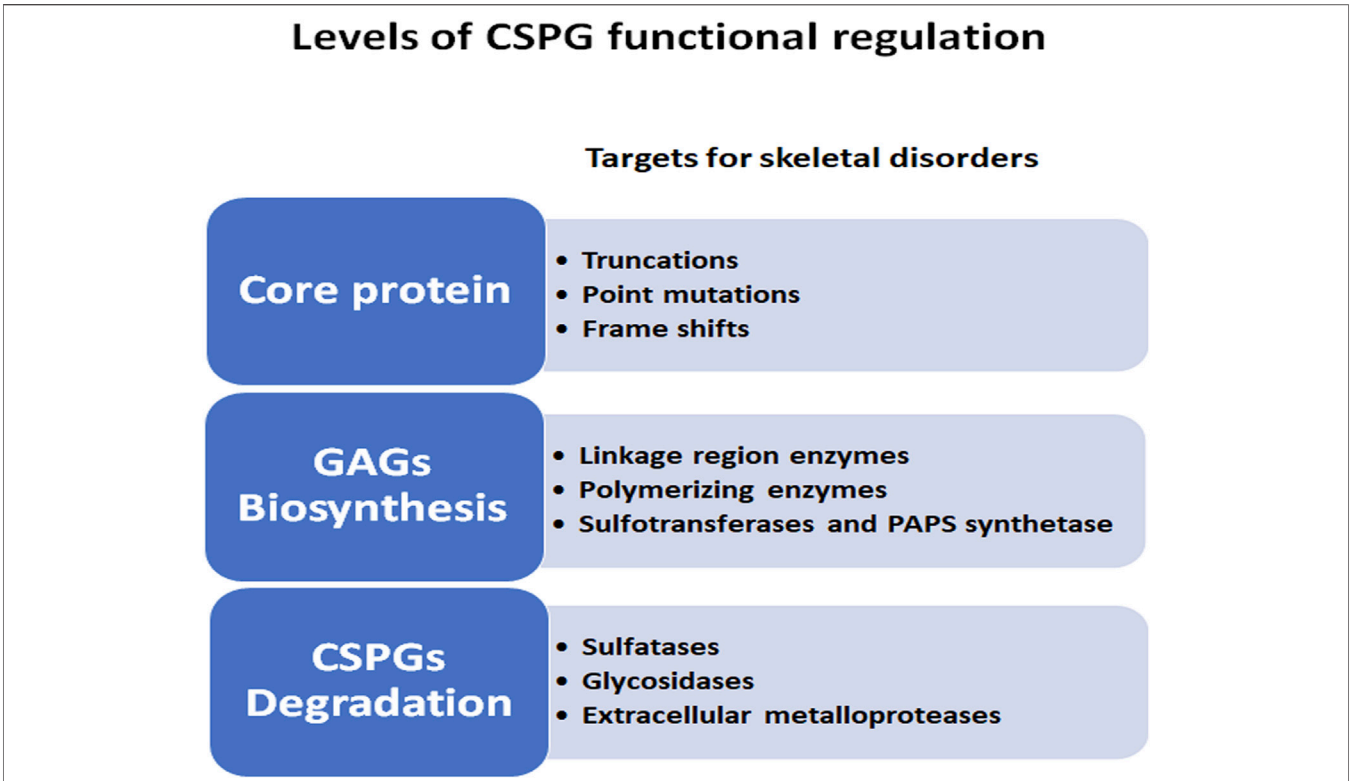


**FIGURE 2 |** Levels of CSPG functional regulations during skeletal development. CSPG complexity is illustrated by the multiple levels at which the synthesis and degradation of these molecules can affect the outcome of normal growth plate development.

and production of *Col2a1* and *Col10a1* in the limb growth plate. As well, transgene expression in rescue mice restored: i) Sox9 expression in resting and proliferative zones similar to wild type; ii) an increase in *Ihh* mRNA production in more chondrocytes in the pre-hypertrophic region; iii) relatively normal expression of *Ptch1*, the receptor of IHH within the bone marrow near the chondro-osteo junction, perichondrium and proliferative zones similar to wild type; iv) strong re-expression of *Fgfr3*, which encodes the receptor for negative regulators of chondrocyte proliferation such as FGF9 and FGF18 in the proliferative and early hypertrophic zones of the growth plate; all these features closely resemble those found in wild-type embryos. Taken together, the data obtained from RT-PCR, immunochemistry and mRNA *in situ* analyses confirm that the presence of aggrecan in the growth plate ECM is fundamental to maintaining normal expression and spatial localization of the essential signaling molecules that regulate chondrocyte organization, morphology, and maintenance during growth plate development (Lauing et al., 2014) (**Figure 3**).

## ROLE OF GAG CHAIN SYNTHESIS

These cited examples clearly present a requirement for CSPGs as demonstrated by mutations in the core protein, which lead to reduced or total absence of CSPGs. However, the complexity of CS/DSPGs and potential interplay with signaling molecules may also be due to interactions involving the long, linear GAG chains of repeating disaccharide units, as well as the contribution of sulfation components of proteoglycans. GAG chain initiation for CS, DS, HS, and heparin begin with addition of Xyl to a serine hydroxyl embedded in a specific core protein peptide sequence (Bourdon et al., 1987; Krueger et al., 1990), catalyzed by the chain-initiating enzyme xylosytransferase (Kearns et al., 1993; Schwartz, 1995). CS/DSPG GAG chain synthesis continues with addition of two galactose (Gal) residues and a GlcA residue, catalyzed by unique-glycosyltransferases (Schwartz and Rodén, 1974; Schwartz and Roden, 1975; Schwartz, 1976). In contrast to the common linkage region structures shared by most proteoglycans, their structural diversity and functional complexity derives from the long linear unbranched GAG chains comprised of unique repeating disaccharide units, which are then substituted with O- or N- linked sulfate groups. GAG chains engage in regulation of biological processes by interacting with various ligands; however, very little is known about these interactions since structural analysis of GAGs is difficult (Song et al., 2021).

### Xylosylation-Initiation of CS Chains

The first step of GAG chains initiation is catalyzed by one of two paralogs XYLT1 AND XYLT2 (Voglmeir et al., 2007). Interestingly, five homozygous *XYLT1* mutations were reported in individuals with Desbuquois dysplasia (DBQD) type 2, leading to severe chondrodysplasias which suggests a requirement for

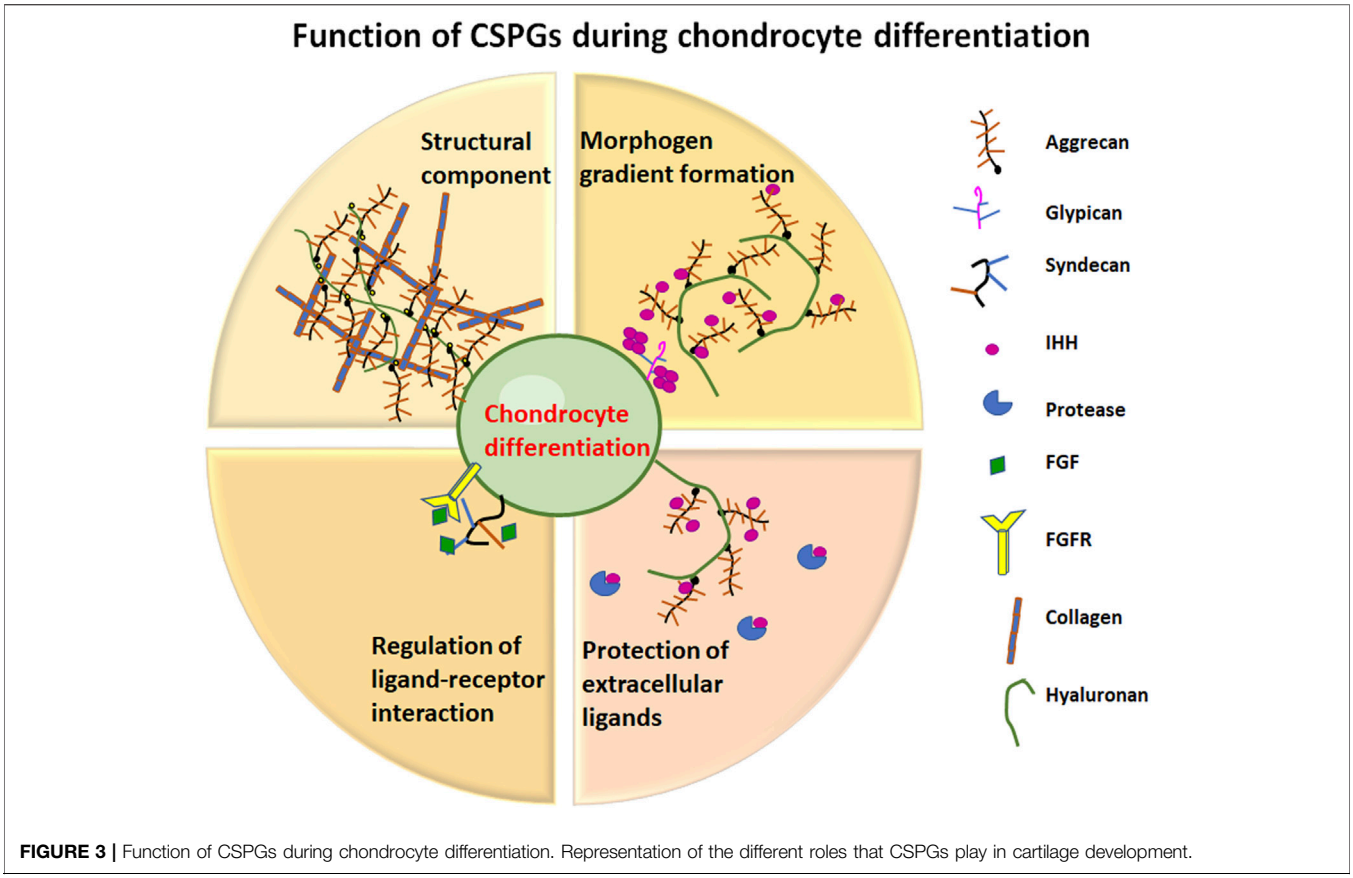


**FIGURE 3 |** Function of CSPGs during chondrocyte differentiation. Representation of the different roles that CSPGs play in cartilage development.

xylosyltransferase during skeletal development (Bui et al., 2014). Sulfate labeling of fibroblast from patients with certain *XYLT1* mutations show predominant sensitivity to CS digestion, suggesting synthesis of CSPGs are affected by partial loss-of-function *XYLT1* (Bui et al., 2014). Another short stature syndrome caused by a homozygous mutation in *XYLT1* exhibited a potential localization defect since the enzyme was diffusely distributed throughout the cytoplasm (Schreml et al., 2014) rather than in the ER and early Golgi (Hoffmann et al., 1984; Vertel et al., 1993). A third type of skeletal disorder, Baratela-Scott syndrome (Baratela et al., 2012) is caused by homozygous mutations in *XYLT1* due to hypermethylation defects (LaCroix et al., 2019). Homozygous mutations in *XYLT2* cause spondyloocular syndrome, which exhibits skeletal defects, as well as ocular, cardiac, auditory system defects, and learning difficulties in patients with this disorder (Munns et al., 2015; Taylan et al., 2016; Taylan et al., 2017; Umair et al., 2018). The different clinical manifestations of *XYLT1* and *XYLT2* disorders, suggest potential functional distinctions between the two enzymes including: use of distinct core protein substrates, differential spatiotemporal expression, and inability to compensate for each other (Mizumoto and Yamada, 2021). These fascinating issues, as well as how signaling pathways are affected as a consequence of these *XYLT* mutations that lead to the devastating phenotypes, remain unexplored in these human hereditary disorders.

A better understanding of the role of xyloxyltransferases has come from the study of an animal model with a xylosyltransferase mutation. The phenotype of the "*pug*" mouse has a missense mutation in *Xylt1*, resulting in skeletal abnormalities (Mis et al., 2014). This recessive dwarf mouse mutant (*pug*) was identified from an N-ethyl-N-nitrosourea (ENU) mutagenesis screen, and exhibits reduced skeletal element lengths, normal growth plate patterning and no change in chondrocyte proliferation; however, *pug* mutants display premature maturation and early ossification leading to the disproportionate dwarfism. The mutation in *Xylt1* disrupts enzyme activity and leads to reduction in the number of GAG chains in *pug* mutant proteoglycans. Furthermore, XYTL1 was mislocalized as it was not observed in the cis-Golgi as previously shown in wild type mice (Kearns et al., 1993; Vertel et al., 1993; Muller et al., 2006; Schön et al., 2006). Thus, this model provides a valuable resource for studying the impact of lack of CS-chains on signaling in growth plate development (Mis et al., 2014). As might be expected, decreased XYLT1 activity in *pug* mutants leads to complex signaling defects, since the *Xylt1* mutation affects synthesis of both HSPGs and CSPGs (shown by sulfate labeling). Furthermore, the phenotype described above (delayed chondrocyte maturation) suggests IHH and FGF signaling pathways may be affected. As predicted, an increase in *Fgfr3* levels, but no downstream changes in MAPK signaling were observed. Concomitantly, an up-regulation of short-range IHH signaling was observed, while long-range IHH signaling through PTHrP, which inhibits chondrocyte maturation, was not affected. These results suggest that the premature maturation of *pug* chondrocytes may not be influenced by changes in IHH and

FGF signaling. Rather proteoglycans, in addition to regulating diffusion of key signaling molecules, may provide maturation cues to chondrocytes independent of IHH and FGF signaling. Furthermore, since the *Xylt1* mutation affects both CSPG and HSPG production, the IHH responses also suggest that these two proteoglycans may function differently in regulating diffusion of IHH through the ECM, with CSPGs expanding the IHH diffusion domain and HSPGs restricting the domain. The premature-maturation *pug* phenotype, in the absence of signaling changes, suggests a novel proteoglycan cue that influences timing of chondrocyte maturation (Mis et al., 2014). Although the *pug* mutant mouse shares characteristics with a human dwarfism (Azouz et al., 1998), the skeletal defects appear more severe in the mouse mutant and thus may serve as a potential candidate for as yet unidentified gene defects underlying short stature or dwarfism phenotypes in humans. Most importantly, understanding how signaling pathways are affected in this mutant may lead to potential new therapeutic targets.

## Synthesis of CS, DS, and HS Linkage Region

In addition to the critical importance of xylosyltransferases to initiating the tetrasaccharide linkage region (GlcA-Gal-Gal-Xyl-o-) of CS, DS, and HS, mutations in the other three enzymes also cause hereditary diseases. Compound heterozygous and homozygous mutations in *B4GALT7*, the enzyme that adds the first Gal residue to -serine-o-xyl- cause Ehlers-Danlos syndrome (EDS) spondylodysplastic type 1 (Malfait et al., 2017; Malfait et al., 2020) which is characterized by short stature, muscle hypotonia and bowing of limbs. Because of multiple mutations in the same gene causing differential substrate selectivity and/or intracellular location, patients may exhibit defects in CS, DS, and even HS GAG chains leading to a wide range of symptoms (Salter et al., 2016; Ritelli et al., 2017; Mihalic Mosher et al., 2019). Larsen syndrome of Reunion Island Syndrome is caused by a homozygous mutation in B4GALT7 and exhibits a clinical spectrum that overlaps with EDS spondylodysplastic (Cartault et al., 2015). Compound heterozygous mutations in B3GALT6 encoding GALT-II which transfers the second Gal residue to the growing linkage region, leads to two disorders: Ehlers-Danlos syndrome spondylodysplastic type 2 (Malfait et al., 2013; Nakajima et al., 2013) which produces less CS, DS, and HS, as well as spondyloepimetaphyseal dysplasia (Nakajima et al., 2013), which predominantely reduces HSPG3 (perlecan), while CS- and DSPGs (versican and decorin) levels are normal (Ritelli et al., 2015). Lastly, multiple homozygous or heterozygous mutations, have thus far been identified in the last linkage region enzyme, B3GAT3 that encodes the glucuronosyltransferase which adds a GlcA residue to the Gal-Gal-Xyl- backbone (Budde et al., 2015; Alazami et al., 2016; Byrne et al., 2020). Again, multiple mutations in the same gene affect synthesis of CS, DS, and HS to varying degrees and lead to syndromes with a broad spectrum of phenotypes (Larsen-like syndrome B3GAT3 type, Spondyloepipheseal dysplasia with congenital joint dislocation and Pseudodiastrophic dysplasia). Unfortunately, no information is yet available on identifying affected signaling pathways, which are required to understand the underlying pathogenic mechanisms.

## GAG Chain Elongation

Following synthesis of the CSPG linkage region, the linear repeating disaccharide units of GalNAC and GlcUA are added, catalyzed by glycosyltransferases that work in concert with sulfotransferases to accomplish polymer elongation and sulfation (Silbert and Sugumaran, 1995; Schwartz, 2000; Schwartz, 2014). Chondroitin sulfate synthase1 (CHSY1) is one of six glycosyltransferases involved in CS chain elongation (Kitagawa et al., 2001). Although all six enzymes are localized to the site of CSPG synthesis only CHSY1, CHSY2 and chondroitin sulfate glucuronyltransferase (CHPF2) catalyze addition of GalNAC and GlcUA saccharide units to elongate CS and DS. These enzymes are co-expressed with aggrecan in the pre-hypertrophic zone of embryonic growth plates (Sakai et al., 2007). Loss of function mutations at the Chsy1 locus have been identified in human Syndromic recessive preaxial brachydactyly (Li et al., 2010; Tian et al., 2010). Mouse mutants for the three CS/DS elongation enzymes have been generated; only *Chsy1−/−* exhibited brachypodism with a patterning defect in distal phalangeal elements, achondrodysplasia and decreased bone density, caused by a reduction in CS chains and a shift in cell orientation. Transcriptome analyses of candidate genes implicated in joint formation, as well as *in vivo* analysis of growth factor signaling by FGF, TGFβ, BMP, WNT3A, NOTCH and HH in mouse embryonic fibroblasts (MEPs) and primary chondrocytes, suggested that IHH distribution was altered and that mutant MEPs are more sensitive to HH stimulation. Together these findings suggest that IHH signaling is disrupted, but differences in signaling may be secondary to changes in chondrocyte orientation (Wilson et al., 2012).

# ROLE OF SULFATION

Lastly, the impact of sulfation molecular diversity and patterning of CS/DS chains on signaling have also been investigated. Sulfation is particularly influential in GAG cross talk either indirectly by regulating protein folding via steric hindrance, exclusion or recruitment, or directly through electrostatic interactions that often are sequence specific. In the skeleton, sulfation plays two main roles: to generate osmotic swelling pressure which enables cartilage to withstand compressive loads and to foster direct cell-proteoglycan interactions with specific growth factors or signaling molecules. Interestingly, sulfation patterns change with maturation of cartilage (Bayliss et al., 1999) with an increasing ratio of CS-6 to CS-4 sulfated GAG chains and a diminished sensitivity to TGFβ (Hickery et al., 2003). Similarly, changes in sulfation patterns greatly influence skeletal development and maintenance by altering interactions with systemic soluble factors (IHH, PTH, FGFs, TGFβ and BMPs) (Klüppel et al., 2005), verifying that imbalance in GAG sulfation can modify the functioning of these signaling pathways. As mentioned, several sulfotransferases are involved in the 4- and 6- sulfation of GalNAC units and the GlcA unit. Examples of altered GAG sulfation involving sulfotransferases that cause abnormalities have been identified for both: mutations in

chondroitin-6-sulfotransferase-1 (C6ST-1) which are associated with chondrodysplasia and progressive spinal involvement (Thiele et al., 2004), while mice deficient in chondroitin-4-sulfotransferase (C4ST-1) exhibit a more severe chrondrodysplasia. Detailed analysis of the mutant growth plate showed abnormal CS localization, chondrocyte differentiation and orientation, and strong up-regulation of TGFβ signaling with concomitant down-regulation of BMP signaling (Klüppel et al., 2002; Klüppel et al., 2005).

In addition to sulfotransferase-caused signaling defects, limiting the sulfate substrate for the sulfotransferases, phosphoadenosine phosphosulfate (PAPS), also leads to chondrodystrophies in mice (Orkin et al., 1976; Schwartz et al., 1978; Kurima et al., 1998) and humans (Faiyaz ul Haque et al., 1998). The brachymorphic (*bm*) mouse model (Sugahara and Schwartz, 1979; Sugahara and Schwartz, 1982a; Sugahara and Schwartz, 1982b; Sugahara and Schwartz, 1982c) has a mutation in the PAPSS2 gene which encodes PAPS synthetase 2 (PAPSS2), one of two isoforms in mammals that catalyze the synthesis of the universal sulfate donor (PAPS) (Kurima et al., 1998). At birth, mice are normal size but as development proceeds *bm* mice exhibit a 50% reduction in limb length, 25% reduction in axial skeleton and a normally organized growth plate but with a reduction in all zones (Schwartz et al., 1978). Aggrecan (*Acan*) and *Col10a1* mRNA expression were comparable in wild type and *bm* mutants. In contrast, using a set of antibodies with specificity for all functional sulfate epitopes, immunohistochemistry revealed reduction in CS-4 and CS-6 epitopes and an increase in the CS-0 epitope in the *bm* growth plate EMC, compared to wild type. In contrast, N-sulfated HS showed comparable staining in wild type and *bm* growth plate. These data were verified by FACE and $^{35}$S-sulfate incorporation experiments; only a reduction of sulfate incorporation into CSPGs of the predominantly CS-4 species and no change in HS-sulfate content in *bm* cartilage was observed; establishing the *bm* mouse as an excellent model for investigating the role of under-sulfated CS interactions with signaling molecules during cartilage development (Cortes et al., 2009).

Analysis of growth plate signaling showed that the PTHrP receptor (*Pthr1*) was expressed at high levels in the pre-hypertrophic zone in both *bm* and wild type. In contrast, *Fgfr3* and *Ihh* (expressed in the pre-hypertrophic zone) and its receptor patched (*Ptch1*) expressed in the proliferative zone exhibited decreases in mRNA levels in *bm* cartilage by three methods, mRNA *in situ*, RT-PCR, and immunohistochemistry. In particular, IHH protein was not uniformly distributed between chondrocytes in *bm* samples, rather a restricted diffusion pattern characterized by protein aggregation was observed. The abnormal IHH distribution was verified by crossing *bm* mice with LacZ *Ptch* ± mice and determining the ratio of Gli activator (*Gli1*/*Gli2*) to Gli repressor (*Gli3*) to measure IHH pathway activation (Hilton et al., 2005). Since, a major function of IHH is to regulate chondrocyte proliferation, cell division was assessed. Significant decreases in BrdU-incorporation were observed, especially in the distal proliferative zone which correlates with the region of restricted IHH diffusion and decreased PTCH1 activation, verifying a decrease in cell division due to a disruption in IHH signaling in the under-sulfated *bm* growth plate (Cortes et al., 2009).

As with most previous studies on reciprocal interactions between signaling factors and CSPGs, the results are compelling, but not biochemically definitive. This ultimate goal was accomplished by three direct approaches. First, quantitative binding curves between IHH-alkaline phosphatase (AP) fusion protein and HS and CS GAG chains (with CS-4, CS-6, and unsulfated CS-0 motifs) showed a gradient of binding affinity (Kd) and binding capacity (Bmax) in order: HS, CS-4, CS-6, CS-0. Since CS-4 is the predominant species in postnatal cartilage and the binding affinity and capacity is higher for the CS-4 to CS-0 motif, a reduction in CS-4 is commensurate with abnormal IHH signaling. Secondly, to demonstrate that IHH interacts with CS specifically and does so through the IHH N-terminal Cardin-Weintraub motif, this motif was mutated which resulted in complete loss of binding to both HS and CS chains, suggesting that the interaction between IHH and CS is primarily mediated through this motif. Lastly, a direct interaction between CSPG and IHH-AP was demonstrated by quantitative immunoprecipitation with a specific aggrecan antibody, demonstrating that the major cartilage CSPG, aggrecan, directly interacts with IHH. Taken together, the biochemical and genetic evidence suggest a biological mechanism whereby undersulfated CSPGs result in restricted IHH diffusion through the ECM leading to a reduction in chondrocyte proliferation, which significantly impacts skeletal growth in the *bm* mutant (Cortes et al., 2009).

## SUMMARY OF CSPG STRUCTURAL COMPONENTS IN REGULATION OF ITS SYNTHESIS

In addition to providing the most definitive evidence to date that molecular interactions occur between signaling factors and CSPGs, these landmark studies extend our understanding of the biological consequences of these interactions. First, the severe-to-mild spectrum of chondrodystrophies observed in CSPG-deficient models correlates directly with the location of the mutations in the CSPG synthetic pathway. Absence of aggrecan core protein (*nanomelic* chick and *cmd* mouse) leads to lethal phenotypes (Li et al., 1993; Krueger et al., 1999; Schwartz and Domowicz, 2002), whereas GAG chain addition (*Pug*) or sulfation (*bm*) models present with milder chondrodyplasia phenotypes (Cortes et al., 2009; Wilson et al., 2012; Lauing et al., 2014; Mis et al., 2014). Secondly, these studies provide a rational for the observations in complex ECMs consisting of more than one proteoglycan. In the cartilage matrix, CSPG is the predominant proteoglycan and contains a large number of CS chains per core protein (Krueger et al., 1990), therefore requiring more PAPS to sulfate the CS chains. In contrast, HSPGs contain fewer HS chains to be sulfated (Knox and Whitelock, 2006). However, HS sulfotransferases have higher affinity for PAPS and therefore result in preferential sulfation of HS chains even if PAPSS2 levels are reduced. Furthermore, the *bm* phenotype, in which only CSPG

sulfation is reduced, is opposite of HS synthesis mutants. In particular, in the *Ext1* gene trap mutant, reduction in HS results in an increased range of HH signaling (marked by increases in *Ptch1* and *Pthrp* mRNA), increased chondrocyte proliferation and expansion of the proliferative zone (Koziel et al., 2004). In another study, additional HH binding sites were found using structural approaches (Whalen et al., 2013) that allowed multimerization of HSPGs close to the cell membrane needed for interaction with its receptor, while CSPGs, that are more broadly distributed in the ECM and have a lower affinity for HH, establish formation of the HH gradients, which may expand several cell-lengths from the site of production (Cortes et al., 2009) (**Figure 1B**). Thus, both CSPGs and HSPGs function as IHH modulators, and in concert, influence long-range HH signaling in the ECM growth plate. Third, it is important to highlight that temporal changes in GAG levels or composition are also critical to the mechanistic consequences in growth plate development. For example, reduction in GAGs during the formation of the growth plate (i.e., *nm*, *cmd*, *pug*) leads to accelerated maturation of chondrocytes, while reduction in GAGs in the mature growth plate (i.e., *bm*) leads to changes in morphogen distribution and altered rate of cell division. Lastly, two other mutant mouse models, a Golgi PAP phosphatase (Frederick et al., 2008) and nucleotidase *Jaws/Bpnt2* (Sohaskey et al., 2008) both show only under-sulfated CSPGs and severe chondrodysphasias. All these findings suggest that sulfated CSPGs function in IHH signaling processes independent of HSPGs, and illustrate how bidirectional communication processes are especially important for regulating cell differentiation during normal tissue development (Gjorevski and Nelson, 2009; Clause and Barker, 2013).

## SIGNALING IN CSPG DEGRADATION

As just summarized, many of the major developmental signaling pathways acting on growth plate cell populations function directly and indirectly through CSPGs, which also reciprocally influence the activity of these signaling pathways. As well, defects in CSPG-GAG metabolism has the potential to disrupt the function of essential regulators and is likely a major underlying mechanism for abnormal skeletogenesis progression (Alliston, 2010).

### Mucopolysaccharidoses

The mucopolysaccharide (MPS) disorders exhibit tissue-specificity for GAG metabolism and function. Those MPSs involving lysosomal storage of CS/DSPG and KSPG families are associated with skeletal disorders (MPS VI, MPS IVA, MPS VII). In contrast, HSPGs are usually associated with central nervous system (CNS) pathology (MPS III), and MPS enzymes common to multiple GAG pathways cause both skeletal and CNS pathology (e.g., MPS I and II). An elegant example of the critical role of CSPG synthetic and catabolic enzymes in growth regulation are the consequences of either deletion of C4ST or MPS VI, both of which lead to skeletal malformations. Although MPS VI and C4ST phenotypes are not identical, there are similarities indicating that both synthesis and degradation of CSPGs cause cellular de-regulation of growth plate development. As discussed earlier, C4ST deficiency hyper-activates TGFβ signaling while down-regulating BMP signaling (Klüppel et al., 2005). MPS VI is due to N-acetylgalactosamine-4-sulfatase deficiency and contributes to degradation of CS-4 and DS, leading to severe skeletal disorders in humans (Litjens and Hopwood, 2001). Since CS-4 is the major GAG in the cartilage growth plate, a mechanistic link between CS-4 and MPS-VI bone shortening and growth plate disorganization is proposed (Alliston, 2010). Although the expression of TGFß and other TGFß-regulated genes are disrupted in both chondroitin-4-sulfotransferase 1 (C4ST-1 also known as CHST11) (Klüppel et al., 2005) and MPS-VI (Simonaro et al., 2005), detailed aspects of the mechanisms controlling disruptions in skeletogenesis in the mucopolysaccharidoses largely remain to be determined.

### Osteoarthritis

Understanding functional interactions between components of the ECM and signaling pathways that control synthesis of the ECM components is also critical to degrative diseases like osteoarthritis (OA), a common degenerative disorder with no current disease-modifying therapies. This skeletal disorder is due to degradation of the major CSPG, aggrecan, mostly by specific enzymes, aggrecanases (ADAMTS-5). These aggrecan degradative enzymes are upregulated by mediators associated with joint inflammation or tissue overloading (Roughley and Mort, 2014). Interestingly, deletion of the TGFβ receptor type II gene, a component of the TGFβ/SMAD3 signaling system which represses chondrocyte hypertrophic differentiation required for maintaining articular cartilage (Yang et al., 2001), leads to a progressive osteoarthritis-like phenotype in mice (Shen et al., 2013), again illustrating disease causation by both CSPG alteration and major signaling pathways. As well, the number of mutations in the TGFβ1 signaling cascade with increased OA risk, provide strong evidence of a protective role for TGFβ. Thus, clinical trials to assess treatment of OA by intra-articular injection of allogenic chondrocytes transduced to express TGFβ1 have shown improved range of movement and reduced pain scores (Ha et al., 2012) and are being continued to assess long term improvement (Lee et al., 2020).

Other approaches have also been attempted to improve the OA pathology: inhibiting the degradative enzymes (Glasson et al., 2005) or increasing the repair capacity of cartilage through delivery of factors that promote ECM synthesis; although challenging the latter approach has been more rigorously investigated [reviewed in (Patel and Lim, 2019)]. To test whether the osteoarthritis degenerative process may be retarded by enhancing production of aggrecan, individual or combinations of growth factors including: FGF2, TGFβ, and members of the BMP family, have been delivered via gene therapy to osteoarthritis models (Trippel et al., 2007; Shi et al., 2013). More recently, direct intra-articular injection of autologous plasma containing high platelet levels, that are activated by cartilage ECM proteins, thereby releasing their

anabolic growth factors (TGFβ1, PDGF, IGF, FGF2) and promoting aggrecan synthesis (Everts et al., 2020) have also been used as therapy. While numerous *in vitro* studies and clinical trials with plasma have produced mixed results (McClurg et al., 2021), intra-articular injection of individual anabolic factors still remains a particularly active area. As example, FGF18 significantly reduced cartilage degeneration in a rat OA model (Moore et al., 2005; Mori et al., 2014). Pharmaceutical companies have produced a modified form of FGF18 (i.e., sprifermin) that stimulates proliferation of chondrocytes, increases GAG production and decreases ADAMTS5 expression (Gigout et al., 2017). Human clinical trials using cartilage structural parameters and patient-reported pain and stiffness scores as outcomes, showed some improvements in cartilage thickness, but no change in function or pain scores (Hochberg et al., 2019). Lastly, WNT signaling promotes hypertrophic differentiation of chondrocytes with deleterious effects on cartilage homeostasis (Usami et al., 2016; Dell'Accio and Cailotto, 2018); thus, inhibition of WNT signaling is also being explored for OA therapy. Several small molecule inhibitors have been developed and are in clinical trials, with promising results (Deshmukh et al., 2019; Yazici et al., 2020). As well, introduction of genetically engineered cells (TissueGene-C) over-expressing TGFβ packaged into a cell line (Lim et al., 2017) has entered Phase 3 Clinical trials (Mobasheri et al., 2020). Clearly, stimulating chondrogenic differentiation with known growth factor genes/proteins is a potential strategy for *ex vivo* gene therapy modalities in the complex cartilage ECM (Uzieliene et al., 2021). Furthermore, on the basis of the lessons learned from the skeletal developmental models, inhibiting chondrocyte maturation and maintaining high levels of CSPG biosynthesis are critical to harnessing the potential of these novel therapies.

## SIGNALING IN REGENERATION

Because of the complexity of the ECM with multiple physical, biological, and chemical interactions involving temporal control of signaling molecule networks, it is challenging to recreate these environments experimentally. As well, growth factors and morphogens are intrinsically unstable, while the ECM is both an active participant and is needed for dimensionality, as the examples in this review have shown. Thus, innovative biomaterial design and tissue engineering strategies are required involving: *i*) autologous or xenographic cells from the tissue to be formed; *ii*) signaling molecules which provide instruction for expressing a desire phenotype; and *iii*) synthetic scaffolds that hold the cells together and shape the tissue formation (Bason et al., 2018). Basically, the goal is to recapitulate the embryonic development and patterning process. Because of the prevalence of skeletal injuries, especially in the pediatric population 15–30% of pediatric skeletal injuries involve the growth plate (Shen et al., 2020), and because injury often results in replacement of cartilage by bone which precludes additional skeletal length growth (Gigante and Martinez, 2019), the growth plate is a highly desirable target for repair. However, in order to successfully re-engineer cartilage tissue, the natural characteristics of the growth plate, i.e., gradients of cell states, composition of ECM, position and function of growth regulators and mechanical properties must be replicated; the growth plate still remains an active model for studying tissue engineering strategies (Wang et al., 2021). Examples include: i) use of various cell types, i.e., bone marrow mesenchymal stem cells (BMSCs) or chondrocytes; ii) and various growth factors (TGFβ, IGF1, and FGF2) (Chen et al., 2020; Wei et al., 2020); iii) as well as different scaffolds composed of natural or synthetic material (Abdollahiyan et al., 2020), all with varying results. Mesenchymal stem cells (MSCs) are widely used in engineering of cartilage due to their capability for self-renewal and their ability to secrete multiple growth factors (Gultekin et al., 2020). As well, there is an influx of MSCs to the injured growth plate site, suggesting that MSCs are naturally vital to the repair process (Zhou et al., 2004). Several studies have shown that MSCs can be derived from multiple sources (Uder et al., 2018), with different regenerative potentials (Maheshwer et al., 2021). Other studies have used autologous chondrocytes which prevent bone formation, build the desired columnar structure and avoid immune rejection (Jin et al., 2006; Tomaszewski et al., 2014; Boopalan et al., 2019). Advances also continue to be made in developing three dimensional cultures that successfully retain the chondrogenic potential (Chow et al., 2011), as well culturing chondrocytes on synthetic hydrogels prior to seeding has been shown to lead to synthesis of Sox-9, aggrecan and collagen, which accumulate over time (Chang et al., 2018). As mentioned, manipulating the microenvironment by addition of chondrogenic-factors (TGFβ1, FGF-2, IGF-1, etc.) stimulates chondrogenesis and synthesis of ECM components (Thielen et al., 2019) (see previous sections). A major improvement in the regeneration process is the introduction of 3D printing technology, which allows different parts of the scaffold to have distinct porosity and mechanical properties, thus more faithfully recapitulating a natural cartilage growth plate (Shaw et al., 2018). In sum, to maintain viable cells, preserve growth factor stability, develop biocompatible as well as degradable natural (or synthetic) scaffolds is an extremely active research area in the field of growth plate regeneration summarized in Wang et al. (2021). Furthermore, many of the concepts are also shared with the bone regeneration field where appropriate combinations of scaffolding and seeding cells with growth factors are also being developed to engineer missing pieces of bone lost due to genetic malformations, trauma, tumors or infections (Perez et al., 2018; Koons et al., 2020; Alonzo et al., 2021). Although results continue to move in promising directions, there are still many challenges and unsolved problems that need to be resolved to benefit clinical application, as might be expected for recapitulating such a complex system such as the skeletal growth plate.

## CONCLUSION

Decades of studies have identified the hierarchical ECM-directed creation of the skeletal growth plate, which involves differentiation and growth of chondrocytes, positioning of

cells, matrix and regulators into a highly integrated, bidirectional and temporally orchestrated process. As well, the reciprocity between ECM components, transcription factors, and signaling molecules that coordinate their expression has been revealed by the plethora of chondrodysplasias due to mutations in these regulatory molecules as well as proteoglycans and their biosynthetic enzymes that disrupt growth plate development and maturation summarized in Guasto and Cormier-Daire (2021). However, a more comprehensive molecular understanding is required to fully understand how chondrogenesis and growth plate expansion are regulated with such exquisite precision. As well, more detailed structural information to define the requisite structural interactions between CSPGs and pathway modulators are necessary to develop novel ECM/signaling paradigms, in order to reverse or ameliorate skeletal pathology.

## AUTHOR CONTRIBUTIONS

All authors listed have made a substantial, direct, and intellectual contribution to the work and approved it for publication.

## FUNDING

This work was funded with grants from the NIH (R01 HD-17332 and R01 AM-00603).

## ACKNOWLEDGMENTS

We are grateful to all the past lab members who contributed to the cited studies.

## REFERENCES

Abdollahiyan, P., Oroojalian, F., Mokhtarzadeh, A., and Guardia, M. (2020). Hydrogel-Based 3D Bioprinting for Bone and Cartilage Tissue Engineering. *Biotechnol. J.* 15 (12), 2000095. doi:10.1002/biot.202000095

Alazami, A. M., Al-Qattan, S. M., Faqeih, E., Alhashem, A., Alshammari, M., Alzahrani, F., et al. (2016). Expanding the Clinical and Genetic Heterogeneity of Hereditary Disorders of Connective Tissue. *Hum. Genet.* 135 (5), 525–540. doi:10.1007/s00439-016-1660-z

Alliston, T. (2010). Chondroitin Sulfate and Growth Factor Signaling in the Skeleton: Possible Links to MPS VI. *J. Pediatr. Rehabil. Med.* 3 (2), 129–138. doi:10.3233/PRM-2010-0117

Alonzo, M., Alvarez Primo, F., Anil Kumar, S., Mudloff, J. A., Dominguez, E., Fregoso, G., et al. (2021). Bone Tissue Engineering Techniques, Advances, and Scaffolds for Treatment of Bone Defects. *Curr. Opin. Biomed. Eng.* 17, 100248. doi:10.1016/j.cobme.2020.100248

Archer, C. W., Dowthwaite, G. P., and Francis-West, P. (2003). Development of Synovial Joints. *Birth Defect Res. C* 69 (2), 144–155. doi:10.1002/bdrc.10015

Argraves, W. S., McKeown-Longo, P. J., and Goetinck, P. F. (1981). Absence of Proteoglycan Core Protein in the Cartilage Mutant Nanomelia. *FEBS Lett.* 131 (2), 265–268. doi:10.1016/0014-5793(81)80381-x

Azouz, E. M., Teebi, A. S., Eydoux, P., Chen, M. F., and Fassier, F. (1998). Bone Dysplasias: an Introduction. *Can. Assoc. Radiol. J.* 49 (2), 105–109.

Baldridge, D., Shchelochkov, O., Kelley, B., and Lee, B. (2010). Signaling Pathways in Human Skeletal Dysplasias. *Annu. Rev. Genom. Hum. Genet.* 11, 189–217. doi:10.1146/annurev-genom-082908-150158

Baratela, W. A. R., Bober, M. B., Tiller, G. E., Okenfuss, E., Ditro, C., Duker, A., et al. (2012). A Newly Recognized Syndrome with Characteristic Facial Features, Skeletal Dysplasia, and Developmental Delay. *Am. J. Med. Genet.* 158A (8), 1815–1822. doi:10.1002/ajmg.a.35445

Bason, C., Gallorini, M., and Berardi, A. C. (2018). "The Extracellular Matrix, Growth Factors and Morphogens in Biomaterial Design and Tissue Engineering," in *ed. A.C. Berardi. (Totowa, NJ: Humana Press, Inc.)*, 3–26. doi:10.1007/978-3-319-77023-9_1

Baur, S. T., Mai, J. J., and Dymecki, S. M. (2000). Combinatorial Signaling through BMP Receptor IB and GDF5: Shaping of the Distal Mouse Limb and the Genetics of Distal Limb Diversity. *Development* 127 (3), 605–619. doi:10.1242/dev.127.3.605

Bayliss, M. T., Osborne, D., Woodhouse, S., and Davidson, C. (1999). Sulfation of Chondroitin Sulfate in Human Articular Cartilage. *J. Biol. Chem.* 274 (22), 15892–15900. doi:10.1074/jbc.274.22.15892

Boopalan, P. J. V. C., Varghese, V., Sathishkumar, S., Arumugam, S., and Amarnath, V. (2019). Similar Regeneration of Articular Cartilage Defects with Autologous & Allogenic Chondrocytes in a Rabbit Model. *Indian J. Med. Res.* 149 (5), 650–655. doi:10.4103/ijmr.IJMR_1233_17

Bourdon, M. A., Krusius, T., Campbell, S., Schwartz, N. B., and Ruoslahti, E. (1987). Identification and Synthesis of a Recognition Signal for the Attachment of Glycosaminoglycans to Proteins. *Proc. Natl. Acad. Sci. U.S.A.* 84, 3194–3198. doi:10.1073/pnas.84.10.3194

Budde, B. S., Mizumoto, S., Kogawa, R., Becker, C., Altmüller, J., Thiele, H., et al. (2015). Skeletal Dysplasia in a Consanguineous Clan from the Island of Nias/Indonesia Is Caused by a Novel Mutation in B3GAT3. *Hum. Genet.* 134 (7), 691–704. doi:10.1007/s00439-015-1549-2

Bui, C., Huber, C., Tuysuz, B., Alanay, Y., Bole-Feysot, C., Leroy, J. G., et al. (2014). XYLT1 Mutations in Desbuquois Dysplasia Type 2. *Am. J. Hum. Genet.* 94 (3), 405–414. doi:10.1016/j.ajhg.2014.01.020

Byrne, A. B., Mizumoto, S., Arts, P., Yap, P., Feng, J., Schreiber, A. W., et al. (2020). Pseudodiastrophic Dysplasia Expands the Known Phenotypic Spectrum of Defects in Proteoglycan Biosynthesis. *J. Med. Genet.* 57 (7), 454–460. doi:10.1136/jmedgenet-2019-106700

Campos-Xavier, A., Saraiva, J. M., Savarirayan, R., Verloes, A., Feingold, J., Faivre, L., et al. (2001). Phenotypic Variability at the TGF-β1 Locus in Camurati-Engelmann Disease. *Hum. Genet.* 109 (6), 653–658. doi:10.1007/s00439-001-0644-8

Cardin, A. D., and Weintraub, H. J. (1989). Molecular Modeling of Protein-Glycosaminoglycan Interactions. *Arteriosclerosis* 9 (1), 21–32. doi:10.1161/01.atv.9.1.21

Cartault, F., Munier, P., Jacquemont, M.-L., Vellayoudom, J., Doray, B., Payet, C., et al. (2015). Expanding the Clinical Spectrum of B4GALT7 Deficiency: Homozygous p.R270C Mutation with Founder Effect Causes Larsen of Reunion Island Syndrome. *Eur. J. Hum. Genet.* 23 (1), 49–53. doi:10.1038/ejhg.2014.60

Chang, C., Yang, C. Y., Yang, C., Hsiao, H., Chen, L., Chu, I., et al. (2018). Cultivation of Auricular Chondrocytes in Poly(ethylene Glycol)/poly(ε-Caprolactone) Hydrogel for Tracheal Cartilage Tissue Engineering in a Rabbit Model. *eCM* 35, 350–364. doi:10.22203/eCM.v035a24

Chen, L., Liu, J., Guan, M., Zhou, T., Duan, X., and Xiang, Z. (2020). Growth Factor and its Polymer Scaffold-Based Delivery System for Cartilage Tissue Engineering. *Int. J. Nanomedicine* 15, 6097–6111. doi:10.2147/IJN.S249829

Choocheep, K., Hatano, S., Takagi, H., Watanabe, H., Kimata, K., Kongtawelert, P., et al. (2010). Versican Facilitates Chondrocyte Differentiation and Regulates Joint Morphogenesis. *J. Biol. Chem.* 285 (27), 21114–21125. doi:10.1074/jbc.M109.096479

Chow, S. K.-H., Lee, K.-M., Qin, L., Leung, K.-S., and Cheung, W.-H. (2011). Restoration of Longitudinal Growth by Bioengineered Cartilage Pellet in Physeal Injury Is Not Affected by Low Intensity Pulsed Ultrasound. *J. Biomed. Mater. Res.* 99B (1), 36–44. doi:10.1002/jbm.b.31869

Clause, K. C., and Barker, T. H. (2013). Extracellular Matrix Signaling in Morphogenesis and Repair. *Curr. Opin. Biotechnol.* 24 (5), 830–833. doi:10.1016/j.copbio.2013.04.011

Cortes, M., Baria, A. T., and Schwartz, N. B. (2009). Sulfation of Chondroitin Sulfate Proteoglycans Is Necessary for Proper Indian Hedgehog Signaling in the Developing Growth Plate. *Development* 136 (10), 1697–1706. doi:10.1242/dev.030742

Dell'Accio, F., and Cailotto, F. (2018). Pharmacological Blockade of the WNT-Beta-Catenin Signaling: a Possible First-In-Kind DMOAD. *Osteoarthr. Cartil.* 26 (1), 4–6. doi:10.1016/j.joca.2017.10.014

Deshmukh, V., O'Green, A. L., Bossard, C., Seo, T., Lamangan, L., Ibanez, M., et al. (2019). Modulation of the Wnt Pathway through Inhibition of CLK2 and DYRK1A by Lorecivivint as a Novel, Potentially Disease-Modifying Approach for Knee Osteoarthritis Treatment. *Osteoarthr. Cartil.* 27 (9), 1347–1360. doi:10.1016/j.joca.2019.05.006

Domowicz, M. S., Pirok, E. W., III, Novak, T. E., and Schwartz, N. B. (2000). Role of the C-Terminal G3 Domain in Sorting and Secretion of Aggrecan Core Protein and Ubiquitin-Mediated Degradation of Accumulated Mutant Precursors. *J. Biol. Chem.* 275 (45), 35098–35105. doi:10.1074/jbc.275.45.35098

Domowicz, M. S., Cortes, M., Henry, J. G., and Schwartz, N. B. (2009). Aggrecan Modulation of Growth Plate Morphogenesis. *Develop. Biol.* 329 (2), 242–257. doi:10.1016/j.ydbio.2009.02.024

Everts, P., Onishi, K., Jayaram, P., Lana, J. F., and Mautner, K. (2020). Platelet-Rich Plasma: New Performance Understandings and Therapeutic Considerations in 2020. *Int. J. Mol. Sci.* 21 (20), 7794. doi:10.3390/ijms21207794

Faiyaz ul Haque, M., King, L. M., Krakow, D., Cantor, R. M., Rusiniak, M. E., Swank, R. T., et al. (1998). Mutations in Orthologous Genes in Human Spondyloepimetaphyseal Dysplasia and the Brachymorphic Mouse. *Nat. Genet.* 20 (2), 157–162. doi:10.1038/2458

Frederick, J. P., Tafari, A. T., Wu, S.-M., Megosh, L. C., Chiou, S.-T., Irving, R. P., et al. (2008). A Role for a Lithium-Inhibited Golgi Nucleotidase in Skeletal Development and Sulfation. *Proc. Natl. Acad. Sci. U.S.A.* 105 (33), 11605–11612. doi:10.1073/pnas.0801182105

Gibson, B. G., and Briggs, M. D. (2016). The Aggrecanopathies; an Evolving Phenotypic Spectrum of Human Genetic Skeletal Diseases. *Orphanet J. Rare Dis.* 11 (1), 86. doi:10.1186/s13023-016-0459-2

Gigante, C., and Martinez, A. I. C. (2019). Desepiphysiodesis and Reconstruction of the Distal Radial Growth Plate with an Autologous Iliac Crest Cartilage Graft: A Case Report and Review of Literature. *J. Orthop. Case Rep.* 10 (1), 70–73. doi:10.13107/jocr.2019.v10.i01.1642

Gigout, A., Guehring, H., Froemel, D., Meurer, A., Ladel, C., Reker, D., et al. (2017). Sprifermin (rhFGF18) Enables Proliferation of Chondrocytes Producing a Hyaline Cartilage Matrix. *Osteoarthr. Cartil.* 25 (11), 1858–1867. doi:10.1016/j.joca.2017.08.004

Gjorevski, N., and Nelson, C. M. (2009). Bidirectional Extracellular Matrix Signaling during Tissue Morphogenesis. *Cytokine Growth Factor. Rev.* 20 (5-6), 459–465. doi:10.1016/j.cytogfr.2009.10.013

Glasson, S. S., Askew, R., Sheppard, B., Carito, B., Blanchet, T., Ma, H.-L., et al. (2005). Deletion of Active ADAMTS5 Prevents Cartilage Degradation in a Murine Model of Osteoarthritis. *Nature* 434 (7033), 644–648. doi:10.1038/nature03369

Gleghorn, L., Ramesar, R., Beighton, P., and Wallis, G. (2005). A Mutation in the Variable Repeat Region of the Aggrecan Gene (AGC1) Causes a Form of Spondyloepiphyseal Dysplasia Associated with Severe, Premature Osteoarthritis. *Am. J. Hum. Genet.* 77 (3), 484–490. doi:10.1086/444401

Guasto, A., and Cormier-Daire, V. (2021). Signaling Pathways in Bone Development and Their Related Skeletal Dysplasia. *Int. J. Mol. Sci.* 22 (9), 4321. doi:10.3390/ijms22094321

Gultekin, A., Ağirdīl, Y., Duman, B. Ö., Demïr, C. S., and Karaöz, E. (2020). Comparison of Mesenchymal Stem Cell Sheets and Chondrocyte Sheets in a Rabbit Growth Plate Injury Model. *Turk J. Med. Sci.* 50 (4), 1082–1096. doi:10.3906/sag-1902-228

Ha, C.-W., Noh, M. J., Choi, K. B., and Lee, K. H. (2012). Initial Phase I Safety of Retrovirally Transduced Human Chondrocytes Expressing Transforming Growth Factor-Beta-1 in Degenerative Arthritis Patients. *Cytotherapy* 14 (2), 247–256. doi:10.3109/14653249.2011.629645

Hickery, M. S., Bayliss, M. T., Dudhia, J., Lewthwaite, J. C., Edwards, J. C. W., and Pitsillides, A. A. (2003). Age-related Changes in the Response of Human Articular Cartilage to IL-1α and Transforming Growth Factor-β (TGF-β). *J. Biol. Chem.* 278 (52), 53063–53071. doi:10.1074/jbc.M209632200

Hilton, M. J., Tu, X., Cook, J., Hu, H., and Long, F. (2005). Ihh Controls Cartilage Development by Antagonizing Gli3, but Requires Additional Effectors to Regulate Osteoblast and Vascular Development. *Development* 132 (19), 4339–4351. doi:10.1242/dev.02025

Hochberg, M. C., Guermazi, A., Guehring, H., Aydemir, A., Wax, S., Fleuranceau-Morel, P., et al. (2019). Effect of Intra-articular Sprifermin vs Placebo on Femorotibial Joint Cartilage Thickness in Patients with Osteoarthritis. *JAMA* 322 (14), 1360–1370. doi:10.1001/jama.2019.14735

Hoffmann, H.-P., Schwartz, N. B., Rodén, L., and Prockop, D. J. (1984). Location of Xylosyltransferase in the Cisternae of the Rough Endoplasmic Reticulum of Embryonic Cartilage Cells. *Connect. Tissue Res.* 12, 151–163. doi:10.3109/03008208408992780

Horiki, M., Imamura, T., Okamoto, M., Hayashi, M., Murai, J., Myoui, A., et al. (2004). Smad6/Smurf1 Overexpression in Cartilage Delays Chondrocyte Hypertrophy and Causes Dwarfism with Osteopenia. *J. Cel Biol.* 165 (3), 433–445. doi:10.1083/jcb.200311015

Iozzo, R. V., and Schaefer, L. (2015). Proteoglycan Form and Function: A Comprehensive Nomenclature of Proteoglycans. *Matrix Biol.* 42, 11–55. doi:10.1016/j.matbio.2015.02.003

Jin, X.-b., Luo, Z.-j., and Wang, J. (2006). Treatment of Rabbit Growth Plate Injuries with an Autologous Tissue-Engineered Composite. *Cells Tissues Organs* 183 (2), 62–67. doi:10.1159/000095510

Karsenty, G., and Wagner, E. F. (2002). Reaching a Genetic and Molecular Understanding of Skeletal Development. *Develop. Cel* 2 (4), 389–406. doi:10.1016/s1534-5807(02)00157-0

Kearns, A. E., Vertel, B. M., and Schwartz, N. B. (1993). Topography of Glycosylation and UDP-Xylose Production. *J. Biol. Chem.* 268 (15), 11097–11104. doi:10.1016/s0021-9258(18)82097-x

Kitagawa, H., Uyama, T., and Sugahara, K. (2001). Molecular Cloning and Expression of a Human Chondroitin Synthase. *J. Biol. Chem.* 276 (42), 38721–38726. doi:10.1074/jbc.M106871200

Klüppel, M., Vallis, K. A., and Wrana, J. L. (2002). A High-Throughput Induction Gene Trap Approach Defines C4ST as a Target of BMP Signaling. *Mech. Dev.* 118 (1-2), 77–89. doi:10.1016/s0925-4773(02)00198-3

Klüppel, M., Wight, T. N., Chan, C., Hinek, A., and Wrana, J. L. (2005). Maintenance of Chondroitin Sulfation Balance by Chondroitin-4-Sulfotransferase 1 Is Required for Chondrocyte Development and Growth Factor Signaling during Cartilage Morphogenesis. *Development* 132 (17), 3989–4003. doi:10.1242/dev.01948

Knox, S. M., and Whitelock, J. M. (2006). Perlecan: How Does One Molecule Do So many Things? *Cell. Mol. Life Sci.* 63 (21), 2435–2445. doi:10.1007/s00018-006-6162-z

Koons, G. L., Diba, M., and Mikos, A. G. (2020). Materials Design for Bone-Tissue Engineering. *Nat. Rev. Mater.* 5 (8), 584–603. doi:10.1038/s41578-020-0204-2

Kozhemyakina, E., Lassar, A. B., and Zelzer, E. (2015). A Pathway to Bone: Signaling Molecules and Transcription Factors Involved in Chondrocyte Development and Maturation. *Development* 142 (5), 817–831. doi:10.1242/dev.105536

Koziel, L., Kunath, M., Kelly, O. G., and Vortkamp, A. (2004). Ext1-dependent Heparan Sulfate Regulates the Range of Ihh Signaling during Endochondral Ossification. *Develop. Cel* 6 (6), 801–813. doi:10.1016/j.devcel.2004.05.009

Krueger, R. C., Fields, T. A., Hildreth, J., and Schwartz, N. B. (1990). Chick Cartilage Chondroitin Sulfate Proteoglycan Core Protein. I. Generation and Characterization of Peptides and Specificity for Glycosaminoglycan Attachment. *J. Biol. Chem.* 265 (20), 12075–12087. doi:10.1016/s0021-9258(19)38509-6

Krueger, R. C., Kurima, K., and Schwartz, N. B. (1999). Completion of the Mouse Aggrecan Gene Structure and Identification of the Defect in the Cmd-Bc Mouse as a Near Complete Deletion of the Murine Aggrecan Gene. *Mamm. Genome* 10, 1119–1125. doi:10.1007/s003359901176

Kurima, K., Warman, M. L., Krishnan, S., Domowicz, M., Krueger, R. C., Jr., Deyrup, A., et al. (1998). A Member of a Family of Sulfate-Activating Enzymes Causes Murine Brachymorphism. *Proc. Natl. Acad. Sci. U.S.A.* 95 (15), 8681–8685. doi:10.1073/pnas.95.15.8681

LaCroix, A. J., Stabley, D., Sahraoui, R., Adam, M. P., Mehaffey, M., Kernan, K., et al. (2019). GGC Repeat Expansion and Exon 1 Methylation of XYLT1 Is a Common Pathogenic Variant in Baratela-Scott Syndrome. *Am. J. Hum. Genet.* 104 (1), 35–44. doi:10.1016/j.ajhg.2018.11.005

Landauer, W. (1965). Nanomelia, a Lethal Mutation of the Fowl. *J. Hered.* 56, 131–138. doi:10.1093/oxfordjournals.jhered.a107392

Lauing, K. L., Cortes, M., Domowicz, M. S., Henry, J. G., Baria, A. T., and Schwartz, N. B. (2014). Aggrecan Is Required for Growth Plate Cytoarchitecture and

Differentiation. *Develop. Biol.* 396 (2), 224–236. doi:10.1016/j.ydbio.2014.10.005

Lee, D., Erickson, A., Dudley, A. T., and Ryu, S. (2019). Mechanical Stimulation of Growth Plate Chondrocytes: Previous Approaches and Future Directions. *Exp. Mech.* 59 (9), 1261–1274. doi:10.1007/s11340-018-0424-1

Lee, B., Parvizi, J., Bramlet, D., Romness, D. W., Guermazi, A., Noh, M., et al. (2020). Results of a Phase II Study to Determine the Efficacy and Safety of Genetically Engineered Allogeneic Human Chondrocytes Expressing TGF-β1. *J. Knee Surg.* 33 (2), 167–172. doi:10.1055/s-0038-1676803

Li, H., Schwartz, N. B., and Vertel, B. M. (1993). cDNA Cloning of Chick Cartilage Chondroitin Sulfate (Aggrecan) Core Protein and Identification of a Stop Codon in the Aggrecan Gene Associated with the Chondrodystrophy, Nanomelia. *J. Biol. Chem.* 268, 23504–23511. doi:10.1016/s0021-9258(19)49491-x

Li, Y., Laue, K., Temtamy, S., Aglan, M., Kotan, L. D., Yigit, G., et al. (2010). Temtamy Preaxial Brachydactyly Syndrome Is Caused by Loss-Of-Function Mutations in Chondroitin Synthase 1, a Potential Target of BMP Signaling. *Am. J. Hum. Genet.* 87 (6), 757–767. doi:10.1016/j.ajhg.2010.10.003

Lim, C.-L., Lee, Y.-J., Cho, J.-H., Choi, H., Lee, B., Lee, M. C., et al. (2017). Immunogenicity and Immunomodulatory Effects of the Human Chondrocytes, hChonJ. *BMC Musculoskelet. Disord.* 18 (1), 199. doi:10.1186/s12891-017-1547-8

Litjens, T., and Hopwood, J. J. (2001). Mucopolysaccharidosis type VI: Structural and clinical implications of mutations in N-acetylgalactosamine-4-sulfatase. *Hum Mutat* 18 (4), 282–295. doi:10.1002/humu.1190

Maheshwer, B., Polce, E. M., Paul, K., Williams, B. T., Wolfson, T. S., Yanke, A., et al. (2021). Regenerative Potential of Mesenchymal Stem Cells for the Treatment of Knee Osteoarthritis and Chondral Defects: A Systematic Review and Meta-Analysis. *Arthrosc. J. Arthroscopic Relat. Surg.* 37 (1), 362–378. doi:10.1016/j.arthro.2020.05.037

Malfait, F., Kariminejad, A., Van Damme, T., Gauche, C., Syx, D., Merhi-Soussi, F., et al. (2013). Defective Initiation of Glycosaminoglycan Synthesis Due to B3GALT6 Mutations Causes a Pleiotropic Ehlers-danlos-syndrome-like Connective Tissue Disorder. *Am. J. Hum. Genet.* 92 (6), 935–945. doi:10.1016/j.ajhg.2013.04.016

Malfait, F., Francomano, C., Byers, P., Belmont, J., Berglund, B., Black, J., et al. (2017). The 2017 International Classification of the Ehlers-Danlos Syndromes. *Am. J. Med. Genet. C Semin. Med. Genet.* 175 (1), 8–26. doi:10.1002/ajmg.c.31552

Malfait, F., Castori, M., Francomano, C. A., Giunta, C., Kosho, T., and Byers, P. H. (2020). The Ehlers-Danlos Syndromes. *Nat. Rev. Dis. Primers* 6 (1), 64. doi:10.1038/s41572-020-0194-9

McClurg, O., Tinson, R., and Troeberg, L. (2021). Targeting Cartilage Degradation in Osteoarthritis. *Pharmaceuticals* 14 (2), 126. doi:10.3390/ph14020126

Melvin, T., and Schwartz, N. B. (1988). Biochemical Correlations in Animal Models of Chondrodysplasias. *Path Immunopathol. Res.* 7 (1-2), 68–72. doi:10.1159/000157096

Mihalic Mosher, T., Zygmunt, D. A., Koboldt, D. C., Kelly, B. J., Johnson, L. R., McKenna, D. S., et al. (2019). Expansion of B4GALT7 Linkeropathy Phenotype to Include Perinatal Lethal Skeletal Dysplasia. *Eur. J. Hum. Genet.* 27 (10), 1569–1577. doi:10.1038/s41431-019-0464-8

Mis, E. K., Liem, K. F., Jr., Kong, Y., Schwartz, N. B., Domowicz, M., and Weatherbee, S. D. (2014). Forward Genetics Defines Xylt1 as a Key, Conserved Regulator of Early Chondrocyte Maturation and Skeletal Length. *Develop. Biol.* 385 (1), 67–82. doi:10.1016/j.ydbio.2013.10.014

Mizuhashi, K., Ono, W., Matsushita, Y., Sakagami, N., Takahashi, N., Saunders, T. L., et al. (2018). Resting zone of the growth plate houses a unique class of skeletal stem cells. *Nature* 563(7730), 254-258. doi:10.1038/s41586-018-0662-5

Mizumoto, S., and Yamada, S. (2021). Congenital Disorders of Deficiency in Glycosaminoglycan Biosynthesis. *Front. Genet.* 12, 717535. doi:10.3389/fgene.2021.717535

Mobasheri, A., Hinton, M., Shaikh, F., and Kubassova, O. (2020). The Role of Advanced MRI in the Development of Treat-To-Target Therapeutic Strategies, Patient Stratification and Phenotyping in Rheumatoid Arthritis. *BMC Rheumatol.* 4, 33. doi:10.1186/s41927-020-00131-w

Moore, E. E., Bendele, A. M., Thompson, D. L., Littau, A., Waggie, K. S., Reardon, B., et al. (2005). Fibroblast Growth Factor-18 Stimulates Chondrogenesis and Cartilage Repair in a Rat Model of Injury-Induced Osteoarthritis. *Osteoarthr. Cartil.* 13 (7), 623–631. doi:10.1016/j.joca.2005.03.003

Mori, Y., Saito, T., Chang, S. H., Kobayashi, H., Ladel, C. H., Guehring, H., et al. (2014). Identification of Fibroblast Growth Factor-18 as a Molecule to Protect Adult Articular Cartilage by Gene Expression Profiling. *J. Biol. Chem.* 289 (14), 10192–10200. doi:10.1074/jbc.M113.524090

Muller, S., Disse, J., Schöttler, M., Schön, S., Prante, C., Brinkmann, T., et al. (2006). Human Xylosyltransferase I and N-Terminal Truncated Forms: Functional Characterization of the Core Enzyme. *Biochem. J.* 394 (Pt 1), 163–171. doi:10.1042/BJ20051606

Munns, C. F., Fahiminiya, S., Poudel, N., Munteanu, M. C., Majewski, J., Sillence, D. O., et al. (2015). Homozygosity for Frameshift Mutations in XYLT2 Result in a Spondylo-Ocular Syndrome with Bone Fragility, Cataracts, and Hearing Defects. *Am. J. Hum. Genet.* 96 (6), 971–978. doi:10.1016/j.ajhg.2015.04.017

Nakajima, M., Mizumoto, S., Miyake, N., Kogawa, R., Iida, A., Ito, H., et al. (2013). Mutations in B3GALT6, Which Encodes a Glycosaminoglycan Linker Region Enzyme, Cause a Spectrum of Skeletal and Connective Tissue Disorders. *Am. J. Hum. Genet.* 92 (6), 927–934. doi:10.1016/j.ajhg.2013.04.003

Orkin, R. W., Pratt, R. M., and Martin, G. R. (1976). Undersulfated Chondroitin Sulfate in the Cartilage Matrix of Brachymorphic Mice. *Develop. Biol.* 50 (1), 82–94. doi:10.1016/0012-1606(76)90069-5

Patel, D. K., and Lim, K. T. (2019). Biomimetic Polymer-Based Engineered Scaffolds for Improved Stem Cell Function. *Materials* 12 (18), 2950. doi:10.3390/ma12182950

Perez, J. R., Kouroupis, D., Li, D. J., Best, T. M., Kaplan, L., and Correa, D. (2018). Tissue Engineering and Cell-Based Therapies for Fractures and Bone Defects. *Front. Bioeng. Biotechnol.* 6, 105. doi:10.3389/fbioe.2018.00105

Ritelli, M., Chiarelli, N., Zoppi, N., Dordoni, C., Quinzani, S., Traversa, M., et al. (2015). Insights in the Etiopathology of Galactosyltransferase II (GalT-II) Deficiency from Transcriptome-wide Expression Profiling of Skin Fibroblasts of Two sisters with Compound Heterozygosity for Two Novel B3GALT6 Mutations. *Mol. Genet. Metab. Rep.* 2, 1–15. doi:10.1016/j.ymgmr.2014.11.005

Ritelli, M., Dordoni, C., Cinquina, V., Venturini, M., Calzavara-Pinton, P., and Colombi, M. (2017). Expanding the Clinical and Mutational Spectrum of B4GALT7-spondylodysplastic Ehlers-Danlos Syndrome. *Orphanet J. Rare Dis.* 12 (1), 153. doi:10.1186/s13023-017-0704-3

Roughley, P. J., and Mort, J. S. (2014). The Role of Aggrecan in normal and Osteoarthritic Cartilage. *J. Exp. Ortop* 1 (1), 8. doi:10.1186/s40634-014-0008-7

Sakai, K., Kimata, K., Sato, T., Gotoh, M., Narimatsu, H., Shinomiya, K., et al. (2007). Chondroitin Sulfate N-Acetylgalactosaminyltransferase-1 Plays a Critical Role in Chondroitin Sulfate Synthesis in Cartilage. *J. Biol. Chem.* 282 (6), 4152–4161. doi:10.1074/jbc.M606870200

Salter, C. G., Davies, J. H., Moon, R. J., Fairhurst, J., Bunyan, D., Foulds, N., et al. (2016). Further Defining the Phenotypic Spectrum ofB4GALT7mutations. *Am. J. Med. Genet.* 170 (6), 1556–1563. doi:10.1002/ajmg.a.37604

Sanford, L. P., Ormsby, I., Gittenberger-de Groot, A. C., Sariola, H., Friedman, R., Boivin, G. P., et al. (1997). TGFbeta2 Knockout Mice Have Multiple Developmental Defects that Are Non-overlapping with Other TGFbeta Knockout Phenotypes. *Development* 124 (13), 2659–2670. doi:10.1242/dev.124.13.2659

Schön, S., Prante, C., Bahr, C., Kuhn, J., Kleesiek, K., and Götting, C. (2006). Cloning and Recombinant Expression of Active Full-Length Xylosyltransferase I (XT-I) and Characterization of Subcellular Localization of XT-I and XT-II. *J. Biol. Chem.* 281, 14224–14231. doi:10.1074/jbc.M510690200

Schreml, J., Durmaz, B., Cogulu, O., Keupp, K., Beleggia, F., Pohl, E., et al. (2014). The Missing "link": an Autosomal Recessive Short Stature Syndrome Caused by a Hypofunctional XYLT1 Mutation. *Hum. Genet.* 133 (1), 29–39. doi:10.1007/s00439-013-1351-y

Schwartz, N. B., and Domowicz, M. S. (1998). "Proteoglycan Gene Mutations and Impaired Skeletal Development," in *Skeletal Growth and Development*. Editors J. A. Buckwalter, M. G. Ehrlich, L. J. Sandell, and S. B. Trippel (Rosemont, IL: American Association of Orthopedic Surgeon Publications), 413–433.

Schwartz, N. B., and Domowicz, M. (2002). Chondrodysplasias Due to Proteoglycan Defects. *Glycobiology* 12 (4), 57R–68R. doi:10.1093/glycob/12.4.57R

Schwartz, N. B., and Domowicz, M. (2014). "Chondrodysplasias," in *Reference Module in Biomedical Sciences*. San Diego, CA: Elsevier Science Inc. doi:10.1016/B978-0-12-801238-3.03764-8

Schwartz, N. B., and Rodén, L. (1974). Biosynthesis of Chondroitin Sulfate. Purification of UDP-D-Xylose:core Protein β-d-xylosyltransferase by Affinity Chromatography. *Carbohydr. Res.* 37 (1), 167–180. doi:10.1016/s0008-6215(00)87072-x

Schwartz, N. B., and Rodén, L. (1975). Biosynthesis of Chondroitin Sulfate. Solubilization of Chondroitin Sulfate Glycosyltransferases and Partial Purification of Uridine Diphosphate-D-galactose:D-Xylose Galactosyltrans. *J. Biol. Chem.* 250 (13), 5200–5207. doi:10.1016/s0021-9258(19)41296-9

Schwartz, N. B., Ostrowski, V., Brown, K. S., and Pratt, R. M. (1978). Defective PAPS-Synthesis in Epiphyseal Cartilage from Brachymorphic Mice. *Biochem. Biophys. Res. Commun.* 82 (1), 173–178. doi:10.1016/0006-291x(78)90592-2

Schwartz, N. B., Hennig, A. K., Krueger, R. C., Krzystolik, M., Li, H., and Mangoura, D. (1993). "Developmental Expression of S103L Cross-Reacting Proteoglycans in Embryonic Chick," in *Limb Development and Regeneration*. Editors J. F. Fallon, P. F. Goetinck, R. O. Kelley, and D. L. Stocum (New York: Wiley-Liss, Inc.), 505–514.

Schwartz, N. B. (1976). Biosynthesis of Chondroitin Sulfate. Role of Phospholipids in the Activity of UDP-D-Galactose: D-Xylose Galactosyltransferase. *J. Biol. Chem.* 251, 285–291. doi:10.1016/s0021-9258(17)33876-0

Schwartz, N. B. (1995). Xylosylation: The First Step in Synthesis of Proteoglycan. *Trends Glycosci. Glycotechnol.* 7, 429–445. doi:10.4052/tigg.7.429

Schwartz, N. B. (2000). Biosynthesis and Regulation of Expression of Proteoglycans. *Front. Biosci.* 5, D649–D655. doi:10.2741/a540

Schwartz, N. B. (2014). Proteoglycan. *Encyclopedia Life Sci.* 3, 1–10. doi:10.1002/9780470015902.a0000623.pub3

Serra, R., and Chang, C. (2003). TGF-beta Signaling in Human Skeletal and Patterning Disorders. *Birth Defect Res. C* 69 (4), 333–351. doi:10.1002/bdrc.10023

Shaw, N., Erickson, C., Bryant, S. J., Ferguson, V. L., Krebs, M. D., Hadley-Miller, N., et al. (2018). Regenerative Medicine Approaches for the Treatment of Pediatric Physeal Injuries. *Tissue Eng. B: Rev.* 24 (2), 85–97. doi:10.1089/ten.TEB.2017.0274

Shen, J., Li, J., Wang, B., Jin, H., Wang, M., Zhang, Y., et al. (2013). Deletion of the Transforming Growth Factor β Receptor Type II Gene in Articular Chondrocytes Leads to a Progressive Osteoarthritis-like Phenotype in Mice. *Arthritis Rheum.* 65 (12), 3107–3119. doi:10.1002/art.38122

Shen, M., Liu, S., Jin, X., Mao, H., Zhu, F., Saif, T., et al. (2020). Porcine Growth Plate Experimental Study and Estimation of Human Pediatric Growth Plate Properties. *J. Mech. Behav. Biomed. Mater.* 101, 103446. doi:10.1016/j.jmbbm.2019.103446

Shepard, J. B., Krug, H. A., LaFoon, B. A., Hoffman, S., and Capehart, A. A. (2007). Versican Expression during Synovial Joint Morphogenesis. *Int. J. Biol. Sci.* 3 (6), 380–384. doi:10.7150/ijbs.3.380

Shi, X., Zhou, J., Zhao, Y., Li, L., and Wu, H. (2013). Gradient-regulated Hydrogel for Interface Tissue Engineering: Steering Simultaneous Osteo/chondrogenesis of Stem Cells on a Chip. *Adv. Healthc. Mater.* 2 (6), 846–853. doi:10.1002/adhm.201200333

Silbert, J. E., and Sugumaran, G. (1995). Intracellular Membranes in the Synthesis, Transport, and Metabolism of Proteoglycans. *Biochim. Biophys. Acta Rev. Biomembr.* 1241 (3), 371–384. doi:10.1016/0304-4157(95)00011-9

Simonaro, C. M., D'Angelo, M., Haskins, M. E., and Schuchman, E. H. (2005). Joint and Bone Disease in Mucopolysaccharidoses VI and VII: Identification of New Therapeutic Targets and Biomarkers Using Animal Models. *Pediatr. Res.* 57 (5 Pt 1), 701–707. doi:10.1203/01.PDR.0000156510.96253.5A

Snow, H. E., Riccio, L. M., Mjaatvedt, C. H., Hoffman, S., and Capehart, A. A. (2005). Versican Expression during Skeletal/joint Morphogenesis and Patterning of Muscle and Nerve in the Embryonic Mouse Limb. *Anat. Rec.* 282A (2), 95–105. doi:10.1002/ar.a.20151

Soares da Costa, D., Reis, R. L., and Pashkuleva, I. (2017). Sulfation of Glycosaminoglycans and its Implications in Human Health and Disorders. *Annu. Rev. Biomed. Eng.* 19, 1–26. doi:10.1146/annurev-bioeng-071516-044610

Sohaskey, M. L., Yu, J., Diaz, M. A., Plaas, A. H., and Harland, R. M. (2008). JAWS Coordinates Chondrogenesis and Synovial Joint Positioning. *Development* 135 (13), 2215–2220. doi:10.1242/dev.019950

Song, Y., Zhang, F., and Linhardt, R. J. (2021). Glycosaminoglycans. *Adv. Exp. Med. Biol.* 1325, 103–116. doi:10.1007/978-3-030-70115-4_4

Stattin, E. L., Wiklund, F., Önnerfjord, P., Jonsson, B.-A., Tegner, Y., Sasaki, T., et al. (2010). A Missense Mutation in the Aggrecan C-type Lectin Domain Disrupts Extracellular Matrix Interactions and Causes Dominant Familial Osteochondritis Dissecans. *Am. J. Hum. Genet.* 86 (2), 126–137. doi:10.1016/j.ajhg.2009.12.018

Sugahara, K., and Schwartz, N. B. (1979). Defect in 3'-phosphoadenosine 5'-phosphosulfate Formation in Brachymorphic Mice. *Proc. Natl. Acad. Sci. U.S.A.* 76 (12), 6615–6618. doi:10.1073/pnas.76.12.6615

Sugahara, K., and Schwartz, N. B. (1982a). Defect in 3'-phosphoadenosine 5'-phosphosulfate Synthesis in Brachymorphic Mice. I. Characterization of the Defect. *Arch. Biochem. Biophys.* 214 (2), 589–601. doi:10.1016/0003-9861(82)90064-9

Sugahara, K., and Schwartz, N. B. (1982b). Defect in 3'-phosphoadenosine 5'-phosphosulfate Synthesis in Brachymorphic Mice. II. Tissue Distribution of the Defect. *Arch. Biochem. Biophys.* 214 (2), 602–609. doi:10.1016/0003-9861(82)90065-0

Sugahara, K., and Schwartz, N. B. (1982c). "Tissue Distribution of Defective PAPS Synthesis and Decreased Sulfoconjugation of a Phenolic Compound in Brachymorphic Mice," in Proceedings of the 6th International Symposium on Glycoconjugates. Editors T. Yamakawa, T. Oswa, and S. Handa (Tokyo, Japan: Sci. Soc. Press), 493–495.

Taylan, F., Costantini, A., Coles, N., Pekkinen, M., Héon, E., Şıklar, Z., et al. (2016). Spondyloocular Syndrome: Novel Mutations in XYLT2 Gene and Expansion of the Phenotypic Spectrum. *J. Bone Miner. Res.* 31 (8), 1577–1585. doi:10.1002/jbmr.2834

Taylan, F., Yavaş Abalı, Z., Jäntti, N., Güneş, N., Darendeliler, F., Baş, F., et al. (2017). Two Novel Mutations in XYLT2 Cause Spondyloocular Syndrome. *Am. J. Med. Genet.* 173 (12), 3195–3200. doi:10.1002/ajmg.a.38470

Thiele, H., Sakano, M., Kitagawa, H., Sugahara, K., Rajab, A., Höhne, W., et al. (2004). Loss of Chondroitin 6- O -sulfotransferase-1 Function Results in Severe Human Chondrodysplasia with Progressive Spinal Involvement. *Proc. Natl. Acad. Sci. U.S.A.* 101 (27), 10155–10160. doi:10.1073/pnas.0400334101

Thielen, N., van der Kraan, P., and van Caam, A. (2019). TGFβ/BMP Signaling Pathway in Cartilage Homeostasis. *Cells* 8 (9), 969. doi:10.3390/cells8090969

Tian, J., Ling, L., Shboul, M., Lee, H., O'Connor, B., Merriman, B., et al. (2010). Loss of CHSY1, a Secreted FRINGE Enzyme, Causes Syndromic Brachydactyly in Humans via Increased NOTCH Signaling. *Am. J. Hum. Genet.* 87 (6), 768–778. doi:10.1016/j.ajhg.2010.11.005

Tomaszewski, R., Bohosiewicz, J., Gap, A., Bursig, H., and Wysocka, A. (2014). Autogenous Cultured Growth Plate Chondrocyte Transplantation in the Treatment of Physeal Injury in Rabbits. *Bone Jt. Res.* 3 (11), 310–316. doi:10.1302/2046-3758.311.2000207

Tompson, S. W., Merriman, B., Funari, V. A., Fresquet, M., Lachman, R. S., Rimoin, D. L., et al. (2009). A Recessive Skeletal Dysplasia, SEMD Aggrecan Type, Results from a Missense Mutation Affecting the C-type Lectin Domain of Aggrecan. *Am. J. Hum. Genet.* 84 (1), 72–79. doi:10.1016/j.ajhg.2008.12.001

Townley, R. A., and Bulow, H. E. (2018). Deciphering Functional Glycosaminoglycan Motifs in Development. *Curr. Opin. Struct. Biol.* 50, 144–154. doi:10.1016/j.sbi.2018.03.011

Trippel, S., Cucchiarini, M., Madry, H., Shi, S., and Wang, C. (2007). Gene Therapy for Articular Cartilage Repair. *Proc. Inst. Mech. Eng. H* 221 (5), 451–459. doi:10.1243/09544119JEIM237

Uder, C., Brückner, S., Winkler, S., Tautenhahn, H.-M., and Christ, B. (2018). Mammalian MSC from Selected Species: Features and Applications. *Cytometry* 93 (1), 32–49. doi:10.1002/cyto.a.23239

Umair, M., Eckstein, G., Rudolph, G., Strom, T., Graf, E., Hendig, D., et al. (2018). Homozygous XYLT2 Variants as a Cause of Spondyloocular Syndrome. *Clin. Genet.* 93 (4), 913–918. doi:10.1111/cge.13179

Usami, Y., Gunawardena, A. T., Iwamoto, M., and Enomoto-Iwamoto, M. (2016). Wnt Signaling in Cartilage Development and Diseases: Lessons from Animal Studies. *Lab. Invest.* 96 (2), 186–196. doi:10.1038/labinvest.2015.142

Uzieliene, I., Kalvaityte, U., Bernotiene, E., and Mobasheri, A. (2021). Non-viral Gene Therapy for Osteoarthritis. *Front. Bioeng. Biotechnol.* 8, 618399. doi:10.3389/fbioe.2020.618399

Vertel, B. M., Walters, L. M., Flay, N., Kearns, A. E., and Schwartz, N. B. (1993). Xylosylation Is an Endoplasmic Reticulum to Golgi Event. *J. Biol. Chem.* 268 (15), 11105–11112. doi:10.1016/s0021-9258(18)82098-1

Vertel, B. M., Grier, B. L., Li, H., and Schwartz, N. B. (1994). The Chondrodystrophy, Nanomelia: Biosynthesis and Processing of the Defective Aggrecan Precursor. *Biochem. J.* 301, 211–216. doi:10.1042/bj3010211

Voglmeir, J., Voglauer, R., and Wilson, I. B. H. (2007). XT-II, the Second Isoform of Human Peptide-O-Xylosyltransferase, Displays Enzymatic Activity. *J. Biol. Chem.* 282 (9), 5984–5990. doi:10.1074/jbc.M608087200

Vortkamp, A. (2001). Interaction of Growth Factors Regulating Chondrocyte Differentiation in the Developing Embryo. *Osteoarthr. Cartil.* 9 (Suppl. A), S109–S117.

Wang, X., Li, Z., Wang, C., Bai, H., Wang, Z., Liu, Y., et al. (2021). Enlightenment of Growth Plate Regeneration Based on Cartilage Repair Theory: A Review. *Front. Bioeng. Biotechnol.* 9, 654087. doi:10.3389/fbioe.2021.654087

Watanabe, H., Kimata, K., Line, S., Strong, D., Gao, L.-y., Kozak, C. A., et al. (1994). Mouse Cartilage Matrix Deficiency (Cmd) Caused by a 7 Bp Deletion in the Aggrecan Gene. *Nat. Genet.* 7 (2), 154–157. doi:10.1038/ng0694-154

Wei, P., Xu, Y., Gu, Y., Yao, Q., Li, J., and Wang, L. (2020). IGF-1-releasing PLGA Nanoparticles Modified 3D Printed PCL Scaffolds for Cartilage Tissue Engineering. *Drug Deliv.* 27 (1), 1106–1114. doi:10.1080/10717544.2020.1797239

Whalen, D. M., Malinauskas, T., Gilbert, R. J. C., and Siebold, C. (2013). Structural Insights into Proteoglycan-Shaped Hedgehog Signaling. *Proc. Natl. Acad. Sci. U.S.A.* 110 (41), 16420–16425. doi:10.1073/pnas.1310097110

Wilson, D. G., Phamluong, K., Lin, W. Y., Barck, K., Carano, R. A. D., Diehl, L., et al. (2012). Chondroitin Sulfate Synthase 1 (Chsy1) Is Required for Bone Development and Digit Patterning. *Develop. Biol.* 363 (2), 413–425. doi:10.1016/j.ydbio.2012.01.005

Yang, X., Chen, L., Xu, X., Li, C., Huang, C., and Deng, C.-X. (2001). TGF-β/Smad3 Signals Repress Chondrocyte Hypertrophic Differentiation and Are Required for Maintaining Articular Cartilage. *J. Cel Biol.* 153 (1), 35–46. doi:10.1083/jcb.153.1.35

Yazici, Y., McAlindon, T. E., Gibofsky, A., Lane, N. E., Clauw, D., Jones, M., et al. (2020). Lorecivivint, a Novel Intraarticular CDC-like Kinase 2 and Dual-Specificity Tyrosine Phosphorylation-Regulated Kinase 1A Inhibitor and Wnt Pathway Modulator for the Treatment of Knee Osteoarthritis: A Phase II Randomized Trial. *Arthritis Rheumatol.* 72 (10), 1694–1706. doi:10.1002/art.41315

Zhou, F. H., Foster, B. K., Sander, G., and Xian, C. J. (2004). Expression of Proinflammatory Cytokines and Growth Factors at the Injured Growth Plate Cartilage in Young Rats. *Bone* 35 (6), 1307–1315. doi:10.1016/j.bone.2004.09.014

**Conflict of Interest:** The authors declare that the research was conducted in the absence of any commercial or financial relationships that could be construed as a potential conflict of interest.

**Publisher's Note:** All claims expressed in this article are solely those of the authors and do not necessarily represent those of their affiliated organizations, or those of the publisher, the editors and the reviewers. Any product that may be evaluated in this article, or claim that may be made by its manufacturer, is not guaranteed or endorsed by the publisher.

# Advantages of publishing in Frontiers

**OPEN ACCESS**
Articles are free to read for greatest visibility and readership

**FAST PUBLICATION**
Around 90 days from submission to decision

**HIGH QUALITY PEER-REVIEW**
Rigorous, collaborative, and constructive peer-review

**TRANSPARENT PEER-REVIEW**
Editors and reviewers acknowledged by name on published articles

**Frontiers**
Avenue du Tribunal-Fédéral 34
1005 Lausanne | Switzerland

**Visit us:** www.frontiersin.org
**Contact us:** frontiersin.org/about/contact

**REPRODUCIBILITY OF RESEARCH**
Support open data and methods to enhance research reproducibility

**DIGITAL PUBLISHING**
Articles designed for optimal readership across devices

**FOLLOW US**
@frontiersin

**IMPACT METRICS**
Advanced article metrics track visibility across digital media

**EXTENSIVE PROMOTION**
Marketing and promotion of impactful research

**LOOP RESEARCH NETWORK**
Our network increases your article's readership